Importance of TRPV3 in the regulation of Sub-cellular organelles and their functions: Implications in health disorders

By

Ram Prasad Sahu

LIFE11201604006

National Institute of Science Education and Research,
Bhubaneswar

A thesis submitted to the
Board of Studies in Life Sciences
In partial fulfilment of the requirements
For the Degree of

DOCTOR OF PHILOSOPHY

of

HOMI BHABHA NATIONAL INSTITUTE

December, 2023

Homi Bhabha National Institute[1]

1. Recommendations of the Viva Voce Committee

As members of the Viva Voce Committee, we certify that we have read the dissertation prepared by **Ram Prasad Sahu** entitled **" Importance of TRPV3 in the regulation of Sub-cellular organelles and their functions: Implications in health disorders"** and recommend that it may be accepted as fulfilling the thesis requirement for the award of Degree of Doctor of Philosophy.

Chairman – Dr. Asima Bhattacharyya	
Guide / Convener – Prof. Chandan Goswami	Chandan Goswami
Co-guide - NA	
Examiner – Prof. Amitabh Chattopadhyay	
Member 1- Dr. Praful Singru	
Member 2- Dr. Kishore CS Panigrahi	
Member 3- Dr. Moloy Sarkar	

Final approval and acceptance of this thesis is contingent upon the candidate's submission of the final copies of the thesis to HBNI.

I/We hereby certify that I/we have read this thesis prepared under my/our direction and recommend that it may be accepted as fulfilling the thesis requirement.

Date: 18.4.2024

Place: NISER, Jatni

Chandan Goswami

Signature 18/04/2024

Guide

[1] This page is to be included only for final submission after successful completion of viva voce.

STATEMENT BY AUTHOR

This dissertation has been submitted in partial fulfilment of requirements for an advanced degree at Homi Bhabha National Institute (HBNI) and is deposited in the Library to be made available to borrowers under the rules of the HBNI.

Brief quotations from this dissertation are allowable without special permission, provided that accurate acknowledgement of the source is made. Requests for permission for extended quotation from or reproduction of this manuscript in whole or in part may be granted by the Competent Authority of HBNI when in his or her judgment the proposed use of the material is in the interests of scholarship. In all other instances, however, permission must be obtained from the author.

Ram Prasad Sahu

DECLARATION

I hereby declare that the investigation presented in the thesis has been carried out by me. The work is original and has not been submitted earlier as a whole or in part for a degree/diploma at this or any other Institution / University.

Ram Prasad Sahu

List of Publications in Refereed Journal:

Published:

1. ***Sahu R.P**. and Goswami C. (2023) Presence of TRPV3 in macrophage lysosomes helps in skin wound healing against bacterial infection. *Experimental Dermatology*, **32**, pp.60-74.
2. *Jain A[1]., **Sahu R. P[1]** & Goswami C. (2022) Olmsted syndrome-causing point mutants of TRPV3 (G568C and G568D) show defects in intracellular Ca2+-mobilization and induce lysosomal defects. *Biochemical and Biophysical Research Communications*. **628**, pp.32-39.

Other Publications:

Book/Book Chapter:

1. *Acharya T.K., **Sahu R.P**., Kumar S., Kumar S., Rokade T.P., Chakraborty R., Dubey N.K., Shikha D., Chawla S. and Goswami C. (2022) Function and regulation of thermosensitive ion channel TRPV4 in the immune system. In *Current Topics in Membranes*. **89**, pp. 155-188. (**Book chapter**)
2. *Dubey N.K., Das N.K., Mahapatra P., Mohanta S., Shikha D., Banerjee A., **Sahu R.P**., Acharya T.K., Mishra S., Kumar S., Rokade T.P., Kumar V., Halder R.R., Sing R., Aswin T., Kumar S., Goswami L., Kumar S.and Goswami C. (2023) Current understanding of TRP channels and their genomics: *Implication in health research*. (Accepted **Book chapter**).

Other Publications:

1. Pany S., **Sahu R.P**., Ranjit M., Pati S., Suar M. and Samal S.K. (**2024**). Bio-fabrication of ZnONPs Using Mimosa pudica Extract to combat Multidrug Resistant

Uropathogens. *Journal of Industrial and Engineering Chemistry.* https://doi.org/10.1016/j.jiec.2024.02.020. (Accepted)

2. Panda S.K., **Sahu R.P**., Goswami C. and Singh A.K. (**2023**) Easily synthesizable molecular probe for the nanomolar level detection of Cd^{2+} in near aqueous media: Theoretical investigations and live cell imaging. *Spectrochimica Acta Part A: Molecular and Biomolecular Spectroscopy*, **302**, p.123098.
3. Panda S.K., **Sahu R.P**, Goswami C. and Singh A.K. (**2023**) Robust Optical Detection of Ga^{3+} by a Rhodamine-and Coumarin-Based Proficient Probe: Theoretical Investigations and Biological Applications. *ACS Applied Bio Materials*. (Accepted)
4. Mahanta S., Prusty M., Sivakumar P.S., Mishra D., **Sahu R.P**., Goswami C., Chawla S., Goswami L., Elangovan S. and Panda S.K. (**2022**) Novel Levilactobacillus brevis-based formulation for controlling cell proliferation, cell migration and gut dysbiosis. *LWT*, **154**, p.112818.
5. Sengupta S., Singh A., Dutta, K., **Sahu R.P**., Kumar S., Goswami C., Chawla S., Goswami L. and Bandyopadhyay A. (2021) Branched/hyperbranched copolyesters from poly (vinyl alcohol) and citric acid as delivery agents and tissue regeneration scaffolds. *Macromolecular Chemistry and Physics*, **222**, p.2100134.
6. Yadav C., Chhajed M., Choudhury P., **Sahu R.P**., Patel A., Chawla S., Goswami L., Goswami C., Li X., Agrawal A.K. and Saini A. (2021) Bio-extract amalgamated sodium alginate-cellulose nanofibres based 3D-sponges with interpenetrating BioPU coating as potential wound care scaffolds. *Materials Science and Engineering*: *C*, **118**, p.111348.
7. Sanjai Kumar P., Nayak T.K., Mahish C., Sahoo S.S., Radhakrishnan A., De S., Datey A., **Sahu R.P.,** Goswami C., Chattopadhyay S. and Chattopadhyay S. (2021) Inhibition of transient receptor potential vanilloid 1 (TRPV1) channel regulates chikungunya virus infection in macrophages. *Archives of virology*, **166**, pp.139-155.

* = Pertinent to the thesis work, **1** = Co-author

Conference, Symposium and workshops:

1. EMBO Meet, Rockville, Maryland 20852, USA **Cell Biology Virtual-2021, ASCB, EMBO,** presented an **oral poster** titled" Generation of a new *in-vivo* wound healing model in rodents for understanding ion channel & complex cellular functions in skin".
2. **National Virtual Conference on Recent Breakthroughs in Biotechnology (NCRBB-2021), Annual Meet of Society for Biotechnologists (SBTI, India)** Department of Human Genetics and Molecular Biology, Bharathiar University, Coimbatore, presented **oral presentation** entitled" Generation of a new wound healing model in rodents for understanding ion channel and complex cellular functions in skin".
3. Biswa Bangla Convention Centre, Kolkata **India International Science Festival (IISF) 2019** Presented **poster** on the theme 'Frontier areas in research' titled "Role of TRPV3 in Nucleolar functions".
4. National Institute of Science Education and Research (NISER), Odisha **Pre-Conference Workshop Electron Microscope Society of India (EMSI) 2018** Participated in two-day workshop entitled " Light microscopies and Live Cell Imaging". Mode of Participation: Demonstrator 30/11/2017 – 02/12/2017.
5. Institute of Life Sciences, Bhubaneswar. **International Conference on Proteomics in Health and Disease (2017)** Participated in 9th Annual Meeting of Proteomics Society, India and International Conference on "Proteomics in Health and Disease".
6. School of Biological Sciences, National Institute of Science Education and Research (NISER), Odisha **Symposium on Recent Advancement on Neuroscience (2017)** Participated in the symposium on "Recent Advancement on Neuroscience".

Ram Prasad Sahu

Ram Prasad Sahu

Dedicated to...

MY BELOVED FAMILY & FRIENDS

ACKNOWLEDGEMENTS

The journey towards PhD is a unique and life-time experience for me. In this occasion, I acknowledge each and every one who is directly or indirectly associated with me during this journey. Without their guidance, help and blessing, this thesis would not have been completed. I would like to express my gratitude to Dr. Chandan Goswami, my thesis supervisor, for his constant guidance and support during this challenging journey. His continuous encouragement and efforts to push my academic boundaries were instrumental in making this thesis achievable. Without his expertise and mentorship, this undertaking would have seemed impossible.

Also, I would like to acknowledge my thesis monitoring committee and doctoral committee members Dr. Asima Bhattacharyya, Dr. Moloy Sarkar (NISER Bhubaneswar), Dr. Praful Singru, Dr. Kishor Panigrahi (NISER Bhubaneswar), CSIR external member Dr. Soma Chattopadhyay (ILS, Bhubaneswar) and CSIR three-member committee member Dr. Harapriya Mohapatra (NISER, Bhubaneswar) for their scientific advice during this time. A special thanks to Dr. Soma Chattopadhyay and her lab members (especially Dr. Sanjai Kumar) for conducting some of the important viral pathogenesis-related experiments.

I would like to acknowledge Dr. Saurabh Chawla and all the animal house (NCARE NISER) members for their constant support and guidance for the animal experiments. I would like to acknowledge all the faculty members and staff from the School of Biological Sciences for their constant help and support. I acknowledge the Imaging facility and other central instrumentation facilities from the School of Biological Science. Also, I would like to acknowledge the academics sections, and finance sections for constantly helping academically in the process of releasing CSIR fellowship and contingency.

Also, I would like to acknowledge the help from other scientists across the world for providing constructs. Dr. Yong Yang (Beijing China) for providing TRPV3-WT and OS mutant

construct, Dr. Jon D Levine (UCSF, San Francisco) for sending pCDNA 3.1 construct, Dr. Y T Chang (Department of Chemistry, POSTECH Korea) for providing subcellular thermo sensitive dyes, Dr. Don Cleveland (Ludwig Institute for Cancer Research, USA) and Dr. Ben E. Black (Perelman School of Medicine at the University of Pennsylvania, USA) for CENP-A EYFP and CENP-A EGFP. Also, I would like to thank Dr. Dibyendu Bhattacharyya for providing Lamin-RFP and Fibrillarin-GFP constructs. My sincere thanks to Dr. Vinay Kumar Nandicoori (National Institute of Immunology, New Delhi, India) and Dr. Savita Lochab from his lab for helping me with *Mycobacterium* phagocytosis experiments. Also, I would like to thank Dr. Luna Goswami (KIIT University, Bhubaneswar), Dr. Sandeep Panda (KIIT University, Bhubaneswar) for their scientific input and guidance during this period. I would also like to thank Dr. Santosh Chauhan and his labs for providing different cell lines (THP-1, Neuro-2A, HEK cell lines) and certain plasmids (pEGFP-N1hAIM2, P62-GFP, NLRP3-GFP and HA-ASC) for my PhD work. I would also like to thank all funding agencies (DAE) and CSIR for extending their financial support during my PhD tenure.

Special thanks to all my former lab members namely, Dr. Ashutosh Kumar, Dr. Manoj Yadav, Dr. Rakesh Kumar Majhi, Dr. Ankit Tiwari, Dr. Somdatta Saha, Dr. Rashmita Das, Dr. Tusar Kanta Acharya, Ms Divyanshi Verma, Mr. Nikhil Tiwari, Mr. Vivek Sahoo, Dr. Arijit Ghosh, Ms. Anushka Jain, Mr. Tejas Rokade, Mr. Shamit Kumar, Ms. Sherya Soni, Mr. Ritesh Dalai, Mr. Harshit Haldua, Mr. Aniket Modak, Mr. Priyadarshan Pradhan, Ms. Srujanika and present lab members Dr. Satish Kumar, Ms. Sushama Mohanta, Mr. Nishant Kumar Dubey, Ms. Deepsikha, Mr. Nilesh Kumar Das, Mr. Subham Mishra, Ms. Raima Singh, Ms. Tanisha Aswin, Mr. Vikash Kumar, Mr. Ramizur Rahaman Halder, Ms. Parnasree Mahapatra, Ms. Anupriya Chattapadhya and all other lab members. Also, I would like to thank my batchmates, namely Mr. Aranyadip Gayen, Mr. Tathagata Mukherjee, Mr. Chandan Mahish and all other SBS students and friends for their support during my PhD time and for making this journey

wonderful. A special thanks to Ms. Anushka Jain for making pmCherry-tagged TRPV3-WT and TRPV3-OS mutants (G568C and G568D) constructs for the requirement of my PhD work. Also thank to NISER beautiful captivating natural flora and fauna which has kept me calm and grounded in this journey.

I would also like to thank all my close friends from other institutes like Mr. Satya Ranjan Sahu from ILS Bhubaneswar and others for supporting me professionally. And special thank to Ms. Swarnaprabha Pany (PhD Scholar at RMRC Bhubaneswar) for supporting throughout my PhD tenure professionally as well ase emotionally during this period. I would also like to thank my parents, my elder brothers, my elder sisters, and other family members for their continuous help and support in this time of PhD. Without their support, this journey would have been impossible.

I would also like to thank all my spiritual masters who constantly motivated me during this adventurous and beautiful life journey. At the last, I thank the ultimate master who kept me in check and never allowed any obstruction or never allowed any opposing force to dictate my mind during this period and helped me to play my part in this journey.

Ram Prasad Sahu

Table of Contents

Summary

Ion channels evolved as specialized proteins for specific tasks at the cell surface, mainly to detect different stimuli present in the surrounding environments. These channels perform various functions as per the requirements based on the extent of the stimuli present in the surroundings. Among different ions, one of the essential cation is the Ca^{2+}. Ca^{2+} ions perform versatile functions and is essential for numerous cellular functions. Their role as secondary messengers in cellular signalling is unique, influencing processes like neurotransmitter release, muscle movement, enzyme activation, gene activity, and cell division. Ca^{2+} is unique due to its precise control, and its level is maintained by specialized channels and pumps, ensuring specific concentrations in different compartments of the cell. This meticulous regulation makes Ca^{2+} crucial for orchestrating various cellular activities, vital for smooth functioning of the cell and supporting life processes. Dysfunction of Ca^{2+} channels can lead to severe pathophysiological conditions, underscoring their critical role in maintaining cellular homeostasis and overall physiological function. In the year 1969, first time TRP channels function were described (Cosens and Manning 1969). TRP channels are polymodal ion channels, which can also be modulated by physical, chemical and mechanical stimuli TRP channels are mostly permeable to Ca^{2+} and other divalent cations. The divalent cations pass through these channels down their concentration gradients. The polymodal TRP channels are classified in to multiple subfamilies according to their amino acid sequence, sequence homology and similarity. These include TRPC (canonical), TRPM (melastatin), TRPV (vanilloid), TRPA (Ankyrin), TRPML (mucolipin), TRPP (polycystin), and TRPN (NompC), respectively (Himmel et al. 2021). Among these seven subfamilies found in mammals, TRPV (vallinoid) (TRPV1-TRPV4) are thermosensitive in nature. The thermosensitive TRPV1-TRPV4 can be activated in the temperature ranges from 27°C to 52°C (Zhong et al. 2012). The other two members of TRPV (TRPV5- TRPV6) are not thermosensitive but are highly-

selective to Ca^{2+} ions (Liao et al. 2013; Cao et al. 2013). Transient Receptor Potential Vallinoid subtype (TRPV3), is a non-selective cation channel which primarily expresses in the skin tissue (keratinocytes), digestive tissue, oral epithelium, immune cells, brain, spinal cord, testes and other tissues where it regulates various physiological functions (Xu et al. 2002; Peier et al. 2002). TRPV3 is polymodal in nature and can be activated by various physical and chemical stimuli such as 2-APB, FPP (endogenous activator), camphor (from Cinnamon camphora), thymol (a natural compound from thyme), carvacrol (natural modulator from oregano), different metabolites, temperature (at the range of 33°C - 45°C), pH, osmolarity (Bang et al. 2010; Moqrich et al. 2005; Vogt-Eisele et al. 2007; Peier et al. 2002; Xu et al. 2002). Regarding the thermosensitivity of the TRPV3, mutagenesis of S6 and adjacent extracellular regions (I644S, N647Y, and Y661C) leads to the decreased "heat-sensitivity" of the channel (Grandl et al. 2008). The heat-evoked activation of TRPV3 can be distinguished from other thermosensitive ion channels like TRPV4. For example, heat-evoked response of TRPV3 grows progressively upon repetitive heat stimulations (Moqrich et al. 2005). The heat-evoked stimulations can lead to the release of prostaglandin E2 (which is a pain mediator in heat-evoked inflammation), adenosine triphosphate (ATP), and nitric oxide, respectively (Huang et al. 2008; Mandadi et al. 2009; Miyamoto et al. 2011). TRPV3 is pathophysiologically important because its mutations can lead to various and severe pathophysiological conditions like Olmsted Syndrome (OS), atopic dermatitis (AD), cancer, myocardial hypertrophy, cardiac fibrosis, alopecia, pain and others (Su et al. 2023).

Earlier, TRP channels were reported to be present predominantly or exclusively in the plasma membrane. Later studies indicated the presence of many TRP channels in the intracellular compartments required for specific subcellular organelle functions. Some of the intracellular organelles that contain TRP channels are secretory vesicles, late endosomes, lysosomes, mitochondria, endoplasmic reticulum, Golgi apparatus (Dong et al. 2010). Among

all the intracellular organelles, lysosome is one of the important sub-cellular compartments which carryout different functions like recycling of macromolecules, phagocytosis, clearance of pathogens, autophagy, maintenance of intracellular ion homeostasis. Specific TRP channels are known to be present in the lysosomal membrane, and some examples are TRPML1-3 and TRPV3 (Yadav and Goswami 2017; Dong et al. 2008; Vergarajauregui et al. 2008). Olmsted syndrome (OS, a rare genetic disorder) occurs due to point mutations in TRPV3 causing dysregulation of lysosomal functions and distributions. Other than the keratoderma (hyperkeratotic) problem, OS-causing TRPV3 mutants show deformities in the bone as well. Symptoms of OS often varies in patient to patient with certain common features. It often involves issues like pseudoainhum, problems with the skin, hearing difficulties, bone damage, and sometimes the spontaneous loss of the tips of limbs at different severity levels (Zhi et al 2016). These symptoms can range in their seriousness. At the cellular levels, OS-causing TRPV3 mutants show abnormalities in the Ca^{2+}-homeostasis and have abnormal lysosomal pH. Therefore, TRPV3 mutations causing OS, offers a cellular system to study the role of TRPV3 related to lysosomal functions. TRPV3 seems to be associated with various immune functions like wound healing, inflammation as observed in the skin tissue, and associated immune cells. Furthermore, higher expression of TRPV3 leads to skin inflammation and release of various inflammatory mediators such as interleukin 1α (Il-1α), TGF-β, NO, prostaglandin-E2, and ATP. This indicates the importance of TRPV3 in inflammatory functions (Huang et al. 2008; Miyamoto et al. 2011).

TRPV4, a functional homologous of the TRPV3 channel, is activated at temperature ranging from 27°C to 35°C. TRPV4 is also polymodal in nature and can be activated through various physical, mechanical stimuli and chemical (exogenous and endogenous compounds). Endogenous compounds include arachidonic acid metabolites, ATP, cholesterol, even steroids and cytoskeletal elements can modulate TRPV4 activity (Landoure et al. 2010; Watanabe et al.

2003; Das and Goswami. 2019; Dubey et al. 2023). Exogenous or synthetic agonist include compounds like phorbol esters, 4αPDD and GSK1016790A (Vincent et al. 2009; Baratchi et al. 2019; Vincent and Duncton. 2011; Rosenbaum et al. 2020). Expression of TRPV4 is detected in different tissues, including neurons, skin, lung, bone, bladder, etc. (Nilius et al. 2004; Liedtke et al. 2000; Strotmann et al. 2000; Jia et al. 2004). The wide-spread expression of TRPV4 accords well with its ability to respond against various stimuli, such as changes in the thermal status, mechanical stimuli, osmolarity as well as to endogenous ligands. The activation of TRPV4 with such stimuli also leads to Ca^{2+}-influx, which eventually can regulate several cellular processes such as cell migrations, proliferation, differentiations, immune responses and pain perceptions (Song et al. 2014; Lee et al. 2017; Willette et al. 2008). Any changes in channel structure or mutations can leads to severe pathophysiological conditions such as cancer, immune disorders, bone diseases, muscular dystrophy, pulmonary edema, inflammation, impaired lung function, etc. (Chen et al. 2023; Phan et al. 2009; Leddy et al. 2014; Hamacher et al. 2023).

Both TRPV3 and TRPV4 offer two important molecular targets to investigate various stresses, such as thermal stress, lysosomal stress, pathogenic stress at the cellular and molecular levels. The stress response of the cells coincides with qualitative and quantitative changes in the cellular parameters. Recent findings suggest that subcellular organelles, namely lysosomes, nucleolus, mitochondria, plasma-membrane all act as the stress-response hubs in the cell. The physiological stress or pathogenic stress can lead to various diseases which are related to dysregulation of TRPV3 or TRPV4 channel functions also. This thesis work attempted to investigate cellular stress response along with TRPV3 and TRPV4 channel modulations. For this study, different methods have been used to understand the cellular physiology. These methods include, cell culture-based assays, immunofluorescence, immunohistochemistry, immunomodulation, microbiology, animal histopathology, biochemistry, sensor-based

imaging and a lot of high-end microscopy of live cells. This study investigated the functional presence of TRPV3 in the subcellular organelles, namely in lysosome and in nucleus and also explored its regulations and functions there. The endogenous presence of TRPV3 and TRPV4 in the immune cells has been investigated in relations to subcellular functions. For that the primary macrophages, Raw 264.7 and THP-1 cells have been used. Both these channels are functionally present in the macrophages and localize in the subcellular compartments. This study also investigated few point mutants of TRPV3, which cause Olmsted Syndrome (OS) using HaCaT (a keratinocyte) and SaoS (osteogenic) cells through transient over expression of the TRPV3 mutants or TRPV3-WT. Different cellular parameters, such as lysosomal functions, phagocytosis, lysosomal pH regulations, lysosomal temperature regulations, cellular Ca^{2+} homeostasis, cytosolic ROS level, cytosolic NOS level, mitochondria ATP, mitochondria temperature, plasma membrane temperature have been investigated in details. It has been observed that the cellular, lysosomal, and mitochondrial status alters due to channel modulation and/or under certain conditions, the status of these sub-cellular organelle can be recovered/rescue to normal level through the modulations of any of these two channels. The bacterial clearance in the skin tissue and macrophage cells has been investigated. It has been observed that TRPV3 modulation helps in bacterial clearance at the wound site and results in early closure of wound. In *in vitro* system, TRPV3 modulation helps in early clearance of bacterial pathogen in macrophage cells. Similar trend has been observed in the presence of TRPV4 modulations also where it helps in clearance of microbial pathogens after phagocytosis, both in *in vivo* and in *in vitro* systems. TRPV3 is detected in the nucleolus in certain conditions. The nuclear presence of TRPV3 has also been investigated by using different cell lines that includes HaCaT, MC3T3-E1, Raw 264.7, F-11 respectively. The nucleolar localization of TRPV3 along with nucleolar marker (i.e. fibrillarin) has been observed. Apparently, TRPV3 has a novel nucleolar localization signal that remain fairly conserved in mammals and largely

present in all vertebrates, though at a lower conserved manner. Changes in the nucleolar size, morphology, and nuclear temperature due to TRPV3 modulation have been investigated. TRPV3 modulation seems to help in nucleolar size (according to cellular stress) and nuclear temperature regulation. The temperature of lysosomal, mitochondrial, plasma membrane seems to be elevated/dysregulated at cellular stress and/or TRPV3 modulations. Similarly, these parameters also change in cases of expression of OS-causing TRPV3 mutants as compared to TRPV3-WT

All these observations indicate that under stressful conditions, presence as well as modulation of these two channels help the cells to recover better from the sub-cellular organelle stress. Thus, TRPV3 or TRPV4 channel modulations provides adaptive benefits to the cells, especially in the stressful conditions.

List of figures:

List of tables:

List of Abbreviations:

4αPDD	4α-phorbol 12,13-didecanoate
ΔG	Gibbs free energy
ΔH	Enthalpy
ΔS	Entropy
ACBD	Acyl-CoA binding domain protein
AD	Atopic dermatitis
AFM	Atomic force microscopy
AKAP	A kinase anchor proteins
AKAP150	Artrial myocytes ankyrin protein
ALI	Acute lung injury
AMG517	N (4-(6-(4-(Trifluoromethyl)phenyl)pyrimidin-4-yloxy)benzo[d]thiazol-2-yl)acetamide, N-[4-[[6- [4-(Trifluoromethyl)phenyl]-4-pyrimidinyl]oxy]-2-benzothiazolyl]acetamide
Amp	Ampicillin
Ang2	Angiotensin-2
ANO1	Anoctamin 1
AP1	Activator protein 1
APS	Ammonium persulphate
ARD	Ankyrin repeat domain
ARD	Ankyrin repeat domain
ARDS	Acute respiratory distress syndrome
ATP	Adenosine triphosphate
BCECF-AM	2',7'-Bis-(2-Carboxyethyl)-5-(and-6)-Carboxyfluorescein, Acetoxymethyl Ester
BCYM3	Brachyolmia
Bp	Base pair
BSA	Bovine serum albumin
CaBP1	Ca^{2+} binding protein1
CaM	Calmodulin
CaMKII-ASK1	Calmodulin dependent protein kinase II- Apoptosis signal regulating kinase 1
CBB	Coomassie Brilliant Blue G250
CD	Coupling domain
CGRP	Calcitonin gene related peptide
CIPN	Chemotherapy induced neuropathic pain
CLC-O	Chloride conducting ion channel type O
CMT2C	Charcot mary tooth disease

CNS	Central nervous system
Co-IP	Co-Immuno precipitation
CRAC	Cholesterol-recognition amino-acid consensus
CREB	cAMP response element binding protein
CSK	Cytoskeletal buffer
DAG	Di acyl glycerol
DAPI	4',6-diamidino-2-phenylindole
Del	deletion
DMSO	Dimethyl Sulfoxide
DNA	Deoxyribonucleic acid
dNTP	deoxy Nucleotide Tri Phosphate
DPBA	diphenyl bionic anhydrate
DPTHF	2,2-Diphenyltetraiodofuran
DRG	Dorsal root ganglion
DRG	Dorsal root ganglion
DTT	DL-Dithiothreitol, threo-1,4-Dimercapto-2,3-butanediol
EC	Enzyme code
ECL	Enhanced Chemiluminescence
EDTA	Ethylene diamine tetraacetic acid
EET	Epoxy icosatrinoic acid
EGFR	Epidermal growth factor receptor
EGFR	Epidermal growth factor receptor
EGTA	Ethylene glycol bis(2-aminoethyl ether)tetraacetic acid
EM	Electron Microscopy
EP3	Subtype of prostaglandin E2
ER	Endoplasmic Reticulum
ERK	Extracellular regulated kinase
EtBr	Ethidium Bromide
FBS	Fetal bovine serum
Fluo-4 AM	Fluo-4 acetoxymethyl ester
FPP	Farnesyl pyrophosphate
FRAP	Fluorescence recovery after photobleaching
FRET	Fluorescence resonance energy transfer
GFP	Green Fluorescence Protein
GJB2	Gap junction protein beta 2
GPCR	G protein coupled receptor
GPCR	G-protein coupled receptor
GTP	Guanosine 5′-triphosphate
H	Hour (Time unit)

HaCaT	Human epidermal keratinocytes
HCl	Hydrogen Chloride
HEPES	4-(2-Hydroxyethyl) piperazine-1-ethanesulfonic acid
HRP	Horseradish Peroxidase
HSP	hereditary spastic paraplegia
HTH	Helix Turn Helix Motif
Hz	Hertz
IAV	Inactive Ion channel (TRPV in *drosophila*)
IFN	Interferon
IGF	Insulin growth factor
IGFR	Insulin like Growth Factor
IL6	Interleukin-6
InsP3	Inositol-1,4,5-trisphosphate
IPP	Isopentenyl pyrophosphate
IPTG	Isopropyl thiogalactose
IRTX	5'-iodoresiniferatoxin
JC-1	5,5′,6,6′-tetrachloro-1,1′,3,3′-tetraethylbenzimidazolocarbocyanine iodide
Kan	Kanamycin
Kb	Kilo base
kDa	Kilo Dalton
KO	Knock out
KOH	Potassium Hydroxide
L	Litre (volume unit)
LB	Luria-Bertani
LPS	Lipopoysaccharides
LTG	Lyso Thermo Green
LTS	Lysosomal targeting sequence
LWI	Lipid-water interface
MAPK	Mitogen-activated protein kinase
MBP	Maltose Binding Protein
MFI	Mean Fluorescence Intensity
MFN2	Mito fusion-2
Min	Minutes (Time unit)
Ml	microlitre
μm	micron
MT	Microtubules
MTG	Mito Thermo Green

MTT	3-(4,5-Dimethyl-2-thiazolyl)-2,5-diphenyl-2H-tetrazolium bromide, Methylthiazolyldiphenyl-tetrazolium bromide
mV	millivolt
NA	Numerical aperture
NaCl	Sodium Chloride
NADA	N-arachidonyl dopamine
NADH	Nicotinamide adenine dinucleotide (reduced form)
NAN	Nanchung Ion channel (TRPV in *drosophila*)
NaOH	Sodium Hydroxide
NCS1	Neuronal calcium sensor 1
NFAT	Nuclear factor of activated T-cell
NFκB	Nuclear factor κB
NGF	Nerve growth factor
NHEK	Normal Human Epidermal keratinocytes
NOS	Nitric oxide synthase
NTG	Nuclear Thermo Green
nV	nanovolt
OCR-1-4	osm-9/capsaicin receptor-related (In *Caenorhabditis elegans*)
OS	Olmsted Syndrome
OSM	OSMotic avoidance abnormal family member-9 (In *Caenorhabditis elegans*)
PAGE	Poly Acrylamide Gel Electrophoresis
PAR2	Protease Activator Receptor 2
PBS	Phosphate buffer saline
PCR	Polymerase Chain Reaction
PFA	Paraformaldehyde
PGE2	Prostagladin E2
PI	Complete protease inhibitor
PI3K	Phosphoinositide-3 kinase
PIP_2	Phosphatidylinositol 4,5-bisphosphate
PIPES	1,4-Piperazinediethanesulfonic acid
PKA	Protein Kinase A
pKa	value acid dissociation constant
PKC	Protein Kinase C
PKG	Protein kinase G
PLA2	Phospholipase-A2
PLC	Phospholipase C
PMSF	Phenylmethanesulfonyl fluoride

PNS	Peripheral nervous system
PPK	Palmoplantar Keratoderma
PPM	Parts per million
PTG	Plasma Thermo Green
PTM	Post-translational modifications
PVDF	Polyvinylidene difluoride membrane
Q10	Temperature coefficient
RhoA	Ras homologue protein A
ROS	Reactive oxygen species
RPM	Revolution-Per-Minute
RT	Room temperature
RTK	Receptor tyrosine kinase
RT-PCR	Reverse transcription- polymerase chain reaction
RTX	Resiniferatoxin
SDS	Sodium Dodecyl Sulphate
SH2	Domain Src homology 2
SOC	Store Operated Channel
SOCE	Store operated Ca2+ entry
Sp1	Specific protein 1
SPSMA	Scappulopuro spinal muscular atrophy
STIM	Stromal interaction molecules
TAE	Tris-Acetic Acid-EDTA
TEMED	N,N,N′,N′-Tetramethylethylenediamine
TFEB	Transcription factor-EB
TG	Trigeminal ganglion
TGF-α	Transforming growth factor-α
TGFβ	TGF Beta
Thr	Thereonine
TM	Transmembrane
TMD	Transmembrane domain
TPC	Two pore channels
Tris	TrisHydroxymethylaminoethane
TRP	Transient Receptor Potential
TRPML	Transient Receptor Potential Mucolipin type
Tyr	Tyrosine
UVR	Ultra violet radiation
v/v	Volume per volume
VEGF	Vascular endothelial growth factor
VEGFR2	Vascular endothelial growth factor receptor2
VSLD	Voltage sensor like domain

w/v	Weight per volume
WGD	Whole genome duplication

Chapter 1

Introduction

In the course of evolution, nature transformed specific proteins to carry out different sensory functions for the benefit of organisms. In specific environmental niches, organisms are exposed to various chemicals and diverse stimulus that are mechanical or physical in nature. Organism need to detect all these chemical and physical stimuli (often noxious in nature) properly and accordingly to initiate a set of physiological response/s, and thus ensures the survival of the species in a given environment. In this context, to detect external signals, organisms developed particular sets of proteins which responds to the external stimuli and acts upon them (Clapham DE. 2003).

Ion channels are integral membrane proteins that form a "pore" to allow the passage of specific ions by passive diffusion (ions flow from higher to lower concentration compartment) (Nekouzadeh and Rudy. 2016). Most, if not all, ion channels undergo conformational changes from "closed" to "open" states, and once "opened", channels allow the passage of ions (López-Romero et al. 2019). Ion channels allow transport of ions in specific "quanta" (i.e. only one or a specific few at a time, depending on the ion channel) (Luo and Hong. 2010). Pumps need energy of ATP-hydrolysis in order to transport ions and that these specialized proteins perform against the concentration gradient (Alberts et al. 2002). The opening and closing of channels can be controlled by various factors, such as "voltage difference" across the membrane, the binding of ligands (such as extracellular neurotransmitters), presence of different metal ions (such as intracellular Ca^{2+}) and/or post-translational modifications such as phosphorylation, glycosylation etc. (López-Romero et al. 2019; Barker et al. 2017). The insertion of the channel into the target membrane provides further levels of control. The surface expression of any channel is also regulated by vesicle recycling, retrieval, level of glycosylation and specific pathway-dependent protein degradation (Rizzoli SO. 2014; Ivanova and Cousin. 2022). Many functional ion channels represent protein complexes of identical or homologous subunits that participate in forming the functional "pore" (Pérez-Hernández et al. 2018).

Among all the physical factors, temperature is a critical factor that affects all physiological processes and macromolecular structures within living systems (Bernal J.D. 1951). Temperature also affects the molecular vibrations, conformational changes and thus molecular stability. Organisms must be able to "sense" their thermal environment, which varies greatly in different environments and is subject to fluctuate in spatio-temporal manner. To reliably respond to ecologically and physiologically relevant thermal variations, organisms have evolved sensory mechanisms based on specialized proteins such as ion channels, heat-shock factors, specific sets of stress-response proteins, etc. which transduce environmental changes into chemical and electrical signals within the cell. In this context, different ion channels have evolved in the organisms in different evolutionary time points primarily to adjust various environments ranging from lowest to the extreme adverse conditions.

In order to survive and minimize the damage of cells/tissues, organisms have adapted to "sense" the environment around them quickly and accurately. For such functions, one group of ion channels are present in animals, termed as Transient Receptor Potential (TRP) ion channels. TRP channels are a class of non-selective cation channels that act as a signal transducer by altering membrane potential or intracellular Ca^{2+}-concentration. TRP channels are mainly present in metazoans. These are specifically present in animals and also in fungi, but are largely absent in plants (Himmel and Cox. 2020; Peng et al. 2015).

Transient Receptor Potential (TRP) channels are the well-studied large-sized protein molecules that have specific thermosensory abilities. These are ancient channels and some of these have evolved more than 1.5 billion years ago, and is even detected in the single-cell eukaryotic ancestors (Venkatachalam and Montell. 2007). Most of the TRP channels are typically "non-specific" in nature, i.e. these channels represent cation channels that conduct influx of different mono- and divalent-cations such as K^{+}, Na^{+}, Ca^{2+}, Sr^{2+}, Mg^{2+} Mn^{2+}, Zn^{2+}, Fe^{2+}, Cu^{2+}, etc. TRP channels consist of four subunits, each with at least six-transmembrane

domains. Recent findings suggest that there are ten subfamilies of TRP channels (TRPA, TRPC, TRPM, TRPML, TRPN, TRPP, TRPS, TRPV, TRPVL, and TRPY/TRPF), of which seven are found in metazoans (Martinac et al. 2008; Peng et al. 2015; Himmel et al. 2021). In contrast, temperature-sensitive TRP channels (i.e. thermo TRPs) have been identified in several subfamilies. Thermo TRPs are polymodal channels that can be activated by diverse stimuli, such as heat, ligands, light, pH, pressure, voltage, or a combination thereof in a synergetic manner (Vay et al. 2012). In higher animals, thermo TRPs are highly expressed in the sensory nerves, where these channels "gate" the permeability of ions in response to a temperature change (Hong and Siemens. 2015; Kashio M. 2021; Singh et al. 2019). Modulation of TRP channels alter the membrane voltage, causing neuronal excitation. These channels are also present in the lower invertebrates to developed metazoans. In many cases, these channels are highly conserved in vertebrates, i.e. remain conserved in fishes to higher vertebrates like human.

1.1 A general introduction on TRP ion channel super family

1.1.1 A brief history of TRP channel research

Research on TRP channel began in 1969 when Cosens and Manning discovered a *Drosophila* mutant that exhibited blindness phenotype in the presence of constant bright light (Cosens and Manning. 1969). And later this mutant *Drosophila* strain was named as trp (transient receptor potential), and cloning of the mutated *trp* gene identified the first member of the TRP superfamily (Wes et al. 1995). Subsequently, a large number of related genes were identified in different animals. This superfamily constitutes a diverse group of polymodal ion channels that are fairly conserved (in terms of sequence, structure and functions) from nematodes to human. Throughout the 1970s and 1980s, the groundwork for understanding TRP channels was laid. In 1976, researchers identified a mutation in *Drosophila* photoreceptor cells that led to the discovery of the first TRP-related gene. This gene was linked to visual signaling

and phototransduction. Subsequently, in 1989, the *trp* gene was cloned from *Drosophila*, providing initial insights into the molecular basis of TRP channels (Montell and Rubin. 1989). The 1990s marked a significant progress for TRP channel research. In 1995, the cloning of the mammalian TRPC1 gene introduced the first mammalian TRP channel (Wes et al. 1995). This channel, known for its Ca^{2+}-permeability, was activated by signaling pathways mediated by cell surface receptors. In 1997, the identification of TRPV1, also known as the "Vanilloid Receptor 1 (referred as VR1 in several earlier publications), revealed its responsiveness to heat as well as Capsaicin (the compound responsible for the spiciness of chili peppers) also in a synergistic manner (Caterina et al. 1997). This discovery linked TRP channels to temperature-sensing and pain perception. Furthermore, in 1998, the TRPM family of channels was identified, with various members serving roles in cell proliferation and magnesium transport (Duncan et al. 1998).

As the new century began, the functional diversity and mechanisms of TRP channels gained more attention. In 2002, TRPV4 was identified as a mechanosensitive ion channel involved in responding to mechanical force and osmotic changes. In 2003, TRPA1 was discovered as a channel activated by noxious cold and irritants, connecting TRP channels to both chemical and thermosensing (Story et al. 2003). In the same year, the structural elucidation of TRPV1 offered first insights into the architecture and possible gating mechanisms of TRP channels. Additionally, in 2008, mutations in TRPML channels were linked to lysosomal storage diseases, highlighting their role in lysosomal functions (Dong et al. 2008; Vergarajauregui et al. 2008).

In 2008, Rock et al. identified one missense mutation in the TRPV4 gene within two families exhibiting autosomal dominant phenotype described as *Brachyolmia* (BCYM3; 113500) (Rock et al. 2008). These findings indicated that both missense mutations led to a gain-of-function phenotype by increasing the proportion of channels that were constitutively

open and enhancing their response to agonists. The study from Rock et al. provided the sufficient evidence suggesting that TRPV4 plays a pivotal role in the regulation of the growth plate and mutations in critical residues of the TRPV4 channel can be detrimental. This marks the emergence of TRP channels involved in severe pathophysiological conditions.

The 2010s emphasized the clinical implications and therapeutic potential of TRP channels. Mutations in TRPC6 were found to be associated with kidney disorders, suggesting the clinical relevance of TRP channels (Krall et al. 2010). In 2012, TRPM8 was implicated in prostate cancer progression, revealing a connection between TRP channels and cancer biology. In 2013, TRPV1-expressing sensory neurons were recognized as regulators of body temperature, metabolism, and energy expenditure. The much-detailed structural insights were reported in 2016 with the use of cryo-EM as the technique to reveal the structure of TRPV1 and shedding light on its gating mechanism/s (Gao et al. 2016).

In the recent time, a large volume of research has been conducted into the regulation and signaling of TRP channels. In this era, success of human genome project and other similar genome projects indicates the presence of multiple *trp* genes in different species, their relationship and overall evolutionary selection and specific changes. In the ongoing decade, the exploration of TRP channels' regulatory mechanisms and their contributions to neurological disorders remains an active area of research. Notably, the year 2021 witnessed a significant milestone as the Nobel Prize in Physiology or Medicine was awarded to Prof. David Julius and Prof. Ardem Patapoutian (Noble committee announcement. 2021). Their pioneering discoveries in the field of sensory biology, notably their investigations into TRP channels and Piezo channels respectively, were acknowledged with this esteemed accolade. Their work, focused on deciphering the molecular underpinnings of temperature and touch sensation, which also encompassed the roles of TRP channels, garnered them this prestigious recognition.

In 2021, studies unveiled the roles of TRP channels in neurological disorders like migraines and neuropathic pain (Feigin et al. 2020; Kuppusamy et al. 2021). Current research continues to explore the intricate regulatory mechanisms of TRP channels, including their modifications, interactions with other proteins and characterizing the unique roles of these different TRP channels relevant in various physiological and pathological processes. Advances in structural biology have provided atomic details of TRP channels in different functional states, contributing to our understanding of how these channels operate. Moreover, the therapeutic potentials of TRP channels are being explored as promising targets for diverse conditions, ranging from pain and inflammation to cancer and metabolic disorders. Over the past half-century, research on TRP channels has evolved significantly, uncovering their roles in sensory perception, cellular signalling, disease pathways and in many other disciplines.

1.1.2 Structural features of TRP channels

In the year 1995, researchers initiated the investigation into the structural attributes of Transient Receptor Potential (TRP) channels. At that time, a method called homology modeling, which involved deriving insights from the established structure of a widely recognized potassium channel named KcsA was applied. Through this strategy, they achieved preliminary insights into the fundamental structural framework of TRP channels (TRPC1 as an example) (Wes et al. 1995). This approach helped to make initial predictions about the fundamental architecture of TRP channels. The initial model proposed that TRP channels consist of four identical subunits, forming a tetrameric arrangement (Schaefer M. 2005; Strubing et al. 2003). Each subunit was envisioned to have six segments, termed transmembrane helices (S1 to S6), that span the plasma membrane. Importantly, a region called the “pore-forming loop” was identified between the 5th (S5) and 6th (S6) TM segments (**Fig 1**).

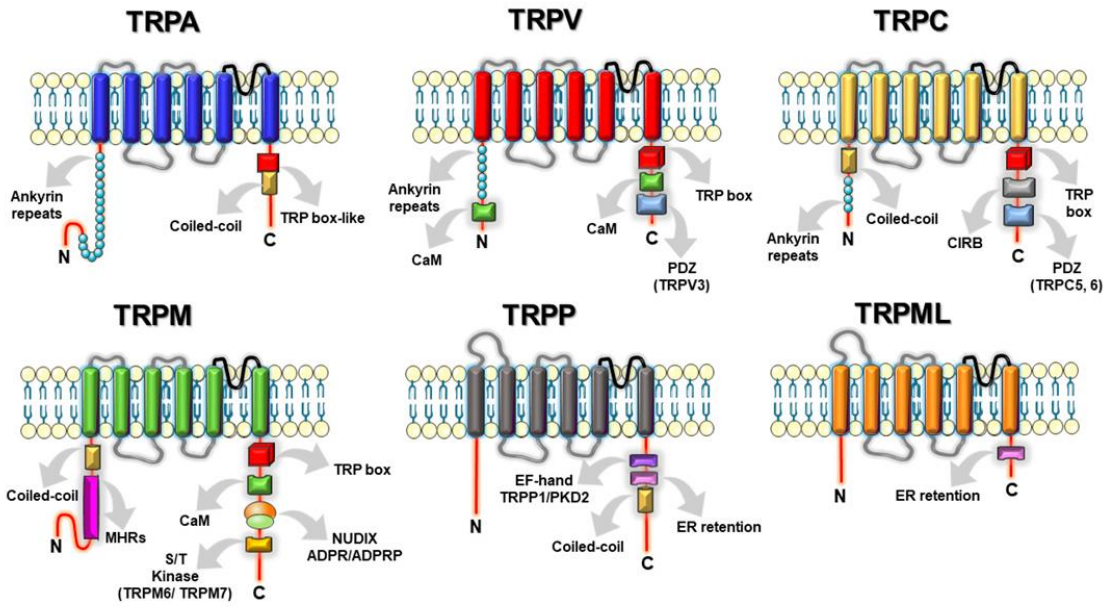

Figure 1: General architecture of TRP channels. This figure is adapted from Méndez-Reséndiz et al. 2020.

This "loop" was projected to contribute to the formation of a "functional pore" at the central through which ions could flow. These early predictions laid the groundwork for subsequent investigations into the functional properties of TRP channels. Although simplified, this model provided a foundational understanding of the architecture of TRP channel, which was later refined with more advanced techniques detailing the structure (**Fig 2**). TRP channels share high sequence homology as well as structural and functional similarities. TRP channels share common structural features that include six transmembrane segments flanked by intracellular N- and C-termini cytosolic domains. The "pore"-forming portion is located between the 5th- and 6th-transmembrane region. In many TRP channels (but not in all), the intracellular N-terminus contains multiple Ankyrin-repeat (AR) motifs, which are important for protein-protein interactions (Owsianik et al. 2006).

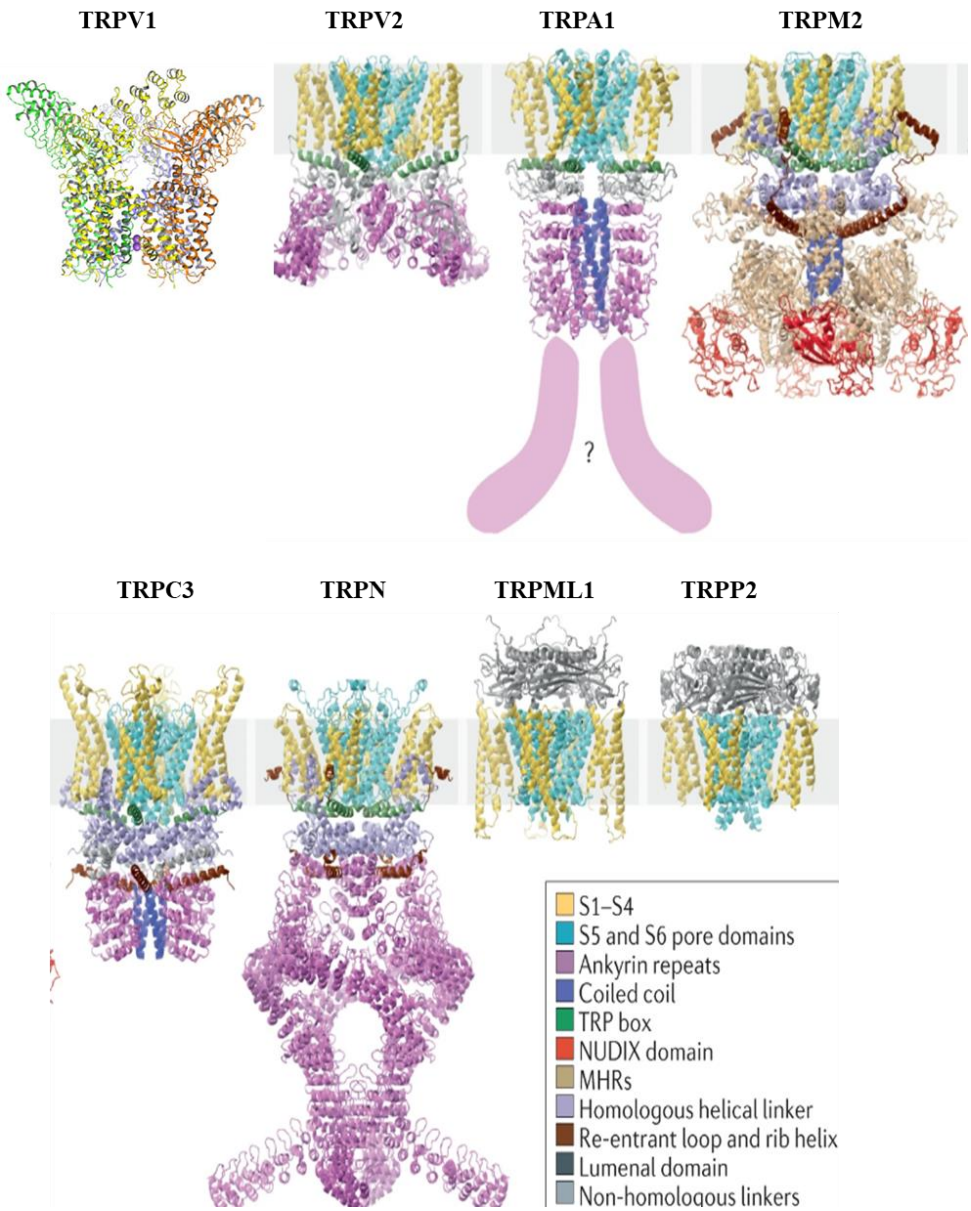

Figure 2: 3D constructed structure of TRP channels. (This figure is adapted from Koivisto et al. 2022).

In addition, the extracellular loops, transmembrane regions, and unstructured loops of TRP channels contain binding sites for different ligands, such as lipids, other membranous components, different proteins and often specific ligands. These ligands can modulate the conformational change of the channels and thus regulate their activities. The C-terminal region of TRPs often contains a motif sequence called the "TRP-box", which is functionally relevant and present in all Canonical members but less conserved in Vanilloid and Melastatin families.

Ankyrin repeats are mainly present in the N-terminal portion of members belonging to TRPC, TRPV, and TRPA families (Putney J.W. 2004; Vazquez et al. 2004).

Fetching structural information of TRP channels was difficult in the earlier time due to the multiple challenges associated with purification of TRP proteins, crystallization and/or diffraction. In spite of these challenges, limited progress was made on specific TRP channels. For example, in 2008, using Cryo-EM technique for the first time, the structure of TRPV1 was determined to a resolution of 19Å, revealing two distinct regions (Zheng J. 2013; Moiseenkova-Bell et al. 2008). The first region represents a large open "basket-like" structure that represents the cytoplasmic N- and C-termini of the protein, while the second region is a compact structure that represents the transmembrane region. This structure also show that the majority of the protein is hanging towards the cytoplasmic side, with only about one-third of the protein present in the membrane. Such a structure was termed as "hanging basket"-like structure of TRPV1. A diagram illustrating this structure is shown (**Fig 3**).

Subsequently, Cryo-EM techniques for resolving structure, especially for membrane proteins were developed. This leads to significant progress in the understanding of the structure of TRP channels. So far, only a few TRP channels have been analysed for their high-resolution structure (covering their almost full-length sequences), and this has been mainly achieved through the use of single particle cryo-electron microscopy. In 2012-2013, the activation mechanism of TRPV1 was revealed through cryo-electron microscopy of the ligand-free and ligand-bound form of TRPV1, which allowed to compare both the open- and closed-structures of the channel at a resolution of 3.4Å (Liao et al. 2013). These structures also provided insight into the channel's "opening" and "closing" mechanisms, as well as the importance of its "selectivity filter". The subunits of all TRP channels are predicted to have six transmembrane domains (S1-S6) with a hydrophobic stretch between S5 and S6 forming the "pore region". However, only TRPM4, TRPM5, TRPV5, and TRPV6 channels are highly "selective" (to Ca^{2+}

ions), whereas the rest are non-selective cation channels. Such specificities are mainly due to the pore region, selective-filters and residues present in such regions.

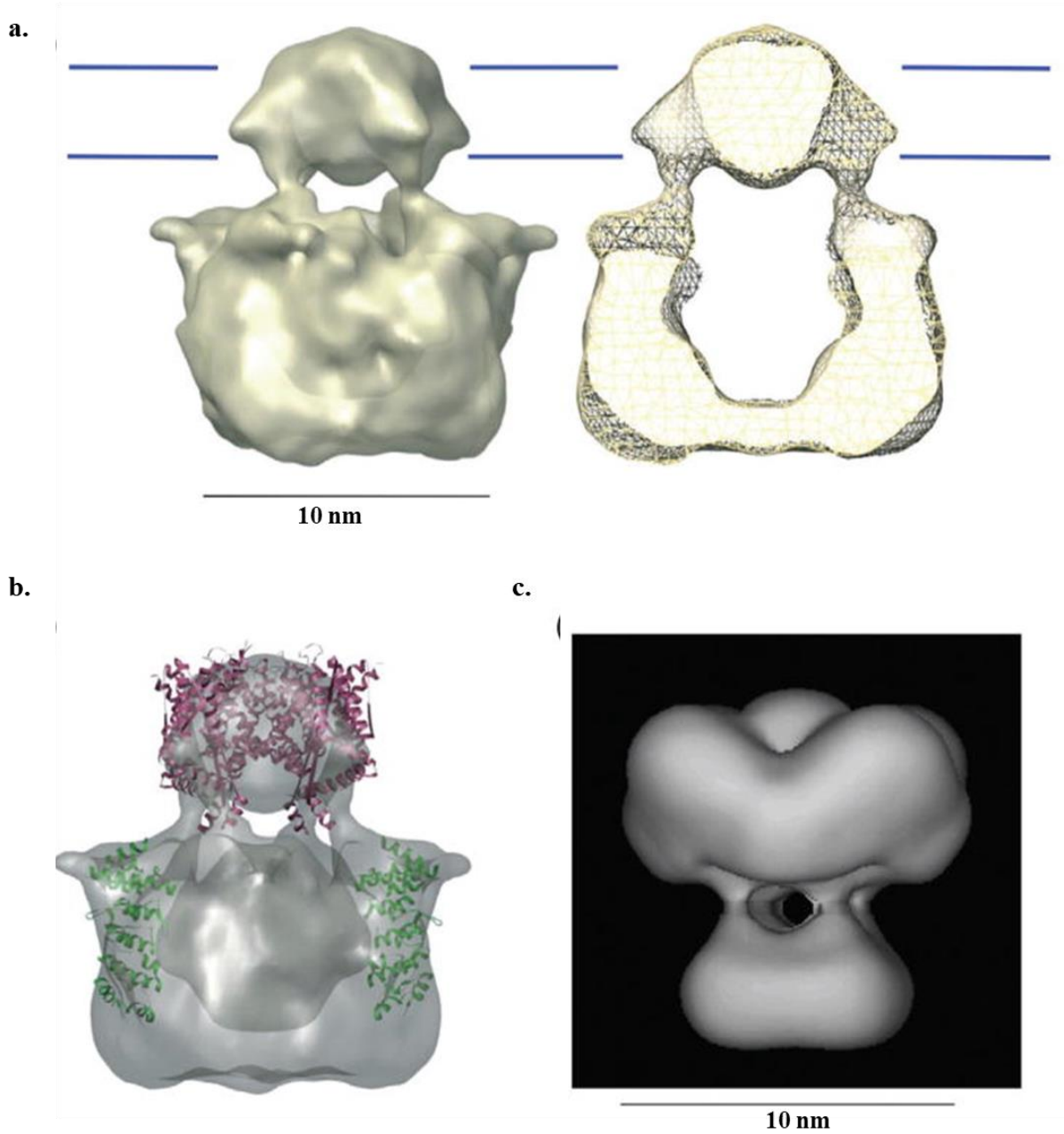

Fig. 3. **The cryo-EM structure of TRPV1(Hanging basket model**). **a.** Three-dimensional map of TRPV1 and its cut section derived from Cryo-EM structure of TRPV1 (solved at 19Å). **b.** The figure shows the crystal structures of Kv2.1 transmembrane domain (PDB 2A79) and TRPV1 ankyrin-like repeat domains (PDB 2PNN) docked into the TRPV1 cryo-EM structure. **c.** Cryo-EM structure of Shaker potassium channel. (These figures have been adapted from Moiseenkova-Bell et al. 2008; Sokolova et al. 2001).

1.1.3 Distributions of TRP ion channels

1.1.3.1 Tissue-wise distribution of TRP channels

The tissue and cell-specific expression of TRPs is difficult to summarize as the expression of TRPs are dynamic that changes with respect to developmental age, disease and also with the context. In addition, different techniques, such as RT-PCR, Western blot, immunofluorescence etc. used to understand the expression varies in their specificity and detection limits. Often, the expression of TRPs or their absence in a cell/tissue is concluded based on the specific technique/s used and the probes that are targeted such as mRNA, total protein or protein at the cell surface only, etc. Thus, understanding the expression patterns of TRP channels is crucial for comprehending their functions. Although much has already been discovered, the distribution of TRP channels in various tissues and cell types remains an area that requires further exploration. According to various reports, these channels are expressed in a range of tissues throughout the body. In the skin, TRPV1, TRPV3, TRPV4, TRPM8, and TRPA1 channels are involved in sensing temperature, pain, itch, and mechanical stimuli (Su et al. 2023; Tóth et al. 2014). TRPA1 and TRPV1 channels in the respiratory system detect irritants and inflammatory stimuli, while in the gastrointestinal tract, TRPA1, TRPV1, TRPV4, and TRPM8 sense various stimuli, including temperature, pain, and mechanical stress (Qian et al. 2019; McGaraughty et al. 2017; Huang et al. 2011). In the cardiovascular system, TRPV1, TRPV4, TRPC1, and TRPM4 regulate vascular tone, blood pressure, and cardiac function (Yue et al. 2015). TRPC3, TRPC6, TRPM2, and TRPM7 express in the central nervous system and play a role in regulating intracellular Ca^{2+}-levels and neuronal excitability. TRPV1, TRPV4, and TRPM8 channels in the urinary system sense bladder distension and regulate urinary function (Andersson K.E.2019; van der Wijst et al. 2019; Peng et al. 2018). In the reproductive system, TRPV1, TRPV4 and TRPM8 channels regulate sperm motility and ejaculation in males, while TRPV4 and TRPM8 channels regulate uterine contractility and menstrual pain in

females. In the immune system (e.g. monocytes, macrophages, T-cells), TRPV1, TRPV2, TRPV4, and TRPM7 channels play a role in regulating immune responses (Koivisto et al. 2022; Tian C. et.al. 2020; Majhi et al. 2015). TRPV channels are also found on sensory neurons and epithelial cells. TRPM is primarily expressed on c-fibres in peripheral nerves. TRPC expresses mainly in smooth muscle and in heart cells where it regulates responses in the central nervous system and vasculature (Scotland et al. 2004; Yang et al. 2006; Wang et al. 2008).

A detailed exploration of the distribution of each TRP channel surpasses the scope of this study and the expression level can vary upon certain physiological conditions. For comprehensive and updated insights into individual TRPs distribution across tissues, the protein atlas website (https://www.proteinatlas.org/ENSG00000167723-TRPV3) serves as a valuable resource. The table below provides an in-depth overview of TRP channel distribution across various tissues (**Table 1**).

Tissues distributions	**TRPs channels**	**References**
Nervous system	TRPV1, TRPA1, TRPM8, TRPV3, TRPC1, TRPC3, TRPC4, TRPC5, TRPC6	Qian et al. 2019; McGaraughty et al. 2017; Huang et al. 2011
Skin	TRPV3, TRPV4, TRPV1, TRPA1, TRPV6, TRPM1, TRPM8, TRPC1, TRPC4, TRPC5, TRPC6 and TRPC7	Su et al. 2023; Tóth et al. 2014
Respiratory system	TRPV1, TRPA1, TRPV4, TRPM8	Grace et al. 2014
Cardiovascular system	TRPV1-V6, TRPC1-C7, TRPM1-TRPM8, TRPA1, TRPP2, TRPP3, TRPP5, TRPML1-TRPML3	Yue et al. 2015
Gastrointestinal system/ Digestive system	TRPV1-V6, TRPA1, TRPM4-M8, TRPP2, TRPC, TRPC1, TRPC3, TRPC4, TRPC6, TRPC7	Holzer et al. 2011
Urinary system	TRPV1, TRPV4, TRPM4, TRPM8, TRPA1, TRPV2, TRPV5	Andersson K.E.2019; van der Wijst et al. 2019; Peng et al. 2018
Reproductive system	TRPV1-TRPV6, TRPC (C2, C3, C7), TRPM, TRPP, TRPM8	Ghavideldarestani et al. 2016; Asghar and Törnquist 2020; Dörr and Fecher-Trost. 2011; Mohandass et al. 2020; De Blas et al. 2009

Table 1. The principal tissue distribution of all the TRPs channels.

1.1.3.2 Subcellular distribution of TRP channels

Ion channels are well-known regulators for the movement of ions across the plasma membrane in response to various stimuli. However, these also serve important functions in intracellular membranes (IMs). These channels can be temporarily located in IMs as these are transported to their final destination or as part of endocytic pathways for recycling or degradation. Some IM ion channels participate in intracellular signal transduction, with the IP_3 receptor in the endoplasmic reticulum being a prominent example (Berridge et al. 2003). Other organellar IM channels help to maintain ionic homeostasis within their respective organelles. Recently discovered IM Ca^{2+} channels have been shown to play active roles in membrane trafficking. The TRPY1 in yeast localizes to the vacuole compartment (Palmer et al. 2001; Zhou et al. 2003). Similarly, many mammalian TRP channels are also found in IMs. Emerging evidence indicates that IM-localized TRP channels play important roles in regulating membrane traffic, signal transduction, and vesicular ion homeostasis.

The distribution of most of the TRP channels are primarily in the plasma membrane. TRP channels, such as TRPV1, TRPV3, TRPV4, TRPM2, TRPM3, TRPM4, TRPM5, TRPM6, TRPM7, TRPC1, TRPC3, TRPC4, TRPC5, TRPC6, and TRPA1 are primarily located at the PM and perform various functions, including sensing external stimuli and regulating the homeostasis for Ca^{2+} and other ions. Being transmembrane proteins, presence of TRP channels in ER and in vesicles/golgi are expected. Yet specific expressions and functions are recorded at different sub-cellular organelles. Apart from sub-membranous localization, TRP channels (TRPV1 and TRPV4 as examples) are also localizes at the filopodia tips which is required for the initiation and regulation of filopodial functions (Goswami and Hucho. 2007; Goswami et al. 2010).

Studies on subcellular localization indicate that TRPV1, both when expressed endogenously or exogenously, can also be found in the Golgi and ER compartments (Turner et

al. 2003). In mast cells, TRPA1 is present in both secretory vesicles (SVs) and secretory granules (SGs). Additionally, it interacts with vesicular proteins found within SGs (Prasad et al. 2008). TRP channels, namely TRPP1, TRPM8, TRPV1, and TRPA1 are active intracellularly, such as within ER, trans-golgi, and secretory vesicles (Koulen et al. 2002; Geng et al. 2008; Thebault et al. 2005; Turner et al. 2003; Prasad et al. 2008).

While the activation of several vesicular TRPs has not yet been documented, there is evidence suggesting that some TRPs, such as TRPC3 and TRPC7, play an active role in trafficking and exocytosis (Lavender et al. 2008). TRPM7 has been shown to complex with synaptotagmin I (Krapivinsky et al. 2006). It seems that TRPM7-mediated Ca^{2+}-release further enhances the interaction of synaptotagmin and the plasma membrane which is necessary for bilayer fusion.

In addition to the ER or vesicles, TRP channels are specifically detected in other sub-cellular organelles. For example, TRPML proteins have been identified as a strong candidate for serving as Ca^{2+} channels in the endo-lysosomal system, as demonstrated by the fact that cells lacking TRPML1 exhibit enlarged endo-lysosomes (Chen et al. 1998; Piper & Luzio 2004). Mammals possess three TRPML proteins (TRPML1-3 or MCOLN1-3) (Puertollano & Kiselyov. 2009). TRPML1 is expressed in most tissues and exclusively colocalizes with late endosomal and lysosomal (LEL) markers (Slaugenhaupt S.A. 2002; Cheng 2010).

TRPMLs are found within specific organelles that vary depending on the cell type. These organelles, other than lysosomes are called lysosome-related organelles (LROs) and are similar to late endosomal and lysosomal (LEL) compartments but differ in their appearance, contents, and functions (Blott and Griffiths. 2002). Another example is TRPML3, which is located within the melanosomes of melanocytes (Xu et al. 2007). When exposed to light, the melanosomes rapidly relocate to the plasma membrane and release melanin (Blott and Griffiths. 2002). The TRPC1, TRPC3, TRPC4, TRPC5, TRPC6, TRPM2, and TRPM7

channels are located on the endoplasmic reticulum and modulate Ca^{2+}-signalling and homeostasis. The TRPV6 channels are located on the nuclear envelope and regulate Ca^{2+}-homeostasis within the nucleus. The TRPC3 and TRPV4 are located on mitochondria and play multiple roles in regulating the uptake of Ca^{2+} by mitochondria and the functional aspect of mitochondria (Acharya et al. 2022; Farfariello et al. 2022).

In conclusion, TRP channels' subcellular distribution is diverse and still poorly characterized, corresponding to their roles in various cellular processes.

1.1.4 Different functions of TRP channels

TRP channels play crucial roles in sensory signalling, and thus are largely involved in the perception of temperature, pain, and taste. Some of the uniqueness of TRP channels make these channels as key molecules responsible for certain function at the cellular as well as organism level. At cellular context, TRP channels regulate ion concentration and homeostasis, particularly for Ca^{2+}, Mg^{2+}, and Zn^{2+}, especially in response to certain stimuli. TRP channels also have important functions in cell growth, differentiation, metabolism, cardiovascular regulation, and immune response, including immune cell activation and cytokine production. Furthermore, TRP channels participate in embryonic development and tissue differentiation. Also, these channels are involved in detecting various stimuli, such as temperature, touch, pain, pheromones, osmolarity, and taste. For instance, yeast uses TRP channels to sense hypertonicity, male mice use TRPs for pheromone sensing, nematodes use to detect noxious chemicals, and humans use these to perceive sweet, bitter, and umami tastes as well as temperature changes (Palmer et al. 2001; Ishimaru et al. 2006; Huang et al. 2006; Zhang et al. 2023). TRP channels also play a crucial role in selecting an appropriate environmental niche and are often critical for the “pray-predator” relationship (Gracheva et al. 2010). TRP channels are known to be heat sensing as well as UV- and IR-sensing proteins. Snakes possess a

remarkable ability to detect infrared thermal radiation through specialized TRPA1 channels, particularly in pit-bearing snake species like vipers, pythons, and boas. And in case of vampire bats, TRPV1 channel act as a detector of noxious heat through somatic afferent neurons (Gracheva et al. 2011; Panzano et al. 2010). These channels are highly sensitive to heat, making them the key players in sensing infrared stimuli. Vampire bats, on the other hand, have also evolved a unique system for detecting infrared radiation (through TRPV1), which they use to locate warm-blooded prey.

By mediating the influx of Na^+ and Ca^{2+} across the plasma membrane and into the cytoplasm, TRP channels induce depolarization and action potentials in excitable cells such as neurons. In non-excitable cells, depolarization by TRP channels activates voltage-dependent channels (Ca^{2+}, K^+, Cl^-) and modulates various cellular events such as transcription, translation, contraction, and migration (Vandewauw et al. 2018; Launay et al. 2002).

TRPM, TRPA, and TRPV channels respond to temperature changes in different ranges, with TRPM and TRPA responding to cold and TRPV to warmth and noxious heat (Hu et al. 2004; Weil et al. 2005; Bandell et al. 2004). TRPP channels regulate intracellular Ca^{2+} and ciliary function, while TRPML channels control lysosomal Ca^{2+} release (Grimm et al. 2012; Wilson PD. 2001).

TRPCs has been suggested to function as store-operated channels (SOCs) or as components of complexes that form SOCs. However, most evidence indicates that they are not directly activated by conventional store-operated mechanisms, which are well-established for STIM-gated Orai channels (also known as CRAC channels) (Liu et al. 2003; Ambudkar IS. 2007). Overall TRPs channels carryout various cellular functions and some of the functions mentioned above. The functions may change according to the cellular stress or any physiological changes. The functions may add in near future according to the discovery of the channel functionality.

1.2 The Differential regulations of TRP channels (cellular regulations)

Transient Receptor Potential (TRP) channels, acting as versatile cellular sensors, are governed by a multitude of regulatory mechanisms that modulate their activity and responsiveness to a wide range of internal and external signals. TRP channels can be activated or influenced by various stimuli directly, such as by physical and chemical stimuli as well as indirectly by receptor-mediated intracellular signalling pathways.

1.2 Cellular regulations of TRP channel

1.2.1 *Protein phosphorylation/dephosphorylations*

One of the primary regulatory avenues for TRP channels involve protein phosphorylation or dephosphorylation. This process entails the addition or removal of phosphate groups from specific amino acid residues within the channels' structure, mainly cytosolic domains, intracellular-loop regions and in all possible intracellular regions that are exposed. This reversible modification dynamically influences TRP channel behaviour, molecular vibrations, localization, protein-protein interaction, etc. all affecting the channel activity. The interplay of different kinases and phosphatases with distinct TRP channel isoforms grants a remarkable degree of fine-tuned control over various cellular processes. There are many examples where the TRPs channel phosphorylated at specific residue in the channel modulate channel activity, like at N-terminus threonine 264 position, which is an ERK-dependent modulation of TRPV3 channel activity (Vyklicka et al. 2017). TRPV4 phosphorylation at serine-824 by PKA (Protein kinase A) enhances its activation by arachidonic acid (Cao et al. 2018). Another example is Phosphorylation of TRPV1 by PKC at S801 position leads to enhancement of inflammation-mediated sensitization of TRPV1 to ligand like capsaicin (Joseph et al. 2019).

1.2.2 *Growth factors*

TRP channel activity is also influenced by growth factors, which are vital signaling molecules relevant for cellular communication. These factors can interact with TRP channels through multiple mechanisms, such as by direct binding to the channels or by indirect effects. Some growth factors can induce changes in channel expression levels, altering their abundance on the cell membrane and consequently impacting cellular responsiveness to certain stimuli (Van den Eynde et al. 2021). Moreover, growth factors can trigger phosphorylation events that modify TRP channel activity, resulting in diverse cellular outcomes based on the context of the signaling. Various growth factors have been revealed to influence the opening behaviour of TRP channels. Examples include Vascular Endothelial Growth Factor (VEGF), which activates TRP channels (TRPM2, TRPC3, TRPC6 and TRPV1), leading to an increase in intracellular Ca^{2+}-concentration in endothelial cell vital for blood vessel formation (Mittal et al. 2015). Epidermal Growth Factor (EGF) modifies TRPV1 channel behaviour by phosphorylating specific residues, impacting cell growth and differentiation (Turker et al. 2018; Walcher et al. 2018; Garreis et al. 2016). Nerve Growth Factor (NGF) activates TRPV1 channels, influencing neuron growth and survival (Zhang et al. 2005; Winter et al. 1998; Puntambekar et al. 2005). Similarly, Hepatocyte Growth Factor (HGF) triggers TRPC6 channel activation through phosphorylation, regulating cell growth, movement, and morphogenesis (Wang et al. 2010). One of the proteins named Klotho, which has been recognized for its anti-aging properties, plays a pivotal role in modulating Ca^{2+}-influx mediated by Vascular Endothelial Growth Factor Receptor 2 (VEGFR2) and TRPC1 through direct interactions (Kusaba et al.2010; Fakhar et al. 2022). This interplay between growth factors and TRP channels serves as a significant mechanism in controlling cellular communication and sensory functions. Irregular TRP channel activity can result in ailments such as pain, inflammation, cancer and many other

diseases. Exploring how growth factors regulate TRP channels remains a subject of ongoing investigation, promising insights into their roles in human health.

1.2.3 *Steroids*

TRP channels are susceptible to modulation by both synthetic and naturally occurring compounds. Notably, endogenous steroids can affect these channels through two primary mechanisms (i.e. by functional regulation by control of their expression and/or their cellular/subcellular localization), shedding light on how hydrophobic molecules influence cellular function (Kumar et al. 2015).

Endogenous steroids have been found to regulate TRP channels in ways that impact pain perception, bone homeostasis, kidney function, insulin secretion, and even diseases like prostate cancer. For instance, certain steroids such as PregS (pregnenolone sulfate) and androstenedione act as "algogenic" molecules, enhancing the expression and activity of pain-sensing TRPM3, TRPA1, and TRPV1 channels (Majeed et al. 2010; Drews et al. 2014; Ortiz-Renteria et al. 2018; De Logu et al. 2016). TRPV4 is also known to interacts with progesterone at the mutational “hot-spot” of TRPV4, which acts as a ligand relevant for fast Ca^{2+}-signalling (Dubey et al. 2023). Another report shows the loss of interaction with cholesterol in the TRPV4 R616Q mutants (causing brychyolmia) in the bone cell lineages (Das and Goswami. 2019).

At least three TRP channels (namely TRPV1, TRPA1, TRPM3) are crucial for sensing noxious heat and plays a central role in pain perception. Importantly, the regulation of these channels by steroids may contribute to the observed sexual dimorphism in pain sensitivity, as the abundance of these steroids varies between genders (Vandewauw et al. 2018). Sexual dimorphism is also apparent in renal Ca^{2+}-reabsorption, where males excrete more Ca^{2+} than females. Androgens negatively regulate the expression of TRPV5 channels, which are involved in Ca^{2+}-reabsorption, potentially explaining this gender difference. In postmenopausal

osteoporosis, elevated androgen levels may further downregulate TRPV5 channels, exacerbating Ca^{2+}-loss and bone mass reduction. Estrogens also impact bone health by influencing TRPV5 channels, and the interplay between estrogens and these channels maintains bone homeostasis. Consequently, the reduction of estrogens and the increase in androgens during menopause can lead to downregulated TRPV5 expression, contributing to osteoporosis (Chen et al. 2014). Estrogen replacement therapy can restore TRPV5 function and mitigate this condition. Moreover, the relationship between estrogens and TRPV5-6 and TRPM6 channels positively influences renal function by favouring the reabsorption of Ca^{2+} and Mg^{2+} (Nijenhuis et al. 2005; Schlingmann et al. 2007). A decline in estrogen levels can, therefore, affect renal function. Aldosterone, another steroid hormone, regulates the expression of TRPM6-7 channels in the kidney, further emphasizing the role of steroids in renal electrolyte balance (Schlingmann et al. 2007).

In summary, TRP channels play pivotal roles in various physiological processes, and endogenous steroids have complex regulatory effects on these channels, impacting pain perception, bone health, kidney function, and more. This intricate interplay between steroids and TRP channels highlights their significance in maintaining physiological balances.

1.2.4 *Store-depletion and Ca^{2+}-influx*

A distinctive mode of TRP channel regulation involves Ca^{2+}-store depletion-induced activation. In this condition, the depletion of intracellular Ca^{2+} stores serve as a signal for the activation of TRP channels, particularly exemplified by TRPC1 (Cheng et al. 2011). The decrease in intracellular Ca^{2+}-levels following store depletion leads to the opening of Ca^{2+}-permeable TRP channels, facilitating Ca^{2+}-influx from the extracellular space. As many TRP channels are known to be de-sensitized due to higher-intracellular Ca^{2+}, the enhanced TRP channel activity due to depletion of intracellular Ca^{2+} is most-likely due to the reduced (or even

loss of) Ca^{2+}-mediated desensitization of TRPs. This process plays a pivotal role in maintaining Ca^{2+}-homeostasis and supporting various cellular functions, including neurotransmission and muscle contraction (Xibao et al. 2018). The effects of Ca^{2+} on TRP channel gating can be both stimulatory and inhibitory, occurring through direct channel-Ca^{2+} interaction or via Ca^{2+}-sensing CaM that undergoes conformational changes to interact with other proteins. Moreover, Ca^{2+}-dependent hydrolysis, driven by Ca^{2+}-dependent enzymes, can also regulate TRP channels through the modification of phosphoinositides, pivotal regulators of their activity.

1.2.5 *CaM's role in regulating TRP channels*

Calmodulin (CaM) plays a vital role in governing transient receptor potential (TRP) channels through multiple pathways. It can directly bind to specific channels like TRPV1, TRPV4, TRPV5, and others influencing their function by different mechanisms (Grycova et al. 2008; Hughes et al. 2018; Strotmann et al. 2003). This direct interaction modulates channel activity. Additionally, CaM indirectly influences TRP channel functions by impacting regulatory proteins, including kinases and phosphatases. For instance, it can downregulate TRPM8 channel function, either directly through binding or indirectly via other regulatory proteins, such as bradykinin a pro-inflammatory mediator (Sarria et al. 2011; Yang et al. 2023).

Collectively the intricate interplay of these regulatory factors allows TRP channels to fine-tune their responses to a diverse array of stimuli. Dysregulation of TRP channel activity has been linked to a spectrum of physiological and pathological conditions, including sensory disorders, pain, inflammation, cardiovascular diseases, cancer, etc. (Kaneko and Szallasi. 2014). And the understanding of TRP channel regulation deepens, new avenues for therapeutic interventions and drug development emerge, holding promise for mitigating health-related challenges by modulating TRP channel activity in a targeted manner.

1.3 The regulation of TRP channel (Activation)

The TRP channel can be regulated by various means mentioned below:

1.3.1 Voltage differences and voltage-gating

Voltage-dependent activation is a well-understood and common form of ion channel gating, primarily involving a series of positively charged amino acids in the fourth transmembrane segment (S4) of voltage-gated potassium, sodium, and calcium channels (Bezanilla F. 2008; Sigworth F.J. 1994; Yellen G. 1998). These charged amino acids sense changes in the electric field across the plasma membrane and respond by moving in response to the force exerted by the electric field. The movement of S4 and its surrounding structures contributes to the gating charges that move across the transmembrane electric field (Schoppa et al. 1992). Recent studies have provided a structural basis for the voltage-sensing process and the subsequent coupling process between the "voltage-sensor" and the "activation gate". TRP channels, are also voltage-sensitive, but exhibit some unique features. Firstly, their voltage-sensitivity is comparatively lower than classic voltage-gated Na^+, K^+, and Ca^{2+} channels. For example, TRPV1 has an apparent gating charge of only 0.5 to 0.7 e^0. Secondly, most TRP channels lack the series of charged amino acids seen in the classic voltage-gated channels, which may explain their low-voltage sensitivity. Thirdly, the voltage range in which TRP channels exhibit sensitivity often falls far beyond the physiological range a cell normally experiences. For instance, TRPV1 has a threshold voltage for activation at around 0mV, with a half-activation voltage of about 150mV at room temperature and physiological pH (Voets et al. 2004).

TRP channels have a low sensitivity to voltage changes, which may initially seem unimportant for their function. However, their response to changes in membrane potential is significant due to the influence of other channel-specific stimuli and temperature. This coupling between the weak voltage-dependent activation gating and other gating processes results in a

shift in the voltage range at which the channel responds, thus making even small voltage changes in the physiological range relevant to the channel's function. Additionally, voltage-dependent gating plays a role in the macroscopic current rectification of many TRP channels, such as for TRPM4 (Nilius et al. 2003).

Voltage-dependent gating is particularly important for TRPV1 and TRPM8, which are temperature sensors. These channels are thought to achieve temperature-dependent gating by shifting their voltage-dependent gating process (Nilius et al. 2003). It has been shown that at room temperature, TRPV1's half-activation voltage is around +100 mV. However, when the temperature is raised to 42°C, the half-activation voltage is lowered to near -50 mV, a level that can be easily reached by a sensory neuron (Nilius et al. 2003). A similar negative shift in the activation voltage is observed in TRPM8 (Voets et al. 2007). This shift is achieved because the opening and closing transitions of these channels are differentially affected by temperature. For example, heating rapidly increases the rate of the opening transition of TRPV1, leading to a shift in equilibrium toward the open state. Conversely, cooling decreases the rate of the closing transition of TRPM8 more strongly than the rate of the opening transition, leading to a shift in equilibrium toward the open state. Mutations that neutralize charged amino acids in S4 and in the S4-S5 linker region of TRPM8 reduce the apparent gating charge, suggesting a mechanism similar to classic voltage-gated ion channels (Voets et al. 2007). A similar mechanism has been proposed for the activation of TRPM4 and TRPM5, which also exhibit voltage-dependence and high temperature sensitivity (Talavera et al. 2005; Hofmann et al. 2003).

The mechanism underlying the functional coupling between voltage-dependent gating and temperature-dependent gating in ion channels is currently a topic of debate. Some studies suggest that a shared machinery is involved in both gating processes, while others propose an allosteric mechanism (Schoppa and Sigworth. 1998; Zagotta et al. 1994). As ion channels are

known to behave as allosteric proteins, this hypothesis seems plausible, especially given the large conformational changes associated with the temperature-dependent gating process (Voets et al. 2004; Brauchi et al. 2004). In support of the allosteric hypothesis, certain mutations) have been found that selectively affect individual activation modalities of certain ion channels, such as TRPV1 and TRPV3. For example, mutations in the pore turret region of TRPV1 (namely P608S, S613P, P623S, S609P, P614S, S624P aa) are relevant for this (Cui et al. 2012; Grandl et al. 2008; Du et al.2020). Furthermore, analyses of gating kinetics and equilibrium suggest that separate channel structures may support various gating processes. Overall, understanding the molecular basis of ion channel gating remains an active area of research.

1.3.2 Heat and thermo-gating

The activation of TRPs by temperature is a unique process that has been extensively studied since it was first discovered in case of TRPV1 by the Julius group (Caterina et al. 1997). Temperature-sensing is a fundamental sensory mechanism that is crucial for homeotherms to maintain a stable body temperature. Both homeotherms and poikilotherms use temperature cues to detect changes in their environment, locate favourable conditions, and avoid tissue damage. Some temperature-sensitive TRP channels are known to act as nociceptors, responding to extreme temperatures (and harmful chemicals too) and causing pain when peripheral neurons are activated. Additionally, temperature-sensitive TRP channels are believed to play a role in dynamic local regulations such as the dilation or constriction of blood vessels and the growth of neurites.

TRP channels that are highly sensitive to temperature are often referred to as thermo-TRPs. TRP channels are known to act as molecular thermosensors that get activated at different temperatures. Among them, TRPV1 is activated when the temperature reaches around 40°C, while TRPV2, TRPV3, and TRPV4 have distinct activation thresholds. TRPV2 activates at

over 50°C, whereas TRPV4 is activated at ranges from 27-37°C and TRPV3 is activated at temperatures around 33°C-39°C. However, TRPV5 and TRPV6 are not activated by heat and thus are not thermosensitive in nature. Additionally, TRPM2, TRPM4, and TRPM5 are reported to be sensitive to high temperatures. In certain snake species and in the *Drosophila*, the TRPA1 channel is heat-sensitive, with different splice variants exhibiting distinct temperature activation thresholds. For example, in the multi-dendritic nociceptor neurons of the fly, the A and D forms activate at 24-29°C and 34°C, respectively, while the B and C forms are not activated by heat. These differences are associated with regions flanking the N-terminal ARD (Zhong et al. 2012). Viper snakes express a TRPA1 in their pit organ that gets activated at 30°C (Gracheva et al. 2010).

TRPM8 is best understood as the "cold-sensitive" TRP channel, and it is activated when the temperature drops below approximately 20°C (McKemy et al. 2002; Peier et al. 2002). Another cold-activated TRP channel is TRPC5, which exhibits high sensitivity to cold in the temperature range of 37°C to 25°C. Although TRPC5 can co-assemble with TRPC1, the heteromeric channel does not display cold-induced activity as such (Zimmermann et al. 2011). Initially, mammalian TRPA1 was believed to also acts as a cold-sensor with an extremely low threshold temperature below 10°C (Story et al. 2003). However, the cold activation of TRPA1 is still debated and alternate evidence suggests that its cold-sensitivity is not a direct phenomenon (Chen et al. 2013).

It is important to note that thermo-TRPs are not the only the channels that exhibit high-sensitivity to temperature. For example, the Torpedo chloride channel CLC-0 has a gating process that is extremely sensitive to temperature, although it is unlikely to play a significant physiological role in fish as they do not typically experience temperatures that affect this process (Pusch et al. 1997). STIM1, an endoplasmic reticulum-based Ca^{2+}-sensor, is also activated by heat, with temperatures above 35°C leading to clustering of STIM1 (Xiao et al.

2011). This process may be important for regulating intracellular Ca^{2+} in response to temperature changes. Highly temperature-sensitive other channels include two-pore potassium channels and voltage-gated proton channels (Kang et al. 2005; Ramsey et al. 2006).

To understand the high temperature sensitivity of a channel, few important aspects are considered. Firstly, for channels that are exclusively sensitive to temperature changes, such as thermo-TRP channels, their activity can be triggered by a change in temperature alone. For example, TRPV1 opens at near 40°C without any agonists present at physiological pH levels (Hille B. 2001). In contrast, the Shaker potassium channel, a voltage-gated channel, would not open upon temperature increase at resting membrane potential, although its gating and ion permeation processes would be affected upon channel activation by membrane depolarization (Hille B. 2001; Zheng J. 2013).

Secondly, the activity level of a thermo-TRP channel is much more sensitive to temperature changes compared to an ordinary channel. The sensitivity of temperature is often characterized by the Q_{10} value (**Table 2**), which measures the fold-change in the rate of increase or decrease with a 10°C temperature change. The Q_{10} value is related to the activation energy by the Arrhenius equation. In general, thermo-sensitive TRP channels have very high Q_{10} values which range from 10 to 27, corresponding to an activation energy of 4.2 to 6.0 kcal/mol between 25 and 35°C (Hille B. 2001).

Protein	T range °C	Q10
TRPA1	26-16	~10
TRPM8	27-18	24
TRPC5	25-40	~10
TRPV4	25-37	10, 19 (at low and higher temperature, >25°C)
TRPV3	25-39	33
TRPV1	41-50	40
TRPV2	50-60	>100

Table 2. Q-10 values of selected TRP channels. Table adapted from Clapham and Miller. 2011.

In comparison, an ordinary channel has a Q_{10} value of 3 to 7, while the CLC-0 common gating has a Q_{10} value of 40. Furthermore, Q_{10} values are now commonly used to describe temperature-dependent changes in current amplitude, which reflect temperature-dependent changes in both permeation and gating (Hille B. 2001). However, it should be noted that the current amplitude-based Q_{10} values cannot be directly converted to an energy term, as they are merely a descriptive parameter.

Thermo-TRP channels' heat activation has been thoroughly studied through equilibrium measurements of macroscopic and single-channel currents, as well as kinetic measurements of current activation (Brauchi et al. 2004). The studies indicate that the heat-induced gating process for these channels can be reasonably described by a single transition between two gating states, “C” and “O” (representing close and open state respectively). This simple situation is described by the Gibbs free energy equation, where the transition energy between C and O is ΔG, and ΔH and ΔS are the corresponding enthalpic and entropic changes. Thermo-TRPs have been found to have a large ΔS in the range of 100 to 300 cal/mol/K, and a large ΔH in the range of 30 to 80 kcal/mol. The balance between these two large quantities is crucial, as it allows the $C \rightarrow O$ transition to occur under physiological conditions. The fine balance between ΔH and ΔS determines the functional temperature range and threshold temperature of each thermo-TRP channel (Yang et al. 2010). This balance is essential as a small deviation from it can cause the system to be stuck indefinitely in either the “C” or “O” state, rendering the channel non-functional (also in case of mutations that induce either constitutively off or constitutively on channels). This fine balance is utilized by biology to regulate the function of these channels under physiological and pathophysiological conditions.

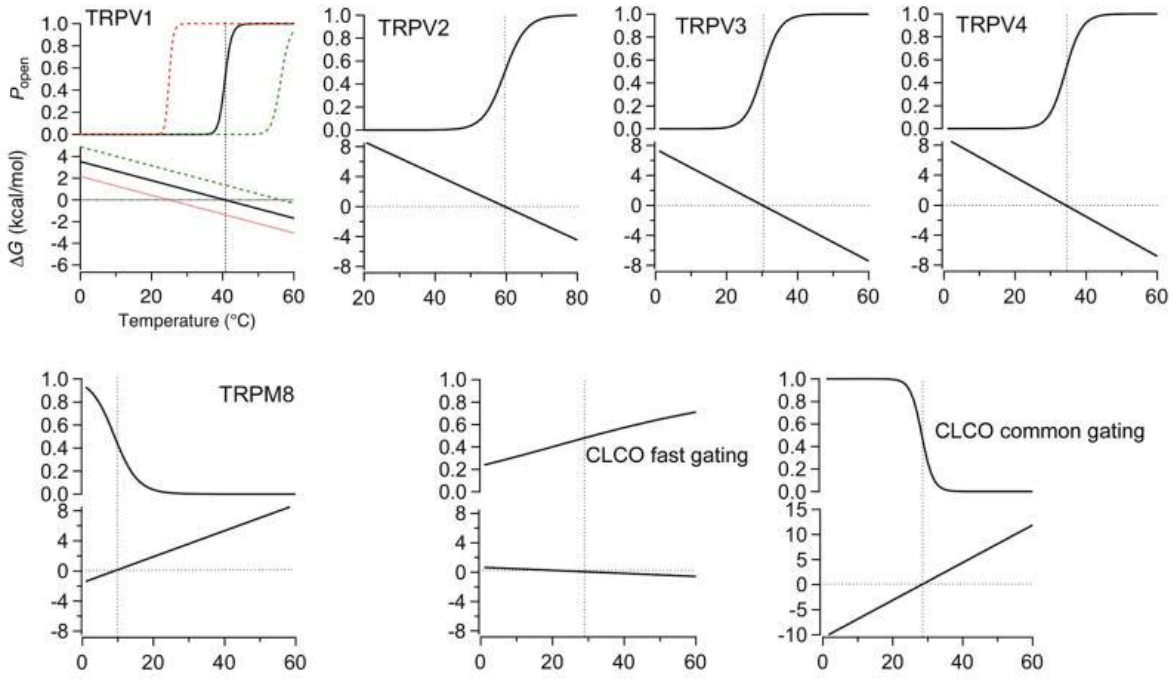

Fig 4: Temperature-dependent activation of thermo TRP channels. This figure is taken from Zheng J. 2013.

The observation that heat-sensing may involve multiple protein areas, each contributing to the overall changes in enthalpy and entropy, suggests that the conformational changes in ion channels are highly cooperative. This is supported by studies on heteromeric channels and random mutation screenings of TRPV1 and TRPV3 (Cheng et al. 2012). While the combination of multiple transitions is theoretically feasible, it does not explain why the activity of TRP channels from the same subfamilies as thermo-TRPs is not highly temperature sensitive. Nevertheless, cooperative gating likely contributes to the synergistic effects of various stimuli on the activation of these polymodal sensors. The relationship between Capsaicin (the ligand) and heat (physical stimuli) in activating TRPV1 suggests that they may act on the same gating process (Vlachova et al. 2003; Voets et al. 2004). In other words, Capsaicin reduces the thermal thresholds needed for activation causing opening of TRPV1 at much lower and physiological temperature ranges. Recent research, however, suggests that functionally connected, structurally distinct activation pathways exist. Experimental data reveals that even at high Capsaicin concentrations, biophysical measurements have demonstrated that Capsaicin and

heat have “additive gating effects”, which is unexpected if these two stimuli operate on the same gating mechanism. The hypothesis of distinct activation pathways is further supported by the fact that the fluorescence resonance energy transfer (FRET) signal from fluorophores attached to the turret changes solely following heat activation and not Capsaicin activation (Yang et al. 2010).

Recent studies on TRPA1 heat activation have revealed important findings. While the viper snake TRPA1 is heat-activated and functions as the snake's infrared sensor, TRPA1 in rats is not heat-activated (Gracheva et al. 2010). Through the creation of chimeric TRPA1 channels between the snake and rat, it was determined that the large ankyrin repeat domain (ARD) is responsible for heat activation in the snake channel. Studies on fruit fly TRPA1 channels suggest that the regions adjacent to the ARD can also regulate the heat activation process, leading to certain splice variants of dTRPA1 being insensitive to heat (Zhong et al. 2012). Whether a similar mechanism applies to TRPV1 is still unclear, as studies have suggested that the ARD region of TRPV1 is not involved in heat sensing (Zhong et al. 2012).

TRPA1 has 14 ankyrin-like repeats, while TRPV1-4 channels have only six. Even if the TRPV1 ARD is found to be responsible for heat activation, the search for a cold sensor in TRPM8 would continue, as it lacks an N-terminal ARD (Zheng J. 2013). Alternate research also suggests that the hot and cold sensitivity of TRPV1 and TRPM8 is due to their C-terminal regions (Yao et al. 2011). This is suggested due to the fact that exchange of C-terminal region of TRPV1 to the TRPM8 and *vice versa* cause hot channel TRPV1 to behave as cold-sensitive and cold-channel TRPM8 as hot sensitive channel (Brauchi et al. 2006).

All these data show the direct role of heat as an activator for the TRP channel and the TRP channel act as a cellular temperature sensor, though the exact molecular mechanisms are not very clear and seems to differ from channel to channel, species to species, remain cell and tissue-dependent manner, thus remain highly context-dependent phenomena.

1.3.3 Mechanical force

Ion channels in the plasma membrane can be activated by various types of mechanical stimuli. These stimuli can be caused by differences in osmolarity, pressure applied to the cell, membrane stretching, or shear stress from fluid flow in blood vessels (Kloda et al. 2008; Sachs and Sokabe.1990; Spencer et al. 1999). When the membrane tension reaches a sufficiently high level, it can affect all proteins embedded in the membrane. Although some ion channels are specialized in sensing mechanical stimuli, several mammalian TRP channels can also respond to mechanical force either at physiological or pathological levels. Interestingly, in some cases, TRP channels can be activated not by the mechanical force itself, but by intracellular signaling molecules generated due to mechanical stimuli by the cell such as hypotonicity-induced cell swelling which activates the Src family tyrosine kinase that phosphorylates TRPV4 protein (Sachs and Sokabe. 1990; Spencer et al. 1999; Xu et al. 2003).

TRPV4 is an osmosensitive TRP channel that responds to hypotonicity-induced cell swelling. TRPV4 can be activated by a decrease in extracellular osmolarity (which in turn alter the membrane stretch) within the physiological range, while it is inhibited by an increase in extracellular osmolarity. TRPV4 may represent a vertebrate osmoreceptor. TRPV4 is highly heat-sensitive, and an increase in temperature potentiates the channel's response to osmotic stress. However, it is suggested that TRPV4's activation by osmotic stress is achieved biochemically, mediated by intracellular signaling molecules produced by membrane-bound mechanosensitive molecules (Nilius et al. 2003; Wu et al. 2007; Gao et al. 2003). Several potential pathways have been proposed, such as the activation of the Src family tyrosine kinase that phosphorylates TRPV4 (Xu et al. 2003). The candidate tyrosine residue involved in TRPV4's mechanical stress response is identified as the Tyr^{253} located in the ARD region (Xu et al. 2003). Another tyrosine residue, i.e. Tyr^{110}, is also found to be involved in the mechano-sensing. In addition, phosphorylation of Ser824 (located at the C-terminus), by PKC and PKA,

sensitizes TRPV4's stress response. Furthermore, the PLA2-dependent formation of arachidonic acid and its conversion to 5′,6′-EET by cytochrome P450 epoxygenase is also involved in TRPV4's mechanical stress response.

In addition to TRPV4, extracellular hypotonicity can also activate TRPM7 and TRPV2 by increasing the channel's open probability. Membrane tension can also affect the activity of TRPM4, TRPM7, TRPC1, and TRPC6 (Numata et al. 2007; Morita et al. 2007; Maroto et. al. 2005; Spassova et al. 2006; Inoue et al. 2009). Conversely, a splice variant of TRPV1 is found in arginine-vasopressin neurons of the supraoptic nucleus is activated by hypertonicity-induced cell shrinkage (Sharif et al. 2006). This activation of splice variant of TRPV1 in organum vasculosum (highly vascularised hypothalamus) lamina terminalis neurons is thought to serve as the osmosensory transduction mechanism underlying thirst responses (Ciura and Bourque. 2006).

Shear stress is a type of mechanical stimulus that can directly activate TRP channels or enhance their responses to other activators too. TRPV4, TRPC6, TRPM7, and TRPP1/TRPP2 all have been reported to be activated by shear stress (Gao et al. 2004; Inoue et al. 2009; Numata et al. 2007; Nauli et al. 2003). Although activation of TRP channels by shear stress is important for vascular physiology, it is unclear how mechanical force is converted into channel conformational changes in most cases.

TRP channels not only exhibit altered functions in response to mechanical stimuli, but they may also undergo changes in their distribution across the cell membrane. For instance, exposure of cells expressing TRPM7 to physiological levels of laminar fluid flow can induce rapid translocation of the channel protein to the plasma membrane, leading to an increase in both TRPM7 current and fluorescence signal near the plasma membrane from attached GFP in less than 100 seconds. Similarly, when myocytes are stretched, TRPV2 channels are known to translocate to the sarcolemma, resulting in increased Ca^{2+}-influx and cell damage. Notably, the

translocation response of TRP channels to mechanical force varies among cell types (Oancea et al. 2006; Iwata et al. 2003).

This shows that sheer stress or mechanical stimulus can activate the channel as well as the distribution of the TRP channel which can affect the functionality of the TRP channel.

1.3.4 Chemical stimuli

Exogenous and endogenous compounds

TRP channels can be activated or regulated not only by physical stimuli but also by different exogenous as well as endogenous compounds including different hydrophobic compounds and lipids. The range of molecules that interact with TRP channels is diverse, and many of them have physiological and pathological significance. Due to the large number of TRP channel-interacting molecules, it is difficult to discuss them all here, but a few main issues are summarized here. TRPV1 being the most studied TRP channel, a large number of compounds have been tested against TRPV1. For example, a long list of natural and synthesized chemicals known that alter TRPV1 channel function, and this list continues to expand with time (some of these are given below, **Figure 5, Figure 6**). Some chemicals that interact selectively with specific TRP channels are mentioned as examples in this section.

TRPV1 is activated by Capsaicin, a natural plant product but an exogenous ligand. TRPV1 is also activated by PIP_2, bradykinin, and nerve growth factor (NGF) as endogenous ligands. Different "endovanilloids" like anandamide and arachidonic acid metabolites, and N-arachidonoyl-dopamine (NADA, a dopamine derivative), can also activate TRPV1 (Basbaum et al. 2009). Additionally, several plant products like Resiniferatoxin, Piperine, Gingerol, Zingerone, and Eugenol, as well as essential oils and other compounds like Camphor, can act as exogenous ligands for TRPV1 (Andrei et al. 2023).

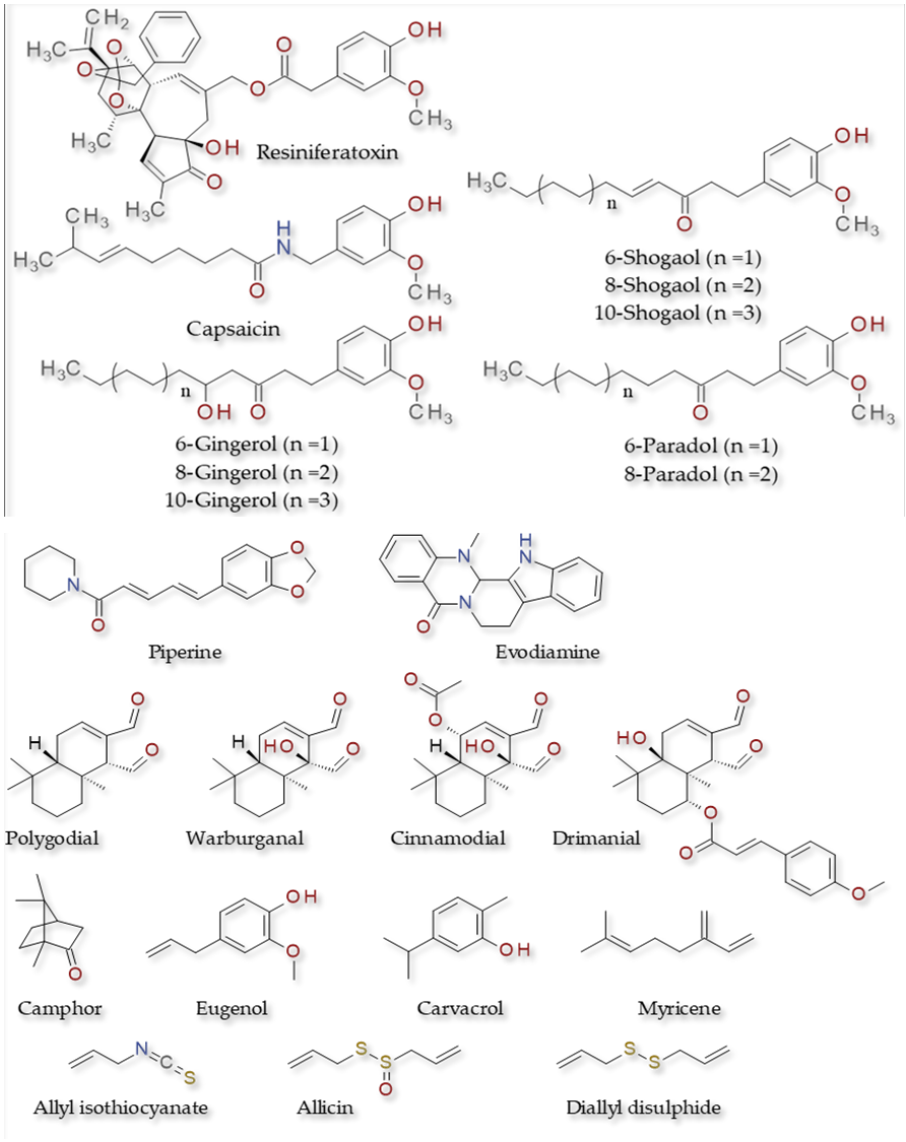

Figure 5. **TRPV1 agonists—various structures**. (Adapted from Andrei et al. 2023).

TRPV2 is activated by insulin growth factor-1 (IGF-1), an endogenous stimulant, while TRPV3 can be activated by endogenous ligands like farnesyl pyrophosphate (FPP, metabolite present in the steroid biosynthesis pathway) and synthetic ligands such as 2-APB (Hu et al. 2004). TRPV4 can be activated by synthetic ligands like 4α-phorbol 12,13-didecanoate (4αPDD), RN1747, and inhibited by compounds like, RN1734, and natural bioactive compound Citral (Watanabe et al. 2002; Vincent et al. 2009). Metal ions like ruthenium red (ammoniated ruthenium oxychloride- $H_{42}C_{l6}N_{14}O_2Ru_3$), gadolinium, and Lanthanum (III) ion

(La^{3+}) can inhibit TRPV4 and other TRP channels by "mis-fitting" into the actual pore and causing "open-channel-block," which may or may not be reversible (Blair et al. 2023).

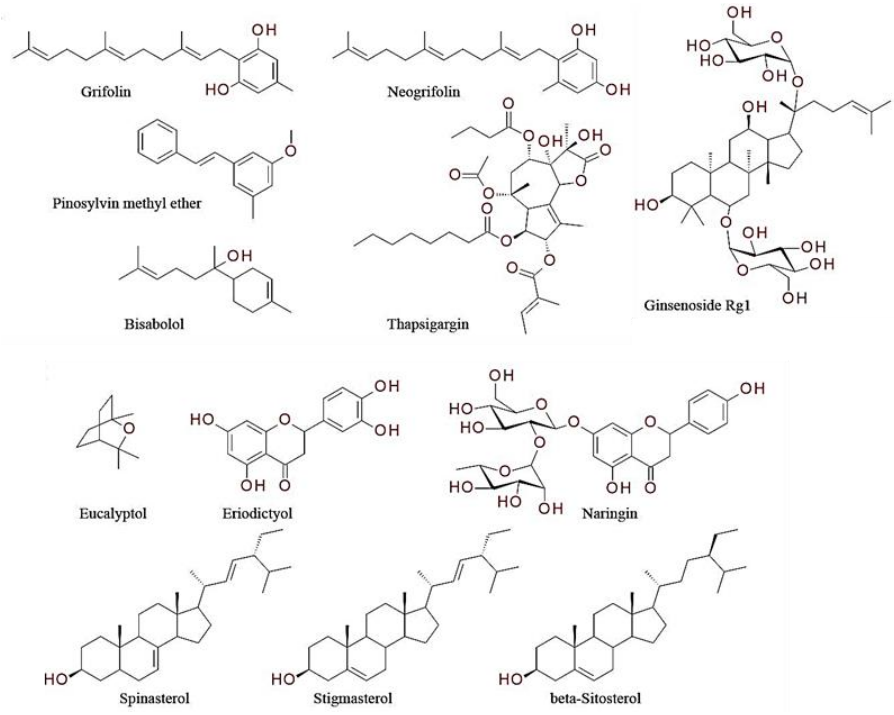

Figure 6. **TRPV1 antagonists—various structures**. (Adapted from Andrei et al. 2023).

In addition, there are several toxins and small peptides from natural sources (such as poisonous animals) known that binds to specific or multiple TRP channels and cause either activation or inhibition of TRP channels. Such toxins and venoms and small peptides set the ‘pray-predator relationship” and “arms-race” due to mutations in ion channels that are selected as toxin-resistant channels (Vriens et al. 2008).

Capsaicin is the main active vanilloid compound responsible for the spiciness of chili peppers. It has a pungent and irritating effect on mammals, including humans, causing a strong burning sensation upon contact. As a result, it has been used in animal experiments (though mainly in mammals) to establish pain models. The existence of the so called “Capsaicin receptor” had been predicted for years, and search for this Capsaicin receptor led the discovery of TRPV1 channel (Caterina et al. 1997). Most of the mammalian TRPV1 channels are highly-

sensitive to Capsaicin, with EC50 values often less than 1μmol/L, whereas those from birds are insensitive to capsaicin due to the point mutation at the Capsaicin-binding position (Jordt and Julius. 2002; Correll et al. 2004). Other TRPV channels from many other species with substantial sequence homology are Capsaicin-insensitive. These findings suggest that Capsaicin binds to specific binding sites on mammalian TRPV1 channels with high affinity. Studies confirmed that these binding sites are located in the S2-S4 region by generating chimeric channels between rat TRPV1 and chicken TRPV1 (Jordt and Julius. 2002).

Several molecules that may activate TRPV1 have been suggested, including anandamide and 12-HPETE. Resiniferatoxin, a potent TRPV1 activator isolated from a cactus, also binds to the same binding sites as Capsaicin. Capsazepine, a capsaicin analogue, inhibits TRPV1 by competing for the same binding sites (McIntyre et al. 2001; Blair et al. 2023).

Activation of TRPV1, a heat sensor in sensory neurons, by Capsaicin, is believed to underlie the "hot" sensation produced by consuming chili peppers. At the cellular level, both chemical energy (Capsaicin-binding) and physical energy (heat) activate TRPV1 and excite the same sensory neurons, resulting in the convergence of the two modalities. Studies in animals and humans have demonstrated that Capsaicin administration causes hypothermia while administering TRPV1 inhibitors such as AMG517 has the opposite effect of inducing hyperthermia (Blum et al. 2010; Blair et al. 2023).

Similar to Capsaicin-mediated activation of TRPV1 leading to hot sensation, there are chemical compounds that activate TRPM8, the “cold-sensor” to produce a cooling sensation. Menthol is one of the most well-studied TRPM8 activators, with an EC50 value of less than 100 μmol/L (though menthol has many other off targets other than TRPM8).

There are various agonists that may activate TRPM8 in a similar manner to menthol. Eucalyptol, which is the active compound in eucalyptus oil, has a high EC50 value of 3.4 mmol/L and low potency. In contrast, the synthetic supercooling agent Icilin (or AG-3-5)

strongly activates TRPM8 with a very low EC50 value of less than 1μmol/L (McKemy et al. 2002). Although menthol and Icilin can also activate other TRP channels there have been reports of more selective menthol derivatives that activate TRPM8 (Myers et al. 2009).

1.3.5 Ca^{2+}-CaM regulations

In line with TRP channels ability to conduct Ca^{2+}, it is not surprising that TRP channels also share regulatory process which is similar to other Ca^{2+} channels. Activation of TRP channels can lead to Ca^{2+}-influx that activates CaM, which can then indirectly affect the channel's function by binding to other proteins like CaM-sensitive kinases. Additionally, the binding of CaM to a TRP channel can occur in Ca^{2+}-dependent as well as Ca^{2+}-independent manner. Some TRP channels, like TRPV1, may have apo-CaM (CaM without Ca^{2+}) associated with them, and the binding of Ca^{2+} to CaM can act as a molecular switch to initiate the regulation process, as also observed in voltage-gated Ca^{2+} channels.

The C-terminal CaM-binding sites often overlap with proposed PIP_2-binding sites. Therefore, it is probable that the competitive binding of CaM and PIP_2 is responsible for some of the observed effects of CaM on channel gating, at least for TRPV channel (Clapham DE. 2003; Phillips et al. 1992).

In addition to CaM, other proteins that bind to Ca^{2+} may also play a role in mediating the effects of Ca^{2+} on TRP channel functions. One such protein is CaBP1, which binds to Ca^{2+} and can inhibit TRPC5 activation by binding to sites on the N- and C-terminals that are different from the sites where CaM binds (Kinoshita-Kawadaet al. 2005).

1.3.6 pH change

Physiological processes such as respiratory and metabolic acidosis and alkalosis, as well as pathological conditions like tissue damage, inflammation, and ischemia, can cause

variations in pH levels. Acid-sensitive ion channels play a crucial role in facilitating cellular responses to changes in environmental pH. Several TRP channels are also highly sensitive to both intracellular and environmental pH levels. pH changes can potentiate a TRP channel's response to other stimuli, thus may directly activate TRPs, or suppress the amplitude of the single-channel current.

TRPV1 was shown to be regulated by extracellular pH (Caterina et al. 1997; Tominaga et al. 1998). Protons can both activate and potentiate TRPV1. TRPV1's sensitivity to acidification is thought to be a mechanism for detecting painful conditions, particularly in deep tissues where the temperature remains constant. TRPV1 activation induced by acidification plays an important role in neuronal pain and cardio protection under various pathological conditions. By using electrophysiology, one study indicated that primary afferent nociceptors in naked mole rats are insensitive to acid stimuli, which is consistent with the animal's lack of acid-induced behaviour (Park et al. 2008).

Acidosis at or below pH 7.0 is perceived as painful in humans, while acidosis between pH 7.1 and 6.7 initiates cardiac pain (Ugawa et al. 2002). At this pH range, TRPV1 activity is affected. Tissue damage can lead to the release of protons from intracellular organelles like lysosomes. Similarly, inflammation-induced pain can result from TRPV1 activation triggered by proton release from affected tissues. TRPV1 subunits contain two primary pH-sensing sites, E600 and E648, (both located at the extracellular region) along with several other potentially pH-sensitive sites, including E536, D601, E610, E636, D646, and E651 (Jordt et al. 2000; Kuzhikandathil et al. 2001; Ryu et al. 2007). These other residues are highly conserved among TRPV1 channels and are mostly located in the pore-loop region (Hellmich and Gaudet. 2014). The pH-dependent curve for TRPV1 peaks at around pH 5.5 due to the known pKa values of these acidic residues. Mutations at several pH-responsive sites in the TRPV1 pore significantly affect heat activation, indicating that pH regulation of TRPV1 may be associated with the heat-

activation pathway also. This observation also matches well with the findings from other pH-sensitive TRP channels.

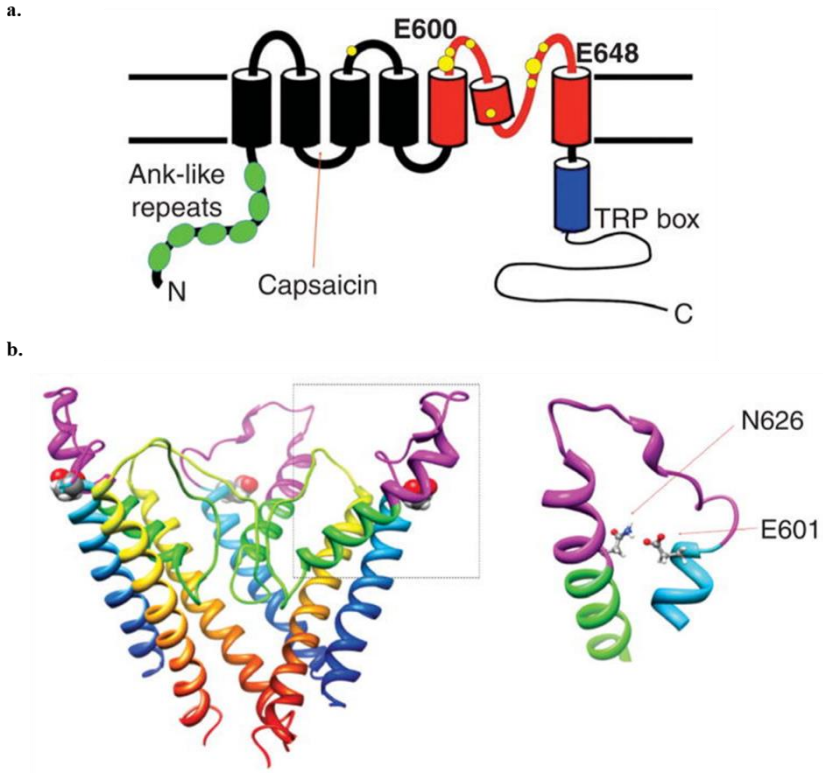

Figure 7: TRPV1 acts as a pH-sensitive ion channel. The TRPV1 subunit has two primary pH-sensing sites, E600 and E648, along with other pH sites, as depicted in the topology plot in panel A. In panel B, a structural model of the mouse TRPV1 channel displays the position of E601 (equivalent to E600 of rat TRPV1), highlighted in space-filling mode. The right panel in panel B suggests a possible interaction between E601 and N626. The figures are adapted from Zheng J. 2013.

Aside from TRPV1, several other TRP channels from various subfamilies, such as TRPV, TRPM, TRPC, TRPML, TRPA, and TRPP, are responsive to alterations in pH levels A large volume of research has been conducted to understand how TRP channels react to acidification. It is worth noting that alkalization can also impact these channels. Studies have shown that both TRPV1 and TRPA1 currents can be intensified (potentiated) by the presence of extracellular NH^{4+} (Dhaka et al. 2009; Fujita et al. 2008). This effect is believed to have resulted from intracellular alkalization (e.g. For TRPM7 its through charge screening by internal pH and polyvalent cations like Mg^{2+}, Ca^{2+}, Mn^{2+} and Zn^{2+}) (Kozak et al.2005). All these findings suggest that the pH changes in the extracellular or intracellular region, the

functions of the TRPs change accordingly. And the regulation by pH changes can also be directly related to thermal variation in the cells (**Table 3**).

Channel type	pH effect	Side	Site of action
TRPV1	Potentiation (gating) Inhibition (permeation)	Extracellular	Pore turret (E600), pre-S6 loop (E648), others
TRPV5	Inhibition (permeation, gating)	Extracellular	Pore turret (E°2)
	Inhibition (permeation, gating)	Intracellular	Proximal C-terminal (K607)
TRPM2	Inhibition (permeation)	Extracellular	Pore turret (H958, R960), pre-S6 loop (E994)
	Inhibition (gating)	Intracellular	S4-S5 linker (R933)
TRPM5	Inhibition (permeation, gating)	Extracellular	S3-S4 linker (E830), pore turret (H896), pre-S6 loop (H934)
TRPM7	Potentiation (permeation)	Extracellular	Selectivity filter ((E1047, E1052, D1054, E1059)
TRPM6	Potentiation (permeation)	Extracellular	Selectivity filter (E1024, E1029)
TRPC4	Potentiation	Extracellular	Unknown
TRPC5	Potentiation (gating), inhibition (permeation)	Extracellular	Pore turret (E543), pre-S6 loop (E595)
TRPC6	Inhibition	Extracellular	Unknown
TRPML1	Potentiation	Luminal (lysosome)	Unknown
TRPML2	Potentiation	Luminal (lysosome)	Unknown
TRPP3/PKD1L3	Potentiation (gating, permeation?)	Extracellular	Unknown
TRPA1	Potentiation (gating)	Extracellular	Unknown

Table 3. Summary of pH-mediated effects on TRP channels. This table is reproduced from Zheng J. 2013.

1.4 TRP channels in inflammatory functions

TRP channels have a significant impact on immune cells, influencing a range of processes like cell movement, engulfing foreign particles, and releasing cytokine levels. Communication between nerve cells, surface cells, and immune cells is facilitated by TRP channel activation required for coordinating immune responses. Specifically, TRPV1 and TRPV4 activation through certain triggers results in Ca^{2+}-influx in isolated T cells (Majhi et al. 2017). This discovery suggests that T cells most likely employ TRPV channels to regulate immune activity. TRP channels act as crucial signal mediators, detecting various physical and chemical changes like shifts in pressure, temperature, and acidity. This makes TRP channels

important for managing immune reactions. TRP channels are broadly distributed within the immune system, serving diverse functions such as managing Ca^{2+} communication, producing cytokines, and guiding immune cell movement. Because TRPs appear on both in immune cells and in other cells, such as in neurons, TRPs become promising targets for addressing inflammatory-related illnesses as well as inflammation through the release of neuropeptides.

In non-neuronal cells, TRP channels play critical roles in tissue development, maintenance, and inflammation regulation. Specifically, a subset of TRP channels, namely TRPV1, TRPV4, TRPM3, TRPM8, and TRPA1, are known to modulate immune responses and can induce either pro- or anti-inflammatory effects depending on the disease context (Silverman et al. 2020; Bousquet et al. 2021; Backaert et al. 2021). In somatosensory neurons, TRP channels mediate pain and temperature sensation, and TRPV1 and TRPV4 are implicated in inflammatory pain. These channels have diverse effects on immune cells, regulating cell migration, phagocytosis, production and release of inflammatory mediators. Additionally, TRP channels facilitate communication between epithelial cells, neuronal tissue, with immune cells involved in immune responses to tissue damage or infection. *In vitro* studies have shown that some TRPs can be sensitized by the activation of other receptors, making them susceptible to activation by processes such as inflammation. Therefore, TRPs can either trigger pro- or anti-inflammatory mechanisms, depending on the context of the inflammatory disease, by directly affecting cation levels or indirectly modulating intracellular pathways (Schumacher M.A. 2010). Recent advances in TRP research have highlighted their significant role in immune and inflammatory cells and their involvement in inflammation-mediated and immune-mediated diseases (Schumacher M.A. 2010).

The most studied TRP channel in relation to inflammation is TRPV1. The activation or sensitisation of TRPV1 can enhance peripheral inflammatory responses by promoting the expression and release of other inflammatory mediators, such as IL-6 and IL-8 through

transactivation of MAPK and NF-kB (Pan et al. 2011). The overexpression of TRPV1 in inflamed tissues, the reduction of inflammation by using TRPV1 antagonists or through genetic ablation, and the correlation between TRPV1 activation and the expression of proinflammatory cytokines all suggest that TRPV1 is involved in the inflammatory process. Additionally, TRPV1 contributes to inflammatory pain by interacting with other TRP channels through co-expression and putative functional interaction (Bujak et al. 2019). Despite the availability of various pharmacologic therapies, chronic inflammatory conditions continue to cause pain and disability, posing a significant challenge in management. TRPV1 was initially thought to play a limited role in nociceptive transduction by responding to thermal stimuli and detecting noxious heat. However, further research has revealed that TRPV1 is not just a thermal sensor but also an essential component of a signaling system that alerts the body to potential or ongoing pathophysiological conditions that could result in irreversible cellular injury.

1.5 TRP channels in sensory functions, pain and other pathophysiology

TRP channels play a vital role in sensory functions, particularly in nociception, i.e. the detection of noxious stimuli that produce pain (Bautista et al. 2013). Nociceptive TRP channels contribute to various pain types, including inflammatory, neuropathic, visceral, and cancer. These channels can be sensitized by the activation of other receptors, allowing them to be activated by processes such as inflammation that contribute to pain. Activated nociceptive TRP channels serve as the primary mode of pain detection/transduction under physiological and pathological conditions (Szallasi et al. 2007). TRPV1, TRPV4, TRPM3, TRPM8, and TRPA1 are expressed on peripheral nerves and neurons that communicate with the immune system and major peripheral organs, regulating inflammatory responses. These channels are potential targets for pain management and other pathophysiological conditions. Specifically, TRPV1 serves as a key player in detecting noxious stimuli and pain transduction under physiological

and pathological conditions. Through the expression and release of inflammatory mediators, TRPV1 activation and/or sensitization can also intensify peripheral inflammatory responses, and contribute to the development of inflammatory pain.

TRP channels play a pivotal role in pain perception and diverse pathological states (Jardin et al. 2017). These channels act as sensors, translating chemical, thermal, and mechanical stimuli into pain sensations. Nociceptive TRP channels contribute significantly to various types of pain, such as inflammation-driven, nerve-related, organ-associated, and cancer-induced pain. Among these, TRPA, TRPM, and TRPV subgroups have been extensively studied, revealing their involvement in pain initiation and persistence. For instance, TRPA1 has implications in a genetic channel disorder and is a potential target for drugs to alleviate associated pain. TRPV1–4, with their strong affinity for Ca^{2+} ions, have widespread connections to nociception. Beyond pain, TRP channels are also implicated in neurodegenerative disorders, diabetes, and cancer (Fernandes et al. 2020; Duitama et al. 2020). Involvement of TRP channels in pain perception and pathophysiology is crucial for devising effective targeted therapies (Szallasi and Cortright. 2007; Bautista et al. 2018).

1.6 The evolutionary aspect of the TRP channel

Life on earth originated about 3.5 billion years ago with the emergence of prokaryotes (bacteria and archaea) and some eukaryotes (protozoa, algae, and fungi) later on. Over time, plants and animals evolved, adapting to different environments and expanding their ranges. The development of sensory abilities was crucial for organisms to navigate their surroundings. Transient receptor potential (TRP) channels are important for perception in most living organisms, serving as "cellular sensors" that respond to various environmental stimuli by allowing cation flow down their electrochemical gradients (Clapham D.E. 2003). TRP channels have been found in a wide range of organisms, from single-cell organisms to multicellular ones.

However, higher plants do not seem to have TRP channels. On the other hand, TRP genes have been discovered in various unicellular parasites, fungi, and marine organisms.

Despite the widespread occurrence of TRP channels in different species, their evolutionary significance remains largely unexplored. However, some conserved sequences have been identified in certain TRP channels, which may be linked to their specific regulation and function, particularly in a species-specific manner. For instance, a study conducted in 2009 by Matsuura et al. examined the conservation and importance of insect TRP channels. The researchers investigated the presence of different TRP genes in *Drosophila* and several other insect species with sequenced genomes. They discovered that all the insect species contained six TRP subfamily members belonging to TRPA, TRPV, TRPN, TRPM, TRPC, and TRPML. This indicates that mechanosensation, phototransduction, and lysosomal functions are well-conserved in insects. In another example, tubulin-binding sequences are present in TRPV1 (Saha et al. 2017), and these sequences have been conserved in all vertebrates for around 450 million years. Likewise, cholesterol-binding sequences are present in TRPV4, but these sequences are selectively present only in vertebrates and not in functional homologues present in invertebrates (Kumari et al. 2015).

1.6.1 Evolution of TRPs according to different characteristics and properties

The importance of “temperature sensitivity” in TRP superfamily members was recognized by the Nobel Prize in Physiology or Medicine awarded to Prof. David Julius and Prof. Ardem Patapoutian in 2021. This indicates the crucial role of these receptors in the interactions of organisms with their surroundings. TRPs are multifunctional cell membrane proteins expressed in various tissues, involved in many sensory and physiological functions. It's worth noting that while ankyrin domains are present in the TRPA family, such domains are also found in the TRPC and TRPV family members.

1.6.1.1 Diversification of TRP channel

The diversification of TRP channels is captivating within their biological realm. Notably, TRP channels exhibit structural distinctiveness, with each channel in the TRP family having a unique structure that enables specific interactions, execute different functions, and thus responses to different stimuli in a unique manner. The regulation and selectivity mechanisms are also diverse, as these can be influenced by factors like temperature, voltage, pH, and signaling molecules, allowing these channels to engage in various physiological roles. Functionally, TRPs are integral to sensory perceptions like pain, temperature, and taste, as well as cellular processes including ion balance, cell movement, and immune reactions. Moreover, the presence of TRPs across species showcases their phylogenetic diversity, implying their evolution and diversification across the animal kingdom. Some of the examples are mentioned below with details.

TRP channels can be categorized into two major groups, Group 1 and Group 2, which consist of TRPA, TRPM, TRPN, TRPS, TRPV, TRPVL and TRPP, TRPML, and possibly TRPY/TRPF, respectively (Venkatachalam and Montell. 2007; Montell C. 2005). These channels are present in a wide range of eukaryotes, including animals, choanoflagellates, apusozoans, alveolates, and green algae (chlorophyta) (Peng et al. 2015). Notably, so far there is no evidence of presence of TRPs in *Archaea* or bacteria, suggesting that these channels emerged during the evolution of early eukaryotes (Fujiu et al. 2011; Huang et al. 2007).

The Group 1 family of TRP channels, which include TRPA, TRPC, TRPM, TRPN, TRPS, TRPV, and TRPVL, are believed to have existed before the Cnidaria-Bilateria split that occurred more than 750 million years ago (Himmel et al. 2020). In fact, many of these families are thought to have existed before the emergence of animals, as some single-celled organisms like *choanoflagellates* have at least three types of Group 1 channels, namely TRPM, TRPC, and TRPA (Cai X. 2006). Interestingly, some algae (such as *Chlamydomonas*) also have

channels that resemble the Group 1 channels, including a TRPV-like channel that has been postulated to exist (Fujiu et al. 2011). Additionally, some other channels, namely TRPN, TRPM, TRPC, and TRPS have also been discovered in algae and form a sister clade to the Group 1. Notably, evidence suggests that TRPM channels may have existed before the bikont-unikont split, as evidenced by the presence of two TRPM-like channels in *Lingulodinium polyedra*, a type of alveolate (Himmel et al. 2020; Peng et al. 2015; Cai X. 2006; Fujiu et al. 2011; Lindström et al. 2017)

The Group 2 family comprises of TRPML and TRPP, which were likely split early on, as evidenced by their expression in animals, amoebozoans, and alveolates. While some eukaryotes such as fungi express only one of these families, both TRPML and TRPP are expressed in the aforementioned groups (Palovcak et al. 2015). Interestingly, there is evidence suggesting that earlier splits occurred within the TRP family, resulting in families that were lost in many taxa but still present in algae and alveolates. These channels are referred to as Other Group 2 channels. Based on current evidence and assuming the hypothesis that the root of the TRP channel tree is between Group 1 and Group 2, it is believed that the split between other Group 2-TRPML/TRPP and the subsequent TRPML-TRPP split occurred in a common eukaryotic ancestor (Lindström et al. 2017; Arias-Darraz et al. 2015).

1.6.1.2 TRP channel diversification and gene-duplications

The number, origin, and evolution of TRPV genes in metazoans were analysed, particularly in the context of vertebrate whole-genome duplication events (WGD). Search for genes followed by phylogenetic tree and synteny analyses revealed the presence of several previously unidentified TRPV genes (Nakatani et al. 2007; Putnam et al. 2008).

The common ancestor of *Bilateria* and *Cnidaria* had three TRPV genes, which increased to four in the *Deuterostome* ancestor. Two of these genes were lost in the vertebrate

ancestor, leaving two genes that gave rise to two TRPV subfamilies in vertebrates. These subfamilies consisted of subtypes 1, 2, 3, 4, 9, and 5, 6, 7, 8, respectively. The gene expansion was due to the two basal vertebrate WGD events (1R and 2R) and three local duplication events before the gnathostome radiation (Simakov et al. 2020). TRPV1, TRPV4, and TRPV5 have been retained in all gnathostomes studied, suggesting their vital roles. TRPV7 and TRPV8 have been independently lost in various lineages but exist in *cyclostomes, actinistians, amphibians, prototherians,* and basal *actinopterygians* (Meyer and Van De Peer. 2005; Lien et al. 2016).

TRPV3 and TRPV9 are present in extant elasmobranchs, while TRPV9 was lost in the osteichthyan ancestor and TRPV3 in the actinopterygian ancestor. The *Coelacanth* has retained the ancestral osteichthyan-derived TRPV repertoire. TRPV2 emerged in the tetrapod ancestor. TRPV5 duplication occurred independently in various lineages, such as in cyclostomes, chondrichthyans, anuran amphibians, sauropsids, mammals, and actinopterygians. After the teleost-specific WGD (3R), only TRPV1 retained its duplicate, whereas TRPV4 and 5 remained single genes. Some teleost species kept both TRPV1 paralogs, while others lost one. The salmonid-specific WGD (4R) duplicated TRPV1, TRPV4, and TRPV5, resulting in six TRPV genes. *Xenopus tropicalis* has the most significant number of TRPV genes (total 15 TRPV genes) (Morini et al. 2022).

In summary, the comprehensive analysis of genetic sequences, species distribution, and specific features within vertebrates has revealed a greater number of TRPV family members. This includes the identification of three additional subtypes, namely TRPV7, TRPV8, and TRPV9, all originated early in the evolution of vertebrates. The TRPV family's evolution is marked by considerable dynamics, characterized by numerous lineage-specific events involving both local gene duplications and gene losses at the same time (Morini et al. 2022). Thus, TRPV genes seem to be very important for providing additive advantages required for adaptive fitness and further species selection.

1.6.1.3 Evolutions of TRPVs

The thermo TRPV channels, TRPV1 to 4, are a group of thermosensitive channels that are highly conserved among mammals, sharing 40-50% sequence identity (Patapoutian et al. 2003). On the other hand, TRPV5 and TRPV6 are less similar to the other thermo-TRPV channels, with only about 30% sequence identity, but share 75% identity with each other (Plant and Strotmann. 2007). Unlike the thermo TRPVs, TRPV5 and TRPV6 are selective for Ca^{2+} ions over other cations and are not involved in temperature sensing (Van Goor et al. 2017).

TRPV family members have been identified in vertebrates, such as in mammals, birds, amphibians, sauropsids, and fishes. However, little is known about their physiological functions, and only a few studies have investigated TRPV in fish. Teleosts, a type of fish, have been found to express three types of TRPVs, namely TRPV1, TRPV4, and TRPV6 (Morini et al. 2022). TRPV1 has been detected in fish-sperm as well (Majhi et al. 2013). In rainbow trout, TRPV1 and TRPV4 are expressed in various tissues, including the pineal gland, and have been shown to regulate melatonin secretion *in vitro*. Additionally, at least TRPV1 is involved in thermosensing. In Atlantic salmon, TRPV1 and TRPV4 have been found to play a role in thermal sensing during behavioural fever (Nisembaum et al. 2022). In zebrafish, TRPV1 and TRPV4 are expressed in different sensory organs (Hunt et al. 2012; Gau et al. 2013).

A functional homologue of TRPV1, named OSM-9 was found in the ecdysozoan protostome, *Caenorhabditis elegans* (Colbert et al. 1997). Later on, four more OSM-9-like channels were identified and named OCR 1-4. These channels have structure (with multiple ankyrin repeat domains, similar to OSM-9) are similar to TRPV (Colbert et al.1997). In *Drosophila melanogaster*, two TRPV family members have been identified: i.e. Nan and IAV. OSM-9 and OCR-2 in *Caenorhabditis elegans* are essential for some forms of mechano-sensation, such as osmosensation and nose touch, while NAN and IAV in *Drosophila* are necessary for sound transduction by the antennal chordotonal organ (O'Neil and Heller. 2005).

In *Caenorhabditis elegans*, TRPV channels are expressed in neuroendocrine cells and promote neurotransmitter release. In *Caenorhabditis elegans*, mechanosensory defect due to mutation in OSM-9 can be rescued by expressing human TRPV4 (Liedtke et al. 2003). Furthermore, TRPV homologs have also been found in cnidarians, indicating that the TRPV family originated before the emergence of bilaterians (Colbert et al. 1997).

The recent discoveries of previously unknown TRPV family members in various metazoans, especially gnathostomes, and the comprehensive evolutionary model are summarized in detail (**Fig. 8)**.

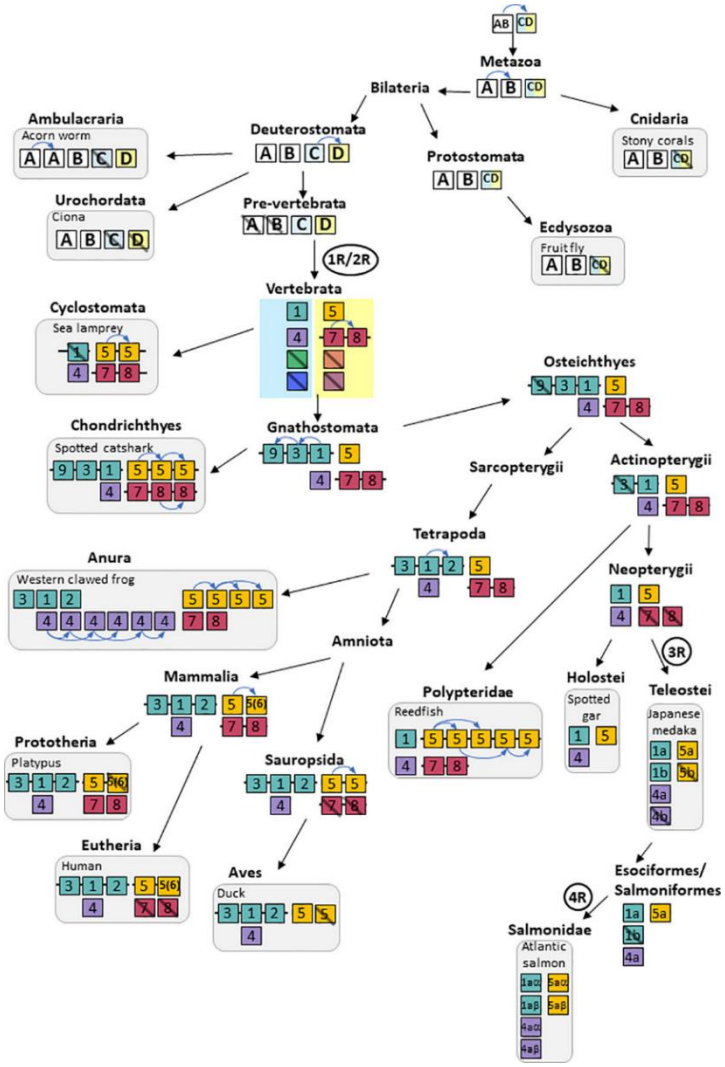

Fig 8: Evolutionary scenario for the TRPV superfamily. The TRPV family's evolution is thought to have occurred through the duplication of local TRPV genes in early metazoans, giving rise to three genes designated as A, B, and C/D. The C/D gene appears to have been lost independently in both the cnidarian and ecdysozoan lineages (Adapted from Morini et al. 2022).

Through global phylogenetic analysis of key metazoan groups, in the previous study, three types of TRPV were identified, i.e. TRPVA, TRPVB, and TRPVC/D, which likely originated in an ancestral metazoan. TRPVA and TRPVB were conserved in cnidarians, protostomes, and non-vertebrate deuterostomes but lost in vertebrates. Duplication events generated TRPVA paralogs in hemichordates, echinoderms, and molluscs, and TRPVB paralogs in nematodes. TRPVC/D was independently lost in cnidarians and ecdysozoans while being duplicated in lophotrochozoan annelids and molluscs. A duplication of TRPVC/D gave rise to TRPVC and TRPVD, which probably occurred in an ancestral deuterostome. TRPVC was independently lost in ambulacraria, cephalochordates, and urochordates, while TRPVD was independently lost in echinoderms and urochordates. TRPVC and TRPVD genes are ancestral to all vertebrate TRPV types (Morini et al. 2022).

1.7 Overview on TRPV3 and TRPV4 channel

TRPV3 and TRPV4 are two closely related ion channels that belong to the TRPV subfamily. These channels play important roles in various physiological processes, including the detection of heat and pain, as well as the regulation of Ca^{2+}-signaling, inflammation, and skin barrier function (Lei et al. 2023).

TRPV3 is predominantly found in the skin, hair follicles, and sensory neurons. It can be activated by several chemical compounds, such as camphor, carvacrol, and eucalyptol and physical factor such as temperatures above 33°C. Upon activation, TRPV3 allows Ca^{2+}-influx. Activation of TRPV3 leads to the release of inflammatory mediators like cytokines and prostaglandins, and causes feelings of warmth and pain (Huang and Chung. 2013; Steinhoff and Biro. 2009; Huang et al. 2008; Cheng et al. 2010).

Expression of TRPV3 in diverse tissues (discussed later) indicates its diverse functions. The most abundant expression of the TRPV3 is in the skin tissue (mainly in keratinocytes).

TRPV4 is expressed in a wide range of tissues, including the skin, lung, bladder, and bone (Nilius et al. 2004; Liedtke et al. 2000; Strotmann et al. 2000; Jia et al. 2004). This wide-spread expression accords well with its ability to respond against different stimuli, such as changes in temperature, mechanical stress, osmolarity, and endogenous compounds such as arachidonic acid and phorbol esters. Activation of TRPV4 also leads to Ca^{2+}-influx, which can regulate several cellular processes, such as cell migration, proliferation, differentiation, immune responses, and pain perception (Song et al. 2014; Lee et al. 2017; Willette et al. 2008).

Both TRPV3 and TRPV4 are implicated in several diseases and disorders, including chronic pain, osteoarthritis, skin disorders, and bladder dysfunction (Masuyama et al. 2012; Girard et al. 2013; Gombedza et al. 2017; Lee and Caterina. 2005; Peier et al. 2002; Barrick et al. 2003; Maccini et al. 2012). Therefore, these channels have become potential therapeutic targets for developing new treatments and drugs.

1.7.1 Structural features and domain structure of TRPV3 and TRPV4

1.7.1.1 Structural features of TRPV3

The typical structure of TRPV3 can be assessed by its protein sequence only. TRPV3 is composed of four subunits that assemble into a tetrameric non-selective cation channel (Deng et al. 2020). Each subunit has six transmembrane domains (S1-S6), a pore-forming loop connecting S5 and S6, and cytoplasmic N- and C-termini. The S5-S6 pore-loop contains several residues that are critical for the channel's ion selectivity and gating, such as a conserved aspartic acid residue (D646 in humans) that affects Ca^{2+}-permeability and other residues like L636 and V642 that influence the channel's sensitivity to heat and chemical compounds.

The N-terminal cytoplasmic domain of TRPV3 has multiple ankyrin repeats, which facilitate protein-protein interactions and channel regulation, while the C-terminal domain features multiple phosphorylation sites (contains ARD, i.e. Ankyrin repeat domain) that can

modify the channel's activity (Rouillard et al. 2016; Singh et al. 2020; Vlachova et al. 2003; Brauchi et al. 2006). Alternative splicing of TRPV3 generates isoforms with distinct characteristics, such as TRPV3b, which lacks the N-terminal ankyrin repeats and exhibits reduced-sensitivity to heat and chemical activators compared to the full-length TRPV3a isoform (Shi et al. 2013). These structural properties of TRPV3 are essential for its physiological functions and regulatory mechanisms and can serve as a basis for the development of drugs and therapies targeting this channel.

1.7.1.2 The cryo-EM structure of TRPV3

Recently, cryo-electron microscopy structures of full-length mouse TRPV3 had been studied in both the closed (i.e. equivalent to apo) and agonist-bound (i.e. equivalent to open) states. The agonist binds to three allosteric sites far away from the pore, and channel opening is accompanied by conformational changes in both the outer pore and in the intracellular gate (Singh et al. 2018). The gate is formed by the S6 helices that line the pore and undergo a transition from α to π helices, elongate, rotate, and spread apart in the open-state (Singh et al. 2018). In the closed-state, the shorter S6 segments are completely α-helical and expose their nonpolar surfaces to the pore, which hydrophobically seals the ion permeation pathway (Singh et al. 2018).

Like other members, TRPV1, TRPV2, and TRPV4 (all belongs to the thermo TRPV family), TRPV3 also forms a homotetramer with four-fold symmetry (Schaefer et al. 2005; Singh et al. 2018; Zubcevic et al. 2018; Smith et al. 2002). Within a tetramer, each monomer consists of an Ankyrin Repeat Domain (ARD) at the amino (N-) terminal cytosolic region and a transmembrane domain (TMD) made up of six transmembrane helices (S1−S6) that undergo a domain-swap configuration (Singh et al. 2018; Zubcevic et al.2018).

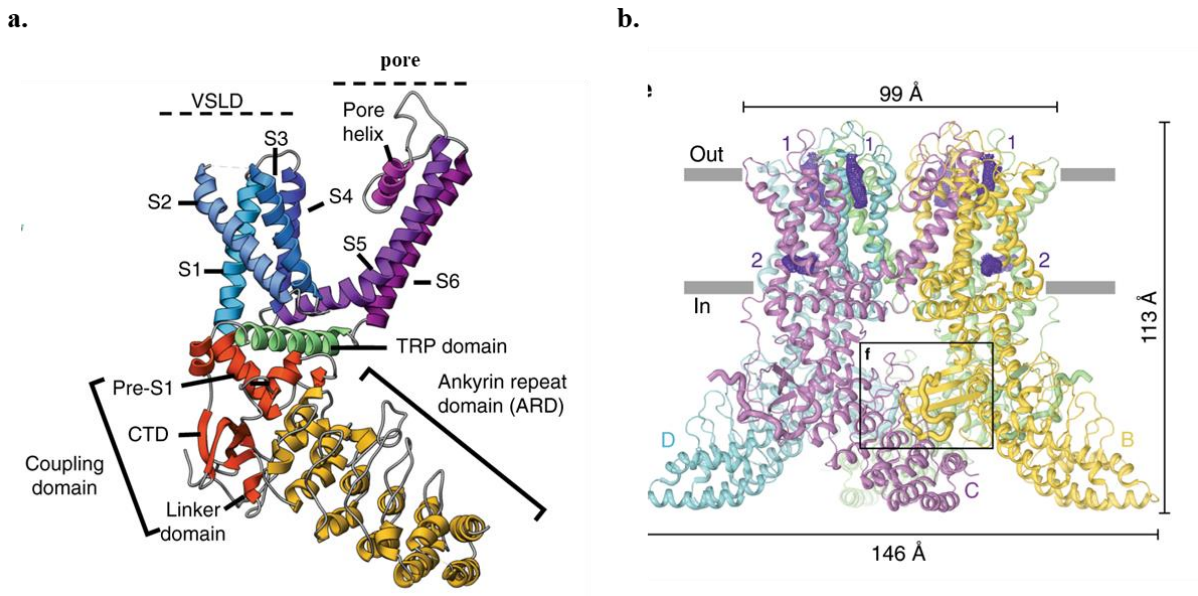

Fig 9: Overview of the structural elements within a single protomer of the TRPV3 channel. a. Overview of the structural elements within a single protomer of the TRPV3 channel: Ankyrin Repeat Domain (ARD) is shown in yellow; coupling domain (CD), consisting of linker domain, pre-S1 and the C-terminal domain, is shown in red; voltage-sensing-like domain (VSLD), consisting of helices S1−S4, is shown in blue, the pore domain, consisting of helices S5−S6 and the pore helix, is coloured in purple; the TRP domain is shown in green). **b.** Side view of the TRPV3(Y564A)-2-APB. This figure has been taken from Zubcevic et al. 2018.

The coupling domain (CD), which comprises the linker domain, pre-S1, and carboxy (C-) terminal domain (CTD), links the TMD and ARD. The TMD consists of a voltage-sensor-like domain (VSLD), containing helices S1-S4, and a pore domain comprising helices S5, S6, and the pore-helix. The S4-S5 linker links the VSLD and the pore domain. Additionally, the channel contains a TRP-domain, as shown (**Fig. 9**). A recent study shows that TRPV3 channels can also form a pentameric (with dilated pore region, **Fig. 10**) structure as observed through AFM and cryo-EM (Lansky et al. 2023). The cryo-EM structure also highlights the presence of a “cap-like” structure on the extracellular side of the channel, which could play a role in temperature and chemical sensing. Additionally, the structure revealed that the ankyrin repeats in the N-terminal domain contribute to the stability of the tetrameric structure of the channel. In summary, the cryo-EM structure of TRPV3 provides valuable information on the channel's architecture and the mechanisms of ion permeation and gating, which could aid in the development of targeted therapies and drugs.

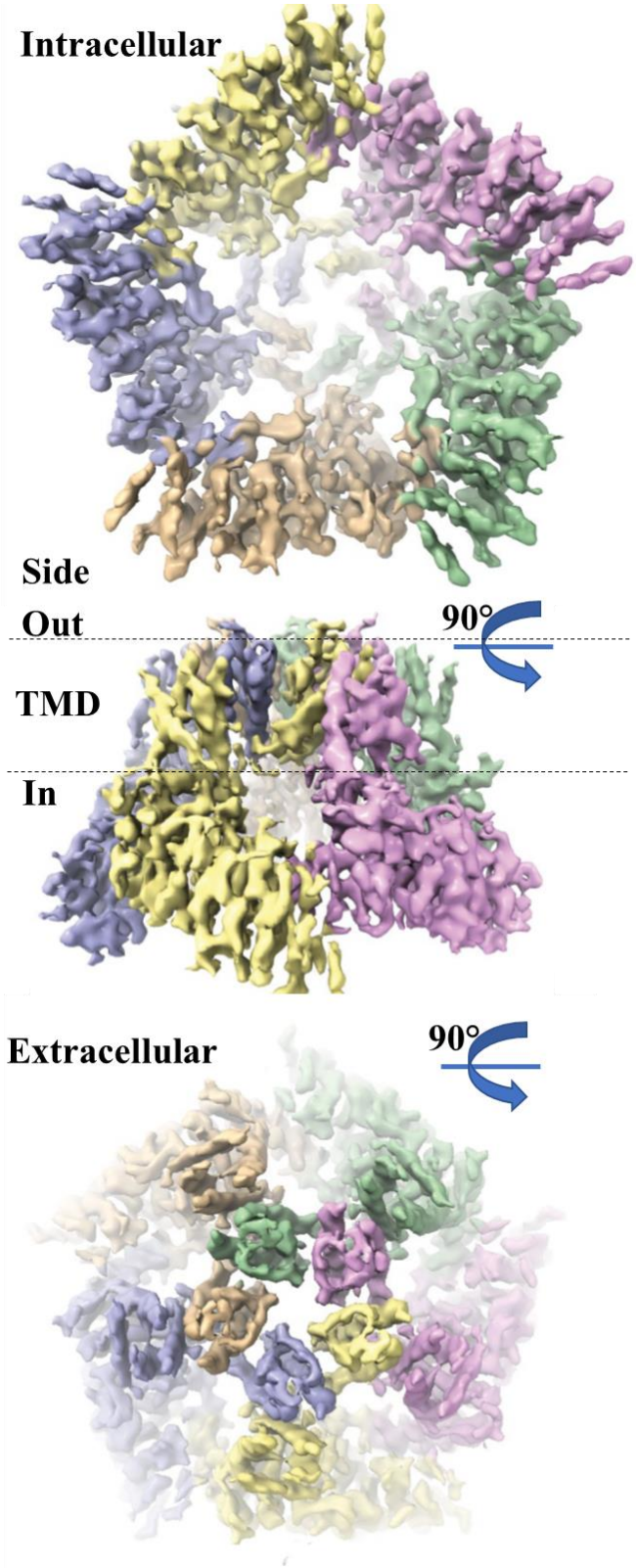

Fig 10: Structure of the pentameric TRPV3 channel. Cryo-EM map of the TRPV3 pentamer, determined to 4.4 Å resolution. The five protein subunits are coloured in wheat, purple, yellow, pink and green. This figure has been taken from Lansky et al. 2023.

1.7.1.3 Structural features of TRPV4

TRPV4 is made up of four subunits that come together to form a functional tetramer (Deng et al. 2018). Each subunit comprises of six transmembrane domains (S1-S6), a pore-forming loop located between S5 and S6, and cytoplasmic N- and C-termini (Strotmann et al.2003; Deng et al. 2018). The "pore-loop" present between S5-S6 has several residues that are crucial for the channel gating and ion-selectivity of TRPV4 (Strotmann et al. 2003). For example, an essential glutamic acid residue (E783 in humans) is responsible for Ca^{2+}-permeability, while other residues such as Y568 and Y572 play a role in the response of TRPV4 to mechanical and osmotic stimuli (Strotmann et al. 2003).

The N-terminal cytoplasmic domain of TRPV4 features ankyrin repeats that take part in protein-protein interactions and the regulation of the channel (Watanabe et al. 2002). The C-terminal domain consists of a TRP-domain, ankyrin repeats, and a coiled-coil domain, which are essential for the modulation of TRPV4 activity by various cellular and environmental factors (Hellwig. et al. 2005). Alternative splicing of TRPV4 generates different isoforms that possess distinct functions and properties. Notably, TRPV4b isoform does not contain the TRP-domain and has lower Ca^{2+}-permeability than the full-length TRPV4a (Kumar et al. 2023).

Recently, the cryo-electron microscopy (cryo-EM) structure of the TRPV4 was determined with a resolution of 3.8Å (Deng et al. 2018). The structure not only provided an overall view of the channel's organization but also uncovered vital information about its mechanisms of ion permeation and gating. The "pore-loop" between the S5-S6 domains contains crucial residues that are essential for ion-selectivity and gating, including the conserved glutamic acid residue (E783), responsible for conferring Ca^{2+}-permeability (Deng et al. 2018; Shigematsu et al. 2010). Moreover, the cryo-EM structure revealed that TRPV4 has a distinctive architecture on the extracellular side, which includes a large cytoplasmic domain and an extended extracellular region (**Fig. 11**). This domain may play a role in sensing a variety

of stimuli such as temperature and mechanical forces (Takahashi et al. 2014; Deng et al.2018). Furthermore, the N-terminal ankyrin repeats were found to be involved in stabilizing the tetrameric structure of the channel (Takahashi N. 2014; Deng et al. 2018).

In the linker domain, a three-stranded beta-sheet composed of beta1, beta2, and beta3 strands not only connects the N-terminal ARD to the C-terminus within each subunit but also interacts with the ARD from an adjacent subunit to create an important subunit-subunit assembly interface. Following the beta-strands, a helix-turn-helix (HTH) motif and a pre-S1 helix tightly accommodate the conserved C-terminal TRP-helix, which regulates channel activity and follows the inner helix S6. The amphipathic TRP-helix is remains parallel to the membrane and in close contact with the S4-S5 linker, which links the S1-S4 and pore-domains (Gregorio-Teruel et al. 2015; Yu and Catterall. 2004). This arrangement situates the TRP-helix between the cytosolic and transmembrane domains, facilitating the conformational changes between these two regions and affects the gating mechanism in response to various stimuli (Gregorio-Teruel et al. 2015; Inada et al. 2012).

Both the TRPV3 and TRPV4 ion channels have been extensively studied, and some notable differences have been observed. Compared to other thermo TRPV channels, TRPV3 has a longer pore helix and a more extended selectivity filter, which results in its unique characteristics (Deng et al. 2020). Additionally, the apo-form of TRPV3 displays some exclusive features. In contrast, TRPV4 has roughly six times greater selectivity for Ca^{2+} over Na^{+} and is a well-suited for initiating Ca^{2+}-influx. The latest TRPV4 structures reveal only one ion-binding site, and it is unclear whether the channel contains multiple ion binding sites in other conformational states (like most other TRP channels), or it has a distinct permeation mechanism based on a single ion binding site (Deng et al. 2018). The structural mechanism of dyclonine-induced inhibition of TRPV3 has also been investigated. This revealed that the

anesthetic (dyclonine) prompts a transition from a low-energy α-helix to a high-energy π-helix in TRPV3 (Neuberger et al. 2022; Liu et al. 2021).

In summary, the cryo-EM structure of TRPV4 provides a detailed view of the channel's architecture and sheds new light on the mechanisms of ion permeation and gating. In future, this can have implications for the development of drugs and therapies targeting this channel.

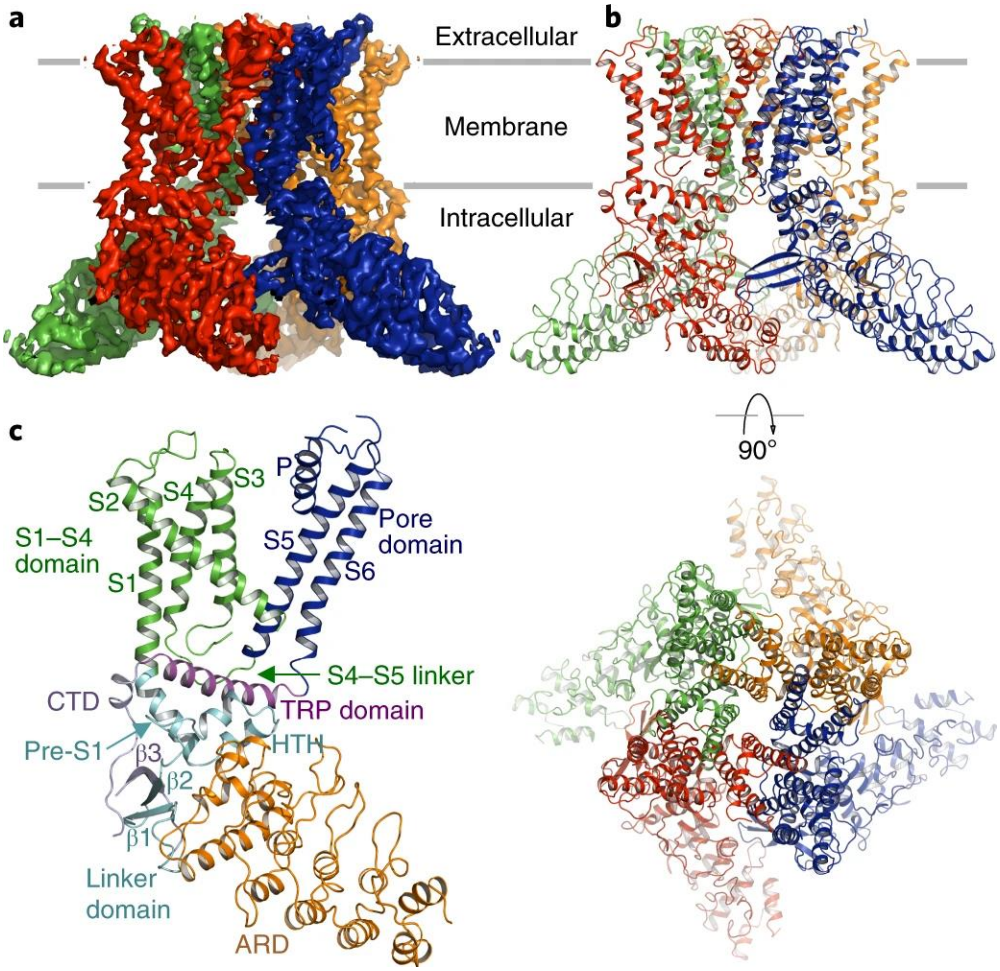

Fig 11.: Cryo-EM structure of TRPV4. **a.** Reconstructed Cryo-EM tetrameric channel. **b.** Overall structure in orthogonal view. **c.** A single subunit structure. This figure has been taken from Deng et al. 2018.

1.7.2 Different interacting proteins of TRPV3 and TRPV4

1.7.2.1 TRPV3 interaction with different proteins

The interaction of TRPV3 with different proteins have been extensively studied, and some of them are listed below.

The interaction between TRPV3 and anoctamin1 (ANO1, a calcium-activated chloride channel) has been shown by using co-IP and patch-clamp methods. An *in vitro* wound-healing assay has demonstrated that TRPV3-ANO1 interaction enhances wound healing in keratinocytes (Yamanoi et al. 2023). ANO1-mediates influx of Cl^- ions, can enhance wound healing in keratinocytes by responding to Ca^{2+}-influx through TRPV3. However, ANO1 activation reduces cell migration and/or proliferation (Yamanoi et al. 2023). It was observed that TRPV3 activation affects ANO1-mediated currents in the mouse skin keratinocytes and in normal human epidermal keratinocytes (NHEKs) (Yamanoi et al. 2023).

TRPV3 has also been found to interact with Calmodulin (CaM), the ancient Ca^{2+}-binding protein responsible for regulating several cellular processes, including muscle contraction and neurotransmitter release (Phelps et al. 2010; Shi et al. 2013). CaM interacts with the ARD (N-terminal ankyrin repeat domain) region of TRPV3 (Phelps et al. 2010; Shi et al. 2013). This interaction may help regulate TRPV3 activity in response to changes in intracellular Ca^{2+}-levels (Beiying et al. 2011). Another Ca^{2+}-binding protein, S100A4, interacts with TRPV3, which is critical in cell proliferation and progression (Deng et al. 2021).

TRPV3 is expressed in sensory neurons and has been shown to interact with the EP3 subtype of the prostaglandin E2 receptor in these cells (Huang et al. 2008). Prostaglandin E2 (PGE2) can cause thermal and mechanical hypersensitivity by binding to G protein-coupled EP receptors in sensory neurons (Huang et al. 2008). In conclusion, the interactions of TRPV3 with various proteins indicate its involvement in complex and diverse physiological processes tightly regulated by intracellular signalling pathways.

1.7.2.2 TRPV4 interaction with different proteins

TRPV4 interacts with different cellular proteins to carry out different cellular functions. That includes as diverse as cytoskeletal proteins, membrane proteins, mitochondrial proteins, nociceptive molecules, Ca^{2+}-sensor proteins and different Kinases.

Previously, it has been shown that the CamKII-ASK1 pathway can regulate the activation of TRPV4 (Yip et al. 2008). Later on, CamKII has been reported to bind TRPV4 (Goswami et al. 2010). In case of TRPV4 variant (R269C, gain-of-function mutation), this can cause an increase in intracellular Ca^{2+}-levels through a mechanism that involves CamKII (Woolums et al. 2020). Essentially, CamKII plays a role in modulating the function of TRPV4, and this interaction can lead to changes in Ca^{2+}-signaling within cells (Goswami et al. 2010).

The regulation of Ca^{2+}-homeostasis involves the participation of Neuronal Ca^{2+}-sensor 1 (NCS1), a protein that binds Ca^{2+}, and TRPV4 in the plasma membrane. These two proteins affect the Ca^{2+}-signaling pathway and play important roles in maintaining Ca^{2+} within cells (Sanchez and Ehrlich. 2021). Other than this, TRPV4 localizes to the microtubule and actin-enriched region and interacts with both, which leads to stabilising the growth cone in the F11 cells (Goswami et al. 2010).

Endoplasmic reticulum-mitochondrial contact points for Ca^{2+}-buffering are facilitated by TRPV4 through its interaction with MFN1 and MFN2, mitochondrial fission-fusion regulatory factors (Acharya et al. 2022).

TRPV4 also interacts with mitochondrial protein like cytochrome C which might be relevant for TRPV4-induced channelopathy. Cytochrome C interacts with TRPV4 (592-630 of TRPV4) in a Ca^{2+} as well as other metal ion-sensitive manner (Das et al. 2022). TRPV4 interacts with different kinases, such as Src kinases (SH2 domain) and it regulates the TRPV4 functions through tyrosine phosphorylation at tyr-253 residue (Xu et al. 2003). Another kinase named PKC (protein kinase C) interacts with TRPV4 and this interaction is essential for its functions. Both the PKC and AKAP150 (arterial myocytes the anchoring protein) were required for AngII-induced (angiotensin II) increases in TRPV4 channels activity (Mercado et al. 2014). It has been recently identified that TRPV4 interact with RhoA (GTpase) which is regulated by Ca^{2+}-influx (Mccray et al. 2021; Bagnell et al. 2022).

These protein interactions highlight the diverse network of regulatory mechanisms that influence TRPV4 function. These also provide insights into the intricate modulation of TRPV4 and its implications in cellular processes and signaling pathways.

1.7.3 Cellular and molecular regulation of TRPV3 and TRPV4

1.7.3.1 Cellular and molecular regulation of TRPV3

The molecular regulation of TRPV3 involves multiple factors that control its expression, activation, and desensitization. Key aspects of TRPV3 regulation include transcriptional control, post-transcriptional modifications, post-translational modifications, intracellular signaling pathways, modulation by ligands, and protein-protein interactions. Transcription factors such as CREB, NFAT, and PPARγ regulate TRPV3 gene expression by binding to its promoter region (Luo et al. 2012; Zhang et al. 2018; Hotta et al. 2010). TRPV3 activation aggravated in pathological condition like cardiac hypertrophy through calcineurin/NFATc3 pathway in rats (Zhang et al. 2018).

TRPV3 mRNA undergoes post-transcriptional modifications like alternative splicing and RNA editing, leading to the generation of different isoforms with distinct properties (which can be either gain-of-function or loss-of-function) (Donaldson and Beazley-Long. 2016). Post-translational modifications, such as phosphorylation by kinases like PKC, PKA, and CaMKII, as well as palmitoylation and glycosylation, impact TRPV3 mostly by activating (potentiate) the channel activity (Karttunen et al. 2015; Mickle et al. 2015). One study indicates that EGFR's sensitizing impact on TRPV3 is mediated by ERK, leading to the phosphorylation of TRPV3. The key site for ERK-dependent modulation is Thr^{264}, the residue located in the N-terminal ankyrin repeat domain and close to a critical region involved in TRPV3 function. In essence, Thr^{264} serves as the pivotal ERK-phosphorylation site responsible for the EGFR-induced

sensitization of TRPV3, promoting signaling pathways crucial for skin homeostasis (Vyklicka et al. 2017).

Intracellular signaling pathways involving GPCRs, RTKs, PLC, PKC, and PI_3K influence TRPV3 activation and sensitization. Protein-protein interactions with heat shock proteins, calmodulin, and 14-3-3 proteins affect TRPV3 trafficking, stability, and channel activity (Park et al. 2017; Wang and Wang. 2017).

Involvement of TRP channels and GPCRs in the transmission of itch sensations has been established. Notably, patients with *Olmsted syndrome*, marked by severe itching have "gain-of-function" mutations in TRPV3. However, the precise mechanisms underlying itch sensation have remained unclear. Studies demonstrates that keratinocytes lacking TRPV3 hinder the functioning of protease activated receptor 2 (PAR2), leading to decreased activation of neurons and reduced scratching responses when exposed to PAR2 agonists. This may suggest the involvement of PAR2 in TRPV3-mediated signalling pathways. Additionally, TRPV3 and PAR2 were found to be elevated in skin biopsies from individuals and mice with atopic dermatitis (AD). Inhibition of these receptors mitigated itching and inflammatory reactions in mouse AD models. These findings uncover an unanticipated connection between TRPV3 and PAR2 in keratinocytes for transmitting itch signals and suggest that targeting PAR2 or TRPV3, either individually or concurrently, may offer a potential avenue for anti-itch therapy in AD (Zhao et al. 2020).

Recent studies have highlighted the significance of the TRPV3 in regulating epidermal homeostasis. TRPV3 forms a signaling complex with epidermal growth factor receptor (EGFR) in keratinocytes, and their proper signaling is crucial for maintaining skin health (Wang et al. 2021). It has been suggested that TRPV3's constitutive activity plays a role in activating EGFR-dependent signaling, creating a positive feedback loop involving the mitogen-activated protein kinase ERK. To investigate the molecular mechanism behind the increased TRPV3 activity

through EGFR activation, mutagenesis and whole-cell patch clamp experiments were performed. ERK, upon activation, mediates the sensitizing effect of EGFR on TRPV3 (Wang et al. 2021). Specifically, Thr^{264}, located in the N-terminal ankyrin repeat domain of TRPV3, has been identified as the critical site for ERK-mediated modulation of the channel's activity (Wang et al. 2021). Notably, this phosphorylation site is situated near a functionally significant region of TRPV3 (Wang et al. 2021). This study highlights the role of Thr^{264} as a key phosphorylation site in TRPV3, which is involved in EGFR-induced sensitization of the channel, thereby influencing signaling pathways crucial for maintaining skin homeostasis (Cheng et al. 2010; Vyklicka et al. 2017).

1.7.3.2 Cellular and molecular regulation of TRPV4

TRPV4 can be regulated by various processes which are described below.

1.7.3.2.1 Transcriptional control: TRPV4 gene expression is influenced by specific transcription factors such as Sp1, NF-κB, and AP-1, which binds to the TRPV4 promoter and regulate its transcription (Woods et al. 2021). This has been shown by using cell-lines from mouse, bovine and human origin.

1.7.3.2.2 Post-transcriptional modifications: TRPV4 mRNA undergoes post-transcriptional modifications like alternative-splicing and RNA-editing, leading to the generation of distinct isoforms. These modifications can impact the channel's function (mostly gain of channel activity) and localization within different tissues and cell types (Arniges et al. 2006).

1.7.3.2.3 Post-translational modifications: TRPV4 activity is subject to various post-translational modifications. Phosphorylation by protein kinases (such as PKA, PKC, and PKG) can modulate TRPV4 sensitivity (more sensitization) and functionality. Additionally, modifications like ubiquitination, N-linked glycosylation (N651) and sumoylation have also been implicated in TRPV4 regulation (influence membrane trafficking, channel activity).

Phosphorylation of Y-253 (which is SRC family kinase-dependent), alters it's the response of TRPV4 to hypotonic stress (Liao et al. 2020; Xu et al. 2003; Xu et al. 2006).

1.7.3.2.4 Intracellular signaling pathways: TRPV4 can be regulated through intracellular signaling cascades involving molecules like PLC, IP_3, and CaMKs. These pathways contribute to TRPV4 activation and sensitization (Zhang et al. 2022; Woolums et al. 2020).

1.7.3.2.5 Modulators and ligands: TRPV4 can be activated or influenced by a variety of ligands, that are either endogenous and exogenous in sources. Endogenous molecules such as arachidonic acid metabolites, ATP, cholesterol, even steroids and cytoskeletal elements can modulate TRPV4 activity (Landoure et al. 2010; Watanabe et al. 2003; Das and Goswami. 2019; Dubey et al. 2023). Exogenous compounds like phorbol esters, GSK1016790A, and 4αPDD act as known agonists of TRPV4 (Fabien et al. 2009; Baratchi et al. 2019; Vincent and Duncton. 2011; Rosenbaum et al. 2020).

TRPV4 can be activated by phorbol esters which are known as potent activators. This activation occurs through the activation of protein kinase C which enhances the sensitization of channels (Watanabe et al. 2002). GSK1016790A is a selective agonist of TRPV4 (IC50 value of GSK1016790A for TRPV4 channel activation is 8.7) and is widely employed to study the physiological functions of TRPV4 both in laboratory settings and in living organisms. Additionally, 4αPDD, a non-protein kinase C–activating phorbol ester, can stimulate TRPV4 directly by binding to the channel itself (Gao et al. 2003; Vriens et al. 2004). PIP_2 also have the ability to modulate TRPV4 activity by binding to the specific sites of TRPV4 (Cao et al. 2018; Garcia-Elias et al. 2013; Pizzoni et al. 2021; Goswami et al. 2010). Binding of all these factors trigger conformational changes, leading to the opening of TRPV4 and subsequent influx of ions. The exploration of these modulators of TRPV4 activity is of great importance in scientific research, as it holds the potential to uncover valuable insights into the normal and abnormal functions of TRPV4.

1.7.3.2.6 Protein-protein interaction

Interactions with other TRP channels: TRPV4 can form hetero-tetrameric complex structures with other TRP channels like TRPV1 or TRPC1. These associations influence TRPV4's biophysical characteristics, leading to modified responses to temperature and chemicals in sensory neurons when compared to TRPV4 homo-tetrameric channels (Zergane et al. 2021).

Calmodulin (CaM): TRPV4 interacts with CaM, a Ca^{2+}-binding protein. When intracellular Ca^{2+}level increases, CaM-Ca^{2+} complex binds to TRPV4, altering its activity. This interaction sensitizes the channel and boosts Ca^{2+}–influx. Such response has roles in regulating vascular tone and blood flow in endothelial cells in response to mechanical forces (Garcia et al. 2008). TRPV4-DeltaCaM-(Delta812-831) important in physical interaction with IP3 receptor 3 and IP3-mediated sensitization. The IP_3-mediated sensitization requires IP_3 receptor binding to a TRPV4 C-terminal domain which overlaps with the calmodulin-binding site.

Cellular Adhesion Molecules: In certain conditions, TRPV4 associates with cellular adhesion molecules such as integrins. These interactions influence TRPV4's function and have significance in processes like cell migration and mechanosensation. In chondrocytes, the interaction of TRPV4 with integrins plays a role in responding to mechanical loading and maintaining cartilage homeostasis. Also, α2β1 integrin complex interacts with TRPV4 and such interaction has been implicated in mechanical transduction, development of mechanical hyperalgesia (Alessandri et al. 2008).

G Protein-Coupled Receptors (GPCRs): TRPV4 can be modulated by GPCRs through different signaling pathways. For example, upon activation of specific GPCRs (like protease-activated receptor PAR2), TRPV4 becomes sensitized. This interaction is relevant in scenarios involving inflammatory pain and heightened sensitivity to mechanical stimuli (Peng et al. 2020).

In summary, TRPV4's function is intricately regulated through diverse protein-protein interactions, allowing it to play pivotal roles in various physiological processes and sensory functions.

1.7.4 Specific activation of TRPV3 and TRPV4 in response to physical and chemical stimuli

1.7.4.1 Activation of TRPV3

TRPV3 is a receptor that can be triggered by a wide range of chemical and physical signals. There are various stimuli that have been identified to activate TRPV3 (Su et al. 2022). In terms of physical stimulation, it responds to temperatures ranging between 31°C and 39°C. TRPV3 activity can be modulated by natural compounds like carvacrol, thymol, and eugenol, which are typically found in certain plants. It also responds to monoterpenoids, which can induce a warm sensation or cause skin sensitization (Vogt-Eisele et al. 2007; Su et al. 2023). Additionally, endogenous substances such as FPP (Farnesyl pyrophosphate), which is a key substance in the isoprene pathway have been shown to activate TRPV3 (Bang et al. 2010). Another endogenous compound, i.e. nitric oxide has also been shown to activate TRPV3. Synthetic compounds like 2-Aminoethoxydiphenyl borate (2-APB) and cysteine nitrosylation activates TRPV3 (Yoshida et al. 2006). Other compounds having a similar structure to 2-APB, such as diphenylboinic anhydride (DPBA) and drofenine, are also effective TRPV3 agonists (Su et al. 2023).

The natural antagonists that act as modulators of TRPV3 include citrusinine II, Osthole, Isochlorogenic acid A and B, Forsythoside B, Pulchranin A, B, C etc. (Han et al. 2021; Neuberger et al. 2021; Qi et al. 2022). And synthetic compounds which are inhibitors of TRPV3 includes Ruthenium Red, 2,2-diphenyltetrahydro-furan (DPTHF), Dyclonine,

Ropivacaine, Mepivacaine and Bupivacaine etc. (Luo et al. 2012; Chung et al. 2012; Vennekens et al. 2012; Horishita et al. 2021).

1.7.4.2 Activation of TRPV4

TRPV4 displays responsiveness to a broad spectrum of stimuli, encompassing both physical cues like cell swelling, heat, and mechanical stimulation, as well as chemical signals such as endocannabinoids, arachidonic acid, and 4α-PDD. TRPV4 is also thermosensitive, meaning it can detect changes in temperature. It possesses a relatively wide temperature sensitivity range, with optimal activation occurring around 25-34°C. When exposed to temperatures above 27°C, TRPV4 opens, allowing Ca^{2+} ions to enter the cell. The activation of TRPV4 by swelling and endocannabinoids involves the metabolic conversion of arachidonic acid to epoxyeicosatrienoic acids (EETs) through the action of cytochrome P450 epoxygenases (Watanabe et al. 2003; Plant and Strotmann. 2007). Although the precise endogenous messenger responsible for heat-induced TRPV4 activation remains unidentified, it appears to share a common mechanism with the activation by 4α–phorbol esters (Gao et al. 2003). TRPV4 exhibits multimodal characteristics, with diverse stimuli regulating its function through various mechanisms. Various mechanical stimuli can also activate TRPV4, such as osmotic swelling, stretching, and shear stress (Vriens et al. 2004; Liedtke et al. 2003; Köhler and Hoyer. 2007). For instance, when cells experience osmotic swelling or stretching, these mechanical forces directly activate TRPV4 channels, resulting in Ca^{2+}-influx into the cell.

1.7.5 Tissue-wise distribution of TRPV3 and TRPV4 channels and its functional role

1.7.5.1 Distribution and regulations of TRPV3

TRPV3 is widely expressed across multiple tissues throughout the body, indicating its involvement in diverse physiological functions. Notably, TRPV3 exhibits prominent expression in the skin, primarily in epidermal keratinocytes, where it plays a role in temperature perception, regulation of hair growth, and maintenance of the skin barrier (Song et al. 2021). High levels of TRPV3 expression have been detected in the esophagus, suggesting its potential influence in that organ (Sulk and Steinhoff. 2014). There is moderate expression of TRPV3 (protein atlas) in the vagina implies its participation in sensory responses and potential impact on sexual function (https://www.proteinatlas.org/ENSG00000167723-TRPV3/tissue/vagina). Moderate expression of TRPV3 have been observed in the bladder, indicating its potential involvement in sensory mechanisms and urinary function (Michael et al. 2012). In the colon, TRPV3 expression has been identified in the distal colon epithelium, suggesting its contribution to sensory processes and gut function in that particular region (Ueda et al. 2009; Bischof et al. 2020). Similarly, within lung tissue, TRPV3 exhibits moderate expression levels, potentially influencing respiratory physiology and sensory responses within the airways (Zhang et al. 2018). The presence of TRPV3 in the corneal epithelial cells of the eye suggests its possible role in corneal sensation and ocular surface health (Yamada et al. 2010). Furthermore, TRPV3 expression has been detected in cardiac muscle cells, indicating its potential contribution to cardiac electrophysiology and contractile function (Liu et al. 2018). Additionally, TRPV3 has been found to be expressed in various cancer types, such as in breast cancer, lung cancer (Li et al. 2016), colorectal cancer (Yu et al. 2022) and prostate cancer (Jariwala et al. 2007), emphasizing its potential involvement in cancer biology. The diverse tissue expression of TRPV3 provides valuable insights into its physiological functions and its potential implications in pathological conditions (Neuberger et al. 2021).

1.7.5.2 Distribution and regulations of TRPV4

TRPV4 exhibits widespread distribution across multiple tissues in the human body, fulfilling diverse physiological roles. Below is the description of distribution of TRPV4 in various tissues which includes as follows:

a) Nervous system: TRPV4 is present in the central nervous system (CNS), encompassing the brain and spinal cord (Li et al. 2013). Their expression within sensory processing regions, like the dorsal root ganglia (DRG) neurons, enables the transmission of sensory information from the periphery to the CNS (Kumar et al. 2018). TRPV4 is also found in the peripheral nervous system (PNS), including sensory nerve fibers and autonomic neurons (Spekker et al. 2022).

b) Sensory organs: TRPV4 is expressed in sensory organs such as in the skin, eyes, and inner ear. Within the skin, they localize to sensory nerve endings, facilitating the detection of temperature, mechanical stimuli, and chemical signals (Suzuki et al. 2003). In the eyes, TRPV4 is found in the cornea and retina, regulating corneal sensitivity and retinal function (Lapajne et al. 2022). The cochlea and vestibular system of the inner ear also house TRPV4, contributing to auditory and balance functions (Wang et al. 2019).

c) Musculoskeletal system: TRPV4 is distributed in various musculoskeletal tissues. It is present in skeletal muscle fibers, impacting muscle contractility and metabolism (Kumar et al. 2018). TRPV4 is also found in bone cells, including osteoblasts and osteoclasts, where it plays a role in bone remodeling and mineralization (Cao et al. 2019). Additionally, expression of TRPV4 in cartilage influences chondrocyte function (Gao et al. 2022).

d) Cardiovascular system: TRPV4 is expressed in endothelial cells lining blood vessels, actively involved in the regulation of vascular tone and blood flow. Smooth muscle cells within blood vessels also harbour TRPV4, contributing to vasodilation and contraction processes (Chen et al. 2021).

e) Respiratory system: Within the respiratory system, TRPV4 is present in airway epithelial cells, participating in the modulation of airway tone and mucus production (Rajan et al. 2021). These are also expressed in sensory nerve fibers, facilitating the detection of irritants and triggering the cough reflex (Ludbrook et al. 2021).

f) Urinary system: TRPV4 plays a role in the urinary system, specifically in the bladder, where it contributes to the bladder sensation and contractility. Furthermore, TRPV4 is found in the kidney, including renal tubules and collecting ducts, aiding in the regulation of fluid balance and renal function (Perkins et al. 2022).

g) Gastrointestinal system: TRPV4 is distributed throughout the gastrointestinal tract, encompassing the stomach and intestines. These play a role in regulating gastrointestinal motility, secretion, and sensation (Matsumoto et al. 2019).

i) Other tissues: TRPV4 has been identified in various other tissues, including the liver, pancreas, adipose tissue, and reproductive organs (Zhan and Jun. 2018; Swain et al. 2020; Hu et al. 2023). In these contexts, TRPV4 contributes to a range of functions, including metabolism, inflammation, and sensory processes (Dutta et al. 2020).

1.7.6. Different physiological functions of TRPV3 and TRPV4 channels

1.7.6.1 Physiological functions of TRPV3

TRPV3 plays a crucial role in maintaining normal physiological functions and have been implicated in temperature and pain perception. Furthermore, TRPV3 is involved in the development of skin and hair (Song et al. 2021). In mice, mutations in the TRPV3 gene result in hair loss, suggesting its participation in hair growth (Song et al. 2021). TRPV3 is expressed in specific subsets of sensory neurons in human that ends in the skin and are responsive to detect warm temperatures (Marics et al. 2014). Notably, mutations in the TRPV3 gene have been observed to cause hair loss in mice too, suggesting its involvement in hair growth. In rats,

TRPV3 is found to modulate nociceptive signaling both in peripheral areas and in supraspinal sites (McGaraughty et al. 2017). Specifically, TRPV3 is involved in temperature perception, particularly the detection of warm temperatures. Activation of TRPV3 occurs when exposed to temperatures between 34 and 39°C (Peier et al. 2002a; Xu et al. 2002).

TRPV3 also contributes to the regulation of blood vessel diameter, particularly in response to heat-induced local vasodilation (Fromy et al. 2018; Singh et al. 2019). TRPV3 is present in the cutaneous region is responsible for initiating this vasoregulatory response by triggering the release of calcitonin gene-related peptide (CGRP) at the local level (Fromy et al. 2018). Disruption of TRPV3 function hinders heat-induced vasodilation and thermoregulation, highlighting the crucial involvement of CGRP in this process. Natural compounds such as carvacrol, thymol, and eugenol directly activate TRPV3, which can lead to specific desensitization of the channels in a Ca^{2+}-independent manner (Fromy et al. 2018). In rats, TRPV3 appears to participate in nociceptive signaling in both peripheral and supraspinal locations (McGaraughty et al. 2017). Overall TRPV3 plays crucial role in regulating different cellular function and in localized tissue.

1.7.6.2 Physiological functions of TRPV4

TRPV4 is engaged in various physiological functions within the body, which comprises as follows:

a) Vasoregulation: TRPV4 contributes to the dilation of local blood vessels in response to heat (Farley et al. 2009). Specifically, cutaneous TRPV4 channels initiate this vasoregulatory response by triggering the calcitonin gene-related peptide (CGRP) release (Filosa et al. 2013). Disruption of TRPV4 function leads to impaired heat-induced vasodilation and thermoregulation, underscoring the critical involvement of CGRP in this process.

b) Bladder physiology and dysfunction: TRPV4 plays a sensory role in the uroepithelium, influencing the release of sensory mediators like ATP, which in turn modulates nerve activity

in response to bladder filling during the urination cycle (Roberts et al. 2020). Accordingly, TRPV4 knockout animals have problems with frequent urination (Tomilin et al. 2019). TRPV4 channels may also directly impact detrusor contractility and urothelial barrier function. Altered expression of TRPV4 has been observed in various pathological bladder conditions.

c) Cardiac function: TRPV4 channels play a role in the development of myocardial infarction and contribute to the cardiac tolerance during ischemia/reperfusion (Goyal et al. 2019). Activation of TRPV4 negatively affects the stability of cardiomyocytes under hypoxia/reoxygenation conditions (Wu et al. 2017). Precise and controlled blocking of TRPV4 may represent a new approach for preventing ischemia/reperfusion injury to the heart.

d) Sensory Transduction: TRPV4 can be activated by different stimuli, including mechanical, thermal, and chemical cues. They participate in sensory transduction, particularly in the uroepithelium, where they are involved in mechanosensation and the development of voiding disorders (Merrill et al. 2014). TRPV4 also contributes to the generation of electrical signals in the nervous and muscular systems (Evangelista et al. 2015).

TRPV4 exhibits a multimodal nature, regulated by various stimuli, suggesting a complex array of mechanisms governing their functions. Ongoing research attempts to understand the cellular pathways that involve TRPV4.

1.7.7 Inflammatory functions of TRPV3 and TRPV4 ion channels

Understanding the functions of TRPV3 and TRPV4 channels in pain perception, thermal sensation, and various pathophysiological conditions is crucial for developing targeted therapeutic approaches to alleviate pain, manage thermal sensitivity, and address associated disorders (Su et al. 2023; Um et al. 2023; Huang et al. 2011). Here some of these issues are discussed.

1.7.7.1 Inflammatory functions of TRPV3

Activation of TRPV3 contributes to the development of skin diseases by triggering a strong proinflammatory response through the NF-κB pathway. TRPV3 is functionally expressed in human epidermal keratinocytes and have been implicated in cutaneous inflammatory processes (Attila et al. 2018). Additionally, downstream elements of the inflammatory cascade, along with endogenous ligands like arachidonic acid and protein kinase C (PKC), can sensitize or activate TRPV3 (Hu et al. 2006). Inhibition of TRPV3 has shown promising results in treating inflammatory dorsal skin conditions, demonstrating a dose-dependent effect (Qu et al. 2019).

Furthermore, excessive expression of TRPV3 has been associated with hair loss, skin inflammation, severe pruritus, and dermatitis (Um et al. 2022). TRPV3 plays a critical role in various aspects of skin physiology, including skin barrier formation, hair growth, wound healing, and itching (Um et al. 2022). All these highlight the importance of TRPV3 in maintaining healthy skin function. Also, when the body sustains an injury from external factors, the damaged tissue site triggers the release of various substances such as prostaglandin E2 (PGE2), ATP, nitric oxide (NO), interleukin 1α (Il-1α), TGF-β, among others. These substances sensitize the sensory nerve endings within the skin, leading to the transmission of signals that result in specific physiological responses. Within keratinocytes, TRPV3 plays a role in facilitating the release of prostaglandins in response to heat stimulation. This influence on prostaglandin release by TRPV3 has implications for both acute pain perception and heightened sensitivity to pain (hyperalgesia), supporting the idea that keratinocytes can actively contribute to sensory functions (Huang et al. 2008; Miyamoto et al. 2011).

Given its involvement in skin diseases and related symptoms, TRPV3 has emerged as a potential therapeutic target for itching and other skin-related disorders (Um et al. 2022). Although the precise mechanisms underlying TRPV3 activation and its contribution to skin

diseases are still under investigation, it is evident that TRPV3 plays a significant role in cutaneous inflammatory processes. This knowledge opens up possibilities for developing targeted interventions and treatments for skin diseases by modulating TRPV3 activity.

In summary, the research suggests that TRPV3 is involved in inflammatory functions and have broad implications in skin physiology and other physiological processes. Further investigations are needed to fully understand the mechanisms underlying TRPV3-mediated inflammation and its potential as a therapeutic target in inflammatory diseases (Szöllősi et al. 2018; Su et al. 2023; Um et al. 2022).

1.7.7.2 Inflammatory functions of TRPV4

TRPV4 has been implicated in inflammatory functions within the body. Here are some examples of key regulation of the inflammatory functions of TRPV4.

a) Regulation of inflammatory responses: TRPV4 may have a critical role in regulating various inflammatory responses, including cytokine production, foam cell formation, and giant cell formation (Goswami et al. 2017). This suggests that TRPV4 is involved in modulating the immune and inflammatory processes.

b) Activations by inflammatory mediators: TRPV4 plays a role in inflammation as it can be activated by inflammatory mediators. Different inflammatory mediators, such as arachidonic acid metabolites, Prostaglandin E2 (PGE2) and histamine, as well as receptors involved in inflammation like protease-activated receptor-2 (PAR2), have been shown to activate or sensitize TRPV4. This indicates the involvement of TRPV4 in inflammation, most-likely also as a part of feedback loop that amplifies inflammatory signals (Watanabe et al. 2003; Alessandri-Haber et al. 2003; Grant et al. 2007; Cenac et al. 2010; Yang et al. 2007).

c) Dual role in inflammation: While TRPV4 activity has generally been associated with pro-inflammatory effects, emerging evidence suggests a more complex role where this channel may

also have anti-inflammatory effects (Dutta et al. 2020). The activation of TRPV4 leads to the release of cytokines such as IL2, IL-6, IL-8, IL-1α and IFNγ (Majhi et al. 2015). TRPV4 activation can also promote the production of anti-inflammatory cytokines, such as IL-10, which enhance the phagocytic activity of macrophages. This shows both of the anti and pro inflammatory role of TRPV4 (Rosenbaum et al. 2020). This highlights the need for further research to understand the intricate mechanisms of TRPV4 in inflammation (Vincent et al. 2011; Nguyen et al. 2022; Acharya et al. 2022).

d) Therapeutic Potential: TRPV4 is considered a potential therapeutic target for inflammatory diseases. Antagonizing TRPV4 is being explored for therapeutic purposes in various areas, such as bone control and inflammation. For example, activation of TRPV4 results in enhanced bio-mineralization by the osteoblasts (Acharya et al. 2023). Targeting TRPV4 could provide new avenues for managing inflammatory conditions (Ye et al. 2023; Dutta et al. 2020).

e) Regulation of cytokine production: TRPV4 regulates cytokine production in macrophages, immune cells that play a crucial role in inflammation (Luo et al. 2017). TRPV4 plays a significant role in multiple biological processes, including the formation of foam cells containing lipid-laden macrophages. Additionally, it is involved in regulating the production of cytokines when human gingival fibroblasts are exposed to lipopolysaccharide from *Porphyromonas gingivalis*. Furthermore, TRPV4 is also linked to the regulation of cytokines in the context of adipose oxidative metabolism (Luo et al. 2017).

The precise mechanisms by which TRPV4 regulates cytokine production are still under investigation. However, it is evident that TRPV4 plays a role in this process and have the potential to be targeted for therapeutic interventions in inflammatory diseases. Further research is needed to fully elucidate the underlying mechanisms and exploit the therapeutic potential of TRPV4 modulation.

1.7.8 The importance of TRPV3 and TRPV4 channels in pain and other pathophysiology

TRPV3 and TRPV4 channels are integral to pain perception and both these two channels contribute to a range of pathophysiological conditions. Both are present in sensory neurons, where these channels are involved in detecting and transmitting pain signals in response to stimuli-like heat, pressure, and chemicals (González-Ramírez et al. 2017).

1.7.8.1 TRPV3 and pathophysiology

In the skin, the TRPV3 is associated with various disorders. Mutations in the TRPV3 gene can lead to channelopathies, such as *Olmsted syndrome* and *erythromelalgia*, characterised by pain, inflammation, and dermatological symptoms.

Since TRPV3 plays an indispensable role in the generation of pain, the research on TRPV3 in early studies mainly focused on pain sensation and thermal sensation. Some of the studies on physiological functions having been conducted, TRPV3 has been found to be associated with a variety of diseases (**Table 4**) (Su et al. 2023).

1.7.8.2 TRPV4 and pathophysiology

TRPV4 plays a crucial role in various physiological processes. Accordingly, dysregulation or dysfunction of TRPV4 has been implicated in several pathological conditions. Here are some examples:

a) Gain-of-function mutations: Rare genetic disorder (missense mutation) known as brychyolmia (BCYM3; 113500) identified by Rock et al, in 2008. They found that when the R616Q mutation (605427.0001) was expressed in human embryonic kidney cells, it resulted in a significantly larger constitutive current even before agonist application. Importantly, the overall characteristics of the current, including the shape of the IV curve and reversal potentials, remained unchanged. The study also revealed a similar pattern for the V620I

Table 4:

Diseases	Research Evidence
Olmsted syndrome (OS)	A series of independent clinical reports are identified mutations in the TRPV3 gene as the cause of Olmsted's syndrome.
Pruritic and atopic dermatitis (AD)	**1**. The expression of TRPV3 is significantly increased in skin lesions and non-diseased skin of patients with specific dermatitis. **2**. The pharmacological activation of TRPV3 leads to the development of AD in wild-type mice, and it has no effect on TRPV3 knockout mice. 3. The inhibition of TRPV3 treats inflammatory dorsal skin in a dose-dependent manner.
Psoriasis	**1.** The expression level of TRPV3 in psoriasis patients is significantly higher than it is in people without psoriasis. **2**. TRPV3 antagonists relieve the symptoms in patients with moderate-to-severe psoriasis in a dose-dependent manner.
Cutaneous pruritus	**1**. TRPV3 knockout mice show no increase in scratching behavior after itch modeling. **2**. The expression of TRPV3 is significantly up-regulated in the epidermis of patients with pruritus after having been burnt.
Rosacea	TRPV3 gene expression is significantly increased in rosacea.
Cancer	**1**. TRPV3 expression is increased in pancreatic, bone, breast, lung and oral squamous cell cancers. **2**. TRPV3 expression is decreased in colorectal cancer.
Myocardial hypertrophy	**1.** The expression of TRPV3 is increased in pathological cardiac hypertrophy. **2**. TRPV3 expression is increased in cardiomyocyte hypertrophy induced by Ang-II in vitro. **3**. TRPV3 inhibitors can significantly aggravate cardiomyocyte hypertrophy and TRPV3 antagonists can slow cardiomyocyte hypertrophy.
Cardiac fibrosis	TRPV3 activation exacerbate cardiac dysfunction and interstitial fibrosis in pressure-overloaded rats.
Myocardial infarction	The expression of TRPV3 is significantly up-regulated in neonatal rat cardiomyocytes after myocardial infarction and in hypoxia-treated rats.
Pain	TRPV3 is overexpressed in skin pain, breast pain, cancer pain and other pain-experiencing tissues.
Alopecia	TRPV3 agonists inhibit hair growth, whereas TRPV3 inhibitors significantly reverse the symptom.

Table 4: TRPV3 and channelopathy. This table taken from Su, et al. 2023

Table 5:

Naturally occurring TRPV3 mutations	References
G573S	Lin et al. 2012
G573C	Lin et al. 2012
G573A	Danso et al. 2013
G568C	Duchatelet et al. 2014
G568V	Choi et al. 2018
G568D	Peters et al. 2020
W692G	Kariminejad et al. 2014
Q216_G262del	Duchatelet et al. 2014
Q580P	He et al. 2014
L673F	Duchatelet and Alain. 2014a
W521S	Mevorah et al. 2005

Table 5: The updated list of TRPV3 mutations causing *Olmsted syndrome*.

mutation (605427.0002), albeit with a somewhat smaller increase in constitutive current compared to the R616Q mutation (Rock et al. 2008).

b) Hereditary Diseases: Mutations in the TRPV4 gene have been linked to hereditary diseases such as Charcot-Marie-Tooth disease type 2C (CMT2C) and scapuloperoneal spinal muscular atrophy (SPSMA). These conditions are characterized by muscle weakness, sensory impairments, and dysfunction of motor neurons (Chen et al. 2023).

c) Osteoarthritis: TRPV4 is expressed in chondrocytes, which are responsible for maintaining cartilage integrity in joints. In case of osteoarthritis, there is evidence of increased TRPV4 activity, leading to excessive Ca^{2+}-influx and activation of downstream signaling pathways that promote cartilage degradation and inflammation. Targeting TRPV4 has been suggested as a potential therapeutic approach for osteoarthritis (Phan et al. 2009; Leddy et al. 2014).

d) Pulmonary Diseases: TRPV4 is expressed in lung epithelial cells and smooth muscle cells. Increased TRPV4 activity has been observed in conditions such as acute lung injury (ALI) and acute respiratory distress syndrome (ARDS) (Sonkusare et al. 2022). This heightened activity contributes to the formation of pulmonary edema, inflammation, and impaired lung function (Hamacher et al. 2023). Inhibition of TRPV4 has shown promise in preclinical models as a potential therapeutic strategy for these lung diseases.

e) Neurological disorders: TRPV4 dysfunction has been implicated in various neurological disorders, including hereditary spastic paraplegia (HSP) and neuropathic pain (Gizem et al. 2021). Mutations in the TRPV4 gene can lead to neurodegeneration and impaired axonal transport in HSP (Elyette et al. 2023). In the case of neuropathic pain, TRPV4 activation in sensory neurons can contribute to the development and maintenance of chronic pain states (Rodrigues et al. 2023). Dysfunction of TRPV4 can give rise to a range of disorders encompassing genetic skeletal and neuromuscular conditions (Andreucci et al. 2011). Additionally, TRPV4 is involved in processes such as endoplasmic reticulum (ER) stress and

inflammation, which have implications for Parkinson's disease (Liu et al. 2022). It also acts as a regulator of adipose oxidative metabolism, inflammation, and energy homeostasis. TRPV4's involvement extends to skeletal dysplasias and peripheral nervous system disorders in terms of pathogenesis (Filosa et al. 2013).

f) Vascular Diseases: TRPV4 is expressed in endothelial cells and smooth muscle cells of blood vessels (Chaigne et al. 2023). Dysregulation of TRPV4 has been implicated in endothelial dysfunction, hypertension, and vascular remodelling (Gizem et al. 2021). TRPV4-mediated Ca^{2+}-influx and subsequent activation of signaling pathways can influence vascular tone, permeability, and inflammatory responses in blood vessels (Gizem et al. 2021; Liu et al. 2022; Ye et al. 2023; Evangelista et al. 2015; Nguyen et al. 2023).

1.8 Specific objectives and aim of this study

This thesis aims to characterize the functionality of two thermosensitive ion channels i.e. TRPV3 and TRPV4 and investigated these channel-mediated functions in the context of sub-cellular organellar specific functions. The subcellular organelles include lysosomes, mitochondria and nucleus. Both these channels are activated at the range of physiological temperature, i.e. at 33-39°C. Both these channels are non-selective in nature, sensitive to noxious heat stimuli and are permeable Ca^{2+}-influx. Both of these channels are presents ubiquitously in many tissue and organ systems. Notably certain TRPs with point mutations results in complex disorders and diseases with numerous manifestations, commonly termed as ‘‘Channelopathies’’. In this context, TRPV3 is very important, as it is associated with various pathophysiology that includes cancer, cardiovascular diseases and skin pathology. TRPV3 overexpression is also associated with various pain pathophysiology that includes skin pain, cancer pain, breast pain and others pain tissues (Su et al. 2023; Huang et al. 2008; Aouizerat et al. 2011; Gopinath et al. 2005). Mutations in TRPV3 is associated with a rare genetic disorder named Olmsted syndrome (*OS*). In this context, the cellular basis of *OS* causing mutants (G573C, G573A, G573S, G568C, G568D, and W692G) have been explored to understand the severity of these mutants. TRPV4 is also associated with various life-threatening diseases due to its point mutations with different penetration level. Mutations in TRPV4 is associated with range of disorders that include skeletal displasia, osteoarthritis, defective neurological motor functions and more. In this context both TRPV3 and TRPV4 are pathophysiologically very important for the investigations of intracellular functions related to various cellular stress. The sub-cellular organelle functions associated with TRP channels have are not yet explored (Dong et al. 2010). So, in this thesis, intracellular organelle functions associated with TRPV3 and TRPV4 have been explored.

TRP channel-mediated functions are -associated with tissue injury and inflammations. Thermal, mechanical and chemical stimuli play role in the underlying tissue injury or inflammations. In this thesis work proinflammatory and anti-inflammatory role of TRPV3 and TRPV4 has been explored. The expression of TRPV3 and TRPV4 in the immune cells and its relations to immune functions has been investigated. The presence of TRPV3 and TRPV4 in the intracellular compartments like lysosome, and specific functions like phagocytosis, bacterial clearance, wound healing, inflammation-associated with skin and immune cells has been explored.

This study focused on exploring how TRPV3 and TRPV4 respond to different types of stress like heat, toxins, infections (*in vivo* and *in vitro*). These molecules play a role in how cells react to stress, leading to changes in cell behaviour. Recent research indicates that parts of cells like lysosomes, mitochondria, and the outer cell layer (plasma membrane) are key players that respond to cellular stress. The thesis aimed to investigate how cells respond to different stress stimuli and how TRPV3 and TRPV4 are involved in all such effects. To address this, different microscopic methods were used to understand how cells work under stress.

The specific aims of the present studies are:

1. Understanding the tissue-specific presence and inflammatory functions of TRPV3.
2. Characterization of TRPV3 in the context of lysosomal functions in different conditions.
3. Role of TRPV3 as a cellular stress response element.
4. Characterization of nucleolar localization sequence present in TRPV3.
5. Understanding the role of TRPV3 in the regulation of intracellular organelle-specific temperature.
6. Comparatives of TRPV3 with TRPV4 in the context of inflammatory functions.

Chapter 2

Results

2.1 Understanding of the tissue-specific presence and inflammatory functions of TRPV3

TRPV3 is a tissue-specific ion channel mainly found in the skin, hair follicles, and related tissues, with a significant presence in the skin's outermost layer, i.e. in the epidermis (Szöllősi et al. 2018). Its primary role is temperature detection, particularly for warmth and heat (Chung et al. 2005). When skin temperature rises, TRPV3 becomes active, allowing ions such as Ca^{2+} and Na^{+} to enter skin cells (Mandadi et al. 2009; Schrapers et al. 2018). This activation transmits signals to the nervous systems also, notifying the brain of the warmth or heat sensation (Schrapers et al. 2018).

Beyond temperature sensing, TRPV3 also has an inflammatory function. Inflammation is the body's natural response to injury and infection, serving as a protective mechanism. When TRPV3 is activated, it can release chemical signals that promote inflammation. While inflammation is essential for healing, an overactive or chronic inflammatory response can lead to various skin conditions and diseases. Other than skin, TRPV3 is also present in the gastrointestinal tract (GI) where it can be crucial for controlling inflammatory function in the colon tissue or clearance of pathogens (Rizopoulos et al. 2018; Bischof et al. 2020). Here the inflammatory role of TRPV3 in skin tissue as well as colon tissue is discussed in elaborate way.

2.1.1 TRPV3 activation helps in reducing *Salmonella* infection in the colon

“Colitis” is a major health problem and is also called as inflammatory bowel disease/syndrome (IBD). This generally causes due to bacterial infection through food or water sources. The primary candidate for this infection or disease is the *Salmonella* strains. To understand the involvement of TRPV3 in IBD, inflammation in the gut (i.e. IBD) was introduced by *Salmonella typhimurium* infection, leading to the formation of colitis in mice. For the colitis induction, around six weeks old animals were used. Streptomycin has been used

before the induction of colitis, i.e. introducing the *Salmonella typhimurium* infection. These animals were subject to antibiotic treatment for five days and the infection were introduced through oral gavaging after the antibiotic treatment. The experimental conditions that have been used are DMSO (colitis-induced), activation of TRPV3 with Thymol and Carvacrol (natural activators), and DPTHF as TRPV3 inhibitor. All the samples (animal) were colitis-induced *Salmonella*-infected which are with or without TRPV3 modulations.

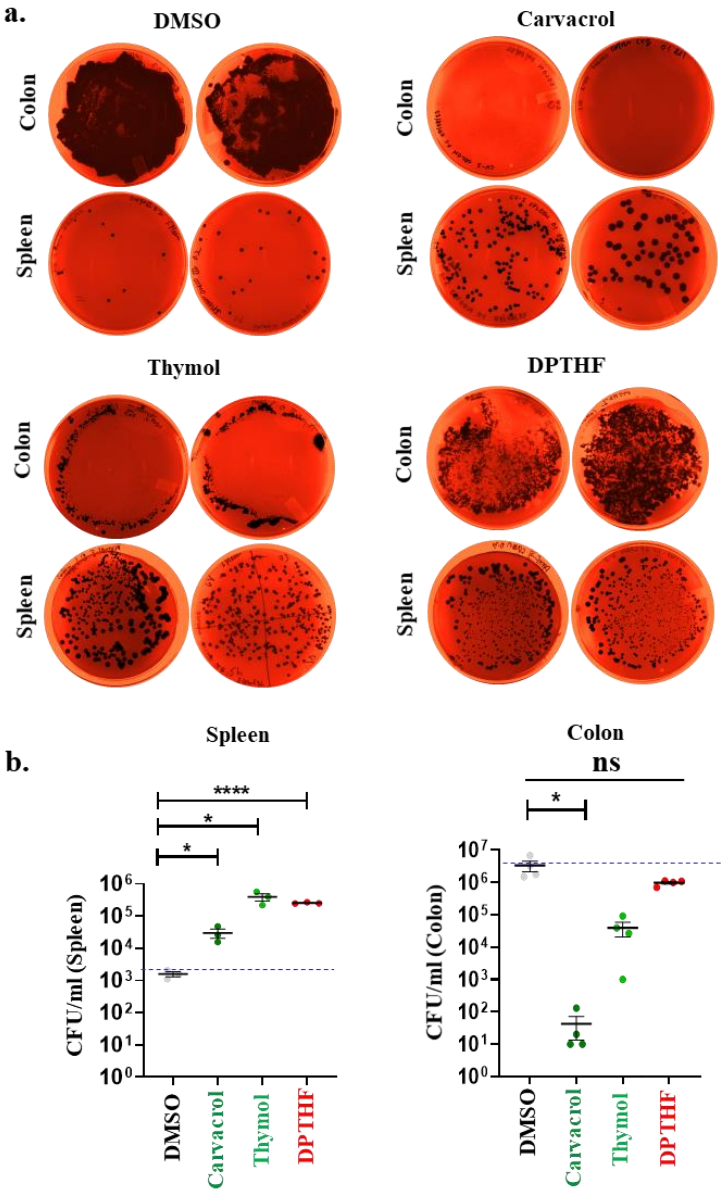

Fig 12. Colitis induction by *Salmonella typhimurium* and CFU count of colon and spleen. **a.** The figure shows the SS agar bacterial plates with *Salmonella* colonies appeared from spleen and colon tissues collected from different conditions like DMSO control, Carvacrol, Thymol and DPTHF-treatment, respectively. **b.** The DMSO (control), as well as DPTHF-treated samples, show more CFU than Carvacrol or Thymol (TRPV3 activation) condition in the colon samples (6 days). In contrast, more CFU is observed when TRPV3 is activated by Carvacrol or Thymol in the spleen sample (6 days). Unpaired t-test, * = $p \leq 0.05$, **** = $p \leq 0.0001$, ns = non-significant.

After *Salmonella* infection to the animal, the CFU counts from colon and spleen were observed. After 5th days of infection, the colon samples were collected for CFU count. The results show that the CFU has been significantly less in case of TRPV3 activation as compared to the DMSO (colitis-induced) or inhibition conditions. There is no major difference in the CFU count of the DPTHF- or vehicle control-treated conditions **(Fig. 12a-b)**.

2.1.2 TRPV3 activation helps to trap the bacteria in the spleen

The spleen has two crucial functions in protecting against bacterial infections in the bloodstream. Firstly, it acts as a phagocytic filter that eliminates bacteria from the bloodstream (Borges da Silva et al. 2015). Secondly, it produces antibodies that are essential for fighting against bacteria (Brendolan et al. 2007). Although the liver removes most of the well-opsonized bacteria, the spleen is essential in sequestering less well-opsonized bacteria, making it a vital in non-immune hosts (Bohnsack and Brown. 1986). Additionally, the spleen plays a critical role in producing opsonizing antibodies, which aid in the rapid and efficient removal of bacteria from the bloodstream. Thus, CFU in the spleen samples (after the bacterial infection has been introduced through oral gavage) in different conditions provide useful information.

As previously mentioned, the colon tissue has a smaller CFU count as compared to the vehicle control (DMSO with colitis induction), but in the spleen sample, the CFU was found to be more in case of TRPV3 activation. This indicates that upon TRPV3 activation animal able to clear the pathogen from colon, and the pathogen gets trapped in the spleen tissue. In other words, the results suggest that when the animals are exposed to the Carvacrol or Thymol, the bacteria are cleared with a better efficiency at the colon and, through the bloodstream, and got trapped at spleen. That is why the CFU is significantly increased in the spleen as compared to the control or in the inhibition conditions (**Fig. 12a-b**).

2.1.3 Physiological parameters are altered by TRPV3 modulation in colitis conditions

The loss of body weight, as well as spleen weight percentage per body weight and colon length, are important indicators for the colitis infection and inflammation. Body weight reduction has been evident in colitis infection. All these animals were subject to colitis induction and subsequently treated with TRPV3 modulators (Carvacrol, Thymol, DPTHF) or DMSO. The body weight reduction is found to be more in case of colitis control (DMSO) as well as in the DPTHF conditions (**Fig. 13a**). The mortality rate is also more in case of DMSO and DPTHF conditions (TRPV3 inhibitor) (**Fig. 13a**).

The colon length and spleen weight have also changed significantly in different treatment conditions. The average colon length in the absolute control group (without colitis induction) remains ~9.25 cm (**Fig. 13b**). However, in DMSO-treated group, (i.e. the vehicle control group with colitis) the colon length become smaller (average colon length remains ~7 cm). Thus, the colon length becomes shorter in the vehicle control group (with colitis) as compared to the absolute control condition (**Fig 13b**). In contrast, the percentage value for spleen weight per body weight is least in case of absolute control group and become more in all other groups. Notably, the spleen weight is found to be more in the vehicle control (with colitis) as compared to the absolute control condition (**Fig. 13c**). When compared with DMSO-treated samples, Thymol-treated samples show significantly low value for spleen weight (**Fig. 13d)**. In Carvacrol and DPTHF-treated conditions the spleen weight value remain almost same with the DMSO-treated conditions.

In colitis condition, the average colon length become significantly large in case of TRPV3 activation (Carvacrol =7.73, Thymol = 8.3 cm) as compared to the DMSO-treated group. In DPTHF-treated group average colon length remains ~7.46 cm (**Fig. 13e**). This indicates that in colitis condition, the colon length is compromised in DMSO as well as in DPTHF-treated conditions, but become almost normal (or not so compromised) in case of

TRPV3 activation. All these changes can be correlated with the rate of infection in all these treatment conditions.

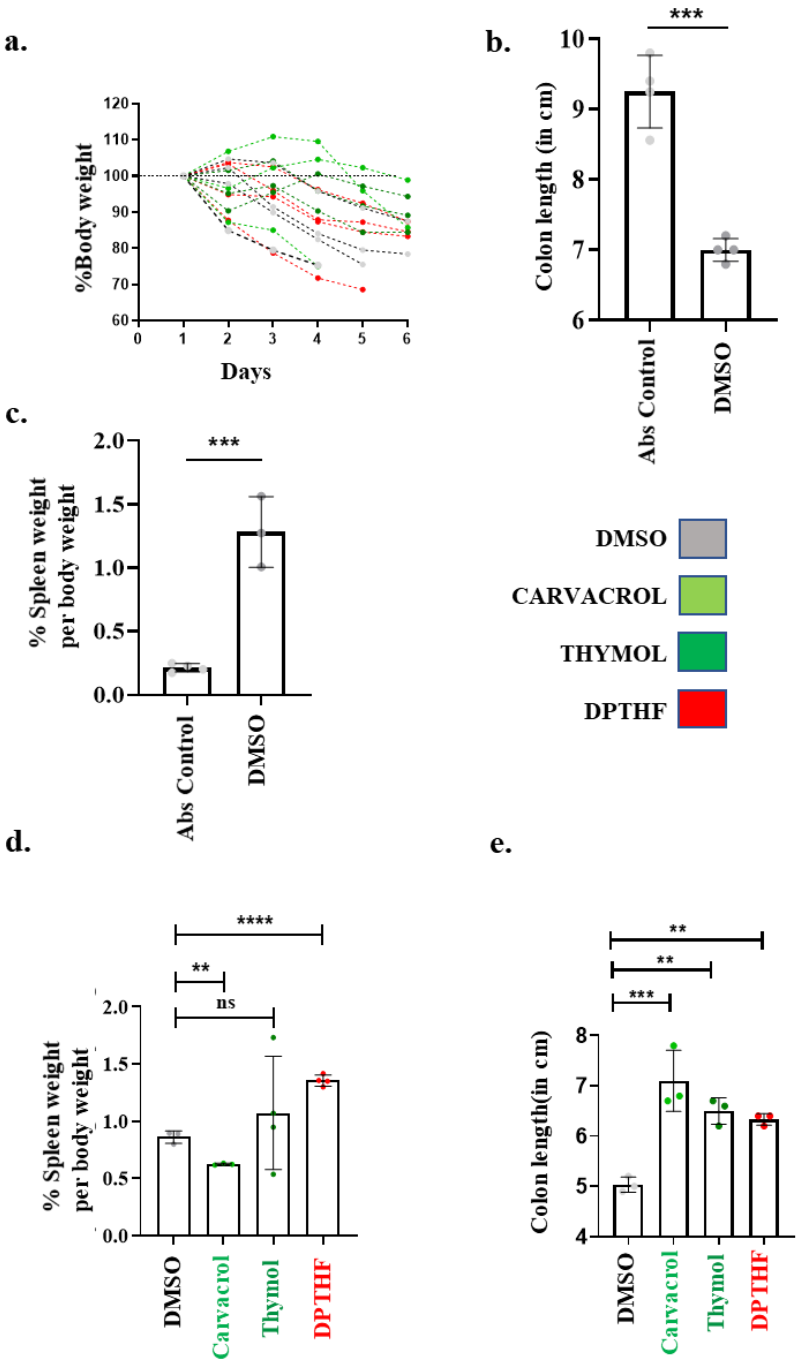

Fig 13. Physiological parameters such as body weight, spleen weight/body weight and colon length in colitis conditions are altered due to TRPV3 modulation. a. The graph shows the day-wise changes in percentage of body weight in different treatment conditions. The loss of body weight seems to be more in the colitis control and in DPTHF treatment conditions**. b.** The graph shows the colon length in cm in DMSO-treatment group (with colitis) as compared to the absolute control group. **c.** The graph shows the comparative spleen weight per body weight of the animal in absolute control group with DMSO-treated group (with colitis). **d.** The graph represents the spleen weight percentage per body weight as compared with the DMSO-treated group. In all these comparative conditions, colitis is induced. **e.** The graph represents the colon length (in cm) as compared with the DMSO-treated group. In all these comparative conditions, colitis is induced. One-way ANOVA, * = $p \leq 0.05$, ** = $p \leq 0.01$, *** = $p \leq 0.001$, **** = $p \leq 0.0001$.

And also, the mortality rate of the animal where it is found that the rate is more in the DMSO sample or DPTHF treated conditions (data not shown). All these data show the loss of body weight is less in the case of activation, and it is evident that TRPV3 activation is able to rescue (at least partially) the animal from colon infection.

2.1.2 TRPV3 in skin wound healing and bacterial clearance in the wound area

It is well known that TRPV3 is abundant in the skin and in intestine. In the skin tissue keratinocytes expresses TRPV3, and TRPV3 modulation is involved with the migration of cells required during the wound healing process (Toledo Mauriño et al. 2020). Apart from keratinocytes, there are other immune cells like macrophages which associate with the keratinocytes. So, effect of TRPV3 modulation on skin wound healing parameters were tested.

2.1.2.1 TRPV3 activation enhances skin wound healing and reduces bacterial infection

The impact of TRPV3 activation or inhibition on the skin wound healing process has been explored. For that purpose, a skin wound (5 mm) developed in mice and infected the same wound with 100µl of 1×10^8 CFU/ml MRS (*Staphylococcus aureus*) bacteria on day 1 of the wound. It was observed that topical application of TRPV3 activator FPP (2µM) daily enhances the skin wound healing by the 10^{th} day while TRPV3 inhibition (DPTHF, 200µM) does not result in enhanced healing of skin wound at the same duration (**Fig. 14a**). Subsequently, the percentage of wound healing and the rate of wound healing in different conditions were also calculated. In the TRPV3-inhibited condition (DPTHF treatment) mostly matches with control, i.e. DMSO-treated condition (**Fig. 14b**). In contrast, TRPV3 activation enahces the skin wound healing process. To confirm that the TRPV3-activation-induced enhanced skin wound healing is indeed due to TRPV3-mediated function, the bacterial numbers in the pus were counted and compared accordingly. The bacterial number present in

the unit volume (100µl) of pus (on the 10th day) becomes significantly low in case of TRPV3 activation (**Fig. 14c-d**). The bacterial number at the 4-day old wound is less in case of activation of TRPV3 than in DMSO- or DPTHF-treated condition (**Fig. 14e**). The wound healing on day 4th was not well visible in all conditions though the bacterial CFU is less in case of TRPV3 activation (**Fig. 14d**).

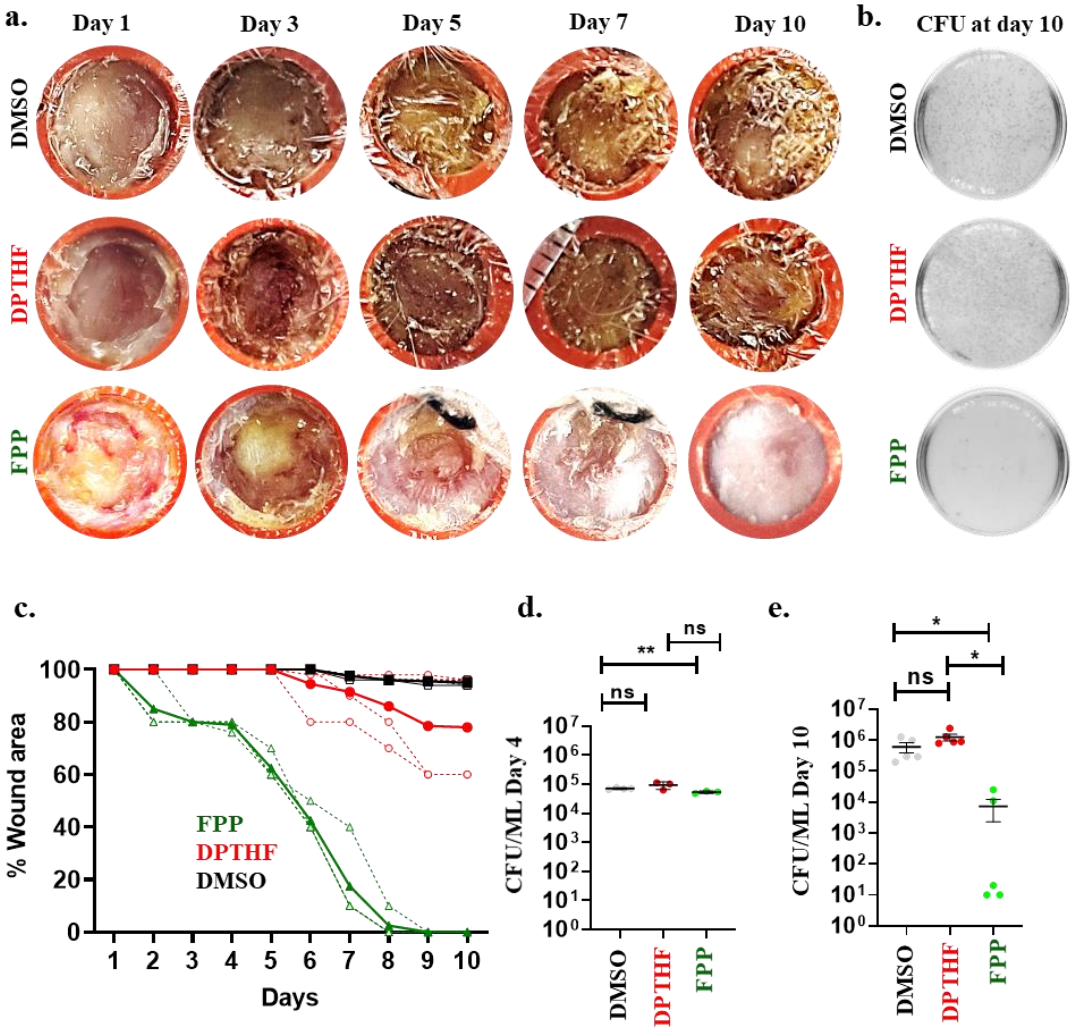

Fig 14. TRPV3 regulates skin wound healing and bacterial infection in the wound. a. Shown are the skin wounds that are infected with MRS (multidrug-resistant *Staphylococcus aureus*) bacteria followed by topical application of DMSO, TRPV3-activator (FPP, 2µM = 100µl) and Inhibitor (DPTHF, 200µM = 100µl) once per day. TRPV3 activation enhances wound healing. **b.** The percentage of wound closure on different days is shown. The thick line indicates the average values of 3 independent experiments. **c.** Topical activation of TRPV3 by FPP significantly reduces the bacterial numbers present in the pus at skin wounds on day 4th. **d-e.** Shown are the number of colonies formed from the pus [serially diluted from 1ml sample (pus + PBS)] sample on the 10th day in the plate as well as in the bacterial CFU graph. (* = p <0.05, n = 5), ** = p <0.01, n =3).

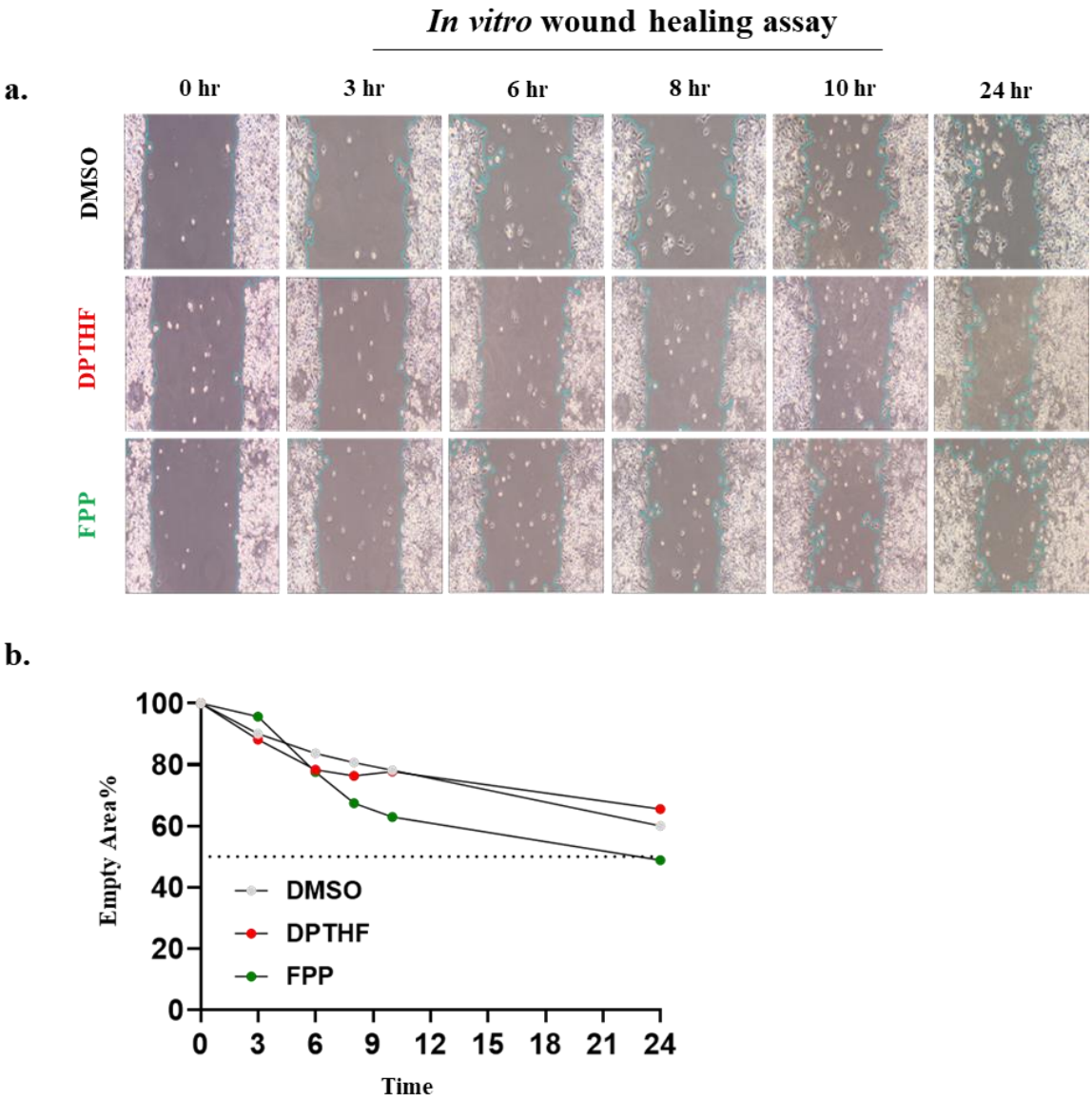

Fig 15. Regulation of *in vitro* wound healing through TRPV3 modulations. a. The figure shown here shows the *in vitro* wound healing assay in the Raw 264.7 cells. **b.** Percentage of area remain empty due to TRPV3 activation or inhibition in 24 hours are shown. The TRPV3 activation covers the empty area quickly. Average of 3 data sets are shown.

The *in vitro* wound healing in the RAW 264.7 cells shows that the percentage of area remains empty after 24 hours is less in case of activation of TRPV3 (i.e. 48.90% for FPP, 60.05% for DMSO, and 65.53% for DPTHF) (**Fig. 15a-b**). This shows that migration efficiency is more in case of activation of TRPV3.

To understand the status of the wound tissue healing process, the histochemistry of the wound tissue was analyzed on day 4^{th} and day 10^{th} (**Fig. 16**). There it is observed that the

healing was almost complete in case of TRPV3 activation on day 10th, but not so prominent on day 4th. Endogenous expression of TRPV3 in such tissues was also analyzed (**Fig. 17**). The expression of TRPV3 is observed in the wound tissue section, mainly at a low level in the keratinocytes. On the 10th day, expression of TRPV3 is observed in the tissue (in the wounded area or wound healed), especially in the keratinocytes and in the macrophages (positive for CD11b marker). TRPV3-activator treated sample has better-healed tissue with more blood vessels there. Notably, in case of TRPV3 activation, more CD11b positive cells are observed, especially within the blood vessels, suggesting that TRPV3 activation results in more migration of macrophages in the wound area. The histochemistry of the 4-day wound samples were analysed. Number of macrophage marker (CD11b) positive cells in the wound area was more, especially in case of TRPV3 activation condition, which indicates more recruitment of macrophage cells in the TRPV3 activation condition (**Fig. 17d**).

To understand the localization of keratinocytes, α keratin (k3/k76) along with TRPV3 was used, where it was found that both the proteins co-localized in the near wound area on the 10th day. And in the case of almost healed tissue that is in FPP-treated condition, migrated keratinocytes were found to be localized with TRPV3 (**Fig. 17b-c**).

2.1.2.2 TRPV3 activation causes more phagocytosis and bacterial clearance by macrophages

To explore if TRPV3 activation/inhibition affects the ability of macrophages towards bacterial phagocytosis and subsequent bacterial survivability within the cell, the CFU count analysis in different conditions was performed. For that, MRSA to the macrophages was added and at the same time TRPV3 is modulated for 15 min and 60 min followed by CFU count analysis (**Fig. 18a**).

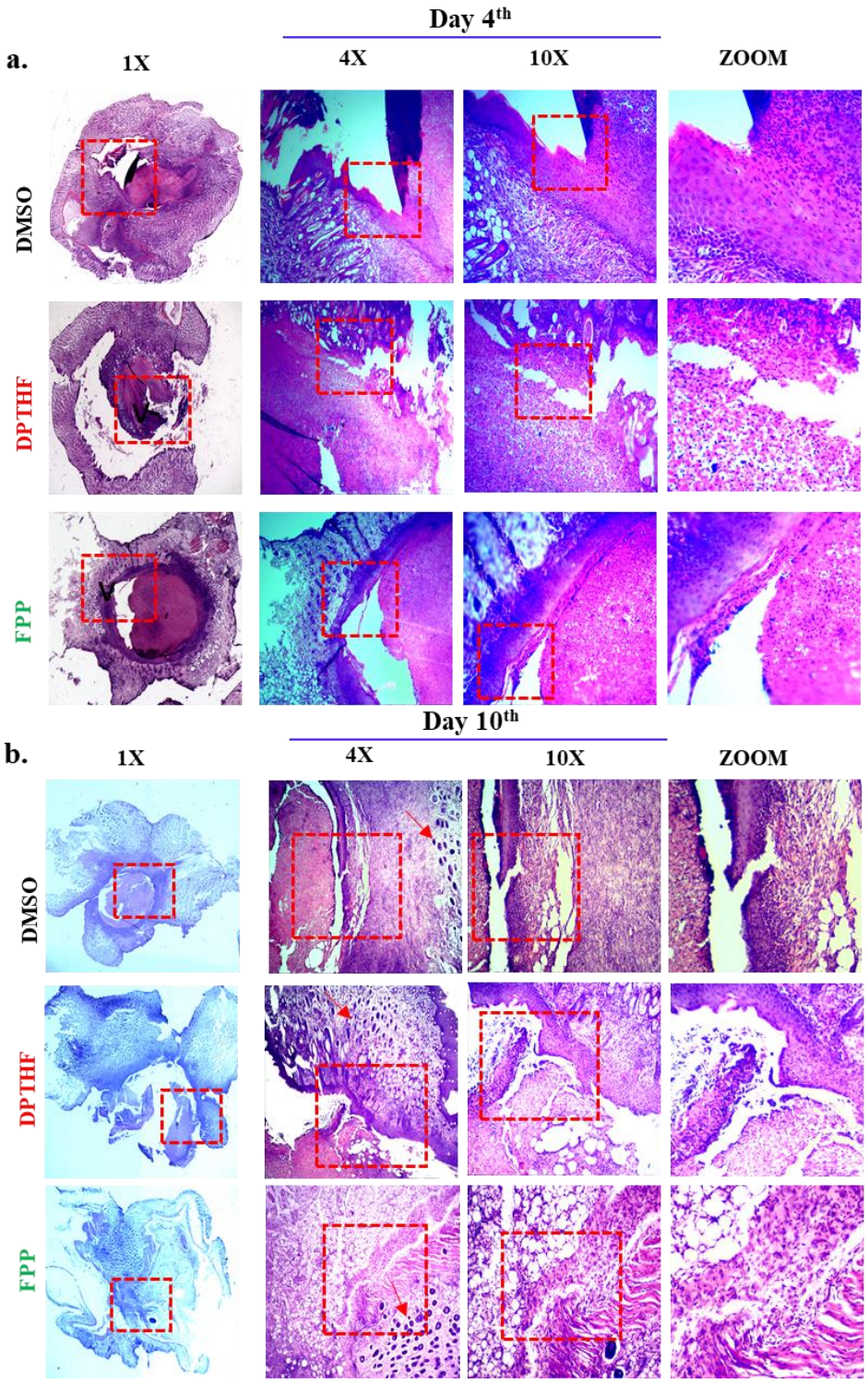

Fig 16. TRPV3 activation enhances rapid wound healing by recruiting more immune cells through blood vessels to the wound area. a. Shown are the tissue sections with haematoxylin and eosin stained of the wounded area on the 4th day of animals treated with DMSO, DPTHF, and FPP daily at the wound area. TRPV3 activation by FPP enhances wound healing. **b.** Shown are the wounded tissue on 10th day of animals treated with DMSO, DPTHF, and FPP daily at the wound area. Arrows indicateblood vessels within the tissue sections.

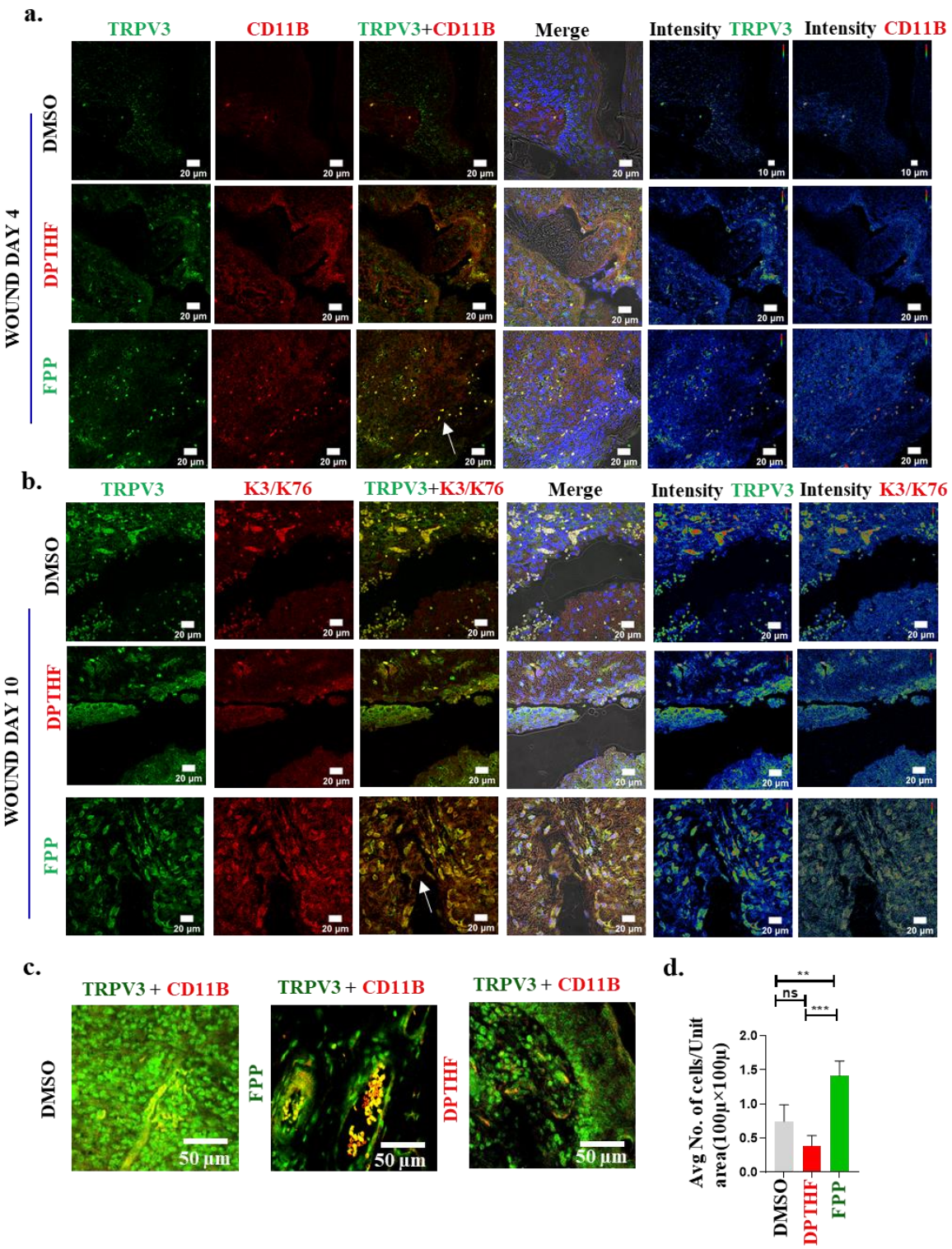

Fig 17. TRPV3 activation enhances the wound healing by recruiting more immune cells as well as keratinocytes migration to the wound area. **a.** Immuno-cytochemistry of the skin section shows the staining of TRPV3 (green) with macrophage marker CD11B (red) at day 4th. **b** Shown are the immune-cytochemistry of wound tissue at day 10th with TRPV3 (green) and α keratin k3/k76 (red) staining**. c.** Immuno-cytochemistry of wound tissue section showing TRPV3 (green) and CD11B (red, macrophage marker) at 10th day tissue sample. Scale bar 20µm, 20µm and 50µm. **d**. At day 10th the numbers of CD11B-positive cells per unit area (quantified through tile images) become much more in TRPV3-activated conditions. One-way ANOVA test, the P values are: ** = p <0.01, *** = p <0.001 and ns = non-significant.

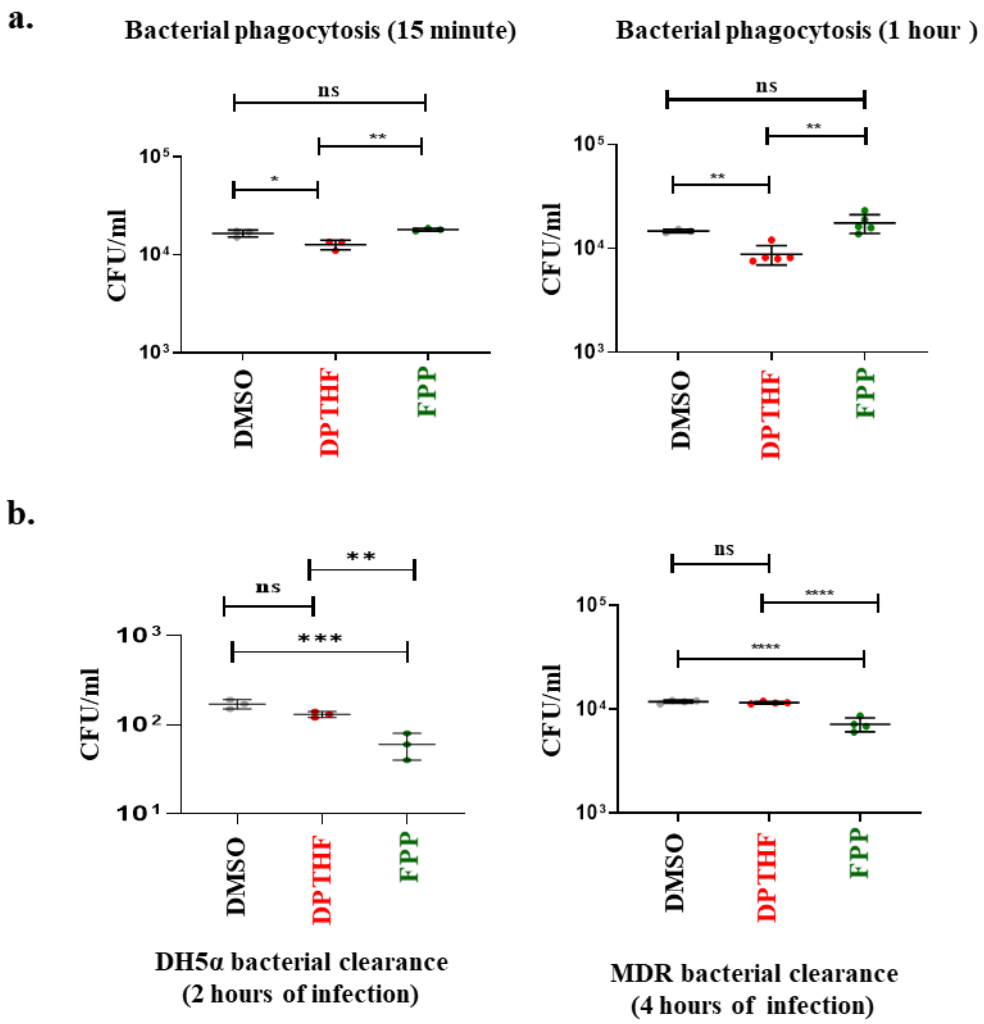

Fig 18. Effect of TRPV3 modulation on bacterial phagocytosis and bacterial clearance. **a.** Endogenous TRPV3 of peritoneal macrophages was modulated by TRPV3-specific activator (FPP, 1μM) or inhibitor (DPTHF, 100μM) and the cells were simultaneously challenged with MRSA (MOI ~at 10 bacteria per cell) for phagocytosis within 15 minutes or 1 hour and followed by CFU count. Less CFU counts is observed in case of DPTHF treatment conditions, suggesting that TRPV3 inhibition results in less bacterial phagocytosis. **b.** TRPV3 activation increases bacterial clearance. Primary macrophages were challenged with MRSA followed by washing. Subsequently, the cells were treated with TRPV3-specific drugs for 4 hours and CFU counts were taken. At the TRPV3-activated condition (FPP, 1μM), the CFU count is significantly less than the DPTHF- or DMSO-treated conditions.

TRPV3 activation (FPP, 1μM) gave more CFU (though the value remains non-significant) than control (DMSO) conditions and TRPV3 inhibition (DPTHF 100μM) produced less CFU than control conditions (**Fig. 18a**). This suggests that TRPV3 activation results in more phagocytosis (as 15 min and 60 min duration is not sufficient for bacterial clearance). To confirm these possibilities, the macrophages were challenged for the bacterial infection for 4 hours (in order to have a saturation of phagocytosis) and then washed out the extracellular

bacteria with gentamycin. Subsequently, the macrophages were treated with TRPV3 modulators for another 4 hours followed by the CFU count analysis. The results show that in the TRPV3 activated condition, the CFU/mL is much less than in the control and inhibited condition, confirming that TRPV3 activation enhances bacterial clearance (**Fig. 18b**). Similar trends were obtained with *Escherichia coli* also (**Fig. 18b**). Taken together, the data suggest that TRPV3 activation results in bacterial clearance from wound areas by recruiting more macrophages there. TRPV3 modulation affects both bacterial phagocytosis as well as bacterial cell clearance by macrophages.

2.2 Characterization of TRPV3 in the context of cellular and lysosomal functions

The entire biological function of cell and sub-cellular organelles are critically optimized with the certain pH and ionic balance that is maintained in the cytosol as well as in the respective subcellualr particles. In this context, the cytosol is mainly maintained at pH 8 and lysosomes are maintained at acidic pH, at a range of 4.5- 5 (Casey et al. 2009; Martina et al. 2020). So far, few ion channels and pumps have been detected in the lysosomes that are involved in the maintenance of lysosomal low pH and thereby ensure the function of lysosomes (Festa et al. 2022). Notably, higher Ca^{2+} concentration is important for maintaining lysosomal low pH (Garrity et al. 2016). In this context, TRP ion channels seems to have significant roles. TRPML group of ion channels are known to regulate lysosomal pH, and mutation in TRPML cause lysosomal defects (Dong et al. 2010; Dong et al. 2008). Work done in this chapter explores the presence and function of TRPV3 in the regulation of lysosomal Ca^{2+} and pH-homeostatsis.

2.2.1 TRPV3 is endogenously expressed in primary macrophages and macrophage cell lines

The presence of TRPV3 in the lysosome and its role in lysosomal functions have been characterized in different cellular systems where TRPV3 is expressed endogenously. The expression of TRPV3 in primary macrophages has been explored. Using TRPV3-specific antibodies and by immunofluorescence analysis, the TRPV3 expression and localization have been detected in the primary macrophages (**Fig. 19a**). This TRPV3-specific signal can be abolished by using a specific peptide that represents the epitope (REEEAIPHPLALTHK-amino acid residues 464-478) of the antibody (**Fig. 19a**). The functional expression of TRPV3 in these primary macrophages was explored. For that purpose, the cells were loaded with a

Ca^{2+}-indicator dye (Fluo 4) and performed Ca^{2+}-influx assay. The Ca^{2+}-level increases with time in response to the application of TRPV3-specific agonist, i.e. FPP (1µM) (**Fig. 19c-d**).

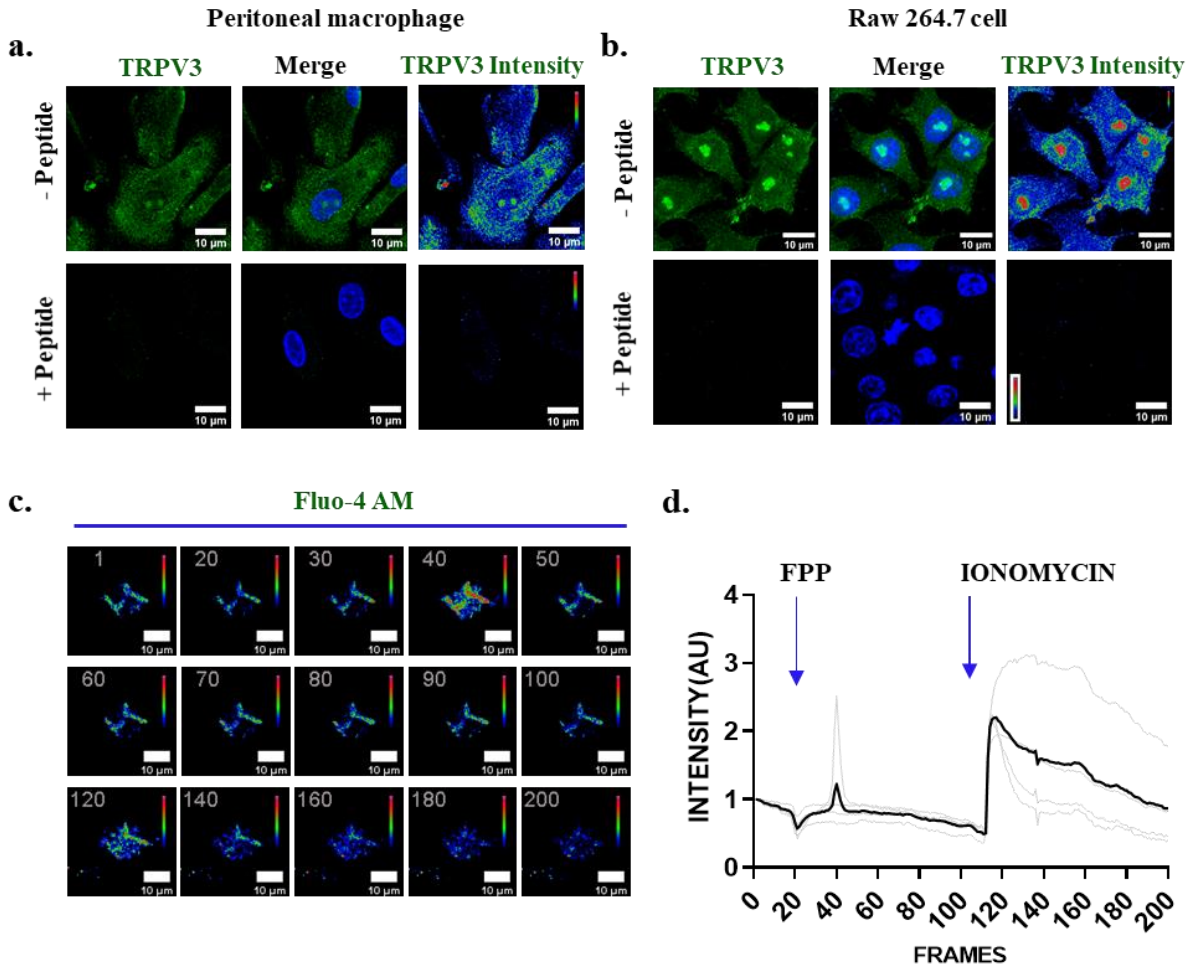

Fig 19. The endogenous expression of TRPV3 in macrophage cells. **a-b.** The representative figure shows the expression of TRPV3 in the peritoneal macrophages and Raw 264.7 cells as detected by antibody staining in the absence or in the presence of blocking peptide. **c.** These images show the Ca^{2+}-signals in peritoneal macrophages in different time points after TRPV3 is activated by FPP (at the 20th frame) and at the end of ionomycin stimulation (120th frame). Scale bar 10µm. **d.** The increased Ca^{2+}-signal is represented in the graph, which is detected through Fluo-4-AM dye.

Next, the expression of TRPV3 has been explored in macrophage cell lines, namely in RAW 264.7 cells. Using TRPV3-specific antibodies and by immunofluorescence analysis, the endogenous expression of TRPV3 in the RAW 264.7 have also been detected (**Fig. 19b**). The TRPV3-specific signal is observed in the cell surface as well as in the cytoplasm and also within the nucleus (**Fig. 19b**). All these TRPV3-specific signals can be blocked by using a TRPV3 antigen-specific peptide (**Fig. 19b**).

The Ca^{2+}-level also checked by using Ca^{2+}-sensor construct GcamP6f in RAW 264.7 cells in response to FPP stimulus (1µM) instantly at 20^{th} frame. The cells respond to TRPV3 activations and exert Ca^{2+}-influx both in primary macrophage and RAW 264.7 cells. The "area –under-the-curve" (equivalent to total Ca^{2+}-influx) analysis shows significant increase in the TRPV3 activation (FPP, 1µM) condition (**Fig. 20-21**).

2.2.2 TRPV3 modulation alters cellular morphology

The expression of TRPV3 in the macrophages has been observed, and then the expression level was compared in different conditions where cells were stimulated with different TRPV3 modulators in presence or in absence of LPS (**Fig. 22 a-b**). The enhanced expression of TRPV3 through LPS-stimulation (for 14 hours) can be observed (**Fig. 22a**). The expression increases significantly (1.5844 fold) with LPS-stimulation (for 14 hours) in the peritoneal macrophages (**Fig. 22b**).

The length, width and perimeter have also been quantified subsequently after TRPV3 modulation and LPS-stimulations. The perimeters of the TRPV3 modulation and LPS-stimulation have increased significantly (**Fig. 22c)**. The width of the cells in DPTHF-treated condition decreases significantly, and there is no change in case of FPP treatment. The width has been increased significantly in the LPS-stimulation (both with TRPV3 modulation by FPP- or DPTHF-treatments) (**Fig. 22c)**. In case of length/width, the case was found to be reversed where the ratio has increased significantly in DPTHF-treated conditions and non-significantly in FPP-treated conditions. And the ratio has decreased significantly in the LPS-stimulated conditions along with TRPV3 modulations (both activations and inhibition) (**Fig. 22c**).

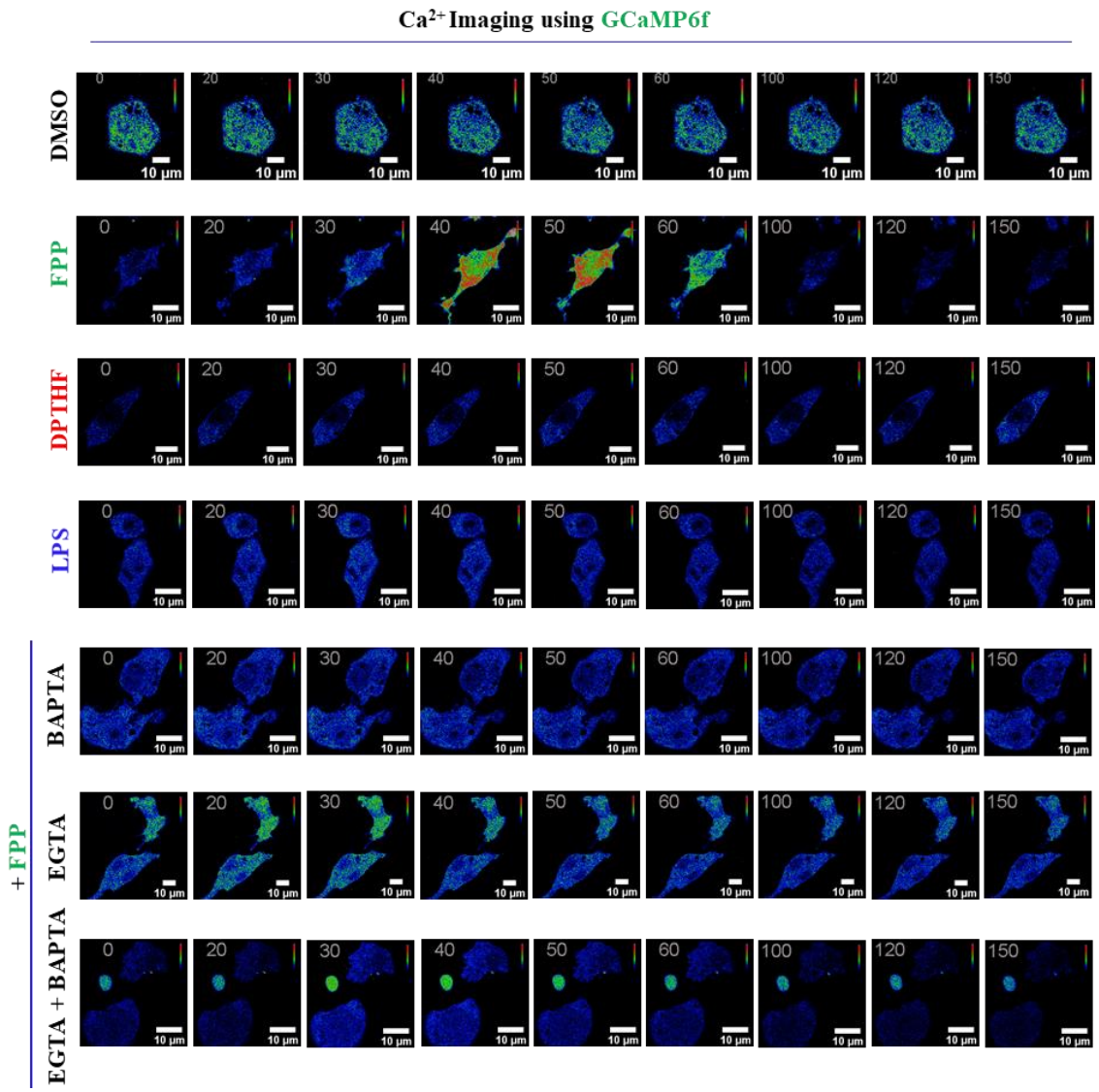

Fig 20. The endogenously express TRPV3 respond to FPP stimulation in Raw 264.7 cells and exert Ca^{2+}-influx. The Raw 264.7 cell transiently transfected with Ca^{2+}-sensor (GCaMP6f) and TRPV3 activator, inhibitor, LPS and chelated with BAPTA and EGTA. The FPP (TRPV3 activator) exert Ca^{2+}-influx when added instanstly at 20th frame. The cells also responsive to LPS stimulus and to some extent in the Ca^{2+}-chelated conditions. The cells is do not show any response to DMSO which was added at 20th frame as well. Scale bar 10µm.

2.2.3 TRPV3 acts as a lysosomal protein in primary macrophages

If TRPV3 co-localizes with lysosomal markers i.e., lysotracker red as well as LAMP1 (as detected by antibody) was explored. This experiment confirms the presence of TRPV3 in the lysosomes (**Fig. 23**). To confirm the localization of TRPV3 in lysosome by another method, lysosomes were isolated from macrophages and were subject to immunostainig of the same with TRPV3-specific antibody. The presence of TRPV3 is detected in a sub-population of the isolated lysosome only, but not in all isolated lysosomes (see later in the discussion section).

2.2.4 TRPV3 regulates lysosomal pH

If the endogenous expression and localization of TRPV3 depends on the stimulation or modulators like LPS (Lipopolysaccharides), FPP (Farnesylpyrophosphate), DPTHF (2,2-diphenyl tetrahydro-furan), that was tested. TRPV3 localizes in different areas of the macrophage, and the exact localization seems to be context dependent and thus depends mainly on the stimulation state of the cells.

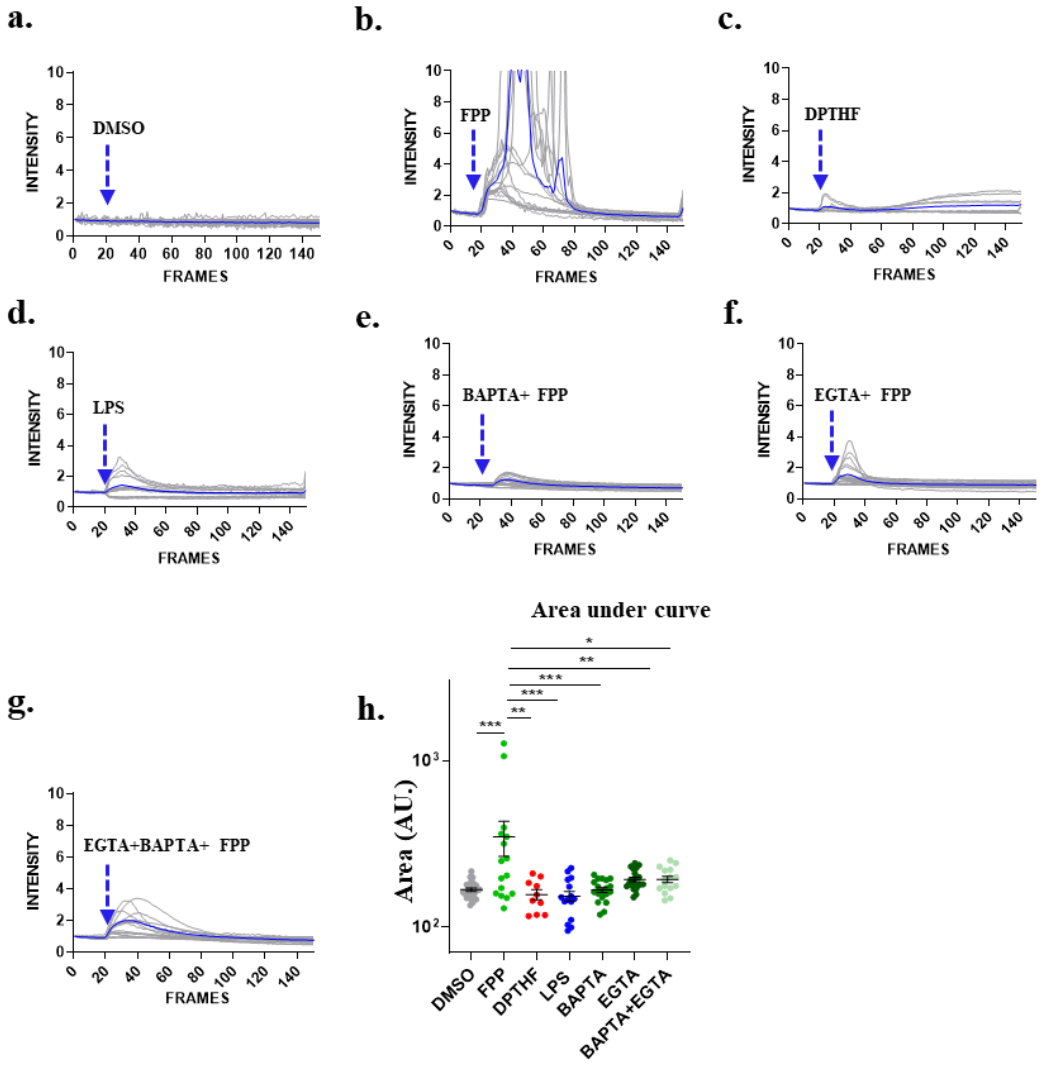

Fig 21. TRPV3 in Raw 264.7 cells respond to TRPV3 activation and exert Ca^{2+}-influx. a-g. The representaive graph shows the quantified responsive cells modulated by TRPV3 activator, inhibitor, LPS and activator along with Ca^{2+}-chealated condition. FPP (1µM) was able to exert Ca^{2+}-influx in Raw 264.7 cells. **h.** The graph represents quantified area under the curve (Arbitrary Unit, AU) in TRPV3 modulated conditions, LPS stimulus as well as Ca^{2+}-chelated condition with FPP stimulus. One-way ANOVA test, * = $p \leq 0.05$, ** = $p \leq 0.01$ and *** = $p \leq 0.001$.

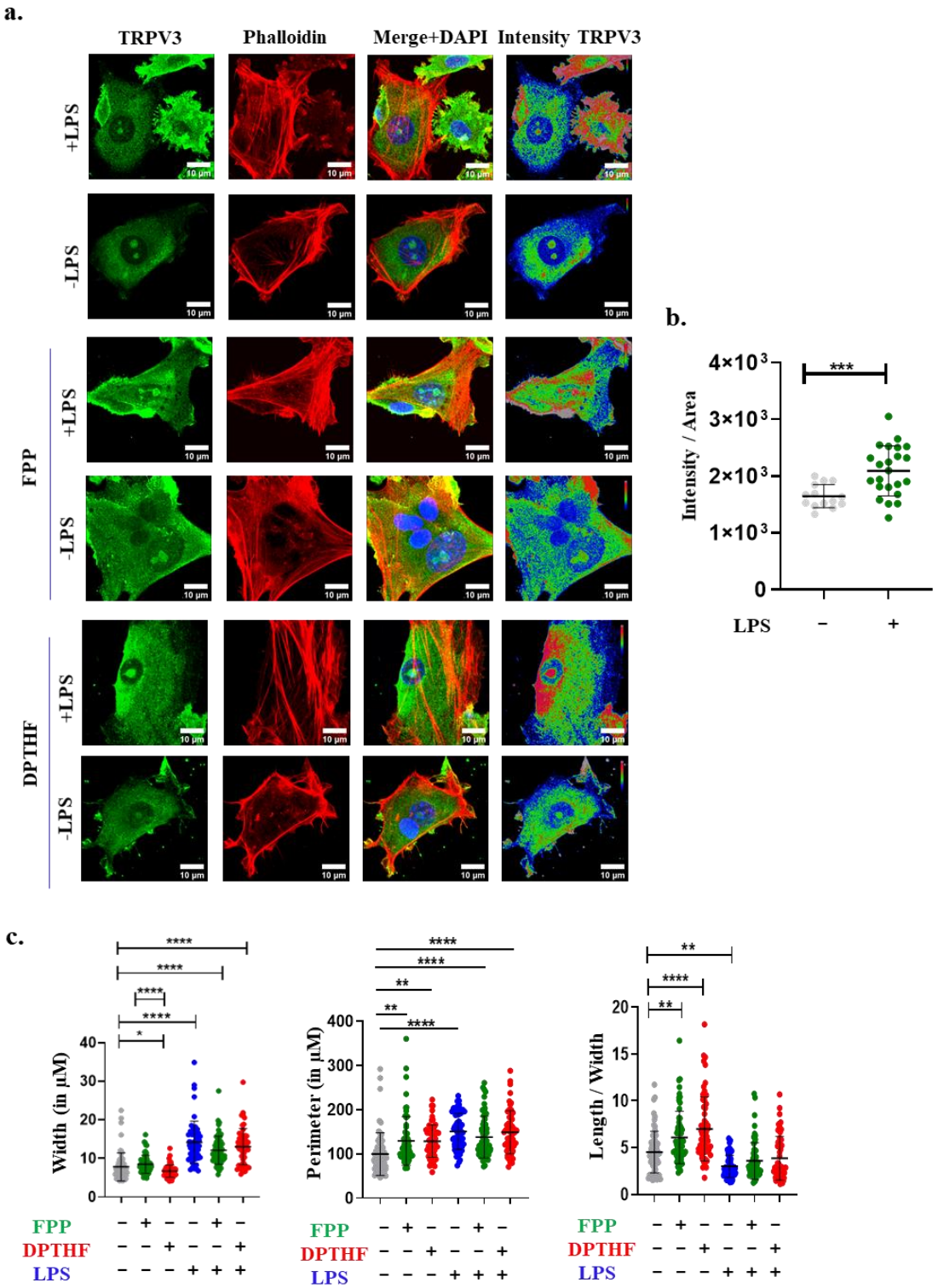

Fig 22. TRPV3 modulations and its role in peritoneal macrophages morphological aspect. **a.** The representative figure shows the expression of TRPV3 in the peritoneal macrophages stimulated with or without LPS stimulations along with TRPV3 modulators (i.e. FPP as activator and DPTHF as inhibitor). The peritoneal macrophages were stained with phalloidin-594 along with TRPV3 extracellular antibody tagged 488. Here the localization of TRPV3 has been throught the cell as well as specifically highlighted in the nucleus. Scale bar 10µm**. b.** The expression of TRPV3 is enhanced upon LPS-stimulations. The graph represent the enhanced intensity of TRPV3 probe with TRPV3 antibody. **c.** The graph represents change in morphological parameters such as perimeters, width, length/width measurements of peritoneal macrophages stimulated with TRPV3 modulators along with or without LPS stimulations. One-way ANOVA, **** = p <0.0001, *** = p <0.001, ** = 0.01. * = 0.05, non-significant = ns).

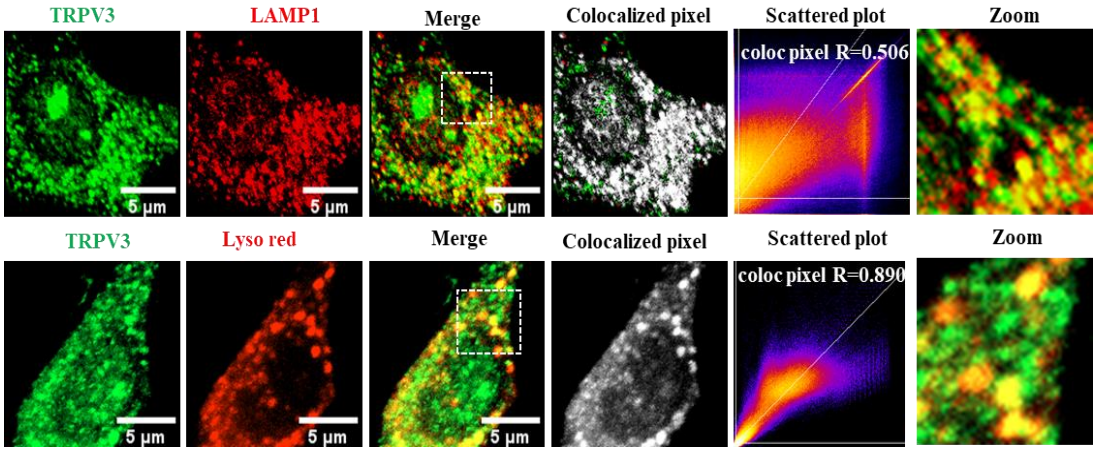

Fig 23. Presence of TRPV3 in lysosomes in peritoneal macrophages. a. The representative figure shows the presence of endogenous TRPV3 (green, detected by antibody staining) in the peritoneal macrophages that colocalizes to lysosomal markers, namely with LAMP1 (red, detected by antibody staining) as well as with lysotracker Red (red, labelled by dye). Scale bar 5µm.

As mentioned earlier that TRPV3 localizes in the lysosome, it is expected to have some functional role in the maintenance of lysosomal functions, like regulation of its pH. It is found that cells maintain acidic lysosomal pH upon TRPV3 activation through FPP (1µM), while on the other hand, the cytosolic pH, which was measured by pH rodo red, seems to be the opposite of lysosomal pH (**Fig. 24a-c**). The cytosolic pH became less acidic in the activated condition, but lysosomal pH was found to be more acidic in the activated state. On the other hand, the cytosolic pH became more acidic and lysosomal pH became less acidic in the TRPV3-inhibited (DPTHF, 100µM) condition (**Fig 24b-c**).

As all the cells were loaded with both sensors for lysosomal pH and cytoslic pH, correlation between lysosomal pH and cytosolic pH in different conditions were tested (**Fig 24d**). It is observed that at control condition, the lysosomal pH and cytosolic pH have modest correlation (r = 0.40) and all the data sets remain clustered. This may suggest that at control condition, lysosomal pH is partially dependent on the cytosolic pH. However, at TRPV3 activation condition, the correlation value drops drastically (r = 0.00). This suggests that at TRPV3 activation condition, lysosomal pH regulation become mostly independent of the cytosolic pH. However, at DPTHF condition, the correlation value become heighest (r = 0.62).

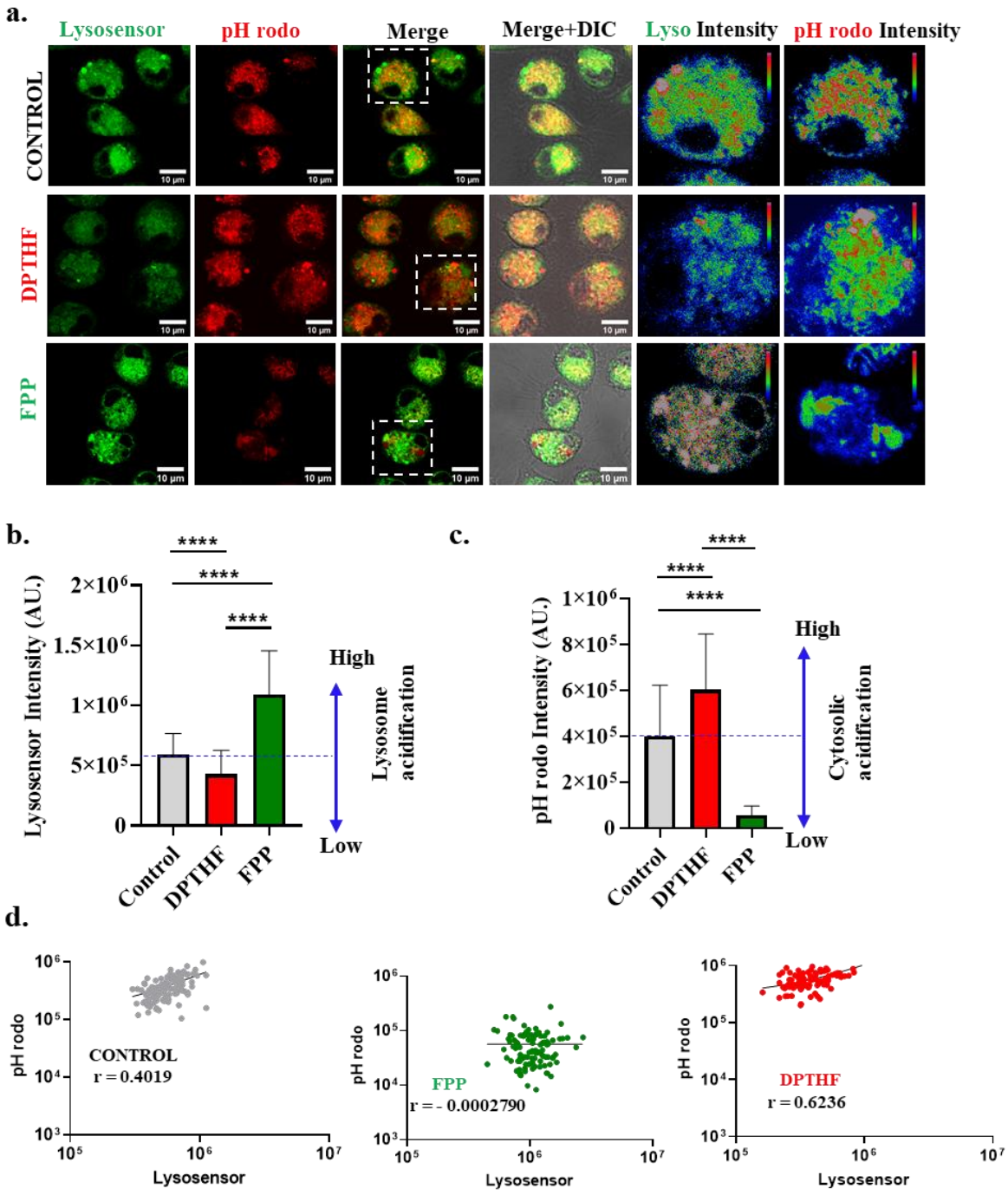

Fig 24. TRPV3 regulates lysosomal pH. a. These representative images of primary macrophages show the fluorescence intensity of lysosomal pH (green, as detected by lysosensor green dye) and cytosolic pH (red, as labelled by pH rodo) dyes. Cells were treated with TRPV3 activator or inhibitors (for 2 hours) of left untreated (control) before labelling with the dyes. Scale bar 10 µM. **b-c.** The graph (b) shows the lysosensor green intensity in conditions where TRPV3 is activated or inhibited. The increased intensity of lysosensor green means more acidification of lysosome. The lower panel (c) shows the changes in the cytosolic pH (pH rodo) due to TRPV3 modulations (p **** ≤ 0.0001). **d.** The figure represents correlation graph between lysosensor green (X-axis) and pH rodo (Y-axis) in different modulated conditions. Unpaired t-test, **** = p ≤0.0001.

This suggests that TRPV3 inhibition compromises the lysosomal pH maintenance mechansim/s drastically and makes lysoosmal pH dependent on the cytosolic pH. This

indicates that TRPV3 have important role in the maintenance of overall cellular and lysosomal pH. Thus, TRPV3 may have a role in balancing lysosomal pH dependent on the cytosolic pH.

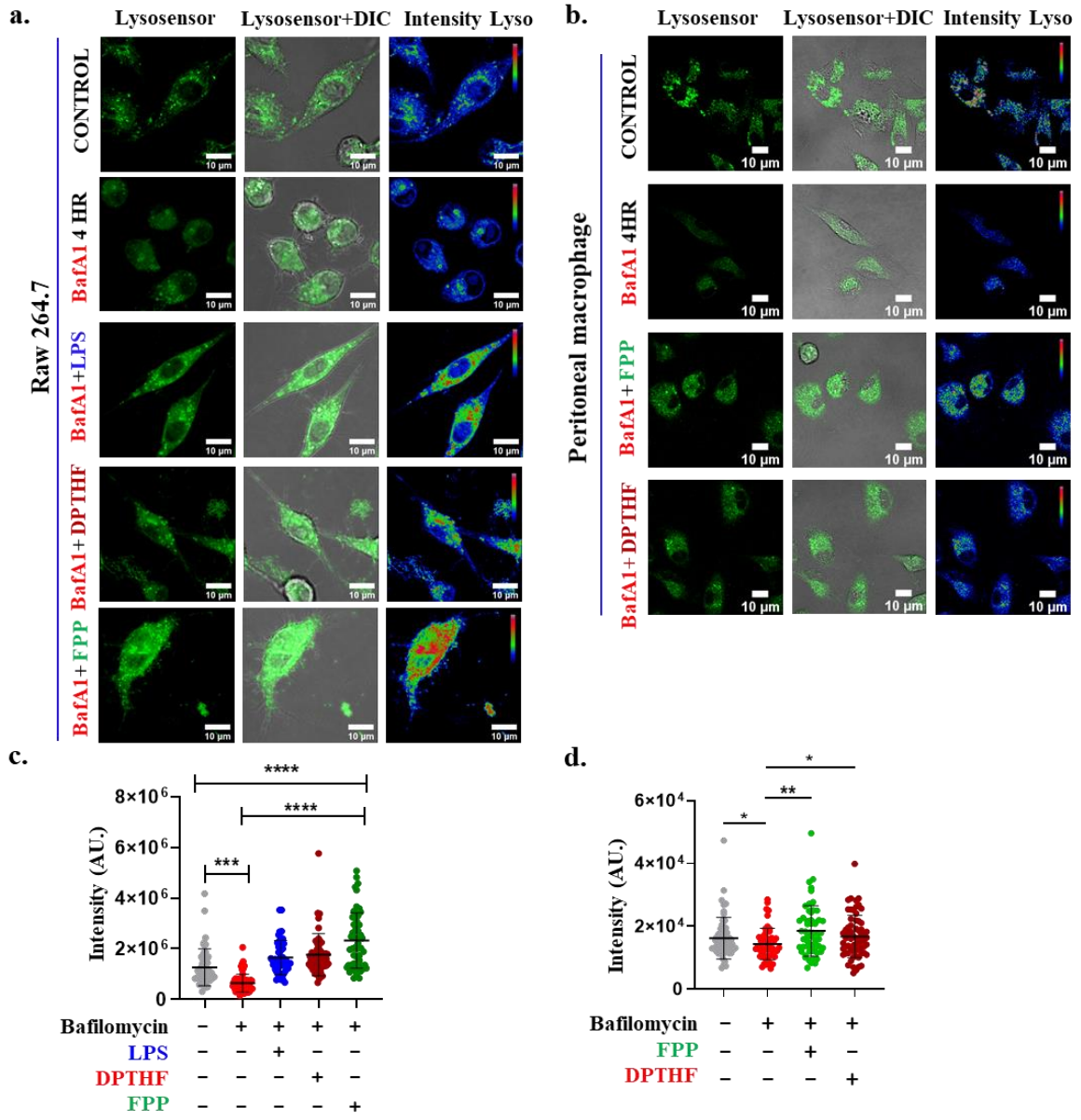

Fig 25. TRPV3 modulation helps to maintain lysosomal pH during lysosomal stress. a-b. The representative image shows the lysosensor dye staining after Raw 264.7 cells and peritoneal macropahges are stressed with BafA1 (400ng, for 4 hours) in absence or presence of TRPV3 modulators (FPP or DPTHF) or LPS. TRPV3 modulation helps to recover lysosomal acidic pH better. Scale bar 10 µm. **c-d.** The quantitative analysis shows the variation in lysosomal pH as measured by using lysosensor green dye in Raw 264.7 cells and primary macrophages respectively. One-way ANOVA, **** = $p \leq 0.0001$, ** = $p \leq 0.01$, * = $p \leq 0.05$.

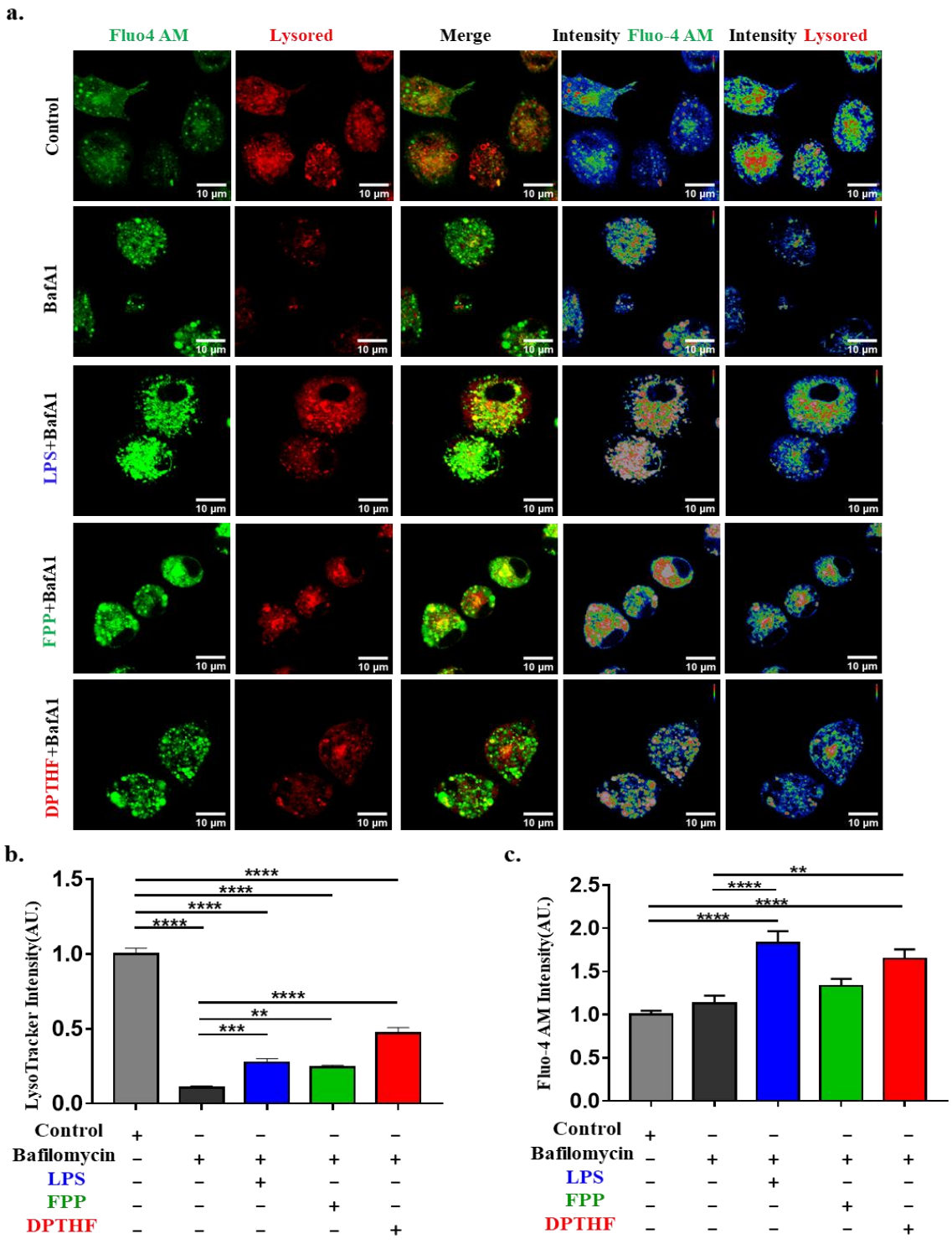

Fig 26. TRPV3 modulation rescue the cytosolic Ca^{2+} and Lysosomal pH level in Bafilomycin-induced stressed conditions. a-c. Qualitative and quantitative representation and analysis of live macrophages loaded with Fluo-4 AM (Green) with LysoTraker Red (Red). Cells were left untreated (as control) or treated with Bafilomycin and further modulated by either FPP, DPTHF or LPS. Scale bar: 10 µm. Values are means ± SEM; one-way ANOVA; ns: non-significant, *p < 0.05, **p < 0.01, ***p < 0.001, ****p < 0.0001.

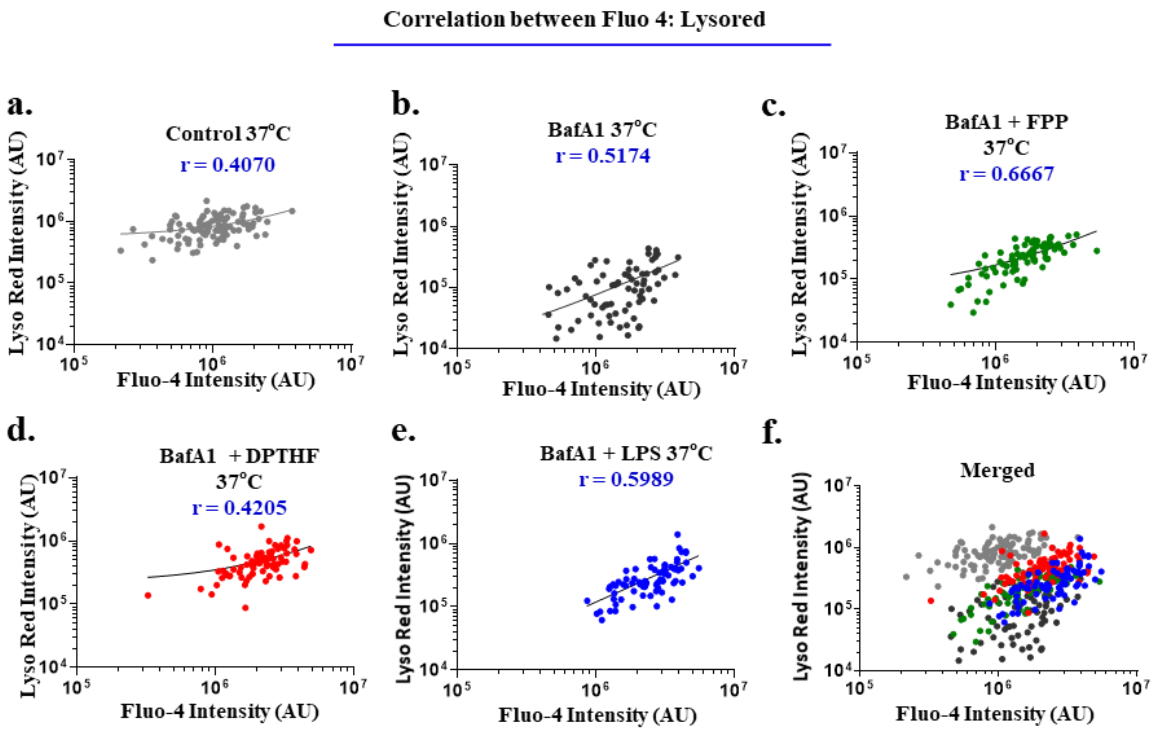

Fig 27. TRPV3 modulation rescue the correlation between cytosolic Ca^{2+} and Lysosomal pH in Bafilomycin-induced stressed conditions. a-f. Correlation analysis between Fluo-4 AM with LysoTraker Red intensity of PM in different conditions are shown.

2.2.5 TRPV3 modulation improves the lysosomal functions stressed by Bafilomycin

Bafilomycin is an antibiotic produced by *Streptomyces* and blocks lysosomal functions (Bowman et al. 1988). To test if TRPV3 functions improve lysosomal functions, Bafilomycin at a "sub-optimum" level has been used to induce lysosomal stress (**Fig. 25**).

The cytosolic Ca^{2+} and lysosomal pH status measured from same cells by using Fluo4-AM and Lyso-Red dyes (**Fig.26a**). The macrophage cells were treated with BafA1, which is expected to hamper the lysosomal pH by blocking V-type ATPase, and accordingly, the lysosomal pH becomes less acidic after 4 hours of treatment.

Bafilomycin at a "sub-optimum" level cause change in lysosomal pH (loss of lysosomal acidity) drastically, however modulation of TRPV3 as well as LPS-treatment rescues this lysosomal pH significantly (**Fig. 25c&d; Fig. 26b**). Ca^{2+}-level increases in FPP, DPTHF and LPS-treated conditions significantly (**Fig. 26c**).

The correlation analysis between the cytosolic Ca^{2+} with lysosomal pH in different conditions were analysed (**Fig.27 a-f**). In Bafilomycin-treated condition, the correlation becomes more significant when TRPV3 is activated (FPP-treated condition, r = 0.6667) as compared to TRPV3-inhibited condition (DPTHF-treated condition, r = 0.4205) as compared to the control (r = 0.4070) or only Bafilomycin-treated condition (r = 0.5174). LPS-treatment also increases the correlation between Fluo4 and Lyso-Red fluorescence (r = 0.5989) (**Fig.27 a-f**). This data indicates that the TRPV3 activation particularly rescues the lysosomal pH levels affected by Bafilomycin treatment. Altogether, this data suggests that TRPV3 activation provides benefits to the cells to restore the low pH in lysosomes, especially in stressed conditions**.**

2.3 Nucleolar localization of TRPV3

This chapter discusses the presence of TRPV3, within cellular organelles like the nucleolus and their role in cellular stress responses. TRPV3 is found in both the nucleolus and the lysosome, both organelles are involved in transmitting information during stressful conditions. Other than genetic organization, nucleus is also a resident of various stress regulatory proteins (Voellmy and Richard. 2004). The main structure which is known as one of the stress-responsive unit is the nucleolus that also takes part in cellular stress response. The nucleolus is a crucial substructure within the nucleus that plays a vital role in the production of ribosomes that synthesize proteins (Hao et al. 2022). During cellular stress, the nucleolus changes its structure and function which allows the cells to adapt to the stressor. The results provided in this chapter further characterize the TRPV3 localization within the nucleolus. Data provided here confirms that TRPV3 has a unique NoLS sequence, which is conserved in warm-blooded organisms and suggests TRPV3's involvement in responding to cellular stress and temperature changes, possibly more precisely in mammals only. Using a recently developed specific thermos-sensor dye, this chapter also investigates the thermal patterns of the nucleus in different conditions (Xiao et al. 2022). Data provided in this chapter suggests that the thermal pattern of nucleus is influenced by TRPV3 modulation as well as by LPS stimulation. Expression of NoLS of TRPV3 also alters this thermal pattern. However, the exact role of TRPV3 in the nucleolus and its responsiveness to different cellular conditions remain unclear, highlighting the need for further investigation into its role in nucleolar stress responses and interactions with other molecules. Never-the-less, the data provided in this chapter confirms the presence of TRPV3 in nucleolus and indicates its possible role in the nucleolar functions, stress response and possibly thermosensation at the nucleolar region.

2.3.1 The presence of TRPV3 in the nucleolus: Relevance for stress response

It has been observed that the TRPV3 is present endogenously in the lysosome of primary macrophages and that, upon certain conditions, TRPV3-specific signal can also be detected in the nucleolus (Sahu and Goswami. 2022). In order to characterize the condition-dependent presence of TRPV3 in the nucleus, the Raw 264.7 cells were treated with or without LPS (Lipopolysaccharides) for 16 hours and subject to subcellular fractionation. Cells were fractionated to cytoplasmic and nuclear fraction by using nuclear enrichment kit, followed by Coomassie staining and Western blot analysis (**Fig. 28**). Full-length TRPV3 protein is detected in the nuclear fraction, both in LPS-treated and untreated samples. However, the presence of TRPV3 in the nuclear fraction is more prominent in the LPS-treated samples (**Fig. 28c)**. More amount of fibrillarin is also seen in the nuclear fraction in the LPS-treated samples (**Fig. 28d**). The TRPV3-specific signal can be abolished when a specific blocking peptide is used, suggesting the detected signal is specific for TRPV3.

To validate this finding in another manner, both LPS-treated and untreated cells were subject to *in situ* nuclear preparation. For that purpose, the cells were fractionated *in situ* as a cytoplasmic and loosely held nuclear fraction, tightly held nuclear fraction (NU), chromatin fraction (CH), and nuclear matrix fraction (NM) by treating the cells sequentially with cytoskeletal buffer [50ml CSK buffer, composition-PIPES/KOH (10mM at pH 6.8), NaCl (100mM), Sucrose (300mM), EGTA (1mM), $MgCl_2$ 1mM, DTT (1mM), in presence of complete Protease inhibitor] along with Triton X100 (0.1% and 0.5%). Subsequently, the coverslips containing different fractions of cells were fixed, and immunostaining was performed. It has been observed that endogenous TRPV3 is present in the nucleolar region (**Fig. 29a**). More amount of TRPV3 is visible in the nucleolar region in case of LPS treatment. Quantification of the fluorescence intensity also indicates that LPS treatment causes the presence of more TRPV3 (~2.12 fold) in the nucleolus (**Fig. 29b**).

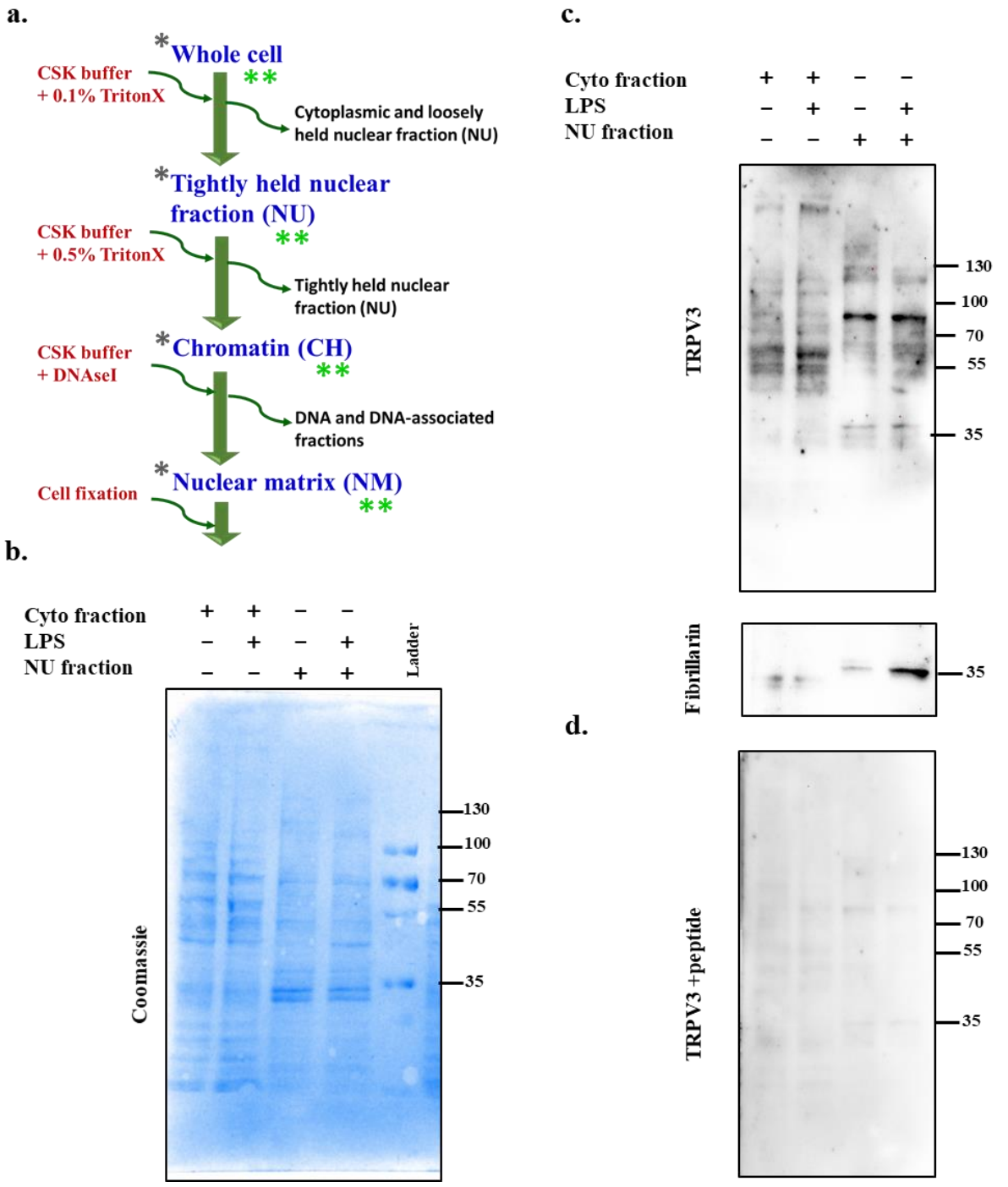

Fig 28. Full-length TRPV3 is present in the nuclear fraction. **a.** Cultured Raw 264.7 cells were fractionated to NU (nuclear protein), CH (chromatin) and NM (nuclear matrix), respectively, using CSK (cytoskeletal buffer) as shown schematically. **b.** The Coomassie staining of the nuclear and cytoplasmic fraction of the Raw 264.7 cells stimulated with or without LPS (Lipopolysaccharides) is shown. **c.** The Western blot analysis of cell fractions probed with TRPV3- and Fibrillarin-specific primary antibodies is shown. Full-length TRPV3 is detected in the nuclear fraction. **d.** Shown is the Western blot of the same samples (as shown in c) with the same TRPV3-specific antibody but in the presence of a specific peptide raised against the antibody. The TRPV3-specific reactivity is not detected in the presence of the blocking peptide.

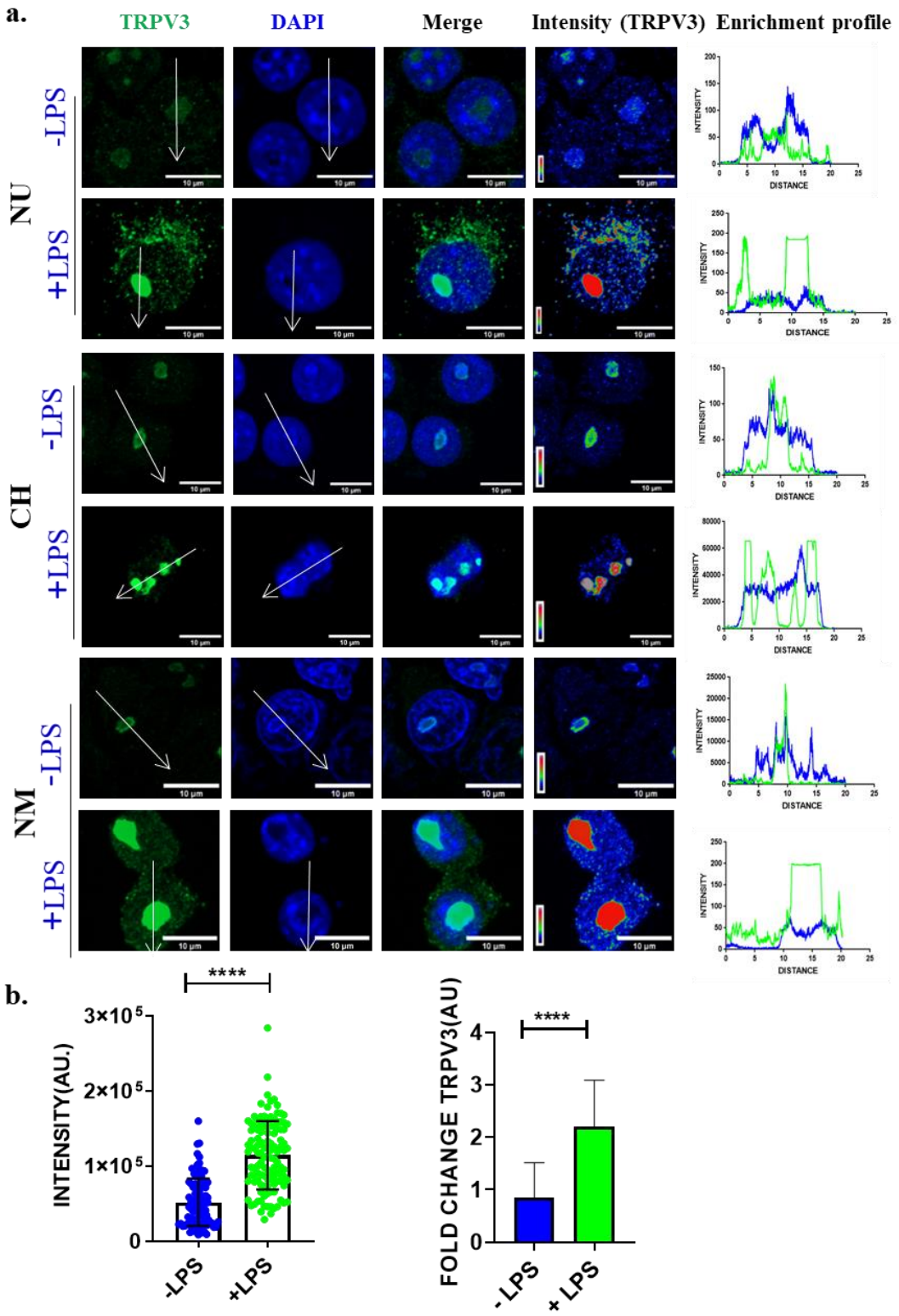

Fig 29. TRPV3 is detected in *in situ* nuclear preparation. a. Raw 264.7 cells were treated with or without LPS (Lipopolysaccharides) and subsequently were fractionated to NU (nuclear protein), CH (chromatin) and NM (nuclear matrix), respectively, using standard buffer treatments. Shown are the confocal images detecting TRPV3 by antibody (green) and DNA by using DAPI (Blue). The intensity profiles (across the white arrow) are shown to indicate the enrichment of TRPV3 in different regions, including in the nucleolus. Scale bar 10μm. **b.** The intensity of TRPV3 in the nucleus is compared. The presence of TRPV3 in the nucleolus is more when cells are exposed to LPS. At least 100 (118 for LPS-treated and 100 for without LPS-treatment) nucleus is quantified in each condition. The fold-change value is shown in right side. Unpaired t-test, **** = $p \leq 0.0001$.

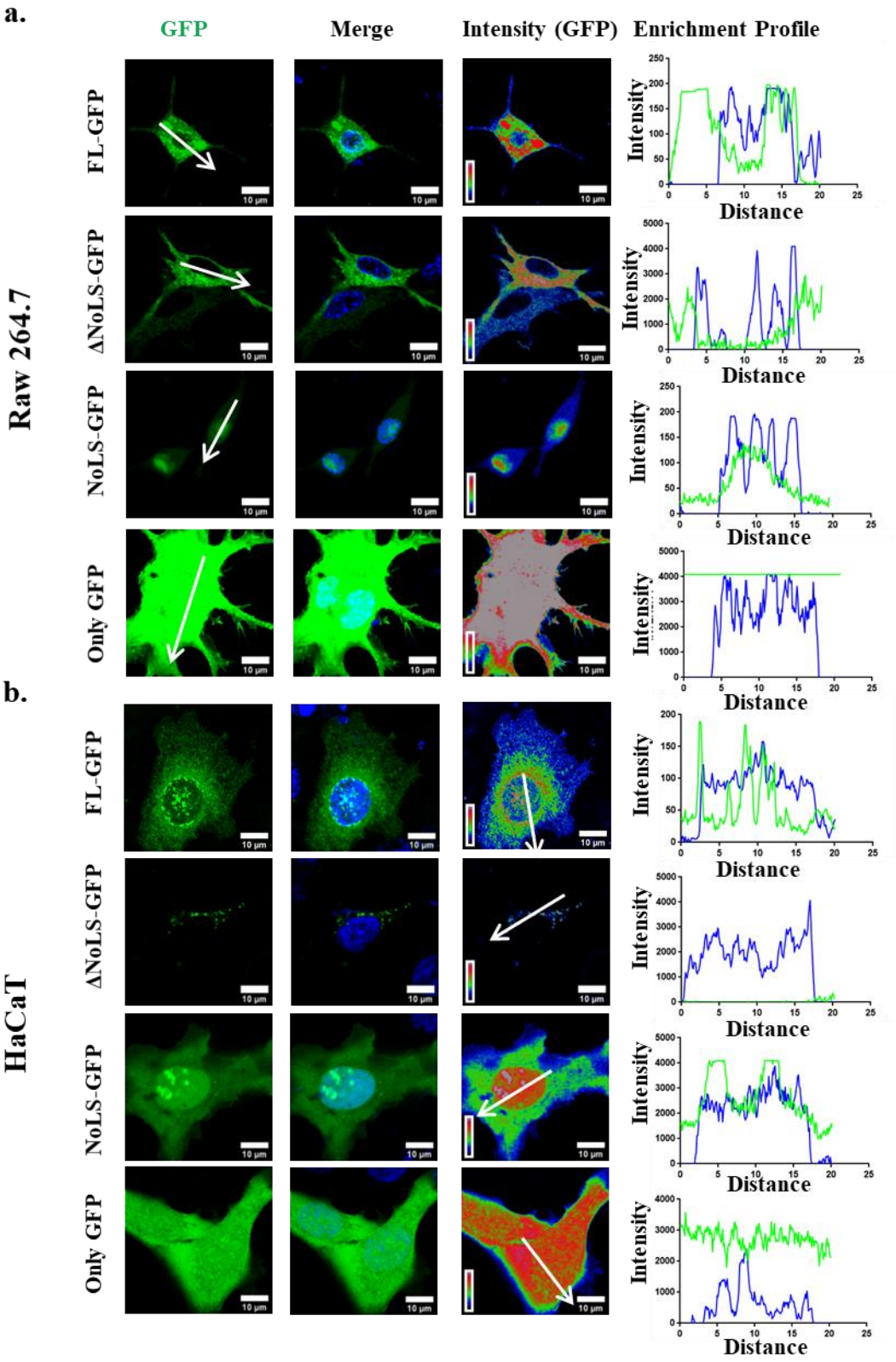

Fig 30. NoLS of hTRPV3 is sufficient to localize in the nucleolus. Expression and localization pattern of full-length hTRPV3 (TRPV3-FL), or only NoLS region (hTRPV3-NoLS), or TRPV3 without the NoLS region (TRPV3-ΔNoLS) in Raw 264.7 (a) and HaCaT (b) cells are shown. The enrichment profile of TRPV3 and DAPI across the white arrows are shown. Only GFP is used as a control. Scale bar 10μm.

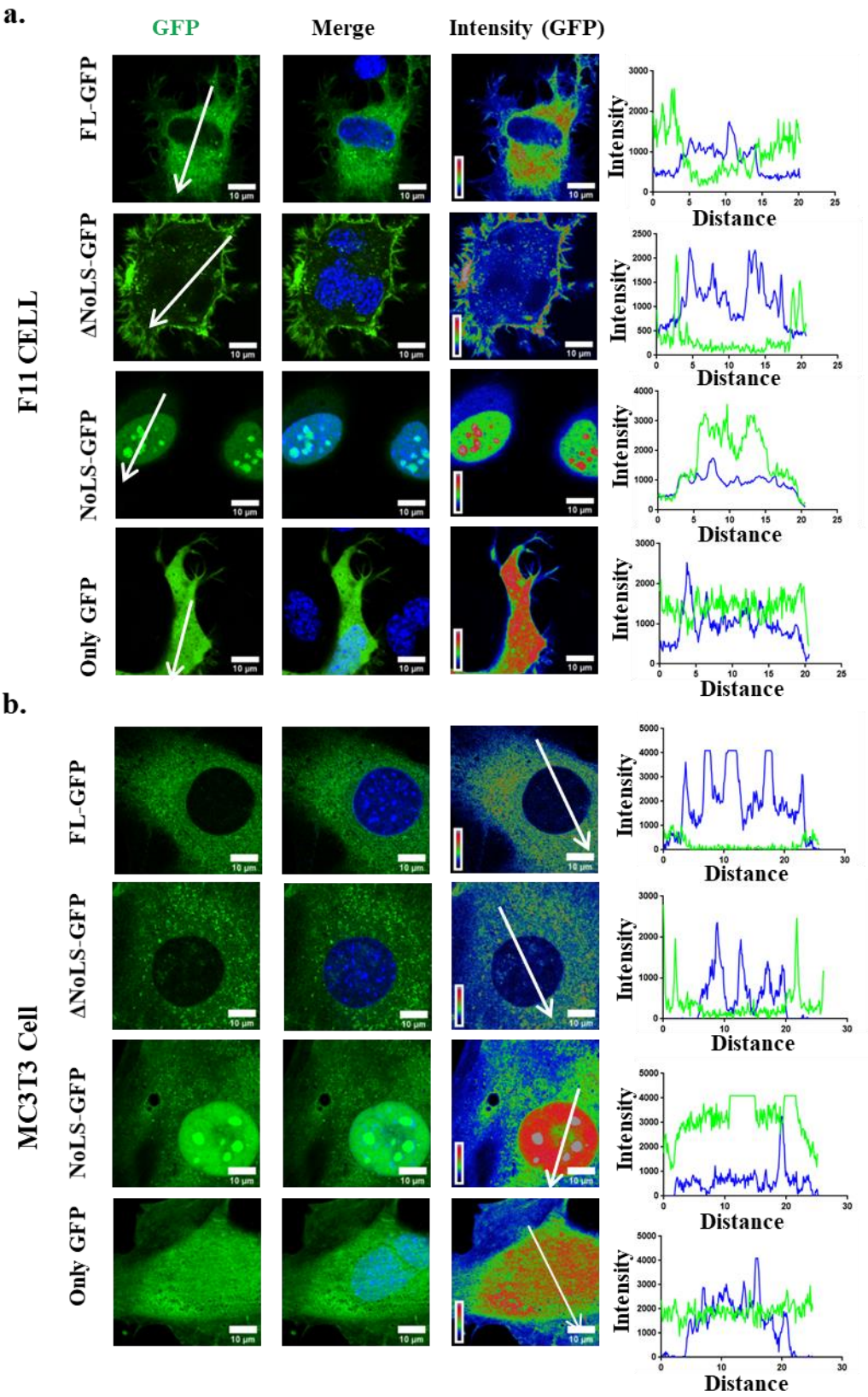

Fig 31. NoLS of hTRPV3 is sufficient to localize in the nucleolus. Expression and localization pattern of full-length hTRPV3 (TRPV3-FL), or only NoLS region (hTRPV3-NoLS), or TRPV3 without the NoLS region (TRPV3-ΔNoLS) in F11 (**a**) and MC3T3(**b**) cells are shown. The enrichment profile of TRPV3 and DAPI across the white arrow are shown. Only GFP is used as a control. Scale bar 10μm.

2.3.2 Prediction of NoLS sequence in hTRPV3

Next it was explored if TRPV3 has any NLS or similar sequence/s. For that purpose, the hTRPV3 protein sequence was scanned. A stretch of 13 amino acids (Amino acid 112-124) appears to have a good score and can be considered as a NoLS. This fragment was separately sub-cloned and tagged with GFP or RFP for expression in mammalian cell lines. However, upon expression, it was noted that this fragment of TRPV3 specifically localizes to the nucleolus. Therefore, this region we termed as "NoLS" and these constructs were termed asTRPV3-NoLS-GFP or TRPV3-NoLS-RFP. Only GFP (PSGFP2-C1 vector), TRPV3-NoLS-GFP, and full-length TRPV3 were expressed in Raw264.7 and in HaCaT cells. TRPV3 without the 112-124 region (hTRPV3-ΔNoLS-GFP) construct was also prepared and expressed. It was observed that hTRPV3-ΔNoLS-GFP does not localize to the nucleolus or even to the nucleus, whereas TRPV3-NoLS-GFP localizes to the nucleolus effectively (**Fig. 30a-b**). Similar results were also observed in other cells also, such as in F11 and MC3T3-E1 cells (**Fig. 31a-b**). In all these cases, TRPV3-NoLS-GFP is also enriched in the nucleolus. Histogram analysis also suggests the same.

2.3.3 hTRPV3-NoLS colocalizes with nucleolar markers but not with other nuclear markers

To confirm the localization of TRPV3-NoLS at the nucleolus, TRPV3-NoLS-GFP or TRPV3-NoLS-RFP in different cells were expressed and probed with different nuclear markers (**Fig. 32**). TRPV3-NoLS-GFP does not colocalize with Lamin A-RFP when co-expressed in MC3T3-E1 cell (**Fig. 32a**). In the same cell line, TRPV3-NoLS-RFP colocalizes well with Fibrillarin-GFP (**Fig. 32b**). In HaCaT cells, TRPV3-NoLS-RFP colocalises with Fibrillarin-GFP, exclusively in the nucleolus (**Fig. 32c**). Similarly, TRPV3-NoLS-GFP colocalizes with endogenous Fibrillarin in Raw264.7 cells as detected by the antibody staining (**Fig. 32d**).

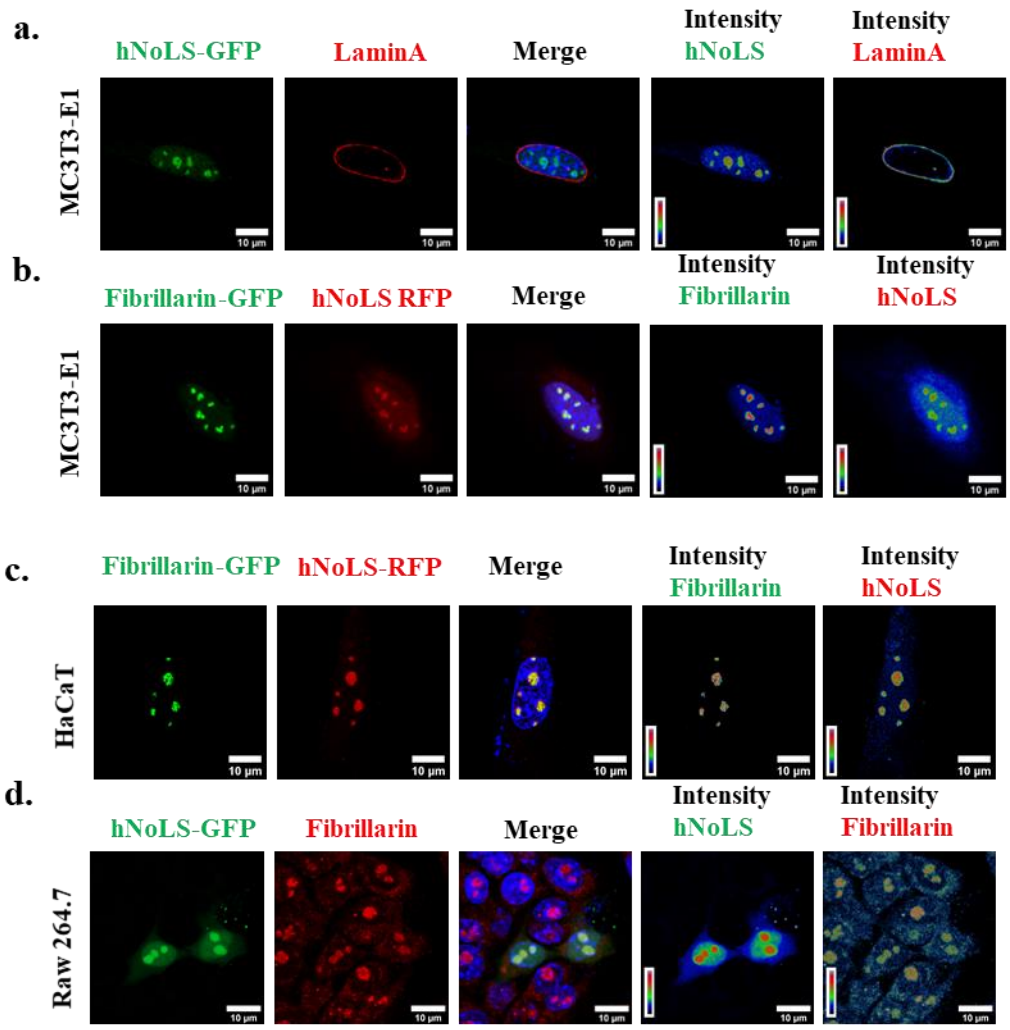

Fig 32. hTRPV3-NoLS colocalizes with the nucleolar markers in different cells. a-b. hTRPV3-NoLS-GFP colocalized with nucleolar marker fibrillarin, both in RAW 264.7 (a) and HaCaT (b) cells. The intensity profile of TRPV3 along with fibrillarin shown in the extreme right panel. **c.** TRPV3-NoLS does not co-localized with Lamin A in MC3T3 cells. **d.** hTRPV3-NoLS-RFP colocalized with nucleolar marker fibrillarin-GFP in MC3T3 cells. Scale bar 10µm.

To confirm if the localization of TRPV3-NoLS is predominantly in the nucleolus and not in other parts of the nucleolus, TRPV3-NoLS-RFP along with CENPA-YFP or H2A-GFP were co-expressed in HaCaT cells. In both cases, TRPV3-NoLS-RFP does not colocalize with these two markers (**Fig. 33a-b**). TRPV3-NoLS-GFP does not colocalize with Lamin A-RFP either (**Fig. 33c**). However, TRPV3-NoLS-GFP significantly colocalizes with Fibrillarin, as detected by the antibody staining (**Fig. 33d**).

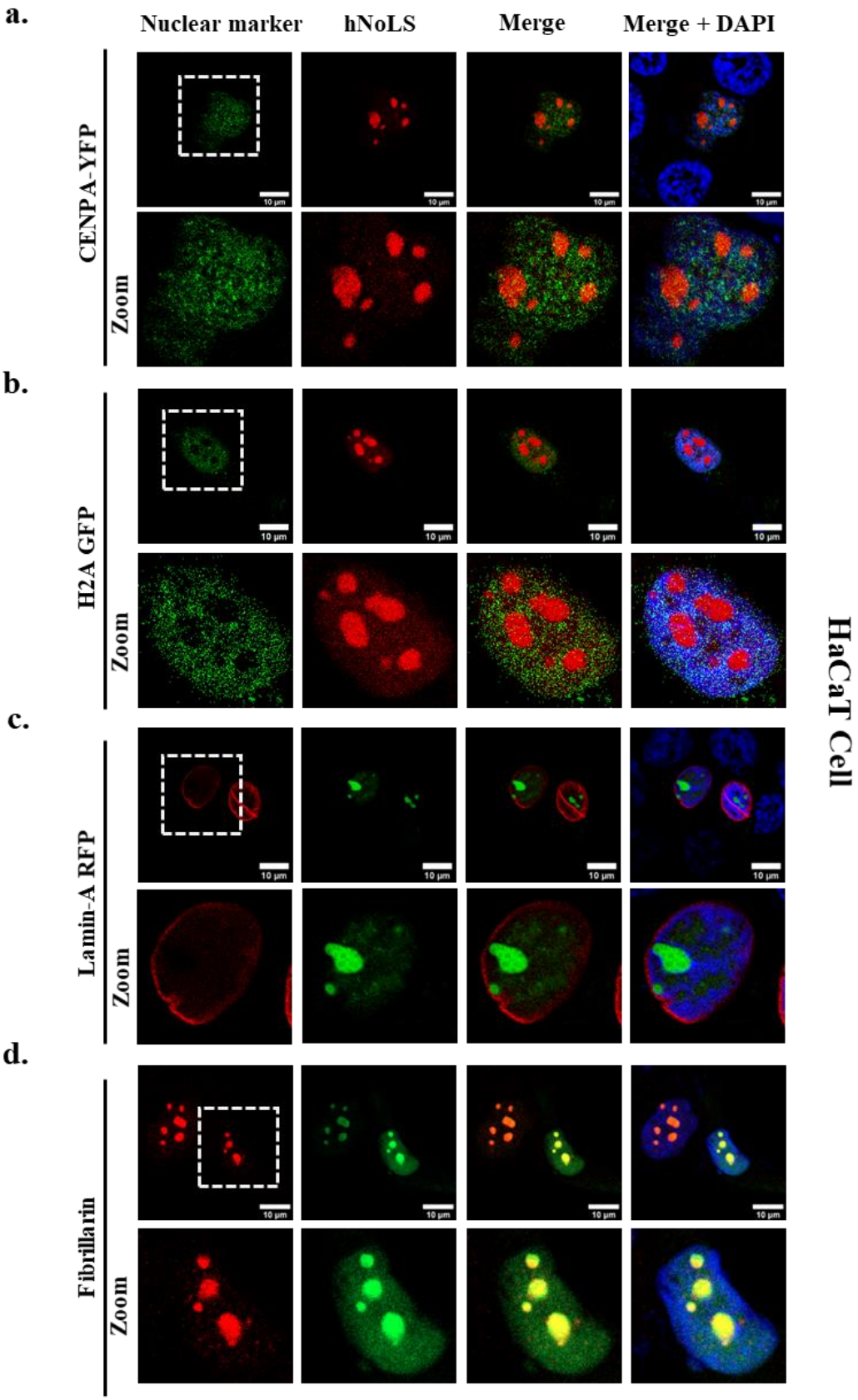

Fig 33. hTRPV3-NoLS colocalizes with nucleolar markers only. Shown are the confocal images of HaCaT cells expressing hTRPV3-NoLS (either as GFP- or RFP-tagged) along with different markers, such as CENP-A-YFP, LaminA-RFP, H2A-GFP or Fibrillarin-RFP. Extensive colocalization between hTRPV3-NoLS-GFP with Fibrillarin-RFP is observed. Scale bar 10μm.

2.3.4 The hTRPV3-NoLS-GFP is modestly static within the nucleolus

Next the dynamics of TRPV3-NoLS-GFP within the nucleolus of HaCaT cells were analysed. For that purpose, Fluorescence Recovery After Photobleaching (FRAP) experiment was performed and TRPV3-NoLS-GFP was expressed in HaCaT cells (**Fig. 34**). As control, Fibrillarin-GFP and only GFP were used. It was observed that TRPV3-NoLS-GFP gets bleached efficiently and recovers late. Comparative analysis suggests that TRPV3-NoLS-GFP is more static that only GFP but less static than Fibrillarin-GFP. Analysis of lowest intensity point after bleaching, fluorescence intensity at the end of the experiment and $t_{1/2}$, all suggests that TRPV3-NoLS-GFP is fairly static within the nucleolus (**Fig. 34a-d**).

2.3.5 NoLS of TRPV3 has evolutionary origin and is more conserved in mammals

To analyse the evolutionary nature of this NoLS, sequence alignment of hTRPV3-NoLS among many vertebrates was performed. It was found that this sequence is fairly conserved in higher vertebrates, especially in mammals (**Fig. 35)**. This NoLS motif is either not conserved or not present in many lower vertebrates (with some rare exceptions). Comparative analysis of sequence analysis indicates that of TRPV3-NoLS is less conserve than the full-length TRPV3 when all vertebrates were analysed (**Fig. 35c**). However, in mammals, the same TRPV3-NoLS region is more conserved than full-length TRPV3 (**Fig. 35d**). These findings suggest that the NoLS region is under strong selection pressure in mammals as compared to other species.

2.3.6 TRPV3-NoLS from different species are able to localize in the nucleolar region:

In order to understand the true potential of TRPV3-NoLS region from different species to be localized in the nucleolus, NoLS sequences from different species (human, chicken, turtle, amphibian and fish) were generated and expressed all these NoLS as GFP-tagged proteins in

HaCaT cells and monitored their localization as well as enrichment within the nucleolus (**Fig. 36**). In all cases (except human), the expressed proteins are also present in cytosol, often in nucleolus. But the best enrichment is observed in case of TRPV3-NoLS (Human). This data also indicates that the enrichment within the nucleolar region matches to some extent on the predicted score of the NoLS.

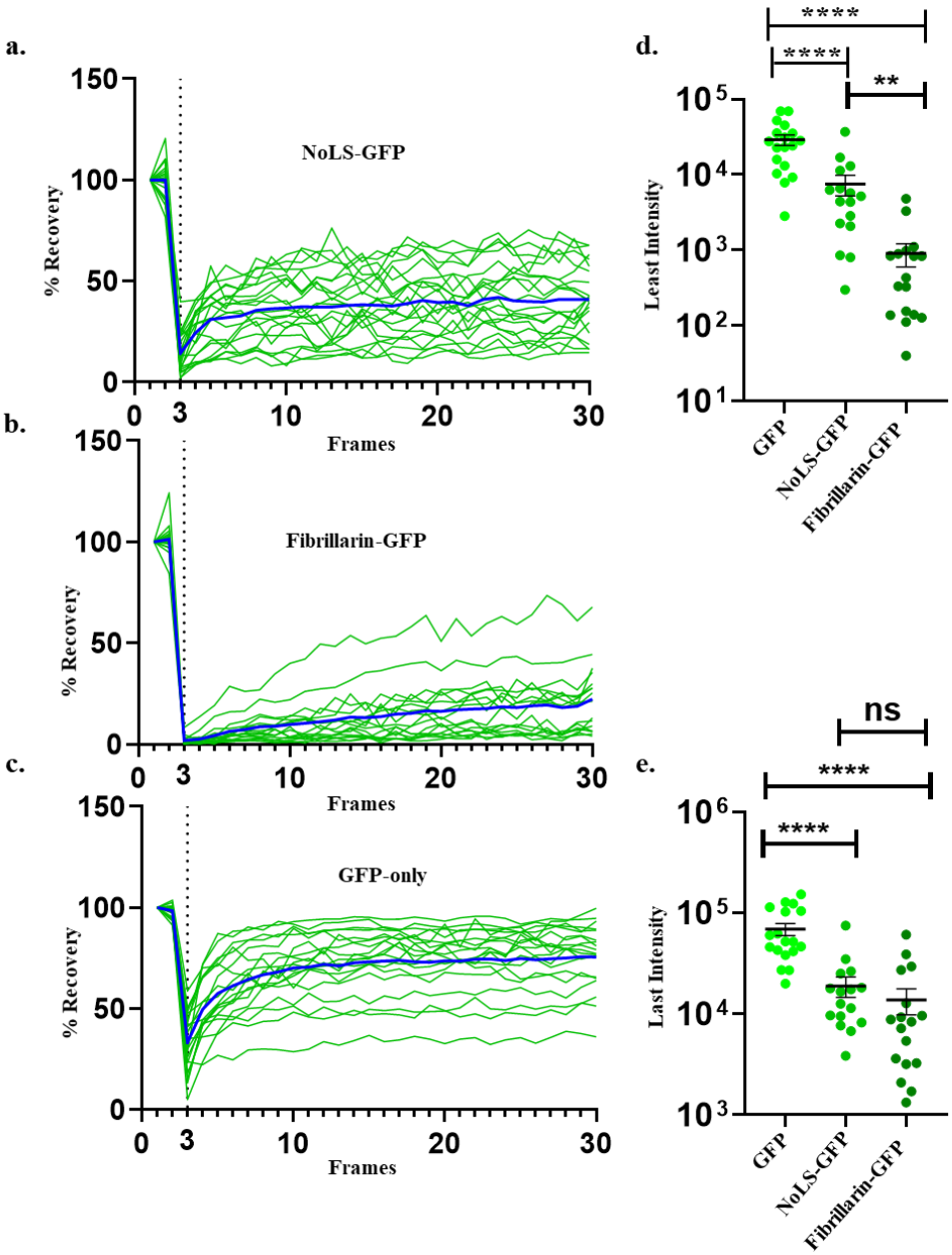

Fig 34. The hTRPV3-NoLS-GFP is modestly static within the nucleolus. a-c. Shown are the FRAP analysis of hTRPV3-NoLS-GFP (a) or Fibrillarin-GFP (b) and only-GFP (c) in Raw 264.7 cell. The recovery rate of hTRPV3-NoLS-GFP is more than Fibrillarin-GFP, but less than only GFP. **d-e.** These graphs represent the comparatives among hTRPV3-NoLS-GFP, Fibrillarin-GFP and only-GFP fluorescence intensities. The "least fluorescence intensity" (just after photo bleaching) (d) and "fluorescence intensity at the end of the experiment" (e) are shown. The least fluorescence intensity of hTRPV3-NoLS-GFP is significantly more than Fibrillarin GFP but less than only GFP. Unpaired t-test. **** = p <0.0001, ** = p <0.01.

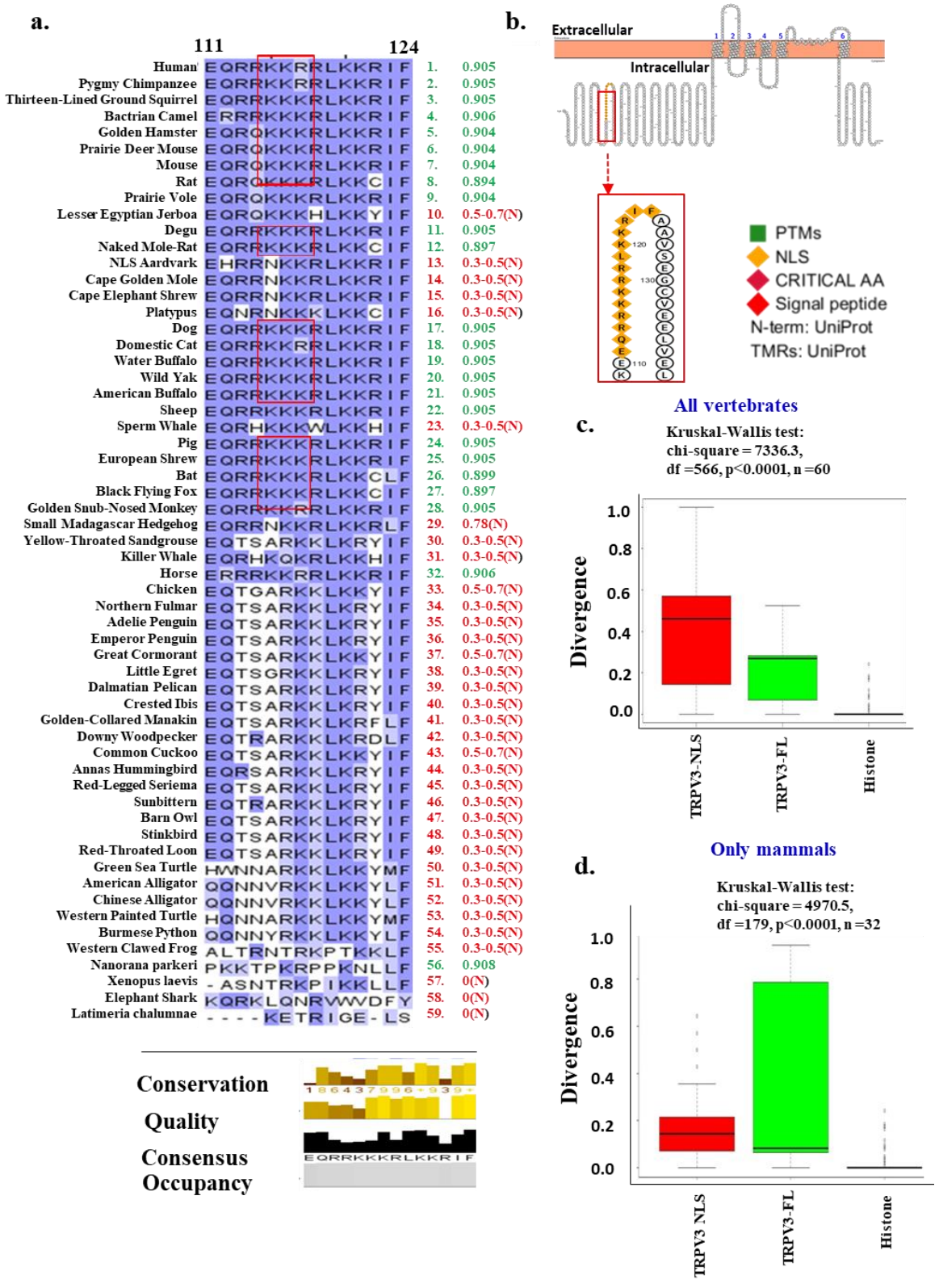

Fig 35. The NoLS of TRPV3 is conserved in mammals and semi-conserved in lower vertebrates. **a.** hTRPV3-NoLS motif is mostly conserved in mammals. **b.** A schematic representation of the NoLS sequence (aa 112-124) in hTRPV3 is shown. **c-d.** Conservation analysis of the NoLS and full-length TRPV3 from multiple vertebrates (total 59 sequences) and only mammals (32 sequences) are shown. A Full-length Histone sequence is used as a reference for a highly conserved protein. The NoLS of TRPV3 is highly conserved in mammals.

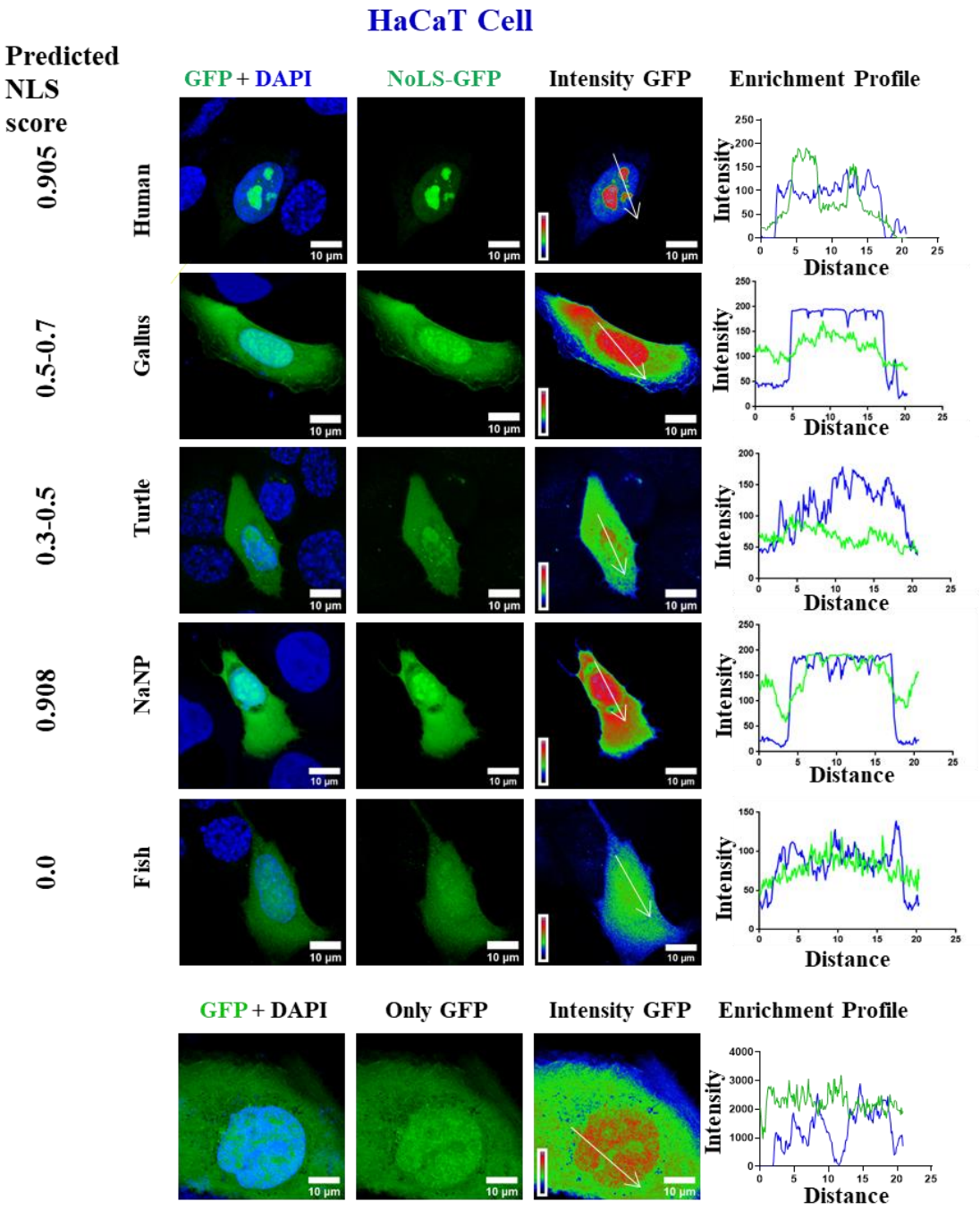

Fig 36. The NoLS from different species are able to localize and or gets enriched in the nucleolar region. Expression of TRPV3-NoLS-GFP of different species in HaCaT cell are shown. The enrichment profile through the nucleolar area is also shown in the right side. The predicted score of different species indicated in the left side. Scale bar 10µm.

2.3.7 Both TRPV3 modulation and LPS-signalling alters the spatio-temporal thermal map of the nucleus

In order to understand if TRPV3 modulation and/or LPS-signalling alter nuclear temperature, a Nuclear Thermo Green dye (NTGs, which is thermo-sensitive and localize

within the nucleus) was used. The fluorescence of this NTGs dye is inversely related to the temperature, thus fluorescence signal become more if the nuclear temperature become low (Liu et al. 2022). Isolated primary peritoneal macrophages were treated for TRPV3 activation as well as for inhibition by using specific pharmacological agents (FPP and DPTHF respectively), both in presence and absence of LPS. The NTGs signals from these cells were quantified, classified and compared (**Fig. 37a-b**). At resting condition, that NTGs signal within nucleus remain heterogeneous (suggesting differences in the temperature) and is mainly absent at the nucleolus region. In resting condition, both TRPV3 activation as well as inhibition results in increased fluorescence per nucleus, suggesting lowering of the overall temperature of the nucleus. Only LPS-stimulation results in increased fluorescence, thus temperature decreased as compared to control. In LPS-stimulated condition, TRPV3 inhibition results in increased fluorescence, thus lowering the temperature. However, in LPS-stimulated condition, TRPV3 activation does not results in any change in the fluorescence.

The entire NTG fluorescence from individual nucleus were classified in 6 categories based on the pixel-wise fluorescence intensity. In Gr I: the number of pixels per nucleus that have no fluorescence intensity was quantified. This number mainly represents the part of the nucleus where NTG-fluorescence is completely absent (such as nucleolus, NTG dye does not label the nucleolus region). In GrII: the pixels per nucleus which has fluorescence intensities in the range of 1-50 was quantified. Similarly, values for GrIII, GrIV, GrV and GrV1 were quantified and these groups have fluorescence intensities in the range of 51-100, 101-150, 151-200, 201 and above respectively. Thus, the entire NTG fluorescence of the nucleus is contributed by GrII, GrIII, GrIV, GrV, and GrVI. In this classification, GrII represents hotter region of the nucleus and GrV1 represent the coldest region of the nucleus. The comparative data suggests that both LPS-stimulation/signalling alters the thermal map of the nucleus significantly (**Fig. 37**).

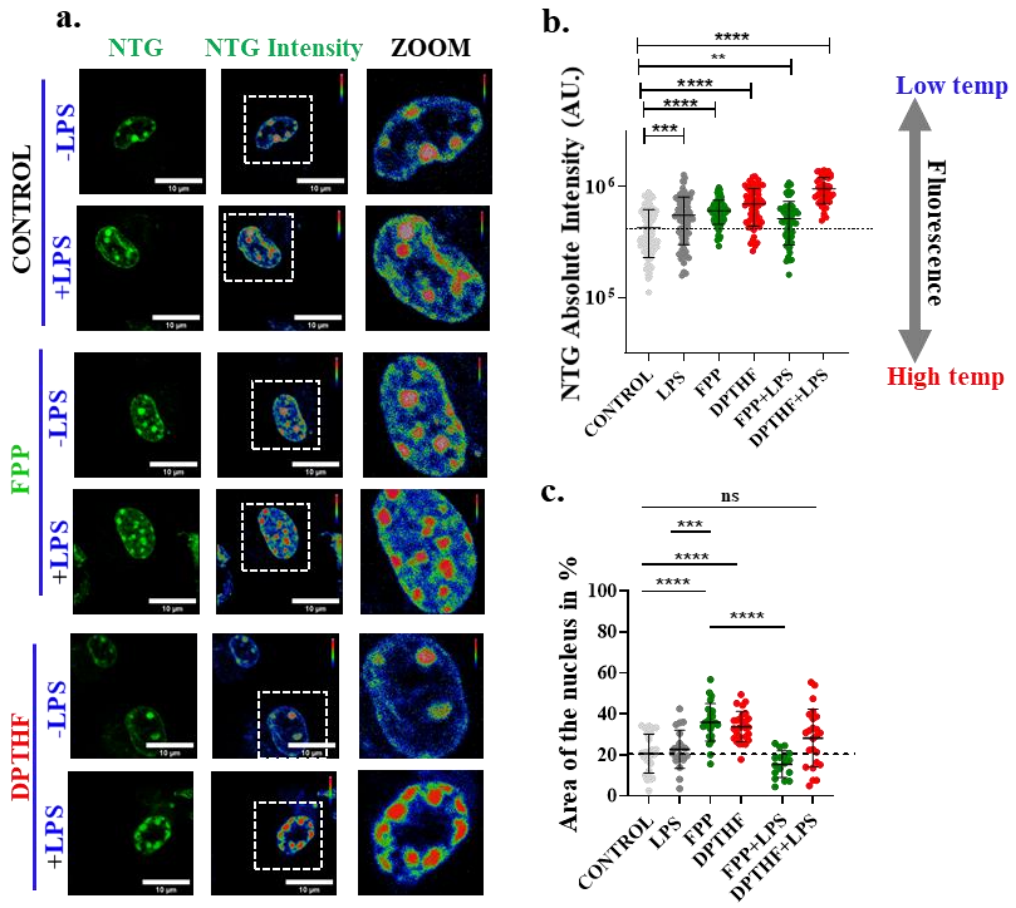

Fig 37. TRPV3 activation alters spatio-temporal thermal pattern of the nucleus. a. These live cell confocal images show the fluorescence pattern of peritoneal macrophage cells loaded with NTG-dye. The fluorescence pattern within the nucleus varies according to the TRPV3 modulation (FPP, DPTHF) and/or LPS stimulation. Red region indicates the highest fluorescence and thus lowest temperature. In opposite, blue regions indicate lowest fluorescence and thus highest temperature. The black regions indicate areas where NTG-dye is most-likely not present. Scale bar 10µm. **b.** The graph shows the fluorescence intensity of NTG dye per nucleus in different conditions. The increases in intensity indicates less temperature and lower fluorescence intensity represents higher temperature. On an average, both TRPV3 modulation and/or LPS stimulation cools the nucleus (n≥50). **c.** The graph represents the area of the nucleus (expressed in %) that has "zero-intensity" (derived from individual pixel values) of NTG in different modulated conditions (n≥18). One-way ANOVA test, **** = $p \leq 0.0001$, *** = $p \leq 0.001$, ** = $p \leq 0.01$, ns = non-significant.

The number of pixels per nucleus which has no NTG signal was quantified and this value remain variable in different conditions. Especially, in LPS-stimulated condition, due to TRPV3 activation, more number of pixels become cooler and less number of pixels become hotter. The local temperature of regions where TRPV3-NoLS is localized were analysed. For that purpose, TRPV3-NoLS-RFP or only RFP were expressed in HaCaT cells (**Fig. 38a-d)**.

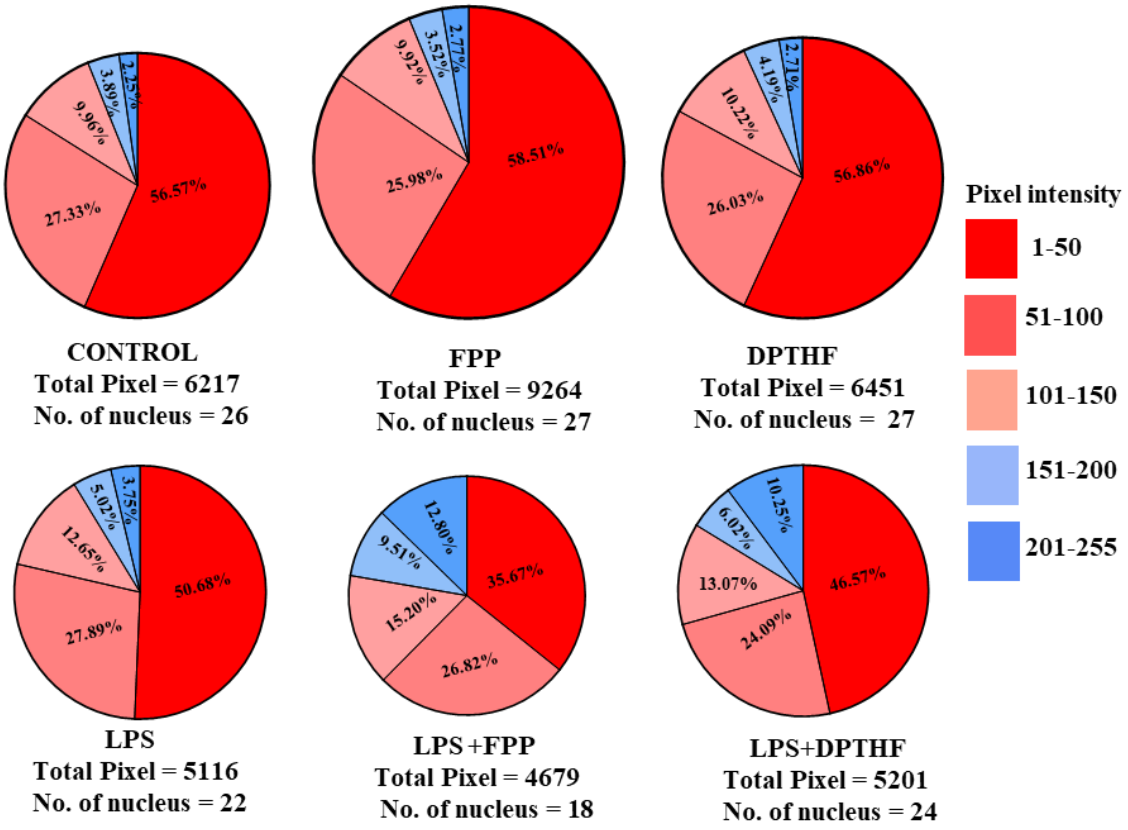

Fig 38. TRPV3 activation in LPS-stimulated condition cools larger area of nucleus. The graph shows the pie-chart plot of % of average pixel numbers with different NTG fluorescence intensities in different conditions (resting as well as TRPV3 activation or inhibition, in absence or in presence of LPS stimulations). The entire NTG-fluorescence spectrum (range 1-255) is classified in five groups as per the values (indicated in the right side). In case of LPS stimulation and TRPV3 activation, majority of the nuclear area becomes cool and less regions remain hot.

Only RFP is more homogenously distributed within the nucleus. Notably, the immediate vicinity of the nucleolar region has more NTG fluorescence, suggesting that the nucleolar periphery is “relatively cold”. In contrast, TRPV3-NoLS-RFP is mainly localized in the areas where NTG-dye-mediated fluorescence is very low or absent. The overall NTG fluorescence of the cells expressing TRPV3-NoLS-RFP is more, suggesting lowering the temperature.

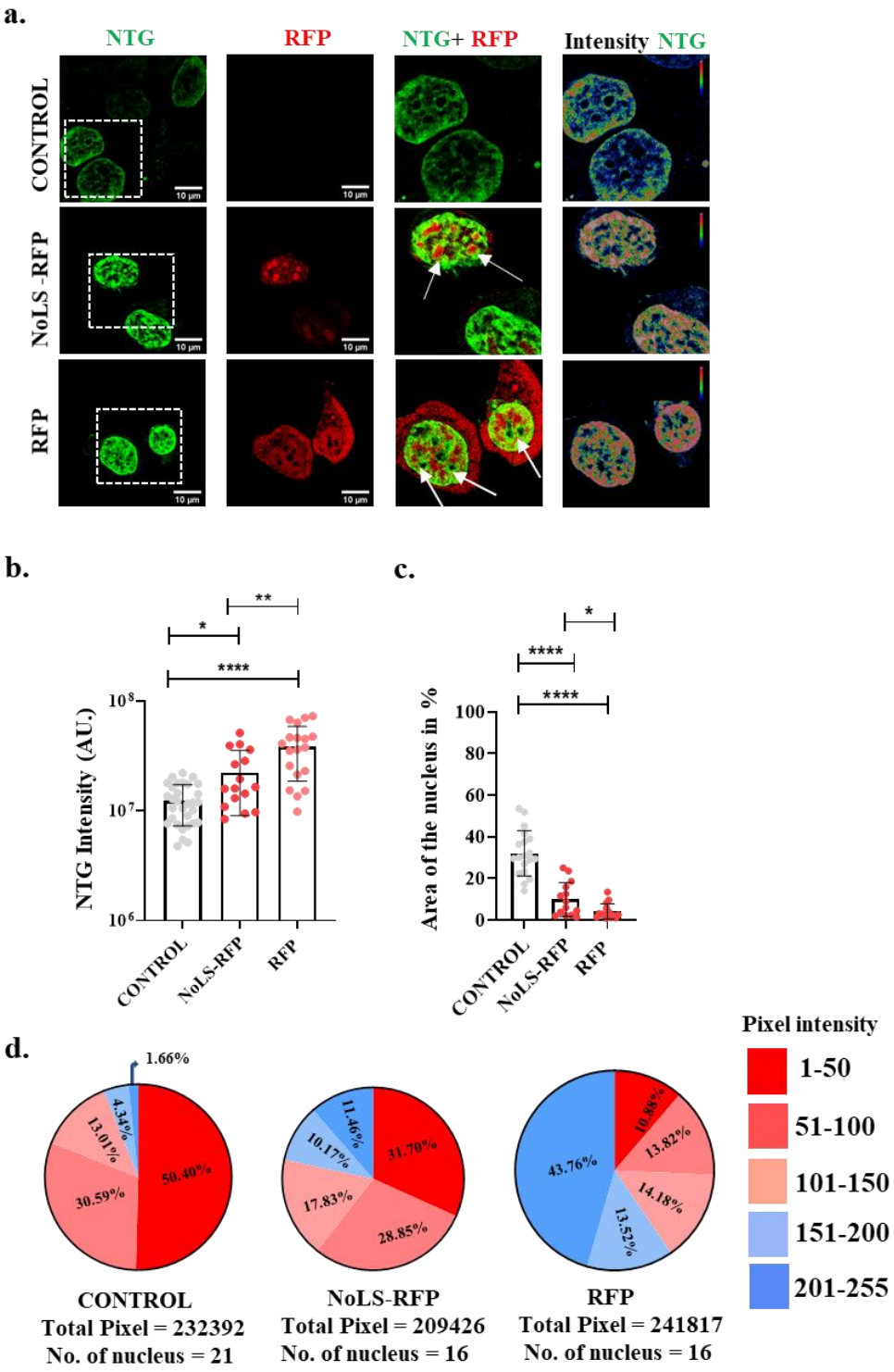

Fig 39. Expression of NoLS-GFP alters the spatio-temporal thermal pattern of the nucleus. a. These live cell confocal images represent NTG-fluorescence (green) within the nucleus of non-transfected HaCat cells or cells expressing transiently NoLS-RFP or RFP only (Liu et al.2022). Scale bar 10µm. **b.** The graph shows the NTG fluorescence intensity in control nucleus or nucleus expressing NoLS-RFP or RFP-only. The increase in fluorescence intensity means lowering of temperature, and decrease in fluorescence intensity represents increment in temperature. **c.** The graph represents the area of the nucleus (expressed in %) that has "zero-intensity" (derived from individual pixel values) of NTG in different modulated conditions. **d.** The graph shows the pie-chart plot of % of total pixel with different NTG fluorescence intensities in control cells or cells expressing NoLS-RFP or RFP-only. The red indicates the % of area that is hottest and blue indicates the % of nuclear area that is coolest. Unpaired t-test. * = $p \leq 0.05$; ** = $p \leq 0.01$; **** = $p \leq 0.0001$).

2.4 The importance of TRPV3 as a regulator of the cellular stress response

TRP channels, known as Transient Receptor Potential channels, are essential cellular sensors for stress responses, including hyperthermia (elevated body temperature). When cells face stressors like temperature changes, TRP channels become active and trigger various reactions in the cell. In the context of hyperthermia, they can affect inflammatory responses, immune activation, and the production of reactive oxygen species and cytokines like IL-6 and TNF-α (Welc et al. 2012). TRP channels, such as TRPV3 seem to be involved in sensing heat stress. While their exact role in human heat stress is not fully understood, studies suggest they might play a part in temperature regulation, with potential implications for cooling and overheating mechanisms. Further research is needed to clarify their precise involvement in human heat stress responses.

2.4.1 The cellular parameter changes according to increasing temperature-induced stress

The activation temperature of TRPV3 is around 33-39°C (Chung et al. 2005; Xu et al. 2002). When the macrophage cells are treated with different temperatures at the range of 37°C to 42°C (hyperthermic temperature), the cells behave differently (and parameters change accordingly) due to thermal stress. As the temperature increased from 37°C to 42°C, the viability of the cells as well as the adhered cell numbers decreased.

It has also been found that as the temperature increased to 42°C (hyperthermic temperature), the lysosomal status (lysosomal pH) compromised drastically, i.e., the lysosomal intensity (detected by using LysoSensor Green) decreased (**Fig. 40c**). At the same temperature, the cytosolic pH also decreased (**Fig. 40a&e**). This data shows that as the temperature increased to a hyperthermic condition, the cellular pH level compromised (less acidic), and lysosomal pH became less acidic (**Fig. 40c&e**). Few other cellular parameters were also tested, and it was found that both the cytosolic Ca^{2+}-level and the cytosolic ROS level increased at

hyperthermic stress (**Fig. 40b & d**). All these data show that as the temperature increased to hyperthermic (42°C) condition, the lysosomal pH and cytosolic pH alters, i.e., the pH became less acidic at cytosol and become more basic in lysosome.

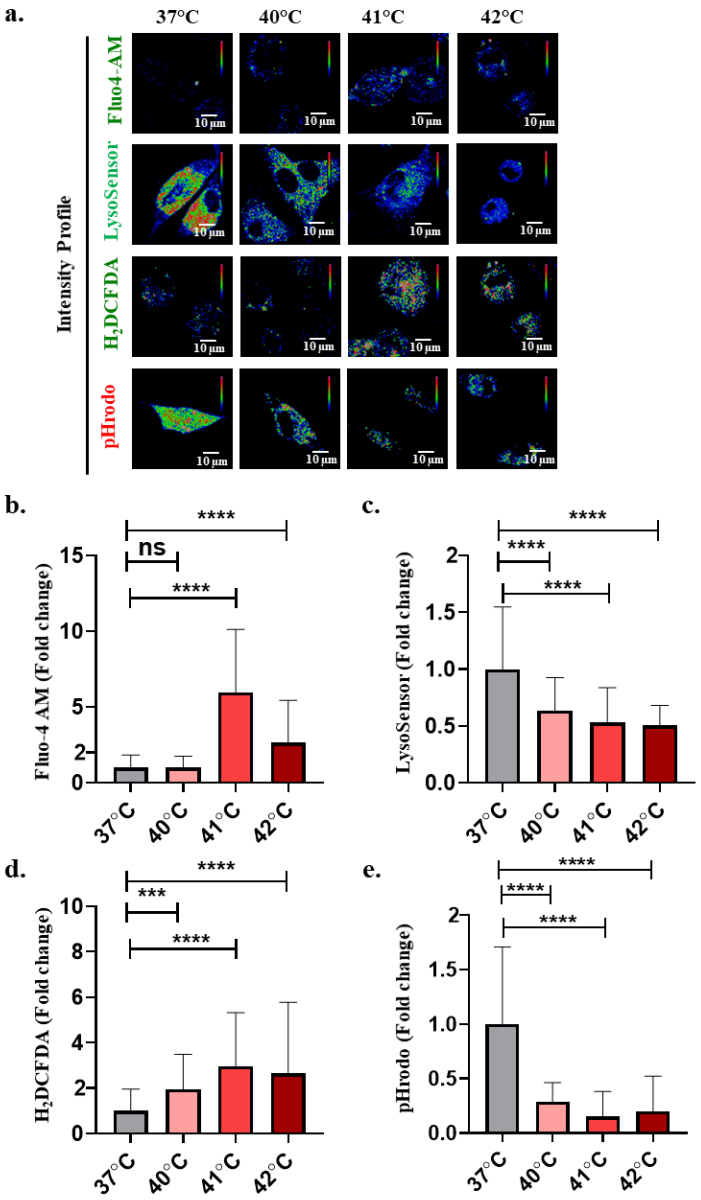

Fig 40. Temperature-sensitivity of the murine peritoneal macrophages (PM). a. Representative images of Fluo4-AM, LysoSensor Green, H_2DCFDA, or pHrodo-loaded PM at different temperature conditions; Scale bar: 10µm. **b.** Quantification of Fluo-4-AM in different hyperthermic conditions for different time interval are shown. **c.** Quantification of LysoSensor Green fluorescence intensity (fold change) in PM exposed to different temperature and for different durations are shown. **d-e.** Quantification of pHrodo and H_2DCFDA intensity in each temperature condition (fold-change) are shown. Values are means ± SD, n = 100 or more cells per conditions; One-Way ANOVA; *** = $p \leq 0.001$, **** = $p \leq 0.0001$ and ns = non-significant).

2.4.2 At hyperthermic stress, the lysosomal status is compromised, which is rescued by TRPV3 modulation

As mentioned earlier, at hyperthermic stress, the lysosomal status is compromised and most of the lysosomes remain undetectable (by using LysoTracker Red dye) at 42°C conditions. To explore the effect of TRPV3 modulation on the lysosome, the cells were subject to heat shock at 42°C for 2 hours along with the TRPV3 modulations by pharmacological agents (FPP as activator, DPTHF as inhibitor, and DMSO as vehicle control) (**Fig. 41, Fig. 42, Fig. 43**). It has been found that TRPV3 activation rescues lysosomes, thus the lysosomal intensity is recovered and become comparable to the normal level, suggesting TRPV3 activation causes lysosomes to be more acidic (**Fig. 41, Fig. 42**). At 42°C, TRPV3 activation also increases the lysosomal number. This is confirmed by using two different approaches, i.e. by Lamp1 antibody-based staining as well as by using the LysoTracker Red labelling (**Fig. 41, Fig. 42**). The number of lysosomes decreased as the cells were treated with hyperthermic stress. However, as the cells were simultaneously treated with the TRPV3 modulator, especially TRPV3 activator (FPP, 1μM), the lysosomal numbers increased (**Fig. 41c**). Apart from that, the colocalized pixel number also become more in case of TRPV3 modulation as compared to the vehicle control condition (**Fig. 41b**). Thus, the data suggests that TRPV3 activation helps in rescuing the lysosomal acidic pH and thus helps in maintaining the lysosomal status.

In the same hyper-thermic shock condition, the lysosomal function (as measured by total LysoTracker Red labelling within the cell as a factor of their acidic environments) is lowest (i.e. in the absence of any pharmacological modulation), suggesting a drastic loss of lysosomal function at hyper-thermic conditions. This loss-of-lysosomal function can be rescued partially by the presence of LPS only, and almost fully by TRPV3 modulation by pharmacological means (**Fig. 42**). This suggests that pharmacological modulation of TRPV3 is beneficial (if not crucial) in hyper-thermic conditions. Quantification of individual

lysosomes for their LysoTracker Red labelling suggests overall loss of lower pH in all lysosomes, at 42°C. However, in other conditions, the lysosomes with low pH (i.e. lysosomes with higher signal, i.e. AU > $2x10^4$) is observed, suggesting that TRPV3 modulation, both in the absence or in presence of LPS helps in the acidification of individual lysosomes (**Fig. 42d**). Notably, TRPV3 intensity in individual lysosomes are lowest in the resting condition (**Fig. 43e**). In hyper-thermic shock conditions, no significant difference is observed in the fluorescence intensity of TRPV3 in the lysosome, both in the absence or presence of LPS (**Fig. 43e**). However, the TRPV3-specific signal increases in both TRPV3 modulated conditions, i.e. in presence of activator or inhibitor (both in absence as well as in presence of LPS), reconfirming that pharmacological modulation of TRPV3 is helpful for the lysosomal functions (**Fig. 43e**). Accordingly, the ratio of lysosomal intensity with TRPV3 intensity is lowest in the resting condition and highest in the case of LPS stimulation (**Fig. 43f**).

To confirm if there is any correlation exists between lysosomal function and the presence of TRPV3 there, a correlation analysis has been performed. It has been observed that in all conditions, there is a strong correlation ($r > 0.9$) between lysosomal function (i.e. LysoTracker Red fluorescence intensity) and TRPV3 intensity (**Fig. 43g**). This strongly suggests that TRPV3 plays an important role in the lysosomal functions in all conditions tested in this work. However, the slope is least in case of resting conditions and steepest in the case of LPS-stimulation.

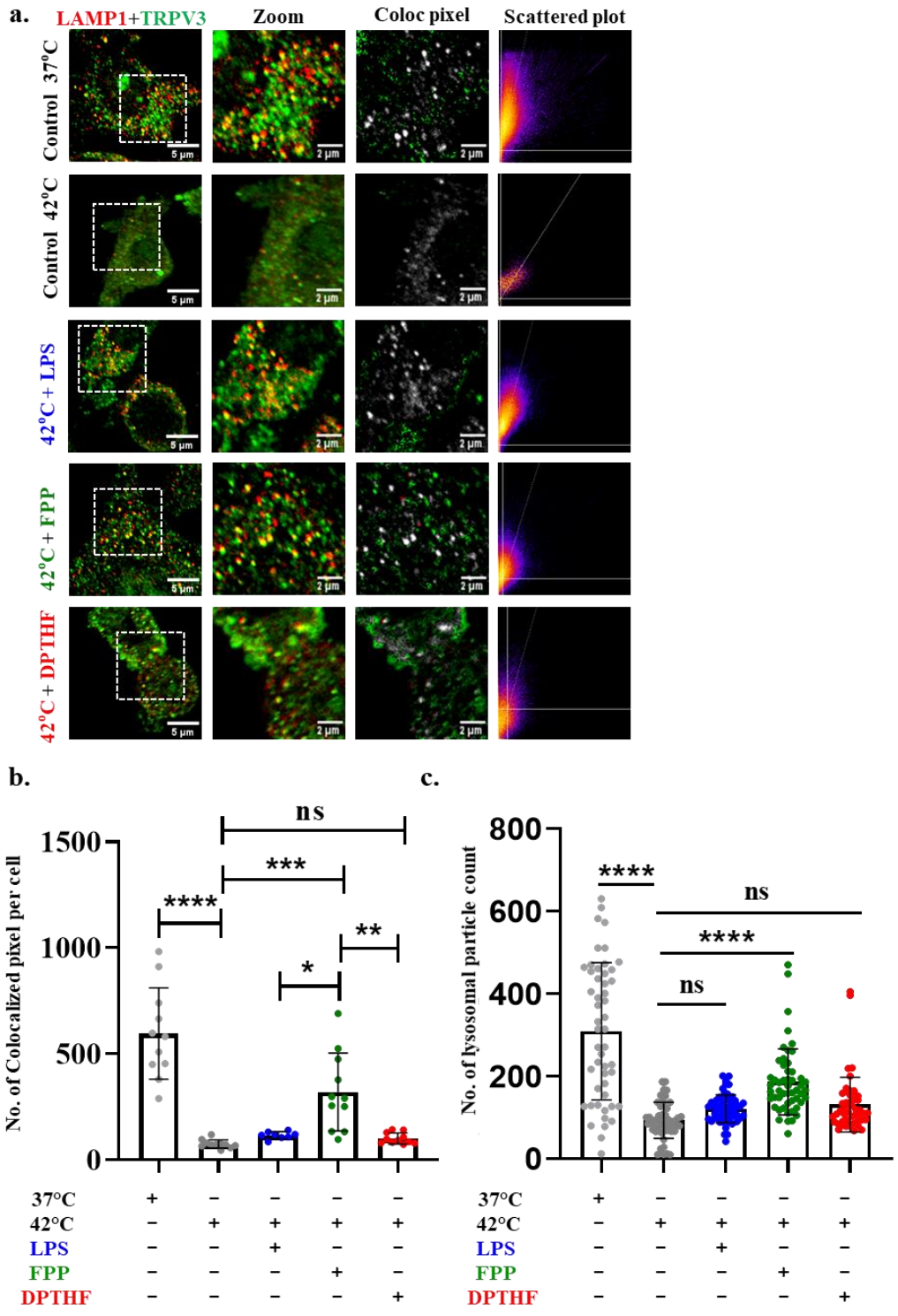

Fig 41. At 42°C, the majority of lysosomes are stressed and TRPV3 modulation rescues lysosomal count and colocalization with LAMP1. a. PM were exposed to 42°C, treated with TRPV3 modulators in different conditions, fixed and were subsequently immunostained for LAMP1 (red) and TRPV3 (green). TRPV3 modulation improves the lysosomal structure at 42°C. Scatter plots represent distribution of colocalised pixels and colocalized pixel are shown in grey color. Scale bar: 5µm; in zoom: 2µm. **b.** The quantification of colocalised pixels of TRPV3 and LAMP1 are shown in the graph. **c.** The graph shows the lysosomal particle numbers (counting LAMP1-positive particles) per cell as measured. The number of lysosomal particles per cell was counted through thresholding and using the particle counting plugin in the Fiji software. Values are means ± SEM, N ≥40 cells per group; one-way ANOVA; ns: non-significant, * = p ≤0.05, ** = p ≤ 0.01, *** = p ≤ 0.001, **** = p ≤ 0.0001.

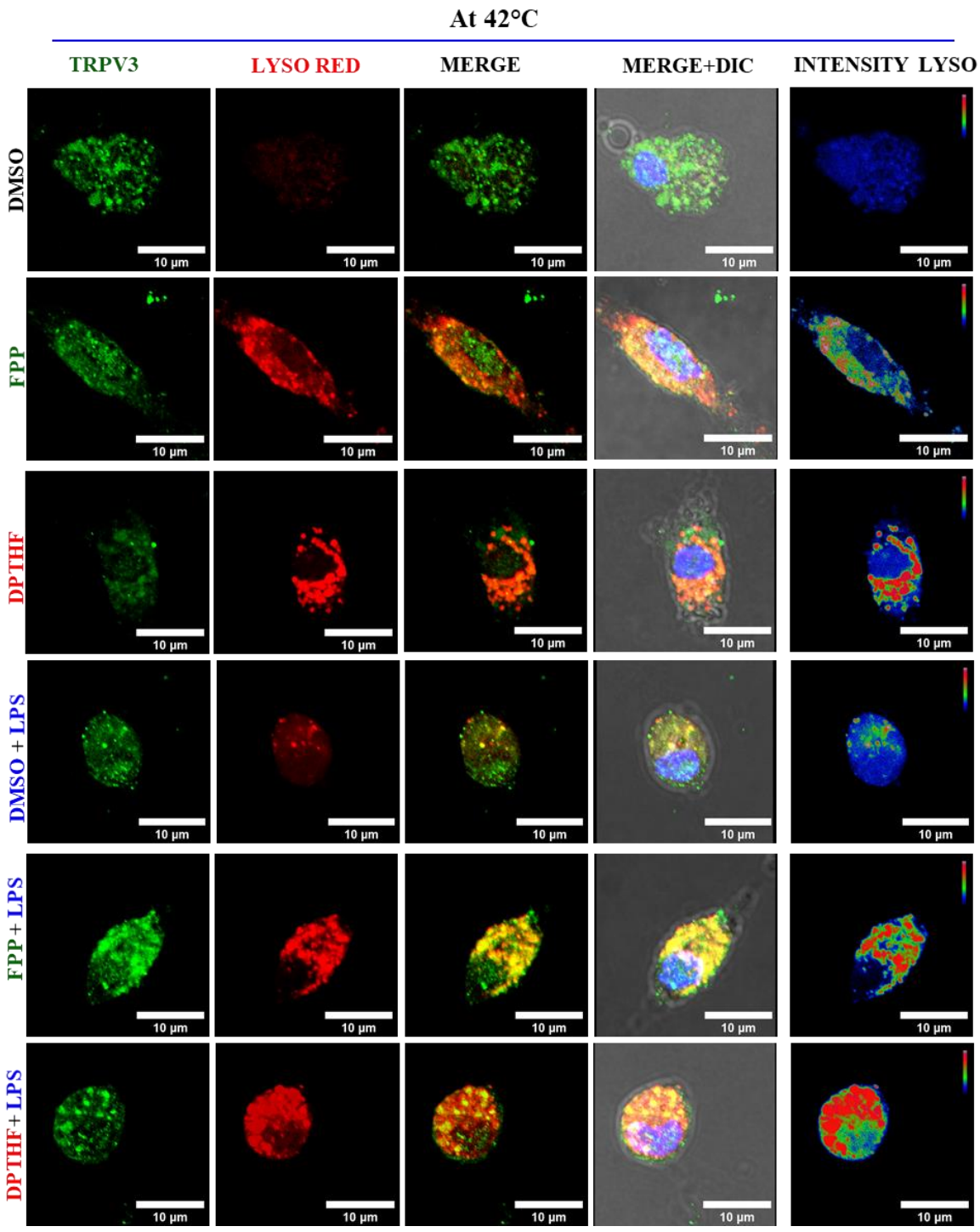

Fig 42. TRPV3 modulation rescue the lysosomal abnormalities induced by heat stress at 42°C. Shown are the confocal images of primary macrophages that are treated with or without LPS and modulated by TRPV3-specific activators or inhibitors. At 42°C, the primary macrophages lose the ability to get labelled by LysoTracker Red dye. This effect can be rescued by either activation or inhibition of TRPV3 by specific pharmacological modulators. The intensity of the LysoTracker Red is shown in pseudo color (the right most panel). Scale bar 10µm.

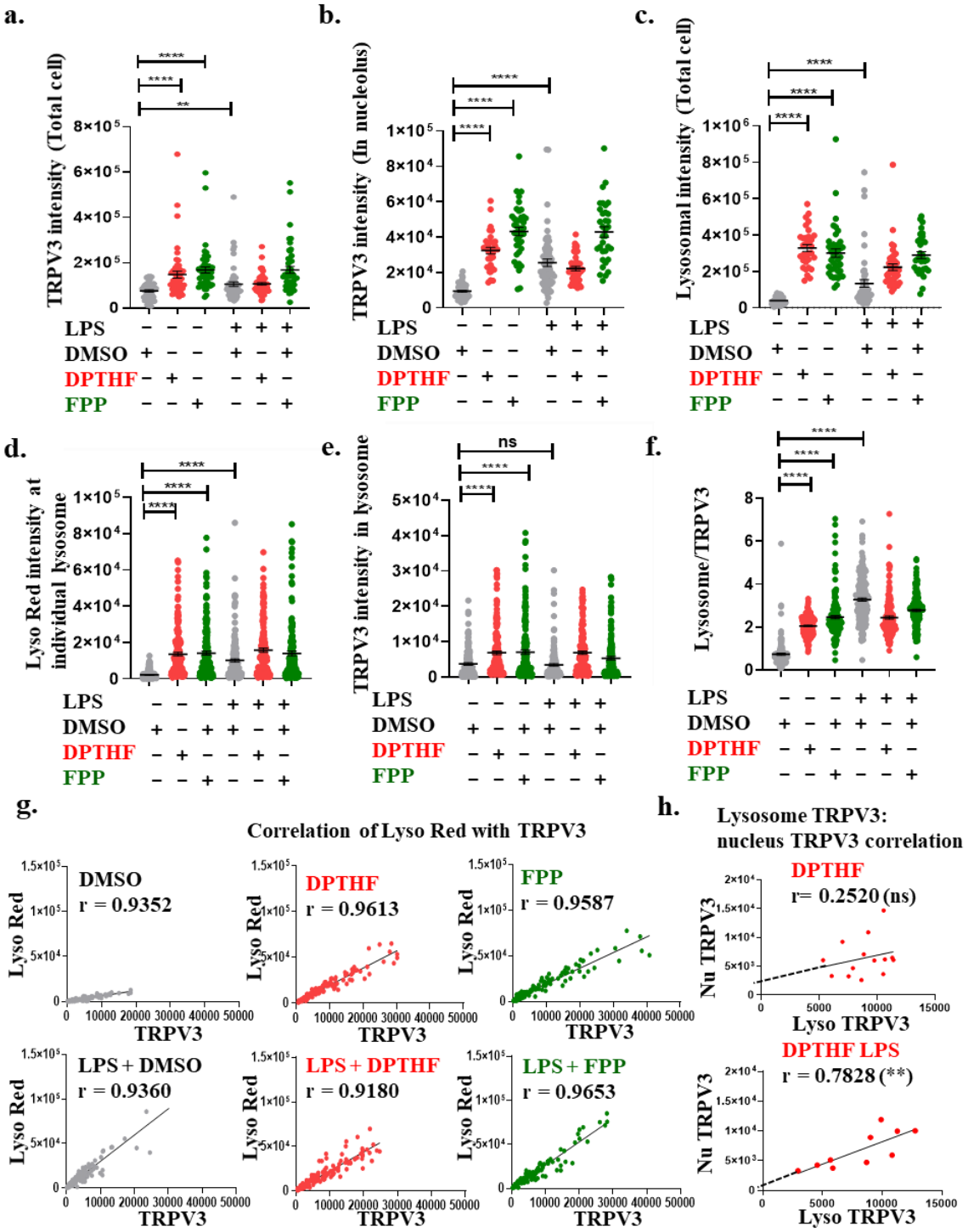

Fig 43. At higher temperature (hyperthermic condition), enrichment of TRPV3 in the nucleolus is dependent on the TRPV3 at the lysosome. For all these experiments, cells were maintained at 42°C. **a-c.** Shown are the intensity of the TRPV3 in the lysosome and nucleolus in the total cell in different conditions respectively. **d-e.** At 42°C, the labelling of lysosome by LysoTracker Red is minimum. This can be rescued by pharmacological modulation of TRPV3 and/or by LPS treatment. Shown are the total fluorescence intensities of lysosomes in individual lysosomes (d) and TRPV3 intensity in lysosomes in different conditions, respectively. **f.** In hyper-thermic condition, the lysosomal/TRPV3 intensity differs in different conditions. It is lowest in resting condition. In case of pharmacological modulation or LPS treatment, the Lysosomal/TRPV3 intensity increases, suggesting that lysosome function (equivalent to LysoTracker Red labelling) is dependent on TRPV3 modulation. **g.** Shown are the correlation between LysoTracker Red labelling with the presence of TRPV3 in the lysosome. In all cases, a tight correlation is observed with the lowest slope at resting condition. Shown are the correlation between TRPV3 in lysosome with the presence of TRPV3 in the nucleus (In case of DPTHF with and without LPS stimulations). One-way ANOVA, ** = $p \leq 0.01$, **** = $p \leq 0.0001$ and ns = non-significant).

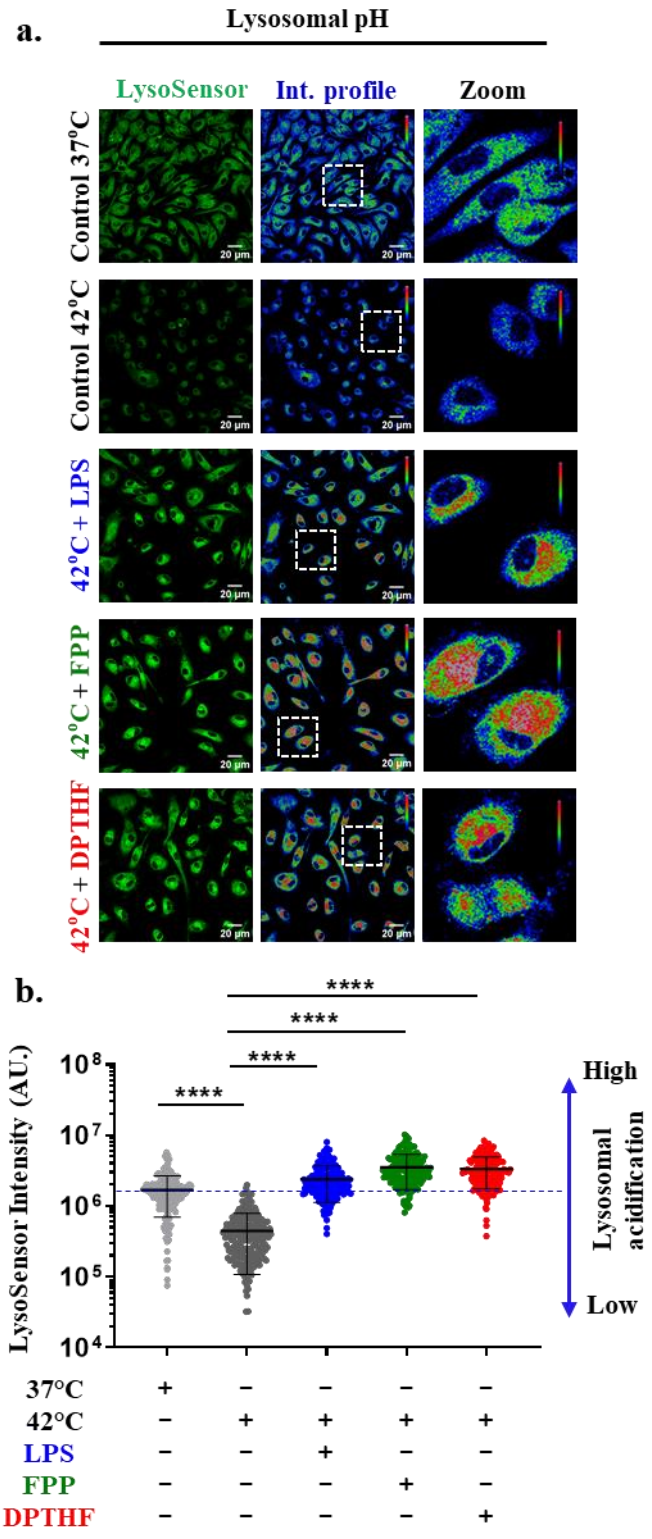

Fig 44. TRPV3 regulates lysosomal pH in hyperthermic conditions. a. Representative confocal images of cells labelled with LysoSensor Green in different conditions. Scale bar: 20µm. **b.** Quantitative analysis of cells labelled with LysoSensor Green in FPP, DPTHF or LPS-treated conditions at heat shock are shown. Values are means ± SEM, N ≥100 cells per group; one-way ANOVA; ns: non-significant, **** = < 0.0001.

2.4.3 TRPV3 modulation improves the lysosomal pH stressed by hyperthermic condition

At 42°C conditions, the lysosomal functions are compromised. So, the lysosomal pH has been measured by using LysoSensor Green dye in different conditions where TRPV3 function is modulated at hyperthermic conditions (**Fig. 44**). At 42°C, the LysoSensor Green intensity is low, indicating loss of lysosomal acidification. However, TRPV3 activation, as well as inhibition both causes significant increments in LysoSensor Green intensity, suggesting that at hyperthermic condition (42°C), pharmacological alteration of TRPV3 causes more acidification of lysosomes (**Fig. 44a-b**). Similarly, LPS-treatment (at 42°C) also increases the LysoSensor Green intensity, suggesting more acidification of lysosomes (**Fig. 44a-b**).

2.4.4 TRPV3 modulation helps in the maintenance of Ca^{2+} and pH levels in isolated lysosomes

Maintenance of lysosomal pH and lysosomal Ca^{2+} have been studied in lysosomes isolated from Raw 264.7 cells. The lysosome was isolated using the lysosomal enrichment kit (Thermo fisher scientific). Isolated lysosomes were labelled with the Ca^{2+}-indicator (Rhod 3) and lysosomal pH indicator (LysoSensor Green) (**Fig. 45a-c**). For this study, the isolated lysosomes were subjected to hyperthermic stress for 2 hours along with the TRPV3 modulators. The lysosomal pH increases (i.e., the LysoSensor Green-based fluorescence intensity reduces) when the lysosomal particles were subjected to 42°C stress. However, the fluorescence intensity increases significantly upon the TRPV3 modulation like FPP-treatment, as well as in the DPTHF conditions (**Fig. 45b**). Thus, the decreased LysoSensor Green intensity at 42°C hyperthermic condition can be rescued by the administration of TRPV3 modulatory agents. Along with the lysosomal pH, simultaneously the Ca^{2+}-status has been observed with the help of Rhod-3 dye. The Ca^{2+}-level decreased/dropped significantly while the lysosome was subjected to hyperthermic stress at 42°C.

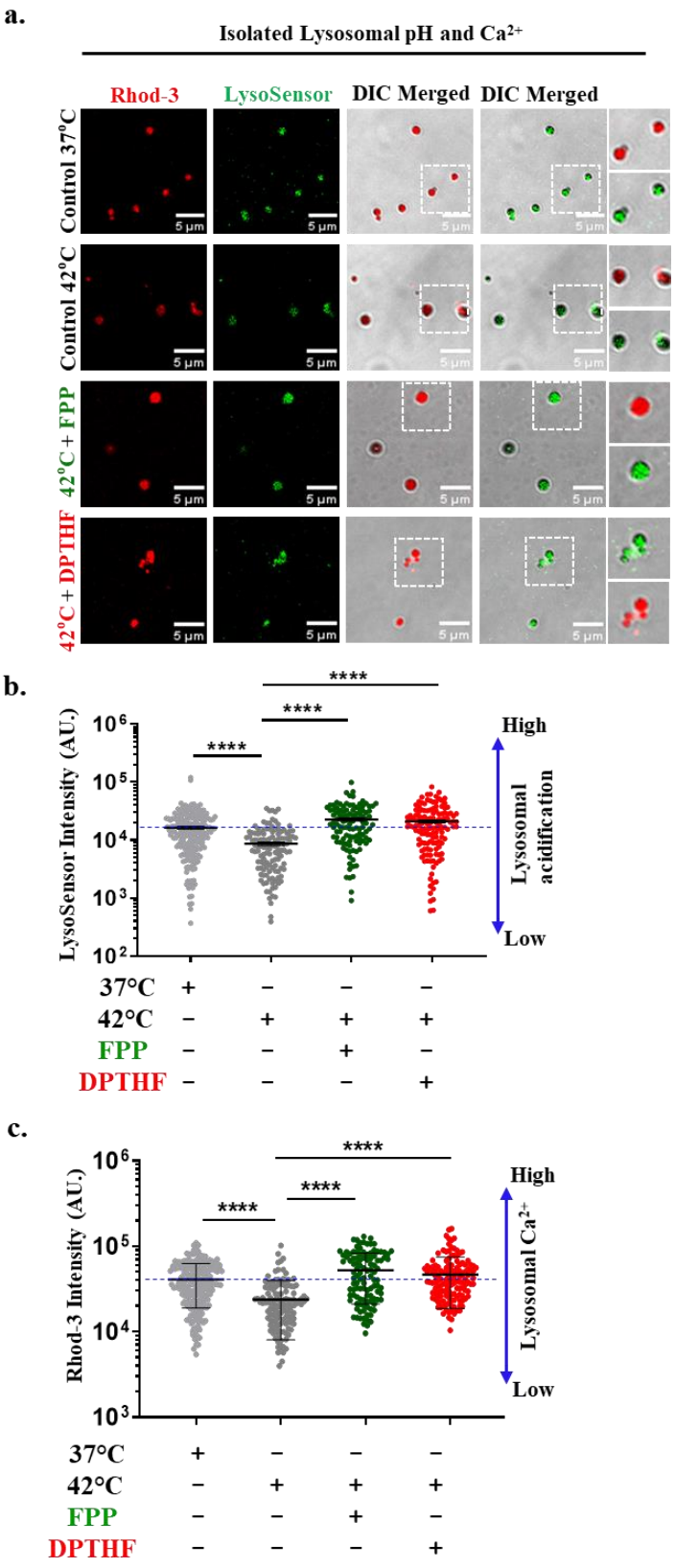

Fig 45. TRPV3 regulates lysosomal Ca^{2+} and pH in cell-free conditions. a. Representative confocal images of isolated lysosomes labelled with Rhod-3 and LysoSensor Green are shown. Lysosomes isolated from macrophages are maintained in control condition, at 42°C alone or in presence of FPP or DPTHF are shown. Scale bar: 5µm. **b-c.** Quantification of LysoSensor Green and Rhod-3 fluorescence intensities are shown. Values are means ± SEM; one-way ANOVA; ns: non-significant, and **** = $p < 0.0001$.

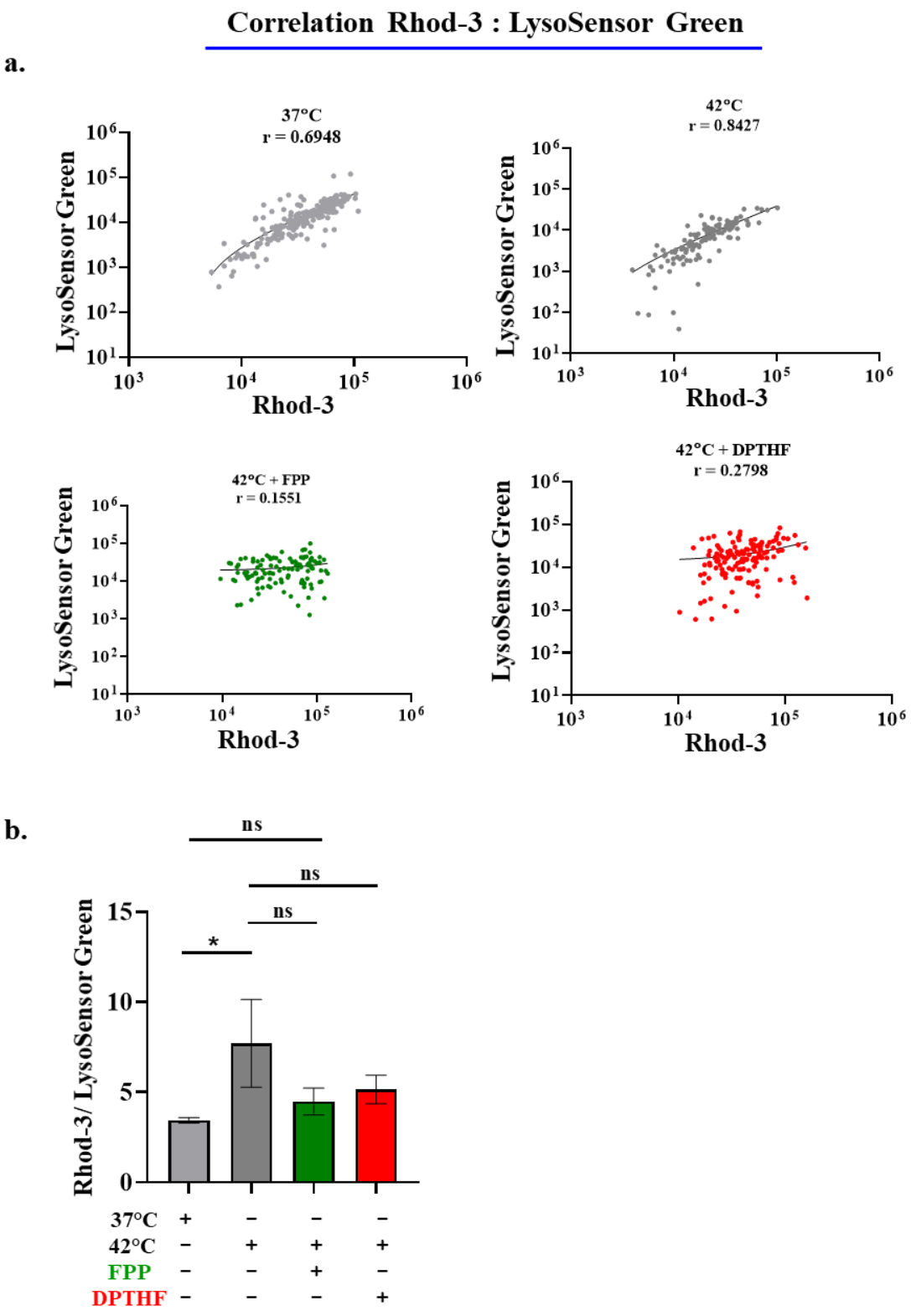

Fig 46. TRPV3 regulates lysosomal Ca^{2+} and pH in cell-free conditions. a. Correlation analysis of isolated lysosomes labelled with Rhod-3 and LysoSensor Green are shown. Lysosomes isolated from macrophages and were maintained in control condition, at 42°C alone or in presence of FPP or DPTHF. Correlation become stronger at 42°C control (r =0.8427) condition. **b.** Ratio of Rhod-3 and LysoSensor Green are shown. Values are means ± SEM; one-way ANOVA; ns: non-significant, and * = $p < 0.05$.

However, the Rhod-3 dye intensity increases significantly in the TRPV3 modulatory conditions, i.e. activation by FPP and inhibition by DPTHF-treated conditions (**Fig. 45c**). Correlation data of isolated lysosomes shows the Rhod-3 dye labelling and LysoSensor Green labelling are well correlated in all these conditions, but the maximum correlation is observed at 42°C and 37°C control conditions. The correlation was significantly lower in case of FPP at as well as in DPTHF at 42°C condition. Correlation was found to be more in case of 42°C control (r =0.8427) and 37°C control (r =0.6948) (**Fig. 46a**). The ratio between Rhod-3 and LysoSensor Green shows the significant changes in the 42°C hyperthermic stress but not in other conditions (**Fig. 46b**). Thus, collectively the results show that the TRPV3 modulations help in rescuing the lysosomal pH as well as the Ca^{2+}-level within the isolated lysosomes.

2.4.5 TRPV3 modulation is beneficial during inflammatory conditions

To check the status of damaged response proteins or the inflammatory response proteins, three markers have been explored. The characterized markers are NLRP3, TFEB, and NF-kB P65 respectively. NLRP3 is known to be an inflammatory marker whose expression increases upon cellular stress like thermal shock or bacterial stress (Kelley et al. 2019). Accordingly, the expression of NLRP3 puncta is more prominent or significant in the 42°C conditions as well as in the DPTHF or LPS at 42°C stress conditions. However, the expression level or the puncta's (particle counts) were not so prominent and significantly lower in case of TRPV3 activation at 42°C stress conditions (**Fig. 47a-b**).

Another lysosomal or cellular stress marker characterized is TFEB, whose expression/presence depends on the stress level (Sardiello. M. 2016). The TFEB protein translocates from cytosol to the nucleus upon cellular stress conditions. The TFEB localizes in the nucleus upon stress conditions, such as nutrient-deficient state and lysosomal dysfunction. Accordingly, more TFEB in the nucleus and less in the cytosol indicate more stress to the cell.

More TFEB in the cytosol then the nuclear TFEB is observed in healthy cells. In the activated condition, the TFEB nuclear localization is minimal, and the TFEB puncta were mostly found in the cytosol. This indicates that at activation condition, the cellular stress level is minimized, whereas in the DPTHF or control 42°C conditions are not able to rescue the cells from stress conditions as compared to FPP-treated conditions (**Fig. 49a-b, Fig. 50**).

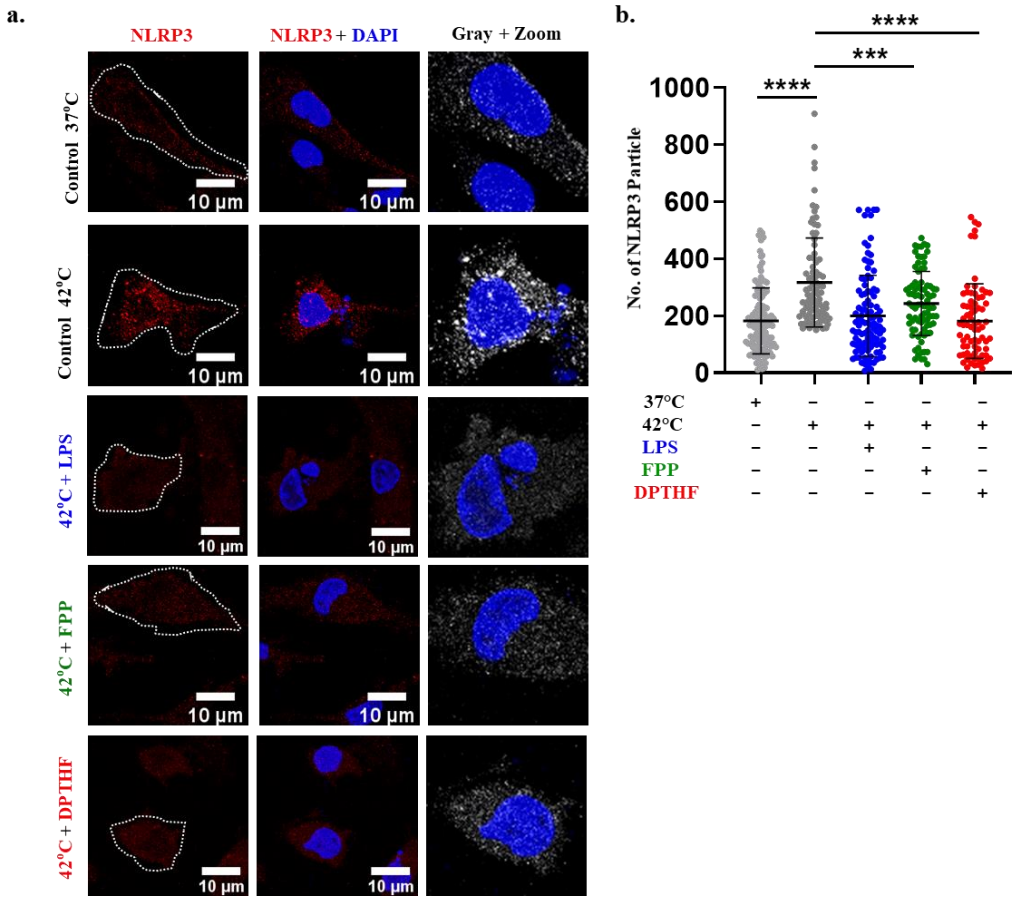

Fig 47. TRPV3 regulates the activity of NLRP3-positive inflammasomes. a. Expression of TRPV3 and NLRP3 at 42ºC in the presence or absence of FPP, DPTHF and LPS are shown. Scale bar: 10µm. **b.** Quantification of the total number of NLRP3 particles per cell is shown. Values are means ± SEM, N ≥30 cells per group; one-way ANOVA; ns: non-significant, *** = $p < 0.001$ and **** = $p < 0.0001$.

Another stress marker characterized in this study is NF-Kb p65 which localized in the nucleus upon cellular stress (Oeckinghaus and Ghosh. 2009). Nuclear localization of NF-Kb p65 correlates well with more stress. NFKB P65 localizes more in the nucleus at the 42°C stress condition. But NFKB P65 expression is significantly lower in case of TRPV3 activation, i.e., in FPP-treated conditions. The nuclear expression of NFKB P65 is significantly low in

case of TRPV3 activation as well as in 37°C control conditions whereas the nuclear expression is more in other conditions, like in DPTHF, LPS, and at 42°C. All these data indicate that TRPV3 activation with FPP helps to rescue the cells from thermal stress (**Fig. 48a-b**).

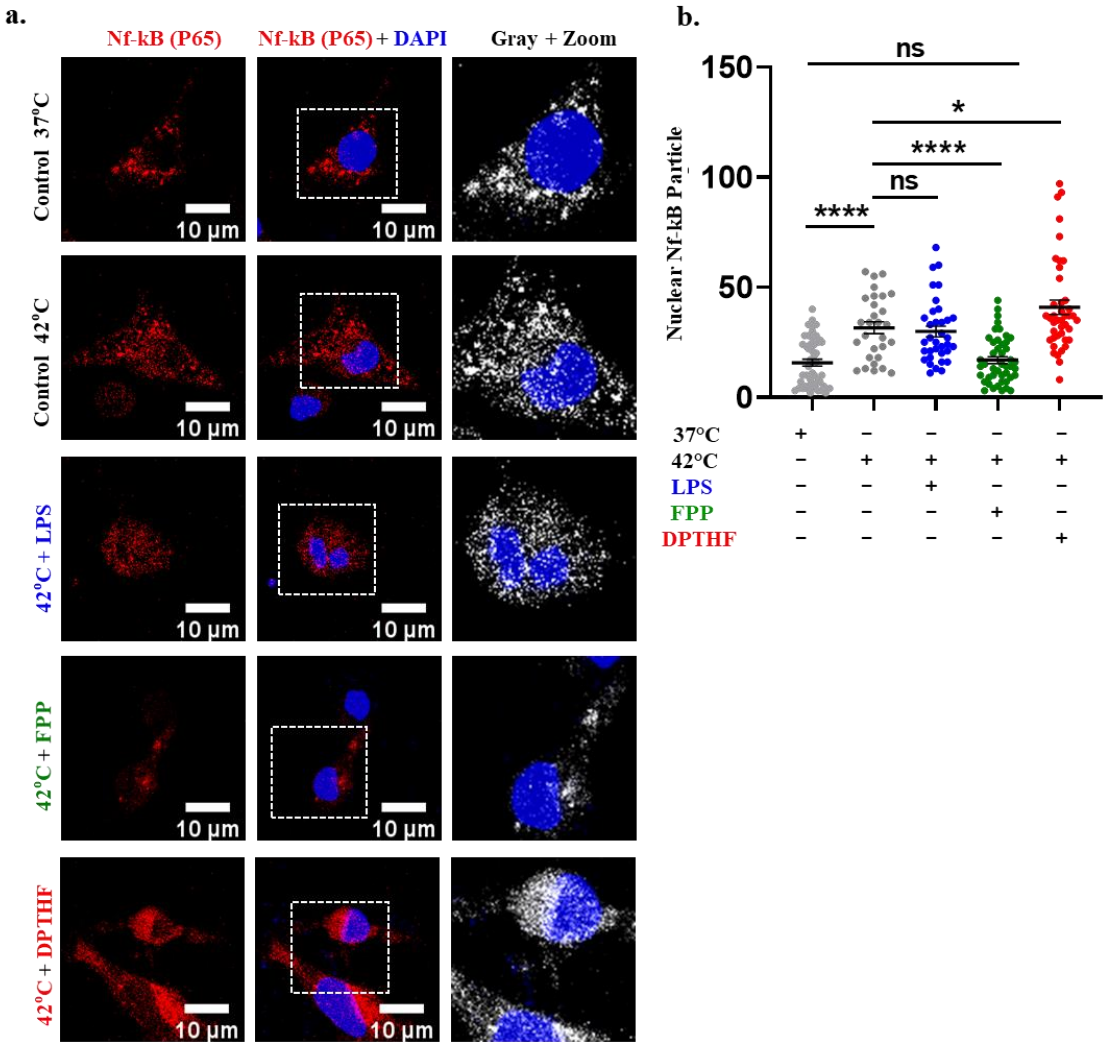

Fig 48. TRPV3 modulation normalizes the expression of stress markers in hyperthermic conditions. a. Confocal images of PM cells immunolabelled for NF-κB (P65) (red) and nucleus (DAPI, blue) show accumulation of NF-κB (P65) in the nucleus at different levels in different conditions. The white dotted border indicates the cell membrane. Scale bar: 10µm. **b.** Quantification of nuclear NF-κB (P65) particle numbers per cell in different conditions are shown. Values are means ± SEM; one-way ANOVA; ns: non-significant, * = $p < 0.05$, **** = $p < 0.0001$.

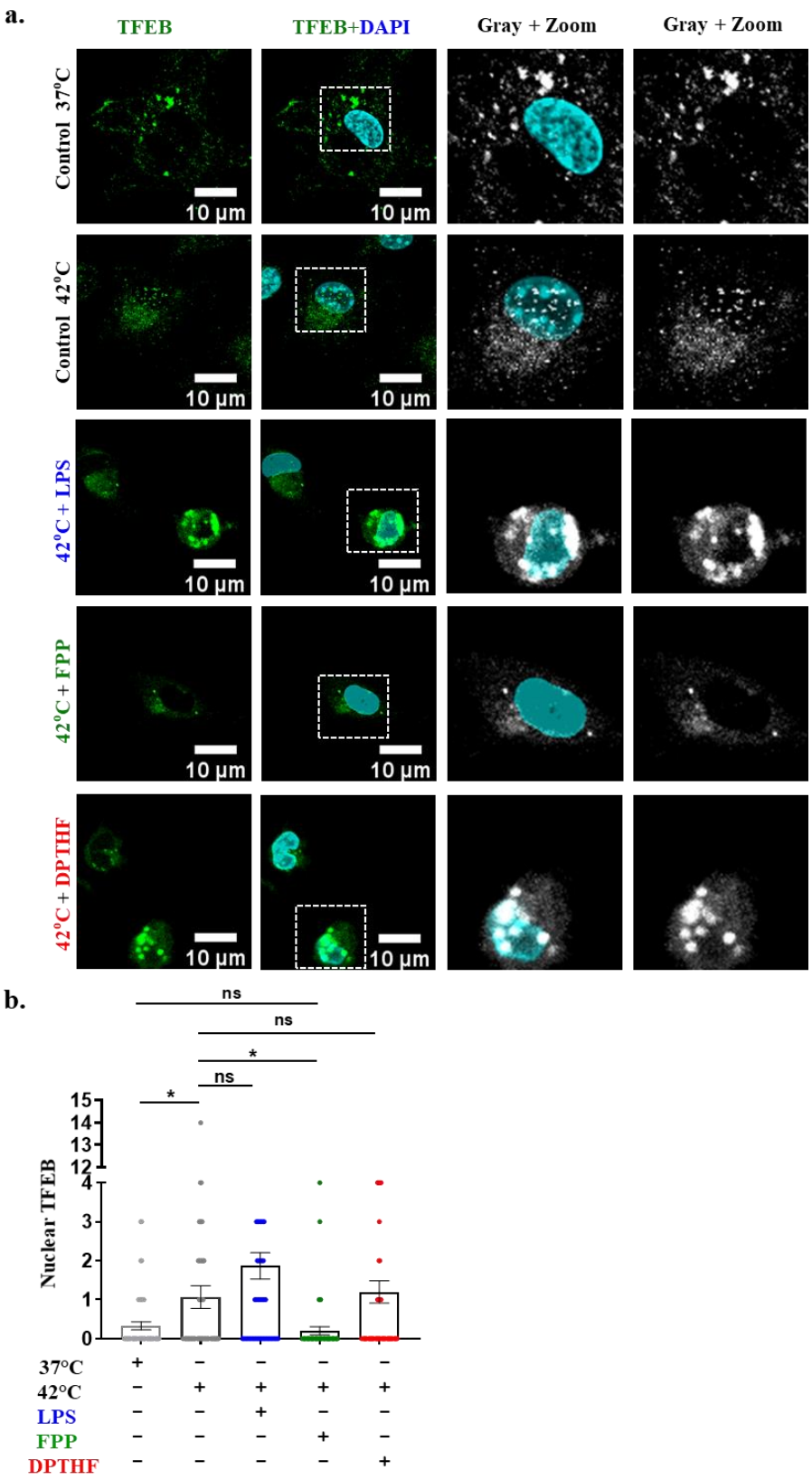

Fig 49. TRPV3 modulation normalizes the expression of stress markers in hyperthermic conditions. a. Shown are the confocal images of PM cells immunolabelled for TFEB (Green). TFEB puncta in cytoplasm and in nucleus are shown in grayscale. Scale bar: 10µm. **b.** Quantified numbers of TFEB spots/puncta in the nucleus of PM in different conditions are plotted.values are means ± SEM; one-way ANOVA; ns: non-significant and * = $p \leq 0.05$.

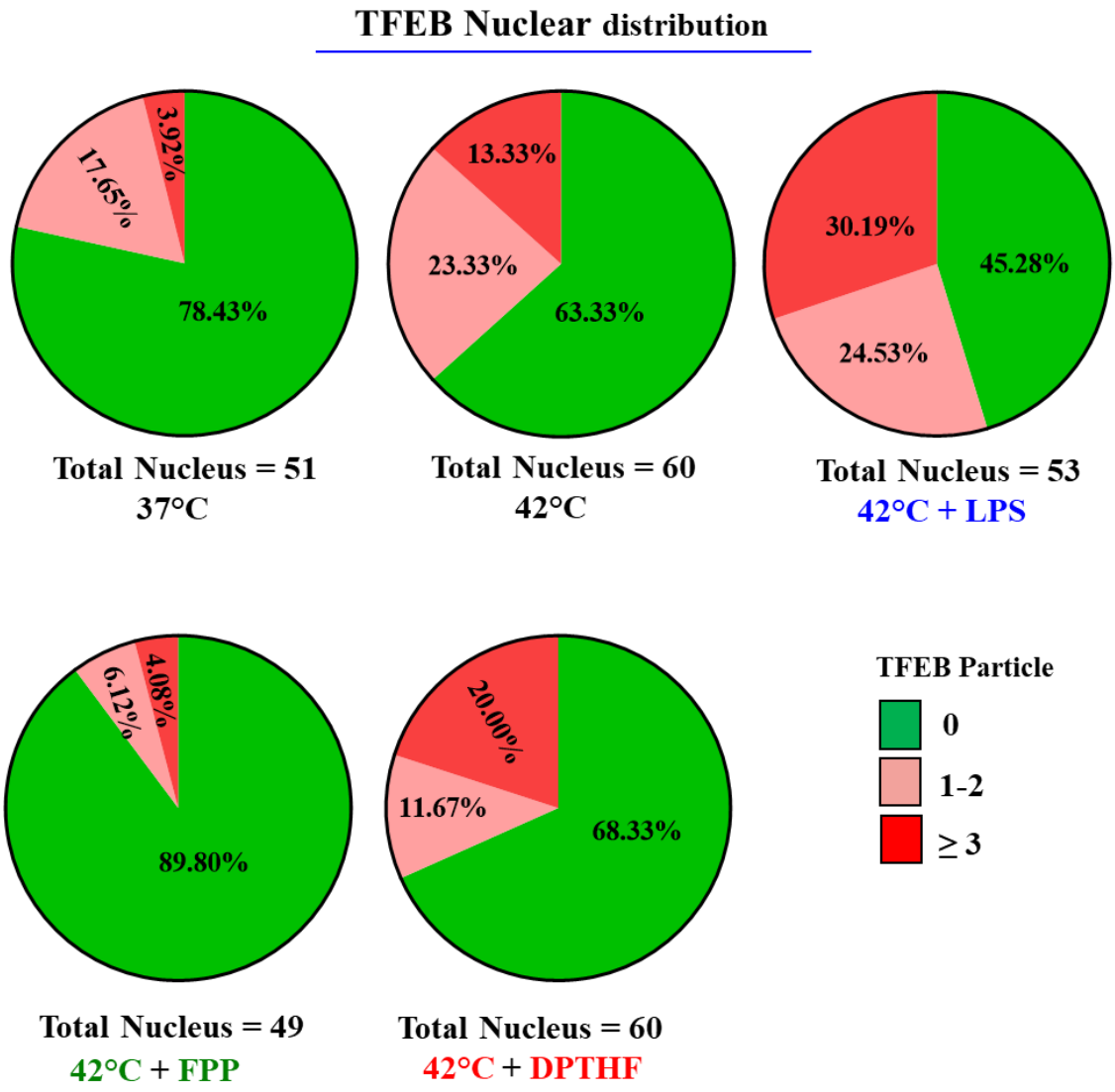

Fig 50. TRPV3 modulation alters the distribution of stress marker (TFEB) in hyperthermic conditions. Shown are the distribution of nuclear TFEB puncta in different conditions. The distribution was categorised as 0, 1 to 2 and ≥3 per nucleus, respectively. The nuclear TFEB distribution in different cells are shown in a percentage scale. Percentage of cells with 0 number of puncta/nucleus are more in case of FPP-treatment at 42°C.

2.4.6 TRPV3 alteration helps in maintaining lysosomal temperature

Lysosomal thermal status is a great determinant for lysosomal health. For that purpose, TRPV3 alteration has been performed to investigate its specific role at different cellular challenges. Using LTG dye, a specific temperature-sensor for lysosome, lysosomal temperature in different conditions were measured. The LTG detection method is based on the fluorescence intensity value that changes with lysosomal temperature (Liu et al. 2022). When

the temperature of the lysosome becomes higher, the fluorescence intensity decreases accordingly. In opposite, if the lysosmal temperature is lower (i.e. when the lysosome becomes cooler), then the LTG-intensity increases accordingly. Based on this, the cells were maintained at 37°C control temperature along with TRPV3 modulators, and the LTG-intensity in diferent conditions were observed accordingly (**Fig. 51a-b**). Lysosomal temperature due to TRPV3 modulation (activation as well as inhibition) and LPS stimulation were investigated. It is observed that LPS stimulation results in a slightly lower lysosomal temperature (shifts ~ 1.10 fold higher fluorescence), but DPTHF treatment tends to maintain the lysosomal temperature towards the hotter side (shifts ~0.78 fold lower fluorescence). When the cells were treated with FPP only (in absence of LPS), it caused ~0.8289 fold reduction in the fluorescence. When cells are treated with FPP or DPTHF in the presence of LPS, lysosomes become cooler. A significant increment in fluorescence intensities were observed (~ 1.27 fold in FPP + LPS and ~ 1.54 fold in DPTHF + LPS conditions) (**Fig. 51b**). This data indicates that only DPTHF (i.e. TRPV3 inhibition) makes the lysosomes hotter, a situation where lysosomal temperature regulation is probably compromised. But the TRPV3 activator or inhibitor, in the presence of LPS as well as LPS alone, makes the lysosomes cooler.

Apart from the 37°C control condition, when cells were treated with the hyperthermic temperature at 42°C or even subjected to lysosomal stress by treatment of BafA1, the LTG fluorececne become different. When cells were treated at 42°C for 2 hours (heat stress), LTG intensity decreased, indicating that the lysosomes became hotter as compared to the control condition at 37°C (**Fig. 52a-b**). But at 37°C. as soon as the TRPV3 activation was introduced through FPP (1µM), the intensity increased significantly, which shows that the lysosomal became cooler after activation (**Fig. 52b**). This data shows the TRPV3 role in maintaining the lysosomal temperature at extreme temperature stress or physiological temperature. And TRPV3 modulation helps rescue the cell from different physiological conditions.

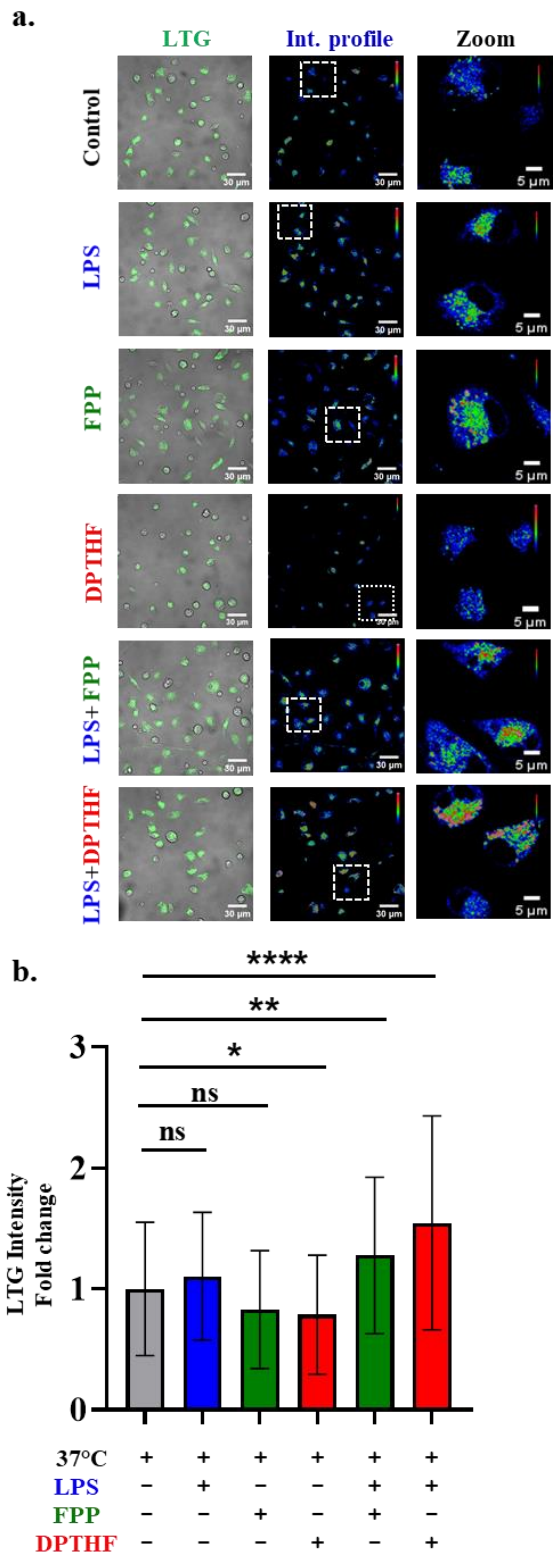

Fig 51. TRPV3 regulate the lysosomal temperature in the PM. a. Shown are the confocal images of live PM cells loaded with lysosomal temperature-sensitive dye LysoThermo Green (LTG) that were treated with FPP (TRPV3 activator), DPTHF (TRPV3 inhibitor) or LPS at 37ºC. The LTG intensity is also shown in rainbow scale. Scale bar: 30µm and 5µm (for enlarged picture). **b.** Quantitative analysis (in fold change) or LTG fluorescence is shown. The LTG intensity has been converted to fold change where the 37°C control is taken as average 1. Values are means ± SEM, N ≥100 cells per group; one-way ANOVA; ns: non-significant, * = $p < 0.05$, ** = $p < 0.01$, *** = $p < 0.001$, **** = $p < 0.0001$.

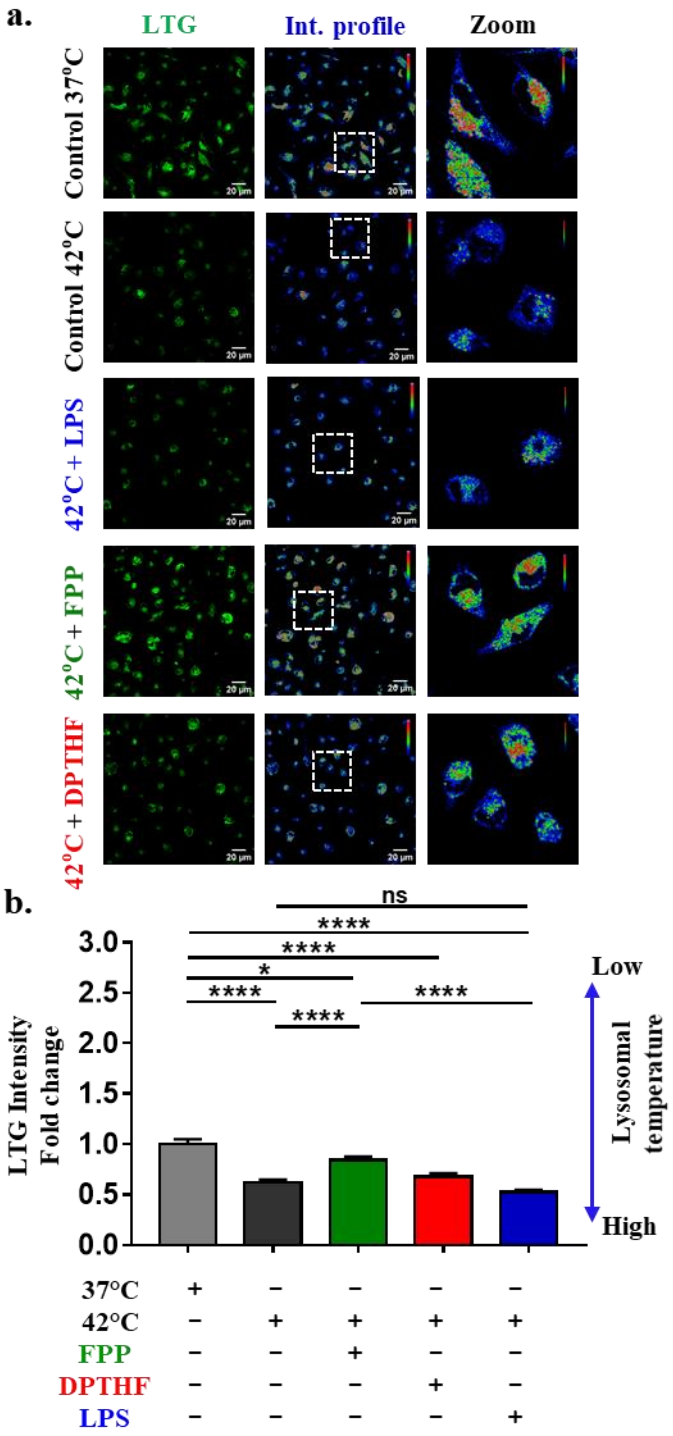

Fig 52. TRPV3 regulates lysosomal temperature in the PM in hyperthermia conditions. a. Representative confocal images and corresponding intensity profile of cells labelled with LTG and maintained in different conditions at 42ºC are shown. Scale bar 20µm. **b.** Quantification of LTG intensity in different conditions are shown. In all cases the average values are represented as fold-change. Values of 37°C is considered as 1. Values are means ± SEM, N ≥100 cells per group; one-way ANOVA; ns: non-significant, * = $p < 0.05$, and **** = $p < 0.0001$.

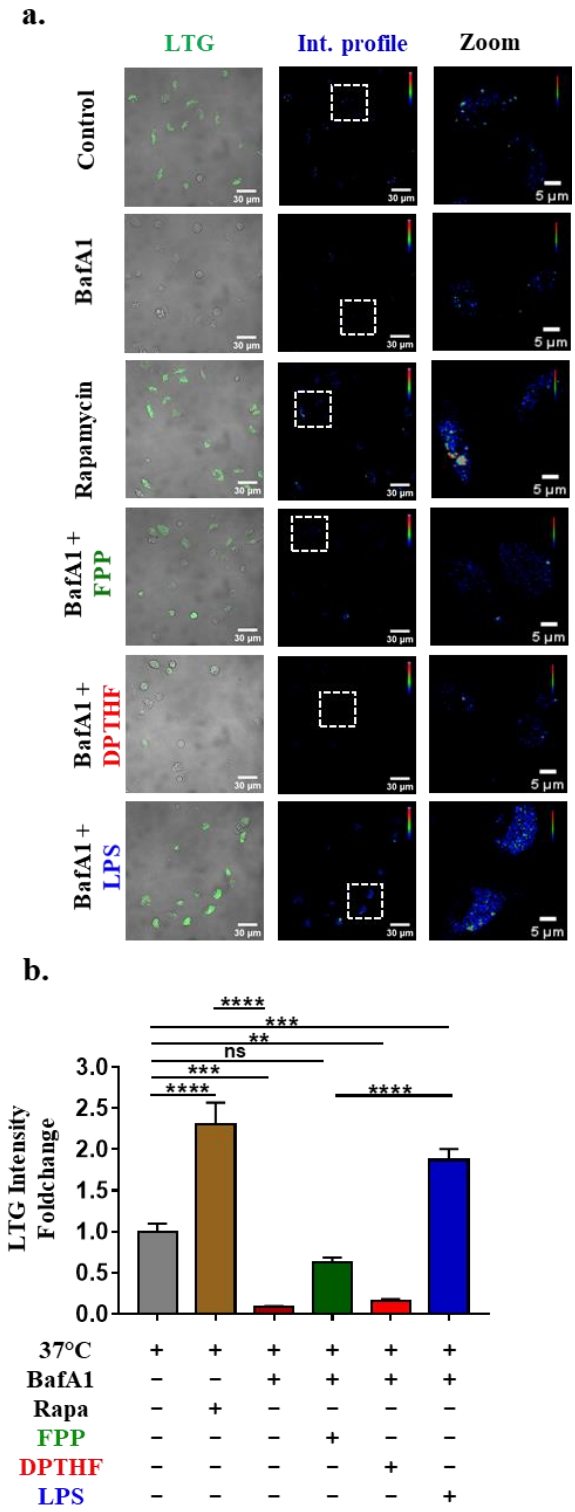

Fig 53. TRPV3 activation rescues lysosomal temperature in BafA1 stressed condition in PM. a. Representative confocal images of LTG fluorescence and corresponding intensity of cells that are treated with FPP, DPTHF, or LPS along with Bafilomycin. Rapamycin is also used as a positive control for this experiment. Scale bar 30µm and 5µm. **b.** Quantification of LTG intensity in different conditions are shown. In all cases the average values are represented as fold-change. Values of 37°C is considered as 1. Values are means ± SEM, N ≥100 cells per group; one-way ANOVA; ns: non-significant, ** = $p \leq 0.01$, *** = $p \leq 0.001$ and **** = $p \leq 0.0001$.

For the lysosomal stress, the cells were treated with BafA1 at a sub-optimal concentration (400ng/ml) and changes in the lysosomal temperature were monitored by using LTG sensor dye (**Fig. 53a-b**). When cells were treated with BafA1, the LTG-fluorescence lowered significantly (~ 0.08-fold), indicating that the lysosmes became hotter (**Fig. 53b**). However, in case of rapamycin treatment (was also used as another control), LTG-fluorescence increases significantly (~2.29-fold), indicating that rapamycin cools the lysosomal temperature (**Fig. 53b**). When the TRPV3 activator was used in the presnce of BafA1, the LTG fluorescence increased significantly (~ 0.62 fold) (**Fig. 53b**). The increased fluorescence indicates that TRPV3 activation causes cooling effect of lysosomes. Similar results were observed when LPS stimulation was performed in the presnce of BafA1. DPTHF treatment along with BafA1 causes no significant changes in the LTG-fluorescence (**Fig. 53b**).

2.4.7 TRPV3 activation lowers the temperature of isolated lysosomes

As mentioned earlier TRPV3 plays a significant role in maintaining lysosomal temperature when subjected to various challenges. It is evident that TRPV3 modulation helps in maintaining lysosomal thermal homeostais that is also directly linkd to lysosomal health. Even isolated lysosomes (in a cell-free system) were utilized to further investigate the influence of TRPV3 modulation on maintaining lysosomal temperature. For that purpose, temperature of isolated lysosomes in a cell-free system was measured using lysothermo green (LTG) dye. The lysosomes were isolated from Raw 264.7 cells with the lysosome enrichment kit. Experiments were conducted in Ca^{2+}-free medium (HBSS) buffer supplemented with ATP (1mM). The lysosomal particles were exposed to 42ºC for 2 hours in the presence of TRPV3 modulators (**Fig. 54a-b**). The isolated lysosomes were labelled with LTG dye and were subjected to 42°C thermal stress along with TRPV3 modulators. The LTG intensity decreased

slightly upon heat stress as compared to 37°C conditions (~ 0.1 fold, which remain non-significant).

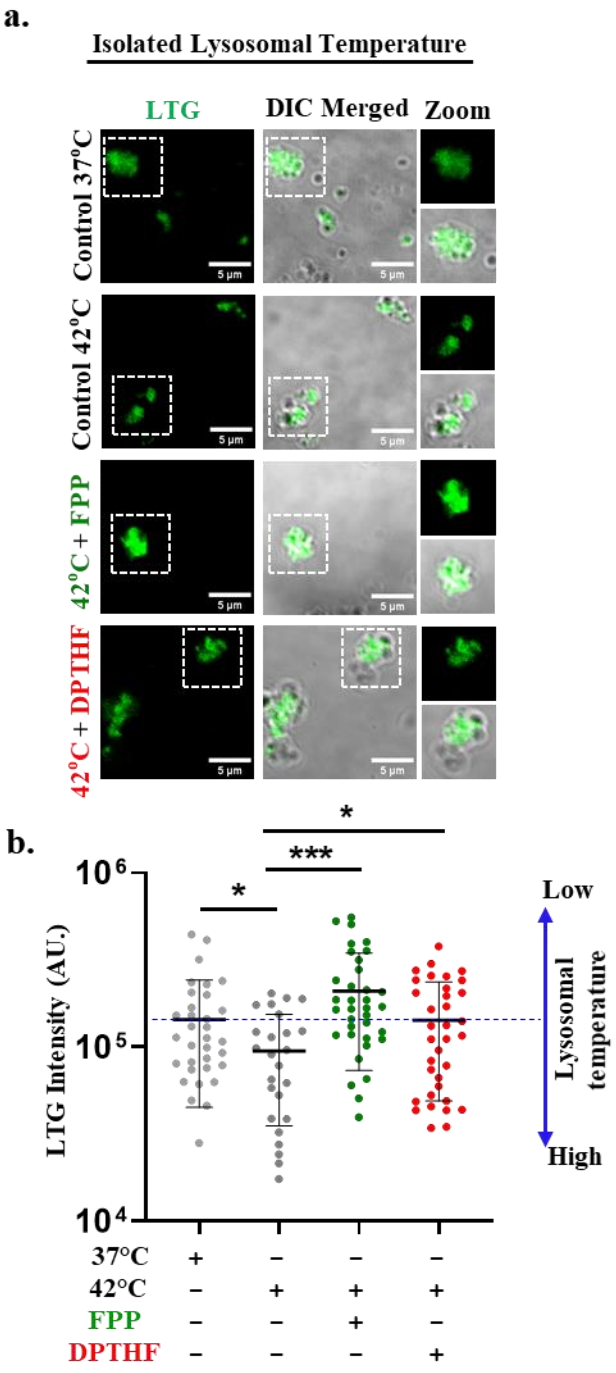

Fig 54. TRPV3 regulates lysosomal temperature in cell-free condition. a. Confocal images of freshly isolated lysosomes (isolated from RAW 264.7 cells) that are labelled with LysoThermo Green dye. Scale bar: 5µm. **b.** Quantitative analysis of LysoThermo Green intensity of isolated lysosome. Values are means ± SEM; one-way ANOVA; ns: non-significant, * = $p \leq 0.05$, and *** = $p \leq 0.001$.

However, when these isolated lysosomes were subjected to 42ºC, LTG intensity decreased by 0.31-fold. In contrast, TRPV3 activation condition, the fluorescent intensity of LTG was increased significantly (0.64-fold) when compared with the 42ºC control condition (**Fig. 54b**). This indicates cooling of isolated lysosome due to TRPV3 activation. However, in DPTHF-treated condition, there is no such significant changes in lysosomal temperature when compared to both 37ºC and 42ºC control conditions. The data suggest that pharmacological modulation of TRPV3 affects lysosomal temperature. TRPV3 activation cools the lysosomal temperature to a certain degree/fold when compared with 37°C or control 42°C conditions.

As reported earlier, the pH rescue by TRPV3 modulation in the lysosome. This indicates that the direct role of lysosomal pH changes could significantly alter the lysosomal temperature, which means the lysosomal temperature and lysosomal pH correlated. Here the data suggest that lysosomal temperature also seems to be rescued through TRPV3 activation as well.

2.4.8 TRPV3 modulations play important role in the maintenance of cytosolic pH and cytosolic Ca^{2+}-levels during hyperthermic stress

The cytosolic Ca^{2+} and cytosolic pH were measured in the peritoneal macrophages in hyperthermic stress conditions. For the cytosolic Ca^{2+}-measurement, Fluo-4 AM has been used and for the cytosolic pH measurement pHrodo red dye was used (**Fig. 55a-d**). The cytosolic Ca^{2+} increased a little bit in 42°C condition in comparison with the 37°C control condition. But at 42°C along with TRPV3 modulation, the basal Ca^{2+}-level in the cytosol increased significantly. The Ca^{2+}-level is significantly higher in the FPP, DPTHF, and LPS-treated conditions than the 42°C control condition (**Fig. 55a-b**).

pHrodo dye was used to measure the cytosolic pH changes during 42°C heat shock. The cytosolic pH drops significantly due to hyperthermic shock at 42°C.

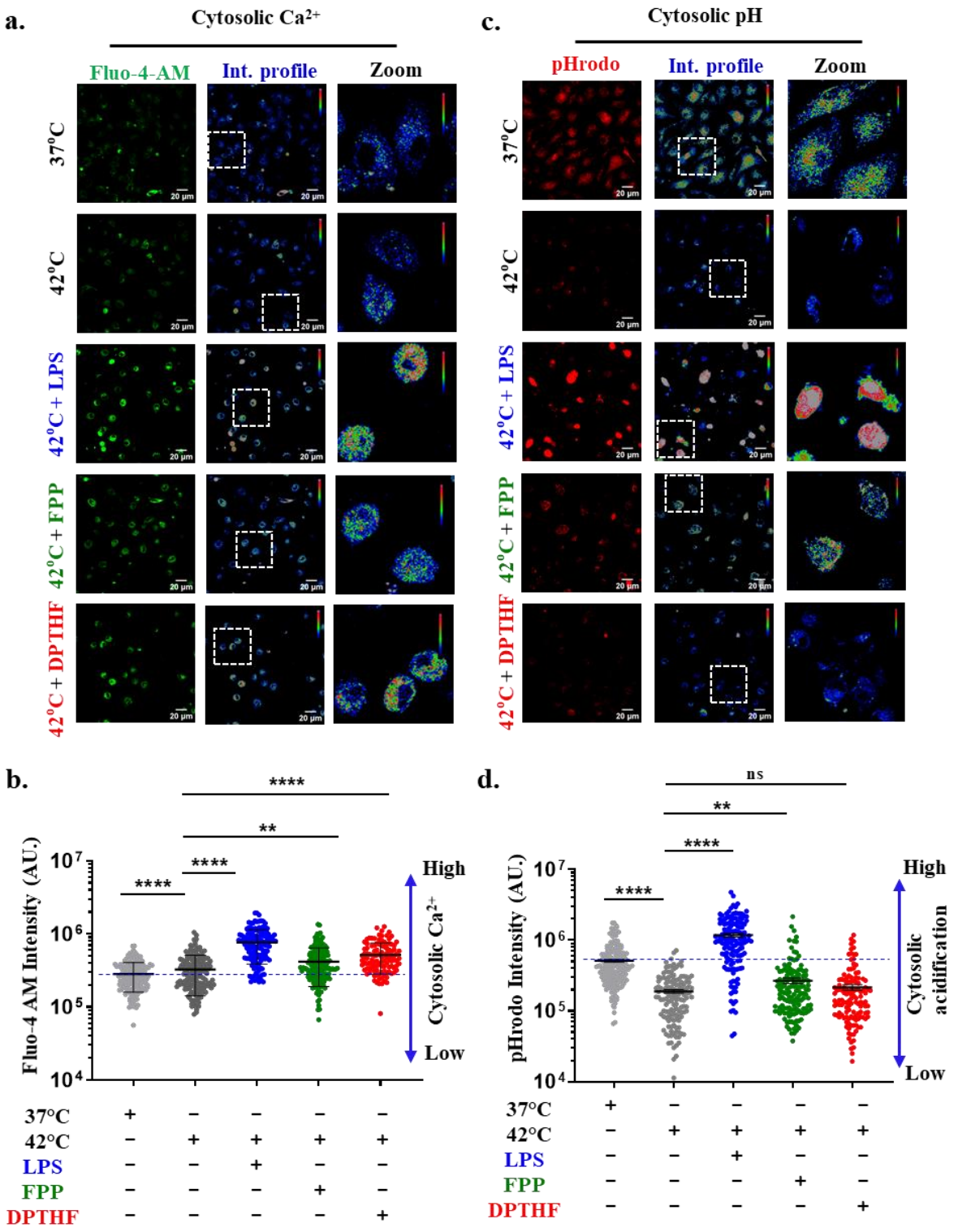

Fig 55. TRPV3 modulation alters cytosolic Ca^{2+} and pH-level of peritoneal macrophages differently in different hyperthermic conditions. a. Representative live-cell images of peritoneal macrophages labelled with Fluo4-AM. PM treated with FPP, DPTHF or LPS at 42ºC are shown. Scale bar 20µm. **b.** Quantitative analysis of Fluo4-AM fluorescence intensity in different conditions is shown. **c.** Representative images of pHrodo red (cytosolic pH) in different conditions are shown. **d.** Quantitative analysis of pHrodo fluorescence intensity in different conditions is shown. Values are means ± SEM, N ≥100 cells per group; one-way ANOVA; ns: non-significant, * = $p \leq 0.05$, ** = $p \leq 0.01$, *** = $p \leq 0.001$ and **** = $p \leq 0.0001$.

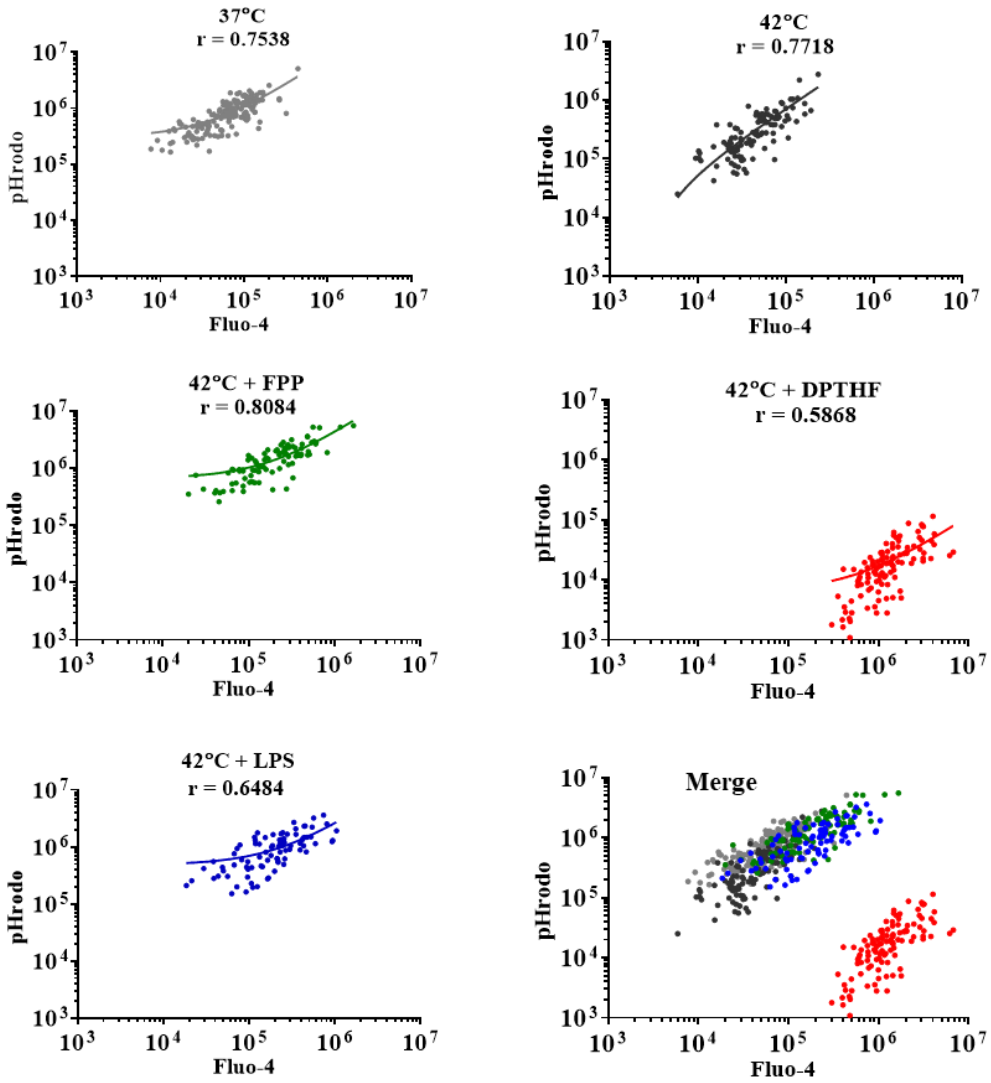

Fig 56. TRPV3 modulation alters cytosolic Ca^{2+} and pH-level of peritoneal macrophages differently in different hyperthermic conditions. The representative image shows the quantification of correlation between cytosolic Ca^{2+}-level (Fluo-4) and cytosolic pH level (pHrodo red). The correlation shows more in case of FPP 42°C condition (r = 0.8084) and less in DPTHF 42°C condition (r = 0.5868).

However, if the cells were simultaneously treated with FPP, then the fluorescence intensity increased significantly and indicating rescue of the cytosolic pH due to TRPV3 activation. The change in the fluorescence intensity upon only TRPV3 inhibition is marginal (non-significant) but increased significantly in the presence of LPS (**Fig. 55c-d**). This data shows that TRPV3 modulation plays a crucial role in maintaining the cytosolic pH and Ca^{2+}. The correlation between the cytosolic pH and cytosolic Ca^{2+} has been plotted to analyse the relationship between both cytosolic parameters (**Fig. 56**). The pH changes correlate with the

Ca^{2+} changes in the cytosol. It is found that the correlation between cytosolic pH and cytosolic Ca^{2+} become more significant in case of TRPV3 activation (r = 0.8084) in the 42°C (**Fig. 56**). This data indicates that the TRPV3 activation is able to rescue the cell from heat shock by maintaining the cytosolic calcium and cytosolic pH level.

2.4.9 The cytosolic ROS-level is altered due to TRPV3 modulation at hyperthermic stress condition

The levels of Reactive Oxygen Species (ROS) in the cytosol vary in response to different types of cellular stress and metabolism. Different challenges, like oxidative stress, heat shock, or exposure to toxins, there is typically an increase in ROS levels. Furthermore, during events like heat shock or inflammation, cells initiate pathways that produce ROS as a protective measure. These heightened ROS levels can activate stress response reqired for cellular adaptation. So, the ROS level in the cells directly determined the level of cellular stress. Based on this consideration, ROS level was measured in hyperthermic stress conditions. To investigate the importance of TRPV3 and its specific role in maintaining cytosolic ROS level, the TRPV3 modulators has been used.

The cytosolic ROS level has been measured by using H_2DCFDA dye (**Fig. 57a-b**). The ROS level increased at significantly (** = p≤ 0.01) in the 42ºC as compared to the 37ºC control. At 42°C, LPS addition does not increase the ROS level anymore, suggesting that exposure at 42°C for 2 hours is sufficient to increase the ROS level to saturation. However, at 42°C, the ROS-level reduced in FPP-treated condition as compared to the only 42ºC control (** = p≤ 0.01). However, this is not the case for DPTHF treatment at 42°C. Addition of H_2O_2 (as a positive control) increases the ROS-level significantly, at 37°C (**Fig. 57a-b**). The result indicates that TRPV3 activation reduces the cytosolic ROS production at 42°C (in hyper-thermic condition), and thus can be beneficial.

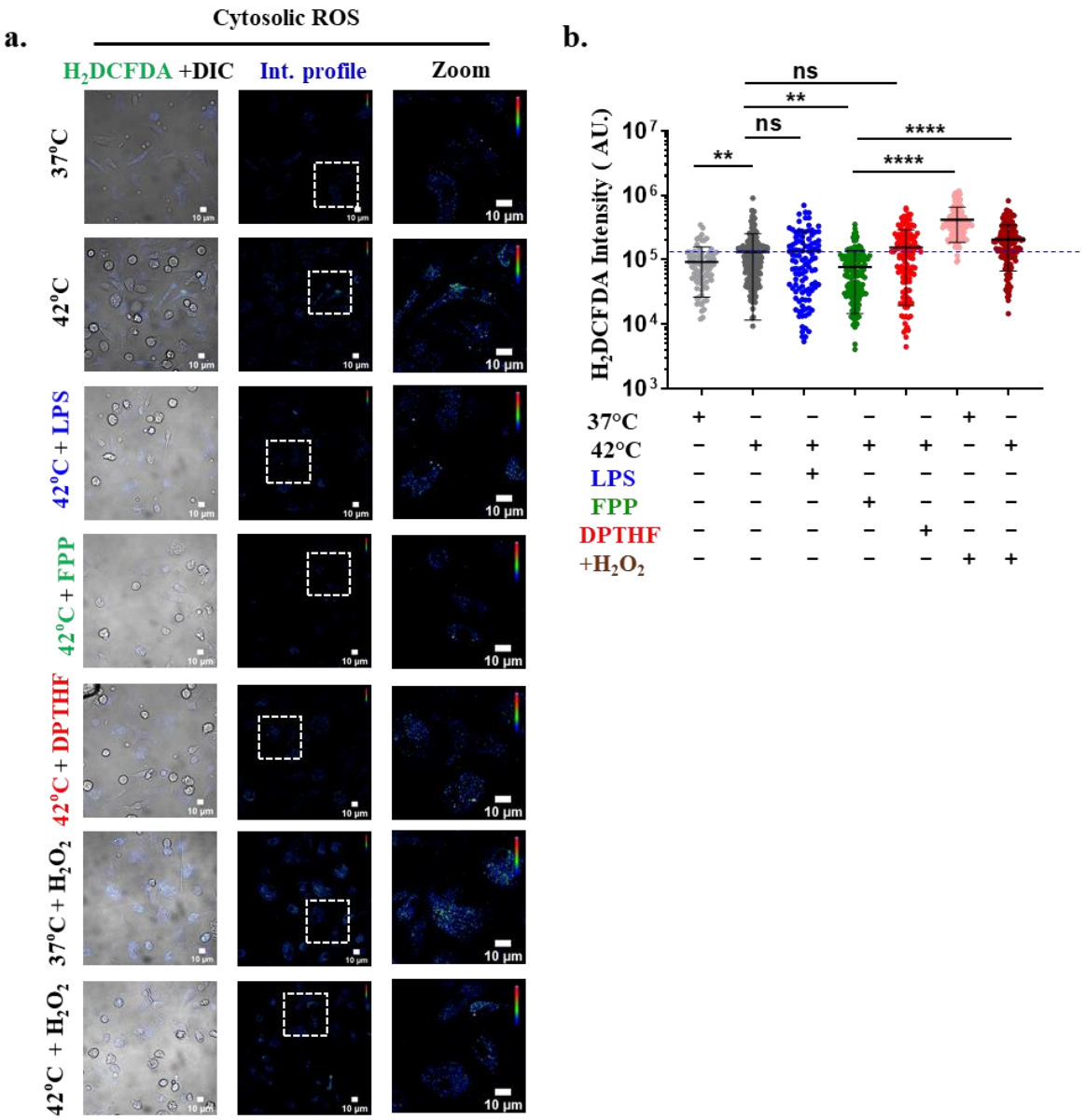

Fig 57. TRPV3 modulation alters cytosolic ROS-level of peritoneal macrophages differently in different hyperthermic conditions. a. Representative live cell staining of H_2DCFDA in different condition at 42ºC are shown. Scale bar 10µm. **b.** Quantitative analysis of H_2DCFDA intensity for different conditions are shown. Values are means ± SEM, N ≥100 cells per group; one-way ANOVA; ns: non-significant, ** = $p \leq 0.01$ and **** = $p \leq 0.0001$.

2.4.10 TRPV3 modulations play a crucial role in the maintenance of mitochondrial stress functions during hyperthermic stress

Mitochondria health is the determinant of overall cellular stress. It plays a vital role in the cellular stress response regulations. During stress conditions, such as oxidative stress, heat shock, or nutrient deprivation, mitochondria actively participate in maintaining cellular

homeostasis. Mitochondria are essential for coordinating the cellular stress response by controlling metabolism, ROS production, signaling pathways, and energy generation. This overall situation aids in promoting cell survival and adaptation during challenging circumstances. In this context different mitochondrial parameters have been explored during the hyperthermic stress at 42°C. Two different mitochondrial parameters, such as mitochondrial temperature (by using MitoThermo Green dye, i.e. MTG) and ATP level (by using ATP-Red dye) were analyzed. Cells were simultaneously labelled with both MTG and ATP-Red dyes to understand the correlation between these two parameters and also to understand the role of TRPV3 modulations at mitochondrial level. Significant changes in the ATP level and mitochondrial temperature are noted due to TRPV3 modulations and LPS stimulation, at 42°C condition. The ATP level reduced significantly at 42°C in comparison to the 37°C control condition. The mitochondrial ATP level seems to be recovered in TRPV3 activation as well as in the LPS stimulatory conditions at 42°C. It seems that the ATP level has changed significantly due to TRPV3 activation but not due to TRPV3 inhibition. The MTG fluorescence was also measured in the heat shock conditions. The MTG-fluorescence intensity reduced significantly during heat shock, suggesting. More fluorescence intensity of MTG indicates reduced mitochondrial temperature. In opposite, less fluorescence intensity of MTG indicates higher mitochondrial temperature. The MTG intensity increased in the FPP and LPS stimulations as compared to the 42°C heat shock (**Fig. 58a-c**). This indicates that TRPV3 activation, as well as LPS stimulation rescue the cells and the mitochondrial temperature, became low in these conditions.

All these data show that the TRPV3 activation plays a crucial role in maintaining the mitochondrial temperature, and ATP level, especially at 42°C stress conditions.

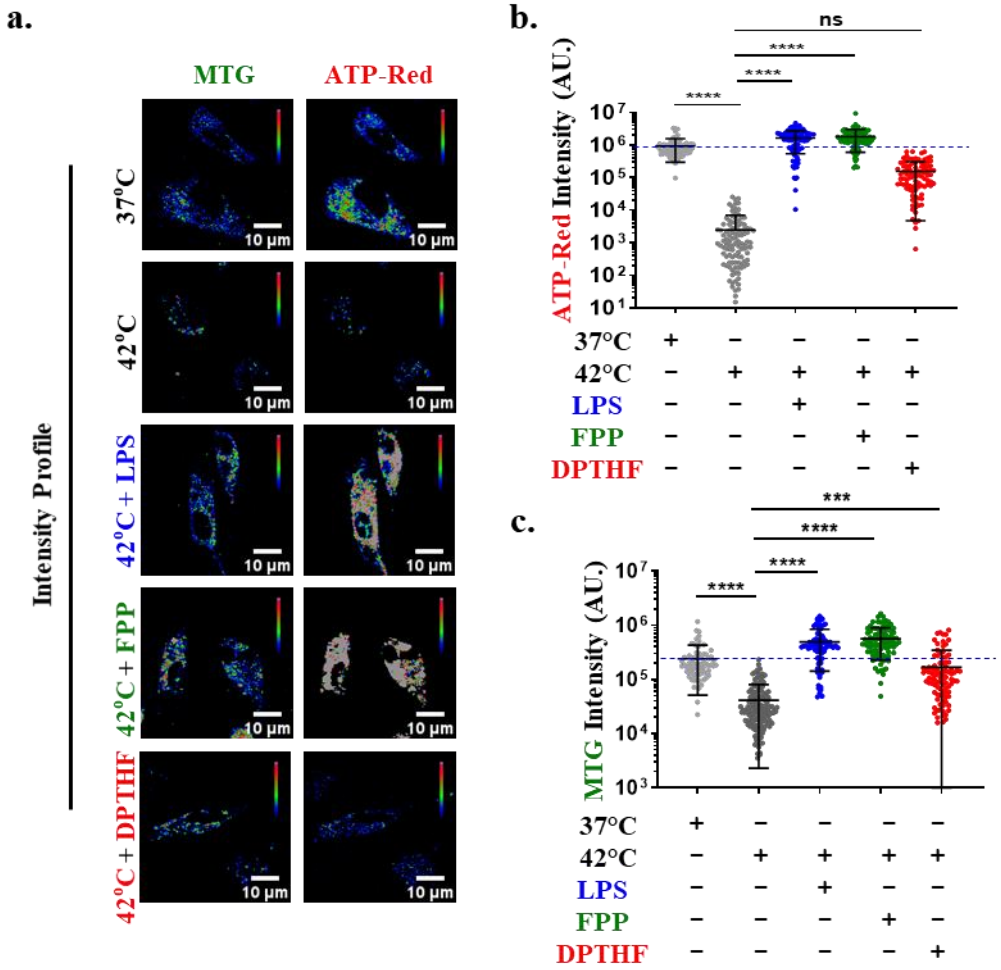

Fig 58. TRPV3 modulation alters mitochondrial temperature and ATP level differently in different hyperthermic conditions in peritoneal macrophages. a. Representative confocal images of peritoneal macrophages labelled with MitoThermo Green (MTG) and ATP-Red dye in different conditions. The MTG and ATP-Red dye used simultaneously to understand the role of TRPV3 modulation at 42°C stress conditions. Scale bar 10µm. **b-c.** Values are means ± SEM, N ≥100 cells per group; one-way ANOVA; ns: non-significant, *** = $p \leq 0.001$ and **** = $p \leq 0.0001$.

2.5 TRPV3 mutants causing lysosomal defects and induce OS syndrome

Recent research has started investigating the involvement of TRP channels in diseases. One notable pathogenic condition is keratoderma. *Olmsted syndrome*, a rare genetic disorder and its phenotypes matached well with sevear forms of keratoderma. *Olmsted syndrome* is caused by the mutations in TRPV3 (G573, G568, L673, Q580, and W692). Previously, few mutants of TRPV3 (G573S, G573C, G573A, W692G) have been detected in lysosomes (Yadav and Goswami. 2017). These mutants cause impaired cell adhesion, reduced lysosome numbers, and altered lysosome distribution. Similar trends have been observed in case of other mutations located in other positions also, such as for G568D and G568C. These findings suggest that mutations in TRPV3 is associated with the development of *Olmsted Syndrome* (OS), a disease which can also be tagged as lysosomal disorder. This finding also highlights the significance of TRPV3 in lysosomal functions. Work added in this chapter explores the TRPV3 and its novel mutants as lysosomal proteins and their role in regulations of lysosomal functions.

2.5.1 TRPV3 OS-mutants (G568C and G568D) have impaired cellular status

Previously our lab has characterized few of these OS-mutants (G573C, G573S, G573A, W692G) that show impaired cell adhesion as well as lysosomal dysfunction (Yadav and Goswami. 2017). These OS-mutants show low lysosomal count as well as reduced cell size. Also these mutants fail to attach to the glass surface (thus remain loosely atached to the nearby non-transfected healthy cells). This study focuses on two other OS-mutants that are G568C and G568D. These two mutants as well as TRPV3-WT were expressed in the HaCaT (Human Keratinocyte cell line) cells as a transient expression system (**Fig. 59**). It has been observed that expression of these two OS-mutants causes defective cell adhesion, rounding of cells (which also cause difficulty of growing these mutant expressing cells on the glass surface), reduced cell perimeter and area, and defective localization at the surface (**Fig. 59a-c**). The data

suggests that the cells expressing these two OS-mutants have more Z-distance than the cells that express TRPV3-WT (**Fig. 59c**).

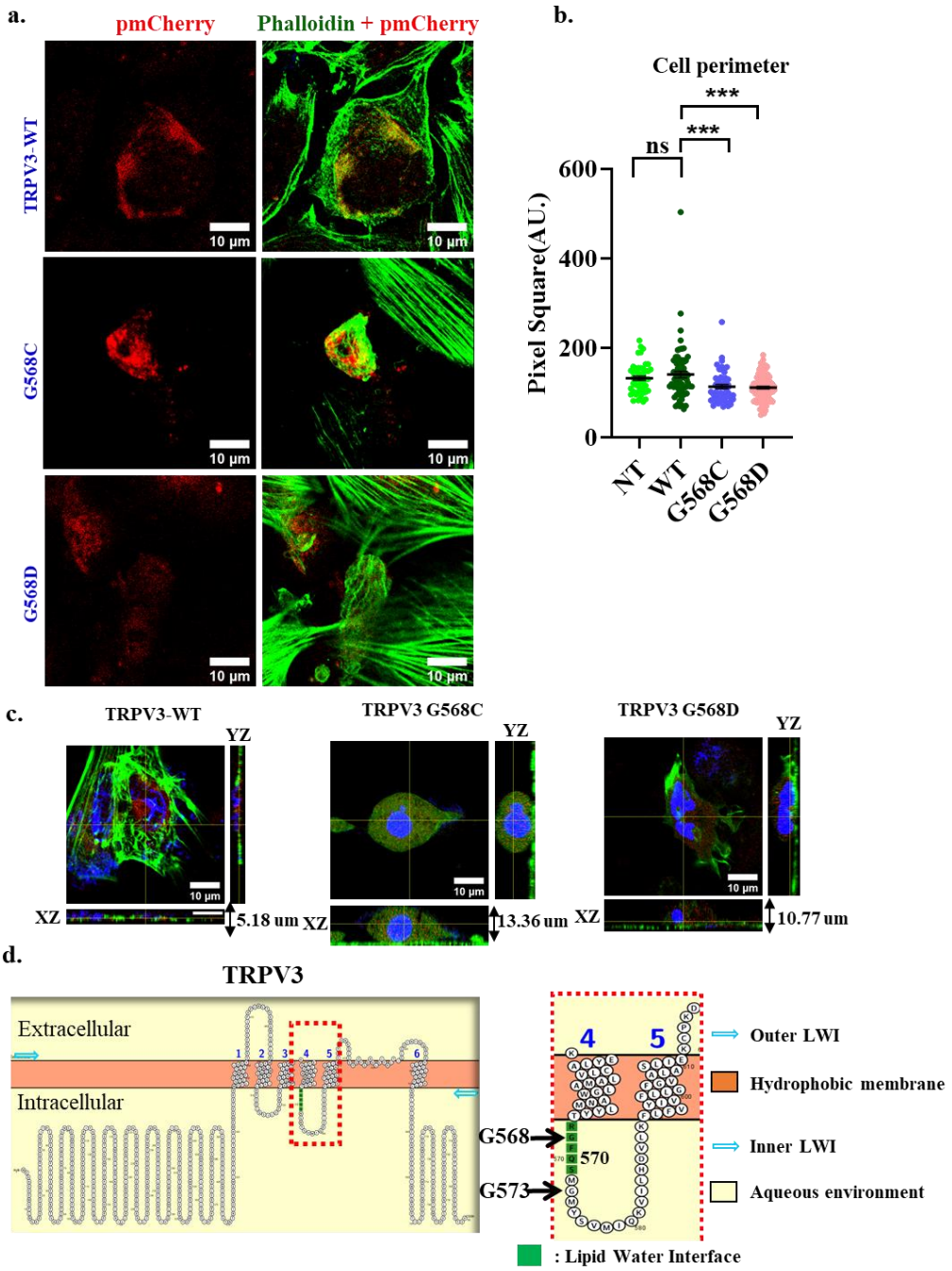

Fig 59. TRPV3 OS-mutants (568C and 568D) have impaired cell adhesion and impaired cellular morphology. a. The representative image shows the HaCaT cell with TRPV3-WT and TRPV3 OS-mutants (mCherry in red) stained with phalloidin antibody (F-actin in green). The OS-mutants shows disrupted Phalloidin labelling as compared to TRPV3-WT cells. Scale bar 10µm. **b.** The graph shows the cellular perimeter in TRPV3 OS-mutants and TRPV3-WT cells. The cells perimeters (pixel square) show significant decrease in case of TRPV3 OS-mutants. (Unpaired t-test, *** = $p \leq 0.001$ and ns = non-significant). **c.** The figure represents orthogonal views of TRPV3-WT and TRPV3 OS-mutants. The cells expressing OS-mutants show less area (XY values) and higher Z-distance than that of TRPV3-WT. Scale bar 10µm. **d.** The schematic figure shows the positioning of TRPV3 OS mutants (G568 and G573) at the lipid-water-interface region.

A schematic representation of TRPV3 OS mutants (namely G568 and G573), which are present in the intracellular lipid water interface region of the TRPV3 is shown (**Fig. 59d**).

2.5.2 OS-mutants have abnormal lysosomal status as well as impaired Ca^{2+}-buffering

The TRPV3-WT and these two OS-mutants (G568C and G568D) have been expressed in the HaCaT and Saos-2 cells. These two OS-mutants also cause changes in the aggregation of ER and loss of lysosomes, suggesting that these OS-mutants induce cellular toxicity that affects general cell health (**Fig. 60**). As expected, the TRPV3-WT is detected in the lysosome. However, though with difficulties, these two OS-mutants have also been detected in the lysosomes (**Fig. 60**). As a "proof-of-concept", this data suggests that these two mutants are localized in the lysosomes. Next, the movement of lysosomes in cells expressing TRPV3-WT or these OS-mutants has been explored. It was noted that the movement of G568C but not the G568D is reduced (**data not shown**). To characterize the details of lysosomal problems, the number of lysosomes per cell expressing TRPV3-WT or these two OS-mutants has been quantified. G568C and G568D mutant-expressing cells have a much-reduced number of lysosomes (**data not shown**). The fluorescence intensity of the lysosomes has been measured by using LysoTracker Red as well as LysoSensor Green. This data suggests less acidification of lysosomes of cells expressing G568D but not for G568C.

TRPV3-WT or OS-mutants along with the GCaMP protein (a fluorescence-based Ca^{2+}-sensor) were expressed. The basal level of Ca^{2+} remains high for cells expressing G568C, while cells expressing either WT or G568D mutant have comparable basal level Ca^{2+} (**Fig. 63b**). Application of FPP (an endogenous activator of TRPV3) causes Ca^{2+}-influx in a considerable number of cells expressing TRPV3-WT (**Fig. 61**). In contrast, the majority of the cells expressing OS-mutants do not respond to the FPP (**Fig. 62, Fig 63**).

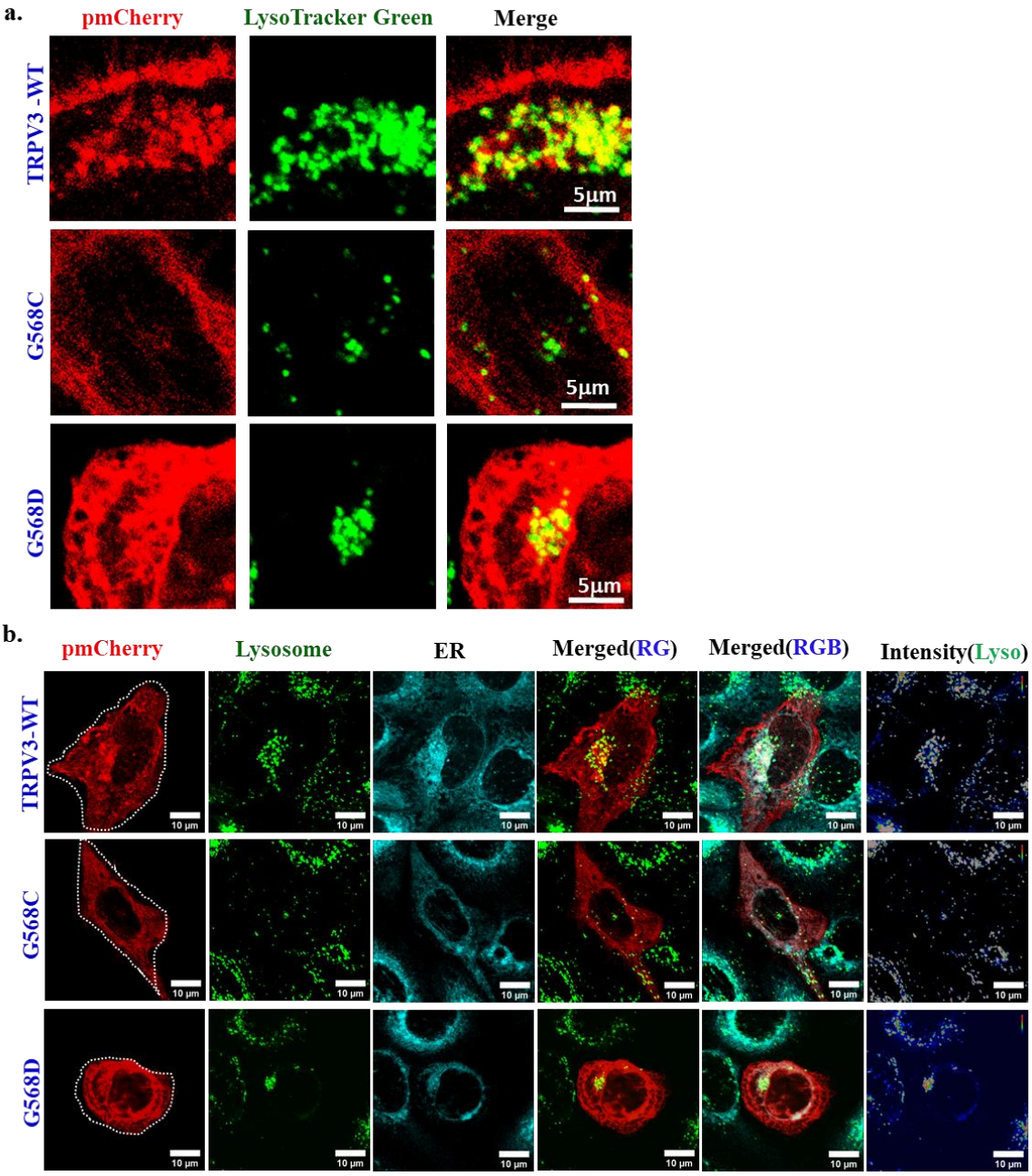

Fig 60. TRPV3 OS-mutants (G568C and G568D) have impaired lysosomal distribution and lysosomal number. a-b. The representative images show lysosomal distribution in TRPV3-WT and TRPV3 OS-mutants in HaCaT (a) and Saos-2 (b) cells. The TRPV3-WT and TRPV3 OS-mutants stained with ERTracker Blue and LysoTracker Green in Saos-2 cell. Scale bar 5μm and 10μm.

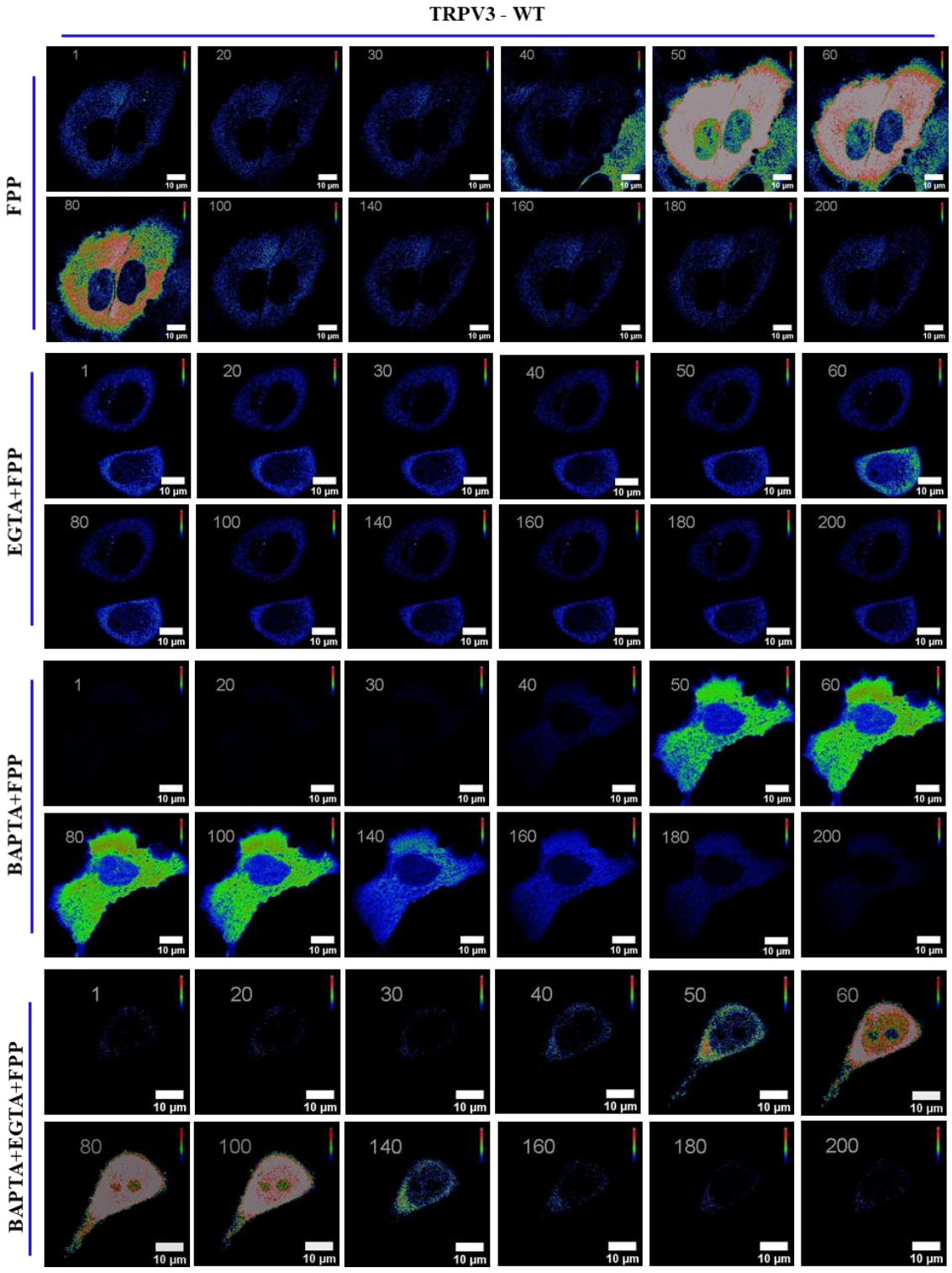

Fig 61. TRPV3-WT cells respond to channel activation even when extracellular or intracellular Ca^{2+} is chelated. The TRPV3-WT expressing HaCaT cells show immediate response to the TRPV3 activation by FPP (Farnesyl pyrophosphate). The Ca^{2+}-level measured by expressing GCaMP6f (a Ca^{2+}-sensitive protein). Intracellular or extracellular Ca^{2+} is chelated with either BAPTA-AM or EGTA respectively or by both agents. Scale bar 10µm.

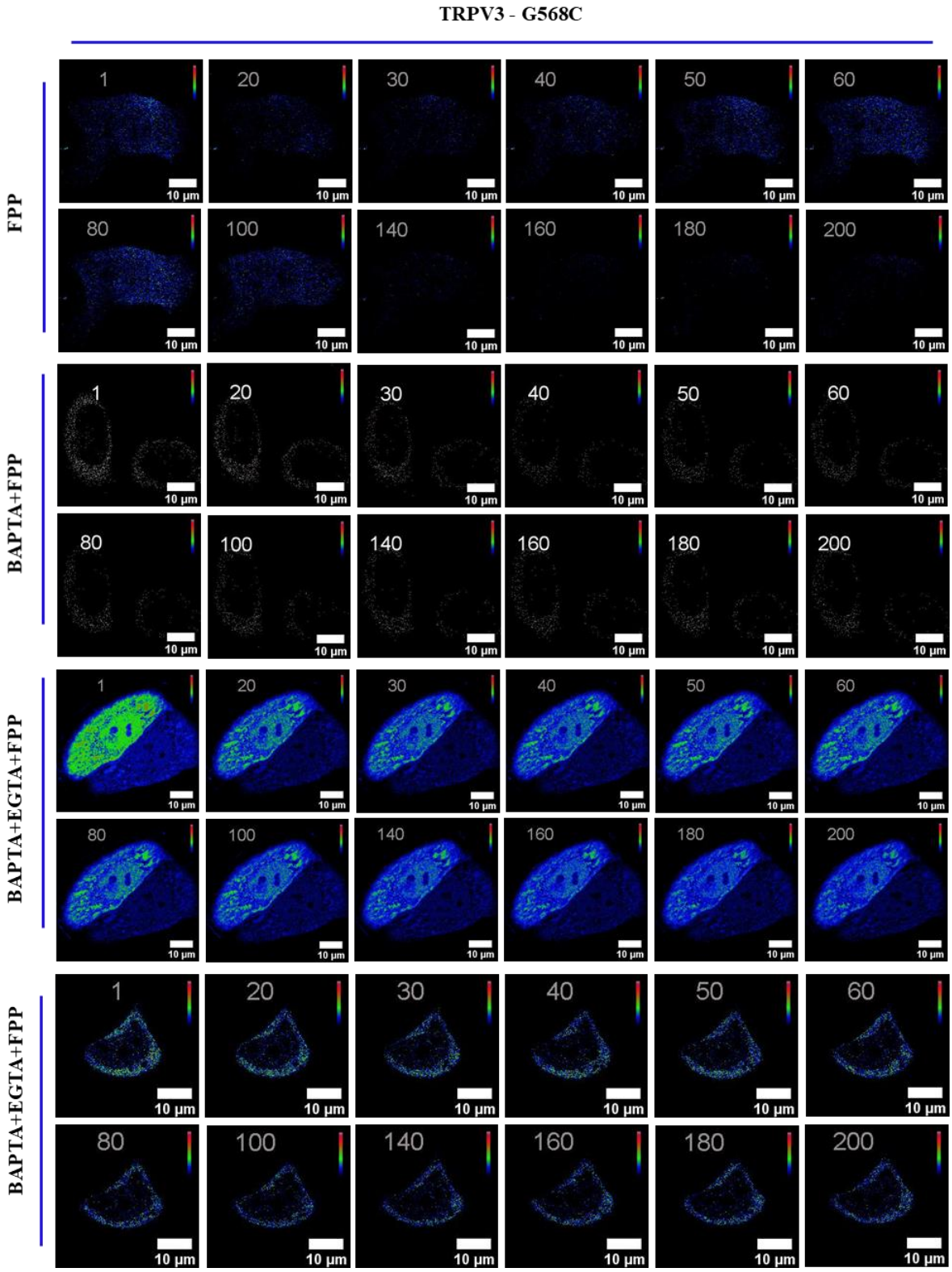

Fig 62. TRPV3 OS-mutant (G568C) expressing cell remain non-responsive to TRPV3 activator in HaCaT cell in Ca^{2+}-chelated conditions also. The TRPV3-G568C did not shows any response to the TRPV3 activation by FPP (Farnesyl pyrophosphate). The Ca^{2+}-level is measured by expressing GCaMP6f (a Ca^{2+}-sensitive protein). Intracellular or extracellular Ca^{2+} is chelated with either BAPTA-AM or EGTA. Scale bar 10µm.

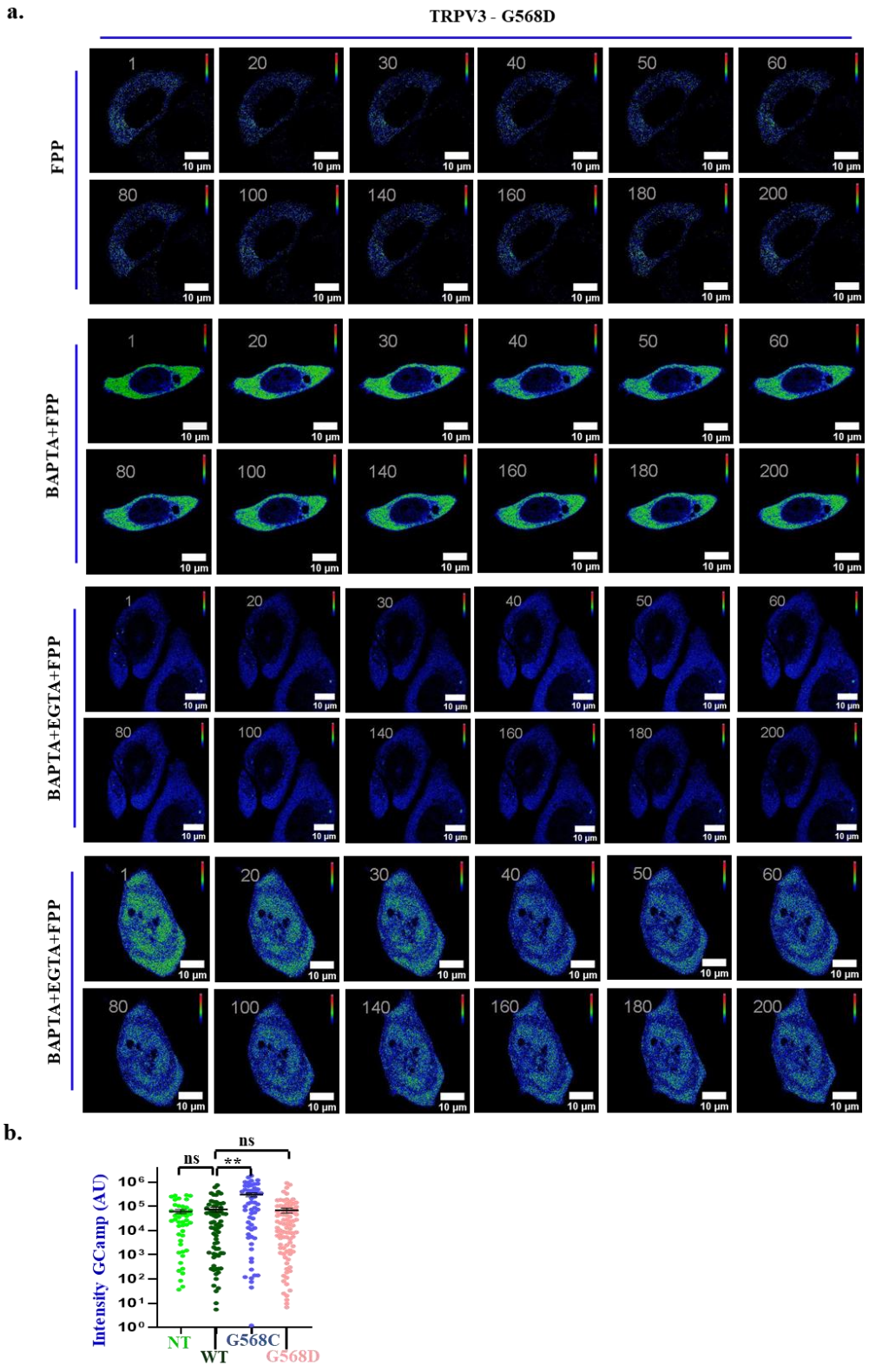

Fig 63. TRPV3 OS-mutant (G568D) expressing cell remain non-responsive to TRPV3 activator in HaCaT cell in Ca^{2+}-chelated conditions also. a. The TRPV3-G568D shows no response to the TRPV3 activation through FPP (Farnesyl pyrophosphate). The Ca^{2+}-level measured through GCaMP6f (a Ca^{2+}-sensitive construct). Intracellular or extracellular Ca^{2+} is chelated with BAPTA-AM and EGTA. Scale bar 10µm. **b.** The basal level Ca^{2+} (GCaMP6f intensity) in the TRPV3 OS-mutants (G568C) shows significantly more than TRPV3-WT and TRPV3-G568D. Unpaired t-test, ** = $p \leq 0.01$ and ns = non-significant.

2.5.3 OS-mutant expressing cells show higher lysosomal temperature and lower lysosomal particle numbers than TRPV3-WT cells

As mentioned earlier, the TRPV3 OS-mutant expressing cells show lesser lysosomal number and impaired lysosomal distribution within the cells than the cells expressing TRPV3-WT. LysoThermo Green (LTG) dye has been used to measure the lysosomal temperature (**Fig. 64; Fig. 65**). This dye shows higher fluorescence if the temperature is low and show lower fluorescence if the temperature is high. The TRPV3 OS-mutant expressing cells show a significant decrease in LTG-intensity as compared to cells expressing TRPV3-WT. Especially the cells expressing W692G and G573A, G573S, and G573C show decreased intensity. But in case of G568C mutant expressing cells, the fluorescence intensity is not much decreased (**Fig. 65a-b**). The decreased LTG-fluorescence intensity in the cells expressing OS-mutants indicate that the lysosomes became hotter than the lysosomes of cells expressing TRPV3-WT. These results show that the OS-mutants have increased lysosomal temperature. The number of lysosomal particles in each cell has been also investigated. It has been observed that the number of LTG-labelled particles is more in case of cells expressing TRPV3-WT than TRPV3 OS-mutants. The TRPV3-WT expressing cells have approximately~ 3-fold more number of lysosomal particles as compared to cells expressing any of these TRPV3 OS-mutants (G573A, G573C, G573S, G568C, G568D and W692G) (**Fig. 65c**). The fluorescent intensity quantified in fold change shows significant decrease in the level in the OS-mutants cells (**Fig. 65d-e**).

2.5.4 Cells expressing OS-mutants show higher plasma membrane temperature:

The plasma membrane quality seems to be very different in cells expressing TRPV3 OS-mutants. For example, adhesion ability is compromised in the cells expressing TRPV3 OS-mutants. Therefore, the plasma membrane temperature has been measured by using plasma thermo green (PTG) dye (**Fig. 66**). Lower fluorescence intensity of PTG dye signifies hotter

temperature and *vice versa*. The fluorescence intensity of PTG dye increases significantly in cells expressing most of the OS-mutants, suggesting lowering the temperature.

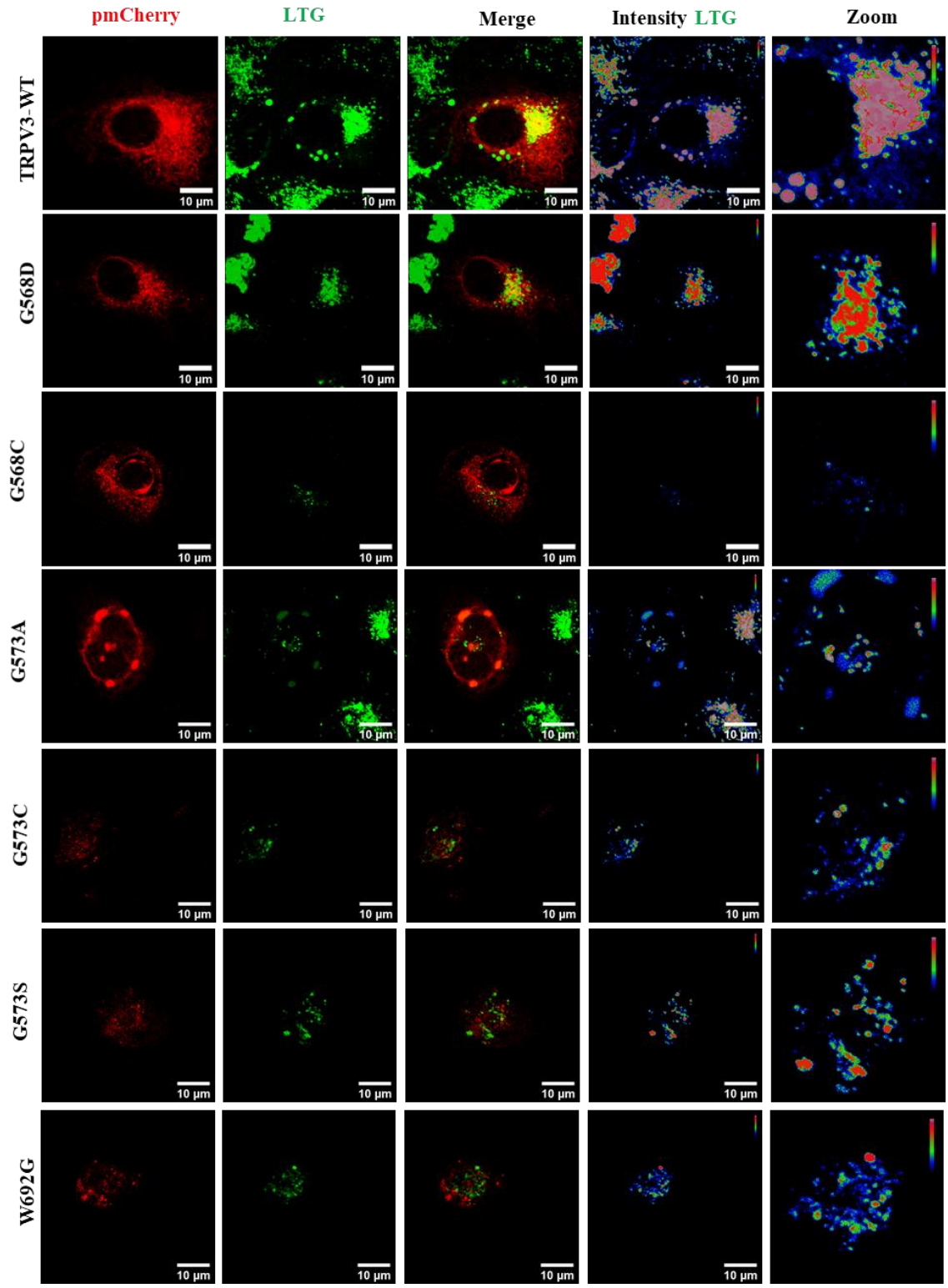

Fig 64. TRPV3 OS-mutants expressing cells show higher lysosomal temperature than cells expressing TRPV3-WT. The representative images show the TRPV3-WT and TRPV3 OS-mutants stained with LTG dye. LTG dye intensity is also shown in rainbow scale. Scale bar 10µm.

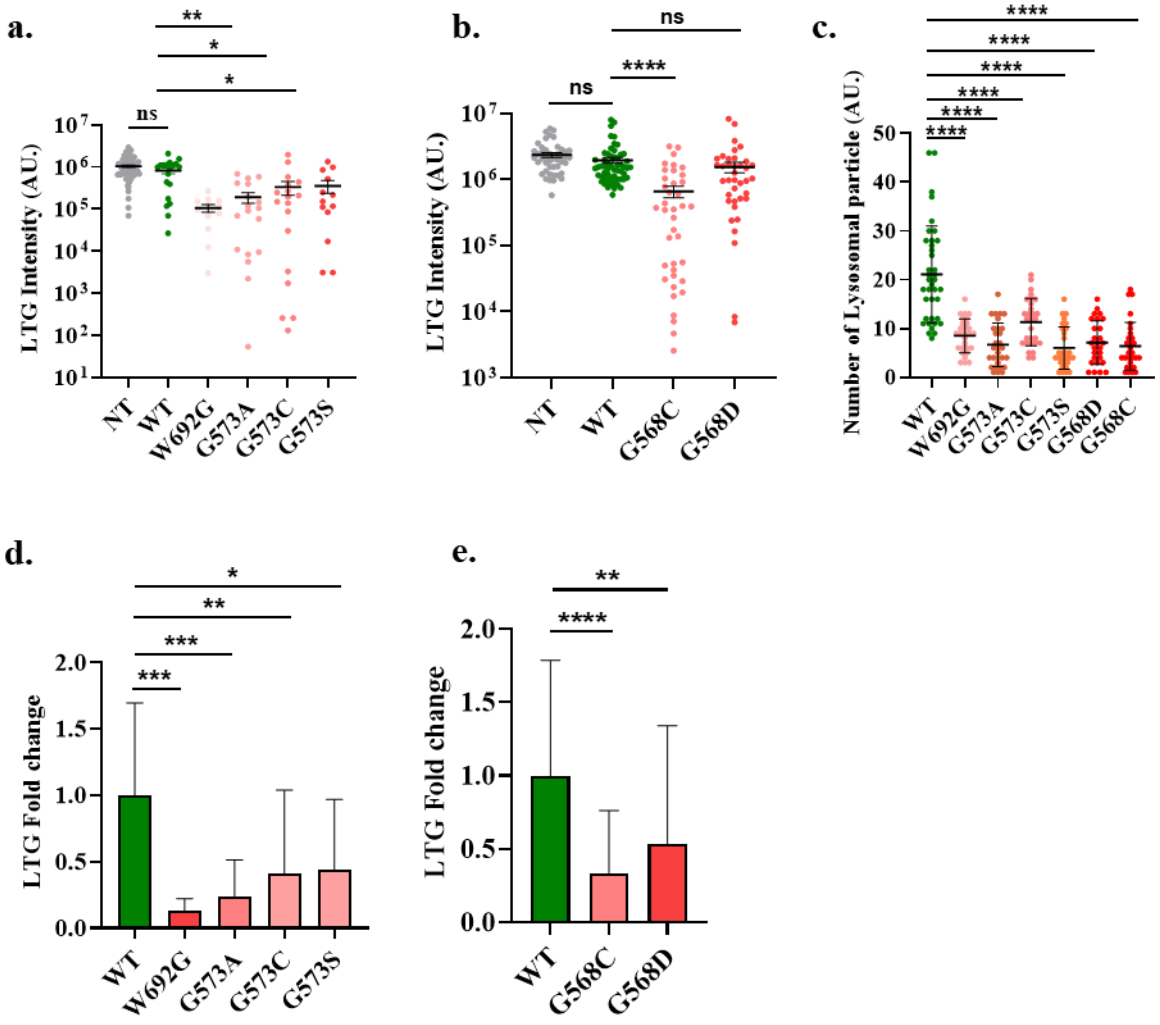

Fig 65. TRPV3 OS-mutants expressing cells show higher lysosomal temperature than cells expressing TRPV3-WT. a-b. The graph shows the LTG intensity is low in the cells expressing TRPV3 OS-mutants (except 568D) as compared to cells expressing TRPV3-WT. **c.** The graph represents lysosomal particle numbers (LTG-dye containing particles) in the cells expressing TRPV3-WT and TRPV3 OS-mutants. Cells expressing OS-mutants have less lysosomal particle counts. **d-e.** The graph represents fluorescent intensity change (in fold) in the cell expressing TRPV3-WT and TRPV3 OS-mutants. The fold change shows significant decrease in OS-mutants as compared with TRPV3-WT cells. One-way ANOVA, * = p≤0.05. ** = p≤0.01, *** = p≤0.001, **** = p≤0.0001 and ns = non-significant.

However, in case of cells expressing W692G, G573S and G568C mutants, the reduction in fluorescence intensity is not so significant. The significant drop in the fluorescence intensity have been observed in case of G573C, G573A and G568D as compared to the TRPV3-WT (**Fig. 66b**). So, the data suggest that the temperature become more at the plasma membrane region in case of TRPV3 OS-mutants as compared with the TRPV3-WT.

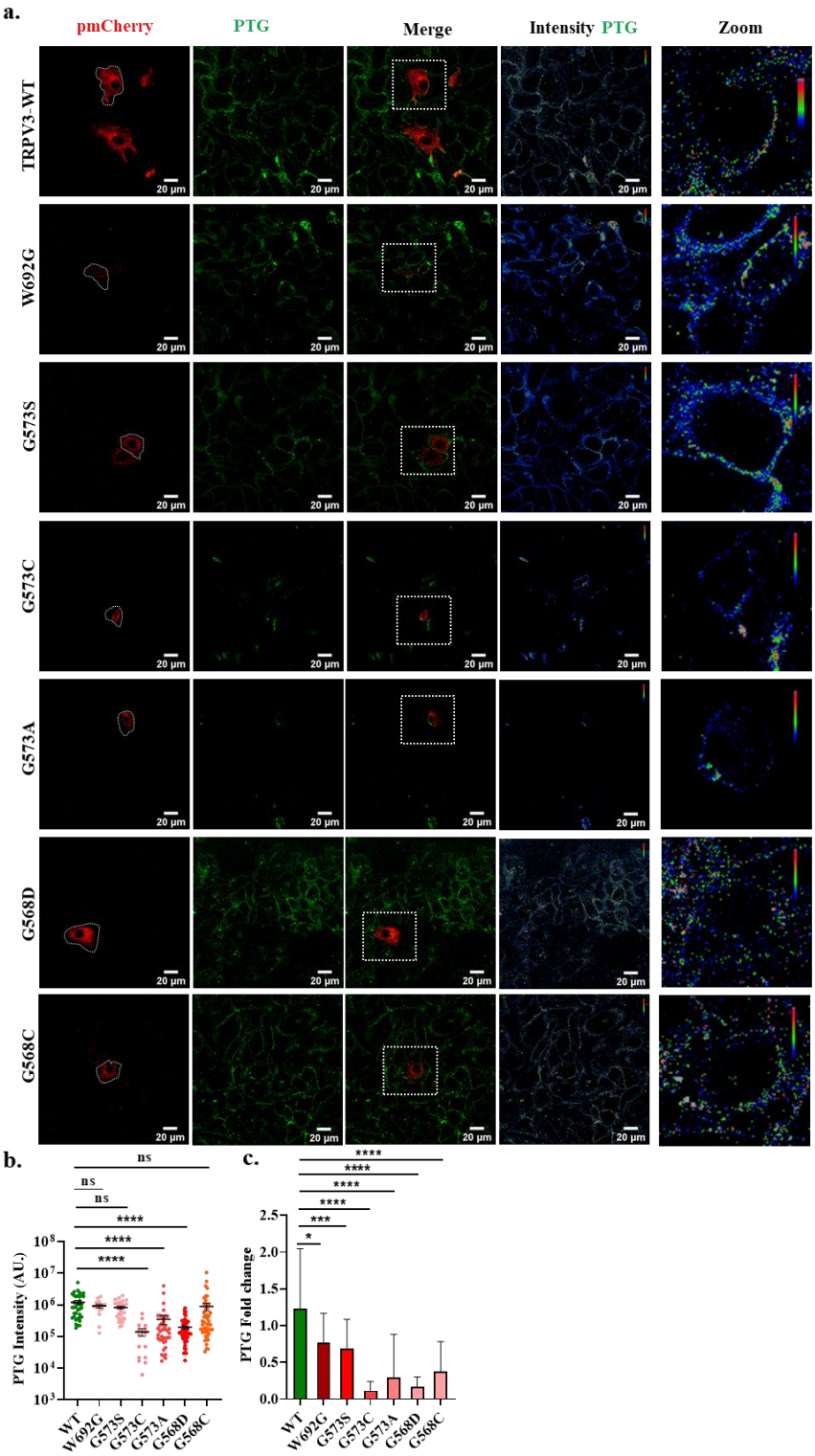

Fig 66. Cells expressing TRPV3 OS-mutants show higher plasma membrane temperature than TRPV3-WT cells. a. The representative images show the cells expressing TRPV3-WT or TRPV3 OS-mutants as RFP-tagged proteins (red) and labelled with PTG dye (green). Scale bar 20µm. **b.** The graph shows the PTG intensity dropped in the TRPV3 OS-mutants (except W692G, G568C and G573S) as compared to TRPV3-WT cells. Here in case of TRPV3-WT the intensity taken as standard and degree of changes in the intensity based on the TRPV3-WT intensity. **c.** The graph represents fluorescent intensity change (in fold) in the cell expressing TRPV3-WT and TRPV3 OS-mutants. The fold change shows significant decrease in OS-mutants as compared with TRPV3-WT cells. One-way ANOVA, * = $p \leq 0.05$, **** = $p \leq 0.0001$ and ns = non-significant.

2.5.5 Cells expressing TRPV3 OS-mutants show higher mitochondria temperature

The mitochondria morphology and temperature has been investigated in the cells expressing TRPV3-WT and different TRPV3 OS-mutants (**Fig. 67, Fig. 68**). The more MitoThermo Green (MTG) fluorescence intensity signifies the less mitochondrial temperature. Here the TRPV3 OS-mutants specially G573S and G568C show less MTG-intensity than other mutants and TRPV3-WT cells (**Fig. 67)**. Thus, the temperature has been significantly more as compared to the TRPV3-WT condition and other mutants. The G568C mutant expressing cells also show significantly more mitochondrial temperature than cells expressing TRPV3-WT (but the degree of significance is less, ***** = $p \leq 0.05$) (**Fig. 68b&c**). Taken together, the data suggest that the mitochondrial temperature in the cells expressing OS-mutants have increased as compared to cells expressing TRPV3-WT cells.

2.5.6 Cells expressing TRPV3 OS-mutants show lower nuclear temperature

The morphology as well as the intracellular compartment functions and distributions are typically disturbed in the cells expressing TRPV3 OS-mutants. The Nuclear Thermo Green (NTG), a nuclear temperature-sensor dye was used to measure the nuclear temperature. The NTG fluorescence intensity distribution varied in different region of nucleus (nucleolar region shows less intensity). This NTG dye primarily localizes in the nucleus (but not in the nucleolus) and its change in the fluorescence properties indicates the change in the nuclear temperature (**see Annexure: 7.1**). Low NTG-fluorescence intensity indicates higher nuclear temperature and *vice versa*. NTG fluorescence intensity provides equivalent information related to nuclear thermal pattern. Cells expressing TRPV3-WT and TRPV3 OS-mutants show differences in fluorescence intensity (**Fig. 69**). These differences remain significant in case of cells expressing any of these TRPV3 OS-mutants with respect to cells expressing TRPV3-WT. The intensity increased significantly in the TRPV3 OS-mutants.

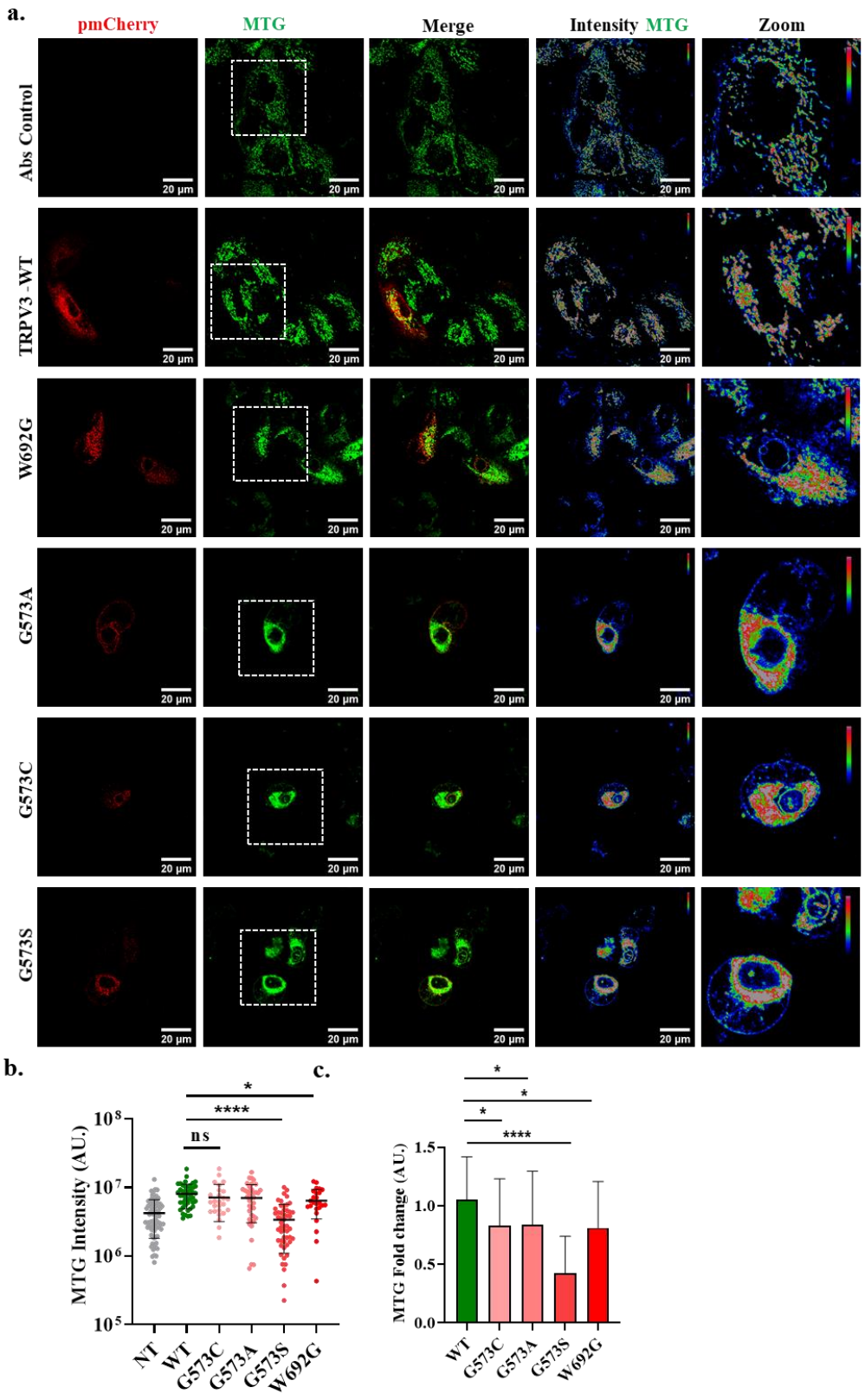

Fig 67. TRPV3 OS-mutants expressing cells show higher Mitochondrial temperature than cells expressing TRPV3-WT. a. The representative images show the cells expressing TRPV3-WT and TRPV3 OS-mutants (red) labelled with MTG dye. The MTG fluorescence is also shown in rainbow scale. Scale bar 20µm. **b.** The graph shows comparatives of MTG fluorescence intensity in cells expressing TRPV3 WT or OS-mutants. MTG fluorescence is low in the cells expressing TRPV3 OS-mutant as compared to cells expressing TRPV3-WT. **c.** The graph shows comparatives of MTG fluorescence intensity (in fold change) in cells expressing TRPV3-WT or OS-mutants. (One-way ANOVA, * = $p \leq 0.05$, **** = $p \leq 0.0001$ and ns = non-significant).

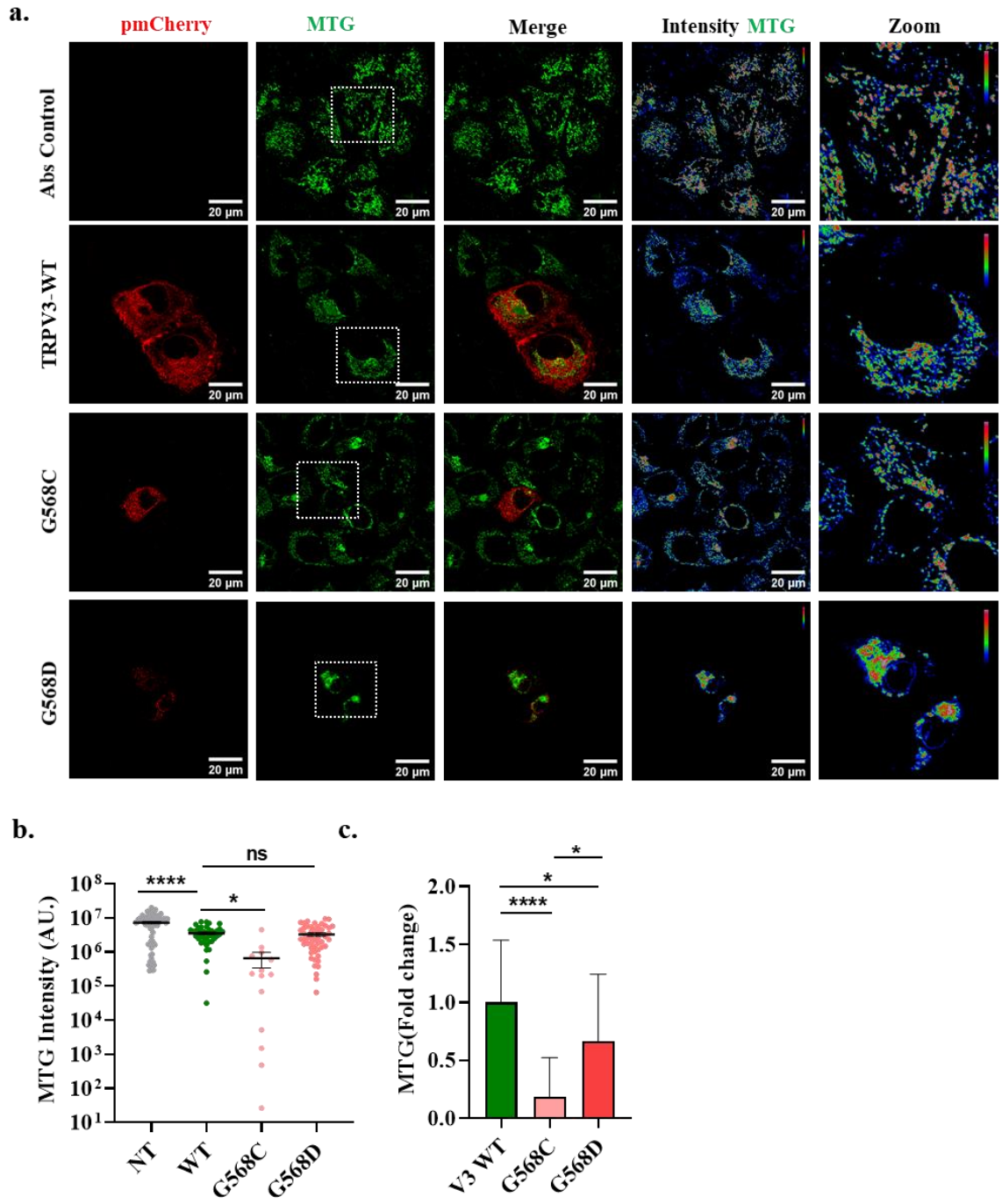

Fig 68. TRPV3 OS-mutant expressing cells show higher mitochondrial temperature than cells expressing TRPV3-WT. a. The representative images show the MTG dye-based fluorescence from live cells expressing TRPV3-WT and TRPV3 OS-mutants (568C and 568D). Scale bar 20µm. **b.** Comparative analysis of MTG fluorescence in cells expressing TRPV3-WT and TRPV3 OS-mutants. The graph shows the MTG intensity is low in the cells expressing TRPV3 OS-mutant as compared to the cells expressing TRPV3-WT. **c**. The graph shows comparatives of MTG fluorescence intensity (in fold change) in cells expressing TRPV3 WT or OS-mutants. One-way ANOVA, * = $p \leq 0.05$ and **** = $p \leq 0.0001$.

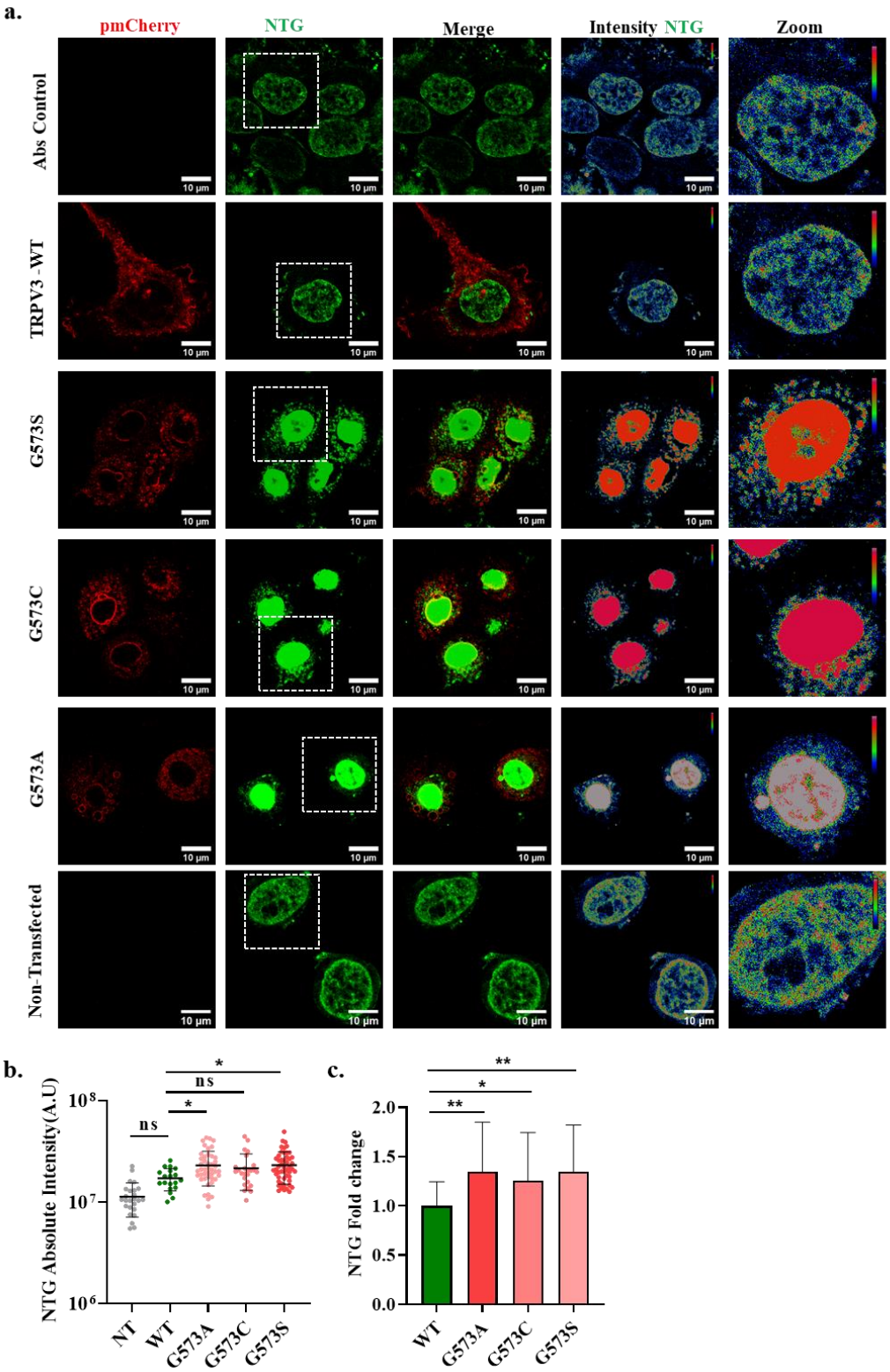

Fig 69: Cells expressing TRPV3 OS-mutants show lower Nuclear temperature as compared to cells expressing TRPV3-WT. a. The representative images show the live cells expressing TRPV3-WT and TRPV3 OS-mutants (red) labelled with NTG dye (green). Scale bar 10µm. **b.** The graph shows that the NTG fluorescence intensity is high in the cells expressing TRPV3 OS-mutant as compared to the cells expressing TRPV3-WT. **c**. The graph represents fluorescent intensity change (in fold) in the cell expressing TRPV3-WT and TRPV3 OS-mutants. The fold-change shows significant decrease in OS-mutants as compared with TRPV3-WT cells. One-way ANOVA, * = $p \leq 0.05$ and ns = non-significant. (NT = Non-transfected).

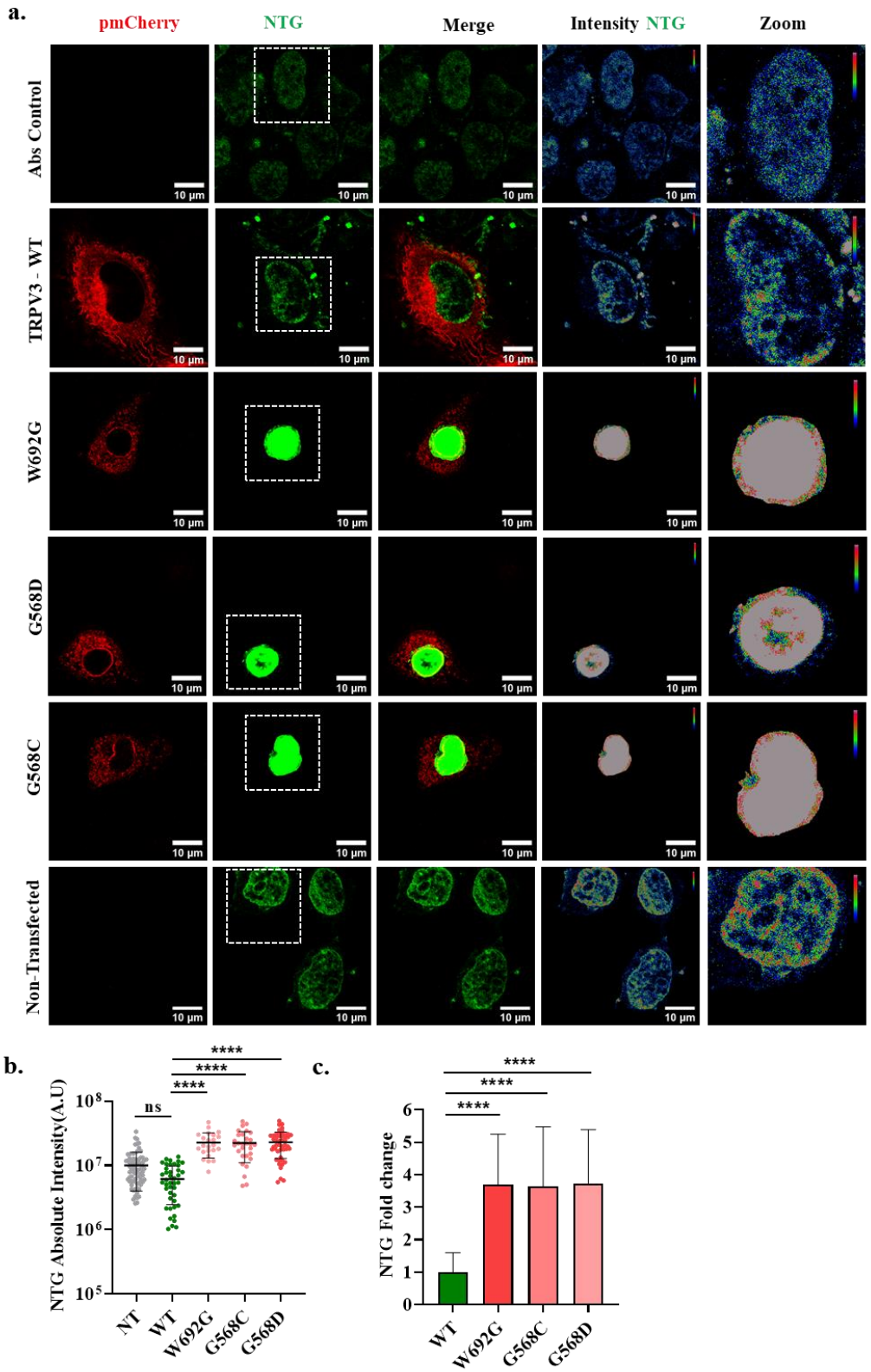

Fig 70. Cells expressing TRPV3 OS-mutants shows lower nuclear temperature than cells expressing TRPV3-WT. a. The representative images show the live cells expressing TRPV3-WT and TRPV3 *OS*-mutants that are further labelled with NTG dye. Scale bar 10µm. **b.** The graph shows the NTG fluorescence intensity is more in the cells expressing TRPV3 OS-mutant as compared to TRPV3-WT cells. **c**. The graph represents fluorescent intensity change (in fold) in the cell expressing TRPV3-WT and TRPV3 OS-mutants. The fold change shows significant decrease in OS-mutants as compared with TRPV3-WT cells. One-way ANOVA, **** = p ≤0.0001 and ns = non-significant. (NT = Non-transfected).

Thus, the temperature is significantly low in the cells expressing G568C, G568D and W692G (******** = p≤0.0001) mutants as well as in cells expressing 573A and 573S mutants (***** = p≤0.05) (**Fig. 70**). This signifies that the reduction in nuclear temperature in the cells expressing TRPV3 OS-mutants (as compared to cells expressing TRPV3-WT) is a hallmark of this pathophysiology. In summary the thermal status of cells expressing TRPV3 OS-mutants show lower temperature in the nuclear region as compared to the cells expressing WT.

Overall, the MTG, PTG, LTG fluorescence intensity reveals that the cells expressing OS-mutants have less fluorescence intensity (i.e. hotter temperature) for most of the sub-cellular organelles as compare to the cells expressing TRPV3-WT cells. However, for nucleus it is opposite. Thus, cells expressing OS-mutants have high fluorescence intensity (i.e. lower temperature) for the nucleus as compared to the cells expressing TRPV3-WT cells. Overall, data suggest a huge thermal imbalance within the sub-cellular regions in case of OS-mutants.

2.6 The importance of TRPV4 in the macrophage cells and the role of TRPV4 in the inflammatory function

In recent studies, the TRPV4 ion channel has been investigated for its role in macrophage functions. It appears that TRPV4 is involved in facilitating exocytosis by using lysosomes as a storage reservoir for cellular cargo. This process relies on interactions between various proteins that regulate cargo distribution within cells. The presence of lysosome-associated membrane protein 2 (LAMP2) has been linked to TRPV4-mediated exocytosis, especially in melanoma cells (Li et al. 2022). Additionally, TRPV4 has been implicated in disrupting the barrier functions of epithelial and endothelial cells, particularly in the context of lung edema formation. It also plays a significant role in inflammatory responses, affecting processes like cytokine production, foam cell formation, and giant cell formation. The evolving understanding of macrophage TRPV4 in conditions like fibrosis, chronic itch, and the foreign body response hints at its multifaceted role (Luo et al. 2015; Dutta et al. 2020). Moreover, TRPV4 is expressed in various macrophage subtypes, influencing their behaviour and phenotype during encounters with pathogens and instances of inflammation. It is also involved in regulating adipose metabolism, inflammation, and energy balance within cells. Furthermore, recent research has focused on TRPV4's role in lysosomal functions. TRPV4 channels are found in lysosomes and can help maintain their acidic pH. They can also influence lysosomal temperature and various cellular stress parameters, including cytosolic pH, cytosolic ROS, and cytosolic NOS levels. This suggests that TRPV4 may have a broader role in cellular and lysosomal functions beyond its previously known functions in macrophages and inflammation. The data provided in this chapter highlights how modulating TRPV4 activity contributes to maintaining various stress levels within cells. Additionally, it confirms that TRPV4 is found in compartments within macrophage cells and suggests its potential involvement in the functions of lysosomes and in managing stress responses in the intracellular environments. Moreover,

the data hints at TRPV4 possibly aiding in clearing bacteria from wound sites and promoting wound healing. Overall, this chapter provides valuable insights into how TRPV4 might play a role in the body's inflammatory responses.

2.6.1 TRPV4 modulation helps in *in vivo* bacterial clearance in the skin tissue

The impact of TRPV4 activation or inhibition on the skin wound healing process has been explored in *in vivo* system. For that purpose, an external skin wound (5 mm) was developed in mice and infected the same wound with 100µL (equivalent to 1×10^8 CFU/mL) MRS (*Staphylococcus aureus*) bacteria on day 1. It was observed that topical application of TRPV4 activator (4αPDD, 5µM) daily enhances the skin wound healing by the 10^{th} day while TRPV4 inhibition (RN1734, 10µM) does not result in enhanced healing of skin wound at the same duration (**Fig. 71**). Both the percentage of wound healing and the rate of wound healing are calculated. Both, in TRPV4-inhibited as well as in TRPV4-activated conditions, the wound closure was significantly faster, and the percentage of wound closure was lesser than in control (DMSO) conditions (**Fig. 71c**). To confirm that the TRPV4-activation-induced enhanced skin wound healing is indeed related to TRPV4-mediated functions, the bacterial numbers in the pus were counted and compared accordingly. The bacterial numbers present in the unit volume (100µl) of pus (on the 10^{th} day collection) becomes significantly low in case of TRPV4 activation and as well as in inhibition conditions if compared to DMSO control (**Fig. 71b**). This suggests that TRPV4 modulations are effective in the clearance of MRSA bacteria at the wound site.

2.6.2 TRPV4 in wound healing and its histopathology significance

To understand the status of the wound tissue healing process, the histochemistry of the wound tissue was analyzed on 10^{th} day (**Fig. 72a-b**). It was observed that the healing was

almost complete in the case of TRPV4 activation on 10th day. Expression of TRPV4 in the wounded or wound-healed tissue was analysed (**Fig. 72a-b**).

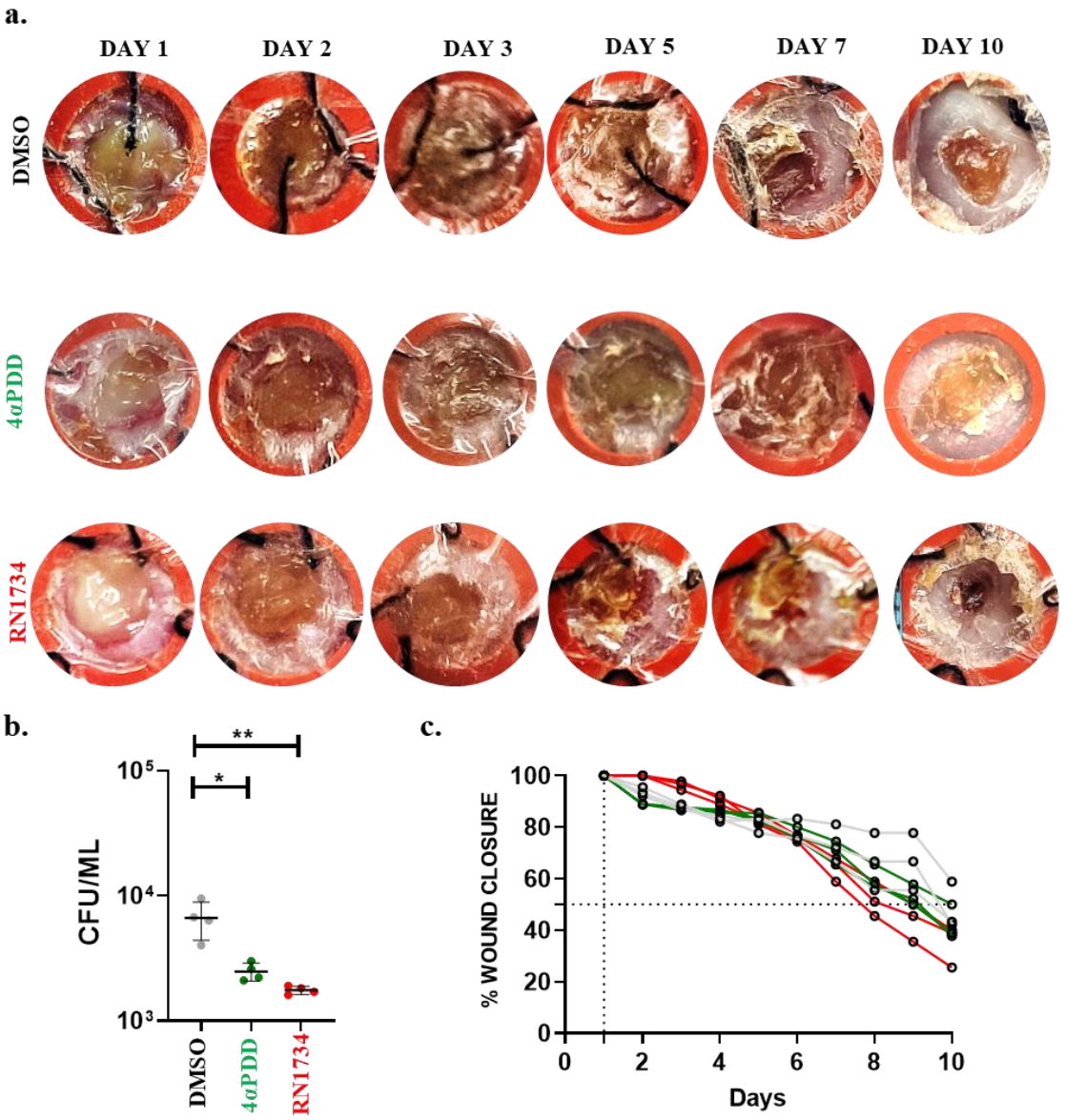

Fig. 71. Role of TRPV4 modulations in wound closure and *in-vivo* bacterial clearance. a. These images show the wound closure in the animal followed till 10th days in different conditions (TRPV4 activation, TRPV4 inhibition, and DMSO control) respectively. **b**. The graph shows the comparative CFU count from the pus collated in the wound site at 10th day. Both the activation as well as inhibition of TRPV4 cause lesser CFU count in comparison with DMSO control. **c.** The graph shows the percentage of wound closure in the TRPV4-modulated conditions. The percentage of wound closure was more in the case of both activation and inhibition in comparison with DMSO control. One-way ANOVA test. * = $p \leq 0.05$, ** = $p \leq 0.01$.

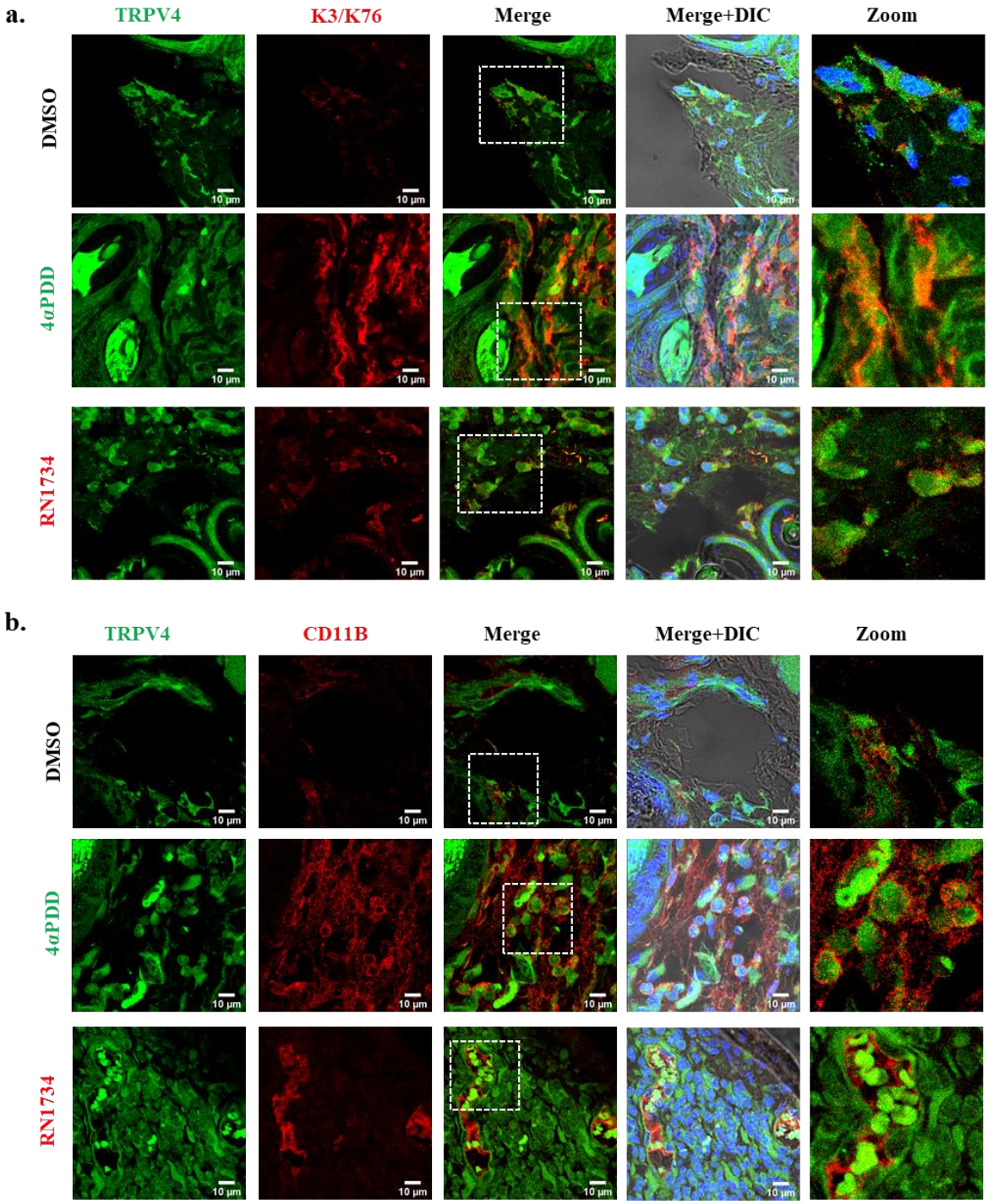

Fig. 72. TRPV4 colocalizes with macrophage and keratinocyte-specific markers in wound-healed tissues. a. The representative confocal image shows the colocalization of TRPV4 along with keratinocytes marker (K3/K76). **b.** The image shows the colocalization of macrophage marker (CD11B) with the TRPV4 in the wound area. Scale bar 10µm.

The expression of TRPV4 was observed in the wound tissue section, mainly at a low level in the keratinocytes. On the 10^{th} day, expression of TRPV4 is observed in the tissue (in the wounded area or wound healed), especially in the keratinocytes and in the macrophages

(positive for CD11b marker) (**Fig. 72b**). Notably, in the case of TRPV4 activation or inhibition, more CD11b-positive cells are observed, especially near wound area, suggesting that TRPV4 modulations results in more migration of macrophages in the wound area (**Fig. 72b**).

To understand the localization of keratinocytes, α keratin (k3/k76) along with TRPV4 was used, where it was found that both the proteins co-localized in the near wound area on the 10^{th} day. And in the case of almost healed tissue in TRPV4 modulated condition, migrated keratinocytes were found to be colocalized with TRPV4, suggesting that macrophages express more TRPV4 during wound healing (**Fig. 72a**).

2.6.3 TRPV4 is endogenously expressed in the macrophage cells and localizes within the lysosome

Expression and localization of TRPV4 (another functional/homologue of TRPV3) has been explored in the peritoneal macrophages and macrophage cell line (Raw 264.7). Endogenous expression of TRPV4 has been observed in these cells and that accords with other reports mentioning the expression of TRPV4 in the macrophage cell (Gupta et al. 2019; Nguyen et al. 2022). Localization of TRPV4 is not limited to the plasma membrane only, and it is reported to be localized in different sub-cellular compartments (Arniges et al. 2006; Acharya et al. 2022; Espadas-Álvarez et al. 2021). The expression level was verified using the TRPV4 antibody stained with other organelle-specific markers. The expression of TRPV4 varies upon macrophage stimulation by LPS (lipopolysaccharides). It has been observed that the expression increases upon LPS-stimulation significantly. Thus, in macrophage cell, expression of TRPV4 in macrophages is LPS-dependent, at least partially (**Fig. 73b**). This TRPV4-specific immunostaining can be blocked by using a specific peptide that binds to the TRPV4 antibody (**Data not shown**). The expression level was also verified by Western blot analysis of the lysosomal fraction as well as of whole cell lysate (**Data not shown**). Lysosomal marker, such

as Lamp1 was also probed. The presence and expression level of TRPV4 was verified along with the LysoTracker Red dye (**Fig. 73a-b**). It has been found that TRPV4 colocalizes with the lysosome that are labelled with the LysoTracker Red dye. Thus, the presence of TRPV4 in lysosome can be visualized as yellow dots or colocalized pixels (**Fig. 73a**). The presence of TRPV4 within the lysosome is observed for a subset of lysosomes and not in all lysosomes.

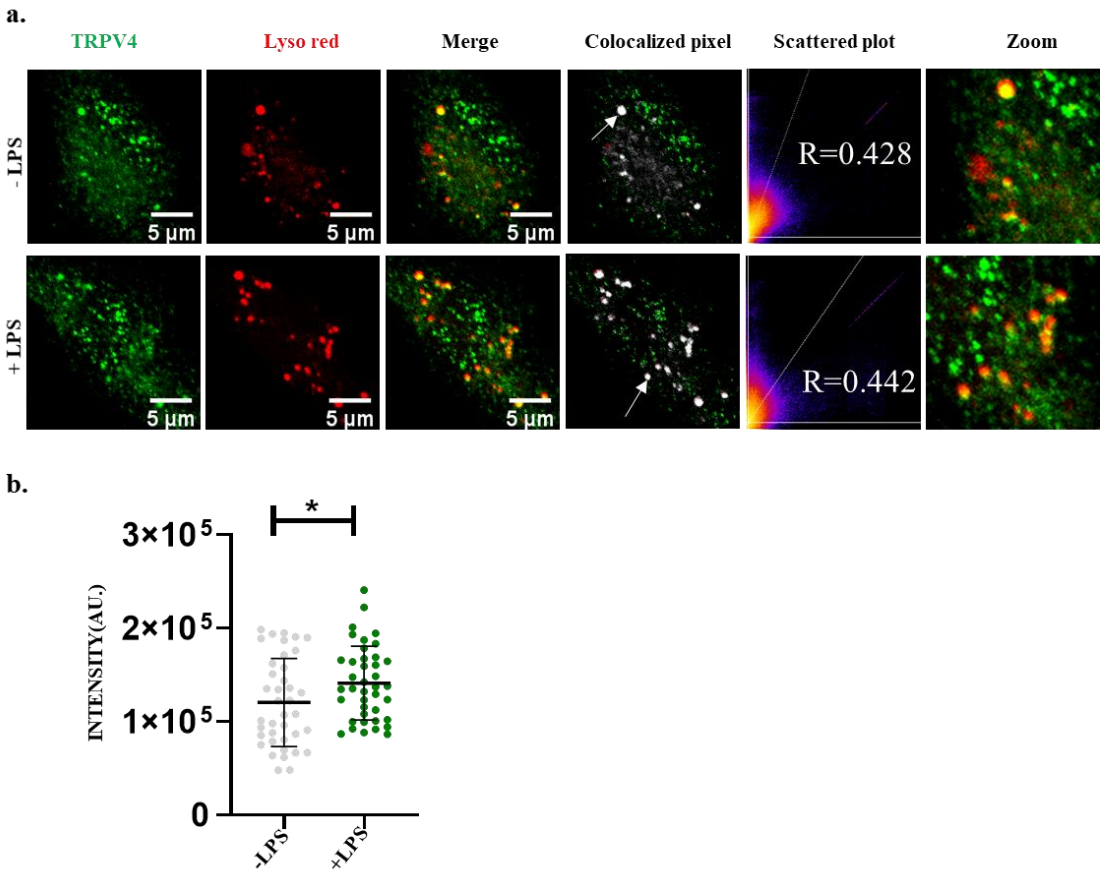

Fig. 73. Endogenous expression of TRPV4 in peritoneal macrophages. a. The representative image shows the TRPV4 (in green) expression in PM with and without LPS-stimulation. The colocalization of the lysosome (labelled with LysoTracker Red stain) with TRPV4 (detected by antibody staining, green) is shown. Colocalized pixels and the scattered plot are also shown. Scale bar 5µm. **b.** The graph shows the intensity plot of TRPV4 expression in the PM with and without LPS treatment (14 hours). The intensity of TRPV4 (total cell) increased in LPS-stimulated cells. Unpaired t-test, * = $p \leq 0.05$.

2.6.4 TRPV4 activation causes Ca^{2+}-influx in the macrophage cells

To check the impact of TRPV4 on Ca^{2+}-homeostasis of macrophage cells, TRPV4 modulation has been carried out on resting cells as well as in cells where intracellular or extracellular Ca^{2+} has been chelated by BAPTA-AM or EGTA respectively (**Fig. 74a-b**).

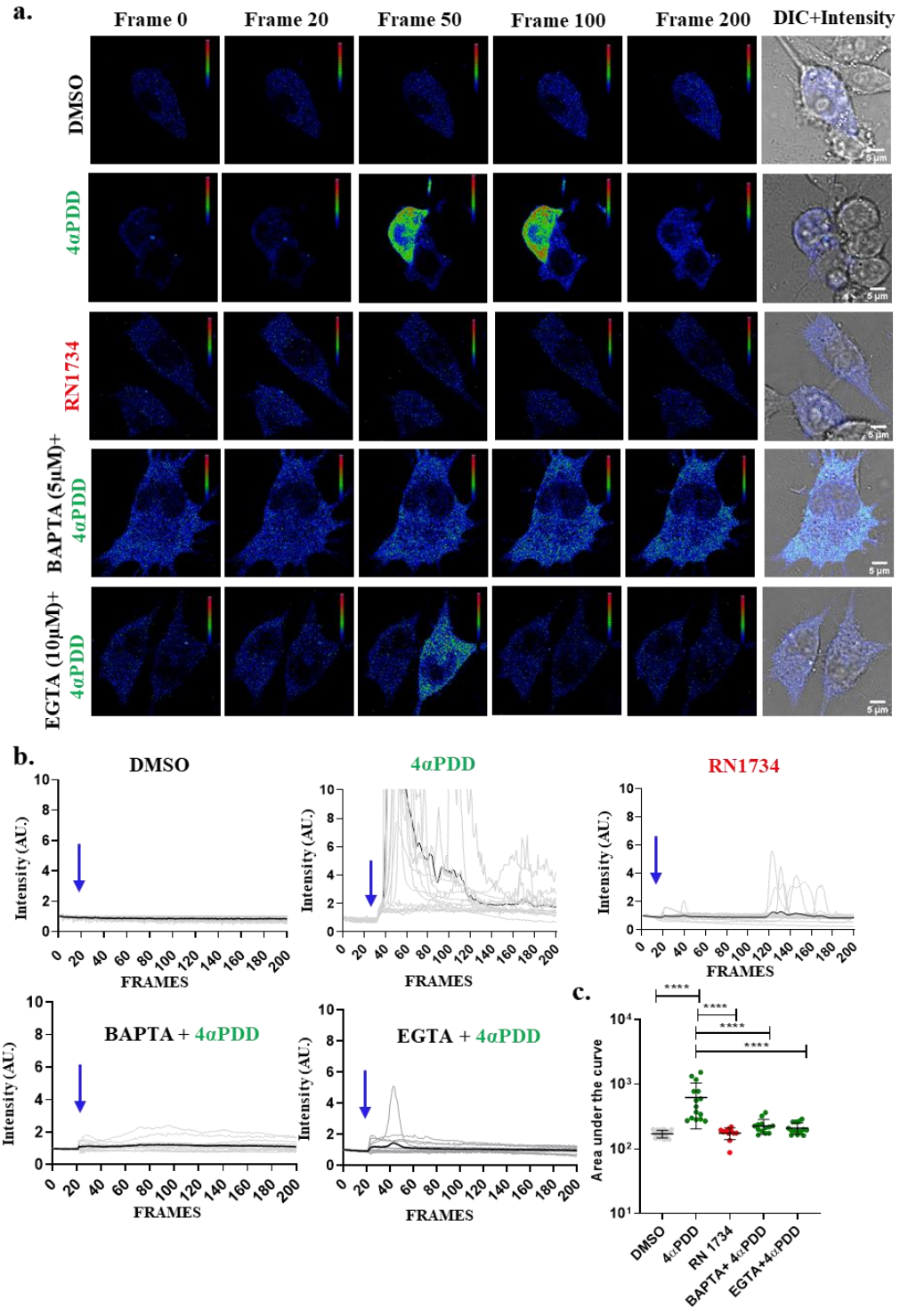

Fig. 74. TRPV4 activation increases the cytosolic Ca^{2+}-level. a. The representative images show the Ca^{2+}-influx in the Raw 264.7 cells after TRPV4 activation, inhibition, and at TRPV4 activation in Ca^{2+}-chelated conditions (BAPTA or EGTA). Fluorescence intensity of GCaMP6F is represented in pseudo colors (blue indicates low and red indicates high Ca^{2+}-levels respectively). Scale bar 5μm. **b.** The graphs represent the cytosolic Ca^{2+}-influx at TRPV4-modulated and Ca^{2+}-chelated conditions. TRPV4 activation causes a significant increase in the Ca^{2+}-level due to 4αPDD added at the 20th frame. **c**. The graph represents the "area under the curve" in different conditions. The TRPV4 activations show significantly more (AUC) value than other conditions. One-way ANOVA test. **** = $p \leq 0.01$.

For Ca^{2+}-imaging, Ca^{2+}-sensitive construct i.e., GCaMP6F has been used which is sensitive to fluctuations in intracellular Ca^{2+}-level. Different conditions were used where TRPV4 is activated (by 4αPDD), inhibited (by RN1734), or different sources of Ca^{2+} has been chelated. Total 200 time-series image frames were acquired to assess the impact of TRPV4 modulation on cytosolic Ca^{2+}-levels. The Ca^{2+}-influx has been significantly increased in the TRPV4-activated condition, when the 4αPDD has been added in the 30^{th} frame (**Fig. 74b**). The sudden Ca^{2+}-influx has been observed upon TRPV4 activation at 30^{th} frame but there was no Ca^{2+}-influx upon RN1734-treatment (**Fig. 74b**). The 4αPDD-treatment enhances Ca^{2+}-influx, but such response is reduced upon chelation of intracellular cytoplasmic or extracellular Ca^{2+}-sources by using BAPTA or EGTA respectively (**Fig. 74b**).

To assess the extent of total Ca^{2+}-influx in a given duration in each condition, the "total area under the curve" (AUC) was analysed. It is observed that the AUC is significantly higher in case of the 4αPDD-treatment (**Fig. 74c**). This 4αPDD-mediated total Ca^{2+}-influx is reduced when Ca^{2+}-chelators such as BAPTA-AM or EGTA were used. These data signify that the TRPV4 activation helps in enhanced Ca^{2+}-influx in the macrophage cells.

2.6.5 TRPV4 modulations maintain lysosomal as well as cytosolic pH in macrophage cells

At control condition, i.e. at 37°C, alteration of lysosomal pH has been checked by using LysoSensor Green dye (lysosomal pH-sensitive sensor) by pharmacological modulation of TRPV4 (**Fig. 75a-b**). It has been found that the intensity of the LysoSensor Green dye increased significantly due to TRPV4 activation. The LPS which is a macrophage cell stimulator, also tends to increase the fluorescence intensity of TRPV4 activations. But on the contrary, the TRPV4 inhibitor was not able to increase the intensity level rather it was lower than the control condition (**Fig. 75b**). This shows that at the TRPV4 activation as well as LPS-stimulation for 2 hours conditions, the lysosomal pH level maintains to a more acidic level.

But when the cells were probed with pHrodo dye (cytosolic pH-indicators) the TRPV4 activation did not show any changes on the contrary the TRPV4 inhibition shows a similar trend as lysosomal pH (lowered intensity) like a significant decrease in the intensity level (**Fig. 76**). The LPS-stimulation shows increased intensity in comparison with DMSO-control conditions (**Fig. 76b**).

Similar experiments have been investigated in the Raw 264.7 cells for lysosomal pH and cytosolic pH regulation. The cytosolic and lysosomal pH levels have been investigated with different treatments, like TRPV4 activation, inhibition, LPS-stimulation, TRPV4 activation or inhibition in case of pre-treatment with LPS, and TRPV4 activation by 4αPDD in case of pre-treatment with an inhibitor (RN1734) (**Fig. 77&78**). The TRPV4 activations seems to increase the fluorescence intensity significantly whereas inhibition have decreased intensity, both in the case of cytosolic pH and lysosomal pH. The intensity level has also significantly increased in case of LPS-stimulation (**Fig. 78a&b**). To understand the relationship of lysosomal pH with cytosolic pH, the ratio of LysoSensor Green fluorescence intensity with pHrodo fluorescence intensity per cell was calculated (**Fig. 78c**). Notably, the ratio values do not remain same or constant in all conditions, suggesting that TRPV4 modulation and/or LPS-treatment alters the pH regulation of lysosome and cytosol differently. The ratio become significantly low in case of TRPV4 inhibition and more in case of TRPV4 activation as well as in LPS-stimulated condition. However, in presence of LPS, TRPV4 modulation lowers this ratio (**Fig. 78c**).

In order to understand the relationship of lysosomal pH with cytosolic pH in details, the correlation between lysosomal pH with cytosolic pH in different conditions were analysed (**Fig. 79a-b**). Notably, these correlations remain variable in different conditions.

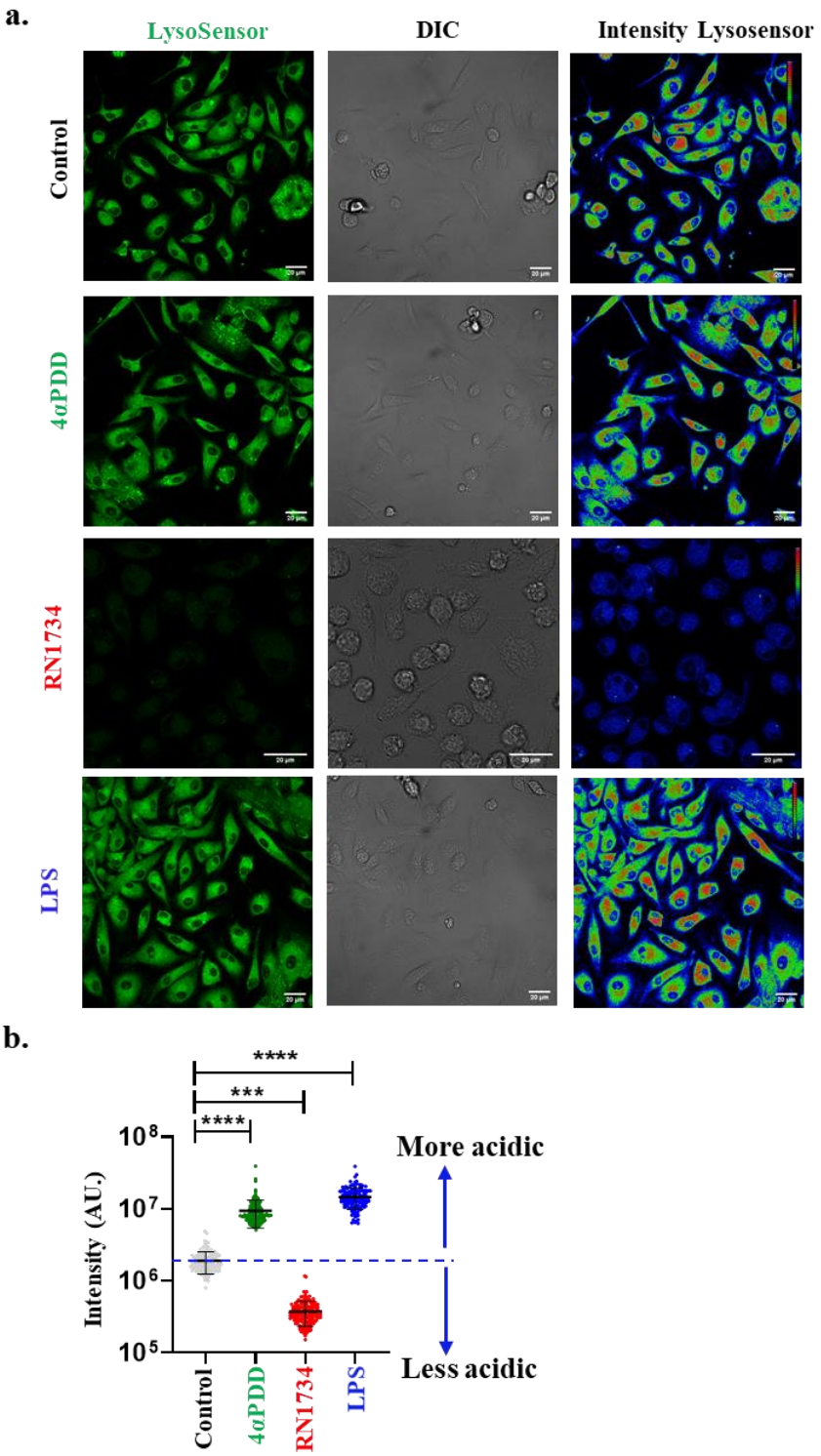

Fig 75. TRPV4 modulation helps maintain lysosomal pH in the macrophage cells (PM). a. The above figure shows the LysoSensor Green dye-based fluorescence intensity at different modulated conditions like TRPV4 activation, TRPV4 inhibitions and LPS stimulations**.** Scale bar 10µm. **b.** The graph represents varied intensity upon TRPV4 modulation and LPS stimulations. The graph shows increased LysoSensor Green intensity at TRPV4 activation and significant decreased intensity at TRPV4 inhibitions. One-way ANOVA test. (**** = $p \leq 0.0001$, *** = $p \leq 0.001$).

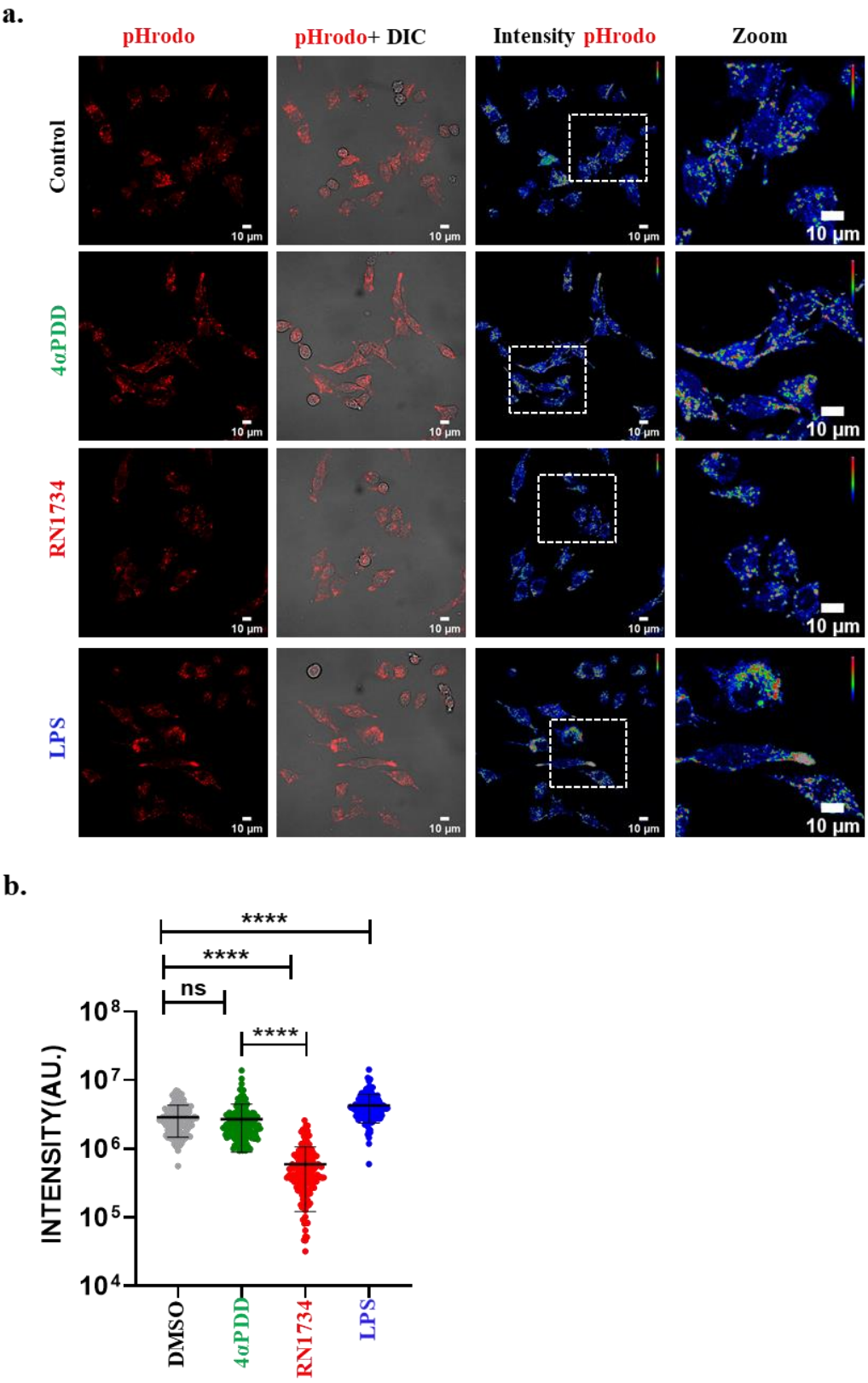

Fig 76. TRPV4 modulation helps maintain cytosolic pH in the in PM. a. The figure shows cytosolic pH difference in TRPV4 modulated conditions as well as in LPS stimulated conditions. Scale bar 10µm. **b.** The graph here represents intensity difference at TRPV4 modulated conditions as well as in LPS-stimulated conditions. The cytosolic pH intensity shows no difference between control and TRPV4 activation conditions. One-way ANOVA test. (**** = p≤ 0.0001; *** = p≤0.001; ** = p≤ 0.01, ns = non-significant).

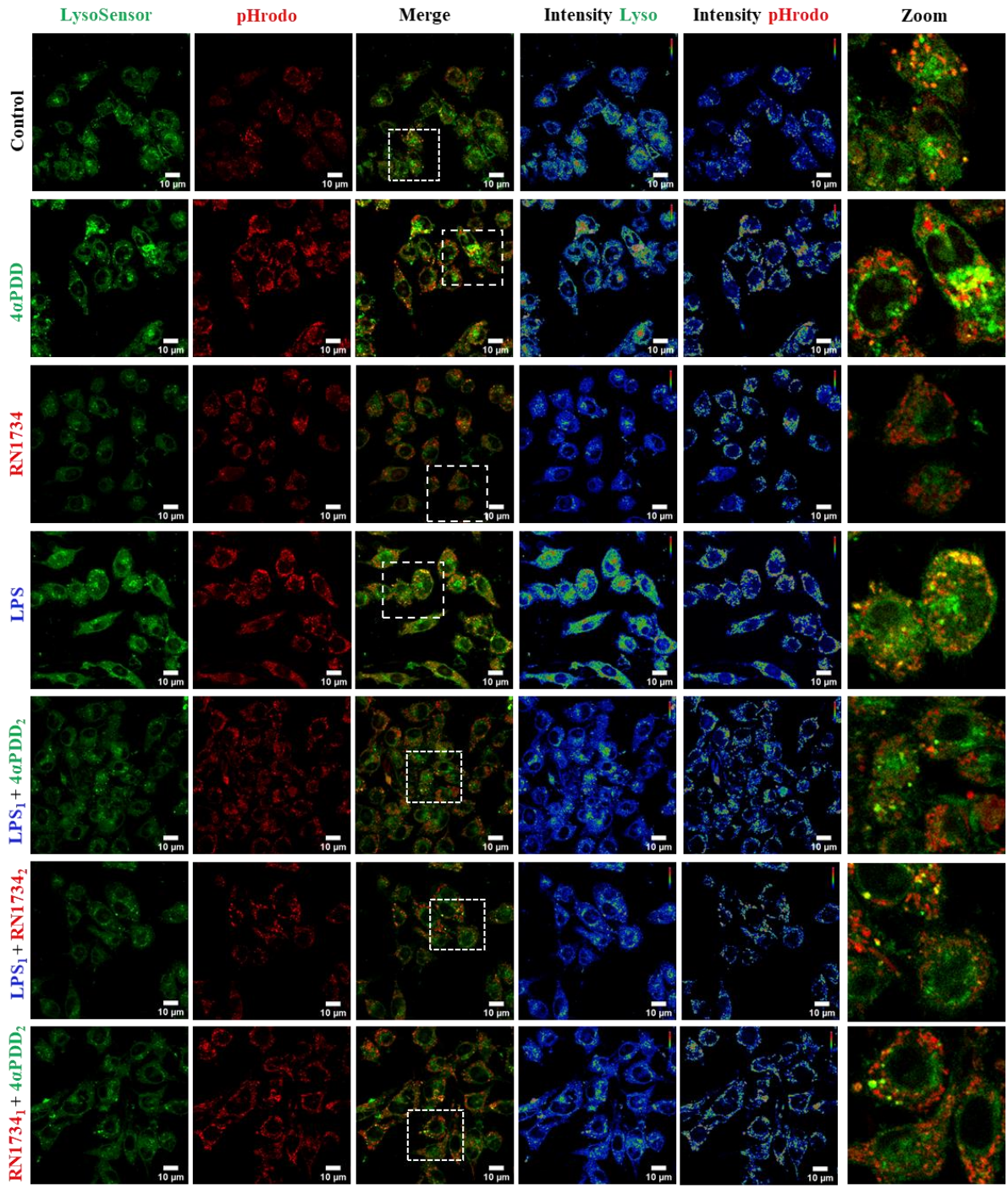

Fig 77. TRPV4 modulation helps in maintaining lysosomal and cytosolic pH in the in Raw 264.7 cells. The above figure shows the LysoSensor Green fluorescence intensity at different modulated conditions like TRPV4 activation, TRPV4 inhibitions, LPS stimulations, pre-treated LPS with 4αPDD or RN1734, and pre-treated RN1734 with 4αPDD (Total duration was 2 hours pre-treated LPS/RN1734 + 2 hours 4αPDD). Scale bar 10µm.

The correlations between cytosolic and lysosomal pH show high correlation in case of TRPV4 activation 4αPDD (r = 0.8642) and LPS (r = 0.8719) and low value in case of TRPV4

inhibition (r = 0.3389). The correlation value remains modest in case of TRPV4 activation in LPS pre-treated as well as in RN1734-pre-treated cells (**Fig. 79a**).

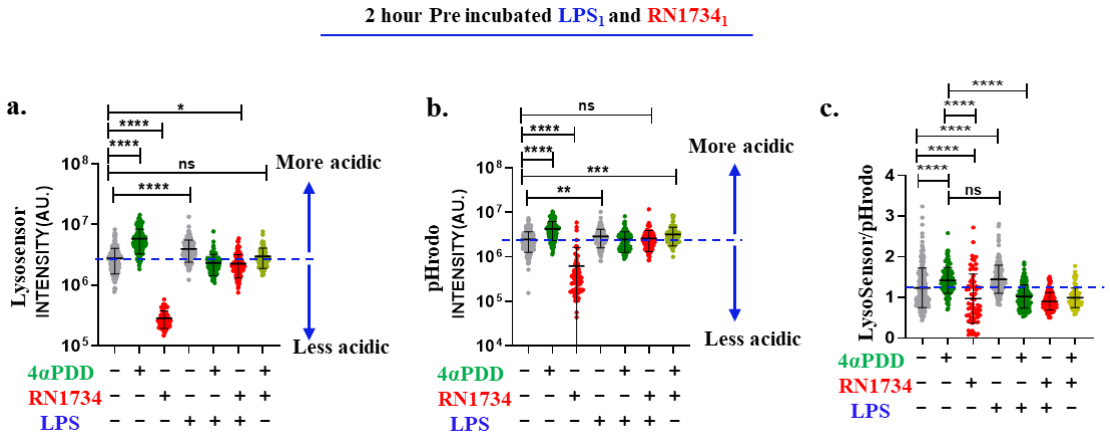

Fig 78. TRPV4 modulation helps to maintain lysosomal as well as cytosolic pH in the in Raw 264.7 cells. a & b. The graph represents varied intensity upon TRPV4 modulation and LPS stimulations. The graph shows increased LysoSensor Green intensity at TRPV4 activation and significant decreased intensity at TRPV4 inhibitions. **c**. The graph shows ratio of LysoSensor Green (lysosomal) and pHrodo (cytosolic) fluorescence intensity in different conditions. One-way ANOVA test, **** = p≤ 0.0001, *** = p ≤0.001, ** = p ≤0.01, * = p ≤ 0.05, ns = non-significant.

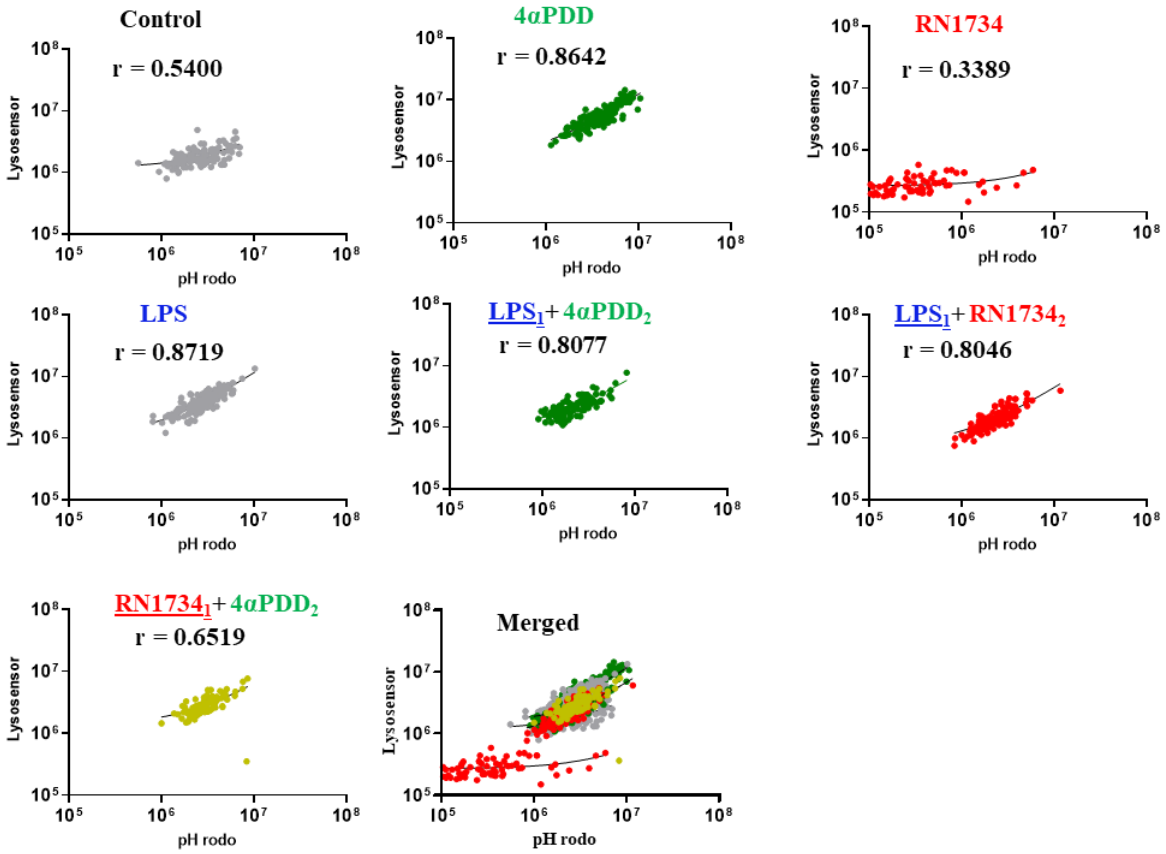

Fig 79. TRPV4 modulation alters the correlation between lysosomal and cytosolic pH. The correlation data shows the significance correlations between cytosolic pH and lysosomal pH in case of TRPV4 activation but lower significance in case of TRPV4 inhibitions.

2.6.6 TRPV4 modulations helps in maintaining cytosolic ROS and NOS-level

Cytosolic ROS level has been checked by using H_2DCFDA dye, and it has been observed that TRPV4 activation is able to increase the ROS level (**Fig. 80a**). When cells were stimulated with LPS, the ROS level increased significantly. TRPV4 activation in the presence of LPS also remains high. The cytosolic NOS level has been studied with the help of DAPFM dye. It has been found that the NOS level increases significantly at the TRPV4-activated conditions. The NOS level also increased significantly with LPS stimulation alone or in combination with TRPV4 modulations (**Fig. 80b**). It has been observed that all these dyes detecting cytosolic ROS, or NOS tend to lower their fluorescence intensity upon TRPV4 inhibition. All these data indicate that TRPV4 modulation play an important role in the maintenance of cytosolic ROS, and cytosolic NOS level.

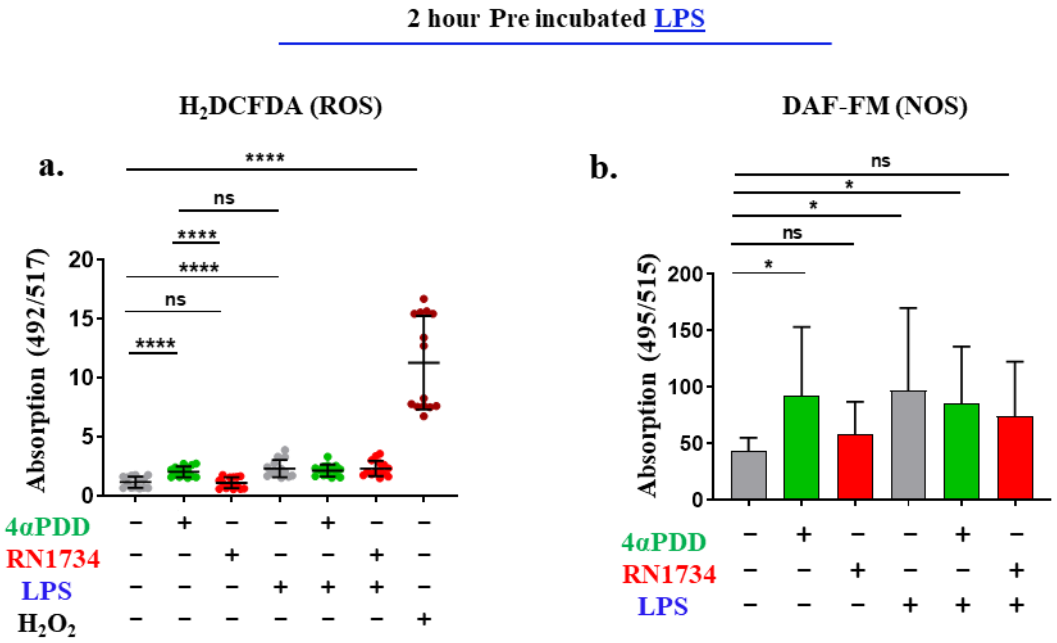

Fig 80. TRPV4 modulation helps maintain cytosolic ROS and NOS in the in PM. a-b. The graph shows the cytosolic ROS and NOS level changes upon TRPV4 modulations and also with LPS stimulation and H_2O_2 treatment (for ROS). There is significant change (increase) in intensity at TRPV4 activation in the cytosolic ROS level (H_2DCFDA) as well NOS level (DAPFM). Unpaired t-test, * = $p \leq 0.05$, **** = $p \leq 0.0001$ and ns = non-significant.

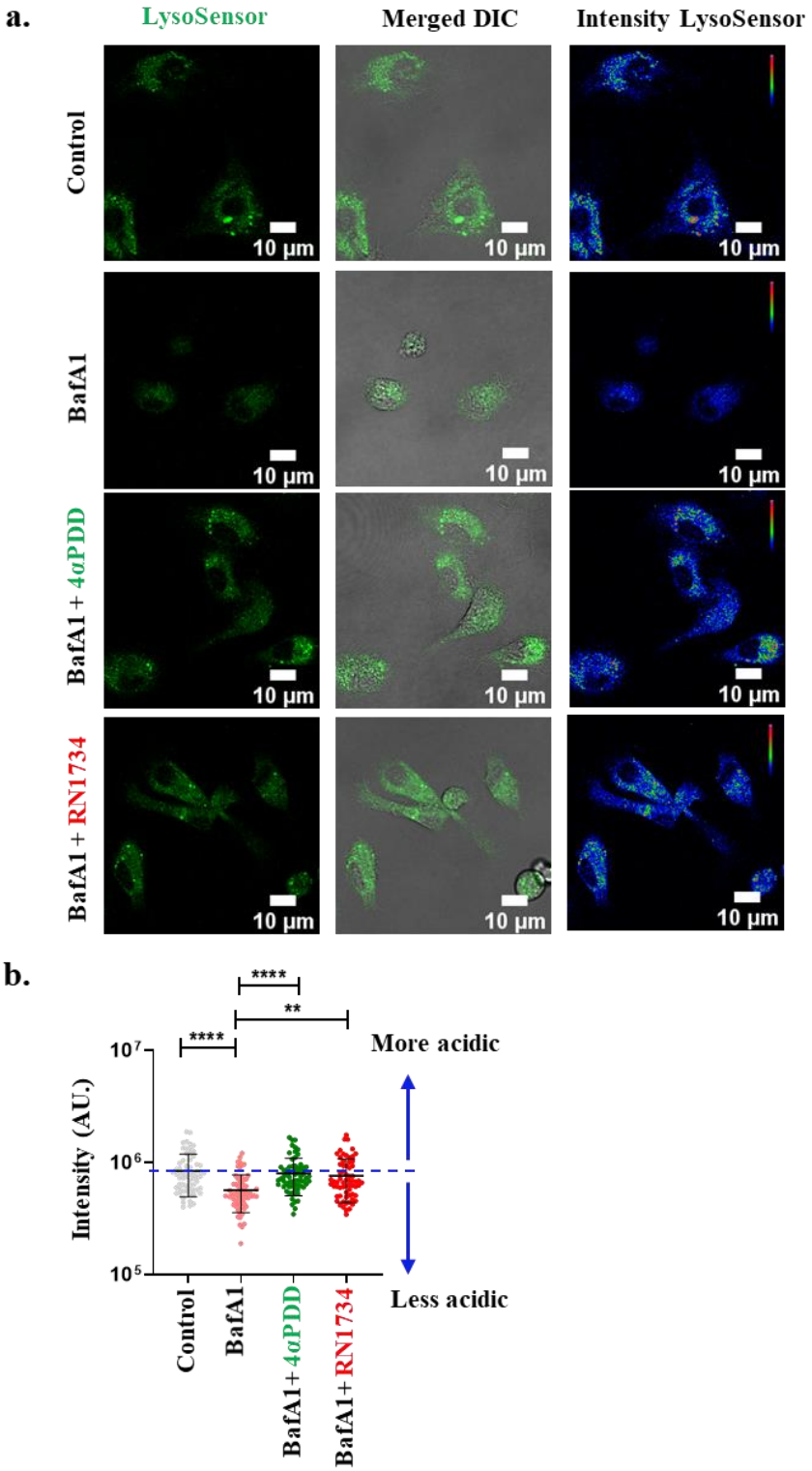

Fig 81. TRPV4 modulation helps maintain acidic pH in the cells in the lysosomal stress condition. a. The above representative image shows the intensity difference when peritoneal macrophage cells were treated with lysosomal pH-disrupting agents (BafA1). The conditions considered are TRPV4 activation (4αPDD), TRPV4 inhibitions (RN1734) and BafA1-treatment respectively. Scale bar 10µm. **b.** The graph represents intensity plot of LysoSensor Green at TRPV4 modulated conditions along with BafA1 treatment (4 hours). One-way ANOVA test, **** = $p \leq 0.0001$, ** = $p \leq 0.01$.

2.6.7 The lysosomal and cytosolic pH are restored by TRPV4 activation in peritoneal macrophages

When the cells were subjected to disruption of lysosomal pH by treating BafA1, the lysosomal pH changed to less acidic and cause lysosomal stress (**Fig.81a-b**). The fluorescence intensity of LysoSensor Green drops significantly upon BafA1 treatments because it blocks the V-Type ATPase present in the lysosomes. But when the BafA1-treated cells were subjected to TRPV4 modulation, the lysosomal pH level return to a more acidic level (**Fig.81b**).

This suggests that TRPV4 is involved in maintaining the cellular pH level and it helps the cells to rescue from the lysosomal stress conditions.

2.6.8 TRPV4 modulation helps in maintaining cellular pH in the macrophage cells

The pH-sensor construct has been used to monitor the pH of the phagocytosed compartments (**see Annexure-2 for more details**). As the macrophages are exposed to pH-sensor tagged bacteria, the cells engulf the bacteria and phagocytosed bacteria move to the endosome and lysosomes. So, the pH red –tagged bacteria was used to measure the changes in lysosomal pH due to TRPV4 modulations.

The fluorescence intensities of the individual phagocytosed particles were analysed, in control and TRPV4 activated as well as in inhibited conditions. The data suggests that TRPV4 activation makes more acidification for most of the particles as the distribution of particle-based florescence indicates lowering of pH (**Fig. 82**). TRPV4 inhibition also causes acidification, but to a lesser extent than that of the TRPV4 activation (**Fig. 82**).

It has been observed that TRPV4-GFP or TRPV4-488 colocalizes with phagocytosed pH–Red-tagged bacteria within the macrophage. Both, TRPV4-GFP and as well as antibody-probed TRPV4 colocalize with the pH–Red-tagged bacteria. The specific enrichment of TRPV4-GFP has been observed in the pH–Red-tagged bacteria localized areas (**Fig. 83**).

Next it was explored if TRPV4 is involved in the phagocytosis event. TRPV4 seems to be involved in the phagocytosis event, as enriched TRPV4 in the filopodial region next to pH-red-tagged bacteria is seen. The line-graph shows both the TRPV4-GFP and pH-Red are enriched at the regions of bacteria during the phagocytosis events (**Fig. 83**).

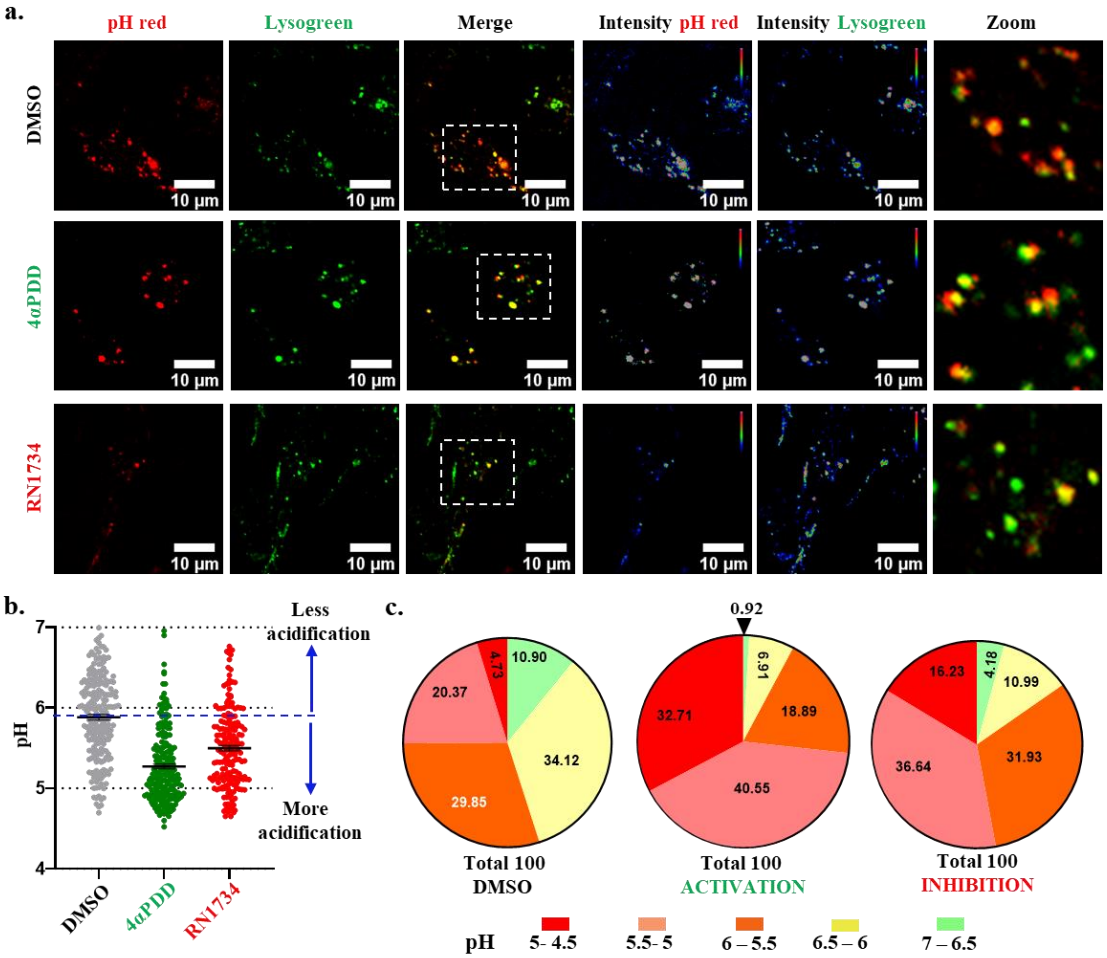

Fig 82. TRPV4 modulation helps to maintain the acidic pH of the lysosome. a. Shown are the confocal images of live Raw 264.7 cells that engulfed the pH–Red-tagged bacteria and further labelled with the LysoTracker Green dye. The engulfed pH-Red-tagged bacteria colocalized well with the lysosomes. Scale bar 10µm. **b.** The graph represents the pH variations upon the cells treated with 4αPDD and RN1734 in comparison with DMSO control. **c.** The pie-chart represents the different pH distributions of phagocytosd bacterial particles upon TRPV4 modulations (4αPDD, RN1734). Unpaired t-test, ** = $p \leq 0.01$.

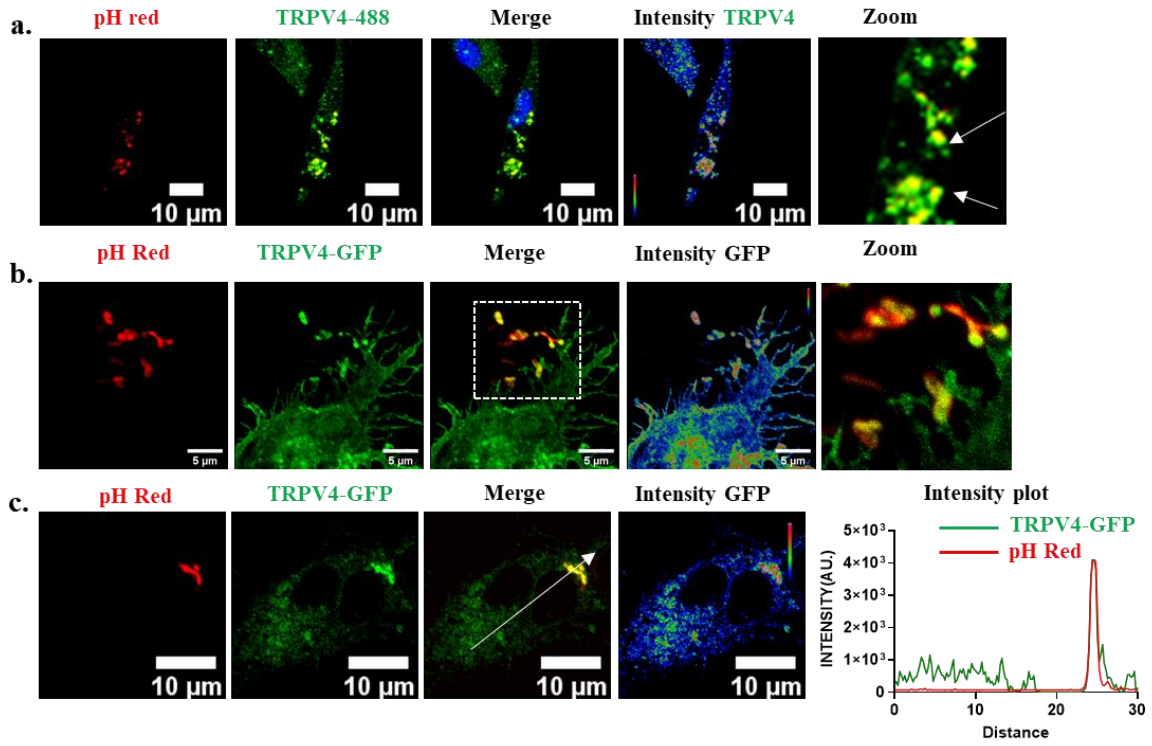

Fig 83. TRPV4 is enriched and colocalized with phagocytosed bacteria in macrophage cell. a-b. These confocal images show the TRPV4-AF 488 (a, green) or TRPV4-GFP (b, green) enrichment and localizations with pH-Red (red)-labelled bacteria at the membrane and inside the cell. Enrichment of TRPV4 at the filipodia-like structures engaged in phagocytosis are more prominent in live cell (b) imaging. **c.** The figure represents the enrichment and colocalization of TRPV4-GFP with engulfed pH Red bacteria. The line graph shows the enrichment of TRPV4-GFP at the bacteria localization site. Scale bar 10µm.

2.6.9 TRPV4 modulation helps in bacterial clearance in isolated macrophage cell *in vitro*

The functional significance of TRPV4 modulation on bacterial clearance was tested. For that, the macrophage-specific function, i.e. bacterial clearance in the *in vitro* system was checked. Here bacterial strains used are DH5α (*Escherichia coli*) and MRSA (*Staphylococcus aureus*) respectively. After 4 hours of infection, the cells were incubated with 4αPDD (activator) and RN-1734 (inhibitors) for 4 hours (for MRSA strain) or 2 hours (for *Escherichia coli*), respectively. It has been observed that the CFU become significantly lesser in the TRPV4-modulated condition in comparison with the DMSO control. This is more prominent in RN1734-treated condition, i.e., in TRPV4 inhibition. It seems that TRPV4 inhibition plays a major role in bacterial clearance (**Fig. 84a&b**).

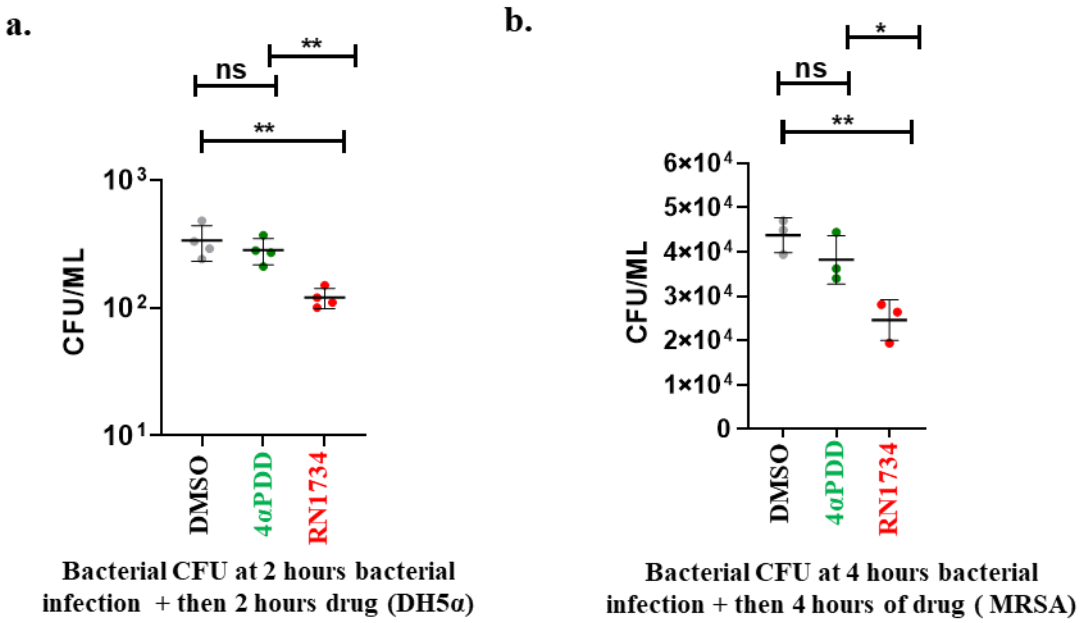

Fig. 84. Role of TRPV4 modulations in *in vitro* bacterial clearance. a-b. These graphs show the *in vitro* bacterial clearance by the peritoneal macrophage cells. The bacterial strain used for the infections are *Escherichia coli* (2 hours, a) and MRSA (4 hours, b), respectively. One-way ANOVA test. * = $p \leq 0.05$, ** = $p \leq 0.01$, *** = $p \leq 0.001$, ns = non-significant.

Chapter 3

Discussion

Lysosomes are one of the major stress response organelles besides Endoplasmic reticulum and mitochondria. The theory of lysosome as a stress response compartments or in general lysosomal stress was first mentioned in 1968. In next 50 years many lysosomal functions and regulations were identified which are related to cellular stress and/or cause diseases (Lapka et al. 2021; Saftig P. and Puertollano R. 2021). The important points that need to be considered is the "lysosomal stress". The lysosomal stress is related to different complex changes, such as the impairments in lysosomal size, in and out movement of certain substances to the lysosome, pH imbalance, membrane integrity, membrane loss, enzyme functions, clumping of proteins, build-up of cholesterol, and an increase in harmful reactive molecules. A great example of lysosomal impairment is lysosomal storage disorders (LSDs) (Parenti et al. 2021; Saftig P. and Puertollano R. 2021).

In the 1882, scientists first recognized the clinical signs of diseases, later known as LSDs (Gaucher P. 1882). The understanding of these diseases advanced significantly in the 1950s (1955-56) when lysosomes were discovered in cells. Then, in the 1960s (1963), researchers uncovered the specific biochemical issues causing LSDs. From the 1970s to the 1990s, studies were conducted mainly into how enzymes reach lysosomes and identified the genetic roots of LSDs. Efforts to treat these disorders with enzyme replacement therapy began in the 1990s (Parenti et al. 2021). Presently, scientists are exploring how lysosomes impact cell functions that are beyond the waste disposal. Such understandings will have implications to find new ways to treat these disorders. Ion channel present in the lysosome are the major contributors of maintaining lysosomal integrity and ion homeostasis. Earlier there was a preconceived notion that ion channels are physically restricted at the plasma membranes only and transport ions through its concentration gradients. But, later it is well established that these channels are not only present in several intracellular organelles (like lysosomes, mitochondria) but also responsible for various cellular processes through these organelles. Lysosomal ion

channels are major contributors of maintaining metal ion concentration which tends to maintain the lysosomal functions in total. The optimal lysosomal Ca^{2+} level (0.5μM) contributes to the process of exocytosis, phagocytosis, pH and maintenance of ion homeostasis within lysosomes (Tancini et al. 2020). Recent findings strongly suggest that TRPs (nonselective Ca^{2+}-permeable channel) are major contributors of lysosomes. Since lysosomes are major contributors of cellular stress response, TRPs seem to play major role in maintenance of lysosomal integrity at cellular level. Notably, lysosome and nucleolus are major structures defined as "stress hub" for the cells. In other words, the health of a cell can be estimate by the structural integrity and size of the nucleolus. Presence of channel proteins in nucleolus also correlates with the significance in cellular health and its status (Latonen L. 2019). In this context, the status of both lysosomes and nucleolus provides detail information of the stress regulatory functions in relation to TRPV3 modulations. So, the present study is relevant to understand about stress regulatory inflammatory functions of lysosomes in relation to TRPV3/ TRPV4 channels which are known to be present functionally in the intracellular compartments. The study is relevant to understand the functions of TRPV3 and TRPV4 in relations to pathogenic stress, lysosomal stress, thermal stress, both in *in vivo* and *in vitro* systems. This study is relevant for the detailed understanding of stress physiology in the context of lysosome and TRPV3/TRPV4 channel functions.

3.1 TRPV channels in the lysosomes and their importance

3.1.1 Lysosomal ion channels

Lysosome as a sub-cellular organelle contains many digestive enzymes and mainly acts as a degradation machine. Many properties of lysosomes are not well characterized, though its existence as a cell organelle has been demonstrated long back, in the year 1955 (De Duve et al. 1955). As lysosome in higher animals refer to highly dynamic and functional organelles,

it has clear evolutionary history as such functions are also required in all cell types and even in the lower organisms (Katzmann et al. 2001; Bouhamdani et al. 2021) It was found that the acidic enzymes (acid phosphatases) are present in the granules-like structure. That is why, these structures were named as lysosomes. Lysosome contains enzymes to facilitate catabolism of the macromolecules, especially in the acidic pH. Because of this requirement of low pH, lysosomal pH maintenance become a critical challenge for all the cells. The lysosome is made from the combination of both endocytic and secretory pathways from the endoplasmic reticulum vesicle, further laden with endocytic enzymes in the Golgi apparatus (De Duve. C and Wattiaux. R 1966). Lysosomes maintain their acidic pH and its buffering through V-type ATPase, various ion channels and carrier proteins present in their membrane (Forgac M. 2007). The endocytic or exocytotic pathway requires Ca^{2+}-efflux as well as Ca^{2+}-influx in the cellular system, and proper lysosomal functions require precise maintenance of lysosomal Ca^{2+}-levels all the time.

Functionally important lysosomal proteins are specifically targeted to the lysosomes due to the presence of specific target sequences. Previous study has identified potential peptide signals that can direct different ion channels to the lysosomes. These signals include specific motifs like DxxLL, [DE] xxxL [LI], DxxLM, DxxMV, IMxxYxxL (in plants), and YxxL (in yeast) (ref). Recent development in sequencing techniques not only allow to summarize th e information about lysosomal target sequences or their targeting mechanisms, but also helps to understand the origin of such target sequences during the evolution.

Lysosomal ion channels are crucial for the optimal performance of lysosomes, maintenance of low pH and thus degradation and recycling of proteins. These ion channels facilitate the controlled movement of ions within the lysosome, thereby modulating the ion-influx and efflux crucial for lysosomal functions. Acting as key regulators of ion balance, these channels are indispensable for lysosomal integrity and functions. Therefore, dysfunctional ion

channels, transporters and related transport proteins are often associated with lysosomal malfunctions and are the “root cause” of the onset of several diseases commonly known as “lysopathy”. Such diseases also include different rare genetic disorders, lysosomal storage disorders, neurodegenerative conditions, and cancer (Bonam et al. 2019). In addition, lysosomes perform diverse critical functions, such as material digestion, cellular clearance, nutrient-sensing, and Ca^{2+}-signalling. Specific TRP channels, like TRPML1 participate in regulating endo-lysosomal trafficking, ion homeostasis, autophagy, and lysosomal exocytosis (Kiselyov et al. 2005).

In the last decade, both electrophysiological recordings and studies focusing on molecular and structural aspects have revealed several distinct ion channels and transporters present in lysosomes. These include TPCs, TMEM175, TRPMLs, CLN7, and CLC-7 (Wang et al. 2023). These channels play a crucial role in allowing various ions such as potassium (K^+), sodium (Na^+), hydrogen (H^+), calcium (Ca^{2+}), and chloride (Cl^-) to pass through the lysosomal membrane. Their activity is regulated by a multitude of cellular factors, including the acidity (H^+) within the lysosome, the voltage across its membrane, ATP levels in the cytosol, and external growth factors (Riederer et al. 2023). In essence, lysosomal ion channels have evolved to be essential contributors to various cellular processes, and disruptions in their structure or function can lead to a range of diseases.

3.1.2 Lysosomal TRP channels

Lysosomal ion channels play crucial roles in cellular processes like endo-lysosomal trafficking, autophagy, pH regulation, lysosomal exocytosis and others. All these have sparked research interest due to their complexity and relevance in health disorders. So far members belong to TRPML and TPC families were reported to be involved in the context of lysosomal diseases (Jaślan et al. 2020). These families of ion channels play crucial roles in various cellular

processes such as endo-lysosomal trafficking, autophagy (the cell's self-cleaning process), regulating pH within lysosomes, and even the release of substances from lysosomes into the cell.

Disturbances in the structure or function of these ion channels have far-reaching consequences, leading to the development of disorders like lysosomal storage diseases, neurodegenerative diseases, and cancer. These channels, acting as selective pores only for certain ions in the lysosomal membranes, thereby ensuring the optimal functioning of lysosomes. In recent times, involvement of TRP channels in various diseases have been studied in details. One such disease is "*Olmsted syndrome*", a rare genetic disorder characterized by palmoplantar keratoderma, nail abnormalities, and potentially other skin-related symptoms. Point mutations in the TRPV3 gene (at G573, G568, L673, Q580 and W692 positions) are strongly linked with the development of OS (Lai-Cheong et al.2012; Lin et al. 2012; Duchatelet et al. 2014; Duchatelet et al. 2014). In this rare disorder, individual's quality of life is significantly affected. As TRPV3 has been detected in the lysosome, these mutants, namely G573S, G573C, G573A, W692G show impaired cell adhesion, lower lysosomal number, and impaired distribution of lysosomes (Yadav and Goswami 2017; Jain et al. 2022; Duchatelet et al. 2015). The spectrum of abnormalities in the lysosome due to TRPV3 mutants (as observed in case of *Olmsted syndrome*) are qualitatively and quantitatively different, suggesting that though these mutants affect lysosomal functions grossly, the "mode-of-action" and the exact cellular phenotypes are not same. Never-the-less, all these mutants show a similar trend (Yadav and Goswami. 2017; Jain et al. 2022). Specifically, the Ca^{2+}-buffering, lysosomal pH and lysosomal distribution have been disrupted in the G568C and G568D mutants. Specifically, the expression of these mutants induces a notable reduction in lysosomal count, spatial distribution, and movement, high-lighting the potential influence of TRPV3 on lysosomal dynamics. This aspect insists that other mutants of TRPV3 that cause OS, also need to be characterized in

future to understand the TRPV3-mediated lysosomal functions in details. Never-the-less, endogenous TRPV3 has also been detected in isolated lysosomes (**Fig 85**). Therefore, in future, precise distribution, topology as well as TRPV3-mediated lysosomal functions can also be tested in the isolated lysosomes in a cell-free conditions.

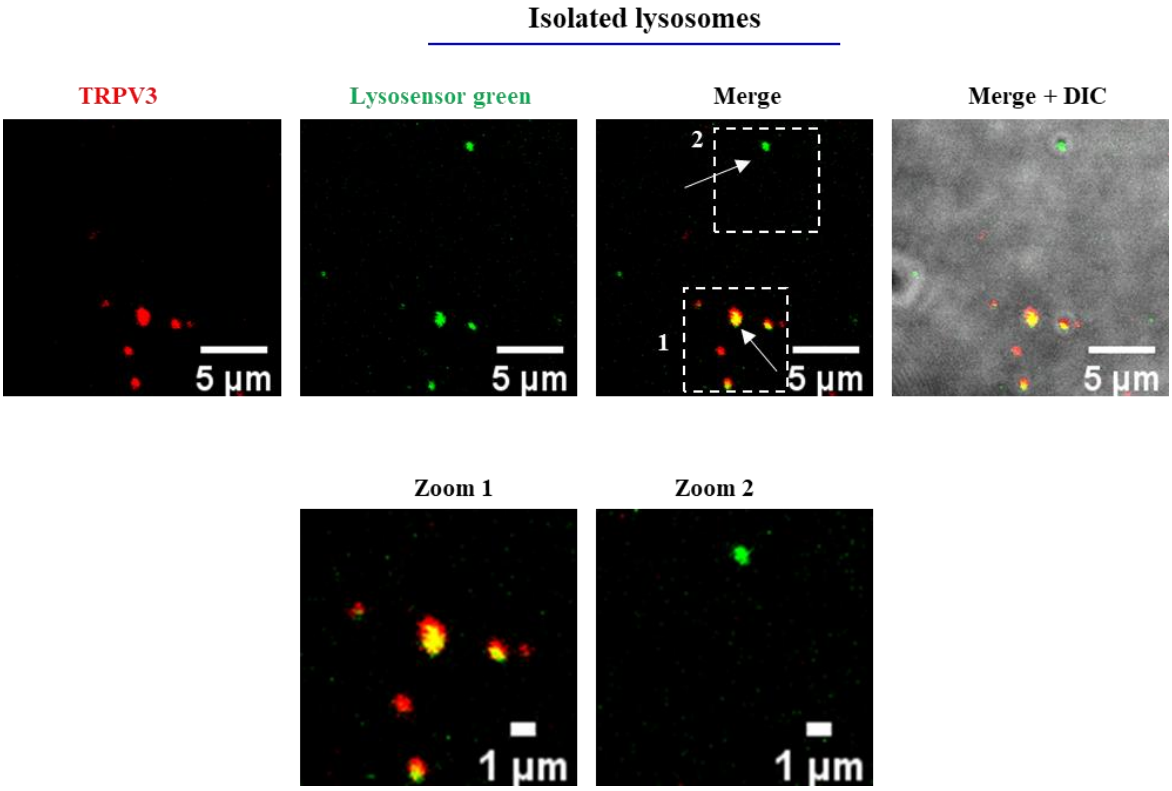

Fig 85. Presence of TRPV3 in lysosomes. The image shows the presence and localization of endogenous TRPV3 in the lysosomes isolated from Raw264.7 cells. TRPV3 is detected in a subset of the lysosomes (shown in arrow). TRPV3 is probed with an extracellular epitope-specific antibody (red), while the lysosome is labelled with lysotracker green dye. Not all, but certain lysosomes are detected by this antibody. Scale bar 5µm and 1µm (for enlarged images).

3.1.3 Importance of TRPV3 and TRPV4 in lysosomal functions

Conventionally, TRP channels are known to be plasma membrane proteins. But recent advancement shows their presence and diverse roles in different subcellular organelles as well (Dong et al. 2010). Different membrane proteins present in the intracellular region takes part in various functions, such as maintenance of intra-organelle-ion homeostasis, maintenance of pH, stress response, etc. The lysosome is one of the stress-responsive organelles for cells where different key proteins take part in its functions, and maintenance of its ionic- and pH-

homeostasis (Trivedi et al. 2020). Recent reports suggest that TRP channels like TRPML, TRPV3, TRPA1, TRPC1 and TRPC2 are present in this subcellular organelle and maintain ionic balances there and also help in various lysosomal functions like phagocytosis, regulation of pH, and Ca^{2+}-levels (Dong et al. 2010). As TRPV3 is physically present in the lysosome, its role in various lysosomal functions is worthy enough to study in details (Yadav and Goswami 2017). Notably, TRPV4, a homologue of TRPV3 is also relevant in the context of lysosomal functions.

Though so far direct evidence of cross talk between TRPV3 and TRPV4 are lacking, but TRPV3 is known to heterotetramerize with TRPV4 (which is also a thermosensitive TRP channel) (Hu et al. 2022). The molecular mechanisms behind temperature detection, ligand sensitivity, and the assembly of temperature-sensitive functional units may differ in the heteromeric complexes from the individual homomeric complexes. However, it remains unclear if the warmth-sensitive TRPV3 and TRPV4 channels, though endogenously expressed in the skin, can indeed combine to form such heteromeric functional units. In this context, Hu et al addressed this by demonstrating that TRPV3 and TRPV4 channels can co-assemble into functional heterotetrameric channels with unique properties (Hu et al. 2022). Using confocal imaging, the co-localization has been established and association of TRPV3 and TRPV4 proteins in the cell membrane is also established. Further analysis via co-immunoprecipitation revealedprotein-protein interaction between TRPV3 and TRPV4 subunits, particularly through their C-termini. Co-expression of TRPV3 and TRPV4 channels resulted in the formation of heterotetrameric channel complexes with intermediate single-channel conductance, distinct activation thresholds, and pharmacological profiles (Hu et al. 2022). In this context, further investigations are required to understand functional cross-talk between different TRPV members.

3.1.3.1 TRPV3 in macrophage and its role in lysosomal functions

Though TRPV3 was previously believed to be only targeted to the PM (Plasma membrane), previous thesis work from the lab demonstrated that TRPV3 has four lysosomal target sequences (LTS) (Yadav M. thesis 2018). To establish the presence of TRP channels within lysosomes, a comprehensive *in silico* analysis was conducted, encompassing sequences from various vertebrate species. The sequence investigation identified four distinct lysosomal targeting signal (LTS) sequences (ELVELL, DIAALL, EIVQLL, DMILL) situated in the N-terminus region. This insightful analysis demonstrated that the DMILL sequence exhibits a remarkably high level of conservation across the entire spectrum of vertebrate species. The presence of multiple and conserved LTS in the TRPV3 accords well with the functional presence of TRPV3 in the lysosome, and such sub-cellular localization seem to be evolved long back and is relevant in all vertebrates. Based on the previous reports and investigations, the presence of TRPV3 in the macrophages, and more specifically in the lysosome of macrophages (or macrophage-like cells) are important findings. Presence of TRPV3 in such intracellular compartments, indicates its diverse roles related to lysosomes. The presence of TRPV3 is detected in a sub-population of the lysosome only and not all isolated lysosomes (**Fig 85**). The major findings of this study with macrophages accords well with previous investigations demonstrating a similar lysosomal presence of TRPV3 in HaCaT cells.

For the first time, this study shades light on the lysosomal temperature dynamics. This has been done by using specific fluorescent probe that responds to temperature changes. In addition, this study explores the pH regulations of cell as well as lysosomes and the relationship between these two parameters. It has been observed that the TRPV3 modulations recover the lysosomal homeostasis in stressful/adverse conditions and help in the maintenance of acidic pH at the lysosomes. Experimental data suggests that TRPV3 modulation is helpful in maintaining a slightly lower temperature (of lysosomes).

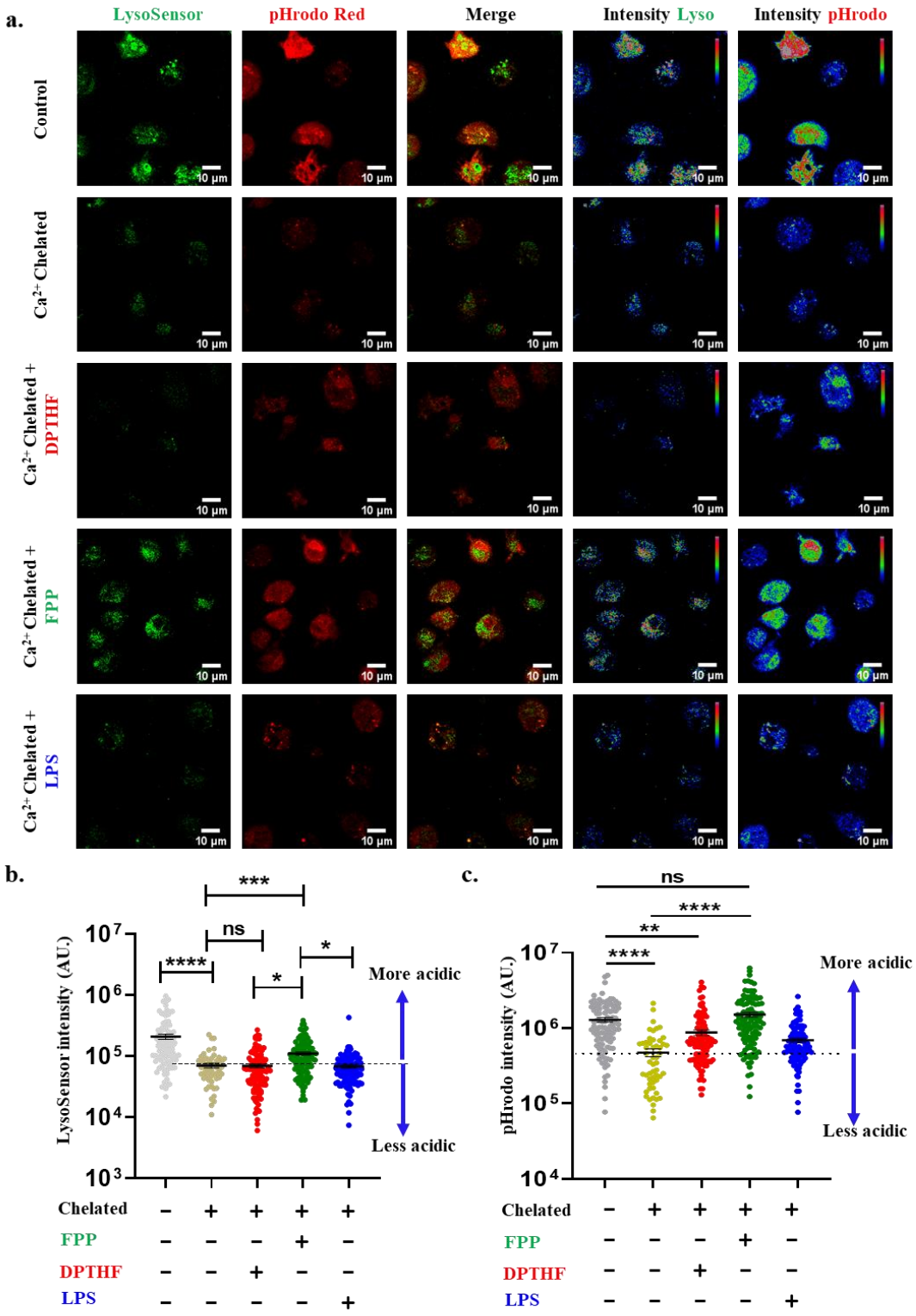

Fig 86 Role of TRPV3 in the regulation of Cytosolic pH and lysosomal pH in different stressful conditions. **a.** The representative image shows cytosolic and lysosomal pH level at Ca^{2+} chelated conditions. Both intracellular as well as extracellular Ca^{2+} is chelated by using BAPTA-AMA (10µM) and EGTA (3 mM). Scale bar 10µm. **b.** The graphs represent the fluorescence intensities of lyso-sensor as a factor of lysosomal pH in different Ca^{2+}-chelated conditions. **c.** The graph represents fluorescence intensities of pHrodo as a factor of cytosolic pH in different Ca^{2+}-chelated conditions. One-way ANOVA test. (* = $p \leq 0.05$, ** = $p \leq 0.01$, *** = $p \leq 0.001$, **** = $p \leq 0.0001$ and ns = non-significant).

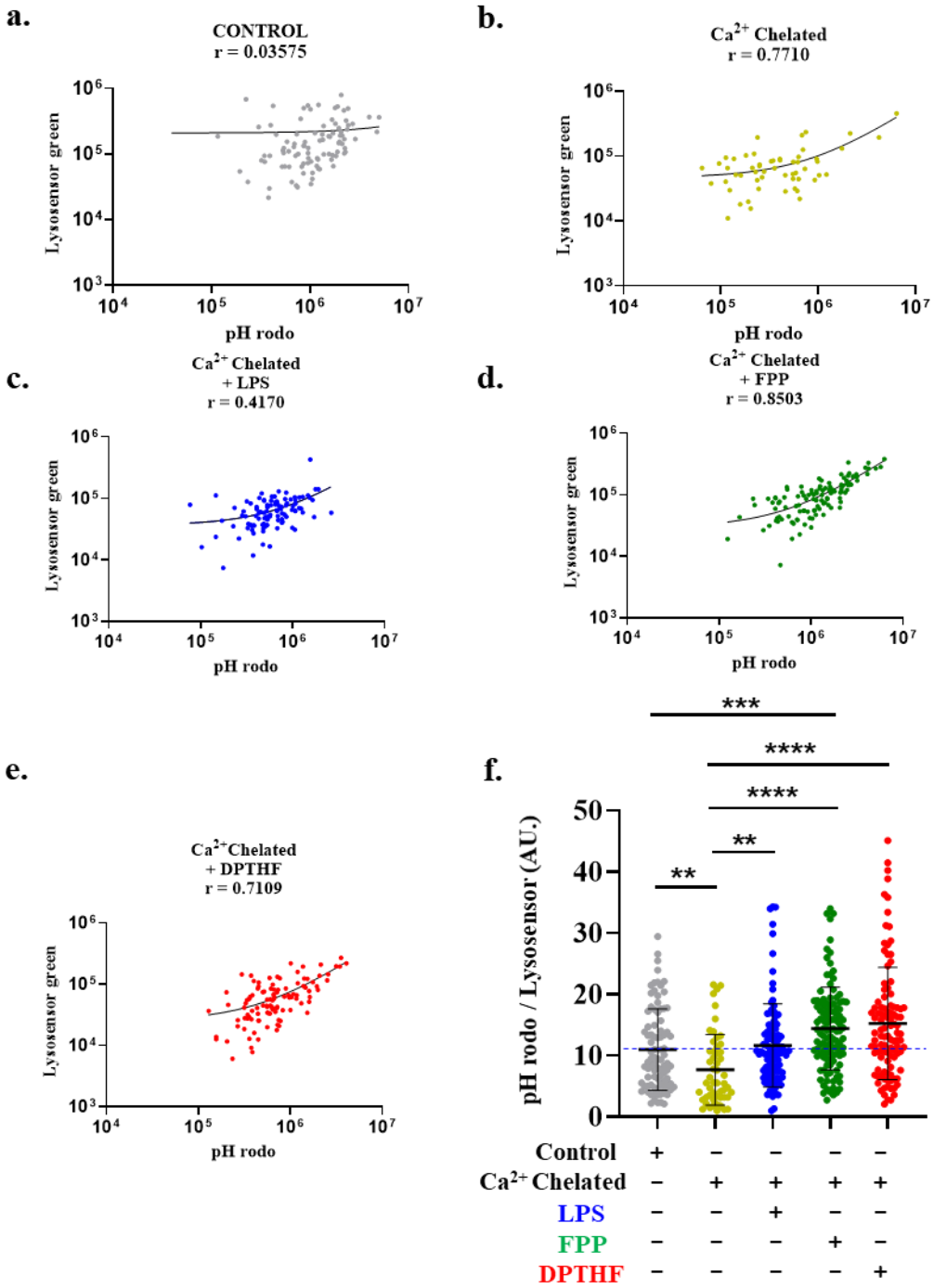

Fig 87. TRPV3 modulation alters lysosomal pH with respect to Cytosolic pH differently different stressful conditions. a-e. These graphs represent the correlation between cytosolic and lysosomal pH intensity in multiple cells at control and different Ca^{2+}-chelated conditions. The correlation value is significantly higher (r = 0.8503) in case of FPP (1µM) with Ca^{2+} chelation. **f.** The graph represents the ratio between cytosolic (pHrodo red) and lysosomal pH (Lysosensor green) intensity in multiple cells at different conditions. Ca^{2+}-chelation causes significant decrease the ratio which can be rescued due to LPS treatment or TRPV3 modulation.

This can be relevant in case of TRPV3 mutants and/or in lysosomal stress conditions.

Collectively, these findings imply that TRPV3 functions as a lysosomal ion channel is involved

in maintaining Ca^{2+}homeostasis as well as lysosomal pH within these organelles.To understand the possible involvement of TRPV3 in controlling lysosomal pH through its modulation overall Ca^{2+}-level have been chelated. In this case of Ca^{2+} chelation-induced stress (chelation of extracellular and intracellular Ca^{2+}), the activation of TRPV3 demonstrates its efficacy in significantly restoring lysosomal as well as cytosolic pH, underscoring its relevance in cellular recovery (**Fig 86, Fig 87**). TRPV3 involves actively in rescuing the lysosomal as well as cytosolic pH through its modulation. This also implies that TRPV3 modulation helps to rescue the cell from different adverse physiological conditions and helps in the maintenance of its integrity.

3.1.3.2 TRPV4 in the regulation of macrophage and lysosomal functions

Presence of TRPV4 in macrophage and its involvement in macrophage functions are not well understood. A recent study has shed light on the involvement of the transient receptor potential vanilloid 4 (TRPV4) ion channel in facilitating exocytosis by utilizing lysosomes as a crucial reservoir for cargo storage (Li et al. 2022). This intricate process relies on the interaction between various vesicle-trafficking proteins and lysosomes to finely regulate the distribution of cargo within cells. Notably, the accumulation of lysosome-associated membrane protein 2 (LAMP2) has been observed to be linked with TRPV4-mediated exocytosis in melanoma cells, specifically the A375 cell line (Li et al. 2022). Another distinct investigation has proposed the involvement of TRPV4 in the disruption of both epithelial and endothelial barrier functions (Weber et al. 2020). This is particularly significant in the context of lung edema formation, suggesting that TRPV4 plays a pivotal role in this pathological condition. Moreover, the significance of TRPV4 in inflammatory responses has been underscored, particularly in the processes like cytokine production, foam cell formation, and the formation of giant cells (Simpson et.al 2019). The expression of TRPV4 in various macrophage subtypes

equips it with the ability to shape macrophage behaviour and phenotype, thereby exerting influence over the innate immune response during pathogen encounters and instances of inflammation. Furthermore, TRPV4 has emerged as a regulator of adipose oxidative metabolism, inflammation, and the delicate balance of energy within the cellular system. It has also become evident that TRPV4 involvement extends to immune functions and the meticulous regulation of lysosomal parameters.

Based on this, the current study focuses on the role of TRPV4 modulations in relation to lysosomal functions. TRPV4 is also functionally present in the lysosome and colocalized with lysosome markers as well. In further investigations, it has been observed that TRPV4 activation helps to maintain lysosomal acidic pH. Thus, lysosomes become more acidic due to TRPV4 activations. However, in case of TRPV4 inhibitions, the lysoSensor intensity decreased significantly, indicating less acidification. Similarly, in case of BafA1-induced stress (lysosomal pH disrupter) conditions, lysosome recovered to their acidic pH if the cells were subjected to TRPV4 modulations. In macrophages, lysosome also maintains a slightly lesser temperature when subjected to TRPV4 modulations. Other than lysosomal pH, the cells show altered and balanced cytosolic pH, cytosolic ROS, and cytosolic NOS levels in case of TRPV4 activations. All these opens a new dimensions of further research where possible involvement of TRPV4 in the regulation of lysosomal functions other cellular stress parameters can be explored in details.

3.2 TRPs as cellular stress response regulators

So far, several reports suggest that TRP channels serve as key molecules relevant for cellular stress responses. This is more because these channels sense and respond to various stress signals within cells, such as change in temperature, oxidative stressors, osmotic pressure, or other environmental challenges. Once TRP channels are activated, cascades of intracellular

events are initiated. Activation of TRPs can lead to alterations in ion concentrations, cell signaling pathways, and gene expression, ultimately helping the cell adapt and survive under stressful conditions. The ability of TRP channels to act as cellular stress response regulators highlights their significance in maintaining cellular homeostasis and ensuring cell viability, especially in adverse conditions. Thus, presence of TRPs in cell or sub-cellular organelle and their functions can provide additive advantages. The role of both TRPV3 and TRPV4 in cellular stress response has been explored and discuss here elaborately.

3.2.1 TRP channels as sensor for nutrient-deprived stress conditions

TRPs are found in important body tissues that are related to metabolism. Thus, alteration is TRPs expression or function affects how the body handles glucose and lipids. For example, TRPV1 can be broken down through a process called autophagy when the body is deprived of food or exposed to glucocorticoid hormones. TRPV channels are also crucial for sensing glucose levels and triggering AMPK activation during glucose shortages (Li et al. 2019). Furthermore, TRPML is essential for controlling cell survival in various situations and for promoting autophagy, during nutrient deprivation (Koivisto et al 2022; Abe K. and Puertollano R. 2011). Notably, TRPML members are present in the lysosome and act as molecular routs that permit influx of Ca^{2+}, provides another layer of complexity to this regulatory process. Intriguingly, the localization of TRPV3 to lysosomes appears to be intricately connected with the overall stress levels experienced by the cell. This interactions and complexity extend beyond temperature-induced stress. Furthermore, even under conditions of starvation, TRPV3 activation proves invaluable in preserving lysosomal pH equilibrium. Notably, the co-localization of TRPV3 with lysosomal markers became more prominent during states of nutrient deprivation. Both mitochondria and lysosome are affected due to nutrient starvation where the distribution and overall organelle status are also compromised (**Fig 89a**).

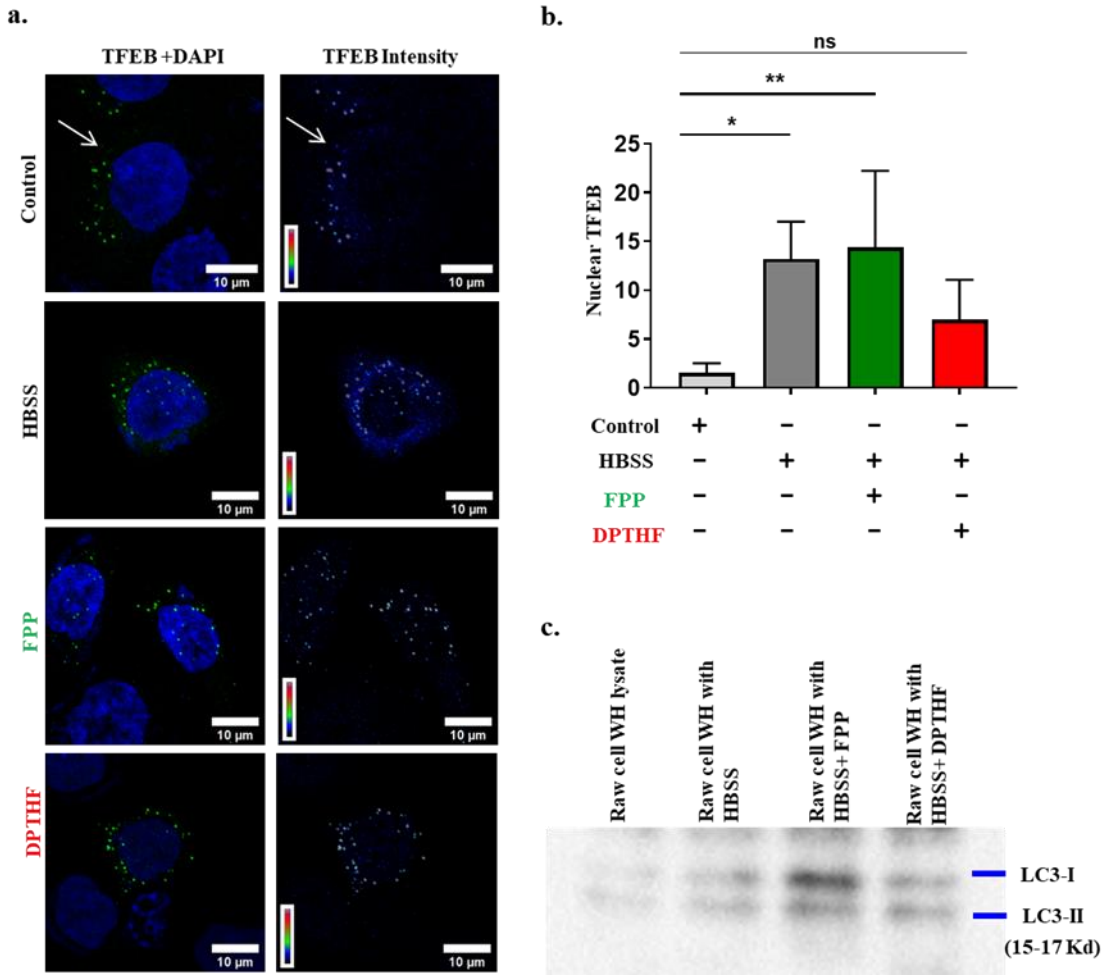

Fig 88. Beneficial role of TRPV3 in starvation conditions. a. These images show the qualitative representation of TFEB levels in cellular starvation condition (HBSS) along with TRPV3 modulations. Scale bar 10µm. **b.** The graph represents nuclear TFEB count in different starvation conditions as shown in figure a. Unpaired t-test (* = $p \leq 0.05$, ** = $p \leq 0.01$, and ns = non-significant). **c.** The figure shows the WB of the LC3B (LC3-I and LC3-II) antibody in starvation conditions.

TRPV3 activation seems to be effective in minimizing the cellular damage in such conditions. Remarkably, activation of TRPV3 also resembles to conditions that are observed in case of autophagy, a process that involves self-degradation and recycling of cell components. This is evidenced by the enhanced expression of LC3B, a marker for autophagy, in starved conditions when TRPV3 is activated (**Fig 88c**). Furthermore, during starvation condition, the intracellular relocation of TFEB (Transcription Factor EB, a regulator of lysosomal biogenesis and autophagy) becomes more enriched in the nucleus when TRPV3 is activated (**Fig 88a&b**). All these observations indicate a multifaceted role of TRPV3 in response to cellular stressors, maintaining lysosomal functionality, and influencing fundamental processes like autophagy.

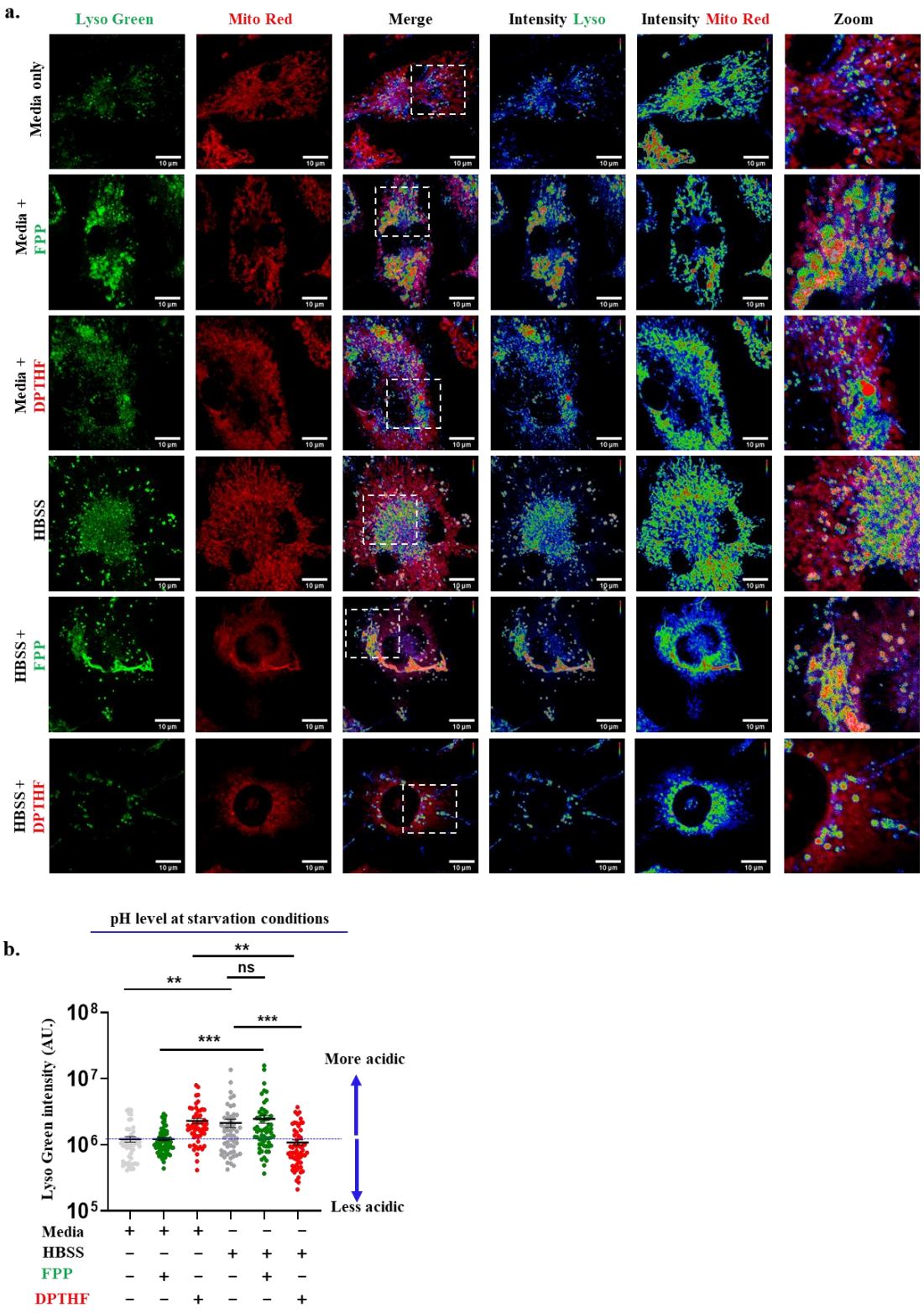

Fig 89. TRPV3 modulation maintains lysosomal and mitochondrial status at starvation conditions. a. The images represent lysosomal and mitochondrial status at HBSS starvation and/or TRPV3 modulation conditions. The merge intensity highlights lysosomes (RGB intensity scale) in contact with mitochondria (red) at different conditions. Scale bar 10µm. **b.** Representative graph shows lysosomal pH intensity upon HBSS-treated conditions which is more in case of TRPV3 activations. One-way ANOVA test, ** = p≤0.01. *** =p≤0.001 and ns = non-significant).

While these findings shed light on the interplay between TRPV3 and cellular responses, certainly there is a need for further research to unravel the precise mechanisms underpinning these interactions and their broader implications for cellular health and survival.

3.2.2 Relevance of TRP channels in hyperthermic stress

Hyperthermia, is referrers to the conditions where the body temperature is elevated, and it can trigger various cellular inflammatory responses. Hyperthermia affects different responses, like adjusting local inflammation, by changing the body's response to inflammation in specific areas. This can also lead to immune activation, cell death, and increased inflammation. Hyperthermia can lead to the production of ROS and also increase the activity of heat shock response proteins. Furthermore, hyperthermia can trigger the production of pro-inflammatory signalling molecules, i.e. cytokines, including interleukin-6 (IL-6) and tumor necrosis factor-alpha (TNF-α) (Lavanderos et al. 2020). These cytokines activate immune cells and attracting them to the sites of infection or inflammation. Hyperthermia can boost the activity of immune cells like macrophages and natural killer (NK) cells. This heightened activity improves their ability to engulf and destroy pathogens, produce more cytokines, and kill infected cells (Lavanderos et al. 2020).

Hyperthermia can also activate TRPs as these are the sensors in the body responsible for detecting temperature changes. Specific channels, like TRPV1, TRPV4, and TRPM8, are associated with various immune processes, including inflammation and pain (Benemei and Dussor. 2019). However, recent studies in various organisms, like *Aphelinus asychis* and rats exposed to stressful conditions, suggest that TRPs are indeed involved in responding to heat stress (Liu et al. 2021). While there isn't any direct evidence for TRPs' role in human heat stress, experiments with TRPV1 receptors have shown interesting effects (Garami et al. 2018). Activation of these receptors can cause cooling, while blocking these can lead to overheating.

Moreover, desensitizing TRPV1 can prolong the body's overheating response by reducing heat release through the skin (Garami et al. 2018). These findings indicate at the potential involvement of TRPs in human heat stress. However, further research is necessary to fully understand how these channels contribute to this process.

In the context of hyperthermic stress, this study focuses on the role of TRPV3 as a thermal stress regulator. In this study, it has been observed that during hyperthermic shock conditions (such as exposure to temperatures of 42°C for a duration of 2 hours), a noteworthy phenomenon emerges: i.e. macrophages lose their susceptibility to being labelled by lysotracker red or other LysoSensor dyes. This clearly suggests the loss of lysosomal low pH. This intriguing observation points towards a compromised ability to maintain a sufficiently low pH within the lysosomes at elevated temperatures. However, either pharmacological activation or inhibition of TRPV3, rescues these lysosomal deficiencies under such harsh conditions. This dynamic interplay between TRPV3 and lysosomal pH regulation proves especially impactful at the cellular level, particularly when cells are under stress or facing challenges. This signifies the importance of TRPV3 channel modulation for the overall survival of the organism. Yet, the precise molecular and cellular mechanisms underlying how TRPV3 exert their influence on lysosomal pH remain unclear, representing an area that requires further investigations.

3.2.3 TRP channel in pathogenic stress

TRPs channels are important in controlling several functions of immune cells (like monocytes and macrophages) including phagocytosis (engulfing foreign particles). These channels influence phagosome maturation, which is a crucial step in the process. TRPs also affects macrophage survival, cellular Ca^{2+}-levels, and cell movement, all of which impact their ability to engulf and digest foreign particles. For instance, TRPV2 is essential for phagocytosis by macrophages as it helps macrophages to bind and uptake particles (Lévêque et al. 2018;

Froghi et al. 2021; Wu et al. 2023; Partida-Sanchez et al. 2021). TRPs also plays roles in immune cell migration, phagocytosis, and the production of signaling molecules called cytokines. In summary, TRPs are important players in phagocytosis, affecting various aspects of this immune cell function. This also suggests that targeting TRPs could be a potential strategy for treating inflammatory and immune-related diseases. All these functions also link TRPs in the Pathogen Associated Molecular Pattern (PAMP) response. In this context the thesis further discussed the possible role of TRPV3 and TRPV4 in pathogen clearance.

3.2.3.1 Importance of TRPV4 in *in vivo* and *in vitro* bacterial clearance

The current study investigated the role of both TRPV3 and TRPV4 ion channels in macrophage functions, specifically on the phagocytosis and bacterial clearance processes, both *in vivo* and *in vitro* systems. The infiltration of macrophage cells at the wound site during early infection (from day 4^{th}) is crucial for effective wound healing and the elimination of bacteria. Among the various factors which influence wound healing, TRPV4 has gained attention for its potential in modulating inflammatory responses and tissue repair. Due to its physical presence in skin cells and sensory nerve endings, TRPV4 acts as a cellular sensor that translates external cues into intracellular signaling cascades. Activation of TRPV4 leads to Ca^{2+}-influx, triggering a range of cellular responses, including inflammation and cell migration. Some studies propose that TRPV4 activation may modulate immune responses against bacterial pathogens, potentially influencing infection clearance and wound healing (Boudaka et al. 2020; Michalick L. and Kuebler W.M. 2020) Additionally, the interplay between TRPV4, microbial colonisation, and biofilm formation presents intriguing prospect for further exploration. In the context of oesophageal keratinocytes wound healing, one of the reports shows that the activation of TRPV4 leads to the release of ATP which further contributes to the decrease in

rate of in *vitro* wound healing (Boudaka et al. 2020). This phenomenon, in turn, exerts an inhibitory influence on the pace of in *vitro* wound healing.

In this regard, the *in vivo* wound healing assay has been carried out by using MRSA (*Staphylococcus aureus*) infection in the wound tissue. The results show unique observations that the TRPV4 inhibition (RN1734) was more efficient in clearing the bacteria rather than DMSO control. The wound closure was also observed to be faster than other two conditions. Interestingly, the activation also seems to be effective in the clearance of bacteria in the wound site, though not as significant as in inhibition conditions, but more efficient in minimizing infection than DMSO control conditions. Thus, TRPV4 modulation seems to play a crucial role in bacterial clearance in the wound site and better wound closure. By modulating the TRPV4, the duration and severity of bacterial infection can be reduced. This finding demonstrates that modulation of TRPV4 significantly enhances wound healing and clearance of MRSA (*Staphylococcus aureus*) bacteria. Furthermore, the *in vitro* experiments revealed a notable decrease in bacterial colony-forming units (CFU) under conditions of TRPV4 modulation, indicating the involvement of TRPV4 in macrophage activation for bacterial clearance through phagocytosis.

The phagocytosis as well as bacterial survival has also been investigated by using Rv and Ra variants of *Mycobacterium tuberculosis*. The total time period taken for the infection was 24 hours. It is observed that these two variants of Mtb has different response to the TRPV4 modulation, i.e. activation or inhibitions. The Rv variant shows well response as compared to Ra variant. The phagocytosis percentage is significantly less in case of Rv sample in TRPV4 activation conditions at initial hours, while at 24 hours of infection the percentage of survival is significantly more in case of TRPV4 activation (as per the CFU count). In this case TRPV4 inhibitions also show better survival in comparison with DMSO control (**Fig.90**). These

observations specifically indicate that TRPV4 is involved in the pathogenic clearance and TRPV4 modulations can be used as a pharmacological target for several pathogenic diseases.

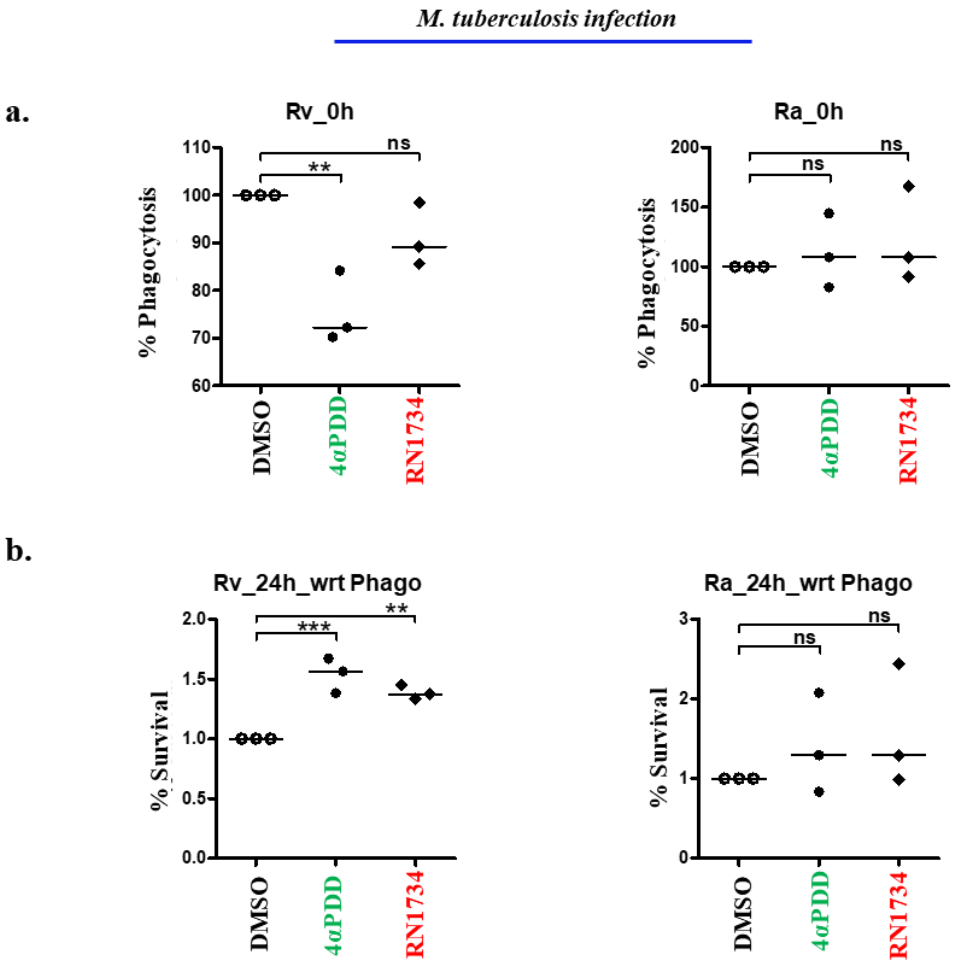

Fig 90. Role of TRPV4 modulations in *in-vitro* bacterial (*Mycobacterium tuberculosis*) clearance in macrophage cells. a & b. The graphs here represent Mtb-infected cells for 24 hours' time periods. Here the graph shows the percentage of phagocytosis and the percentage of survival upon Mtb infection after 24 hours. One-way ANOVA test. (** = p≤ 0.01, *** = p≤0.001 and ns = non-significant). (Acknowledgement to Dr. Vinay Nandicoori and Dr. Sabita from NII, New Delhi for conducting this experiment at their facility).

3.2.3.2 TRPV3 in *in vitro* and *in vivo* bacterial clearance

Because of the abundance in the skin tissue, TRPV3 seems to be important in skin inflammatory functions like dermatitis, skin infections, pruritus, and wound infection. The keratinocytes cells are associated with blood vessels, neuronal cells, and different immune cells like dendritic cells, neutrophils cells, macrophage cells, mast cells, and other immune cells. Keratinocytes and their nearby environments are very important in clearing out pathogens and

repairing of the skin tissue and the re-epithelization. The abundance of macrophages in the wound tissue in the TRPV3 activations as well as bacterial clearance in the wound area are correlated events and shows the significance of TRPV3 in the immune regulation in the wound tissue. The available data collectively imply a noteworthy engagement of TRPV3, and possibly other TRP channels also, in tissues that undergo recurrent encounters with diverse bacterial (and thus pathogenic) challenges. Notably, the modulation of TRPV3 presents a potentially advantageous strategy when contending with various challenges such as pruritus, microbial infections, tissue injuries, and persistent inflammatory processes (Um et al. 2022). Activation of TRPV3 via FPP (Farnesyl pyrophosphate) results in recruiting primary macrophages at the wound tissue, coinciding with the expression of TRPV3 in these immune cell populations. This suggests the potential involvement of TRPV3 to the surveillance of tissue damage and subsequently orchestrate localized immune responses within the microenvironment of wounds. Likewise, in culture conditions, activation of TRPV3 by FPP results in more bacterial phagocytosis and bacterial clearance as confirmed by CFU analysis. This also suggests an efficient lysosomal function; as bacterial clearance needs low pH at the lysosome. This could further indicate the possible involvement of lysosomal acidic pH (at wound tissue microenvironments) regulated by TRPV3.

3.2.3.3 Role of TRPs in chronic intestinal inflammation and bacterial clearance

TRPs play a significant role in inflammatory bowel disease (IBD), a condition characterized by intestinal inflammation. So far, several TRP channels have linked to gut disorders, such as heightened sensitivity in the gut (visceral hypersensitivity) and the immune-related aspects (such as IBD), which can either worsen or alleviate inflammation and sensitivity. Based on the recent findings, TRPV1 and TRPA1, appeared as potential targets for new IBD treatments. TRPV1 is more active in the nerves of the colon in people with IBD as

compared to those without the pathogenic condition. However, the role of TRP channels, particularly TRPV1 and TRPA1, in IBD is still not clearly understood, and studies are ongoing to understand how these channels might be involved in IBD (Chen et al. 2020; Csekő et al. 2019). In summary, few TRP channels, especially TRPV1 and TRPA1, are implicated in IBD and visceral hypersensitivity. These two channels hold promise as potential targets for IBD therapies. Increased TRPV1 activity in the colon of IBD patients is linked to the severity of abdominal pain. Further research is needed to uncover the exact mechanisms by which TRP channels contribute to IBD.

In the context of colon infection and acute infection in the colon, this thesis focuses on TRPV3 as a potential therapeutic target. Other than skin tissue, TRPV3 is also abundant in the gastrointestinal (GI) tract and intestine. Different TRP channels (such as TRPV1-V4, TRPM2, TRPM4, TRPM5, and TRPC) are also present in the intestine, and gastrointestinal (GI) tract and are involved in chronic inflammation and colitis. The abundance of TRPV3 in the GI tract (other than skin tissue) implicates its role in colon infection and inflammation. For instance, TRPV3 activation effectively minimise *Salmonella typhimurium* infection in the colon and divert it to the spleen for its early elimination of the pathogen. The colon length also reduced in case of colitis-induced mice with DMSO or DPTHF (TRPV3 inhibitor) treatment, but there are non-significant changes in case of TRPV3 activation (such as by carvacrol, thymol). This data suggests the crucial role of TRPV3 activation, which helps in reducing and helps in recovering from *Salmonella* infection. The detectable presence of TRPV3 including other TRP channels in both macrophages and in T cells substantiates this notion, implying their potential involvement in immune-related activities (Majhi et al. 2018). Collectively the data suggests that TRPV3 play important role in minimizing bacterial infection and control inflammatory functions of the tissues that are frequently invaded by pathogens.

3.3 TRPV3 in the nucleolus: importance and application of TRPV3 in the nucleolus

3.3.1 Lysosome and nucleus as stress response regulator

Both the nucleolus and lysosomes are vital sub-cellular structures that respond to cellular stress. Nucleolus helps to make ribosomes, and is also acts like a “stress response regulator”. The factors contribute to the nuclear stress are thermal stress, osmotic stress, pathogenic stress, ionic stress, and nutrient stress. Nucleolar size and structure correlate with the nucleolar health, and at molecular level correlates with rRNA transcription, cell growth and the metabolic rate of a cell (Latonen L. 2019). Nucleolus is important for the cell to grow and stay alive. On the other hand, lysosomes also act like control centres for dealing with stress and regulate how the cell uses energy. These can also sense cellular stress happening in the cell and manage it using different pathways. Nucleolus also takes part in controlling autophagy, a process where the cell cleans up and recycles molecules that cell doesn't need. In case of cellular stress, nucleolus can “senses” that and can signal the cell to start this clean-up process faster. This helps cell to cope-up during cellular stress. So, both nucleolus and lysosomes are crucial when the cell faces stress (Saftig P. and Puertollano R. 2021; Dannheisig et al. 2021; Pfister A.S. 2019). The nucleolus detects stress and helps with cleaning up, while lysosomes manage how the cell deals with stress and uses energy, indicating the importance of these subcellular structures for maintaining the cellular balances under challenging conditions. In a molecular level both lysosomes and nucleolus are linked with each other functionally (**Fig. 91**). Both these compartments contribute to the cell’s health, aging of cells, and ultimately combat with various diseases. The nucleolar localization of TRPV3 could be relevant for understanding role of TRPV3 in nucleolar stress.

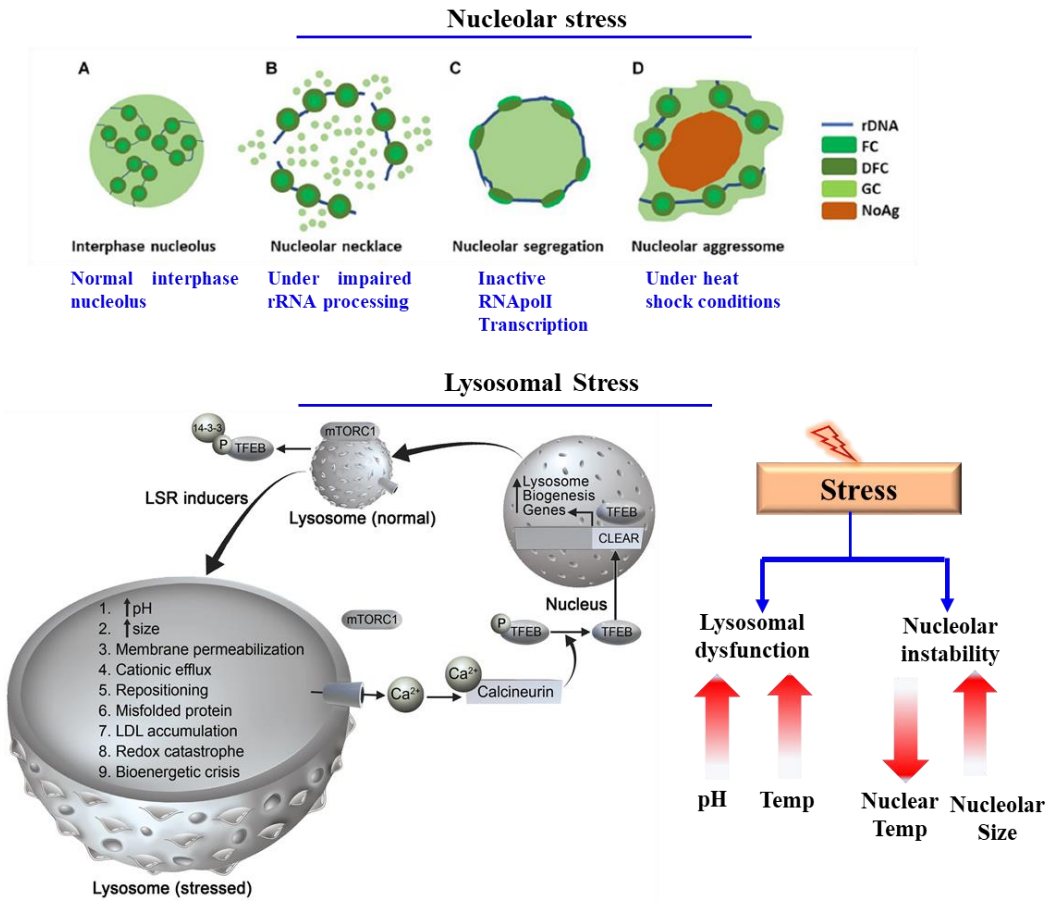

Fig 91. Physiological effects on lysosome and nucleolus in relation to cellular stress. The representative image shows effect of cellular stress on nucleolar and lysosomal structure and functions**. (**Granular components-GC Fibrillar components-FC, Dense fibrillar components-DFC). This image is adapted from Latonen L. 2019 and Lakpa et al. 2021.

3.3.2 Importance of ion channels in the nuclear functions

It is widely known that ion channels are expressed in the plasma membrane. However, a few studies have suggested that several channels including voltage-gated K^+ (Kv) channels also exist in intracellular organelles where these are involved in the biochemical events associated with cell signaling. Kv1.3 channels are primarily localized in the nucleus of several types of cancer cells and human brain tissues where these are capable of regulating nuclear membrane potential and activation of transcription factors, such as phosphorylated CREB and c-Fos (Jang et al 2015). Reports also suggests that upon activation of TRPV4, it binds to the DEAD-box RNA helicase DDX3X and regulates its function (Doñate-Macián et al 2018).

TRPV4-mediated Ca^{2+} influx releases DDX3X from the channel and drives DDX3X nuclear translocation (Doñate-Macián et al 2018). NRs (Nuclear receptors) are intimately involved in macrophage development as well as in macrophage inflammatory response and host defence pathways. Nuclear receptors (NRs) comprise a superfamily of intracellular transcription factors that are key players in macrophage homeostasis, metabolism, and transcriptional regulation (Leopold et al. 2019). All these reports suggest that there are proteins (including K^+ channels) that localizes and accumulates in the nucleus and all have a specific role.

3.3.3 Nucleolar localization of TRPV3

Nucleolar functions are critical for the preservation of cellular homeostasis and prevention of complex diseases. These functions are pivotal in enabling cells to acclimate to challenging conditions while upholding their regular operations. Based on the findings from this thesis work, a unique role of TRPV3 can be proposed. TRPV3 is found in both nucleolus and in the lysosome, the organelles that transmit information regarding cellular stress, and employing distinct proteins. Under stress-induced circumstances, lysosome orchestrates the transmission of information to the nucleolus, which subsequently enacts stress-responsive measures.

A remarkable revelation in this study is the detection of TRPV3 within the nucleolus. Co-localization studies confirm the presence of TRPV3 with fibrillarin-enriched structures, an established nucleolar marker, as opposed to other markers indicative of nuclear compartments. Though full-length TRPV3 is detected in the nuclear fraction, the nature and the structure of TRPV3 within the nucleolus remain unclear. Noteworthy is the identification of a distinct NoLS sequence within TRPV3. This sequence exhibits significant conservation among warm-blooded organisms and originates from a unique evolutionary lineage. Given the nucleolus's specialized engagement in cellular stress and thermal retorts, along with the presence of the

thermosensitive ion channel TRPV3 within this domain, further studies are required to understand the involvement of TRPV3 in stress response.

3.3.4 TRPV3 can be involved in the regulation of nuclear temperature spectrum

The thermal pattern has been investigated through NTG thermal dye. It has been observed that the channel modulations have a specific role in the distribution of thermal patterns in the nucleus. The findings indicate that the nucleus itself has a definite pattern of thermal spectrum. The nucleolus region does not emit any signal. This is mainly due to the lack of Ds-DNA at the nucleolus. The temperature varies according to the TRPV3 modulations or LPS stimulations. It has been observed that the absolute intensity increases according to the TRPV3 modulations as well as LPS stimulations. The % of pixels corresponding to “zero intensity” or “highest intensity” level varies in different conditions. The more the intensity, the less the temperature, so at TRPV3, modulation or LPS stimulation representing the cold temperature level increased significantly while the hot sensing part decreased accordingly. Overall the data suggests that TRPV3 modulation or even expression of NoLS alters the thermal spectrum of the nucleus. Though the change in the nuclear thermal spectrum matches well with the cellular stress levels, further studies are needed in this aspect.

3.3.5 Evolution of TRPV3 NoLS sequence

The NoLS have been screened and scored the NoLS of different species like fish, amphibians, turtles and birds along with humans. The predicted score of NoLS have found to be more in case of mammals but some exception like amphibians (*Nanorana parkeri)*. The predicted score for the human (0.905), bird (0.5-0.7), turtle (0.3-0.5), fish (0.0) and amphibian (0.908) remain variable. All these constructs -tagged with GFP vector and their localization is found to be more in the nucleolar region. It is more for higher scored sequences, i.e. human

and *Nanorana parkeri* but distributed throughout in case of less-scored sequences such as in fish (elephant shark-*Callorhincus milii*). In that context, it has been found that the distribution of TRPV3-NoLS is concentrated in the nucleolar region in case of humans, *Nanorana parkeri*, to some extent in turtles (*Chelonia mydas*) and in *Gallus gallus* but not in case of fish (where it was dispersed throughout the cell). This indicates the enrichment in the nucleolar region depends on the score of the NoLS, at least to some extent and human species NoLS have more enrichment in the nucleus than others. Nevertheless, it is important to mention that the nucleolar localization of TRPV3 is marked by specificity and remain responsive to diverse cellular conditions, particularly in the context of stress stimuli. These findings suggest and provide insight into the role of TRPV3 in the cellular response and its actions as a cellular stress response regulator. Further investigation is required for a better understanding of the molecular basis of TRPV3 in nucleolar stress response and the involvement of other molecules.

3.3.6 Application of TRPV3 NoLS as a novel sensor for studying nucleolar environment

As NoLS of TRPV3 shows specific and exclusive localization within nucleolus, it is possible to use the same for a nucleolus-specific sensor. For that purpose, the NoLS sequence of TRPV3 has been tagged with a Ca^{2+}-sensor (i.e. GCaMP6f). This NoLS sequence tagged with the GCaMP can be useful to study Ca^{2+}-dynamics in the nucleolus. The NoLS-GCaMP is able to localize within the nucleolus and respond to TRPV3 modulations and/or LPS stimulation. This shows great signs of NoLS-GCaMP being able to measure Ca^{2+}-status in the nucleus, and it will be a great prospect for future studies. The construct can be further used as nucleolar Ca^{2+}-sensor in the future and it would be useful for the nucleolar stress study (**Fig. 92**).

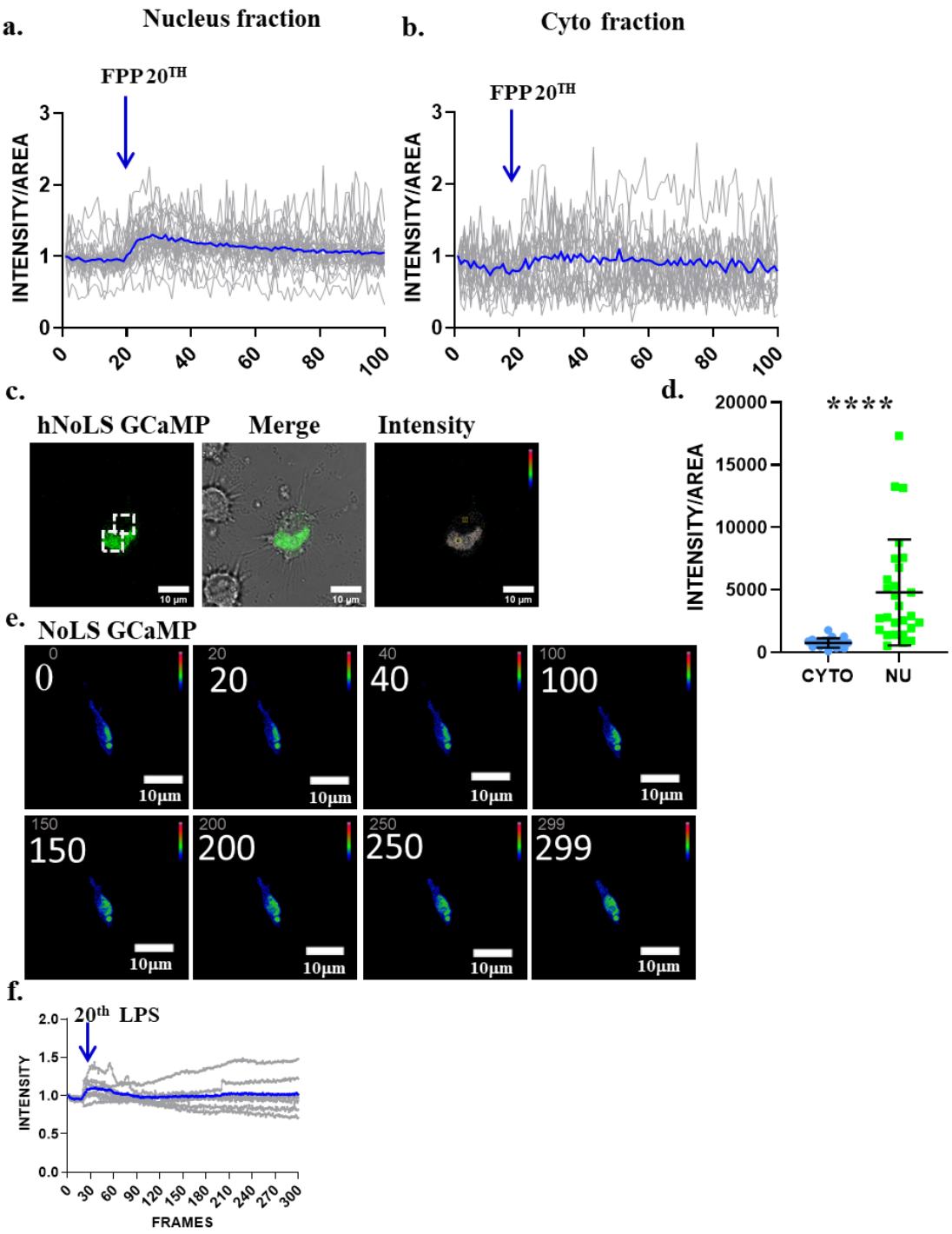

Fig 92. TRPV3 activation increases nuclear Ca^{2+}-level as detected by NoLS-GCaMP. a & b. The graph shows the Ca^{2+}-influx in the Raw 264.7 cells (expressing NoLS-GCAMP) after TRPV3 activation. TRPV3 activation shows a significant increase in the Ca^{2+}-level in the nucleus due to FPP addition at the 20th frame. **c & d.** The representative image and graphs show the NoLS-GCaMP intensity in Raw 264.7 cells. Scale bar 10µm. **(c)** and the quantitative fluorescence intensity observed in the cytosolic and nuclear regions (d). **e & f.** The images represent the nuclear intensity changed upon LPS stimulations at 20th frames along with the intensity plot. The intensity peak shows upon LPS stimulation at 20th frame. Scale bar 10µm. Unpaired t-test. (**** = p≤ 0.01).

3.4 TRP channels as potential regulators of viral infection

3.4.1 TRP channel role in the regulations of viral infections

Viruses primarily engage with host cells at the plasma membrane (PM), which is rich in a variety of ion channels, exchangers, pumps and receptors. These components play crucial roles in maintaining cellular Ca^{2+} homeostasis, mainly due to the engament of certain Ca^{2+} channels. Viruses have evolved mechanisms to manipulate this homeostasis, aiding in successful infections. Consequently, these membrane proteins become direct targets of viral interaction (and also for pharmacological agents for treatment purposes). Moreover, intracellular membrane proteins involved in Ca^{2+} regulation have also been implicated in various stages of viral life cycles. Among these, TRP channels have emerged as significant regulators of Ca^{2+}-dynamics within host cells during viral infections (Kumar et al. 2022). Ca^{2+} plays a pivotal role in viral pathogenesis by regulating host-virus interactions and influencing viral infection processes. The elevation of intracellular Ca^{2+}-levels during viral infection is associated with enhancing viral replication and orchestrating pro-viral responses within host cells. This underscores the importance of Ca^{2+}-signaling pathways mediated by TRP channels in viral pathogenesis, highlighting their potential as targets for developing antiviral strategies. The complex interplay between Ca^{2+} and viral infections emphasizes the necessity of comprehending and targeting these mechanisms to effectively combat viral diseases (Kumar et al. 2022).

TRP channels have an important role in viral infections by controlling Ca^{2+}-levels inside host cells, which impacts various stages of the viral life cycle. These stages include viral fusion, entry, replication, maturation, and release. TRP channels also influence how the virus interacts with host cells because these channels allow Ca^{2+} into the cells and often many interactions are Ca^{2+}-dependent or remain Ca^{2+}-sensitive. During a viral infection, TRP channels like TRPV1, TRPA1, TRPM8, TRPV2, and ASICS3 show higher expression and

activation. This increased activity can affect functions like the “sensitivity of cough reflexes” induced by respiratory viruses and the behaviour of nerve and airway cells (Omar et al 2017; Abdullah et al. 2014).

A recent study revealed that ChikV infected cells have higher TRPV1 activation. Also blocking of TRPV1 in the presence of ChikV, the infection rate decreased significantly. The Ca^{2+}-level in the ChikV-infected cells increased instantaneously and TRPV1 activation contributes in such Ca^{2+}-levels. Such Ca^{2+}-increment was not observed in case of TRPV1 inhibition This indicates the involvement of TRPV1 in viral infection (Kumar et al. 2021).

Another report described that following cleavage, spike glycoproteins have the capability to engage with distinct intracellular receptors like NPC1 (in Ebola virus) or lamp1 (in case of Lassa virus) (Zhao et al 2021). This interaction facilitates fusion between the viral envelope and the endo-lysosomal membrane, a process mediated by spike glycoproteins. Furthermore, lysosomal ion channels such as TPCs and TRPML2 play a role in initiating the fusion process, potentially serving as channels for releasing Ca^{2+} within lysosomes (Zhao et al 2021). In this context, lysosomal TRPs channel involvement in viral pathogenesis seems to be relevant for future investigation.

In summary, TRP channels appears to be important players in the context of viral infections as these channels regulate intracellular Ca^{2+}-levels within host cells and imitates a series of Ca^{2+}-dependent as well as Ca^{2+}-independent signalling events which influence various stages of the viral life cycle. These channels, because of their involvement, could be potential molecular targets for developing antiviral therapies.

3.4.2 TRPV3 in the regulations of ChikV infection

In this context of Chikungunya Virus (ChikV) infection, the potential role of the TRPV3 has been investigated along with the possible antiviral responses. A dynamic

relationship between TRPV3 expression and ChikV infection seems to be plausible. Experimental manipulation of TRPV3 expression levels reveals a compelling pattern: i.e. under conditions of TRPV3 inhibition, a significant reduction in TRPV3 expression is observed. At the same time, the significantly heightened intensity of the E2 protein, a component of ChikV, is detected upon TRPV3 inhibition (DPTHF 100µM). Remarkably, the application of pharmacological agents to inhibit TRPV3 yields notably more (PFU/ml) viral particles as compared to TRPV3 activation as quantified through the plaque assay (more PFU/ml). Though the PFU/ml is found to be more in the case of both TRPV3 activation as well as inhibition conditions, but TRPV3 inhibition shows a more significant increase in viral plaque as compared to TRPV3 activations. The correlation data of TRPV3 expression with E2 protein from ChikV infection in different conditions also suggests that TRPV3 modulation alters such relationship (**Annexure 7.3**). The Ca^{2+}-efflux also varies upon TRPV3 modulatory conditions along with ChikV administration. The Ca^{2+}-levels change significantly in TRPV3 activation (FPP, 1µM) and more Ca^{2+}-influx upon further administration of ChikV in the live cell system. However, in case of TRPV3 inhibition, the Ca^{2+}-efflux was non-detectable, which further increased upon addition of ChikV particles in the live cell. These findings collectively indicate the intricate interplay between TRPV3 and ChikV infection dynamics. Further research in this direction can be beneficial to introduce targeted therapeutic strategies harnessing TRPV3 modulation to combat ChikV and potentially other viral infections.

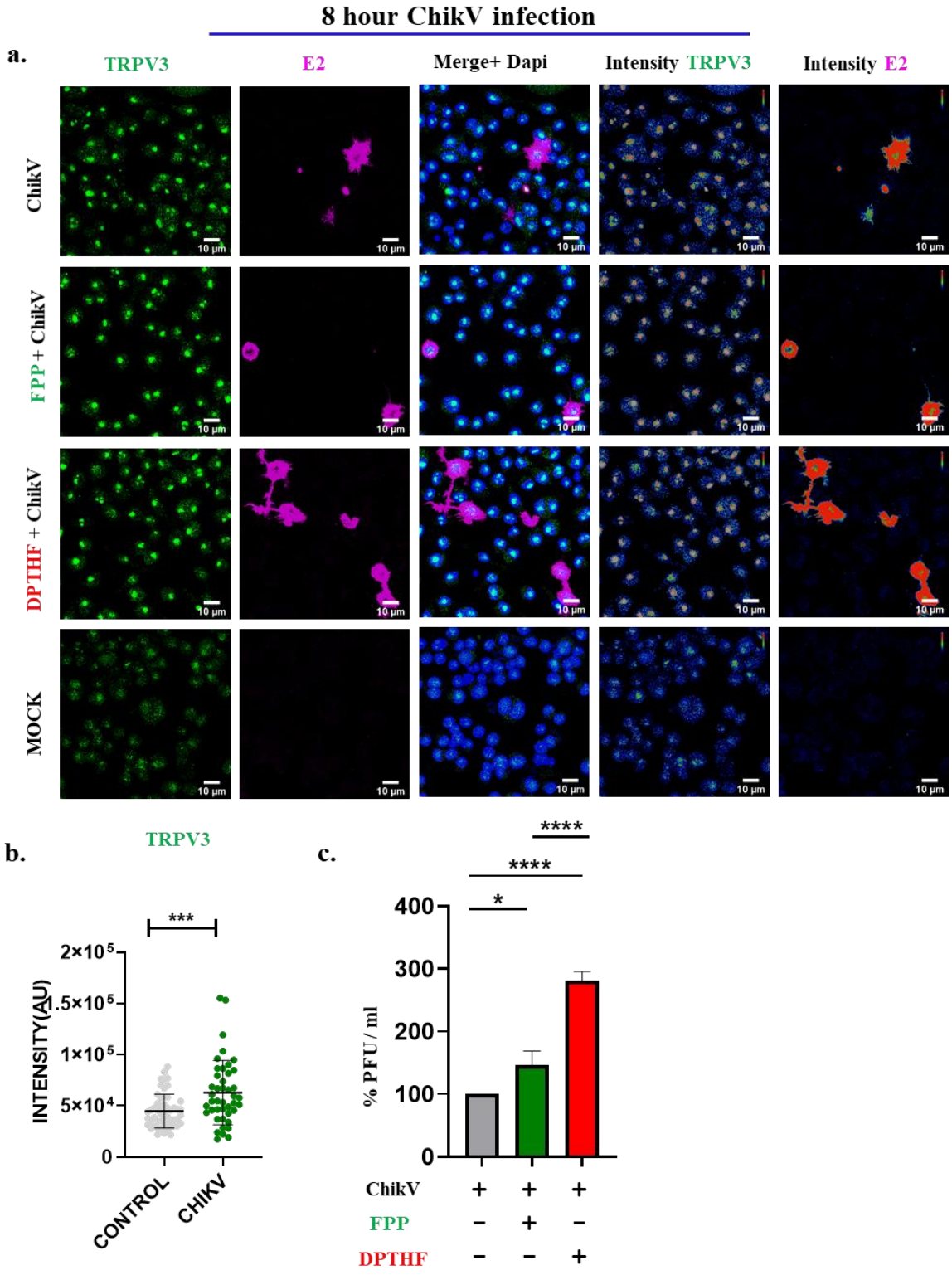

Fig 93. ChikV infection is more in TRPV3 inhibitory conditions. a. The representative image shows E2 protein and TRPV3 protein localization in Raw 264.7 cells after ChikV infection over certain period of time (8 hour infection). Scale bar 10µm. **b.** The graph represents intensity plot of TRPV3 in the ChikV infected macrophage cells **c.** The representative graph shows percentage of viral particle (PFU/ml) with and without TRPV3 modulations. TRPV3 inhibition shows increase percentage of PFU/ml significantly. The values are normalized with control condition as 100%. Unpaired t-test, * = p ≤0.05, *** = p ≤0.001, and **** = p ≤0.0001. (Acknowledgement to Dr. Soma Chattopadhay and her lab members).

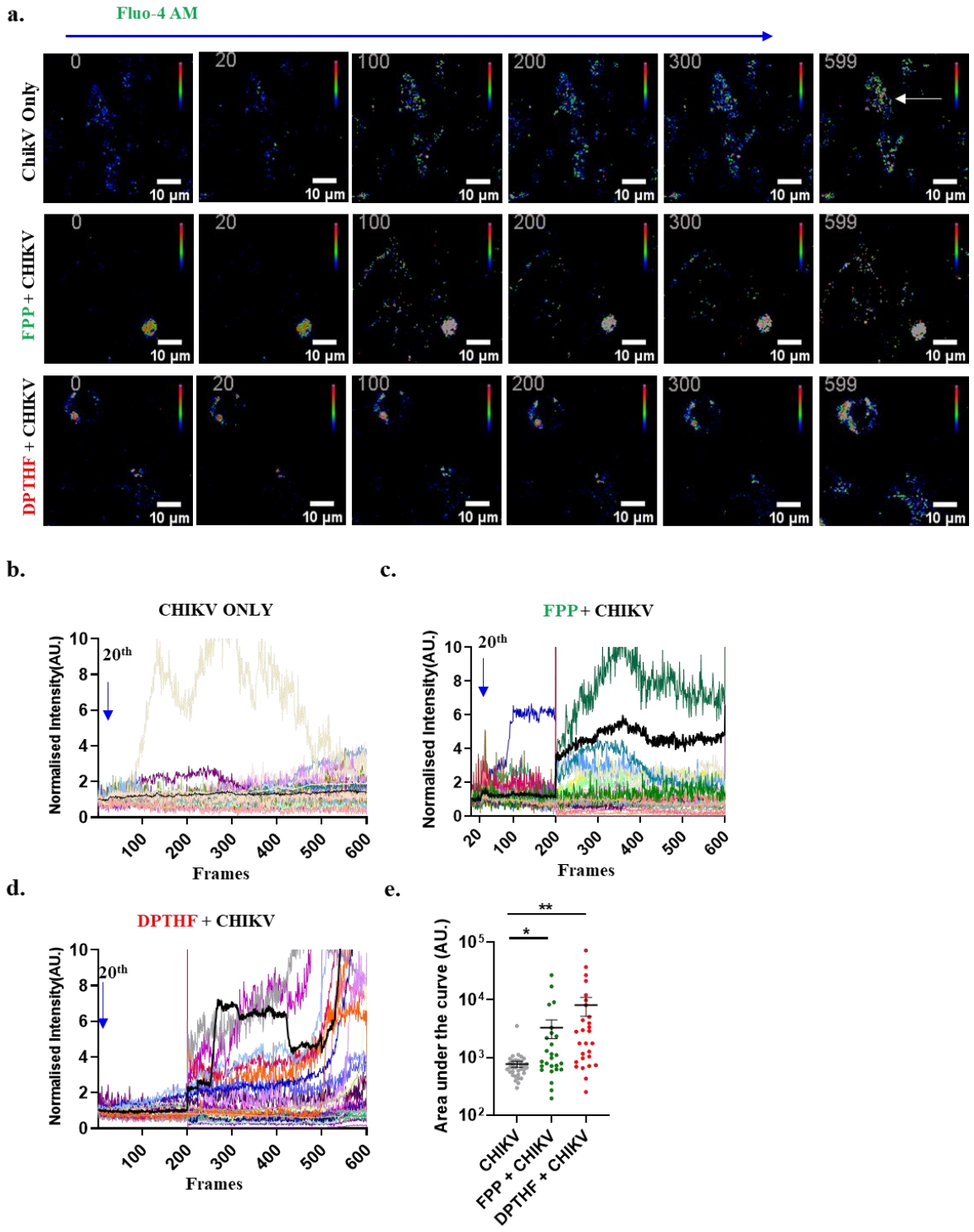

Fig 94. Ca^{2+}-influx is more due to TRPV3 activation and addition of ChikV. a. The representative image shows Ca^{2+}-influx upon TRPV3 modulations and ChikV administration respectively. Scale bar 10µm. **b-d.** The representative graph shows the changes in the Ca^{2+}-level upon different treatments. Administration of ChikV causes instant increases the Ca^{+2}. However, such increases in Ca^{2+}-become more when TRPV3 is activated by FPP (1µM) or inhibited by (DPTHF, 100µM). e. The graph represents the area-under-curve values (equivalent to total Ca^{2+}-influx in a cell during the experiment) in different condition of ChikV infection, i.e. with or without TRPV3 modulation. Unpaired t-test, * = $p \leq 0.05$ and ** = $p \leq 0.01$. (This experiment was performed in collaboration with Dr. Soma Chattopadhay and her lab members, ILS Bhubaneswar).

Chapter 4

Conclusion

Conclusion and future prospects

This work demonstrates the effective role of TRPV3 in clearance of invading pathogens in the skin wound and in colon tissue. As per previous report, specific expression of TRPV3 is most abundant in the skin tissue and in the gastrointestinal tract (GI tract). Notably, both skin and GI act as the protective barriers and GI maintains the gut microenvironments. These two tissues act as the barrier for invading pathogen from external sources. It seems that molecular evolution of TRPV3 is influenced by its protective role. The protective functions of TRPV3 is mainly due to its presence in the immune cells and its subcellular localization and functions in lysosomes. Other than carrying out ion-influx in the cell and in the sub-cellular compartments, TRPV3 plays much bigger role. Lysosome is crucial for cellular homeostasis by controlling pathogen clearance, waste management, ion homeostasis, and pH regulations. These regulations of lysosomal functions are critical for cellular stress response. Both TRPV3 and TRPV4 seems to be involved in the regulation of lysosomal functions. Both TRPV3 and TRPV4 are involved in the cellular homeostasis and stress management.

TRPV3 acts as a protective barrier in the colon tissue as well as skin keratinocytes and helps in pathogen clearance through its modulations. TRPV3 modulation, mainly activation helps to clear bacterial pathogen (*Salmonella typhimurium* and *Staphylococcus aureus*) in both colon tissue and skin tissue effectively. The activation of TRPV3 also recruits immune cells in the wound site, which seem to be involved in better bacterial clearance. TRPV3 in the macrophage cells helps in the maintenance of wound site repair management through its modulations. TRPV3 modulation results in early clearance of bacteria and early closure of the wound. This indicates the protective role of TRPV3 in terms of handling bacterial infections in the wound site and in colitis conditions. Accordingly, in case of TRPV3 activation, the spleen (which filtered out bacterial pathogens) show more CFU counts and colon sample show

significantly lesser CFU. This signifies the effective role of TRPV3 activations in clearing out bacteria in the colitis-induced animal.

Regulating inflammatory functions like wound healing and bacterial clearance, the presence of TRPV3 in the immune cells like macrophages is more relevant. The cytosolic Ca^{2+} level is enhanced through TRPV3 activation in macrophage cells. The cells respond to TRPV3 activations (FPP, 1 mM) and exert Ca^{2+}-influx both in primary macrophage and RAW 264.7 cells. The presence of TRPV3 both in the primary macrophage cells as well as in macrophage cell lines are clear indicative of its role in macrophage functions. Notably its presence in the subcellular compartment like lysosome and nucleus helps in the regulation of cellular stress response. TRPV3 modulations help in the maintenance of lysosomal function in the hyperthermic stress as well as in the LPS-induced stress conditions. TRPV3 modulation rescues the cells from lysosomal stress and nuclear stress at LPS stimulations or at hyperthermic conditions. Lysosomes tend to lose their integrity and low pH when lysosomal stress in induced (BafA1, 4 hours) or hyperthermic stress (42°C, 2 hours) in introduced. TRPV3 modulation helps in the maintenance of lysosomal low pH and lysosomal integrity in hyperthermic stress and/or in lysosomal stress conditions. Generally, the cytosolic ROS-level, cytosolic Ca^{2+}-level, ATP-level, and other cellular parameters are disrupted due to hyperthermic stress, which is effectively maintained in case of TRPV3 modulations.

The temperature gradient may be dysregulated in case of cellular stress. The relative temperature of different subcellular organelles and temperature gradient at the subcellular level also play significant roles in cellular homeostasis. The temperature differences within the cells are crucial for maintaining cellular balance. To understand such issues in details, various lysosomal parameters were characterized especially in conditions where TRPV3 is modulated. The TRPV3 modulations play a significant role in maintaining lysosomal temperature at heat stress or lysosomal stress conditions, and is able to rescue the cells to maintain its temperature

gradient. At hyperthermic stress (42°C for 2 hours) or lysosomal stress (V-ATPase blocked by BafA1), the temperature in the lysosome fluctuates and mostly increases as compared to the control condition. TRPV3 modulations in cellular stress conditions maintain the lysosomal temperature more comparable to the control level.

The status of cells expressing TRPV3 OS mutants or TRPV3-WT have also been explored. TRPV3-WT cells have a better chance of survivability as compared to TRPV3 OS mutants. The cellular Ca^{2+}-level changes upon TRPV3 activation (increased at 1 mM FPP). However, cells expressing TRPV3 OS-mutants fail to exert any response in the activation state. The nuclear temperatures of individual cells are measured by using NTG dye. TRPV3-OS mutant expressing cells seem to be maintained with lower nuclear temperatures (more fluorescence intensity) as compared to cells expressing TRPV3-WT. Such changes may affect the transcription of genes drastically. Similarly, the plasma membrane thermal status (by using PTG dye), lysosomal thermal status (by using LTG dye), and mitochondrial thermal status (by using MTG dye) were compared in different conditions where TRPV3 were modulated. The temperature of the lysosome, plasma membrane and mitochondria drastically increased in the cells expressing TRPV3 OS-mutants as compared to cells expressing TRPV3-WT. Such altered temperatures accord well with the low survival rate of the cells expressing OS-mutants

TRPV4 has also been investigated in this study as a functional homologous of the TRPV3 ion channel. TRPV4 is involved in immune functions and regulating lysosomal stress conditions. TRPV4 plays significant roles in both pro-inflammatory and in anti-inflammatory processes. TRPV4, helps in clearing bacteria at the wound site and fastens wound closure through its modulations. TRPV4 helps to maintain various cellular factors like ROS, NOS, Ca^{2+}, and pH during cellular stress or any pathogenic stress.

The data indicate that TRPV3 and TRPV4 can react to signals associated with both pathogens and cell/tissue damage. Understanding this response is crucial in the context of

pathogen infection and inflammation responses. As pathogen infection is followed by increase in body temperature, activation of these thermosensitive channels seems to be obvious during infection and cellular stress and thus indicating their essential role in recruiting feedback signaling suitable for combating invading pathogens both at the cellular and tissue levels. The temperature variations at the subcellular level are crucial for maintaining cellular homeostasis. TRPV3 modulations cause altered lysosomal temperature during heat or lysosomal stress, thus rescuing the cells and ensuring the maintenance of their temperature gradient (**Fig.95 and Fig 96**).

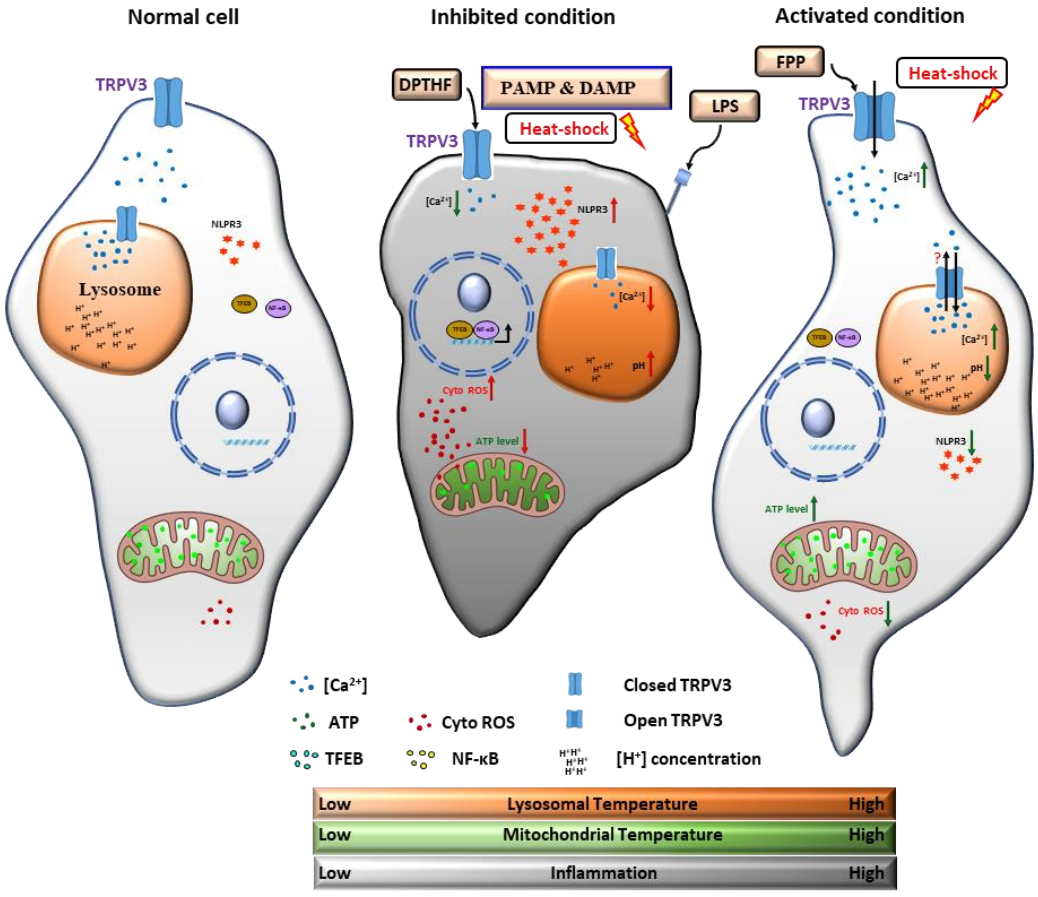

Fig 95. Schematic representation of TRPV3 regulated cellular stress managements.

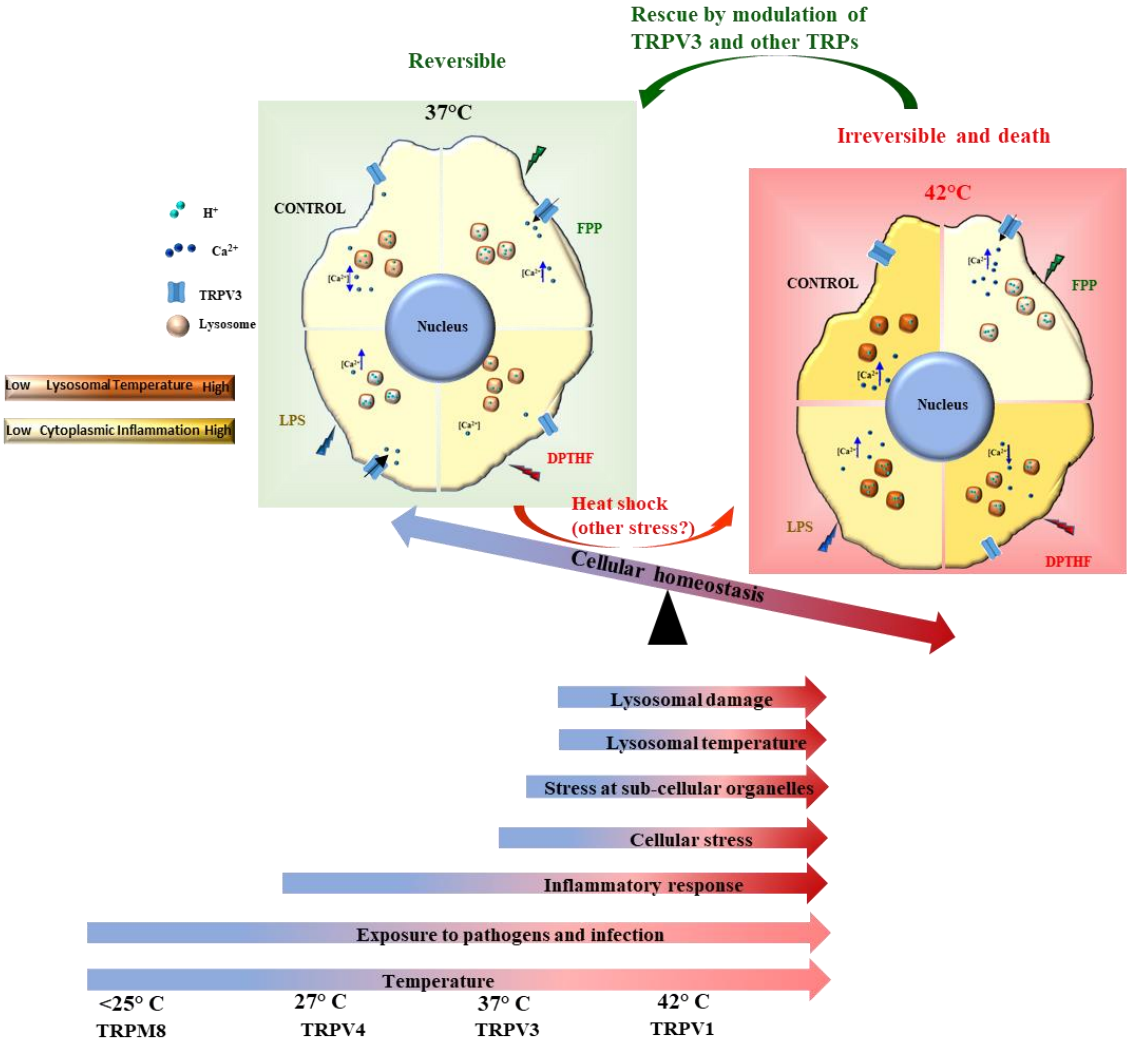

Fig 96. Overview of TRPV3 and TRPV4 channel as cellular stress response regulators.

In future, this study may form the basis to understand the functions related to stress in lysosomes, nuclei, and in other sub-cellular organelles. This study also relevant to understand the involvement of these two organelles in stress-induced conditions. These aspects may become relevant in various health issues such as cancer, inflammatory diseases, pain, and other physiological conditions.

Chapter 5

Materials and Methods

5.1 Materials

5.1.1 Chemicals used

Chemical used	Source
4αPDD	Sigma - Aldrich
Acetic Acid	Merck Millipore
Acrylamide	Sigma – Aldrich
Agar	Himedia
Agarose	Lonza
Ampicillin	Sigma – Aldrich
Amphotericin-B	Sigma – Aldrich
Amylose resin	NEB
APS (Ammonium persulphate)	Sigma – Aldrich
ATP	Sigma – Aldrich
Bafilomycin A1	CST
BAPTA-AM	Sigma – Aldrich
Bis-acrylamide	Sigma – Aldrich
Bromophenol Blue	Sigma – Aldrich
BSA	Sigma – Aldrich
Carvacrol	Sigma-Aldrich
Complete protease inhibitor	Sigma – Aldrich
Coomassie Brilliant Blue G250	MP biomedical
Cover Slip	Himedia, VWR,
DAPI	Invitrogen
DDT	Sigma – Aldrich
DMSO	Sigma – Aldrich
dNTPs	NEB
DPTHF	Sigma – Aldrich
EDTA	Sigma – Aldrich
EGTA	Sigma – Aldrich
Ethanol	Merck
Ethidium Bromide	Sigma – Aldrich
Fluoromount- G	Southern Biotechnology
Paraformaldehyde	Sigma – Aldrich

F12	Himedia
FPP	Sigma – Aldrich
G418	Sigma – Aldrich
Glutamate	MP biomedical
Gluteral dehyde (4%)	Sigma-Aldrich
Glycerol	Sigma – Aldrich
Glycine	Sigma – Aldrich
HBSS (1X)	Invitrogen
HEPES	Sigma – Aldrich
Hydrogen Chloride	Merck
Hydrogen peroxide (H_2O_2)	Sigma-Aldrich
Ionomycin	Sigma-Aldrich
IPTG	MP biomedical
Kanamycin	MP biomedical
LB powder	Himedia
Leupeptin Hemisulfate	Sigma – Aldrich
Lipofectamine 3000	Invitrogen
Lysosome Enrichment Kit for Tissues and Cultured Cells	ThermoFisher
LPS	Invivogen
Maltose	Sigma – Aldrich
Methanol	Merck
$MgCl_2$	Sigma – Aldrich
MitoTracker Red	Invitrogen
$NaBH_4$	MP biomedical
NADH	Sigma – Aldrich
NE-PER™ Nuclear and Cytoplasmic Extraction Reagents	ThermoFisher
Paraformaldehyde	Sigma – Aldrich
PBS (10X)	Invitrogen
PIPES	Sigma – Aldrich
PMSF	Sigma – Aldrich
Potassium Hydroxide	Sigma – Aldrich
Potassium phosphate monobasic	Sigma – Aldrich
Power load (100X)	Invitrogen
Probenecid	Sigma – Aldrich
PVDF membrane	Millipore

Rapamycin	Invivogen
RN1734	Sigma – Aldrich
RPMI	Invitrogen
Skimmed milk powder	Himedia
Sodium acetate	Sigma- aldrich
Sodium Azide	Sigma- aldrich
Sodium Chloride	Sigma – Aldrich
Sodium Dodecyl Sulphate	Sigma – Aldrich
Sodium Hydroxide	Sigma – Aldrich
SS Agar	Himedia
Streptomycin	Sigma – Aldrich
Sucrose	Sigma – Aldrich
TEMED	Sigma – Aldrich
Thymol	Sigma-Aldrich
Tris base	Sigma – Aldrich
Triton X100	Sigma – Aldrich
Tryptone	Himedia
Tween 20	Sigma – Aldrich
Whatman paper	Whatman
Xylene cyanol	Sigma – Aldrich
Yeast extracts	Himedia
β-mercaptoethanol	Sigma – Aldrich

5.1.2 Kits and Markers

Reagents	Source
Plasmid DNA isolation (midi prep) kit	Qiagen
Plasmid DNA isolation (mini prep) kit	Qiagen
Gel extraction kit	Qiagen
Lipofectamine Cell transfection kit	Invitrogen
Lysosome enrichment kit	ThermoFisher Scientific
ECL	Thermo Scientific
Bradford protein estimation kit	Sigma-Aldrich
SDS-PAGE protein marker High-range	Thermo Scientific
1 kb DNA ladder	NEB

100 bp DNA ladder	NEB
Restriction Enzyme	NEB
Q5 DNA polymerase	NEB
Q5 buffer	NEB
T4 DNA ligase	NEB

5.1.3 Primary antibody used

Antibodies	Host	Source	Application/s	Dilution
MBP	Mo	NEB	WB	1:30,000
Lamp1	Mo	GeneTex	WB, IF	1:500
TRPV4-Ct	Rb	Alomone	WB, IF	1:500
TRPV4-Ext. loop	Rb	Alomone	WB, IF	1:500
TRPV3-Ct	Rb	Alomone	WB, IF	1:500
TRPV3-Ext. loop	Rb	Alomone	WB, IF	1:200, 1:500
TRPV3-Ext. loop Atto-633	Rb	Alomone	IF	1:400
P62	Mo	CST	WB, IF	1:500
NLRP3	Rb	CST	WB, IF	1:500
NFkB-P65	Mo	Santacruz	IF	1:500
TFEB	Rb	CST	WB, IF	1:500
Fibrillarin	Mo	CST	WB, IF	1:500
Fibrillarin	Rb	Abcam	WB, IF	1:500
α Keratin k3/k76	Mo	DSHB	IF	1:500
CD11b	Mo	DSHB	IF	1:500
Atto-630-labeled TRPV3	Rb	Alomone	IF	1:500
LC3B	Rb	CST	WB, IF	1:500

Mo: Mouse monoclonal; **Rb:** Rabbit polyclonal; **WB:** Western Blot; **IF**: Immunofluorescence;

Dilution with respect to Western Blot analysis and Immunofluorescence assay.

5.1.4 Secondary antibody used in immunofluorescence

Description	**Host**	**Source**	**Dilution**
Alexa-594-labelled anti-mouse	Chicken	Molecular Probe	1:750
Alexa-594-labelled anti-rabbit	Chicken	Molecular Probe	1:750
Alexa-488-labelled anti-rabbit	Chicken	Molecular Probe	1:750
Alexa-488-labelled anti-mouse	Chicken	Molecular Probe	1:750
Alexa-647 labelled anti-mouse	Chicken	Molecular Probe	1:500
Alexa-647 labelled anti-rabbit	Chicken	Molecular Probe	1500

5.1.5 Dyes used for live and fixed cells

Description	**Source**
AF-488 Phalloidin	Thermo Fisher Scientific
AF-594 Phalloidin	Thermo Fisher Scientific
BCECF	Molecular Probe
DAPI	Molecular Probe
ER Tracker blue	Thermo Fisher Scientific
Fluo4-AM	Molecular Probe
LysoSensor Green	Thermo Fisher Scientific

LysoTracker Green	Thermo Fisher Scientific
LysoTracker Red	Thermo Fisher Scientific
Mito CMX Ros	Thermo Fisher Scientific
MitoSox Red	Thermo Fisher Scientific
MitoTracker Red	Thermo Fisher Scientific
Rhod-3	Thermo Fisher Scientific
LTG	Kind gift from Prof Y T Chang lab (South Korea)
MTG	Kind gift from Prof Y T Chang lab (South Korea)
NTG	Kind gift from Prof Y T Chang lab (South Korea)
PTG	Kind gift from Prof Y T Chang lab (South Korea)

5.1.6 Secondary antibody used in western blotting

Description	**Host**	**Source**	**Dilution**
HRP labelled anti-mouse	Donkey	GE Healthcare	1:10,000
HRP labelled anti-rabbit	Donkey	GE Healthcare	1:10,000

5.1.7 Blocking peptide

Peptide Sequence	**Blocking activity against**	**Source**
Extracellular loop 1st extracellular loop (464-478aa) REEEAIPHPLALTHK	TRPV3	Alomone
1st extracellular loop (647-662) (C)EDQSN(S)TVPSYPA(S)RD	TRPV4	Alomone

5.1.8 Vectors

Vectors	**Source**
H2A-GFP	Addgene

pCDNA3.1	Prof. Jon D Levine (UCSF, San Francisco)
pRsetB-pHRed	Addgene
pSGFP2-C1	Addgene
pCMV6-AC-GFP	Dr. Yong Yang (Peking University, Beijing, China)
pGP-CMV-GCamP6f	Addgene

5.1.9 Cell line

Cell lines	**Source**
F11	Prof. F. Hucho (FU, Berlin)
HaCaT	Prof. F. Hucho (FU, Berlin)
MC3T3-E1	Kind gift from Dr Naibedya Chattopadhyay (CDRI, Lucknow)
Saos-2	NCCS Pune
Raw 264.7	NCCS Pune
THP1	Dr Santosh Chauhan Lab (ILS, Bhubaneswar)

5.1.10 Bacterial cell line

Bacterial cell line	**Source**
BL21DE3	CG-Lab, NISER, India
DH5α	CG-Lab, NISER, India
Staphylococcus aureus (MRSA)	ATCC-33591, India
Salmonella typhimurium	A kind gift from Dr. Sandeep Panda Lab, KIIT, Bhubaneswar, India

5.1.11 Constructs

Constructs used	**Vector**	**Expression system**	**Source**
TRPV3-NoLS GFP	pSGFP2-C1 and pCDNA3.1 (backbone)	Mammalian	Prepared in CG lab
TRPV3-GFP	pCMV6-AC-GFP	Mammalian	Dr. Yong Yang
MBP-TRPV3-Ct	pMalc2x	*Escherichia coli*	Prof. F. Hucho (FU, Berlin)

TRPV3-mutant-GFP (*OS*)	pCMV6-AC-GFP	Mammalian	Dr. Yong Yang, Beijing, China
hTRPV3 NoLS GFP	pSGFP2-C1	Mammalian	Prepared in CG lab
TRPV3 NoLS RFP	pmCherry-C1	Mammalian	Prepared in CG lab
TRPV3 NoLS NTD GCAMP	pGP-CMV-GCaMP6f	Mammalian	Prepared in CG lab
TRPV3 WT(*OS*) Mcherry	pmCherry-C1	Mammalian	Prepared in CG lab

5.1.12 Construct Gift from other lab

Constructs used	Source
Fibrillarin-GFP	Dr. Dibyendu Bhattacharyya Lab, ACTREC Mumbai
LaminA-RFP	Dr. Dibyendu Bhattacharyya Lab, ACTREC Mumbai
CENPA-YFP	Dr. Ben E. Black and Dr. Clevland lab, USA

5.1.13 Primers used

Species	***Forward primer***	***Reverse primer***
NoLS GFP *Gallus gallus* (bird)	5'CACCGGATCCGCCACCATGGAGCAGACCGGCGCCCGCAAGAAGCTGAAGAAATACATCTTCAGCAAGGGCGAGGAGCTGTTC3'	5'CACCGAATTCTTACTTGTACAGCTCGTCCATGCC3'
NoLS GFP *Nanorana parkeri* (Amphibian)	5'CACCGGATCCGCCACCATGCCGAAGAAAACACCAAAAAGGCCACCAAAAAATCTTCTGTTCAGCAAGGGCGAGGAGCTGTTC3'	5'CACCGAATTCTTACTTGTACAGCTCGTCCATGCC3'
NoLS GFP (*Callorhinchus milii)* Fish	5'CACCGGATCCGCCACCATGAAACAAAGGAAGCTTCAAAACAGGGTATGGGTAGACTTCTATAGCAAGGGCGAGGAGCTGTTC3'	5'CACCGAATTCTTACTTGTACAGCTCGTCCATGCC3'
NoLS GFP *Chelonia mydas* (Turtle)	5'CACCGGATCCGCCACCATGCACTGGAACAATGCCCGAAAAAAGCTGAAGAAATATATGTTTAGCAAGGGCGAGGAGCTGTTC3'	5'CACCGAATTCTTACTTGTACAGCTCGTCCATGCC3'
NoLS GFP Human	5'CACCGGATCCGCCACCATGGTGCAGAGGAGGAAAAAGAGGCGGCTGAAGAAGCGCATCTTTAGCAAGGGCGAGGAGCTGTTC3'	5'CACCGAATTCTTACTTGTACAGCTCGTCCATGCC3'
TRPV3-hNoLS-mCherry	5'CACCGCTAGCATGGTGCAGAGGAGGAAAAAGAGGCGGCTGAAGAAGCGCATCTTTAGCAAGGGCGAGGAGGATAACATG3'	5'CCTTGGATCCTTACTTGTACAGCTCGTCCATGCC3'

TRPV3-Δ112-124 hNLS-GFP, TRPV3-Δ112-124 hNLOS-GFP	TRPV3 F1-5'CACCAGATCTATGAAAGCCCACCCCAAGGAG3', TRPV3 F2-5'CTGGCCAAGGAAGAGGCAGCCGTGTCTGAGGGCTG3'	TRPV3 R1-5'TCAGACACGGCTGCCTCTTCCTTGGCCAGCTGTGC3', TRPV3 R2-5'CACCGTCGACCTACACCGAGGTTTCCGGGAATTC3'

5.2 Methods

5.2.1 Methods related to molecular biology

5.2.1.1 Construct preparation

DNA fragments corresponding to the desired coding regions were obtained using two methods: cutting the available cDNA with restriction enzymes or amplifying the desired sequence by PCR with specific primers. Following this, both the PCR-amplified DNA fragments and the vectors were treated with restriction enzymes to create complementary overhanging ends. The resulting insert (fragment) and vector were then separated and purified from the agarose gel using DNA purification kits. After purification, the desired insert and vector fragments were joined together through ligation. The ligated product was then introduced into *Escherichia coli* cells through transformation. To ensure a successful transformation, the *Escherichia coli* cells were plated on a LB medium supplemented with a specific antibiotic (as selection marker present in the ligated vector). From the transformed colonies, plasmid DNA was isolated using plasmid DNA purification kits. The extracted plasmid DNA was further subjected to various analyses to confirm the presence of the desired insert. These analyses involved restriction digestion to check for the correct fragment size and PCR amplification to confirm its presence. To conclusively validate the insert's identity, the constructs were confirmed through sequencing.

5.2.1.2 Agarose gel electrophoresis

The process of separating double-stranded DNA (dsDNA) was carried out using horizontal agarose gel electrophoresis in the presence of 1X TAE buffer. To prepare the gel, agarose powder was mixed with electrophoresis buffer (1X TAE) at a concentration ranging from 0.8% to 1.2% (depending on the size of the DNA). The mixture was then heated in a microwave until the agarose completely melted. The exact percentage of agarose used in the gel was determined based on the length of the dsDNA fragments to be separated (Lower size DNA needs higher percentage of agarose gel and *vice versa*). To aid in DNA visualization, Ethidium Bromide (EtBr) was added to the liquefied gel at a final concentration of 0.1 to 0.5μg/ml. A casting tray was placed horizontally on the workbench. The hot and molten gel solution was poured into the casting tray containing a sample comb and allowed to solidify at room temperature (25°C). The comb was then carefully removed from the gel without damaging the bottom of the wells. The solidified gel was placed into an electrophoresis chamber and covered with electrophoretic buffer. DNA samples were mixed with loading buffer and loaded into the sample wells. A constant current source was connected to the apparatus for electrophoresis. The DNA loading buffer contained tracking dyes, such as a mixture of Bromophenol blue and Xylene Cyanol, which help to visualize the migration of DNA within the gel during electrophoresis. After sufficient migration, the DNA fragments were visualized using an ultraviolet transilluminator, as DNA emits fluorescence in response to UV excitation. This is due to the presence of Ethidium Bromide in the DNA which got incorporated during electrophoresis. Gel images were captured using a camera and documented using a gel documentation system.

Solutions and buffer required:

(1X) TAE buffer: 40mM Tris/Acetic acid, pH7.8; 1mM EDTA pH 8.0

(5X) DNA loading buffer: 40% (w/v) Sucrose, 240mM Tris/Acetic acid, pH7.8, 5mM EDTA, pH 0.8, 0.25% (w/v) Bromophenol blue, 0.25% (w/v) Xylene Cyanol FF.

5.2.1.3. Polymerase chain reaction (PCR)

In order to create various constructs within specific expression vectors, PCR reactions were employed to accurately amplify different coding regions while incorporating specific restriction sites at the ends. This was necessary for transferring a particular insert from one expression vector to another. The PCR master mix, used for these reactions, included Template DNA, specific forward and reverse primers, dNTPs, 1X Q5 buffer, Q5 DNA polymerase, and miliQ water. The PCR master mix was then subjected to PCR amplification. Throughout all PCR reactions, the following standardized conditions were applied. Q5 DNA-polymerase from NEB served as the enzyme for these procedures.

PCR reaction conditions:

Forward Primer (100nM) = 1µl Reverse Primer (100nM) =1µl Template = 0.5µl dNTPs (10mM) = 2µl 10x buffer = 2.5µl H_2O = 17µl Enzyme = 1µl
Total Volume = 25µl

The mixture was subjected to a temperature change in an Eppendorf thermocycler instrument, as described below.

Step	**Process**	**Temperature and duration**
1.	Denaturation	95°C for 5 minutes
2	Denaturation	94°C for 30 sec
3	Annealing	55°C for 30 sec
4	Extension	72°C for 1 minute/Kb

5	Repeat step 2 for 29 Cycles	
6	Extension	72°C for 10 minutes
7	End and store	4°C

All PCR-amplified DNAs were further confirmed by agarose gel electrophoresis.

5.2.1.4 Restriction digestion of dsDNA

About 1µg of double-stranded DNA (dsDNA) was utilized for restriction digestion in each 20µl reaction mixture. The restriction digestion mixture consisted of a specific restriction buffer at a concentration of 1x, along with double-distilled autoclaved water. The addition of restriction enzymes was based on a ratio of 1 unit per µg of DNA, depending on their activity. The reaction mixtures were then incubated at 37°C for either 3 hours or overnight, depending on the enzymes' activity. In the case of double restriction digestion, a compatible buffer was selected as per the instructions provided by the manufacturer (NEB).

5.2.1.5 Ligation of dsDNA:

Following the restriction digestion of both the insert and vector DNA, the resulting fragments were analyzed on a 0.8% agarose gel, and the bands of appropriate sizes were excised from the gel. The double-stranded DNA (dsDNA) was then purified from the gel using a DNA gel extraction kit from Qiagen, following the manufacturer's protocol. Subsequently, the concentration of both the insert and vector DNA was determined using Nanodrop from Thermo Scientific. For the ligation process, the insert DNA and vector DNA were mixed in a ratio of 3:1, based on their respective concentrations. Additionally, T4-DNA ligase compatible buffer (1X) was included in the ligation mix, and double-distilled autoclaved water was added to achieve the final desired reaction volume. T4-DNA ligase

was then introduced into the reaction mixture, which was incubated for 12 hours at 16°C to facilitate the ligation process.

5.2.2 Methods related to bacterial cell

5.2.2.1 Competent *Escherichia coli* cell preparation by $CaCl_2$ Method

To prepare competent *Escherichia coli* cells, both DE3 and DH5α strains, single colony of bacterial cells from respective LB plates with either strain was taken and incubated in 3ml of Luria-Bertani (LB) broth and cultured overnight at 37ºC and 220 RPM. From this starter culture, 1ml was transferred to 100ml of fresh LB liquid medium, and the broth culture was further incubated at 37°C and 220 RPM. The cells were allowed to grow until the OD (at 600 nm) of the culture reached 0.4-0.5. Once the desired OD was reached, the culture was placed on ice for 10 minutes and then subjected to centrifugation at 3000 RPM for 5 minutes at 4°C. The resulting pellet containing the bacterial cells was resuspended in 30ml of ice-cold $CaCl_2$ solution (100mM) and incubated for an additional 30 minutes on ice. Following this, the suspension was centrifuged again for 5 minutes at 4°C and 5000 RPM.

Finally, the pellet was resuspended in ice-cold $CaCl_2$ solution (100mM) supplemented with 10% glycerol. The competent *Escherichia coli* cells were then distributed into tubes and stored at -80°C for future use.

5.2.2.2 Competent *Escherichia coli* cell preparation by RbCl method

To prepare competent *Escherichia coli* cells (DH5α or DE3), a single colony was introduced into 3ml of Luria-Bertani (LB) broth and allowed to grow overnight at 37°C in a shaker at 220 RPM. From this initial culture, a 1ml inoculum was transferred to 100 ml of fresh LB liquid medium and incubated at 37°C and 220 RPM. The cells were cultivated until the broth's optical density (OD) reached the range of 0.4-0.5 at 600nm.

Next, the bacterial culture was subjected to incubation on ice for 10 minutes, followed by centrifugation at 4500 RPM for 10 minutes at 4°C. After centrifugation, the supernatant was discarded, and the entire 100ml culture was pelleted by centrifugation once more. The resulting pellet was then resuspended in 30ml of TfbI buffer and incubated on ice for 15 minutes. Subsequently, the cells were subjected to another round of centrifugation at 4000 RPM for 5 minutes at 4°C.

The obtained pellet was resuspended again, but this time in 6 ml of TfbII buffer. The bacterial cells suspended in TfbII buffer were divided into aliquots and placed into microcentrifuge tubes. These competent cell-containing tubes were rapidly chilled using liquid nitrogen and then stored at -80°C for future use.

Solutions and buffer required

LB media: 10g Bacto Tryptone, 5g Bacto Yeast extract, 10g NaCl dissolved in 1 litre of double distilled water and autoclave at 121°C at 15 lbs for 20 minutes.

TfbI buffer: Rubidium Chloride (RbCl, 100mM), Manganese Chloride ($MnCl_2$, 50mM), Potassium Acetate (CH_3CO_2K, 30mM), Calcium Chloride ($CaCl_2$, 10mM), Glycerol (15%). Adjusted the pH to 5.8 with diluted acetic acid (0.2%; 1.0M). Filter sterilized (not by autoclaving) and stored at 4°C.

TfbII buffer: MOPS (10mM), Rubidium Chloride (RbCl, 10mM), Calcium Chloride ($CaCl_2$, 75mM), Glycerol (15%). Adjusted the pH to 6.5 with KOH. Filter sterilize (not by autoclaving) and stored at 4°C.

5.2.2.3 Transformation of *Escherichia coli*

For the transformation of *Escherichia coli*, competent cells (DH5α or DE3 strain) containing aliquots were taken out from -80°C and thawed in ice for 10 minutes. Purified

plasmid DNA (~100ng/µl) or ligated DNA products were then added to 50µl of competent cell-containing vials. This mixture was incubated for 10 minutes in ice. After incubation, this mixture was given a heat shock at 42ºC for 45 seconds by dipping the tube in a water bath. Immediately after heat shock, the tube was kept in ice for 2 minutes. After subsequent cooling, 800µL of LB media was added to the mix. The cells were allowed to grow for 1 hour at 37°C and 220 RPM in an incubator shaker with constant shaking. After 1 hour, the bacterial suspension was centrifuged at 13,500 RPM for 30 seconds. The resulting pellet was resuspended in 100µL supernatant and plated on LB plates containing the desired antibiotic. Subsequently, the plates were kept at 37°C for 12 hours and single colonies were obtained after 12 hours of incubation.

5.2.2.4 Bacterial expression of pRsetB-pHRed

pRsetB-pHRed DNA construct from addgene transformed into competent cells (*Escherichia coli* BL21-DE3) and transformed bacteria plated in an Ampicillin plate. The colony obtained was picked and cultured with Ampicillin in a 4ml culture LB broth media. The culture was grown up to OD (optical density) around 0.4-0.8, and then IPTG was added for induction for at least 4 hours. Then the culture was pellet down at RPM 13000 for 2 minutes. The pellet was resuspended with PBS and spread in a glass slide to test the fluorescence of pH-Red. And for the bulk production of the protein, the colony picked from the plate was grown overnight in a 5ml LB culture medium with antibiotics. In the morning, the culture was grown in the 50ml 2xYT LB medium (Tryptone 5gm, Yeast extract 3gm, NaCl 1.25gm dissolved in 250ml 2xYT media). From 5ml culture, 100µl primary culture was taken and mixed with 50ml 2xYT medium till the OD reached 0.8. Then the culture was grown for at least 4 hours, pellet down, and proceeded for chemical fixation.

5.2.2.5 Live imaging of pH-sensor bacteria in Raw 264.7 cells

The especially fixed *Escherichia coli* cells with pH-Red were used for the imaging of pH changes in the phagocytosed compartments. The Raw 264.7 cell was used for the live cell imaging of phagocytosed bacteria. The cells were grown in the humified incubator chamber with 5% CO_2 at 37°C. Then the cells were seeded in the 25 mm coverslip and kept for 24 hours till the cells reached 70-80% confluency before the experiment. The especially fixed bacteria expressing pH-Red were incubated with the cells for 30 minutes before imaging. The bacteria expressing pH-Red was first allowed to phagocytosis by the macrophage cell line, i.e., Raw 264.7 cell. Subsequently, the engulfed bacteria eventually transferred to the lysosome. The engulfed bacteria emit fluorescence intensity as per the pH of the respective environment, i.e. the phagocytosed compartment. The more acidic organelle, like the functional lysosome, will have more fluorescence intensity of engulfing bacteria than compartments that have a neutral or basic pH. However, the endocytosed bacteria finally disintegrate in the lysosome due to the lytic activities there and thus lose their fluorescence intensity.

5.2.3 Methods related to protein chemistry

5.2.3.1 Separation of denatured proteins by SDS-PAGE

SDS-PAGE, a widely used technique for protein separation, involves electrophoretic separation of denatured proteins. The incorporation of Sodium Dodecyl Sulphate (SDS), a strong anionic detergent, aids in denaturing the proteins, leading to their separation based on molecular size, hence the term SDS-PAGE. U.K. Laemmli first introduced this valuable protein separation technique (Laemmli U.K. 1970; Kashino Y. 2003). SDS-PAGE was performed by using 10% acrylamide gels in a BioRad mini-apparatus, unless stated otherwise.

To prepare the protein samples for SDS-PAGE, they were fully denatured by adding Laemmli protein loading buffer in a 1:4 v/v ratio (from a 5x stock of Laemmli buffer) and then heating

the mixture at 95°C for 5 minutes. The SDS-PAGE cassettes were assembled using clean glass plates (10cm wide and 7cm high) separated by spacers (1mm thick). Resolving gel (about 5 ml) was poured into the cassettes and allowed to polymerize. A thin layer of water was gently added to the top of the resolving gel to create a smooth surface. After polymerization, the excess water was removed, and a stacking gel mixture (approximately 2ml) was poured on top of the resolving gel. To form wells for loading protein samples, a 10-well or 15-well comb was inserted into the stacking gel. After the stacking gel solidified, the combs were carefully removed without disturbing the wells.

The assembled cassette was placed vertically into an electrophoresis chamber, which was then filled with an electrophoresis running buffer. Denatured protein samples were loaded into the wells using a Hamilton syringe. The apparatus was connected to a constant current source (10mAmp) to facilitate electrophoresis. The tracking dye (bromophenol blue), present in the protein loading buffer aided in visualizing the migrated proteins within the gel. Once the dye-front neared the end, electrophoresis was stopped, and the separated proteins in the gel were visualized through Coomassie Brilliant Blue (CBB) staining.

For Western blot analysis, the unfixed gel was used to transfer the separated proteins onto a PVDF membrane.

Buffers required:

SDS-PAGE running buffer (1x): Glycine 196mM, SDS 0.1%, Tris-HCl (pH 8.3, 50mM)

Laemmli protein loading buffer (5x): Tris HCl (pH 6.8, 62.5mM), β-mercaptoethanol (5%, v/v), Glycerol (50%, v/v), SDS (2%, w/v), Bromo phenol Blue (0.1%, w/v). All the time, the final volume was adjusted by adding water.

Resolving gel mixture: Bis-Acrylamide (10%, v/v), Tris HCl (pH 8.8, 375mM), SDS (0.1%, w/v), Ammonium persulfate (0.1%, w/v), TEMED (0.005%, v/v) in water.

Stacking gel mixture: Bis-Acrylamide (4%, v/v), Tris HCl (pH 6.8, 125mM), SDS (0.1%, w/v), Ammonium persulfate (0.1%, w/v), TEMED (0.005% v/v) in water.

Bis-Acrylamide stock solution (30%), APS stock solution (10%), TEMED solution (100%), SDS solution (10%) and Tris-HCl (pH 8.8, 1.5M solution for separating gel)/or Tris-HCl (pH 6.8, 0.5M solution for stacking gel) were used to prepare separating and stacking gel solutions. APS and TEMED were added just prior to pouring the liquid.

5.2.3.2 Coomassie staining of the protein bands in gel

Coomassie staining is a commonly used method for visualizing proteins separated by SDS-PAGE. For that, a solution of 0.1% Coomassie Brilliant Blue dye in methanol (50%, v/v) and glacial acetic acid (10%, v/v) was employed. This staining solution helped to selectively stain proteins in the gel after the SDS-PAGE separation. The addition of acidified methanol in the staining process facilitated the precipitation of the proteins.

Staining typically took place overnight with gentle agitation of the gel in the staining solution. Agitation aided in the uniform circulation and penetration of the dye throughout the gel. Although the dye diffused through the entire gel, it binds specifically to the proteins, resulting in permanent staining of the protein bands. After staining, the gel was transferred to a de-staining solution composed of acetic acid/methanol to remove excess dye. Gentle agitation during de-staining effectively washed out the excess dye.

To achieve optimal results, a two-step de-staining process was employed. The gel was first de-stained in a solution containing 50% methanol and 10% acetic acid for 1-2 hours. This step caused the gel to shrink, expelling much of the liquid component. In the second de-staining step, a solution containing 7% methanol and 10% acetic acid was used. This step allowed the gel to swell and clear up, resulting in better visualization of the stained protein bands against a clear background.

During the staining process, the original dye front, represented by bromophenol blue dye, disappeared. Bromophenol blue, acting as a pH indicator, turned light yellow under acidic conditions before being washed out.

It's important to note that Coomassie blue staining has its limitations. It may not effectively stain proteins present in very low amounts or proteins with high carbohydrate content. Nevertheless, Coomassie staining remains a widely used and valuable technique for

protein visualization in SDS-PAGE gels. The stained gels were scanned using a scanner connected to a computer to document the stained protein bands.

5.2.3.3 Western blot analysis

Following the separation of proteins by SDS-PAGE, the electrotransfer to a PVDF membrane was performed using the semi-dry transfer method. Initially, unfixed gels were briefly incubated in a transfer buffer, while Whatman paper and PVDF membranes were soaked and equilibrated in the same transfer buffer. The PVDF membrane was then carefully placed on top of the gel, and two layers of Whatman papers were added on each side of the gel-membrane combination. To ensure the transfer set was free of air bubbles, the entire assembly was rolled over with a glass rod.

Next, the transfer set was placed on a transfer apparatus, with the gel connected to the cathode and the membrane connected to the anode. The apparatus was then connected to a power supply, and the electro-transfer was conducted at a constant current of 50 mA (for a single gel) for 1 hour. The efficiency of protein transfer from the gel to the membrane was verified by staining the membranes with Coomassie solution.

After the transfer, the PVDF membranes were subjected to blocking with 5% non-fat milk dissolved in 1xTBS-T buffer. Following the blocking step, the membrane was incubated with the primary antibody in TBS-T buffer for 1 hour at room temperature or overnight at 4°C. This was followed by three washes with TBS-T buffer to remove any unbound primary antibody. Subsequently, the membrane was incubated with a secondary antibody in TBST buffer for 1 hour, followed by another round of washing with TBST buffer three times.

To detect the protein bands, the membranes were developed using the chemiluminescence method (using Super Signal™ West Femto Maximum Sensitivity Substrate from Thermo Scientific) and detected using a chemidoc apparatus from Bio-Rad.

In some experiments, the membrane blots were "stripped-off" by incubating the blots in a stripping buffer at 50°C for 30 minutes. This stripping step allowed for the removal of previously bound antibodies, enabling the re-probing of the membranes with a different primary antibody if needed.

Buffers and solutions required:

Transfer buffer: SDS (0.1%, w/v), MeOH (20%, v/v), TRIS/HCl (48mM), Glycine (39 mM)
Ponceau Red solution: Ponceau S dye (5%, w/v), Acetic acid (5%, v/v)
TBS-T: Tris (20mM), NaCl (150Mm). Tween-20 (0.1%, w/v)
Stripping buffer: SDS (1%, w/v), TRIS/HCl (pH 6.8, 20mM), β-Mercaptoethanol (1%, v/v)

5.2.3.4 Protein estimation method

For the estimation of protein concentration, the Bradford reagent was used (Kruger N.J. 2009). Pure BSA protein standards (Sigma-Aldrich) were purified at concentrations of 20, 40, 60, 80, and 100µg in 100µL of PBS solution was used. Bradford reagent (Sigma-Aldrich) was added to the tubes containing different BSA concentrations and incubated for 5 minutes. The OD was measured at 595 nm, and Aa blank solution was made by adding 100µL of PBS and 900µL of Bradford reagent without any protein. All measurements were acquired using a Beckman Coulter spectrophotometer at 595 nm.

5.2.4 Cellular fractionation methods

5.2.4.1 Isolation of lysosome from Raw 264.7 cells

The Raw 264.7 cells were grown in 100mm cultured dishes in a humidified chamber maintained at 5% CO_2 and 37°C for 24 hours. Subsequently the cells were subjected to different modulators before harvesting in 1.5ml centrifuge tubes. Protease inhibitor 1x was used during the scrapping of cells. The cells were immediately resuspended with an ice-cold homogenisation buffer [HEPES (10mM, pH 7.4), EDTA (1mM), Sucrose (320mM)]). Briefly,

the cells present in the suspension were ruptured by passing the cells at least 20 times through 2.5ml syringe with a needle (23Gx25mm). The resuspended solution in a lysosome isolating buffer contains a complete protease inhibitor cocktail (Sigma-Aldrich). After complete rupture, the suspension was centrifuged for 20 minutes at 1200g (Benchtop centrifuge- MicroClick 24x2 rotor). Subsequently, the S1 fraction was collected, which contains cell organelle like ER, Mitochondria, lysosome etc. Subsequently, the S1 fraction was centrifuged at 12000g for 30 minutes, and the pellet contain mitochondria and loosely attached fraction contains lysosome. The pellet was resuspended with homogenisation buffer and centrifuged again at 20000g for 20 minutes. After 20 minutes, the loosely attached pellet was collected which contains predominantly lysosomes. Subsequently, the lysosomal pellet was resuspended in isolating buffer, aliquoted and kept at -80°C for long-term storage. All isolation procedures and centrifugation steps were carried out at 4°C.

5.2.4.2 Isolation of lysosomes from macrophage (KIT-based method)

Lysosome fractions were isolated from 90% confluent RAW 264.7 cells by density gradient-based separation. The lysosomes from cells were isolated through the lysosome-enrichment kit (ThermoFisher) for tissue and cultured cells. The kit contents include lysosome-enrichment reagent A, lysosome-enrichment reagent B, OptiPrep cell separation media and PBS. The gradient solution was made by gradient dilution buffer and OptiPrep gradients buffer. The final gradient per cent were 17, 20, 23, 27, and 30% respectively. After proper homogenized cell suspension is made (by sonication at 6-9W of power), the sample was processed for the gradient centrifugation and isolation of lysosome. The cell samples were ultracentrifuged at 145,000×g for 2 hours at 4°C using the lysosome enrichment kit for tissue and cultured cells according to the manufacturer's protocol (89839, Invitrogen). Fractions

isolated from lysosome enrichment were re-suspended in an HBSS buffer, loaded with different fluorescence probes followed by time-series imaging as and when required.

5.2.4.3 *In situ* subcellular fractionation (nuclear matrix fractionation)

In situ, sub-cellular fractionation of RAW 264.7 cells for immunofluorescence (IF) was done through cytoskeletal (CSK) buffer by using protocol from (Sawasdichai et al., 2010). First, the cells were grown on glass coverslips in 6 well plates for 24 hours with or without LPS stimulation. Subsequently, the cells were fractionated by CSK buffer. Before the fractionation through CSK buffer the cells were washed with ice-cold 1x PBS two times by tilting the plate. After the extraction with CSK buffer, the portion of the cells remain attached to the coverslips were fixed with 4% PFA and were further processed for antigen detection. Then the rest of the coverslip washed with PBS and then PBS was removed gently from the rest of the well plates, and gently placed 200µl CSK buffer with 0.1% Triton-X 100 was in the well for further fractionation. The CSK solution in the coverslip was incubated for 1 minute in ice and removed from the well subsequently. Then the coverslip containing well was washed with ice-cold PBS twice by tilting. Then the coverslip was removed, representing tightly held nuclear material and fixed for further processing. Then the remaining well went for further processing by placing CSK buffer with 0.5% triton x 100 and incubated for 20 minutes in ice. Then the coverslip was washed with PBS (ice-cold) after removing CSK buffer solutions, and chromatin fractions were collected and fixed in 4% PFA. In the end, the rest coverslip was incubated with CSK buffer with 100µg of DNAse I onto the remaining coverslip and incubated for 30 minutes at 37°C. Then the coverslip was washed, representing the nuclear matrix fraction. Then the nuclear matrix fraction went for fixation in 4% PFA and was processed for immunofluorescence assay.

After fractionation, cells present in the coverslips were fixed by adding 4% paraformaldehyde (PFA) in PBS and incubated for 30 minutes at 37°C in humidified CO_2 incubator chamber. Then coverslips were washed with PBS 3 times, and 0.1% Triton-X was added for 5 minutes. Subsequently, the coverslips were washed three times using PBS and blocked by incubating the cells with 5% BSA in PBS for 1 hour. Subsequently, TRPV3 primary antibody (1:200, Alomone Lab) in PBS was added and incubated overnight at 4°C. The coverslips were washed with PBST (With Tween 20 0.1%) 3 times and incubated with fluorophore-tagged rabbit secondary antibody (1:750 dilution) for 1 hour. Again, the coverslips were washed three times with PBST for 5 minutes each and incubated with DAPI in PBS (1:1000) solution and washed with PBST. Finally, the coverslips were mounted in a glass slide by using Fluromount-G.

Cytoskeletal (CSK) Buffer recipe (50ml volume):

Reagent	**Quantity (for 50 mL)**	**Final concentration**
PIPES/KOH (1M, pH 6.8)	0.5mL	10mM
NaCl (5M)	1mL	100mM
Sucrose	5.135gm	300mM
EGTA (250mM)	0.2mL	1mM
$MgCl_2$ (1M)	50µL	1mM
DTT (1M)	50µL	1mM
Protease Inhibitor	1 tablet	

5.2.5 Methods related to cell biology

5.2.5.1 Cell culture and transfection

Different cell lines, namely F11, Raw 264.7, Saos-2, MC3T3-E1 and HaCaT were cultured in Ham's F12 medium and RPMI medium, respectively and were supplemented with FBS (10%), L-glutamine (2mM), Streptomycin (100µg/ml), and Penicillin (100U/ml). The cells were grown in a humidity-controlled incubator maintained with 5% CO_2 set at 37°C. For transient transfection, lipofectamine (Invitrogen) was used according to the manufacturer's protocol. MC3T3-E1 cell was cultured in αMEM medium and was supplemented with FBS (10%), L-glutamine (2mM), Streptomycin (100µg/ml), and Penicillin (100U/ml).

5.2.5.2 Isolation of murine peritoneal macrophage

All animal experiments were performed as per the guideline and approval (Institutional Animal Ethics Committee no: 213/NISER/SBS/AH). Animals used in this work were in-house at the Animal facility (NCARE) at NISER. PM cells were obtained from the peritoneal cavity of Male BALB/c mice (4-6 weeks) by incubating RPMI-1640 (GIBCO) medium for 5 minutes. After straining the cells with a 70μm cell strainer, adherent PM, cells were cultured in a 60 mm plastic tissue culture dish overnight with RPMI-1640 medium containing 10% Fetal Bovine Serum (with added 1xPen-Strep-GIBCO and Amphotericin-B, 1μg/ml) in a humidity-controlled incubator maintained at 37°C and 5% CO_2.

5.2.5.3 Ca^{2+}-imaging of adherent cells

Adherent cells (HaCaT, F11, Raw 264.7, PM) were seeded on 25mm coverslip in 35mm dishes or 6 well plates and kept in a CO_2 (5%) incubator humidified chamber at 37°C. After 24 hours, Ca^{2+}-sensing dye Fluo-4 AM (5μM) which is a non-fluorescent form of acetoxymethyl ester, was added to culture dishes for 40 minutes. Through the addition, due to esterase activity inside the cell, this acetoxymethyl group gets cleaved off, and it binds to Ca^{2+} and emits fluorescence. Fluo-4 AM shows excitation maxima at 488nm and emission maxima at 520nm, for which an argon laser was used. Subsequently, cells were gently washed two times with PBS (1X), and then cells were used for live cell imaging. Live cell imaging was performed with a confocal microscope 488nm argon laser and fluorescence microscope. During the imaging, Specific drugs for TRPV3 and TRPV4 were added without disturbing the cells.

The Ca^{2+}-imaging is also done through the Ca^{2+}-sensor construct purchased through addgene. The construct has a calmodulin-binding motif, which subsequently binds to the Ca^{2+} in the intracellular compartment or cytosol. The expressed protein shows high sensitivity to the Ca^{2+} ion in the cells. The GCaMP6f has excitation maximum at 488nm, and emission maxima

at 520nm. For the Ca^{2+}-imaging, adherent's cells like HaCaT, Raw 264.7, and F11, the resuspended cells were seeded in the 25mm coverslips placed within 35mm dishes or in the 6 well plates. Cells were maintained within the CO_2 (5%) incubator at 37°C. Then around 70% confluency, the cells were transfected with GCaMP6f. After 24 hours, the cells were stimulated with cell/channel modulators and time series images were acquired. The live image was taken for at least 200 frames for a total duration of ~3 minutes 36 seconds.

5.2.5.4 MitoTracker Red and Mito CMX ROS staining in adherent cells

Adherent cells (HaCaT) were grown and/or transfected on 18mm, or 25mm glass coverslips. Approximately 24 hours after seeding or transfection, MitoTracker Red (1µM)/ MitoTracker Red CMXRos was added to cells for 30 minutes. Subsequently, the cells were either washed with 1xPBS and used for live cell imaging, or cells were fixed by 4% PFA at room temperature (RT, ~25°C). Both of the dyes (i.e. MitoTracker Red and MitoTracker Red CMXRos Red) are dyes that can penetrate through the cell membrane and accumulate within the mitochondria of living cells. This dye's accumulation level is linked to the membrane potential of the mitochondria (Pendergrass et al. 2004; Poot et al. 1996). Additionally, these dyes can be fixed with aldehyde and remains detectable even after fixation. These dyes have an excitation maximum of 580±10 nm and an emission maximum of 620±10 nm.

5.2.5.5 LysoTracker Red staining in adherent cells:

To visualize lysosomes of live cells, peritoneal macrophages, HaCaT, and Raw 264.7 cells were grown on 25 mm glass coverslips in a 35mm culture dish for 24 hours and LysoTracker Red (1µM) was added for 30 minutes. After washing with 1xPBS, the coverslips were imaged using a confocal microscope (FV3000 Olympus). LysoTracker Red is a fluorescent dye that can freely permeate cells due to its weak base partially protonated at pH

7. LysoTracker Red selectively accumulates within the acidic organelles, with an excitation maximum of 590nm and emission maxima at 620nm.

For fixed cell imaging, cells were grown on 12mm or 18mm glass coverslips and incubated with LysoTracker Red (1μM) for 30 minutes before being washed with 1xPBS and fixed with PFA (4%) at room temperature.

5.2.5.6 LysoSensor Green staining in adherent cells

To visualize lysosomes in live cells, peritoneal macrophages, HaCaT, and Raw 264.7 cells were grown on 25mm glass coverslips in 35mm culture dishes or in the 6-well plates for 24 hours before adding LysoSensor Green DND-189 (1μM) for 30 minutes. The LysoSensor Green DND-189 dye is capable of sensing the pH changes of acidic organelles like lysosomes because its fluorescence increases in acidic environments. This is due to the dye's weak base side chain being relieved of fluorescence quenching by protonation, causing an increase in fluorescence intensity (Lin et al. 2001). The LysoSensor dyes are “acidotropic” probes that accumulate in acidic organelles through protonation, resulting in a pH-dependent increase or decrease in fluorescence intensity. In contrast, the LysoTracker probes exhibit fluorescence that is weakly affected by pH. The pKa value of LysoSensor Green DND-189 is~5.2.

After washing with 1xPBS, the coverslips were imaged using a confocal microscope (FV3000 Olympus). It selectively binds to acidic organelles, with an excitation maximum of 443nm and emission maxima of 505nm.

5.2.5.7 Tetramethyl rhodamine (TMRM)-based imaging of mitochondrial membrane potential

For imaging of mitochondrial membrane potential or its changes in live cells, macrophage cells were seeded in 35mm culture dishes or in six-well plates in the 25mm

coverslip for 24 hours before the addition of Tetramethyl rhodamine, methyl ester (TMRM) reagent (100nM) for 30 minutes. TMRM is a dye that can penetrate cells and accumulate in active mitochondria with intact membrane potentials. If the cells are healthy and have functioning mitochondria, the signal will be strong. However, if the mitochondrial membrane potential is low or lost, TMRM accumulation will stop, and the signal will become weaker or disappear. It can be detected with RFP/TRITC filter set (absorbance maxima: 548nm, emission maxima: 574nm). After the cells reached to required confluency (~70-80%), the cells were loaded with TMRM dye (100nm) for 30 minutes. Then the cells were used for live cell imaging by using confocal microscopy (FV 3000 OLYMPUS).

5.2.5.8 Thermosensitive dyes (LTG, PTG, MTG, NTG) imaging

To visualise live cells, the peritoneal macrophages, HaCaT cells and Raw 264.7 cells were grown on 25mm glass coverslips in a 35mm culture dish or in the six-well plates for 24 hours before adding thermosensitive dyes for 30 minutes. All these probes were synthesized and kindly provided by Dr Y.T Chang Lab.

Fluorescence based thermosensors are highly effective molecular tools for detecting minor changes in temperature by measuring alterations in fluorescence signals, including fluorescence intensity, anisotropy, and/or lifetime. This allows for precise and accurate temperature readings. To create TGs, various organelle-targeting motifs were added to the unsymmetrical BODIPY (boron-dipyrromethene) structure which has a temperature sensitivity of 3.9%/°C (intensity) and 26 ps/°C (lifetime) in live cells. The TGs, which are added to the BODIPY derivatives are as follows Lipid Droplet Thermo Green (DTG) with an n-undecanoyl group, Mitochondria Thermo Green (MTG) with a triphenylphosphonium group, Lysosome Thermo Green (LTG) with a 4-(2-aminoethyl) morpholine group, Plasma Membrane Thermo Green (PTG) with a 3-(dodecyl(methyl)amino) propane-1-sulfonate group, Golgi Thermo

Green (GTG) with a d-sphingosine group, and Nucleus Thermo Green (NTG) with Hoechst 33,258. The absorption and emission wavelengths of all the TGs dyes are all around 496 nm and 512 nm, and for NTG, the excitation is around 353/395nm, and the emission is 511nm. The expected percentage of temperature sensitivity of the TGs dyes per degree temperature is as follows PTG 2.9%/°C, NTG 1.4%/°C, LTG 3.8%/°C, MTG 4.1%/°C respectively. Here LTG, NTG, PTG and MTG have been used for the detection of lysosomal, nuclear, plasma membrane and mitochondrial temperature upon TRPV3 modulations or LPS stimulations. These thermosensing dyes share an inverse relationship with the temperatures. Thus, higher the temperature, lower will be the fluorescence intensity and *vice versa*. The TGs dye, after being loaded in the cells, was imaged after 30 minutes of incubation in a live cell chamber in the confocal microscopy (FV 3000).

5.2.5.9 Cell viability assay (MTT assay)

For cell viability assay, $1x10^5$ cell/well suspensions were prepared at a volume of 100µL/well seeded in 48 well plates (Corning) and cultured along with drugs for 2 hours and exposed with HS in different temperature. This is followed by removing the medium, and 100µL MTT (tetrazolium salt 3-[4, 5-dimethylthiazol-2-yl]-2,5-diphenyltetrazolium bromide) solution was added in each well in 37°C incubator for 3 hours. Then, MTT was removed, and crystals dissolved in 100µL DMSO (Sigma). Then the absorbance has been checked at 570nm using a Varioskan multi-plate reader. All the experiments were performed in triplicates.

5.2.5.10 Multiplate reading assay

For the multiple reading of cellular parameters like cellular ROS and NOS measurements, or MTT-cell viability assay, the adherent cells were seeded in the 48 well plates 24 hours before the desired experiments. The cells were grown in a CO_2 (5%) humidified

chamber at 37°C before the assays. After the cells reached 70-80% confluency, the cells were subjected to different experimental treatments as per the plan. Subsequently, the cells were loaded with H_2DCFDA (ROS) or DAPFM (NOS) dye and incubated for 30 minutes. Then the plate was taken for multi-plate reading in the varioskan multi-plate reader. The excitation filter for the ROS and NOS dyes was set at ~492-495nm, and the emission range was set at ~517-527nm.

5.2.6 Methods related to immunocytochemistry and microscopy

5.2.6.1 Immunocytochemistry

For immunocytochemistry, cells were grown and/or transfected on glass coverslips. 24 to 48 hours after seeding or transfection, the cells were fixed with paraformaldehyde (4%) at room temperature (RT), followed by permeabilization with Triton X-100 (0.1%) in 1xPBS for 5 minutes. Subsequently, the cells were gently washed with PBS-T (0.1% Tween 20) for 5 minutes. The cells were blocked with bovine serum albumin (BSA, 5%). After blocking, the cells were incubated with primary antibody for 1 hour at RT. The primary antibody was added in a solution of BSA (5%) and PBS-T (1:1). The cells were then washed three times with PBS-T buffer. Cells were further incubated with a secondary antibody diluted in PBS-T buffer and BSA (1:1). After incubation with the secondary antibody, the cells were washed three times with PBS-T buffer. Subsequently, DAPI was added in PBS-T buffer at 1:1000 dilution for 10 minutes. Finally, the cells were washed with PBS-T for three times. Coverslips containing the stained cells were mounted onto glass slides with Fluoromount G (Southern Biotech). Alexa 594-labelled Phalloidin was used to label and visualize the actin cytoskeleton. Images were taken with a confocal laser-scanning microscope (Zeiss LSM780, FV 3000 OLYMPUS) with a 63x objective and analysed by the FIJI software.

5.2.6.2 Immunohistochemistry/Animal experiments

5.2.6.2.1 *In vivo* wound healing experiments

In this study, the healthy Balb/c mice (6-8 weeks old) were used for wound healing experiments. All animals were housed in standard polysulfone cages with floor area covered with autoclaved corncob bedding. The animals were kept in a controlled environment with a temperature range of 24 ± 3°C and humidity between 40-70%. Before the experiment, the mice were acclimatized for 7 days in separate cages and had access to food and water *ad-libitum*. Only mice without any skin injury or inflammation were selected for the study. All animal experiments were conducted following the guidelines of CPCSEA (Committee for the Purpose of Control and Supervision of Experiments on Animals, Govt. of India), and the protocols were approved by the Institute Animal Ethics Committee constituted by CPCSEA (Protocol no SBS/NISER/AH-195).

For the experiments, the mice were anesthetized using Isoflurane administered through a precision vaporizer with oxygen. The dorsal skin area of the animals was shaved and cleaned three times with a weak antiseptic solution (Savlon- Cetrimide 0.5% w/w, Chlorhexidine Digluconate 0.1%). Next, the shaved area was treated with a sterile gauge and a 5% povidone-iodine solution. Excision wounds of 5 mm diameter were created on the back skin of the mice using biopsy punches. These wounds were later infected with multidrug-resistant *S. aureus* (MRSA) strains (100µL; equivalent to $1x10^8$ CFU/mL in 24 hours) following the method described before (Kumar et al. 2019).

The treatment with TRPV3-specific drugs commenced 24 hours after the inoculation. The test substance was applied to the wound site every 24 hours. To protect the wounds, a silicone splint of 7mm inner diameter and 0.5mm thickness, with suture sites (Grace Biolabs, USA), was fixed around the outer diameter of the wound using commercially available topical skin adhesive (Dermabond). The splinted wound was further secured by an interrupted suture

pattern using 4-0 black braided silk sterile suture. Finally, the splinted wound was covered with a polyurethane film dressing (Tegaderm).

5.2.6.2.2 *In vitro* wound healing assay

In vitro wound healing assay was conducted in RAW 264.7 cell line. The cell was seeded 24 hours before the experiment in 12 well plates. Once the desired confluency in the well is achieved, a scratch in a "plus-shape" was made. Before the scratch cells were treated with TRPV3 modulators. Subsequent readouts were taken by taking images in different time intervals like 3, 6, 8,10 and 24 hours. Then the graph was plotted in the percentage of area covered from 0 to 24 hours. The data suggested that TRPV3 activation promotes better migration of macrophage cells.

5.2.6.2.3 Bacterial CFU count

***In vivo*:** The CFU of MRSA (*Staphylococcus aureus,* ATCC-33591) was determined by examining the bacterial load in the infected wound area on 4^{th} and 10^{th} day. Wounds were swabbed with a sterile cotton swab which was serially diluted in PBS and subsequently cultured on a Tryptic Soy agar plate overnight. Bacterial load was expressed as CFU by a standard plate count method.

***In vitro*:** The CFU of MRSA (*Staphylococcus aureus,* ATCC-33591) in the *in vitro* study was carried out for analyzing bacterial phagocytosis as well as intracellular bacterial clearance assay. To analyze the bacterial phagocytosis, cells were infected with MRSA (10 MOI) for 15 minutes as well as for 1 hour, respectively, along with the TRPV3 modulators, and subsequently, the colony numbers were determined.

For the bacterial clearance assay, cells were first infected with MRSA for 4 hours and then washed with cold PBS. Subsequently, the cells were incubated with gentamycin

(200μg/ml) solution for half an hour and washed with cold PBS again. Then cells were incubated with channel modulators for 4 hours and then processed for colony counting. In all these cases, cells were washed with cold PBS and permeabilized with Triton-X-100 (0.1%) for 10 minutes. Subsequently the cells were taken out through scrapping and serially diluted with the PBS and cultured on a Tryptic soy agar plate overnight. Then CFU was determined by the standard plate count method.

5.2.6.2.4 Immunohistochemistry (IHC)

For immunohistochemistry, the tissue was fixed with 10% formalin buffer for long term fixation (5 days). The tissue was subsequently kept in 4% PFA overnight before the paraffin embedding in the tissue is performed. The next day the tissue sample was washed and dehydrated repeatedly with different percentages of alcohol like 50%, 70%, 90% and finally 100% ethanol, respectively. Subsequently, the sample was transferred to acetone and eventually to xylene. The tissue sample after xylene wash went for paraffin wax embedding for 3 to 6 hours, according to the tissue sample (Skin tissue). Then the sample went for further processing like sectioning with a 5μm thickness sample. The paraffin-embedded tissue sample in a poly-lysine coated charged slide then went for Hematoxylin-Eosin (H&E) staining. The hematoxylin and eosin staining was used for the nucleic acid and protein in the extracellular matrix and cytoplasm, respectively. The H&E-staining shows deep blue-purple colour, whereas the eosin stain shows pink colour. The H&E staining protocol involves different steps like dewaxing the sections in xylene and then rehydrating in alcohol (100%, 95%, 70%). Subsequently, the tissue sections were dipped in distilled water and stained with hematoxylin (nucleic) for 4-10 minutes. Then the section was rinsed in tap water and stained with eosin for cytoplasm and extracellular matrix staining. These tissue sections were processed for

dehydration in alcohol (70%, 95%, 100%) and finally cleared in xylene and mounted with the mounting agent.

For immunohistochemistry, the paraffin-embedded skin section was first deparaffinized, dehydrated and then heated at 70°C (12 hours) for the antigen retrieval process. Then the tissue was washed with PBS and was permeabilized with Triton X-100 (0.5%) in PBS (15 minutes) and subsequently blocked with BSA (5%). For co-immunostaining with cellular markers, specific antibodies were used [TRPV3 extracellular loop-specific antibody (1:300, Alomone, conjugated with Atto dye); TRPV3 extracellular loop antibody (1:200, Alomone); Fibrillarin (1:300, Abcam); CD11b (1:500, DSHB); α Keratin k3/k76 (1:500, Merck)]. In most cases, Alexa-488 labelled anti-rabbit, was used as the secondary antibody. In some experiments, Atto-630-labeled TRPV3 extracellular anti-rabbit was used to detect TRPV3. TRPV3 extracellular antibody peptide as antigen is also used for blocking the antibody to check the specificity of the antibody. For comparative analysis, all imaging parameters were kept constant, and images were acquired by confocal microscope (FV3000, Olympus and LSM780, Zeiss). Fluorescence intensities of individual images were analyzed by Fiji software and represented in pseudo colour. Fluorescence intensity was quantified by Fiji software with manually marking the region-of-interest (ROI).

5.2.7 Live cell imaging

5.2.7.1 Live cell subcellular imaging

Live cell imaging was performed using an inverted confocal microscope. After seeding the cells on 25 mm cover glass, the coverslip was transferred to a metal chamber, and slowly media was added. Live cell imaging was performed using 63x Oil-immersion objective at 25ºC. Different genetically encoded proteins (GFP and RFP) and cell-permeant dyes, such as

LysoTracker Red, MitoTracker Red etc., were used to observe cellular dynamics and organelle movement.

5.2.7.2 Fluorescent Recovery After Photobleaching experiment (FRAP) Imaging

To visualise the localization and intracellular dynamics of hTRPV3-NoLS-GFP, live cell imaging and/or FRAP assay were performed. Cells were grown on 25mm glass coverslips overnight and transfected with hTRPV3-NLS-GFP construct. 24-48 hours after the transfection, the cells were used for live-cell and/or FRAP assay. For all FRAP analysis, a specific region of interest (ROI) with a circular shape and a fixed area (according to nucleolar size) was selected. In all cases, the ROI was selected at the appropriate position in the nucleolus, which was subject to photo bleach and subsequent recovery. For FRAP, time series images were acquired. A total of 30 frames (~34 sec) were taken for FRAP analysis and subjected to bleaching on the 3rd frame. The laser used here is a 488nm laser for 100% bleaching in point focus. In each case, at least 20 or more region-of-interest (ROI) were measured. During imaging, cells were maintained at a constant temperature (25°C) with the help of a controlled chamber. Images were acquired by a confocal microscope (FV 3000, Olympus) using a 63x objective. All these images were analyzed and quantified through Olympus CellSens imaging software.

5.2.8 Image processing, analysis, and quantification by different software

5.2.8.1 Microscopy image processing

All confocal images were processed using LSM image examiner software, while live cell time series images and movies were analyzed using Image J and Fiji software. Changes in lysosomal movement and numbers were calculated using TrackMate (Fiji software), while cell

size, morphology, cell shape, neurite number, etc. were calculated manually using LSM image examiner. Image resolution and labeling were done using Adobe Photoshop software.

5.2.8.2 Statistical analysis

Graph pad prism software was used for statistical analysis. An unpaired t-test (non-parametric) was performed to calculate the significance of the two data sets. The P-values are as follows: **** = P <0.0001, *** = P <0.001, ** P = <0.01, * P = <0.05, ns = non-significant. The correlation coefficient calculation was done with the help of GraphPad prism software. Correlation analysis between two parameters were analysed. For that Pearson correlation calculations were performed with the assumption that both X and Y values are sampled from populations that follow a Gaussian distribution. The non-linear curve fit was put in the correlation graph through the non-linear regression (curve fit) dialog.

5.2.8.3 Quantification

The colocalization study was done with the help of coloc-2 in the Fiji software. The "r"- value (colocalization coefficient) was taken into the consideration in the present study.

5.2.8.4 Bioinformatics analysis

All the sequences of TRPV3 from vertebrates were obtained from NCBI or UniProt database (**Supplementary Table 1**). All the sequences were stored in FASTA format and the MUSCLE alignment tool in MEGA 5.1 software suite was used for the alignment of the proteins as described before (Sardar et al. 2012). ENSEMBL database was used for Histone H4 sequence (as a reference of highly conserved protein) retrieval. Box-plot analysis (conservation pattern of TRPV3) was done by using R software. Multiple sequence alignment of NLS (Nuclear Localization Sequence) was performed by Jalview software. NLS scoring was

performed through SeqNLS prediction (http://mleg.cse.sc.edu/seqNLS/) software available online.

Chapter 6

References

References:

Abdullah H., Heaney L.G., Cosby S.L. and McGarvey L.P.A. (2014) Rhinovirus upregulates transient receptor potential channels in a human neuronal cell line: implications for respiratory virus-induced cough reflex sensitivity. *Thorax*, **69**, pp.46-54.

Abe K. and Puertollano R. (2011) Role of TRP channels in the regulation of the endosomal pathway. *Physiology*, **26**, pp.14-22.

Acharya T.K., Kumar A., Kumar S. and Goswami C. (2022) TRPV4 interacts with MFN2 and facilitates endoplasmic reticulum-mitochondrial contact points for Ca^{2+}-buffering. *Life Sciences*, **310**, p.121112.

Acharya T.K., Kumar A., Majhi R.K., Kumar S., Chakraborty R., Tiwari A., Smalla K.H., Liu X., Chang Y.T., Gundelfinger E.D. and Goswami C. (2022) TRPV4 acts as a mitochondrial Ca^{2+}-importer and regulates mitochondrial temperature and metabolism. *Mitochondrion*, **67**, pp.38-58.

Acharya T.K., Pal S., Ghosh A., Kumar S., Kumar S., Chattopadhyay N. and Goswami C. (2023) TRPV4 regulates osteoblast differentiation and mitochondrial function that are relevant for channelopathy. *Frontiers in Cell and Developmental Biology*, **11**, p.1066788.

Ahn S., Park J., An I., Jung S.J. and Hwang J., (2014) Transient receptor potential cation channel V1 (TRPV1) is degraded by starvation-and glucocorticoid-mediated autophagy. *Molecules and cells*, **37**, p.257.

Alberts B., Johnson A., Lewis J., Raff M., Roberts K. and Walter P. (2002) Carrier proteins and active membrane transport. In *Molecular Biology of the Cell. 4th edition*. Garland Science.

Alessandri-Haber N., Dina O.A., Joseph E.K., Reichling D.B. and Levine J.D. (2008) Interaction of transient receptor potential vanilloid 4, integrin, and SRC tyrosine kinase in mechanical hyperalgesia. *Journal of Neuroscience*, **28**, pp.1046-1057.

Alharbi M.O., Dutta B., Goswami R., Sharma S., Lei K.Y. and Rahaman S.O. (2021) Identification and functional analysis of a biflavone as a novel inhibitor of transient receptor potential vanilloid 4-dependent atherogenic processes. *Scientific Reports*, **11**, p.8173.

Ambudkar I.S. (2007) TRPC1: a core component of store-operated calcium channels. *Biochem Soc Trans*. **35**, pp.96-100.

Andersson K.E. (2019) TRP Channels as Lower Urinary Tract Sensory Targets. *Medical sciences* (Basel, Switzerland), **7**, p.67.

Andrei C., Zanfirescu A., Nițulescu G.M., Olaru O.T. and Negreș S. (2023) Natural Active Ingredients and TRPV1 Modulation: Focus on Key Chemical Moieties Involved in Ligand–Target Interaction. *Plants*, **12**, p.339.

Andreucci E., Aftimos S., Alcausin M., Haan E., Hunter W., Kannu P., Kerr B., McGillivray, G., Gardner R.J., Patricelli M.G. and Sillence D. (2011) TRPV4 related skeletal dysplasias: a phenotypic spectrum highlighted byclinical, radiographic, and molecular studies in 21 new families. *Orphanet journal of rare diseases*, **6**, pp.1-8.

Aneiros E., Cao L., Papakosta M., Stevens E.B., Phillips S. and Grimm, C. (2011) The biophysical and molecular basis of TRPV1 proton gating. *The EMBO journal*, **30**, pp.994-1002.

Aouizerat B., Dunn L., Cooper B., Paul S., West C. and Miaskowski C. (2011) Association between of temperature-sensitive transient receptor potential cation channel, subfamily V, member 3 (TRPV3) with preoperative pain in women with breast cancer. *The Journal of Pain*, **12**, p.P25.

Arniges M., Fernández-Fernández J.M., Albrecht N., Schaefer M. and Valverde M.A. (2006) Human TRPV4 channel splice variants revealed a key role of ankyrin domains in multimerization and trafficking. *Journal of Biological Chemistry*, **281**, pp.1580-1586.

Asghar M.Y. and Törnquist K. (2020) Transient Receptor Potential Canonical (TRPC) Channels as Modulators of Migration and Invasion. *International Journal of Molecular Sciences*, **21**, p.1739.

Asuthkar S., Elustondo P.A., Demirkhanyan L., Sun X., Baskaran P., Velpula K.K., Thyagarajan B., Pavlov E.V. and Zakharian E. (2015) The TRPM8 protein is a testosterone receptor: I. Biochemical evidence for direct TRPM8-testosterone interactions. *Journal of Biological Chemistry*, ***290***, pp.2659-2669.

Backaert W., Steelant B., Hellings P.W., Talavera K. and Van Gerven L. (2021) A TRiP through the roles of transient receptor potential cation channels in type 2 upper airway inflammation. *Current Allergy and Asthma Reports*, **21**, pp.1-13.

Bagnell A.M., Sumner C.J. and McCray B.A. (2022) "TRPV4: A trigger of pathological RhoA activation in neurological disease," *BioEssays: news and reviews in molecular, cellular and developmental biology*, **44**, p. e2100288.

Bai X.C., Fernandez I.S., McMullan G. and Scheres S.H. (2013) Ribosome structures to near-atomic resolution from thirty thousand cryo-EM particles. *elife*, ***2***, p. e00461.

Bakthavatchalam R. and Kimball S.D. (2010) "Modulators of transient receptor potential ion channels," in *Annual Reports in Medicinal Chemistry*. *Elsevier*, **45**, pp. 37–53.

Bandell M., Story G.M., Hwang S.W., Viswanath V., Eid S.R., Petrus M.J., Earley T.J. and Patapoutian A. (2004) Noxious cold ion channel TRPA1 is activated by pungent compounds and bradykinin. *Neuron*, **41**, pp.849-857.

Bang S., Yoo S., Yang T.J., Cho H. and Hwang S.W., (2010) Farnesyl pyrophosphate is a novel pain-producing molecule via specific activation of TRPV3. *Journal of Biological Chemistry*, **285**, pp.19362-19371.

Barker B.S., Young G.T., Soubrane C.H., Stephens G.J., Stevens E.B. and Patel M.K. (2017) Ion channels. In *Conn's translational neuroscience*. pp. 11-43. Academic Press.

Barrick S.R., Lee H., Meyers S., Caterina M.J., Kanai A.J., Zeidel M.L., Chopra B., De Groat W.C. and Birder L. (2003) Expression and function of TRPV4 in urinary bladder urothelium. *In Society for Neuroscience Abstracts*, **608**, pp. 608–614.

Basbaum A.I., Bautista D.M., Scherrer G. and Julius D. (2009) Cellular and molecular mechanisms of pain. Cell, **139**, pp.267-284.

Bassi M.T., Manzoni M., Monti E., Pizzo M.T., Ballabio A. and Borsani G. (2000) Cloning of the gene encoding a novel integral membrane protein, mucolipidin—and identification of the two major founder mutations causing mucolipidosis type IV. *The American Journal of Human Genetics*, **67**, pp.1110-1120.

Bautista D.M., Pellegrino M. and Tsunozaki M. (2013) "TRPA1: A gatekeeper for inflammation," *Annual review of physiology*, **75**, pp. 181–200.

Bautista D.M., Jordt S.E., Nikai T., Tsuruda P.R., Read A.J., Poblete J., Yamoah E.N., Basbaum A.I. and Julius D. (2006) TRPA1 mediates the inflammatory actions of environmental irritants and proalgesic agents. *Cell*, **124**, pp.1269-1282.

Baylie R.L. and Brayden J.E. (2011) "TRPV channels and vascular function: Vascular TRPV channels," *Acta physiologica* (*Oxford, England*), **203**, pp. 99–116.

Becker D., Bereiter-Hahn J. and Jendrach M. (2009) "Functional interaction of the cation channel transient receptor potential vanilloid 4 (TRPV4) and actin in volume regulation," *European journal of cell biology*, **88**, pp. 141–152.

Benemei S. and Dussor G. (2019) TRP channels and migraine: recent developments and new therapeutic opportunities. *Pharmaceuticals*, **12**, p.54.

Bernal J. D. (1951). *The Physical Basis of Life*. London: Routledge and Paul.

Bernal J.D. (1949) The physical basis of life. *Proceedings of the Physical Society*. *Section B*, **62**, p.597.

Berridge M.J., Bootman M.D. and Roderick H.L. (2003) Calcium signalling: dynamics, homeostasis and remodelling. *Nature reviews Molecular cell biology*, **4**, pp.517-529.

Bezanilla F. (2008) How membrane proteins sense voltage. *Nature reviews Molecular cell biology*, **9**, pp.323-332.

Birder L.A. (2007) "TRPs in bladder diseases," *Biochimica et biophysica acta. Molecular basis of disease*, **1772**, pp.879–884.

Bischof M., Olthoff S., Glas C., Thorn-Seshold O., Schaefer M. and Hill K. (2020). TRPV3 endogenously expressed in murine colonic epithelial cells is inhibited by the novel TRPV3 blocker 26E01. *Cell Calcium*, **92**, p.102310.

Blair N.T., Caceres A.I., Carvacho I., Chaudhuri D., Clapham D.E., De Clerq K., Delling M., Doerner J.F., Fan L., Grimm C.M., Ha K., Hu M., Jabba S.V., Jordt S.E., Julius D., Kahle K.T., Liu Q., Liu B., McKemy D., Nilius B., Oancea E., Owsianik G., Riccio A., Sah R., Stotz SC., Tian J., Tong D., Vriens J., Wu L.J., Xu H., Yang F., Yang W., Yue L. and Zhu M.X (2023) Transient Receptor Potential channels (TRP) in GtoPdb v.2023.2. *IUPHAR/BPS guide to pharmacology CITE*, **2**, p.2023.

Blair N.T., Carvacho I., Chaudhuri D., Clapham D.E., De Clerq K., Delling M., Doerner J.F., Fan L., Grimm C.M., Ha K. and Hu M. (2023) Transient Receptor Potential channels (TRP) in GtoPdb v. 2023.1. *IUPHAR/BPS Guide to Pharmacology CITE*, **1**, p.2023.

Blott E.J. and Griffiths G.M. (2002) Secretory lysosomes. *Nature reviews Molecular cell biology*, **3**, pp.122-131.

Blum C.A., Caldwell T., Zheng X., Bakthavatchalam R., Capitosti S., Brielmann H., De Lombaert S., Kershaw M.T., Matson D., Krause J.E. and Cortright D. (2010) Discovery of novel 6, 6-heterocycles as transient receptor potential vanilloid (TRPV1) antagonists. *Journal of medicinal chemistry*, **53**, pp.3330-3348.

Bohnsack J.F. and Brown E.J. (1986) The role of the spleen in resistance to infection. *Annual review of medicine*, **37**, pp.49-59.

Bonam S.R., Wang F. and Muller S. (2019) Lysosomes as a therapeutic target. *Nature Reviews Drug Discovery*, **18**, pp.923-948.

Borges da Silva H., Fonseca R., Pereira R.M., Cassado A.D.A., Álvarez J.M. and D'Império Lima M.R. (2015) Splenic macrophage subsets and their function during blood-borne infections. *Frontiers in immunology*, **6**, p.480.

Boudaka A., Saito C.T. and Tominaga M. (2020) Deletion of TRPV4 enhances in vitro wound healing of murine esophageal keratinocytes. *Scientific Reports*, **10**, p.11349.

Bouhamdani N., Comeau D. and Turcotte S. (2021) A Compendium of Information on the Lysosome. *Frontiers in Cell and Developmental Biology*, **9**, p.798262.

Bousquet J., Czarlewski W., Zuberbier T., Mullol J., Blain H., Cristol J.P., De La Torre R., Pizarro Lozano N., Le Moing V., Bedbrook A. and Agache I. (2021) Potential interplay between Nrf2, TRPA1, and TRPV1 in nutrients for the control of COVID-19. *International archives of allergy and immunology*, **182**, pp.324-338.

Bowman B.J. and Bowman E.J. (1986) H^+-ATPases from mitochondria, plasma membranes, and vacuoles of fungal cells. *The Journal of membrane biology*, **94**, pp.83-97.

Brauchi S., Orio P. and Latorre R. (2004). Clues to understanding cold sensation: thermodynamics and electrophysiological analysis of the cold receptor TRPM8. *Proceedings of the National Academy of Sciences*, **101**, pp.15494-15499.

Brauchi S., Orta G., Salazar M., Rosenmann E. and Latorre R. (2006) A hot-sensing cold receptor: C-terminal domain determines thermosensation in transient receptor potential channels. *Journal of Neuroscience*, **26**, pp.4835-4840.

Brederson J.D., Kym P.R. and Szallasi A. (2013) "Targeting TRP channels for pain relief," European journal of pharmacology, **716**, pp. 61–76.

Brendolan A., Rosado M.M., Carsetti R., Selleri L. and Dear T.N. (2007) Development and function of the mammalian spleen. *Bioessays*, **29**, pp.166-177.

Brożyna A.A., Guo H., Yang S.E., Cornelius L., Linette G., Murphy M., Sheehan C., Ross J., Slominski A. and Carlson J.A. (2017) TRPM1 (melastatin) expression is an independent predictor of overall survival in clinical AJCC stage I and II melanoma patients. *Journal of cutaneous pathology*, **44**, pp.328-337.

Cai X. (2006) Unicellular Ca^{2+} Signaling 'Toolkit' at the Origin of metazoa. *Mol. Biol. Evol*. **25**, 1357–1361.

Cao B., Dai X. and Wang W. (2019) "Knockdown of TRPV4 suppresses osteoclast differentiation and osteoporosis by inhibiting autophagy through Ca^{2+} -calcineurin-NFATc1 pathway. *Journal of cellular physiology*, **234**, pp. 6831–6841.

Cao E., Cordero-Morales J.F., Liu B., Qin F. and Julius D., (2013) TRPV1 channels are intrinsically heat sensitive and negatively regulated by phosphoinositide lipids. *Neuron*, **77**, pp.667-679.

Cao E., Liao M., Cheng Y. and Julius D., (2013) TRPV1 structures in distinct conformations reveal activation mechanisms. *Nature*, **504**, pp.113-118.

Cao S., Anishkin A., Zinkevich N.S., Nishijima Y., Korishettar A., Wang Z., Fang J., Wilcox D.A. and Zhang D.X. (2018) Transient receptor potential vanilloid 4 (TRPV4) activation by arachidonic acid requires protein kinase A–mediated phosphorylation. *Journal of Biological Chemistry*, **293**, pp.5307-5322.

Casey J.R., Grinstein S. and Orlowski J. (2010) Sensors and regulators of intracellular pH. *Nature reviews Molecular cell biology*, **11**, pp.50-61.

Caterina M.J., Rosen T.A., Tominaga M., Brake A.J. and Julius D., (1999) A capsaicin-receptor homologue with a high threshold for noxious heat. *Nature*, **398**, pp.436-441.

Caterina M.J., Schumacher M.A., Tominaga M., Rosen T.A., Levine J.D. and Julius D. (1997) The capsaicin receptor: a heat-activated ion channel in the pain pathway. *Nature*, **389**, pp.816-824.

Catterall W.A. (2010) Ion channel voltage sensors: structure, function, and pathophysiology. *Neuron*, **67**, pp.915-928.

Cenac N., Altier C., Motta J.P., d'Aldebert E., Galeano S., Zamponi G.W. and Vergnolle N. (2010) Potentiation of TRPV4 signalling by histamine and serotonin: an important mechanism for visceral hypersensitivity. *Gut*, **59**, pp.481-488.

Chaigne S., Barbeau S., Ducret T., Guinamard R. and Benoist D. (2023) Pathophysiological Roles of the TRPV4 Channel in the Heart. *Cells*, **12**, p.1654.

Chauvet V., Tian X., Husson H., Grimm D.H., Wang T., Hieseberger T., Igarashi P., Bennett A.M., Ibraghimov-Beskrovnaya O., Somlo S. and Caplan M.J. (2004) Mechanical stimuli induce cleavage and nuclear translocation of the polycystin-1 C terminus. *The Journal of clinical investigation*, **114**, pp.1433-1443.

Chen C.S., Bach G. and Pagano R.E. (1998) Abnormal transport along the lysosomal pathway in mucolipidosis, type IV disease. *Proceedings of the National Academy of Sciences*, **95**, pp.6373-6378.

Chen F., OuYang Y., Ye T., Ni B. and Chen A. (2014) Estrogen inhibits RANKL-induced osteoclastic differentiation by increasing the expression of TRPV5 channel. *Journal of cellular biochemistry*, **115**, pp.651-658.

Chen H., Sun C., Zheng Y., Yin J., Gao M., Zhao C. and Lin J. (2023). A TRPV4 mutation caused Charcot-Marie-Tooth disease type 2C with scapuloperoneal muscular atrophy overlap syndrome and scapuloperoneal spinal muscular atrophy in one family: *a case report and literature review*.

Chen J., Kang D., Xu, J., Lake M., Hogan J.O., Sun C., Walter K., Yao B. and Kim D. (2013) Species differences and molecular determinant of TRPA1 cold sensitivity. *Nature communications*, **4**, p.2501.

Chen M. and Li X. (2021) "Role of TRPV4 channel in vasodilation and neovascularization," *Microcirculation* (New York, N.Y.: 1994), **28**, p. e12703.

Chen Y., Mu J., Zhu M., Mukherjee A. and Zhang H. (2020) Transient receptor potential channels and inflammatory bowel disease. *Frontiers in immunology*, **11**, p.180.

Cheng X., Jin J., Hu L., Shen D., Dong X.P., Samie M.A., Knoff J., Eisinger B., Liu M.L., Huang S.M. and Caterina M.J. (2010) TRP channel regulates EGFR signaling in hair morphogenesis and skin barrier formation. *Cell*, **141**, pp.331-343.

Cheng K.T., Liu X., Ong H.L., Swaim W. and Ambudkar I.S. (2011) Local Ca^{2+} entry via Orai1 regulates plasma membrane recruitment of TRPC1 and controls cytosolic Ca^{2+} signals required for specific cell functions. *PLoS biology*, **9**, p.e1001025.

Cheng W., Yang F., Liu S., Colton C.K., Wang C., Cui Y., Cao X., Zhu M.X., Sun C., Wang K. and Zheng J. (2012) Heteromeric heat-sensitive transient receptor potential channels exhibit distinct temperature and chemical response. *Journal of Biological Chemistry*, **287**, pp.7279-7288.

Cheng X., Jin J., Hu L., Shen D., Dong X.P., Samie M.A., Knoff J., Eisinger B., Liu M.L., Huang S.M. and Caterina M.J. (2010) TRP channel regulates EGFR signaling in hair morphogenesis and skin barrier formation. Cell, **141**, pp.331-343.

Cheng X., Shen D., Samie M. and Xu H. (2010) Mucolipins: intracellular TRPML1-3 channels. *FEBS letters*, **584**, pp.2013-2021.

Choi J.E. and Di Nardo A. (2018) "Skin neurogenic inflammation," *Seminars in immunopathology*, **40**, pp. 249–259.

Choi J.Y., Kim S.E., Lee S.E. and Kim S.C. (2018) Olmsted syndrome caused by a heterozygous p. Gly568Val missense mutation in TRPV3 gene. *Yonsei medical journal*, **59**, pp.341-344.

Chung M.K., Güler A.D. and Caterina M.J. (2005) "Biphasic currents evoked by chemical or thermal activation of the heat-gated ion channel, TRPV3," *The journal of biological chemistry*, **280**, pp.15928–15941.

Chung M.K., Güler A.D. and Caterina M.J. (2008) TRPV1 shows dynamic ionic selectivity during agonist stimulation. *Nature neuroscience*, **11**, pp.555-564.

Ciura S. and Bourque C.W. (2006) Transient receptor potential vanilloid 1 is required for intrinsic osmoreception in organum vasculosum lamina terminalis neurons and for normal thirst responses to systemic hyperosmolality. *Journal of Neuroscience*, **26**, pp.9069-9075.

Clapham D.E. (2003) "TRP channels as cellular sensors," *Nature*, **426**, pp. 517–524.

Clapham D.E. and Miller C. (2011) A thermodynamic framework for understanding temperature sensing by transient receptor potential (TRP) channels. *Proceedings of the National Academy of Sciences*, **108**, pp.19492-19497.

Clapham D.E. (2003) TRP channels as cellular sensors. *Nature*, **426**, pp.517-524.

Clapham D.E., Julius D., Montell C. and Schultz G. (2005) International Union of Pharmacology. XLIX. Nomenclature and structure-function relationships of transient receptor potential channels. *Pharmacological reviews*, **57**, pp.427-450.

Cohen M.R., Johnson W.M., Pilat J.M., Kiselar J., DeFrancesco-Lisowitz A., Zigmond R.E. and Moiseenkova-Bell V.Y. (2015) Nerve growth factor regulates transient receptor potential vanilloid 2 via

extracellular signal-regulated kinase signaling to enhance neurite outgrowth in developing neurons. *Molecular and Cellular Biology*, **35**, pp.4238-4252.

Colbert H.A., Smith T.L. and Bargmann C.I. (1997) "OSM-9, A novel protein with structural similarity to channels, is required for olfaction, mechanosensation, and olfactory adaptation in *Caenorhabditis elegans*," *The Journal of neuroscience: the official journal of the Society for Neuroscience*, **17**, pp. 8259–8269.

Correll C.C., Phelps P.T., Anthes J.C., Umland S. and Greenfeder S. (2004) Cloning and pharmacological characterization of mouse TRPV1. *Neuroscience letters*, **370**, pp.55-60.

Cosens D.J. and Manning A. (1969) Abnormal electroretinogram from a Drosophila mutant. *Nature*, **224**, pp.285-287.

Csekő K., Beckers B., Keszthelyi D. and Helyes Z. (2019). Role of TRPV1 and TRPA1 ion channels in inflammatory bowel diseases: potential therapeutic targets? *Pharmaceuticals*, **12**, p.48.

Cuajungco M.P., Silva J., Habibi A. and Valadez J.A. (2016) The mucolipin-2 (TRPML2) ion channel: a tissue-specific protein crucial to normal cell function. *Pflügers Archiv-European Journal of Physiology*, **468**, pp.177-192.

Cui Y., Yang F., Cao X., Yarov-Yarovoy V., Wang K. and Zheng J. (2012) Selective disruption of high sensitivity heat activation but not capsaicin activation of TRPV1 channels by pore turret mutations. *Journal of general physiology*, **139**, pp.273-283.

Cvetkov T.L., Huynh K.W., Cohen M.R. and Moiseenkova-Bell V.Y. (2011) Molecular architecture and subunit organization of TRPA1 ion channel revealed by electron microscopy. *Journal of Biological Chemistry*, **286**, pp.38168-38176.

Dannheisig D.P., Schimansky A., Donow C. and Pfister A.S. (2021) Nucleolar stress functions upstream to stimulate expression of autophagy regulators. *Cancers*, **13**, p.6220.

Danso-Abeam D., Zhang J., Dooley J., Staats K.A., Van Eyck L., Van Brussel T., Zaman S., Hauben E., Van de Velde M., Morren M.A. and Renard M. (2013) Olmsted syndrome: exploration of the immunological phenotype. *Orphanet journal of rare diseases*, **8**, pp.1-8.

Das R. and Goswami C. (2019) "TRPV4 expresses in bone cell lineages and TRPV4-R616Q mutant causing Brachyolmia in human reveals 'loss-of-interaction' with cholesterol," *Biochemical and biophysical research communications*, **517**, pp. 566–574.

Das R. and Goswami C. (2022) Role of TRPV4 in skeletal function and its mutant-mediated skeletal disorders. *In Current Topics in Membranes*, **89**, pp. 221-246. Academic Press.

Das R., Kumar A., Dalai R. and Goswami C. (2022) Cytochrome C interacts with the pathogenic mutational hotspot region of TRPV4 and forms complexes that differ in mutation and metal ion-sensitive manner. *Biochemical and Biophysical Research Communications*, **611**, pp.172-178.

De Blas G.A., Darszon A., Ocampo A.Y., Serrano C.J., Castellano L.E., Hernández-González E.O., Chirinos M., Larrea F., Beltrán C. and Treviño C.L. (2009) TRPM8, a versatile channel in human sperm. *PLoS One*, **4**, p.e6095.

De Duve C., Pressman B.C., Gianetto R., Wattiaux R. and Appelmans F. (1955) Tissue fractionation studies. 6. Intracellular distribution patterns of enzymes in rat-liver tissue. *Biochemical Journal*, **60**, pp.604-617.

De Duve C. and Wattiaux R. (1966) Functions of lysosomes. *Annual review of physiology*, **28**, pp.435-492.

De Logu F., Tonello R., Materazzi S., Nassini R., Fusi C., Coppi E., Li Puma S., Marone I.M., Sadofsky L.R., Morice A.H. and Susini T. (2016) TRPA1 mediates aromatase inhibitor–evoked pain by the aromatase substrate Androstenedione. *Cancer research*, **76**, pp.7024-7035.

Deng S., Zhang Y., Liao Z., Huang J., Huang R. and Li Z. (2021) S100A4 plays a key role in TRPV3 ion channel expression and its electrophysiological function. *Neuroscience Letters*, **759**, p.135999.

Deng Z., Maksaev G., Rau M., Xie Z., Hu H., Fitzpatrick J.A. and Yuan P. (2020) Gating of human TRPV3 in a lipid bilayer. *Nature structural & molecular biology*, **27**, pp.635-644.

Deng Z., Maksaev G., Rau M., Xie Z., Hu H., Fitzpatrick J.A. and Yuan P. (2020) Gating of human TRPV3 in a lipid bilayer. *Nature structural & molecular biology*, **27**, pp.635-644.

Deng Z., Paknejad N., Maksaev G., Sala-Rabanal M., Nichols C.G., Hite R.K. and Yuan P. (2018) Cryo-EM and X-ray structures of TRPV4 reveal insight into ion permeation and gating mechanisms. *Nature structural & molecular biology*, **25**, pp.252-260.

Dhaka A., Uzzell V., Dubin A.E., Mathur J., Petrus M., Bandell M. and Patapoutian A. (2009) TRPV1 is activated by both acidic and basic pH. *Journal of Neuroscience*, **29**, pp.153-158.

Dietrich A., Fahlbusch M. and Gudermann T. (2014) Classical transient receptor potential 1 (TRPC1): channel or channel regulator? *Cells*, **3**, pp.939-962.

Donaldson L.F. and Beazley-Long N. (2016) "Alternative RNA splicing: contribution to pain and potential therapeutic strategy," *Drug discovery today*, **21**, pp. 1787–1798.

Doñate-Macián P., Jungfleisch J., Pérez-Vilaró G., Rubio-Moscardo F., Peralvarez-Marin A., Diez J. and Valverde M.A. (2018) The TRPV4 channel links calcium influx to DDX3X activity and viral infectivity. *Nature communications*, **9**, p.2307.

Dong X.P., Cheng X., Mills E., Delling M., Wang F., Kurz T. and Xu H. (2008) The type IV mucolipidosis-associated protein TRPML1 is an endolysosomal iron release channel. *Nature*, **455**, pp.992-996.

Dong X.P., Wang X. and Xu H. (2010) "TRP channels of intracellular membranes," Journal of neurochemistry, **113**, pp. 313–328.

Dörr J. and Fecher-Trost C. (2011). TRP channels in female reproductive organs and placenta. *Transient Receptor Potential Channels*, **704**, pp.909-928.

Drews A., Mohr F., Rizun O., Wagner T.F.J., Dembla S., Rudolph S., Lambert S., Konrad M., Philipp S.E., Behrendt M. and Marchais-Oberwinkler S. (2014) Structural requirements of steroidal agonists of transient receptor potential melastatin 3 (TRPM 3) cation channels. *British journal of pharmacology*, **171**, pp.1019-1032.

Du G., Tian Y., Yao Z., Vu S., Zheng J., Chai L., Wang K. and Yang S. (2020) A specialized pore turret in the mammalian cation channel TRPV1 is responsible for distinct and species-specific heat activation thresholds. Journal of Biological Chemistry, **295**, pp.9641-9649.

Du Q., Liao Q., Chen C., Yang X., Xie R. and Xu J. (2019) The role of transient receptor potential vanilloid 1 in common diseases of the digestive tract and the cardiovascular and respiratory system. *Frontiers in Physiology*, **10**, p.1064.

Dubey N.K., Mishra S. and Goswami C. (2023) Progesterone interacts with the mutational hot-spot of TRPV4 and acts as a ligand relevant for fast Ca^{2+}-signalling. *Biochimica et Biophysica Acta (BBA)-Biomembranes*, **1865**, p.184178.

Duchatelet S. and Hovnanian A. (2015) Olmsted syndrome: clinical, molecular and therapeutic aspects. *Orphanet journal of rare diseases*, **10**, pp.1-10.

Duchatelet S., Guibbal L., De Veer S., Fraitag S., Nitschké P., Zarhrate M., Bodemer C. and Hovnanian A. (2014) Olmsted syndrome with erythromelalgia caused by recessive transient receptor potential vanilloid 3 mutations. *British Journal of Dermatology*, **171**, pp.675-678.

Duchatelet S., Pruvost, S., de Veer S., Fraitag S., Nitschké P., Bole-Feysot C., Bodemer C. and Hovnanian A. (2014) A new TRPV3 missense mutation in a patient with Olmsted syndrome and erythromelalgia. *JAMA dermatology*, **150**, pp.303-306.

Duitama M., Vargas-López V., Casas Z., Albarracin S.L., Sutachan J.J. and Torres Y.P. (2020). TRP channels role in pain associated with neurodegenerative diseases. *Frontiers in Neuroscience*, **14**, p.782.

Duncan L.M., Deeds J., Hunter J., Shao J., Holmgren L.M., Woolf E.A., Tepper R.I. and Shyjan A.W. (1998) Down-regulation of the novel gene melastatin correlates with potential for melanoma metastasis. *Cancer research*, **58**, pp.1515-1520.

Dutta B., Arya R.K., Goswami R., Alharbi M.O., Sharma S. and Rahaman S.O. (2020) Role of macrophage TRPV4 in inflammation. *Laboratory investigation*, **100**, pp.178-185.

Dutta B., Goswami R. and Rahaman S.O. (2020) TRPV4 plays a role in matrix stiffness-induced macrophage polarization. *Frontiers in immunology*, **11**, p.570195.

Espadas-Álvarez H., Martínez-Rendón J., Larre, I., Matamoros-Volante A., Romero-García T., Rosenbaum T., Rueda A. and García-Villegas R. (2021) TRPV4 activity regulates nuclear Ca2+ and transcriptional functions of β-catenin in a renal epithelial cell model. *Journal of Cellular Physiology*, **236**, pp.3599-3614.

European Polycystic Kidney Disease Consortium, (1994). The polycystic kidney disease 1 gene encodes a 14 kb transcript and lies within a duplicated region on chromosome 16. *Cell*, **77**, pp.881-894.

Evangelista T., Bansagi B., Pyle A., Griffin H., Douroudis K., Polvikoski T., Antoniadi T., Bushby K., Straub V., Chinnery P.F. and Lochmüller H. (2015) Phenotypic variability of TRPV4 related neuropathies. *Neuromuscular Disorders*, **25**, pp.516-521.

Everaerts W., Nilius B. and Owsianik G. (2010) The vanilloid transient receptor potential channel TRPV4: from structure to disease. *Progress in biophysics and molecular biology*, **103**, pp.2-17.

Fakhar M., Zahid S. and Rashid S. (2022) Structural basis of Klotho binding to VEGFR2 and TRPC1 and repurposing calcium channel blockers as TRPC1 antagonists for the treatment of age-related cardiac hypertrophy. *Archives of Biochemistry and Biophysics*, **719**, p.109171.

Farfariello V., Gordienko D.V., Mesilmany L., Touil Y., Germain E., Fliniaux I., Desruelles E., Gkika D., Roudbaraki M., Shapovalov G. and Noyer L. (2022) TRPC3 shapes the ER-mitochondria Ca^{2+} transfer characterizing tumour-promoting senescence. *Nature Communications*, **13**, p.956.

Feigin V.L., Vos T., Nichols E., Owolabi M.O., Carroll W.M., Dichgans M., Deuschl G., Parmar P., Brainin M. and Murray C. (2020) The global burden of neurological disorders: translating evidence into policy. *The Lancet Neurology*, **19**, pp.255-265.

Fernandes E.S., Fernandes M.A. and Keeble J.E. (2012) The functions of TRPA1 and TRPV1: moving away from sensory nerves. *British journal of pharmacology*, **166**, pp.510-521.

Festa M., Minicozzi V., Boccaccio A., Lagostena L., Gradogna A., Qi T., Costa A., Larisch N., Hamamoto S., Pedrazzini E. and Milenkovic S. (2022) Current methods to unravel the functional properties of lysosomal ion channels and transporters. *Cells*, **11**, p.921.

Filosa J.A., Yao X. and Rath G. (2013) "TRPV4 and the regulation of vascular tone," Journal of cardiovascular pharmacology, **61**, pp. 113–119.

Flores E.N. and García-Añoveros J. (2011) TRPML2 and the evolution of mucolipins. *Transient Receptor Potential Channels*, pp.221-228.

Fonfria E., Murdock P.R., Cusdin F.S., Benham C.D., Kelsell R.E. and McNulty S. (2006) Tissue distribution profiles of the human TRPM cation channel family. *Journal of Receptors and Signal Transduction*, **26**, pp.159-178.

Forgac M. (2007) Vacuolar ATPases: rotary proton pumps in physiology and pathophysiology. *Nature reviews Molecular cell biology*, **8**, pp.917-929.

Froghi S., Grant C.R., Tandon R., Quaglia A., Davidson B. and Fuller B. (2021) New insights on the role of TRP channels in calcium signalling and immunomodulation: review of pathways and implications for clinical practice. *Clinical reviews in allergy & immunology*, **60**, pp.271-292.

Fromy B., Josset-Lamaugarny A., Aimond G., Pagnon-Minot A., Marics I., Tattersall G.J., Moqrich A. and Sigaudo-Roussel D. (2018) Disruption of TRPV3 impairs heat-evoked vasodilation and thermoregulation: a critical role of CGRP. *Journal of Investigative Dermatology*, **138**, pp.688-696.

Fujita F., Uchida K., Moriyama T., Shima A., Shibasaki K., Inada H., Sokabe T. and Tominaga M. (2008) Intracellular alkalization causes pain sensation through activation of TRPA1 in mice. *The Journal of clinical investigation*, **118**, pp.4049-4057.

Fujiu K., Nakayama Y., Iida H., Sokabe M. and Yoshimura K. (2011) Mechanoreception in motile flagella of Chlamydomonas. *Nat. Cell Biol*. **13**, pp.630–632.

Fujiwara Y. and Minor Jr D.L. (2008). X-ray crystal structure of a TRPM assembly domain reveals an antiparallel four-stranded coiled-coil. *Journal of molecular biology*, **383**, pp.854-870.

Gao W., Hasan H., Anderson D.E. and Lee W. (2022) The role of mechanically-activated ion channels Piezo1, Piezo2, and TRPV4 in chondrocyte mechanotransduction and mechano-therapeutics for osteoarthritis. *Frontiers in Cell and Developmental Biology*, **10**, p.885224.

Gao X., Wu L. and O'Neil R.G. (2003) "Temperature-modulated diversity of TRPV4 channel gating: activation by physical stresses and phorbol ester derivatives through protein kinase C-dependent and -independent pathways," *The journal of biological chemistry*, **278**, pp. 27129–27137.

Gao Y., Cao E., Julius D. and Cheng Y. (2016) TRPV1 structures in nanodiscs reveal mechanisms of ligand and lipid action. *Nature*, **534**, pp.347-351.

Garami A., Pakai E., McDonald H.A., Reilly R.M., Gomtsyan A., Corrigan J.J., Pinter E., Zhu D.X., Lehto S.G., Gavva N.R. and Kym P.R. (2018) TRPV 1 antagonists that cause hypothermia, instead of hyperthermia, in rodents: compounds' pharmacological profiles, in vivo targets, thermoeffectors recruited and implications for drug development. *Acta physiologica*, **223**, p.e13038.

Garcia-Elias A., Lorenzo I.M., Vicente R. and Valverde M.A. (2008) IP3 receptor binds to and sensitizes TRPV4 channel to osmotic stimuli via a calmodulin-binding site. *Journal of Biological Chemistry*, **283**, pp.31284-31288.

Garcia-Elias A., Lorenzo I.M., Vicente R. and Valverde M.A. (2008) IP3 receptor binds to and sensitizes TRPV4 channel to osmotic stimuli via a calmodulin-binding site. *Journal of Biological Chemistry*, **283**, pp.31284-31288.

Garcia-Elias A., Mrkonjić S., Jung C., Pardo-Pastor C., Vicente R. and Valverde M.A. (2014). The TRPV4 channel. *Mammalian Transient Receptor Potential (TRP) Cation Channels:* **I**, pp.293-319.

Garcia-Elias A., Mrkonjić, S., Pardo-Pastor C., Inada H., Hellmich U.A., Rubio-Moscardó F., Plata C., Gaudet R., Vicente R. and Valverde M.A. (2013) Phosphatidylinositol-4, 5-biphosphate-dependent rearrangement of TRPV4 cytosolic tails enables channel activation by physiological stimuli. *Proceedings of the National Academy of Sciences*, **110**, pp.9553-9558.

Garreis F., Schröder A., Reinach P.S., Zoll S., Khajavi N., Dhandapani P., Lucius A., Pleyer U., Paulsen F. and Mergler S. (2016) Upregulation of transient receptor potential vanilloid type-1 channel activity and Ca^{2+} influx dysfunction in human pterygial cells. *Investigative Ophthalmology & Visual Science*, **57**, pp.2564-2577.

Garrity A.G., Wang W., Collier C.M., Levey S.A., Gao Q. and Xu H. (2016) The endoplasmic reticulum, not the pH gradient, drives calcium refilling of lysosomes. *Elife*, **5**, p. e15887.

Gaucher P. (1882) De l'epithelioma primitive de la rate, hypertrophic idiopathique de la rate sans leucemie (doctoral thesis).

Geng L., Boehmerle W., Maeda Y., Okuhara D.Y., Tian X., Yu Z., Choe C.U., Anyatonwu G.I., Ehrlich B.E. and Somlo S. (2008) Syntaxin 5 regulates the endoplasmic reticulum channel-release properties of polycystin-2. *Proceedings of the National Academy of Sciences*, **105**, pp.15920-15925.

Ghavideldarestani M., Atkin S.L., Leese H.J. and Sturmey R.G. (2016) Expression and function of transient receptor potential channels in the female bovine reproductive tract. *Theriogenology*, **86**, pp.551-561.

Giamarchi A., Padilla F., Coste B., Raoux M., Crest M., Honoré E. and Delmas P. (2006). The versatile nature of the calcium-permeable cation channel TRPP2. *EMBO reports*, **7**, pp.787-793.

Gombedza F., Kondeti V., Al-Azzam N., Koppes S., Duah E., Patil P., Hexter M., Phillips D., Thodeti C.K. and Paruchuri S. (2017) Mechanosensitive transient receptor potential vanilloid 4 regulates Dermatophagoides farinae–induced airway remodeling via 2 distinct pathways modulating matrix synthesis and degradation. *The FASEB Journal*, **31**, p.1556.

González-Ramírez R., Chen Y., Liedtke W.B. and Morales-Lázaro S.L. (2017) TRP channels and pain. *Neurobiology of TRP channels*, **1**, pp.125-147.

Gopinath P., Wan E., Holdcroft A., Facer P., Davis J.B., Smith G.D., Bountra C. and Anand P. (2005) Increased capsaicin receptor TRPV1 in skin nerve fibres and related vanilloid receptors TRPV3 and TRPV4 in keratinocytes in human breast pain. *BMC women's health*, **5**, pp.1-9.

Gorbunov A.S., Maslov L.N., Jaggi A.S., Singh N., De Petrocellis L., Boshchenko A.A., Roohbakhsh A., Bezuglov V.V. and Oeltgen, P.R. (2019) Physiological and pathological role of TRPV1, TRPV2 and TRPV4 channels in heart. *Current Cardiology Reviews*, **15**, pp.244-251.

Goswami C., Kuhn J., Heppenstall P.A. and Hucho T. (2010) Importance of Non-Selective Cation Channel TRPV4 Interaction with Cytoskeleton and Their Reciprocal Regulations in Cultured Cells. *PLoS ONE* **5**, e11654.

Goswami C. and Hucho T. (2007) TRPV1 expression-dependent initiation and regulation of filopodia. *Journal of neurochemistry*, **103**, pp.1319-1333.

Goswami C., Kuhn J., Heppenstall P.A. and Hucho T. (2010) Importance of non-selective cation channel TRPV4 interaction with cytoskeleton and their reciprocal regulations in cultured cells. *PloS ONE*, **5**, p.e11654.

Goswami R., Merth M., Sharma S., Alharbi M.O., Aranda-Espinoza H., Zhu X. and Rahaman S.O. (2017) TRPV4 calcium-permeable channel is a novel regulator of oxidized LDL-induced macrophage foam cell formation. *Free Radical Biology and Medicine*, **110**, pp.142-150.

Gouin O., L'herondelle K., Lebonvallet N., Le Gall-Ianotto C., Sakka, M., Buhé V., Plée-Gautier E., Carré J.L., Lefeuvre L., Misery L. and Le Garrec R. (2017) TRPV1 and TRPA1 in cutaneous neurogenic and chronic inflammation: pro-inflammatory response induced by their activation and their sensitization. *Protein & cell*, **8**, pp.644-661.

Goyal N., Skrdla P., Schroyer R., Kumar S., Fernando D., Oughton A., Norton N., Sprecher D.L. and Cheriyan J. (2019) Clinical pharmacokinetics, safety, and tolerability of a novel, first-in-class TRPV4 ion channel inhibitor, GSK2798745, in healthy and heart failure subjects. *American Journal of Cardiovascular Drugs*, **19**, pp.335-342.

Grace M.S., Baxter M., Dubuis E., Birrell M.A. and Belvisi M.G. (2014) Transient receptor potential (TRP) channels in the airway: role in airway disease. *British journal of pharmacology*, **171**, pp.2593-2607.

Gracheva E.O., Cordero-Morales J.F., González-Carcacía J.A., Ingolia N.T., Manno C., Aranguren C.I., Weissman J.S. and Julius D. (2011) Ganglion-specific splicing of TRPV1 underlies infrared sensation in vampire bats. *Nature*, **476**, pp.88-91.

Gracheva E.O., Ingolia N.T., Kelly Y.M., Cordero-Morales J.F., Hollopeter G., Chesler A.T., Sánchez E.E., Perez J.C., Weissman J.S. and Julius D. (2010) Molecular basis of infrared detection by snakes. *Nature*, **464**, pp.1006-1011.

Grandl J., Hu H., Bandell M., Bursulaya B., Schmidt M., Petrus M. and Patapoutian A. (2008) Pore region of TRPV3 ion channel is specifically required for heat activation. *Nature neuroscience*, **11**, pp.1007-1013.

Grant A.D., Cottrell G.S., Amadesi S., Trevisani M., Nicoletti P., Materazzi S., Altier C., Cenac N., Zamponi G.W., Bautista-Cruz F. and Lopez C.B. (2007) Protease-activated receptor 2 sensitizes the transient receptor potential vanilloid 4 ion channel to cause mechanical hyperalgesia in mice. *The Journal of physiology*, **578**, pp.715-733.

Gregorio-Teruel L., Valente P., Liu B., Fernández-Ballester G., Qin F. and Ferrer-Montiel A. (2015) The integrity of the TRP domain is pivotal for correct TRPV1 channel gating. *Biophysical journal*, **109**, pp.529-541.

Grieben M., Pike A.C., Shintre C.A., Venturi E., El-Ajouz S., Tessitore A., Shrestha L., Mukhopadhyay S., Mahajan P., Chalk R. and Burgess-Brown N.A. (2017) Structure of the polycystic kidney disease TRP channel Polycystin-2 (PC2). *Nature structural & molecular biology*, **24**, pp.114-122.

Grimm C., Barthmes M. and Wahl-Schott C. (2014) Trpml3. *Mammalian Transient Receptor Potential (TRP) Cation Channels:* **I**, pp.659-674.

Grimm C., Hassan S., Wahl-Schott C. and Biel, M. (2012) Role of TRPML and two-pore channels in endolysosomal cation homeostasis. *Journal of Pharmacology and Experimental Therapeutics*, **342**, pp.236-244.

Grycova L., Lansky Z., Friedlova E., Obsilova V., Janouskova H., Obsil T. and Teisinger J. (2008) Ionic interactions are essential for TRPV1 C-terminus binding to calmodulin. *Biochemical and biophysical research communications*, **375**, pp.680-683.

Gupta N., Goswami R., Alharbi M.O., Biswas D. and Rahaman S.O. (2019) TRPV4 is a regulator in P. gingivalis lipopolysaccharide-induced exacerbation of macrophage foam cell formation. *Physiological Reports*, **7**, p.e14069.

Güler A.D., Lee H., Iida, T., Shimizu I., Tominaga M. and Caterina M. (2002) Heat-evoked activation of the ion channel, TRPV4. *Journal of Neuroscience*, **22**, pp.6408-6414.

Hamacher J., Hadizamani Y., Huwer H., Moehrlen U., Bally L., Stammberger U., Wendel A. and Lucas R. (2023) Characteristics of inflammatory response and repair after experimental blast lung injury in rats. *Plos one*, **18**, p.e0281446.

Han Y., Luo A., Kamau P.M., Takomthong P., Hu J., Boonyarat C., Luo L. and Lai R. (2021) A plant-derived TRPV3 inhibitor suppresses pain and itch. *British Journal of Pharmacology*, **178**, pp.1669-1683.

Hao Q. and Prasanth K.V. (2022) Regulatory roles of nucleolus organizer region-derived long non-coding RNAs. Mammalian Genome, **33**, pp.402-411.

Hashimoto A. and Kambe, T. (2015) Mg, Zn and Cu transport proteins: a brief overview from physiological and molecular perspectives. *Journal of nutritional science and vitaminology*, **61**, pp.S116-S118.

Haywood N., Ta H.Q., Zhang A., Charles E.J., Rotar E., Noona IV S., Salmon M., Daneva Z., Sonkusare S.K. and Laubach V.E. (2022) Endothelial transient receptor potential vanilloid 4 channels mediate lung ischemia-reperfusion injury. *The Annals of Thoracic Surgery*, **113**, pp.1256-1264.

He Y., Zeng K., Zhang X., Chen Q., Wu J., Li H., Zhou Y., Glusman G., Roach J., Etheridge A. and Qing S., (2015) A gain-of-function mutation in TRPV3 causes focal palmoplantar keratoderma in a Chinese family. *The Journal of investigative dermatology*, **135**, p.907.

Held K., Voets T. and Vriens J. (2015) TRPM3 in temperature sensing and beyond. *Temperature*, **2**, pp.201-213.

Heller S. and O'Neil R. (2006) "Molecular mechanisms of TRPV4 gating," in *TRP Ion Channel Function in Sensory Transduction and Cellular Signaling Cascades*. *CRC Press*, pp. 113–124.

Heller S. and O'Neil R.G. (2007) Molecular mechanisms of TRPV4 gating. TRP Ion Channel Function in Sensory Transduction and Cellular Signaling Cascades, pp.113-125.

Hellwig N., Albrecht N., Harteneck C., Schultz G. and Schaefer M. (2005) Homo-and heteromeric assembly of TRPV channel subunits. *Journal of cell science*, **118**, pp.917-928.

Hille B. (2001) Ion Channels of Excitable Membranes. **Third edition**. Sinauer Press, Sunderland, MA. p.814.

Hille B. (1992) Potassium channels and chloride channels. *In Ionic Channels of Excitable Membrane*, pp.130-133.

Himmel N.J., Gray T.R. and Cox D.N. (2020) Phylogenetics identifies two eumetazoan TRPM clades and an eighth TRP family, TRP Soromelastatin (TRPS). *Mol. Biol. Evol*. **37**, pp.2034–2044.

Himmel N.J. and Cox D.N. (2020) Transient receptor potential channels: current perspectives on evolution, structure, function and nomenclature. *Proceedings of the Royal Society B*, **287**, p.20201309.

Himmel N.J., Gray T.R. and Cox D.N. (2020) Phylogenetics identifies two eumetazoan TRPM clades and an eighth TRP family, TRP soromelastatin (TRPS). *Molecular biology and evolution*, **37**, pp.2034-2044.

Himmel N.J., Letcher J.M., Sakurai A., Gray T.R., Benson M.N., Donaldson K.J. and Cox D.N. (2021) Identification of a neural basis for cold acclimation in Drosophila larvae. *IScience*, **24**.

Hinman A., Chuang H.H., Bautista D.M. and Julius D. (2006) TRP channel activation by reversible covalent modification. *Proceedings of the National Academy of Sciences*, **103**, pp.19564-19568.

Hoenderop J.G.J., Voets T., Hoefs S., Weidema F., Prenen J., Nilius B. and Bindels R.J.M. (2003) Homo- and heterotetrameric architecture of the epithelial Ca^{2+} channels TRPV5 and TRPV6. *The EMBO journal*, **22**, pp.776-785.

Hofmann T., Chubanov V., Gudermann T. and Montell C. (2003) TRPM5 is a voltage-modulated and Ca^{2+}-activated monovalent selective cation channel. *Current biology*, **13**, pp.1153-1158.

Holzer P. (2011) TRP channels in the digestive system. *Current pharmaceutical biotechnology*, ***12***, pp.24-34.

Horishita R., Ogata Y., Fukui R., Yamazaki R., Moriwaki K., Ueno S., Yanagihara N., Uezono Y., Yokoyama Y., Minami K. and Horishita T. (2021) Local Anesthetics Inhibit Transient Receptor Potential Vanilloid Subtype 3 Channel Function in Xenopus Oocytes. *Anesthesia & Analgesia*, ***132***, pp.1756-1767.

http://(https://www.proteinatlas.org/ENSG00000167723-TRPV3/tissue/vagina (Accessed: October 6, 2023).“Beyond hot and spicy: TRPV channels and their pharmacological modulation” (2021) *Cellular physiology and biochemistry: international journal of experimental cellular physiology, biochemistry, and pharmacology*, **55**, pp. 108–130.

https://www.guidetopharmacology.org/GRAC/ObjectDisplayForward?objectId=510

https://www.proteinatlas.org/ENSG00000111199-TRPV4/tissue

Hu H.Z., Gu Q., Wang C., Colton C.K., Tang J., Kinoshita-Kawada M., Lee L.Y., Wood J.D. and Zhu M.X. (2004) 2-aminoethoxydiphenyl borate is a common activator of TRPV1, TRPV2, and TRPV3. *Journal of Biological Chemistry*, **279**, pp.35741-35748.

Hu H.Z., Xiao R., Wang C., Gao N., Colton C.K., Wood J.D. and Zhu M.X. (2006) Potentiation of TRPV3 channel function by unsaturated fatty acids. *Journal of cellular physiology*, **208**, pp.201-212.

Hu F., Cao X., Niu C. and Wang K., (2022) Coassembly of Warm Temperature–Sensitive Transient Receptor Potential Vanilloid (TRPV)3 and TRPV4 Channel Complexes with Distinct Functional Properties. *Molecular Pharmacology*, **101**, pp.390-399.

Hu W., Huang J., Luo L., Chen R., Liu H., Xu J., Chen W., Ding Y. and Yu H. (2023) Study on the role of calcium channel protein TRPV4 in the inflammatory pathway of type 2 diabetic adipose tissue based on gene databases. *Biochemical and Biophysical Research Communications*, **639**, pp.161-168.

Huai J., Zhang Y., Liu Q.M., Ge H.Y., Arendt-Nielsen L., Jiang H. and Yue S.W. (2012) Interaction of transient receptor potential vanilloid 4 with annexin A2 and tubulin beta 5. *Neuroscience Letters*, **512**, pp.22-27.

Huang A.L., Chen X., Hoon M.A., Chandrashekar J., Guo W., Tränkner D., Ryba N.J. and Zuker C.S. (2006) The cells and logic for mammalian sour taste detection. *Nature*, **442**, pp.934-938.

Huang J., Du W., Yao H. and Wang Y. (2011) 10 TRPC Channels in Neuronal Survival. *TRP channels*, p.219.

Huang S.M. and Chung M.K. (2013) Targeting TRPV3 for the development of novel analgesics. *The open pain journal*, **6**, p.119.

Huang S.M., Lee H., Chung M.K., Park U., Yu Y.Y., Bradshaw H.B., Coulombe P.A., Walker J.M. and Caterina M.J. (2008) Overexpressed transient receptor potential vanilloid 3 ion channels in skin keratinocytes modulate pain sensitivity via prostaglandin E2. *Journal of Neuroscience*, **28**, pp.13727-13737.

Huang, S.M., Lee, H., Chung, M.K., Park, U., Yu, Y.Y., Bradshaw, H.B., Coulombe, P.A., Walker, J.M. and Caterina, M.J., 2008. Overexpressed transient receptor potential vanilloid 3 ion channels in skin keratinocytes modulate pain sensitivity via prostaglandin E2. *Journal of Neuroscience*, *28*(51), pp.13727-13737.

Huang S.M., Li X., Yu Y., Wang J. and Caterina M.J. (2011) TRPV3 and TRPV4 ion channels are not major contributors to mouse heat sensation. *Molecular pain*, **7**, pp.1744-8069.

Hughes J., Ward C.J., Peral B., Aspinwall R., Clark K., San Millán J.L., Gamble V. and Harris P.C. (1995) The polycystic kidney disease 1 (PKD1) gene encodes a novel protein with multiple cell recognition domains. *Nature genetics*, **10**, pp.151-160.

Hughes T.E., Pumroy R.A., Yazici A.T., Kasimova M.A., Fluck E.C., Huynh K.W., Samanta A., Molugu S.K., Zhou Z.H., Carnevale V. and Rohacs T. (2018) Structural insights on TRPV5 gating by endogenous modulators. *Nature Communications*, **9**, p.4198.

Huynh K.W., Cohen M.R., Chakrapani S., Holdaway H.A., Stewart P.L. and Moiseenkova-Bell V.Y. (2014) Structural insight into the assembly of TRPV channels. *Structure*, **22**, pp.260-268.

Huynh K.W., Cohen M.R., Jiang J., Samanta A., Lodowski D.T., Zhou Z.H. and Moiseenkova-Bell V.Y. (2016) Structure of the full-length TRPV2 channel by cryo-EM. *Nature communications*, **7**, p.11130.

Inada H., Procko, E., Sotomayor M. and Gaudet R. (2012) Structural and biochemical consequences of disease-causing mutations in the ankyrin repeat domain of the human TRPV4 channel. *Biochemistry*, **51**, pp.6195-6206.

Inoue R., Jensen L.J., Jian Z., Shi J., Hai L., Lurie A.I., Henriksen F.H., Salomonsson M., Morita H., Kawarabayashi Y. and Mori M. (2009) Synergistic activation of vascular TRPC6 channel by receptor and mechanical stimulation via phospholipase C/diacylglycerol and phospholipase A2/ω-hydroxylase/20-HETE pathways. *Circulation research*, **104**, *pp.1399-1409.*

Inoue R., Okada T., Onoue H., Hara Y., Shimizu S., Naitoh S., Ito Y. and Mori Y. (2001) The transient receptor potential protein homologue trp6 is the essential component of vascular α1-adrenoceptor–activated Ca^{2+}-permeable cation channel. *Circulation research*, **88**, pp.325-332.

Ishimaru Y., Inada H., Kubota M., Zhuang H., Tominaga M. and Matsunami H. (2006) Transient receptor potential family members PKD1L3 and PKD2L1 form a candidate sour taste receptor. *Proceedings of the National Academy of Sciences*, **103**, pp.12569-12574.

Islam M.S. ed. (2011) Transient receptor potential channels (Vol. **704**). *Springer Science & Business Media*.

Ivanova D. and Cousin M.A. (2022) Synaptic vesicle recycling and the endolysosomal system: a reappraisal of form and function. *Frontiers in synaptic neuroscience*, **14**, p.826098.

Iwata Y., Katanosaka Y., Arai Y., Komamura K., Miyatake K. and Shigekawa M. (2003) A novel mechanism of myocyte degeneration involving the Ca^{2+}-permeable growth factor–regulated channel. *The Journal of cell biology*, **161**, pp.957-967.

Jang S.H., Byun J.K., Jeon W.I., Choi S.Y., Park, J., Lee B.H., Yang J.E., Park J.B., O'Grady S.M., Kim D.Y. and Ryu P.D. (2015) Nuclear localization and functional characteristics of voltage-gated potassium channel Kv1. 3. *Journal of Biological Chemistry*, **290**, pp.12547-12557.

Jaquemar D., Schenker T. and Trueb B. (1999) An ankyrin-like protein with transmembrane domains is specifically lost after oncogenic transformation of human fibroblasts. *Journal of Biological Chemistry*, **274**, pp.7325-7333.

Jardín I., López J.J., Diez R., Sánchez-Collado J., Cantonero C., Albarrán, L., Woodard G.E., Redondo P.C., Salido G.M., Smani T. and Rosado J.A. (2017) TRPs in pain sensation. *Frontiers in physiology*, **8**, p.392.

Jariwala U., Prescott J., Jia, L., Barski A., Pregizer S., Cogan J.P., Arasheben A., Tilley W.D., Scher H.I., Gerald W.L. and Buchanan G. (2007) Identification of novel androgen receptor target genes in prostate cancer. *Molecular cancer*, **6**, pp.1-15.

Jaślan D., Böck J., Krogsaeter E. and Grimm C. (2020) Evolutionary aspects of TRPMLs and TPCs. *International Journal of Molecular Sciences*, **21**, p.4181.

Ji C. and McCulloch C. A. (2021) "TRPV4 integrates matrix mechanosensing with Ca^{2+} signaling to regulate extracellular matrix remodeling," *The FEBS journal*, **288**, pp. 5867–5887.

Jia Y., Wang X., Varty L., Rizzo C.A., Yang R., Correll C.C., Phelps P.T., Egan R.W. and Hey J.A. (2004) Functional TRPV4 channels are expressed in human airway smooth muscle cells. *American Journal of Physiology-Lung Cellular and Molecular Physiology*, **287**, pp.L272-L278.

Jordt S.E. and Julius D., 2002. Molecular basis for species-specific sensitivity to "hot" chili peppers. *Cell*, **108**, pp.421-430.

Jordt S.E., Bautista D.M., Chuang H.H., McKemy D.D., Zygmunt P.M., Högestätt E.D., Meng I.D. and Julius D. (2004) Mustard oils and cannabinoids excite sensory nerve fibres through the TRP channel ANKTM1. *Nature*, **427**, pp.260-265.

Jordt S.E., Tominaga M. and Julius D. (2000) Acid potentiation of the capsaicin receptor determined by a key extracellular site. *Proceedings of the National Academy of Sciences*, **97**, pp.8134-8139.

Julius D. and Nathans J. (2012) Signaling by sensory receptors. *Cold Spring Harbor perspectives in biology*, **4**, p.a005991.

Kalinovskii A.P., Utkina L.L., Korolkova Y.V. and Andreev Y.A. (2023) TRPV3 Ion Channel: From Gene to Pharmacology. *International Journal of Molecular Sciences*, **24**, p.8601.

Kaneko Y. and Szallasi A. (2014) Transient receptor potential (TRP) channels: a clinical perspective. *British journal of pharmacology*, **171**, pp.2474-2507.

Kang D., Choe C. and Kim D. (2005) Thermosensitivity of the two-pore domain K^+ channels TREK-2 and TRAAK. *The Journal of physiology*, **564**, pp.103-116.

Kanzaki M. and Kojima I. (1999) Translocation of a calcium-permeable cation channel induced by insulin-like growth factor-I. *Nature cell biology*, **1**, pp.165-170.

Karashima Y., Damann N., Prenen J., Talavera K., Segal A., Voets T. and Nilius B. (2007). Bimodal action of menthol on the transient receptor potential channel TRPA1. *Journal of Neuroscience*, **27**, pp.9874-9884.

Kariminejad A., Barzegar M., Abdollahimajd F., Pramanik R. and McGrath J.A. (2014) Olmsted syndrome in an Iranian boy with a new de novo mutation in TRPV3. *Clinical and experimental dermatology*, **39**, pp.492-495.

Kashino Y. (2003) Separation methods in the analysis of protein membrane complexes. *Journal of Chromatography B*, **797**, pp.191-216.

Kashio M. (2021) Thermosensation involving thermo-TRPs. *Molecular and cellular endocrinology*, **520**, p.111089.

Katzmann D.J., Babst M. and Emr S.D. (2001) Ubiquitin-dependent sorting into the multivesicular body pathway requires the function of a conserved endosomal protein sorting complex, ESCRT-I. *Cell*, **106**, pp.145-155.

Kelley N., Jeltema D., Duan Y. and He Y. (2019) The NLRP3 inflammasome: an overview of mechanisms of activation and regulation. *International journal of molecular sciences*, **20**, p.3328.

Kenjiro Matsumoto and Shinichi Kato. (2019) Role of transient receptor potential vanilloid 4 in the physiological function and pathology of the gastrointestinal tract. *Japanese Pharmacological Journal*, **154**, pp.92-96.

Khairatkar Joshi., N.K., Maharaj N. and Thomas A. (2010) The TRPV3 receptor as a pain target: a therapeutic promise or just some more new biology. *The Open Drug Discovery Journal*, **2**, pp. 89-97.

Kinoshita-Kawada M., Tang J., Xiao R., Kaneko S., Foskett J.K. and Zhu M.X. (2005) Inhibition of TRPC5 channels by Ca^{2+}-binding protein 1 in Xenopus oocytes. *Pflügers Archiv*, **450**, pp.345-354.

Kiselyov K., Chen J., Rbaibi Y., Oberdick D., Tjon-Kon-Sang S., Shcheynikov N., Muallem S. and Soyombo A. (2005) TRP-ML1 is a lysosomal monovalent cation channel that undergoes proteolytic cleavage. Journal of Biological Chemistry, **280**, pp.43218-43223.

Kloda A., Petrov E., Meyer G.R., Nguyen T., Hurst A.C., Hool L. and Martinac B. (2008) Mechanosensitive channel of large conductance. *The international journal of biochemistry & cell biology*, **40**, pp.164-169.

Köhler R. and Hoyer J. (2006) "Role of TRPV4 in the mechanotransduction of shear stress in endothelial cells," in TRP Ion Channel Function in Sensory Transduction and Cellular Signaling Cascades. *CRC Press*, pp. 377–388.

Köhler R., Heyken W.T., Heinau P., Schubert R., Si H., Kacik M., Busch C., Grgic I., Maier T. and Hoyer J. (2006) Evidence for a functional role of endothelial transient receptor potential V4 in shear stress–induced vasodilatation. *Arteriosclerosis, thrombosis, and vascular biology*, **26**, pp.1495-1502.

Koivisto A.P., Belvisi M.G., Gaudet R. and Szallasi A. (2022) Advances in TRP channel drug discovery: from target validation to clinical studies. *Nature reviews Drug discovery*, **21**, pp.41-59.

Komiya Y. and Runnels L.W., (2015) TRPM channels and magnesium in early embryonic development. *The International journal of developmental biology*, **59**, p.281.

Koulen P., Cai Y., Geng L., Maeda Y., Nishimura S., Witzgall R., Ehrlich B.E. and Somlo S. (2002) Polycystin-2 is an intracellular calcium release channel. *Nature cell biology*, **4**, pp.191-197.

Kozak J.A., Matsushita M., Nairn A.C. and Cahalan M.D. (2005) Charge screening by internal pH and polyvalent cations as a mechanism for activation, inhibition, and rundown of TRPM7/MIC channels. *The Journal of general physiology*, **126**, pp.499-514.

Kraft R. and Harteneck C. (2005) The mammalian melastatin-related transient receptor potential cation channels: an overview. *Pflügers Archiv*, **451**, pp.204-211.

Krall P., Canales C.P., Kairath P., Carmona-Mora P., Molina J., Carpio J.D., Ruiz P., Mezzano S.A., Li J., Wei C. and Reiser J. (2010) Podocyte-specific overexpression of wild type or mutant trpc6 in mice is sufficient to cause glomerular disease. *PloS one*, **5**, p.e12859.

Krapivinsky G., Mochida S., Krapivinsky L., Cibulsky S.M. and Clapham D.E. (2006) The TRPM7 ion channel functions in cholinergic synaptic vesicles and affects transmitter release. *Neuron*, **52**, pp.485-496.

Kruger N.J. (2009) The Bradford method for protein quantitation. *The protein protocols handbook*, **3**, pp.17-24.

Kumar A., Kumari S., Majhi R.K., Swain N., Yadav M. and Goswami C. (2015) Regulation of TRP channels by steroids: implications in physiology and diseases. *General and comparative endocrinology*, **220**, pp.23-32.

Kumar H., Lee S.H., Kim K.T., Zeng X. and Han I. (2018) TRPV4: a sensor for homeostasis and pathological events in the CNS. *Molecular Neurobiology*, **55**, pp.8695-8708.

Sanjai Kumar P., Nayak T.K., Mahish C., Sahoo S.S., Radhakrishnan A., De S., Datey A., Sahu R.P., Goswami C., Chattopadhyay S. and Chattopadhyay S. (2021) Inhibition of transient receptor potential vanilloid 1 (TRPV1) channel regulates chikungunya virus infection in macrophages. *Archives of virology*, **166**, pp.139-155.

Kumar P.S., Radhakrishnan A., Mukherjee T., Khamaru S., Chattopadhyay S. and Chattopadhyay S. (2023) Understanding the role of Ca^{2+} via transient receptor potential (TRP) channel in viral infection: Implications in developing future antiviral strategies. *Virus Research*, **323**, p.198992.

Kusaba T., Okigaki M., Matui A., Murakami M., Ishikawa K., Kimura T., Sonomura K., Adachi Y., Shibuya M., Shirayama T. and Tanda S. (2010) Klotho is associated with VEGF receptor-2 and the transient receptor potential canonical-1 Ca^{2+} channel to maintain endothelial integrity. *Proceedings of the National Academy of Sciences*, **107**, pp.19308-19313.

Kuzhikandathil E.V., Wang H., Szabo T., Morozova N., Blumberg P.M. and Oxford G.S. (2001) Functional analysis of capsaicin receptor (vanilloid receptor subtype 1) multimerization and agonist responsiveness using a dominant negative mutation. *Journal of Neuroscience*, **21**, pp.8697-8706.

Laemmli U.K. (1970) Cleavage of structural proteins during the assembly of the head of bacteriophage T4. *Nature*, **227**, pp.680-685.

Lai-Cheong J.E., Sethuraman G., Ramam M., Stone K., Simpson M.A. and McGrath J.A. (2012) Recurrent heterozygous missense mutation, p. Gly573Ser, in the TRPV3 gene in an Indian boy with sporadic Olmsted syndrome. *British Journal of Dermatology*, **167**, pp.440-442.

Lakpa K.L. Khan N. Afghah Z., Chen X. and Geiger J.D. (2021) Lysosomal stress response (LSR): physiological importance and pathological relevance. *Journal of Neuroimmune Pharmacology*, **16**, pp.219-237.

Latonen L. (2019) Phase-to-phase with nucleoli–stress responses, protein aggregation and novel roles of RNA. *Frontiers in cellular neuroscience*, **13**, p.151.

Landouré G., Zdebik A.A., Martinez, T.L., Burnett, B.G., Stanescu, H.C., Inada, H., Shi, Y., Taye, A.A., Kong, L., Munns C.H. and Choo S.S. (2010) Mutations in TRPV4 cause Charcot-Marie-Tooth disease type 2C. *Nature genetics*, **42**, pp.170-174.

Lansky S., Betancourt J.M., Zhang J., Jiang Y., Kim E.D., Paknejad N., Nimigean C.M., Yuan P. and Scheuring S. (2023) A pentameric TRPV3 channel with a dilated pore. *Nature*, pp.1-9.

Lapajne L., Rudzitis C.N., Cullimore B., Ryskamp D., Lakk M., Redmon S.N., Yarishkin O. and Krizaj D. (2022) TRPV4: Cell type-specific activation, regulation and function in the vertebrate eye. *In Current topics in membranes*, **89**, pp. 189-219). Academic Press.

Lakpa K.L., Khan N., Afghah Z., Chen X. and Geiger J.D. (2021) Lysosomal stress response (LSR): physiological importance and pathological relevance. *Journal of Neuroimmune Pharmacology*, **16**, pp.219-237.

Latonen L. (2019) Phase-to-phase with nucleoli–stress responses, protein aggregation and novel roles of RNA. *Frontiers in cellular neuroscience*, **13**, p.151.

Launay P., Fleig A., Perraud A.L., Scharenberg A.M., Penner R. Kinet J.P. (2002) TRPM4 is a Ca^{2+}-activated nonselective cation channel mediating cell membrane depolarization. *Cell*, **109**, pp.397–407.

Lavanderos B., Silva I., Cruz, P., Orellana-Serradell O., Saldías M.P. and Cerda O. (2020) TRP channels regulation of Rho GTPases in brain context and diseases. *Frontiers in Cell and Developmental Biology*, **8**, p.582975.

Lavender V., Chong S., Ralphs K., Wolstenholme A.J. and Reaves B.J. (2008) Increasing the expression of calcium-permeable TRPC3 and TRPC7 channels enhances constitutive secretion. *Biochemical Journal*, **413**, pp.437-446.

Leddy H.A., McNulty A.L., Lee S.H., Rothfusz N.E., Gloss B., Kirby M.L., Hutson M.R., Cohn D.H., Guilak F. and Liedtke W. (2014) Follistatin in chondrocytes: the link between TRPV4 channelopathies and skeletal malformations. *The FASEB Journal*, **28**, p.2525.

Lee L.Y. and Gu Q. (2009) Role of TRPV1 in inflammation-induced airway hypersensitivity. *Current opinion in pharmacology*, **9**, pp.243-249.

Lei J., Yoshimoto R.U., Matsui T., Amagai M., Kido M.A. and Tominaga M. (2023) Involvement of skin TRPV3 in temperature detection regulated by TMEM79 in mice. *Nature communications*, **14**, p.4104.

Leopold Wager C.M., Arnett E. and Schlesinger L.S. (2019) Macrophage nuclear receptors: Emerging key players in infectious diseases. *PLoS pathogens*, **15**, p.e1007585.

Lévêque M., Penna A., Le Trionnaire S., Belleguic C., Desrues B., Brinchault G., Jouneau S., Lagadic-Gossmann D. and Martin-Chouly C. (2018) Phagocytosis depends on TRPV2-mediated calcium influx and requires TRPV2 in lipids rafts: alteration in macrophages from patients with cystic fibrosis. *Scientific Reports*, **8**, p.4310.

Li L., Yin J., Jie P.H., Lu Z.H., Zhou L.B., Chen L. and Chen L. (2013) Transient receptor potential vanilloid 4 mediates hypotonicity-induced enhancement of synaptic transmission in hippocampal slices. *CNS neuroscience & therapeutics*, **19**, pp.854-862.

Li M., Jiang J. and Yue L. (2006) Functional characterization of homo-and heteromeric channel kinases TRPM6 and TRPM7. *The Journal of general physiology*, **127**, pp.525-537.

Li M., Zhang C.S., Zong Y., Feng J.W., Ma T., Hu M., Lin Z., Li X., Xie C., Wu Y. and Jiang D. (2019) Transient receptor potential V channels are essential for glucose sensing by aldolase and AMPK. *Cell metabolism*, **30**, pp.508-524.

Li M., Zheng J., Wu T., He Y., Guo J., Xu J., Gao C., Qu S., Zhang Q., Zhao J. and Cheng W. (2022) Activation of TRPV4 induces exocytosis and ferroptosis in human melanoma cells. *International journal of molecular sciences*, **23**, p.4146.

Li X., Mooney P., Zheng S., Booth C.R., Braunfeld M.B., Gubbens S., Agard D.A. and Cheng Y. (2013) Electron counting and beam-induced motion correction enable near-atomic-resolution single-particle cryo-EM. *Nature methods*, **10**, pp.584-590.

Li X., Zhang Q., Fan K., Li B., Li H., Qi H., Guo J., Cao Y. and Sun H. (2016) Overexpression of TRPV3 correlates with tumor progression in non-small cell lung cancer. *International journal of molecular sciences*, **17**, p.437.

Liao M., Cao E., Julius D. and Cheng Y. (2013) Structure of the TRPV1 ion channel determined by electron cryo-microscopy. *Nature*, **504**, pp.107-112.

Liao W.H., Hsiao M.Y., Kung Y., Liu H.L., Béra J.C., Inserra C. and Chen W.S. (2020) TRPV4 promotes acoustic wave-mediated BBB opening via Ca^{2+}/PKC-δ pathway. *Journal of Advanced Research*, **26**, pp.15-28.

Liedtke W. and Friedman J.M. (2003) Abnormal osmotic regulation in trpv4-/-mice. *Proceedings of the National Academy of Sciences*, **100**, pp.13698-13703.

Liedtke W., Choe Y., Martí-Renom M.A., Bell A.M., Denis C.S., Hudspeth A.J., Friedman J.M. and Heller S. (2000) Vanilloid receptor–related osmotically activated channel (VR-OAC), a candidate vertebrate osmoreceptor. *Cell*, **103**, pp.525-535.

Liman E.R. (2007) TRPM5 and taste transduction. *Transient receptor potential (TRP) channels*, **179**, pp.287-298.

Lin H.J., Herman P., Kang J.S. and Lakowicz J.R. (2001) Fluorescence lifetime characterization of novel low-pH probes. *Analytical biochemistry*, **294**, pp.118-125.

Lin Z., Chen Q., Lee M., Cao X., Zhang J., Ma D., Chen L., Hu X., Wang H., Wang X. and Zhang P. (2012) Exome sequencing reveals mutations in TRPV3 as a cause of Olmsted syndrome. *The American Journal of Human Genetics*, **90**, pp.558-564.

Lishko P.V., Procko E., Jin X., Phelps C.B. and Gaudet R. (2007) The ankyrin repeats of TRPV1 bind multiple ligands and modulate channel sensitivity. *Neuron*, **54**, pp.905-918.

Liu B., Yao J., Zhu M.X. and Qin F. (2011) Hysteresis of gating underlines sensitization of TRPV3 channels. *Journal of General Physiology*, **138**, pp.509-520.

Liu N., Bai L., Lu Z., Gu R., Zhao D., Yan F. and Bai J., (2022) TRPV4 contributes to ER stress and inflammation: implications for Parkinson's disease. *Journal of Neuroinflammation*, **19**, pp.1-15.

Liu X., Ong H.L. and Ambudkar I. (2018) TRP channel involvement in salivary glands—some good, some bad. *Cells*, **7**, p.74.

Liu X., Kang Z.W., Yu X.L., Li F., Liu T.X. and Li Q. (2021) Role of TRP channels and HSPs in thermal stress response in the aphid parasitoid Aphelinus asychis (Hymenoptera: Aphelinidae), **19**, p-1530, 2020. *JOURNAL OF INTEGRATIVE AGRICULTURE*, **20**, pp.VII-VII.

Liu X., Singh B.B. and Ambudkar I.S. (2003) TRPC1 is required for functional store-operated Ca^{2+} channels: role of acidic amino acid residues in the S5-S6 region. *Journal of Biological Chemistry*, **278**, pp.11337-11343.

Liu Q., Wang J., Wei X., Hu J., Ping C., Gao Y,, Xie C., Wang P., Cao P., Cao Z., Yu Y., Li D., Yao J. (2021) Therapeutic inhibition of keratinocyte TRPV3 sensory channel by local anesthetic dyclonine. *eLife*, 10, p.e68128.

Liu X., Yamazaki T., Kwon H.Y., Arai S. and Chang Y.T. (2022) A palette of site-specific organelle fluorescent thermometers. Materials Today Bio, 16, p.100405.

Liu Y., Qi H., E M., Shi P., Zhang Q., Li S., Wang Y., Cao Y., Chen Y., Ba L. and Gao J. (2018) Transient receptor potential vanilloid-3 (TRPV3) activation plays a central role in cardiac fibrosis induced by pressure overload in rats via TGF-β 1 pathway. *Naunyn-Schmiedeberg's Archives of Pharmacology*, **391**, pp.131-143.

Liu Z., Wu H., Wei Z., Wang X., Shen P., Wang S., Wang A., Chen W. and Lu Y. (2016) TRPM8: a potential target for cancer treatment. *Journal of cancer research and clinical oncology*, **142**, pp.1871-1881.

Long S.B., Campbell E.B. and MacKinnon R. (2005) Crystal structure of a mammalian voltage-dependent Shaker family K+ channel. *Science*, **309**, pp.897-903.

Long S.B., Tao X., Campbell E.B. and MacKinnon R. (2007) Atomic structure of a voltage-dependent K+ channel in a lipid membrane-like environment. *Nature*, **450**, pp.376-382.

López-Romero A.E., Hernández-Araiza I., Torres-Quiroz F., Tovar-Y-Romo L.B., Islas L.D. and Rosenbaum T. (2019) TRP ion channels: Proteins with conformational flexibility. *Channels*, **13**, pp.207-226.

Lu W., Peissel B., Babakhanlou H., Pavlova A., Geng L., Fan X., Larson C., Brent G. and Zhou J. (1997) Perinatal lethality with kidney and pancreas defects in mice with a targetted Pkd1 mutation. *Nature genetics*, **17**, pp.179-181.

Ludbrook V.J., Hanrott K.E., Kreindler J.L., Marks-Konczalik J.E., Bird N.P., Hewens D.A., Beerahee M., Behm D.J., Morice A., McGarvey L. and Parker S.M. (2021) Adaptive study design to assess effect of TRPV4 inhibition in patients with chronic cough. *ERJ Open Research*, **7**, pp. 00269-2021.

Lugo E., Graulau E., Cortes E.R., Carlo S., Ramírez N., Carlo S. and Ramírez-Lluch N. (2023) Homozygous TRPV4 Mutation Broadens the Phenotypic Spectrum of Congenital Spinal Muscular Atrophy and Arthrogryposis: A Case Report. *Cureus*, **15,** p. e43413.

Luo J., Feng J., Yu G., Yang P., Mack M.R., Du J., Yu W., Qian A., Zhang Y., Liu S. and Yin S. (2018) Transient receptor potential vanilloid 4–expressing macrophages and keratinocytes contribute differentially to allergic and nonallergic chronic itch. *Journal of Allergy and Clinical Immunology*, **141**, pp.608-619.

Luo J., Stewart R., Berdeaux R. and Hu H. (2012) Tonic inhibition of TRPV3 by Mg^{2+} in mouse epidermal keratinocytes. *Journal of Investigative Dermatology*, **132**, pp.2158-2165.

Luo W. and Hong M. (2010) Conformational changes of an ion channel detected through water− protein interactions using solid-state NMR spectroscopy. *Journal of the American Chemical Society*, **132**, pp.2378-2384.

Macpherson L.J., Dubin A.E., Evans M.J., Marr F., Schultz P.G., Cravatt B.F. and Patapoutian A. (2007) Noxious compounds activate TRPA1 ion channels through covalent modification of cysteines. *Nature*, **445**, pp.541-545.

Majeed Y., Agarwal A.K., Naylor J., Seymour V.A.L., Jiang S., Muraki K., Fishwick C.W.G. and Beech D.J. (2010) Cis-isomerism and other chemical requirements of steroidal agonists and partial agonists acting at TRPM3 channels. *British journal of pharmacology*, **161**, pp.430-441.

Majhi R.K., Kumar A., Yadav M., Swain N., Kumari S., Saha A., Pradhan A., Goswami L., Saha S., Samanta L. and Maity A. (2013) Thermosensitive ion channel TRPV1 is endogenously expressed in the sperm of a fresh water teleost fish (*Labeo rohita*) and regulates sperm motility. *Channels*, **7**, pp.483-492.

Majhi R.K., Sahoo S.S., Yadav M., Pratheek B.M., Chattopadhyay S. and Goswami C. (2015) Functional expression of TRPV channels in T cells and their implications in immune regulation. *The FEBS journal*, **282**, pp.2661-2681.

Malhas A.N., Abuknesha R.A. and Price R.G. (2002) Interaction of the leucine-rich repeats of polycystin-1 with extracellular matrix proteins: possible role in cell proliferation. *Journal of the American Society of Nephrology*, **13**, pp.19-26.

Marics I., Malapert P., Reynders A., Gaillard S. and Moqrich A. (2014) Acute heat-evoked temperature sensation is impaired but not abolished in mice lacking TRPV1 and TRPV3 channels. *PLoS One*, **9**, p.e99828.

Maroto R., Raso A., Wood T.G., Kurosky A., Martinac B. and Hamill O.P. (2005) TRPC1 forms the stretch-activated cation channel in vertebrate cells. *Nature cell biology*, **7**, pp.179-185.

Martinac B., Saimi Y. and Kung C. (2008) Ion channels in microbes. *Physiological reviews*, **88**, pp.1449-1490.

Martina J.A., Raben N. and Puertollano R. (2020) SnapShot: lysosomal storage diseases. *Cell*, **180**, pp.602-602.

Martinez J.M. and Eling T.E. (2019) Activation of TRPA1 by volatile organic chemicals leading to sensory irritation. *Altex*, **36**, p.572.

Matsumoto K. and Kato S. (2019) Physiological and pathophysiological roles of TRPV4 channel in gastrointestinal tract. *Nihon yakurigaku zasshi. Folia pharmacologica Japonica*, **154**, pp.92-96.

McCray B.A., Diehl E., Sulliva J.M., Aisenberg W.H., Zaccor N.W., Lau A.R., Rich D.J., Goretzki B., Hellmich U.A., Lloyd T.E. and Sumner C.J. (2021) Neuropathy-causing TRPV4 mutations disrupt TRPV4-RhoA interactions and impair neurite extension. *Nature communications*, **12**, p.1444.

McGaraughty S., Chu K.L., Xu J., Leys L., Radek R.J., Dart M.J., Gomtsyan A., Schmidt R.G., Kym P.R. and Brederson J.D. (2017) TRPV3 modulates nociceptive signaling through peripheral and supraspinal sites in rats. *Journal of neurophysiology*, **118**, pp.904-916.

McIntyre P., McLatchie L.M., Chambers A., Phillips E., Clarke M., Savidge J., Toms C., Peacock M., Shah K., Winter J. and Weerasakera N. (2001) Pharmacological differences between the human and rat vanilloid receptor 1 (VR1). *British journal of pharmacology*, **132**, p.1084.

McKemy D.D., Neuhausser W.M. and Julius D. (2002) Identification of a cold receptor reveals a general role for TRP channels in thermosensation. *Nature*, **416**, pp.52-58.

Méndez-Reséndiz K.A., Enciso-Pablo Ó., González-Ramírez R., Juárez-Contreras R., Rosenbaum T. and Morales-Lázaro S.L. (2020) Steroids and TRP channels: a close relationship. *International Journal of Molecular Sciences*, **21**, p.3819.

Mercado J., Baylie R., Navedo M.F., Yuan C., Scott J.D., Nelson M.T., Brayden J.E. and Santana L.F. (2014) Local control of TRPV4 channels by AKAP150-targeted PKC in arterial smooth muscle. *Journal of General Physiology*, **143**, pp.559-575.

Merrill L. and Vizzard M.A. (2014) Intravesical TRPV4 blockade reduces repeated variate stress-induced bladder dysfunction by increasing bladder capacity and decreasing voiding frequency in male rats. *American Journal of Physiology-Regulatory, Integrative and Comparative Physiology*, **307**, pp.R471-R480.

Mevorah B., Goldberg I., Sprecher E., Bergman R., Metzker A., Luria R., Gat A. and Brenner S. (2005) Olmsted syndrome: mutilating palmoplantar keratoderma with periorificial keratotic plaques. *Journal of the American Academy of Dermatology*, **53**, pp.S266-S272.

Maccini M.A., King B.J., Zvarová K., Mann-Gow T.K., Yared J. And Zvara P. (2012) *The TRPV3 ion channel role in regulation of bladder function and sensory nerve activity in a mouse. Neaua.org*. Available at: https://meeting.neaua.org/abstracts/2012/P16.cgi.

Michalick L. and Kuebler W.M. (2020) TRPV4—a missing link between mechanosensation and immunity. *Frontiers in Immunology*, **11**, p.413.

Mickle A.D., Shepherd A.J. and Mohapatra D.P. (2015) Sensory TRP channels: the key transducers of nociception and pain. *Progress in molecular biology and translational science*, **131**, pp.73-118.

Mickle A.D., Shepherd A.J. and Mohapatra D.P. (2016) Nociceptive TRP channels: sensory detectors and transducers in multiple pain pathologies. *Pharmaceuticals*, **9**, p.72.

Mio K., Ogura T., Kiyonaka S., Hiroaki Y., Tanimura Y., Fujiyoshi Y., Mori Y. and Sato C. (2007) The TRPC3 channel has a large internal chamber surrounded by signal sensing antennas. *Journal of molecular biology*, **367**, pp.373-383.

Mishra C.B., Kumari S., Siraj F., Yadav R., Kumari S., Tiwari A.K. and Tiwari M. (2018) The anti-epileptogenic and cognition enhancing effect of novel 1-[4-(4-benzo [1, 3] dioxol-5-ylmethyl-piperazin-1-

yl)-phenyl]-3-phenyl-urea (BPPU) in pentylenetetrazole induced chronic rat model of epilepsy. *Biomedicine & Pharmacotherapy*, **105**, pp.470-480.

Mittal M., Urao N., Hecquet C.M., Zhang M., Sudhahar V., Gao X.P., Komarova Y., Ushio-Fukai M. and Malik A.B. (2015) Novel role of reactive oxygen species–activated trp melastatin channel-2 in mediating angiogenesis and postischemic neovascularization. *Arteriosclerosis, thrombosis, and vascular biology*, **35**, pp.877-887.

Miyamoto T., Petrus M.J., Dubin A.E. and Patapoutian A. (2011) TRPV3 regulates nitric oxide synthase-independent nitric oxide synthesis in the skin. *Nature communications*, **2**, p.369.

Miyake T., Shirakawa H., Nakagawa T. and Kaneko S. (2015) Activation of mitochondrial transient receptor potential vanilloid 1 channel contributes to microglial migration. *Glia*, **63**, pp.1870-1882.

Mochizuki T., Wu G., Hayashi T., Xenophontos S.L., Veldhuisen B., Saris J.J., Reynolds D.M., Cai Y., Gabow P.A., Pierides A. and Kimberling W.J. (1996) PKD2, a gene for polycystic kidney disease that encodes an integral membrane protein. *Science*, **272**, pp.1339-1342.

Mohandass A., Krishnan V., Gribkova E.D., Asuthkar S., Baskaran P., Nersesyan Y., Hussain Z., Wise L.M., George R.E., Stokes N. and Alexander B.M. (2020) TRPM8 as the rapid testosterone signaling receptor: Implications in the regulation of dimorphic sexual and social behaviors. *The FASEB Journal*, **34**, p.10887.

Moiseenkova-Bell V.Y., Stanciu L.A., Serysheva I.I., Tobe B.J. and Wensel T.G. (2008) Structure of TRPV1 channel revealed by electron cryomicroscopy. *Proceedings of the National Academy of Sciences*, **105**, pp.7451-7455.

Montell C. and Rubin G.M. (1989) Molecular characterization of the Drosophila trp locus: a putative integral membrane protein required for phototransduction. *Neuron* **2**, pp.1313-1323.

Moqrich A., Hwang S.W., Earley T.J., Petrus M.J., Murray A.N., Spencer K.S., Andahazy M., Story G.M. and Patapoutian A. (2005) Impaired thermosensation in mice lacking TRPV3, a heat and camphor sensor in the skin. *Science*, **307**, pp.1468-1472.

Moran M. M., Xu H. and Clapham D. E. (2004) "TRP ion channels in the nervous system," *Current opinion in neurobiology*, **14**, pp. 362–369.

Morini M., Bergqvist C.A., Asturiano J.F., Larhammar D. and Dufour S. (2022) Dynamic evolution of transient receptor potential vanilloid (TRPV) ion channel family with numerous gene duplications and losses. *Frontiers in* Endocrinology, **13**, p.1013868.

Morita H., Honda A., Inoue R., Ito Y., Abe K., Nelson M.T. and Brayden J.E. (2007) Membrane stretch-induced activation of a TRPM4-like nonselective cation channel in cerebral artery myocytes. *Journal of pharmacological sciences*, **103**, pp.417-426.

Myers B.R., Bohlen C.J. and Julius D. (2008) A yeast genetic screen reveals a critical role for the pore helix domain in TRP channel gating. *Neuron*, **58**, pp.362-373.

Myers B.R., Sigal Y.M. and Julius D. (2009) Evolution of thermal response properties in a cold-activated TRP channel. *PloS one*, **4**, p.e5741.

Naeini R.S., Witty M.F., Séguéla P. and Bourque C.W. (2006) An N-terminal variant of Trpv1 channel is required for osmosensory transduction. *Nature neuroscience*, **9**, pp.93-98.

Nagarajan Y., Rychkov G.Y. and Peet D.J. (2017) Modulation of TRP channel activity by hydroxylation and its therapeutic potential. *Pharmaceuticals*, **10**, p.35.

Nauli S.M., Alenghat F.J., Luo Y., Williams E., Vassilev P., Li X., Elia A.E., Lu W., Brown E.M., Quinn S.J. and Ingber D.E. (2003) Polycystins 1 and 2 mediate mechanosensation in the primary cilium of kidney cells. *Nature genetics*, **33**, pp.129-137.

NEAUA - The TRPV3 ion channel role in regulation of bladder function and sensory nerve activity in a mouse (no date) *Neaua.org*. Available at: https://meeting.neaua.org/abstracts/2012/P16.cgi.

Neil R.G. and Heller S. (2005) The mechanosensitive nature of TRPV channels. *Pflügers Archiv*, **451**, pp.193-203.

Nekouzadeh A. and Rudy Y. (2016) Conformational changes of an ion-channel during gating and emerging electrophysiologic properties: Application of a computational approach to cardiac Kv7. 1. *Progress in biophysics and molecular biology*, **120**, pp.18-27.

Neuberger A., Nadezhdin K. D. and Sobolevsky A. I. (2021) TRPV3 expression and purification for structure determination by Cryo-EM, *Methods in Enzymology*. Elsevier, pp. 31–48.

Neuberger A., Nadezhdin K.D., Zakharian E. and Sobolevsky A.I. (2021) Structural mechanism of TRPV3 channel inhibition by the plant-derived coumarin osthole. *EMBO reports*, **22**, p.e53233.

Nguyen T.N., Siddiqui G., Veldhuis N.A. and Poole D.P. (2022) Diverse roles of TRPV4 in macrophages: A need for unbiased profiling. *Frontiers in Immunology*, **12**, p.828115.

Nijenhuis T., Hoenderop J.G. and Bindels R.J. (2005) TRPV5 and TRPV6 in Ca 2+(re) absorption: regulating Ca2+ entry at the gate. *Pflügers Archiv*, **451**, pp.181-192.

Nilius B., Appendino G. and Owsianik G. (2012) The transient receptor potential channel TRPA1: from gene to pathophysiology. *Pflügers Archiv-European Journal of Physiology*, **464**, pp.425-458.

Nilius B., Owsianik G., Voets T. and Peters J.A. (2007) Transient receptor potential cation channels in disease. *Physiological reviews*, **87**, pp.165-217.

Nilius B., Prenen J., Droogmans G., Voets T., Vennekens R., Freichel M., Wissenbach U. and Flockerzi V. (2003) Voltage dependence of the Ca^{2+}-activated cation channel TRPM4. *Journal of Biological Chemistry*, **278**, pp.30813-30820.

Nilius B., Talavera K., Owsianik G., Prenen J., Droogmans G. and Voets T. (2005) Gating of TRP channels: a voltage connection?. *The Journal of physiology*, **567**, pp.35-44.

Nilius B., Vriens J., Prenen J., Droogmans G. and Voets T. (2004) TRPV4 calcium entry channel: a paradigm for gating diversity. *American Journal of Physiology-Cell Physiology*, **286**, pp.C195-C205.

Nisembaum L.G., Loentgen G., L'honoré T., Martin P., Paulin C.H., Fuentès M., Escoubeyrou K., Delgado M.J., Besseau L. and Falcón J. 2022. Transient receptor potential-vanilloid (TRPV1-TRPV4) channels in the Atlantic salmon, Salmo salar. A focus on the pineal gland and melatonin production. *Frontiers in Physiology*, **12**, p.2393.

Noben-Trauth K. (2011) The TRPML3 channel: from gene to function. *Transient Receptor Potential Channels*, pp.229-237.

Numata T., Shimizu T. and Okada Y. (2007) Direct mechano-stress sensitivity of TRPM7 channel. *Cellular Physiology and Biochemistry*, **19**, pp.1-8.

O 'Neil R.G. and Heller S. (2005) The mechanosensitive nature of TRPV channels. *Pflügers Archiv*, **451**, pp.193-203.

Oancea E., Wolfe J.T. and Clapham D.E. (2006) Functional TRPM7 channels accumulate at the plasma membrane in response to fluid flow. *Circulation research*, **98**, pp.245-253.

Oeckinghaus A. and Ghosh S. (2009) The NF-κB family of transcription factors and its regulation. *Cold Spring Harbor perspectives in biology*, **1**, p.a000034.

Omar S., Clarke R., Abdullah H., Brady C., Corry J., Winter H., Touzelet O., Power U.F., Lundy F., McGarvey L.P. and Cosby S.L. (2017) Respiratory virus infection up-regulates TRPV1, TRPA1 and ASICS3 receptors on airway cells. *PloS one*, **12**, p. e0171681.

Ong H.L., de Souza L.B. and Ambudkar I.S. (2016) Role of TRPC channels in store-operated calcium entry. *Calcium entry pathways in non-excitable cells*, pp.87-109.

Ortíz-Rentería M., Juárez-Contreras R., González-Ramírez R., Islas L.D., Sierra-Ramírez F., Llorente I., Simon S.A., Hiriart M., Rosenbaum T. and Morales-Lázaro S.L. (2018) TRPV1 channels and the progesterone receptor Sig-1R interact to regulate pain. *Proceedings of the National Academy of Sciences*, **115**, pp.E1657-E1666.

Owsianik G., D'hoedt D., Voets T. and Nilius B. (2006) Structure–function relationship of the TRP channel superfamily. *Reviews of physiology biochemistry and pharmacology*, **156,** pp.61-90.

Palmer C.P., Zhou X.L., Lin J., Loukin S.H., Kung C. and Saimi Y. (2001) A TRP homolog in Saccharomyces cerevisiae forms an intracellular Ca^{2+}-permeable channel in the yeast vacuolar membrane. *Proceedings of the National Academy of Sciences*, **98**, pp.7801-7805.

Pan Z., Wang Z., Yang H., Zhang F. and Reinach P.S. (2011) TRPV1 activation is required for hypertonicity-stimulated inflammatory cytokine release in human corneal epithelial cells. *Investigative ophthalmology & visual science*, **52**, pp.485-493.

Panzano V.C., Kang K. and Garrity P.A. (2010) Infrared snake eyes: TRPA1 and the thermal sensitivity of the snake pit organ. *Science signaling*, **3**, pp.pe22-pe22.

Parenti G., Medina D.L. and Ballabio A. (2021) The rapidly evolving view of lysosomal storage diseases. *EMBO molecular medicine*, **13**, p. e12836.

Park C.W., Kim H.J., Choi Y.W., Chung B.Y., Woo S.Y., Song D.K. and Kim H.O. (2017) TRPV3 channel in keratinocytes in scars with post-burn pruritus. *International journal of molecular sciences*, **18**, p.2425.

Park T.J., Lu Y., Jüttner R., Smith E.S.J., Hu J., Brand A., Wetzel C., Milenkovic N., Erdmann B., Heppenstall P.A. and Laurito C.E. (2008) Selective inflammatory pain insensitivity in the African naked mole-rat (Heterocephalus glaber). *PLoS biology*, **6**, p.e13.

Park U., Vastani N., Guan Y., Raja S.N., Koltzenburg M. and Caterina M.J. (2011) TRP vanilloid 2 knock-out mice are susceptible to perinatal lethality but display normal thermal and mechanical nociception. *Journal of Neuroscience*, **31**, pp.11425-11436.

Partida-Sanchez S., Desai B.N., Schwab A. and Zierler S. (2021) TRP channels in inflammation and immunity. *Frontiers in Immunology*, **12**, p.684172.

Paul D., Achouri S., Yoon Y.Z., Herre J., Bryant C.E. and Cicuta P. (2013) Phagocytosis dynamics depends on target shape. *Biophysical journal*, **105**, pp.1143-1150.

Paulsen C.E., Armache J.P., Gao Y., Cheng Y. and Julius D. (2015) Structure of the TRPA1 ion channel suggests regulatory mechanisms. *Nature*, **520**, pp.511-517.

Payandeh J., Scheuer T., Zheng N. and Catterall W.A. (2011) The crystal structure of a voltage-gated sodium channel. *Nature*, **475**, pp.353-358.

Peier A.M., Moqrich A., Hergarden A.C., Reeve A.J., Andersson D.A., Story G.M., Earley T.J., Dragoni I., McIntyre P., Bevan S. and Patapoutian A. (2002) A TRP channel that senses cold stimuli and menthol. *Cell*, **108**, pp.705-715.

Pendergrass W., Wolf N. and Poot M. (2004) Efficacy of MitoTracker Green™ and CMXrosamine to measure changes in mitochondrial membrane potentials in living cells and tissues. *Cytometry Part A: the journal of the International Society for Analytical Cytology*, **61**, pp.162-169.

Peng G., Shi X. and Kadowaki T. (2015) Evolution of TRP channels inferred by their classification in diverse animal species. Molecular phylogenetics and evolution, **84**, pp.145–157.

Peng J.B., Suzuki Y., Gyimesi G. and Hediger M.A. (2018) TRPV5 and TRPV6 calcium-selective channels. *Calcium entry channels in non-excitable cells*, pp.241-274.

Peng S., Grace M.S., Gondin A.B., Retamal J.S., Dill L., Darby W., Bunnett N.W., Abogadie F.C., Carbone S.E., Tigani T. and Davis T.P. (2020) The transient receptor potential vanilloid 4 (TRPV4) ion channel mediates protease activated receptor 1 (PAR1)-induced vascular hyperpermeability. *Laboratory Investigation*, **100**, pp.1057-1067.

Pérez-Hernández M., Matamoros M., Alfayate S., Nieto-Marín P., Utrilla R.G., Tinaquero D., de Andrés R., Crespo T., Ponce-Balbuena D., Willis B.C. and Jiménez-Vazquez E.N. (2018) Brugada syndrome trafficking–defective Nav1. 5 channels can trap cardiac Kir2. 1/2.2 channels. *JCI insight*, **3**.

Perkins M. E. and Vizzard M. A. (2022) Transient receptor potential vanilloid type 4 (TRPV4) in urinary bladder structure and function, *Current topics in membranes*, **89**, pp. 95–138.

Peters F., Kopp J., Fischer J. and Tantcheva-Poor I. (2020) Mutation in TRPV3 causes painful focal plantar keratoderma. *Journal of the European Academy of Dermatology and Venereology*, **34**, pp.e620-e622.

Pfister A.S. (2019) Emerging role of the nucleolar stress response in autophagy. *Frontiers in cellular neuroscience*, **13**, p.156.

Phan M.N., Leddy H.A., Votta B.J., Kumar S., Levy D.S., Lipshutz D.B., Lee S.H., Liedtke W. and Guilak F. (2009) Functional characterization of TRPV4 as an osmotically sensitive ion channel in porcine articular

chondrocytes. *Arthritis & Rheumatism: Official Journal of the American College of Rheumatology*, **60**, pp.3028-3037.

Phelps C.B., Wang R.R., Choo S.S. and Gaudet R. (2010) Differential regulation of TRPV1, TRPV3, and TRPV4 sensitivity through a conserved binding site on the ankyrin repeat domain. *Journal of Biological Chemistry*, ***285***, pp.731-740.

Phillips A.M., Bull A. and Kelly L.E. (1992) Identification of a Drosophila gene encoding a calmodulin-binding protein with homology to the trp phototransduction gene. *Neuron*, **8**, pp.631-642.

Piper R.C. and Luzio J.P. (2004) CUPpling calcium to lysosomal biogenesis. *Trends in cell biology*, **14**, pp.471-473.

Pizzoni A., Bazzi Z., Di Giusto G., Alvarez C.L., Rivarola V., Capurro C., Schwarzbaum P.J. and Ford P. (2021) Release of ATP by TRPV4 activation is dependent upon the expression of AQP2 in renal cells. *Journal of Cellular Physiology*, **236**, pp.2559-2571.

Plant T. D. and Strotmann R. (2007) "TRPV4," in Transient Receptor Potential (TRP) Channels. *Berlin, Heidelberg: Springer Berlin Heidelberg*, pp. 189–205.

Poot M., Zhang Y.Z., Krämer J.A., Wells K.S., Jones L.J., Hanzel D.K., Lugade A.G., Singer V.L. and Haugland R.P. (1996) Analysis of mitochondrial morphology and function with novel fixable fluorescent stains. *Journal of Histochemistry & Cytochemistry*, **44**, pp.1363-1372.

Prasad P., Yanagihara A.A., Small-Howard A.L., Turner H. and Stokes A.J. (2008) Secretogranin III directs secretory vesicle biogenesis in mast cells in a manner dependent upon interaction with chromogranin A. *The Journal of Immunology*, **181**, pp.5024-5034.

Puertollano R. and Kiselyov K. (2009) TRPMLs: in sickness and in health. *American Journal of Physiology-Renal Physiology*, **296**, pp. F1245-F1254.

Pumroy R.A., Protopopova A.D., Fricke T.C., Lange I.U., Haug F.M., Nguyen P.T., Gallo P.N., Sousa B.B., Bernardes G.J., Yarov-Yarovoy V. and Leffler A. (2022) Structural insights into TRPV2 activation by small molecules. *Nature communications*, **13**, p.2334.

Puntambekar P., Mukherjea D., Jajoo S. and Ramkumar V. (2005) Essential role of Rac1/NADPH oxidase in nerve growth factor induction of TRPV1 expression. *Journal of neurochemistry*, **95**, pp.1689-1703.

Pusch M., Ludewig U. and Jentsch T.J. (1997) Temperature dependence of fast and slow gating relaxations of ClC-0 chloride channels. *The Journal of general physiology*, **109**, pp.105-116.

Putney J.W. (2004) Box 1. Store-operated channels. *Trends in Cell Biology*, **6**, pp.282-286.

Putney J.W. (2004) The enigmatic TRPCs: multifunctional cation channels. *Trends in cell biology*, **14**, pp.282-286.

Qi H., Ren J., E M., Zhang Q., Cao Y., Ba L., Song C., Shi P., Fu B. and Sun H. (2019) MiR-103 inhibiting cardiac hypertrophy through inactivation of myocardial cell autophagy via targeting TRPV 3 channel in rat hearts. *Journal of Cellular and Molecular Medicine*, **23**, pp.1926-1939.

Qi H., Shi Y., Wu H., Niu C., Sun X. and Wang K. (2022) Inhibition of temperature-sensitive TRPV3 channel by two natural isochlorogenic acid isomers for alleviation of dermatitis and chronic pruritus. *Acta Pharmaceutica Sinica B*, **12**, pp.723-734.

Qian F., Boletta A., Bhunia A.K., Xu H., Liu L., Ahrabi A.K., Watnick T.J., Zhou F. and Germino G.G. (2002) Cleavage of polycystin-1 requires the receptor for egg jelly domain and is disrupted by human autosomal-dominant polycystic kidney disease 1-associated mutations. *Proceedings of the National Academy of Sciences*, **99**, pp.16981-16986.

Qian F., Boletta A., Bhunia A.K., Xu H., Liu L., Ahrabi A.K., Watnick T.J., Zhou F. and Germino, G.G. (2002) Cleavage of polycystin-1 requires the receptor for egg jelly domain and is disrupted by human autosomal-dominant polycystic kidney disease 1-associated mutations. *Proceedings of the National Academy of Sciences*, **99**, pp.16981-16986.

Qu Y., Wang G., Sun X. and Wang K. (2019) Inhibition of the warm temperature–activated Ca^{2+}-permeable transient receptor potential vanilloid TRPV3 channel attenuates atopic dermatitis. *Molecular pharmacology*, **96**, pp.393-400.

Ragamin A., Gomes C.C., Bindels-de Heus K., Sandoval R., Bassenden A.V., Dib L., Kok F., Alves J., Mathijssen I., Medici-Van den Herik E. and Eveleigh R. (2022) De novo TRPV4 Leu619Pro variant causes a new channelopathy characterised by giant cell lesions of the jaws and skull, skeletal abnormalities and polyneuropathy. *Journal of medical genetics*, **59**, pp.305-312.

Rajan S., Schremmer C., Weber J., Alt P., Geiger F. and Dietrich A. (2021) Ca^{2+}-signaling by TRPV4 channels in respiratory function and disease. *Cells*, **10**, p.822.

Ramsey I.S., Delling M. and Clapham D.E. (2006) An introduction to TRP channels. *Annual review of physiology*, **68**, pp.619-647.

Ramsey I.S., Moran M.M., Chong J.A. and Clapham D.E. (2006) A voltage-gated proton-selective channel lacking the pore domain. *Nature*, **440**, pp.1213-1216.

Riederer E., Cang C. and Ren D. (2023) Lysosomal Ion Channels: What Are They Good For and Are They Druggable Targets? *Annual Review of Pharmacology and Toxicology*, **63**, pp.19-41.

Rizopoulos T., Papadaki-Petrou H. and Assimakopoulou M. (2018) Expression profiling of the transient receptor potential vanilloid (TRPV) channels 1, 2, 3 and 4 in mucosal epithelium of human ulcerative colitis. *Cells*, **7**, p.61.

Rizzoli SO. (2014) Synaptic vesicle recycling: steps and principles. *EMBO journal*. **33,** pp.788-822.

Roberts M.W., Sui G., Wu R., Rong W., Wildman S., Montgomery B., Ali A., Langley S., Ruggieri Sr M.R. and Wu C. (2020) TRPV4 receptor as a functional sensory molecule in bladder urothelium: Stretch-independent, tissue-specific actions and pathological implications. *The FASEB Journal*, **34**, p.263.

Rock M.J., Prenen J., Funari V.A., Funari T.L., Merriman B., Nelson S.F., Lachman R.S., Wilcox W.R., Reyno S., Quadrelli R. and Vaglio A. (2008) Gain-of-function mutations in TRPV4 cause autosomal dominant brachyolmia. *Nature genetics*, **40**, pp.999-1003.

Rodrigues P., Ruviaro N. A. and Trevisan G. (2022) “TRPV4 role in neuropathic pain mechanisms in rodents,” *Antioxidants (Basel, Switzerland)*, **12**, p. 24.

Rohacs T. (2013) Regulation of transient receptor potential channels by the phospholipase C pathway. *Advances in biological regulation*, **53**, pp.341-355.

Rosenbaum T., Benítez-Angeles M., Sánchez-Hernández R., Morales-Lázaro S.L., Hiriart M., Morales-Buenrostro L.E. and Torres-Quiroz F. (2020) TRPV4: a physio and pathophysiologically significant ion channel. *International journal of molecular sciences*, **21**, p.3837.

Rouillard A.D., Gundersen G.W., Fernandez, N.F., Wang Z., Monteiro C.D., McDermott M.G. and Ma’ayan A. (2016) The harmonizome: a collection of processed datasets gathered to serve and mine knowledge about genes and proteins. *Database*, 2016.

Ryu S., Liu B., Yao J., Fu Q. and Qin F. (2007) Uncoupling proton activation of vanilloid receptor TRPV1. *Journal of Neuroscience*, **27**, pp.12797-12807.

Sachs F. and Sokabe M. (1990) Stretch-activated ion channels and membrane mechanics. *Neuroscience research supplements*,**12**, p. S1–S4.

Saftig P. and Puertollano R. (2021) How lysosomes sense, integrate, and cope with stress. *Trends in biochemical sciences*, **46**, pp.97-112.

Saha S., Ghosh A., Tiwari N., Kumar A., Kumar A. and Goswami C. (2017) Preferential selection of Arginine at the lipid-water-interface of TRPV1 during vertebrate evolution correlates with its snorkeling behaviour and cholesterol interaction. *Scientific Reports*, **7**, p.16808.

Sahu R.P. and Goswami C. (2023) Presence of TRPV3 in macrophage lysosomes helps in skin wound healing against bacterial infection. *Experimental Dermatology*, **32**, pp.60-74.

Sánchez J. C. and Ehrlich B. E. (2021) “Functional interaction between transient receptor potential V4 channel and neuronal calcium sensor 1 and the effects of paclitaxel,” *Molecular pharmacology*, **100**, pp. 258–270.

Saotome K., Singh A.K., Yelshanskaya M.V. and Sobolevsky A.I. (2016) Crystal structure of the epithelial calcium channel TRPV6. *Nature*, **534**, pp.506-511.

Sardar P., Kumar A., Bhandari A. and Goswami C. (2012) Conservation of tubulin-binding sequences in TRPV1 throughout evolution. *PLoS One*, **7**, p. e31448.

Sardiello M. (2016) Transcription factor EB: from master coordinator of lysosomal pathways to candidate therapeutic target in degenerative storage diseases. *Annals of the New York Academy of Sciences*, **1371**, pp.3-14.

Sarria I., Ling J., Zhu M.X. and Gu J.G. (2011) TRPM8 acute desensitization is mediated by calmodulin and requires PIP2: distinction from tachyphylaxis. *Journal of neurophysiology*, **106**, pp.3056-3066.

Sawamura S., Shirakawa H., Nakagawa T., Mori Y. and Kaneko S. (2017) TRP Channels in the Brain. *Neurobiology of TRP channels*, chapter **16**, p. 288-316.

Sawasdichai A., Chen H.T., Hamid N.A., Jayaraman P.S. and Gaston K. (2010) In situ subcellular fractionation of adherent and non-adherent mammalian cells. *JoVE (Journal of Visualized Experiments)*, **41**, p. e1958.

Schaefer M. (2005) Homo-and heteromeric assembly of TRP channel subunits. *Pflügers Archive*, **451**, pp.35-42.

Scheres S.H. and Chen S. (2012) Prevention of overfitting in cryo-EM structure determination. *Nature methods*, **9**, pp.853-854.

Schlingmann K.P., Waldegger S., Konrad M., Chubanov V. and Gudermann T. (2007) TRPM6 and TRPM7—Gatekeepers of human magnesium metabolism. *Biochimica et Biophysica Acta (BBA)-Molecular Basis of Disease*, **1772**, pp.813-821.

Schoppa N.E., McCormack K., Tanouye M.A., Sigworth F.J. (1992) The size of gating charge in wild-type and mutant Shaker potassium channels. *Science*; **255**, pp.1712–1715.

Schoppa N.E. and Sigworth F.J. (1998) Activation of shaker potassium channels: III. An activation gating model for wild-type and V2 mutant channels. *The Journal of general physiology*, **111**, pp.313-342.

Schumacher M.A. (2010) Transient receptor potential channels in pain and inflammation: therapeutic opportunities. *Pain Practice*, **10**, pp.185-200.

Schrapers K.T., Sponder G., Liebe F., Liebe H. and Stumpff F. (2018) The bovine TRPV3 as a pathway for the uptake of Na^{+}, Ca^{2+}, and NH^{4+}. *PLoS One*, **13**, p.e0193519.

Scotland R.S., Chauhan S., Davis C., De Felipe C., Hunt S., Kabir J., Kotsonis P., Oh U. and Ahluwalia A. (2004) Vanilloid receptor TRPV1, sensory C-fibers, and vascular autoregulation: a novel mechanism involved in myogenic constriction. *Circulation research*, **95**, pp.1027-1034.

Seebohm G. and Schreiber J.A. (2021) Beyond hot and spicy: TRPV channels and their pharmacological modulation. *Cell Physiol Biochem*, **55**, pp.108-130.

Shen P.S., Yang X., DeCaen P.G., Liu X., Bulkley D., Clapham D.E. and Cao E. (2016) The structure of the polycystic kidney disease channel PKD2 in lipid nanodiscs. *Cell*, **167**, pp.763-773.

Shi D.J., Ye S., Cao X., Zhang R. and Wang K. (2013) Crystal structure of the N-terminal ankyrin repeat domain of TRPV3 reveals unique conformation of finger 3 loop critical for channel function. *Protein & cell*, **4**, pp.942-950.

Shigematsu H., Sokabe T., Danev R., Tominaga M. and Nagayama K. (2010) A 3.5-nm structure of rat TRPV4 cation channel revealed by Zernike phase-contrast cryoelectron microscopy. *Journal of Biological Chemistry*, **285**, pp.11210-11218.

Sigworth F.J. (1994) Voltage gating of ion channels. *Quarterly reviews of biophysics*, **27**, pp.1-40.

Silverman H.A., Chen A., Kravatz N.L., Chavan S.S. and Chang E.H. (2020) Involvement of neural transient receptor potential channels in peripheral inflammation. *Frontiers in immunology*, **11**, p.590261.

Simpson S., Preston D., Schwerk C., Schroten H. and Blazer-Yost B. (2019) Cytokine and inflammatory mediator effects on TRPV4 function in choroid plexus epithelial cells. *American Journal of Physiology-Cell Physiology*, **317**, pp.C881-C893.

Singh A.K., McGoldrick L.L. and Sobolevsky A.I. (2018) Structure and gating mechanism of the transient receptor potential channel TRPV3. *Nature structural & molecular biology*, **25**, pp.805-813.

Singh A.K., McGoldrick L.L., Demirkhanyan L., Leslie M., Zakharian E. and Sobolevsky A.I. (2019) Structural basis of temperature sensation by the TRP channel TRPV3. *Nature structural & molecular biology*, **26**, pp.994-998.

Smani T., Gómez L.J., Regodon S., Woodard G.E., Siegfried G., Khatib A.M. and Rosado J.A. (2018) TRP channels in angiogenesis and other endothelial functions. *Frontiers in physiology*, **9**, p.1731.

Smith G.D., Gunthorpe M.J., Kelsell R.E., Hayes P.D., Reilly P., Facer P., Wright J.E., Jerman J.C., Walhin J.P., Ooi L. and Egerton J. (2002) TRPV3 is a temperature-sensitive vanilloid receptor-like protein. *Nature*, **418**, pp.186-190.

Sokolova O., Kolmakova-Partensky L. and Grigorieff N. (2001) Three-dimensional structure of a voltage-gated potassium channel at 2.5 nm resolution. *Structure*, **9**, pp.215-220.

Song Y., Zhan L., Yu M., Huang C., Meng X., Ma T., Zhang L. and Li J. (2014) TRPV4 channel inhibits TGF-β1-induced proliferation of hepatic stellate cells. *PloS one*, **9**, p.e101179.

Song Z., Chen X., Zhao Q., Stanic V., Lin Z., Yang S., Chen T., Chen J. and Yang Y. (2021) Hair loss caused by gain-of-function mutant TRPV3 is associated with premature differentiation of follicular keratinocytes. *Journal of Investigative Dermatology*, **141**, pp.1964-1974.

Sonkusare S. K. and Laubach V. E. (2022). "Endothelial TRPV4 channels in lung edema and injury," in Role of TRPV4 Channels in Different Organ Systems. *Elsevier*, pp. 43–62.

Spassova M.A., Hewavitharana T., Xu W., Soboloff J. and Gill D.L. (2006) A common mechanism underlies stretch activation and receptor activation of TRPC6 channels. *Proceedings of the National Academy of Sciences*, **103**, pp.16586-16591.

Spekker E., Körtési T. and Vécsei L. (2022) TRP channels: Recent development in translational research and potential therapeutic targets in migraine, *International journal of molecular sciences*, **24**, p.700.

Spencer R.H., Chang G. and Rees D.C. (1999) 'Feeling the pressure': structural insights into a gated mechanosensitive channel. Current opinion in structural biology, **9**, pp.448-454.

Spix B., Castiglioni A.J., Remis N.N., Flores E.N., Wartenberg P., Wyatt A., Boehm U., Gudermann T., Biel M., García-Añoveros J. and Grimm C. (2022) Whole-body analysis of TRPML3 (MCOLN3) expression using a GFP-reporter mouse model reveals widespread expression in secretory cells and endocrine glands. *PloS one*, **17**, p.e0278848.

Steinberg X., Lespay-Rebolledo C. and Brauchi S. (2014) A structural view of ligand-dependent activation in thermoTRP channels. *Frontiers in physiology*, **5**, p.171.

Steinhoff M. and Bíró T. (2009) A TR (I) P to pruritus research: role of TRPV3 in inflammation and itch. *Journal of Investigative Dermatology*, **129**, pp.531-535.

Stockand J.D. (2013) "Renal ion channels, electrophysiology of transport, and channelopathies," in *Seldin and Giebisch's The Kidney*. *Elsevier*, chapter **8,** pp. 217–262.

Story G.M., Peier A.M., Reeve A.J., Eid S.R., Mosbacher J., Hricik T.R., Earley T.J., Hergarden A.C., Andersson D.A., Hwang S.W. and McIntyre P. (2003) ANKTM1, a TRP-like channel expressed in nociceptive neurons, is activated by cold temperatures. *Cell*, **112**, pp.819-829.

Strotmann R., Harteneck C., Nunnenmacher K., Schultz G. and Plant T.D. (2000) OTRPC4, a nonselective cation channel that confers sensitivity to extracellular osmolarity. *Nature cell biology*, **2**, pp.695-702.

Strotmann R., Schultz G. and Plant T.D. (2003) Ca^{2+}-dependent potentiation of the nonselective cation channel TRPV4 is mediated by a C-terminal calmodulin binding site. *Journal of Biological Chemistry*, **278**, pp.26541-26549.

Strubing C., Krapivinsky G., Krapivinsky L. and Clapham D.E. (2003) Formation of novel TRPC channels by complex subunit interactions in embryonic brain. *Journal of Biological Chemistry*, **278**, pp.39014-39019.

Su W., Qiao X., Wang W., He S., Liang K. and Hong X. (2023) TRPV3: Structure, diseases and modulators. *Molecules*, **28**, p.774.

Sulk M. and Steinhoff M., (2015) Role of TRP channels in skin diseases. *In TRP channels as therapeutic targets*, pp.293-323. Academic Press.

Suzuki M., Watanabe Y., Oyama Y., Mizuno A., Kusano E., Hirao A. and Ookawara S. (2003) Localization of mechanosensitive channel TRPV4 in mouse skin. *Neuroscience letters*, **353**, pp.189-192.

Svobodova B. and Groschner K. (2016) "Mechanisms of lipid regulation and lipid gating in TRPC channels". *Cell calcium*, **59**, pp.271-279.

Swain S.M., Romac J.M.J., Shahid R.A., Pandol S.J., Liedtke W., Vigna S.R. and Liddle R.A. (2020) TRPV4 channel opening mediates pressure-induced pancreatitis initiated by Piezo1 activation. *The Journal of clinical investigation*, **130**, pp.2527-2541.

Szallasi A., Cortright D.N., Blum C.A. and Eid S.R. (2007) The vanilloid receptor TRPV1: 10 years from channel cloning to antagonist proof-of-concept. *Nature reviews Drug discovery*, **6**, pp.357-372.

Szöllősi A.G., Vasas N., Angyal Á., Kistamás K., Nánási P.P., Mihály J., Béke G., Herczeg-Lisztes E., Szegedi A., Kawada N. and Yanagida T. (2018) Activation of TRPV3 regulates inflammatory actions of human epidermal keratinocytes. *Journal of Investigative Dermatology*, **138**, pp.365-374.

Takahashi N. and Mori Y. (2011) TRP channels as sensors and signal integrators of redox status changes. *Frontiers in Pharmacology*, **2**, p.58.

Takahashi N., Hamada-Nakahara S., Itoh, Y., Takemura K., Shimada A., Ueda Y., Kitamata M., Matsuoka R., Hanawa-Suetsugu K., Senju Y. and Mori M.X. (2014) TRPV4 channel activity is modulated by direct interaction of the ankyrin domain to PI (4, 5) P2. *Nature communications*, **5**, p.4994.

Takahashi N., Kuwaki T., Kiyonaka S., Numata T., Kozai D., Mizuno Y., Yamamoto S., Naito S., Knevels E., Carmeliet P. and Oga T. (2011) TRPA1 underlies a sensing mechanism for O_2. *Nature chemical biology*, **7**, pp.701-711.

Talavera K., Yasumatsu K., Voets T., Droogmans G., Shigemura N., Ninomiya Y., Margolskee R.F. and Nilius B. (2005) Heat activation of TRPM5 underlies thermal sensitivity of sweet taste. *Nature*, **438**, pp.1022-1025.

Tancini B., Buratta S., Delo F., Sagini K., Chiaradia E., Pellegrino R.M., Emiliani C. and Urbanelli L. (2020) Lysosomal exocytosis: the extracellular role of an intracellular organelle. *Membranes*, **10**, p.406.

Thebault S., Lemonnier L., Bidaux G., Flourakis M., Bavencoffe A., Gordienko D., Roudbaraki M., Delcourt P., Panchin Y., Shuba Y. and Skryma R. (2005) Novel role of cold/menthol-sensitive transient receptor potential melastatine family member 8 (TRPM8) in the activation of store-operated channels in LNCaP human prostate cancer epithelial cells. *Journal of Biological Chemistry*, **280**, pp.39423-39435.

Thorneloe K.S., Sulpizio A.C., Lin, Z., Figueroa D.J., Clouse A.K., McCafferty G.P., Chendrimada T.P., Lashinger E.S., Gordon E., Evans L. and Misajet B.A. (2008) N-((1S)-1-{[4-((2S)-2-{[(2, 4-dichlorophenyl) sulfonyl] amino}-3-hydroxypropanoyl)-1-piperazinyl] carbonyl}-3-methylbutyl)-1-benzothiophene-2-carboxamide (GSK1016790A), a novel and potent transient receptor potential vanilloid 4 channel agonist induces urinary bladder contraction and hyperactivity: Part I. *Journal of Pharmacology and Experimental Therapeutics*, **326**, pp.432-442.

Tian C., Han X., He L., Tang F., Huang R., Lin Z., Li S., Deng S., Xu J., Huang H. and Zhao H. (2020) Transient receptor potential ankyrin 1 contributes to the ATP-elicited oxidative stress and inflammation in THP-1-derived macrophage. *Molecular and Cellular Biochemistry*, **473**, pp.179-192.

Tissue expression of TRPV4 - summary - the human protein atlas (no date) Proteinatlas.org. Available at: https://www.proteinatlas.org/ENSG00000111199-TRPV4/tissue (Accessed: October 6, 2023).

Togashi K., Inada H. and Tominaga M. (2008) Inhibition of the transient receptor potential cation channel TRPM2 by 2-aminoethoxydiphenyl borate (2-APB). *British journal of pharmacology*, **153**, pp.1324-1330.

Toledo Mauriño J.J., Fonseca-Camarillo G., Furuzawa-Carballeda J., Barreto-Zuñiga R., Martínez Benítez B., Granados J. and Yamamoto-Furusho J.K. (2020) TRPV subfamily (TRPV2, TRPV3, TRPV4, TRPV5, and TRPV6) gene and protein expression in patients with ulcerative colitis. *Journal of Immunology Research*, **2020**, pp.1-11.

Tomilin V., Mamenko M., Zaika O., Wingo C.S. and Pochynyuk O. (2019). TRPV4 deletion protects against hypokalemia during systemic K+ deficiency. *American Journal of Physiology-Renal Physiology*, **316**, pp. F948-F956.

Tominaga M., Caterina M.J., Malmberg A.B., Rosen T.A., Gilbert H., Skinner K., Raumann B.E., Basbaum A.I. and Julius D. (1998) The cloned capsaicin receptor integrates multiple pain-producing stimuli. *Neuron*, **21**, pp.531-543.

Tóth B.I., Oláh A., Szöllősi A.G. and Bíró T. (2014) TRP channels in the skin. *British journal of pharmacology*, **171**, pp.2568-2581.

Trivedi P.C., Bartlett J.J. and Pulinilkunnil T. (2020) Lysosomal biology and function: modern view of cellular debris bin. *Cells*, **9**, p.1131.

TRPV4 (no date) *Guidetopharmacology.org*. Available at: https://www.guidetopharmacology.org/GRAC/ObjectDisplayForward?objectId=510 (Accessed: October 12, 2023).

TRPV4 protein expression summary - The Human Protein Atlas (no date) *Proteinatlas.org*. Available at: https://www.proteinatlas.org/ENSG00000111199-TRPV4 (Accessed: October 12, 2023).

Tsavaler L., Shapero M.H., Morkowski S. and Laus R. (2001) Trp-p8, a novel prostate-specific gene, is up-regulated in prostate cancer and other malignancies and shares high homology with transient receptor potential calcium channel proteins. *Cancer research*, **61**, pp.3760-3769.

Tsiokas L., Arnould T., Zhu C., Kim E., Walz G. and Sukhatme V.P. (1999) Specific association of the gene product of PKD2 with the TRPC1 channel. *Proceedings of the National Academy of Sciences*, **96**, pp.3934-3939.

Türker E., Garreis F., Khajavi N., Reinach P.S., Joshi P., Brockmann T., Lucius A., Ljubojevic N., Turan E., Cooper D. and Schick, F. (2018) Vascular endothelial growth factor (VEGF) induced downstream responses to transient receptor potential vanilloid 1 (TRPV1) and 3-Iodothyronamine (3-T1AM) in human corneal keratocytes. *Frontiers in Endocrinology*, **9**, p.670.

Turner H., Fleig A., Stokes A., Kinet J.P. and Penner R. (2003) Discrimination of intracellular calcium store subcompartments using TRPV1 (transient receptor potential channel, vanilloid subfamily member 1) release channel activity. *Biochemical Journal*, **371**, pp.341-350.

Ueda T., Yamada T., Ugawa S., Ishida Y. and Shimada S. (2009) TRPV3, a thermosensitive channel is expressed in mouse distal colon epithelium. *Biochemical and biophysical research communications*, **383**, pp.130-134.

Ugawa S., Ueda T., Ishida Y., Nishigaki M., Shibata Y. and Shimada S. (2002) Amiloride-blockable acid-sensing ion channels are leading acid sensors expressed in human nociceptors. *The Journal of clinical investigation*, **110**, pp.1185-1190.

Um J.Y., Kim H.B., Kim J.C., Park J.S., Lee S.Y., Chung B.Y., Park C.W. and Kim H.O. (2022) TRPV3 and Itch: The Role of TRPV3 in Chronic Pruritus according to Clinical and Experimental Evidence. *International Journal of Molecular Sciences*, **23**, p.14962.

Ürel-Demir G., Şimşek-Kiper P.Ö., Öncel İ., Utine G.E., Haliloğlu G. and Boduroğlu K. (2021) Natural history of TRPV4-Related disorders: From skeletal dysplasia to neuromuscular phenotype. *European Journal of Paediatric Neurology*, **32**, pp.46-55.

Van den Eynde C., Vriens J. and De Clercq K. (2021) Transient receptor potential channel regulation by growth factors. *Biochimica et Biophysica Acta (BBA)-Molecular Cell Research*, **1868**, p.118950.

van der Wijst J., van Goor M.K., Schreuder M.F. and Hoenderop J.G. (2019) TRPV5 in renal tubular calcium handling and its potential relevance for nephrolithiasis. *Kidney International*, **96**, pp.1283-1291.

Vandewauw I., De Clercq K., Mulier M., Held K., Pinto S., Van Ranst N., Segal A., Voet T., Vennekens R., Zimmermann K. and Vriens J. (2018) A TRP channel trio mediates acute noxious heat sensing. Nature, **555**, pp.662-666.

Vay L., Gu C. and McNaughton P.A. (2012). The thermo-TRP ion channel family: properties and therapeutic implications. *British journal of pharmacology*, **165**, pp.787-801.

Vazquez G., Wedel B.J., Aziz O., Trebak M. and Putney Jr J.W. (2004) The mammalian TRPC cation channels. *Biochimica et Biophysica Acta (BBA)-Molecular Cell Research*, **1742**, pp.21-36.

Veldhuisen B., Spruit L., Dauwerse H.G., Breuning M.H. and Peters D.J. (1999). Genes homologous to the autosomal dominant polycystic kidney disease genes (PKD1 and PKD2). *European Journal of Human Genetics*, **7**, pp.860-872.

Venkatachalam K and Montell C. (2007) TRP channels. *Annu Rev Biochem*,**76**, pp.387-417.

Venkatachalam K., Wong C.O. and Zhu M.X. (2015) The role of TRPMLs in endolysosomal trafficking and function. *Cell calcium*, **58**, pp.48-56.

Vennekens R., Owsianik G. and Nilius B. (2008) "Vanilloid transient receptor potential cation channels: an overview," *Current pharmaceutical design*, **14**, pp. 18–31.

Vergarajauregui S., Connelly P.S., Daniels M.P. and Puertollano R. (2008) Autophagic dysfunction in mucolipidosis type IV patients. *Human molecular genetics*, **17**, pp.2723-2737.

Vincent F. and AJ Duncton M. (2011) TRPV4 agonists and antagonists. *Current topics in medicinal chemistry*, **11**, pp.2216-2226.

Vincent F., Acevedo A., Nguyen M.T., Dourado M., DeFalco J., Gustafson A., Spiro P., Emerling D.E., Kelly M.G. and Duncton M.A. (2009) Identification and characterization of novel TRPV4 modulators. *Biochemical and biophysical research communications*, **389**, pp.490-494.

Vlachová V., Teisinger J., Sušánková K., Lyfenko A., Ettrich R. and Vyklický L. (2003) Functional role of C-terminal cytoplasmic tail of rat vanilloid receptor 1. *Journal of Neuroscience*, **23**, pp.1340-1350.

Voellmy R. (2004) Transcriptional regulation of the metazoan stress protein response. *Progress in nucleic acid research and molecular biology*, **78**, pp.143-185.

Voets T., Droogmans G., Wissenbach U., Janssens A., Flockerzi V. and Nilius B. (2004) The principle of temperature-dependent gating in cold-and heat-sensitive TRP channels. *Nature*, **430**, pp.748-754.

Voets T., Owsianik G. and Nilius B. (2007) Trpm8. *Transient Receptor Potential (TRP) Channels*, pp.329-344.

Vogt-Eisele A.K., Weber K., Sherkheli M.A., Vielhaber G., Panten J., Gisselmann G. and Hatt H. (2007) Monoterpenoid agonists of TRPV3. *British journal of pharmacology*, **151**, pp.530-540.

Voltz J.W., Weinman E.J. and Shenolikar S. (2001) Expanding the role of NHERF, a PDZ-domain containing protein adapter, to growth regulation. *Oncogene*, **20**, pp.6309-6314.

Vriens J., Nilius B. and Vennekens R. (2008) Herbal compounds and toxins modulating TRP channels. *Curr Neuropharmacol*, **6**, pp.79-96.

Vriens J., Watanabe H., Janssens A., Droogmans G., Voets T. and Nilius B. (2004) Cell swelling, heat, and chemical agonists use distinct pathways for the activation of the cation channel TRPV4. *Proceedings of the National Academy of Sciences*, **101**, pp.396-401.

Vyklicka L., Boukalova S., Macikova L., Chvojka S. and Vlachova V. (2017) The human transient receptor potential vanilloid 3 channel is sensitized via the ERK pathway. *Journal of Biological Chemistry*, **292**, pp.21083-21091.

Walcher L., Budde C., Böhm A., Reinach P.S., Dhandapani P., Ljubojevic N., Schweiger M.W., Von der Waydbrink H., Reimers I., Köhrle J. and Mergler S. (2018) TRPM8 activation via 3-iodothyronamine blunts VEGF-induced transactivation of TRPV1 in human uveal melanoma cells. *Frontiers in Pharmacology*, **9**, p.1234.

Waller D.D., Park J. and Tsantrizos Y.S. (2019) Inhibition of farnesyl pyrophosphate (FPP) and/or geranylgeranyl pyrophosphate (GGPP) biosynthesis and its implication in the treatment of cancers. *Critical reviews in biochemistry and molecular biology*, **54**, pp.41-60.

Wang G. and Wang K. (2017) The Ca^{2+}-permeable cation transient receptor potential TRPV3 channel: an emerging pivotal target for itch and skin diseases. *Molecular Pharmacology*, **92**, pp.193-200.

Wang H. and Siemens J. (2015) TRP ion channels in thermosensation, thermoregulation and metabolism. *Temperature*, **2**, pp.178-187.

Wang S., Geng Q., Huo L., Ma Y., Gao Y., Zhang W., Zhang H., Lv P. and Jia Z. (2019) Transient receptor potential cation channel subfamily vanilloid 4 and 3 in the inner ear protect hearing in mice. *Frontiers in Molecular Neuroscience*, **12**, p.296.

Wang W., Zhang X., Gao Q. and Xu H. (2014) TRPML1: an ion channel in the lysosome. *Mammalian Transient Receptor Potential (TRP) Cation Channels*, **I**, pp.631-645.

Wang H., Zhu Y., Liu H., Liang T. and Wei Y. (2023) Advances in Drug Discovery Targeting Lysosomal Membrane Proteins. *Pharmaceuticals*, **16**, p.601.

Wang Y., Li H., Xue C., Chen H., Xue Y., Zhao F., Zhu M.X. and Cao Z. (2021) TRPV3 enhances skin keratinocyte proliferation through EGFR-dependent signaling pathways. *Cell Biology and Toxicology*, **37**, pp.313-330.

Watanabe H., Vriens J., Prenen J., Droogmans G., Voets T. and Nilius B. (2003) Anandamide and arachidonic acid use epoxyeicosatrienoic acids to activate TRPV4 channels. *Nature*,**424**, pp.434–8.

Watanabe H., Vriens J., Suh S.H., Benham C.D., Droogmans G. and Nilius B. (2002) Heat-evoked activation of TRPV4 channels in a HEK293 cell expression system and in native mouse aorta endothelial cells. *J Biol Chem*, **277**, pp.47044-51.

Watanabe H., Davis J.B., Smart D., Jerman J.C., Smith G.D., Hayes P., Vriens J., Cairns W., Wissenbach U., Prenen J. and Flockerzi V. (2002) Activation of TRPV4 channels (hVRL-2/mTRP12) by phorbol derivatives. *Journal of Biological Chemistry*, **277**, pp.13569-13577.

Watanabe H., Vriens J., Prenen J., Droogmans G., Voets T. and Nilius B. (2003) Anandamide and arachidonic acid use epoxyeicosatrienoic acids to activate TRPV4 channels. *Nature*, 424(6947), pp.434-438.

Watanabe H., Vriens J., Prenen J., Droogmans G., Voets T. and Nilius B. (2003) Anandamide and arachidonic acid use epoxyeicosatrienoic acids to activate TRPV4 channels. *Nature*, **424**, pp.434-438.

Weber J., Rajan S., Schremmer C., Chao Y.K., Krasteva-Christ G., Kannler M., Yildirim A.Ö., Brosien M., Schredelseker J., Weissmann N. and Grimm C. (2020) TRPV4 channels are essential for alveolar epithelial barrier function as protection from lung edema. *JCI insight*, **5,** e134464.

Weil A., Moore S.E., Waite N.J., Randall A. and Gunthorpe M.J. (2005) Conservation of functional and pharmacological properties in the distantly related temperature sensors TRPV1 and TRPM8. *Mol Pharmacol* **68**, pp.518-527.

Welc S.S., Phillips N.A., Oca-Cossio J., Wallet S.M., Chen D.L. and Clanton T.L. (2012) Hyperthermia increases interleukin-6 in mouse skeletal muscle. *American Journal of Physiology-Cell Physiology*, **303**, pp.C455-C466.

Wes P.D., Chevesich J., Jeromin A., Rosenberg C., Stetten G. and Montell C. (1995) TRPC1, a human homolog of a Drosophila store-operated channel. *Proceedings of the National Academy of Sciences*, **92**, pp.9652-9656.

Willette R.N., Bao W., Nerurkar S., Yue T.L., Doe C.P., Stankus G., Turner G.H., Ju H., Thomas H., Fishman C.E. and Sulpizio A. (2008) Systemic activation of the transient receptor potential vanilloid subtype 4 channel causes endothelial failure and circulatory collapse: Part 2. *Journal of Pharmacology and Experimental Therapeutics*, **326**, pp.443-452.

Wilson P.D. (2001) Polycystin: new aspects of structure, function, and regulation. *Journal of the American Society of Nephrology*, **12**, pp.834-845.

Winter J., Forbes C.A., Sternberg J. and Lindsay R.M. (1988) Nerve growth factor (NGF) regulates adult rat cultured dorsal root ganglion neuron responses to the excitotoxin capsaicin. *Neuron*, **1**, pp.973-981.

Woods S., Humphreys P.A., Bates N., Richardson S.A., Kuba S.Y., Brooks I.R., Cain S.A. and Kimber S.J. (2021) Regulation of TGFβ signalling by TRPV4 in chondrocytes. *Cells*, **10**, p.726.

Woolums B.M., McCray B.A., Sung H., Tabuchi M., Sullivan J.M., Ruppell K.T., Yang Y., Mamah C., Aisenberg W.H., Saavedra-Rivera P.C. and Larin B.S. (2020) TRPV4 disrupts mitochondrial transport and causes axonal degeneration via a CaMKII-dependent elevation of intracellular Ca^{2+}. *Nature communications*, **11**, p.2679.

Wu J., Li Z., Deng Y., Lu X., Luo C., Mu X., Zhang T., Liu Q., Tang S., Li J. and An Q. (2023) Function of TRP channels in monocytes/macrophages. *Frontiers in Immunology*, **14**, p.1187890.

Wu L., Gao X., Brown R.C., Heller S. and O'Neil R.G. (2007) Dual role of the TRPV4 channel as a sensor of flow and osmolality in renal epithelial cells. *American Journal of Physiology-Renal Physiology*, **293**, pp.F1699-F1713.

Wu Q.F., Qian C., Zhao N., Dong Q., Li J., Wang B.B., Chen L., Yu L., Han B., Du Y.M. and Liao Y.H. (2017) Activation of transient receptor potential vanilloid 4 involves in hypoxia/reoxygenation injury in cardiomyocytes. *Cell death & disease*, **8**, pp.e2828-e2828.

Wu Y., Qi J., Wu C. and Rong W. (2021) Emerging roles of the TRPV4 channel in bladder physiology and dysfunction. *The Journal of physiology*, **599**, pp.39-47.

Xiao B., Coste B., Mathur J. and Patapoutian A. (2011). Temperature-dependent STIM1 activation induces Ca^{2+} influx and modulates gene expression. *Nature chemical biology*, **7**, pp.351-358.

Xiao R. and Xu X.S. (2011) *C. elegans* TRP channels. *Transient Receptor Potential Channels*, **704**, pp.323-339.

Xu H., Delling M., Li L., Dong X. and Clapham D.E. (2007) Activating mutation in a mucolipin transient receptor potential channel leads to melanocyte loss in varitint–waddler mice. *Proceedings of the National Academy of Sciences*, **104**, pp.18321-18326.

Xu H., Fu Y., Tian W. and Cohen D.M. (2006) Glycosylation of the osmoresponsive transient receptor potential channel TRPV4 on Asn-651 influences membrane trafficking. *American Journal of Physiology-Renal Physiology*, **290**, pp.F1103-F1109.

Xu H., Ramsey I.S., Kotecha S.A., Moran M.M., Chong J.A., Lawson D., Ge P., Lilly J., Silos-Santiago I., Xie Y. and DiStefano P.S. (2002) TRPV3 is a calcium-permeable temperature-sensitive cation channel. *Nature*, **418**, pp.181-186.

Xu H., Zhao H., Tian W., Yoshida K., Roullet J.B. and Cohen D.M. (2003) Regulation of a transient receptor potential (TRP) channel by tyrosine phosphorylation: Src family kinase-dependent tyrosine phosphorylation of TRPV4 on TYR-253 mediates its response to hypotonic stress. *Journal of Biological Chemistry*, **278**, pp.11520-11527.

Yadav M. and Goswami C. (2017) TRPV3 mutants causing Olmsted Syndrome induce impaired cell adhesion and nonfunctional lysosomes. *Channels*, **11**, pp.196-208.

Yadav M. (2018) Importance of thermosensitive ion channel(TRPV2 and TRPV3) in cellular functions,(Doctoral thesis).

Yamada T., Ueda T., Ugawa S., Ishida Y., Imayasu M., Koyama S. and Shimada S. (2010) Functional expression of transient receptor potential vanilloid 3 (TRPV3) in corneal epithelial cells: involvement in thermosensation and wound healing. *Experimental eye research*, **90**, pp.121-129.

Yamanoi Y., Lei J., Takayama Y., Hosogi S., Marunaka Y. and Tominaga M. (2023) TRPV3-ANO1 interaction positively regulates wound healing in keratinocytes. *Communications Biology*, **6**, p.88.

Yang C., Yamaki S., Jung T., Kim B., Huyhn R. and McKemy D.D. (2023) Endogenous inflammatory mediators produced by injury activate TRPV1 and TRPA1 nociceptors to induce sexually dimorphic cold pain that is dependent on TRPM8 and GFRα3. *Journal of Neuroscience*, **43**, pp.2803-2814.

Yang F., Cui Y., Wang K. and Zheng J. (2010) Thermosensitive TRP channel pore turret is part of the temperature activation pathway. Proceedings of the National Academy of Sciences, **107**, pp.7083-7088.

Yao J., Liu B. and Qin F. (2010) Kinetic and energetic analysis of thermally activated TRPV1 channels. *Biophysical journal*, **99**, pp.1743-1753.

Yao J., Liu B. and Qin F. (2011) Modular thermal sensors in temperature-gated transient receptor potential (TRP) channels. *Proceedings of the National Academy of Sciences*, **108**, pp.11109-11114.

Yao L., Chen S., Tang H., Huang P., Wei S., Liang Z., Chen X., Wang H., Tao A., Chen R. and Zhang Q. (2019) Transient receptor potential ion channels mediate adherens junctions dysfunction in a toluene diisocyanate-induced murine asthma model. *Toxicological sciences*, **168**, pp.160-170.

Yao X., Kwan H.Y. and Huang Y. (2006) Regulation of TRP channels by phosphorylation. *Neurosignals*, **14**, pp.273-280.

Ye L., Kleiner S., Wu J., Sah R., Gupta R.K., Banks A.S., Cohen P., Khandekar M.J., Boström P., Mepani R.J. and Laznik D. (2012) TRPV4 is a regulator of adipose oxidative metabolism, inflammation, and energy homeostasis. *Cell*, **151**, pp.96-110.

Yellen G. (1998) The moving parts of voltage-gated ion channels. *Quarterly reviews of biophysics*, **31**, pp.239-295.

Yip M.F., Ramm G., Larance M., Hoehn K.L., Wagner M.C., Guilhaus M., and James D.E. (2008) CaMKII-mediated phosphorylation of the myosin motor Myo1c is required for insulin-stimulated GLUT4 translocation in adipocytes. *Cell Metab*, **8**, pp.384–398.

York J.M. and Zakon H.H. (2022) Evolution of transient receptor potential (TRP) ion channels in Antarctic fishes (Cryonotothenioidea) and identification of putative thermosensors. *Genome Biology and Evolution*, **14**, p.evac009.

Yoshida T., Inoue R., Morii T., Takahashi N., Yamamoto S., Hara Y., Tominaga M., Shimizu S., Sato Y. and Mori Y. (2006) Nitric oxide activates TRP channels by cysteine S-nitrosylation. *Nature chemical biology*, **2**, pp.596-607.

Yu F.H. and Catterall W.A. (2004). The VGL-chanome: a protein superfamily specialized for electrical signaling and ionic homeostasis. *Science's STKE*, **2004**, p.re15.

Yunna C., Mengru H., Lei W. and Weidong C. (2020) Macrophage M1/M2 polarization. *European journal of pharmacology*, **877**, p.173090.

Yu W., Huang J., Yu H., Lin J., Fan F., Xie R., Shen Y., Lin K., Ye Y. and Weng J. (2022) TRPV3 inhibits colorectal cancer cell proliferation and migration by regulating the MAPK signaling pathway. *Journal of Gastrointestinal Oncology*, **13**, p.2447.

Yu X., Jin L. and Zhou Z.H. (2008) 3.88 Å structure of cytoplasmic polyhedrosis virus by cryo-electron microscopy. *Nature*, **453**, pp.415-419.

Yu Z., Wang Y., Qin L. and Chen H. (2017) Functional cooperation between KCa3. 1 and TRPV4 channels in bronchial smooth muscle cell proliferation associated with chronic asthma. *Frontiers in Pharmacology*, **8**, p.559.

Yuasa-Kawada J., Kinoshita-Kawada M., Rao Y. and Wu J.Y. (2009) Deubiquitinating enzyme USP33/VDU1 is required for Slit signaling in inhibiting breast cancer cell migration. *Proceedings of the National Academy of Sciences*, **106**, pp.14530-14535.

Yue Z., Xie J., Yu A. S., Stock J., Du J., & Yue L. (2015) Role of TRP channels in the cardiovascular system. American journal of physiology. *Heart and circulatory physiology*, **308**, pp.H157–H182.

Zagotta W.N., Hoshi T., Dittman J. and Aldrich R.W. (1994) Shaker potassium channel gating. II: Transitions in the activation pathway. *The Journal of general physiology*, **103**, pp.279-319.

Zergane M., Kuebler W.M. and Michalick L. (2021) Heteromeric TRP channels in lung inflammation. *Cells*, **10**, p.1654.

Zhan L. and Li J. (2018) "The role of TRPV4 in fibrosis," *Gene*, **642**, pp. 1–8.

Zhang M., Ma Y., Ye X., Zhang N., Pan L. and Wang B. (2023) TRP (transient receptor potential) ion channel family: Structures, biological functions and therapeutic interventions for diseases. *Signal Transduction and Targeted Therapy*, **8**, p.261.

Zhang Q., Cao Y., Luo Q., Wang P., Shi P., Song C., E M., Ren J., Fu B. and Sun H. (2018) The transient receptor potential vanilloid-3 regulates hypoxia-mediated pulmonary artery smooth muscle cells proliferation via PI 3K/AKT signaling pathway. *Cell Proliferation*, **51**, p.e12436.

Zhang X., Huang J. and McNaughton P.A. (2005) NGF rapidly increases membrane expression of TRPV1 heat-gated ion channels. *The EMBO journal*, **24**, pp.4211-4223.

Zhang X., Jin, L., Fang Q., Hui W.H. and Zhou Z.H. (2010) 3.3 Å cryo-EM structure of a nonenveloped virus reveals a priming mechanism for cell entry. *Cell*, **141**, pp.472-482.

Zhang X., Lee M.D., Buckley C., Wilson C. and McCarron J.G. (2022) Mitochondria regulate TRPV4-mediated release of ATP. *British Journal of Pharmacology*, **179**, pp.1017-1032.

Zhang X., Ren W., DeCaen P., Yan C., Tao X., Tang L., Wang J., Hasegawa K., Kumasaka T., He J. and Wang J. (2012) Crystal structure of an orthologue of the NaChBac voltage-gated sodium channel. *Nature*, **486**, pp.130-134.

Zhao J., Munanairi A., Liu X.Y., Zhang J., Hu L., Hu M., Bu D., Liu L., Xie Z., Kim B.S. and Yang Y. (2020) PAR2 mediates itch via TRPV3 signaling in keratinocytes. *Journal of Investigative Dermatology*, **140**, pp.1524-1532.

Zhao Z., Qin P. and Huang Y.W. (2021) Lysosomal ion channels involved in cellular entry and uncoating of enveloped viruses: Implications for therapeutic strategies against SARS-CoV-2. *Cell Calcium*, **94**, p.102360.

Zheng J. (2013) Molecular mechanism of TRP channels. *Comprehensive Physiology*, **3**, p.221.

Zheng J.S., Hu X.J., Zhao Y.M., Yang J. and Li D. (2013) Intake of fish and marine n-3 polyunsaturated fatty acids and risk of breast cancer: meta-analysis of data from 21 independent prospective cohort studies. *BMJ*, ***346***, p.f3706.

Zhi Y.P., Liu J., Han J.W., Huang Y.P., Gao Z.Q., Yang Y. and Wu R.N. (2016) Two familial cases of Olmsted-like syndrome with a G573V mutation of the TRPV3 gene. *Clinical and Experimental Dermatology*, **41**, pp.510-513.

Zhong L., Bellemer A., Yan H., Honjo K., Robertson J., Hwang R.Y., Pitt G.S. and Tracey W.D. (2012) Thermosensory and nonthermosensory isoforms of Drosophila melanogaster TRPA1 reveal heat-sensor domains of a thermoTRP Channel. *Cell reports*, **1**, pp.43-55.

Zhou X.L., Batiza A.F., Loukin S.H., Palmer C.P., Kung C. and Saimi Y. (2003) The transient receptor potential channel on the yeast vacuole is mechanosensitive. *Proceedings of the National Academy of Sciences*, **100**, pp.7105-7110.

Zimmermann K., Lennerz J.K., Hein A., Link A.S., Kaczmarek J.S., Delling M., Uysal S., Pfeifer J.D., Riccio A. and Clapham D.E. (2011) Transient receptor potential cation channel, subfamily C, member 5

(TRPC5) is a cold-transducer in the peripheral nervous system. *Proceedings of the National Academy of Sciences*, **108**, pp.18114-18119.

Zubcevic L., Herzik Jr M.A., Wu M., Borschel W.F., Hirschi, M., Song A.S., Lander G.C. and Lee S.Y. (2018) Conformational ensemble of the human TRPV3 ion channel. *Nature Communications*, ***9***, p.4773.

Chapter 7

Annexure section

Annexure 1

7.1 Thermo dye characteristics

Fluorescence Intensity-Based Thermometry Using a Palette of Organelle Thermometers is a cutting-edge technique in the field of cellular biology and biophysics. This method allows researchers to precisely measure temperature variations within different subcellular compartments by utilizing a range of specialized fluorescent indicators or dyes. Here's an overview of this technique, its accuracy, and its applications in cellular systems.

7.1.1 Methodology

Within the cell, micro-temperature changes play vital roles in cellular processes. To measure this local temperature inside cells, molecular fluorescent thermometers have been employed. These are fluorescence probes act as temperature sensors and convert information related to change in temperature as detectable fluorescence signals. Investigating intracellular temperature variations in different organelles requires the proper development and characterization of organelle-specific thermosensors. In this study, a new series of fluorescence thermos-sensors, known as Thermo Greens (TGs), has been further characterized and utilized to visualize the temperature changes in almost all common sub-cellular organelles. Using fluorescence lifetime-based cell imaging, some of the TGs have demonstrated their capability to monitor temperature gradients in specific organelles induced by external heating. This thermos-sensors can be utilized to investigate the distinct temperature changes that different sub-cellular organelle experiences, mostly due to change in metabolism or external heating or other unknown factors. TGs can also be utilized for quantitative imaging of heat production in various organelles, such as in mitochondria, lysosome, nucleus, plasma membrane and the endoplasmic reticulum in different cells. As of now, TGs represent the first collection of small molecules that act as “fluorescence-based thermometers” and these molecules can be applied

to virtually all common organelles. These findings hold the potential to inspire the development of new molecular tools and technologies for probing local temperature changes that can contribute to understanding of thermal biology in the future.

Furthermore, TGs have been applied to thermally image heat production in different organelles. This versatile palette of "novel fluorescence-based molecular thermometers" are believed to hold significant value in the exploration of previously unanswered biological questions.

Various organelle-targeting motifs were incorporated into the unsymmetrical BODIPY structure, including the n-undecanoyl group (in Lipid Droplet Thermo Green, DTG), triphenylphosphonium group (in Mitochondria Thermo Green, MTG), 4-(2-aminoethyl) morpholine group (in Lysosome Thermo Green, LTG), 3-(dodecyl(methyl)amino) propane-1-sulfonate (in Plasma Membrane Thermo Green, PTG), D-sphingosine group (in Golgi Thermo Green, GTG), and Hoechst 33, 258 (in Nucleus Thermo Green, NTG). This ensemble of site-specific organelle-based thermometers was collectively named Thermo Greens (TGs).

The introduction of organelle-targeting motifs had minimal impact on the fundamental photophysical properties of these organelle-based thermometers. The absorption and emission wavelengths of the newly developed thermometers remained consistent, typically at around 496 nm and 512 nm, closely resembling the properties of the parent compound, ETG. This alignment of excitation and emission spectra closely matches the standard filter sets of fluorescence/confocal microscopes, such as FITC, Alexa dyes or GFP, a feature not previously achieved by the yellow color-based MTY and ETY. Additionally, the absorption spectrum of NTG displayed a secondary peak at 353nm, attributable to the presence of the Hoechst motif. The quantum yields of TGs exhibited only slight variations, falling within the range of 1.28% to 1.74%. Overall, TGs demonstrated highly similar photophysical properties with relatively low quantum yields.

7.1.2 Accuracy

The accuracy of this method depends on several factors, including the choice of fluorescent indicators, calibration procedures, and the precision of fluorescence measurements. With proper calibration and controls, fluorescence intensity-based thermometry can achieve high accuracy in temperature measurements. However, it's important to note that accurate measurements may be influenced by factors like photobleaching, phototoxicity, and probe-specific variations. Therefore, rigorous experimental design and data analysis are crucial for the accurate measurement of the organelle temperature. Firstly, the organelle-specificity of the newly developed TGs was confirmed, demonstrating that each of these "molecular thermometers" are accurately localized within the intended organelles. Additionally, it was observed that all the TGs had minimal cytotoxic effects on cells.

7.1.3 Characterization of the dye

An investigation into the fluorescence lifetimes of TGs within each organelle under basal conditions ($\Delta T = 0$) was conducted (Liu et al. 2022). The results indicated differences in fluorescence lifetimes between PTG and DTG. This discrepancy can be attributed to the differing rigidity of the plasma membrane compared to lipid droplets, with PTG existing in a planar molecular rotor form, leading to a longer fluorescence lifetime. In contrast, DTG tends to adopt a butterfly-like structure within the more fluidic environment of lipid droplets, resulting in a shorter lifetime. It's worth noting that intracellular membranes (e.g., ER, Golgi, mitochondria, and lysosome) were found to be more flexible than plasma membranes. Given that TGs likely associated with organelle membranes due to their hydrophobic nature, this supports the observation that the fluorescence lifetimes of LTG, ETG, MTG, and GTG were shorter than PTG under basal conditions. Unlike the other thermometers, NTG does not bind

to the membrane but rather adheres to condensed DNA via the Hoechst motif. This interaction restricts the free motion of the rotor, promoting a planar structure with an extended lifetime.

7.1.4 Applications and uses

All these dyes offer great tools for the accurate measurement of temperature variation in subcellular organelle and can estimate the exact % changes (in fold change) per degree change in the temperature. The accuracy will always be dependent upon the sensitivity of the dye, which is reported to exhibit high sensitivity to intracellular temperature. Like for example, the sensitivity for PTG is 125 ps/°C, followed by NTG 74 ps/°C and MTG 60 ps/°C (Yamazaki et al. 2023).

So, by looking at the accuracy and sensitivity of the organelle-specific thermo dye, some of the dyes have been used for the measurement of the thermal status at different cellular conditions. The thermo dyes used here for the study are PTG, LTG, NTG and MTG, respectively.

7.1.5 LTG calibration

The LTG (Lyso-thermo green) dye has been used to measure the lysosomal temperature in the cellular system (Liu et al. 2022). The LTG dye was calibrated for the determination of fluorescent intensity changes per °C change. For that, the peak intensity was converted to a relative percentage scale, and 5°C-50°C temperature range was considered. Temperature-dependent fluorescence spectra were collected using Edinburgh spectrofluorometer FLS 1000, using a quartz cuvette of 10 mm optical path length. Appropriate baseline correction was carried out with their respective blank solvents. A Quantum North West (TC 125) temperature controller was used to maintain the temperature by circulating water through the cell holder. All the samples were excited at 480 nm to collect the corrected fluorescence emission spectra. The average percentage change per degree temperature was around~1.73%.

Temperature (In °C)	Intensity (AU.)	Relative %	Fold change/°C
35	13628.36	100	-
36	13030.75	95.61501	1.60646
37	12811.82	94.00855	1.56207
38	12598.94	92.44648	2.45208
39	12264.76	89.9944	1.58912
40	12048.19	88.40528	1.67152
41	11820.38	86.73376	2.0361
42	11542.9	84.69766	1.78027
43	11300.28	82.91739	0.45158
44	11238.73	82.46581	2.50629
45	10897.17	79.95952	-

Table 6 Relative changes in the intensity (in fold change) per °C change in temperature.

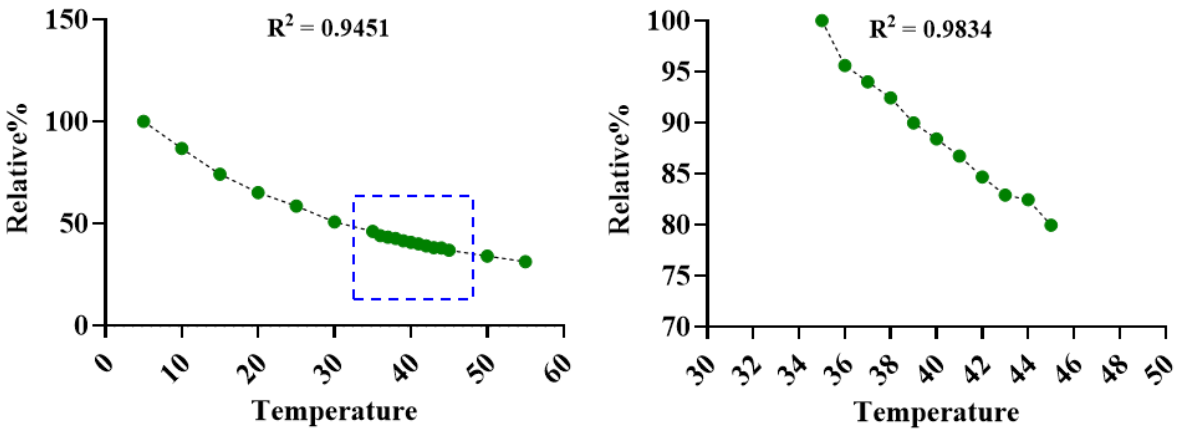

Fig 97. Relative % of intensity changes in every °C change in temperature.

Annexure 2

7.2 Bacterial construct generation

7.2.1 pRsetB pH red pH sensor

DNA construct from Addgene transformed into competent cells (*Escherichia coli*, DE3-BL21) and transformed bacteria plated in Amphicillin plate. The colony obtained was picked and cultured with Ampicillin in a 4ml LB broth media. The culture was grown up to OD (optical density) around 0.4-0.8 and then IPTG was added for induction for at least 4 hours. Then, the culture was pellet down at RPM 13000 for 2 minutes. The pellet was resuspended with PBS and spread in a glass slide to test the fluorescence of pH red bacteria. For the bulk production, a single colony was picked from the plate and grown for overnight in 5ml LB culture medium with antibiotics. In the morning the culture was grown in the 50 ml 2XYT LB medium (Tryptone 5gm, Yeast extract 3gm, NaCl 1.25gm in 250ml 2XYT media). From 5ml culture 100µl primary culture was taken and mixed with 50ml 2XYT medium till the OD reached 0.8. Subsequently, the culture was grown for at least 4 hours, pellet down, and proceeded for cell fixation.

7.2.2 pH calibration of bacterial pH-sensor

For calibration of the pH red bacteria, pH buffer was made to check the efficiency. The pH buffer used is acetate buffer with different pH ranging from pH 3.6-5.6. The solution for making this buffer was 0.1M acetic acid and 0.1M sodium acetate. For 100ml acetic acid of 0.1M, 572.4098µl glacial acetic acid was used, and for 100ml 0.1M sodium acetate solution, 820 milligrams were used from the main stock. The pH buffer that has been prepared ranges from 3.6, 4.0, 4.4, 4.8, 5.2, 5.6, 6 and 7. The mildly-chemically fixed bacteria were then subjected to resuspend with different pH buffers for calibration. The image was taken at

different pH buffers, which were then quantified using Fiji software, and a standard curve was plotted based on the quantified data.

7.2.3 Induction of and storage of bacterial sensor

After induction with IPTG for 4 hours, the culture medium was pellet down and proceeded for fixation and storage. First, the solution was mildly fixed with glutaraldehyde (0.1% for 30 minutes). Then, the bacterial suspension with glutaraldehyde (0.1%) solutions was kept for at least 30 minutes and pellet down to proceed with washing in 1X PBS (3 times). Then, the pellet is stored in sodium azide solution (1mM) for long-term storage at 4°C. The same procedure has been followed for the fixation and storage of pGP-CMV-GCaMP6f bacteria. The glutaraldehyde fixation is perfect for fixation of the bacteria, then methanol: acetone (1:1) fixation.

Annexure 3

7.3 TRPV3 role in regulations of ChiKV infection

In the context of Chikungunya Virus (ChikV) infection, the role of TRPV3 have been studied and its impact on the antiviral responses in the cells has been investigated. It has been found that when TRPV3 is inhibited, there is a significant reduction in its expression, and the intensity of the E2 protein, a key component of ChikV, increases (**Fig 99a**). This leads to a higher number of viral particles in case of TRPV3 inhibition compared to its activation, as measured through a plaque assay (**Fig 99c**).

The relationship between E2 and TRPV3 was examined, and it was observed that the correlation between these two proteins is stronger in the presence of ChikV infection and even stronger when TRPV3 is inhibited. When TRPV3 is activated, the correlation is not as significant. The correlation between E2 and TRPV3 is more correlated in only ChikV infection (r = 5270) and ChikV infection with TRPV3 inhibitions (r = 0.5944). The correlation between E2 protein and TRPV3 protein is correlated (r = 0.5944) in case of TRPV3 inhibition. TRPV3 activation shows a non-significant correlation (r = 0.1011) (**Fig 99d-f**).

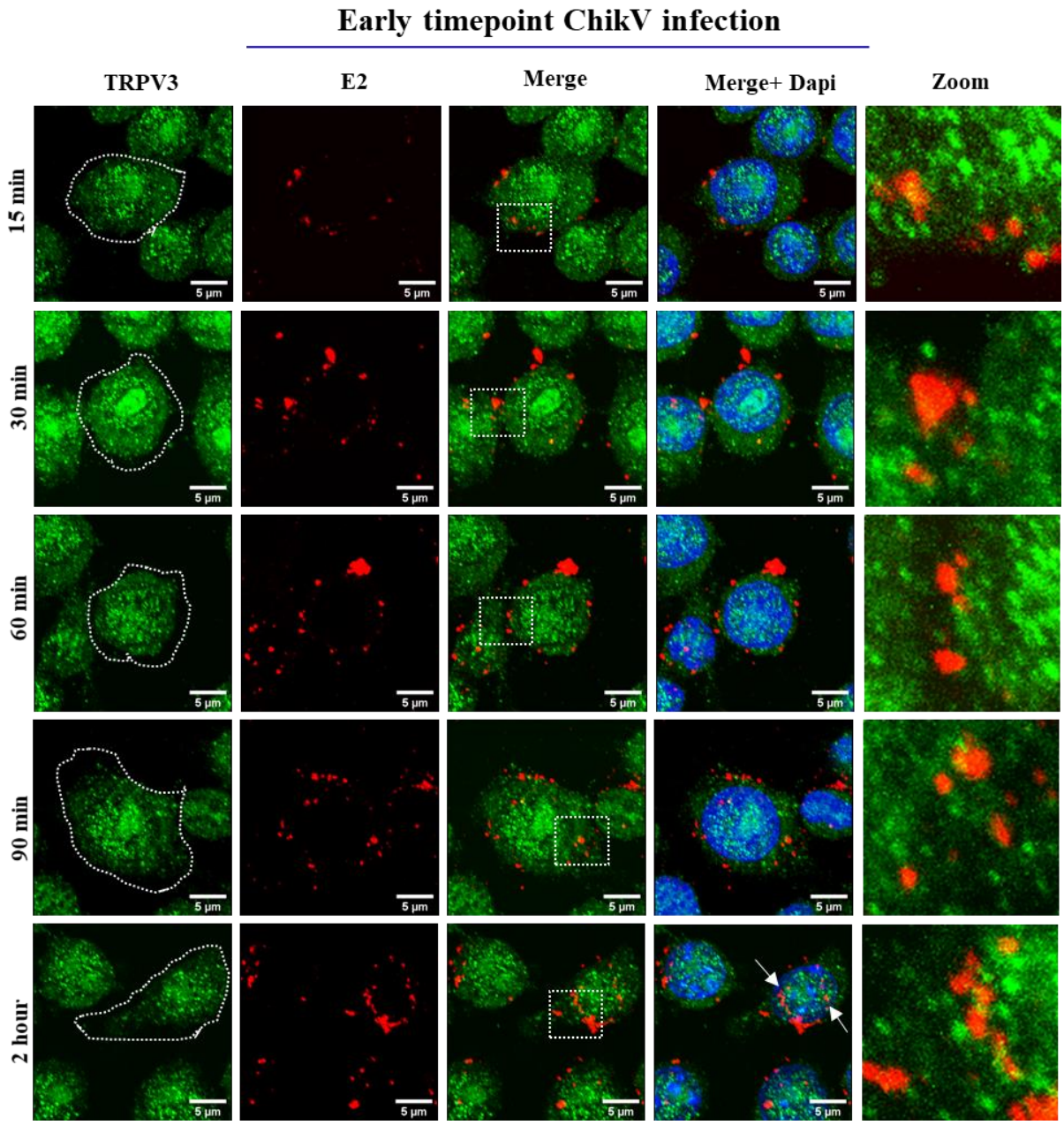

Fig 98. The early time point localization of E2 proteins with TRPV3. The figure shows early time point localization of viral proteins (E2, red) along with TRPV3 (green). Scale bar 5µm.

The early time points of viral infection have been studied, which is from 15 minutes to 2 hours, to investigate the localization of E2 protein along with TRPV3. It has been observed that the colocalization of E2 along with TRPV3 is more inside the cells and become time-dependent. Thus, the colocalization is more at 2 hours. The viral particle (E2) was found more inside the cells at 2 hours than in the periphery as compared to early time points, i.e. at 15 minutes or at 30 minutes (**Fig 98**).

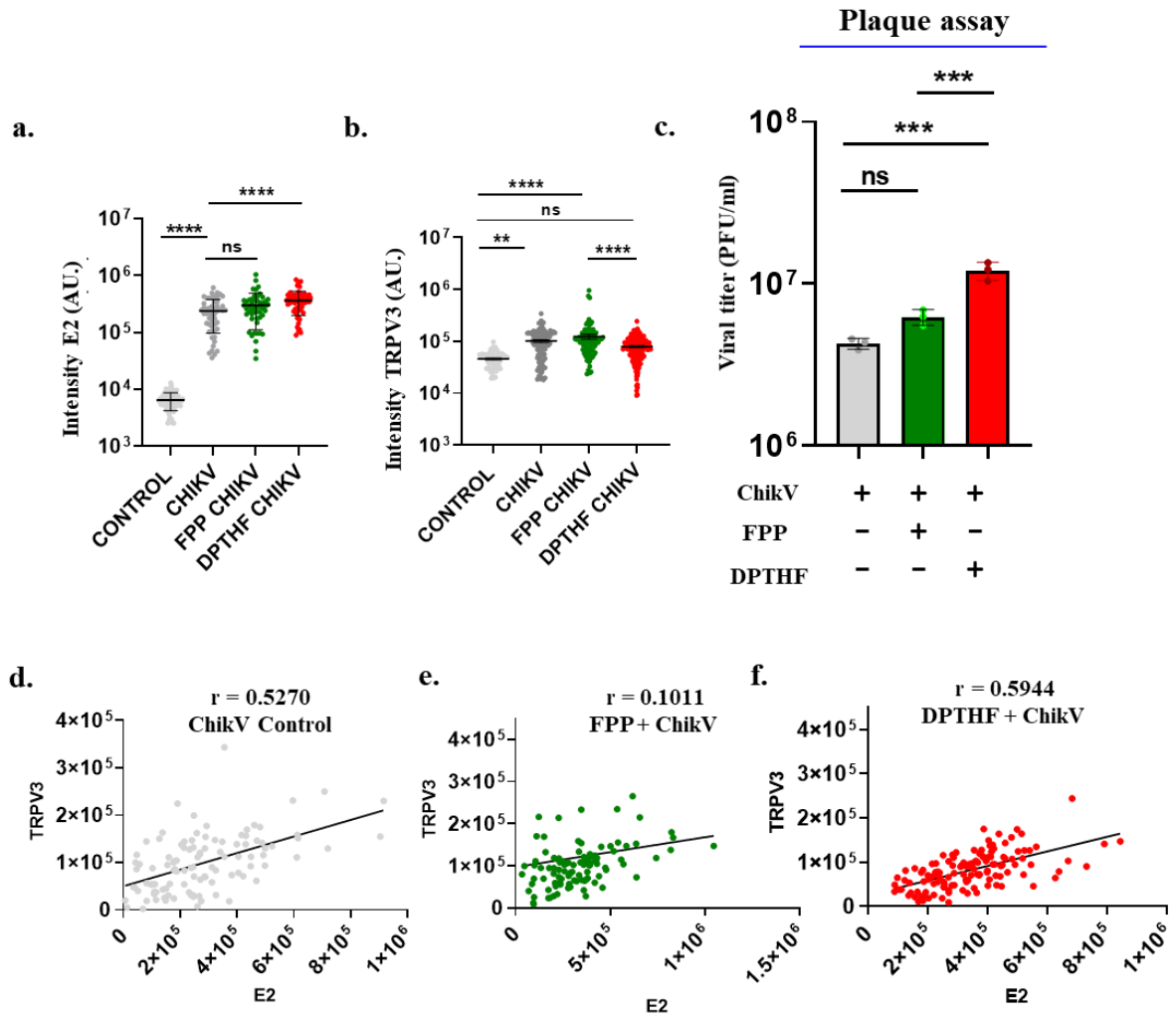

Fig 99. TRPV3 modulations affect ChikV infection. a. The graph shows the E2 protein intensity (in AU.) in TRPV3 modulated conditions along with viral infections. The condition includes TRPV3 activation by FPP(1µm) and inhibition by DPTHF (100µm) along with ChikV infections. **b.** The graph shows the TRPV3 intensity (in AU.) in TRPV3 modulations conditions along with viral infections. **c.** The graph shows viral titer upon TRPV3 modulations. It shows the significant increase in titer (PFU/ml) in TRPV3 inhibition condition. **d-e.** The graph shows correlation between TRPV3 and E2 protein in different conditions The correlation become more in case of TRPV3 inhibition with ChikV infections (r = 0.5944). Unpaired t-test, ** = p ≤0.01, *** = p ≤0.001, **** = p ≤0.0001 and ns = non-significant).

In addition, the intracellular Ca^{2+}-levels have been observed in the cells during TRPV3 modulation and ChikV infection. It has been observed that TRPV3 activation led to an influx of Ca^{2+} when ChikV was administered, and TRPV3 inhibition resulted in an undetectable Ca^{2+}-efflux (Shown in the discussion section).

Overall, these findings highlight the complex relationship between TRPV3 and ChikV infection dynamics, suggesting that TRPV3 modulation could be a potential target for therapeutic strategies against ChikV and other viral infections.

Annexure 4

7.4. Table 7. TRPV3 sequence of difference species

Species	Accession no.	TRPV3 Sequence
>Human	ACA81614.1	MKAHPKEMVPLMGKRVAAPSGNPAVLPEKRPAEITPTKKSAHFFLEIEGFEPNPTVAKTSPPVFSKPMD SNIRQCISGNCDDMDSPQSPQDDVTETPSNPNSPSAQLAKEEQRRKKGRLKKRIFAAVSEGCVEELVEL LVELQELCRRRHDEDVPDFLMHKLTASDTGKTCLMKALLNINPNTKEIVRILLAFAEENDILGRFINAE YTEEAYEGQTALNIAIERRQGDIAALLIAAGADVNAHAREAFFNPKYQHEGFYFGETPLALAACTNQP EIVQLLMEHEQTDITSRDSRGNNILHALVTVAEDFKTQNDFVKRMYDMILLRSGNWELETTRNNDGL TPLQLAAKMGKAEILKYILSREIKEKRLRSLSRKFTDWAYGPVSSSLYDLTNVDTTTDNSVLEITVYNT NIDNRHEMLTLEPLHTLLHMKWKKFAKHMFFLSFCFYFFYNITLTLVSYYRPREEEAIPHPLALTHKMG WLQLLGRMFVLIWAMCISVKEGIAIFLLRPSDLQSILSDAWFHFVFFIQAVLVILSVFLYLFAYKEYLAC LVLAMALGWANMLYYTRGFQSMGMYSVMIQKVILHDVLKFLFVYIVFLLGFGVALASLIEKCPKDNK DCSSYGSFSDAVLELFKLTIGLGDLNIQQNSKYPILFLFLLITYVILTFVLLLNMLIALMGETVENVSKES ERIWRLQRARTILEFEKMLPEWLRSRFRMGELCKVAEDDFRLCLRINEVKWTEWKTHVSFLNEDPGP VRRTADFNKIQDSSRNDSKTTLNAFEEVEEFPETSV
>Mouse	NP_659567.2	MNAHSKEMAPLMGKRTTAPGGNPVVLTEKRPADLTPTKKSAHFFLEIEGFEPNPTVTKTSPPIFSKPMD SNIRQCLSGNCDDMDSPQSPQDDVTETPSNPNSPSANLAKEEQRQKKKRLKKRIFAAVSEGCVEELRE LLQDLQDLCRRRRGLDVPDFLMHKLTASDTGKTCLMKALLNINPNTKEIVRILLAFAEENDILDRFINA EYTEEAYEGQTALNIAIERRQGDITAVLIAAGADVNAHAKGVFFNPKYQHEGFYFGETPLALAACTNQ PEIVQLLMENEQTDITSQDSRGNNILHALVTVAEDFKTQNDFVKRMYDMILLRSGNWELETMRNNDG LTPLQLAAKMGKAEILKYILSREIKEKPLRSLSRKFTDWAYGPVSSSLYDLTNVDTTTDNSVLEIIVYNT NIDNRHEMLTLEPLHTLLHTKWKKFAKYMFFLSFCFYFFYNITLTLVSYYRPREDEDLPHPLALTHKMS WLQLLGRMFVLIWATCISVKEGIAIFLLRPSDLQSILSDAWFHFVFFVQAVLVILSVFLYLFAYKEYLAC LVLAMALGWANMLYYTRGFQSMGMYSVMIQKVILHDVLKFLFVYILFLLGFGVALASLIEKCSKDKK DCSSYGSFSDAVLELFKLTIGLGDLNIQQNSTYPILFLFLLITYVILTFVLLLNMLIALMGETVENVSKES ERIWRLQRARTILEFEKMLPEWLRSRFRMGELCKVADEDFRLCLRINEVKWTEWKTHVSFLNEDPGPI RRTADLNKIQDSSRSNSKTTLYAFDELDEFPETSV
>Pygmy Chimpanzee	XP_008960843.1	MKAHPKEMVPLMGKRVAAPSGNPAVLPEKRPAEITPTKKSAHFFLEIEGFEPNPTVAKTSPPVFSKPMD SNIRQCISGNCDDMDSPQSPQDDVTETPSNPNSPSAHLAKEEQRRKKRRLKKRIFAAVSEGCVEELVEL LVELQELCRRRHDEDVPDFLMHKVTASDTGKTCLMKALLNINPNTKEIVRILLAFAEENDILGRFINAE YTEEAYEGQTALNIAIERRQGDIAAVLIAAGADVNAHAKGAFFNPKYQHEGFYFGETPLALAACTNQP EIVQLLMEHEQTDITSQDSRGNNILHALVTVAEDFKTQNDFVKRMYDMILLRSGNWELETTRNNDGL TPLQLAAKMGKAEILKYILSREIKEKRLRSLSRKFTDWAYGPVSSSLYDLTNVDTTTENSVLEITVYNT NIDNRHEMLTLEPLHTLLHMKWKKFAKHMFFLSFCFYFFYNITLTLVSYYRPREEEAVPHPLALTHKM GWLQLLGRMFVLIWAMCISVKEGIAIFLLRPSDLQSILSDAWFHFVFFVQAVLVILSVFLYLFAYKEYLA CLVLAMALGWANMLYYTRGFQSMGMYSVMIQKVILHDVLKFLFVYIVFLLGFGVALASLIEKCPKDN KDCSSYGSFSDAVLELFKLTIGLGDLNIQQNSKYPILFLFLLITYVILTFVLLLNMLIALMGETVENVSKE SERIWRLQRARTILEFEKMLPEWLRSRFRMGELCKVAEDDFRLCLRINEVKWTEWKTHVSFLNEDPGP VRRTADFNKIQDSSRNNSKTTLNAFEEIEEFPETSV
>Rat	NP_001020928.2	MNAHSKEMVPLMGKRTTAPGGNPAVLTEKRPADLTPTKKSAHFFLEIEGFEPNPTVTKTSPPIFSKPMD SNIRQCLSGNCDDMDSPQSPQDDVTETPSNPNSPSANLAKEEQRQKKKRLKKCIFAAVSEGCVRELRE LLQDLQELCRRRRGLDASDFLMHKLTASDTGKTCLMKALLNINPNTKEIVRILLAFAEENDILDRFINA EYTEEAYEGQTALNIAIERRQGDITAVLIAAGADVNAHAKGVFFNPKYQHEGFYFGETPLALAACTNQ PEIVQLLMENEQTDITSQDSRGNNILHALVTVAEDFKTQNDFVKRMYDMILLRSGNWELETMRNNDG LTPLQLAAKMGKAEILKYILGREIKEKPLRSLSRKFTDWAYGPVSSSLYDLTNVDTTTDNSVLEIIVYNT NIDNRHEMLTLEPLHTLLHMKWKKFAKYMFFLSFCFYFFYNITLTLVSYYRPREDEALPHPLALTHKM SWLQLLGRMFVLIWAMCISVKEGIAIFLLRPSDLQSILSDAWFHFVFFVQAVLVILSVFLYLFAYKEYLA CLVLAMALGWANMLYYTRGFQSMGMYSVMIQKVILHDVLKFLFVYILFLLGFGVALASLIEKCSKDK KDCSSYGSFSDAVLELFKLTIGLGDLNIQQNSTYPILFLFLLITYVILTFVLLLNMLIALMGETVENVSKE SERIWRLQRARTILEFEKMLPEWLRSRFRMGELCKVADEDFRLCLRINEVKWTEWKTHVSFLNEDPGP IRRTADSNKIQDSSRSNSKTTLYAFDELDEFPETSV
>Thirteen-Lined Ground Squirrel	XP_005337351.1	MHAHPKEMVPLVGRRTTGPSGNPVVLTEKRPAEVTPTKKSAHFFLEIEGFEPNPTVAKTSPPIFSKPMD SNIRQCISGNCDDMDSPQSPQDDVTETPSNPNSPSANLAKEEQRRKKKRLKKRIFAAVSEGCVEELVEL LAELQELCKRRRGGMDVPDFLMHKLTASDTGKTCLMKALLNINPNTKEIVRILLAFAEENDILDRFIN AEYTEEAYEGQTALNIAIERRQGDITAVLIAAGADVNAHAKGVFFNPKYQHEGFYFGETPLALAACTN QPEIVQLLMENEQTDITSQDSRGNNILHALVTVAEDFKTQNDFVKRMYDMILLRSGTWELETTRNND GLTPLQLAAKMGKAEILKYILSREIKEKPLRSLSRKFTDWAYGPVSSSLYDLTNVDTTTDNSVLEITVY NTNIDNRHEMLTLEPLHTLLHMKWKKFAKYMFFLSFCFYFFYNITLTLVSYYRPREVEALPHPLALTH KMGWLQLLGRMFVLIWATCISVKEGIAIFLLRPSDLQSILSDAWFHFVFFIQAMLVILSVFLYLFAYKEY LACLVLAMALGWANMLYYTRGFQSMGMYSVMIQKVILHDVLKFLFVYIVFLLGFGVALASLIEKCSE DNKDCSSYGSFSDAVLELFKLTIGLGDLNIQQNSTYPILFLFLLITYVILTFVLLLNMLIALMGETVENVS KESERIWRLQRARTILEFEKMLPEWLRSRFRMGELCKVAEGDFRLCLRINEVKWTEWKTHVSFLNED PGPIKRTADINKMQDSSRNNSKTTLNAFDEMDEFPETSV
>Chicken	XP_004946732.1	MIKDNKEVVPLMGKKTNPPGAPPSNQQEKKPTESTPTKKSSHFFLEIEGFESNATPNNTSPPVFSKPMD SNIRPCASANGEDMDSPQSLQDDVTEYSPNVDSCGANIAQGPEQTGARKKLKKYIFRAVSEGNVEELQ GLLAELKERSNVCTNMTVPDYLMKKFTASDTGKTCLMKALLNINNNTNQIVNMLLSFAEENGILERFI NAAYTEEAYRGQTALNIAIERRQFEITQTLIEKGADVNAHAQGIFFNPKHKHEGFYFGETALALAACTN QPDIIELLMDNTRTNIAAQDSRGNNILHALVTVAEDFKTQNDFVIRMYDMILLKSKDRNLEKVKNKEG

		LTPLQLAAKTGKLEVLKYILSREIRDKPNRSLSRKFTDWAYGPVQSSLYDLTELDTTADNSVLEIIVYNT NIGNRHEMLTLEPLNSLLRMKWKRFARHMLFMSCCFYFLYNVTLTLVSYHRPNENEAPPYPLALTRG VGWLQLSGQVMVMLGAIFLAIKESVAIFLLRPSDLQSILSDAWFHFAFFIQAMLVIFSVFLYLSSYKEHL VCLVLAMALGWANMLYFTRGFQSMGIYSVMIQKVILNDVIKFLVVYIVFLLGFGVALAALIETCQNGG ECLSNSSLGPVLMDLFKLTLGLGDLEIQQNSKYPVLFLLLLITYVVLTFVLLLNMLIALMGETVEDISKE SEHIWKLQRARTILEFEKFLPKSLRKKFQLGERCKVAENDTRVCLRINEVRWTEWKTHVSFINEDPGPT DPSKVQDNSRTNSKNTLNTFEETDDLPETSL
>Blind Mole Rat	XP_008853834.1	MNAHSKEMVPLIGRRATAPSGNPAVLTEKRAAELTPTKKSAHFFLEIEGFEPNPAVTKTSPPIFSKPMDS NIRQCISGNCDDMDSPQSPQDDVTETPSNPNSPSANLAKEEQRRKKKRLKKRIFAAVSEGCVEELVEAL LELQELCKRRRGLDVPDFLMHKLTASDTGKTCLMKALLNINPSTKEIVRILLAFAEENDILDRFINAEY TEEAYEGQTALNIAIERRQGDITALLIAAGADVNAHAKGVFFNPKYQHEGFYFGETPLALAACTNQPEI VQLLMENEQTDITSQDSRGNNILHALVTVAEDFKTQNDFVKRMYDMILLRSSNWELETMRNNDGLTP LQLAAKMGKAEILKYILSREIKEKPLRSLSRKFTDWAYGPVSSSLYDLTNVDTTTDNSVLEIIVYNTNID NRHEMLTLEPLHTLLHMKWKKFAKYMFFLSFCFYFFYNITLTLVSYYRPREEEALPHPLALTHKMGW LQLLGRMFVLIWATCISVKEGIAIFLLRPSDLQSILSDAWFHFVFFVQAVLVILSVFLYLFAYKEYLACLV LAMALGWANMLYYTRGFQSMGMYSVMIQKVILHDVLKFLFVYIVFLLGFGVALASLIEKCSKDNKD CSSYGSFSDAVLELFKLTIGLGDLNIQQNSTYPILFLFLLITYVILTFVLLLNMLIALMGETVENVSKESE RIWRLQRARTILEFEKMLPEWLRSRFRMGELCKVADEDFRLCLRINEVKWTEWKTHVSFLNEDPGPIR RTADLNKIQDSSRSNSKTTLNAFDELDEFPETSV
>Bactrian Camel	XP_010948530.1	MNAHPKEMVPFMGRRATIASGSPAIMQEKRPADITPTKKSAHFFLEIEGFEPNPTVTKTSPPIFSKPMDS NIRQCISGNCDDMDSPQSPQDDATETPSNPNSPSANLAKEERRRKKKRLKKRIFAAVSEGCVEELLELL VELKELCRWRRESDVPDFLMHKLTAMDTGKTCLMKALLNINPNTKEILRILLAFADENDILDRFINAE YTEEAYEGQTALNIAIERRQGDITAALIAAGADVNAHAKGVFFNPKYQHEGFYFGETPLALAACTNQP EIVQLLMENEQTDITSQDSRGNNILHALVTVAEDFKTQNDFVKRMYDMILRRGGNWELETMRNNDG LTPLQLAAKMGKAEILKYILSREIKEKRLRSLSRKFTDWAYGPVSSSLYDLTNVDTTTDNSVLEIIVYNT NIDNRHEMLTLEPLHTLLHMKWKKFAKYMFFLSFCFYFFYNITLTLVSYYRPREEEALPHPLALTHKM GWLQLLGRMFVLIWAMCISVKEGIAIFLLRPSDLQSILSDAWFHFVFFIQAVLVILSVFLYLFAYKEYLA CLVLAMALGWANMLYYTRGFQSMGMYSVMIQKVILHDVLKFLFVYIVFLLGFGVALASLIEKCPKDH EDCSSYGSFSDAVLELFKLTIGLGDLNIQQNSKYPILFLFLLITYVILTFVLLLNMLIALMGETVEDVSKE SERIWRLQRARTILEFEKMLPEWLRSRFRMGELCKVAEEDFRLCLRINEVKWTEWKTHVSFLNEDPGP GRRTADFSKLQDSSRSNSKTTLNAFGEIDEFPETSV
>Prairie Vole	XP_005349656.1	MSWAPAMNAHSKEMVPLMGRRTTAPSGNSVVLTEKRPADLTPTKKSAHFFLEIEGFEPNPTVTKTSLPI FSKPMDSNIRQCMSGNCDDMDSPQSPQDDVTETPSNPNSPSVNLAKEEQRQKKKRLKKRIFAAVSEG CVGELQELLQELEELCRRRRGLDVSDFLMHKLTASDTGKTCLMKALLNINPNTKEIVRILLAFAEENGI LGRFINAEYTEEAYEGQTALNIAIERRQGDITAVLIAAGADVNAHAKGIFFNPKNQHEGFYFGETPLAL AACTNQPEIVQLLMENEQTDITSQDSRGNNILHALVTVAEDFKTQNDFVKRMYDMILLRSGNWELET MRNNDGLTPLQLAAKMGKAEILKYILSREIKEKPLRSLSRKFTDWAYGPVSSSLYDLTNVDTTTDNSV LEIIVYNTNIDNRHEMLTLEPLHTLLHMKWKKFAKYMFFLSFCFYFFYNITLTLVSYYRPREDKDLPHP LALTHKMSWLQLLGRMFVLIWATCISVKEGIAIFLLRPSDLQSILSDAWFHFVFFVQAVLVILSVFLYLF AYKEYLACLVLAMALGWANMLYYTRGFQSMGMYSVMIQKVILHDVLKFLFVYILFLLGFGVALASLI EKCSKDKKDCSSYGSFSDAVLELFKLTIGLGDLNIQQNSTYPILFLFLLITYVILTFVLLLNMLIALMGET VENVSKESERIWRLQRARTILEFEKMLPEWLRSRFRMGELCKVADEDFRLCLRINEVKWTEWKTHVS FLNEDPGPIRRTADVNKIQDSSRSNSKTTLYAFDELEEFPETSV
>Prairie Deer Mouse	XP_006992285.1	MNAHSKEMVPLMGRRTTAPSGNSVVLTEKRPADLTPTKKNAHFFLEIEGFDPNPTVTKTSPPIFSKPMD SNIRQCHSGNCDDMDSPQSPQDDVTETPSNPNSPSANLAKEEQRQKKKRLKKRIFTAVSEGCVEELWG LLQELQELCKRRRGLDVSDFLMHKLTASDTGKTCLMKALLNINPNTKEIVRILLAFAEENGILDRFINA EYTEEAYEGQTALNIAIERRQGDITAVLIAAGADVNAHAKGVFFNPKYQHEGFYFGETPLALAACTNQ PEIVQLLMENEQTDITSQDSRGNNILHALVTVAEDFKTQNDFVKRMYDMILLRSGNWELETMRNNDG LTPLQLAAKMGKAEILKYILSREIKEKPLRSLSRKFTDWAYGPVSSSLYDLTNVDTTTDNSVLEIIVYNT NIDNRHEMLTLEPLHTLLHMKWKKFAKYMFFLSFCFYFFYNITLTLVSYYRPRDDEDLPHPLALAHKM SWLQLLGRMFVLIWATCISVKEGIAIFLLRPSDLQSILSDAWFHFVFFVQAVLVILSVFLYLFAYKVYLA CLVLAMALGWANMLYYTRGFQSMGMYSVMIQKVILHDVLKFLFVYILFLLGFGVALASLIEKCAKDK KDCSSYGSFSDAVLELFKLTIGLGDLNIQQNSTYPILFLFLLITYVILTFVLLLNMLIALMGETVENVSKE SERIWRLQRARTILEFEKMLPEWLRSRFRMGELCKVADEDFRLCLRINEVKWTEWKTHVSFLNEDPGP IRRTADLSKIQDSSRCNSKTTLYAFDELDEFPETSV
>Golden Hamster	XP_005067481.1	MNAHPKEMVPLMGRRTTAPSGNSVVLTEKRPADLTPTKKSAHFFLEIEGFEPNPTVTKTSPPIFSKPMD SNIRQCISGNCDDMDSPQSPQDDVTETPSNPNSPSANLAKEEQRQKKKRLKKRIFAAVSEGCVGELRD LLQELQELCKRRRGLDVPDFLMHKLTASDTGKTCLMKALLNINPNTKEIVRTLLAFAEENDILDRFINA EYTEEAYEGQTALNIAIERRQGDITAVLIAAGADVNAHAKGVFFNPKYQHEGFYFGETPLALAACTNQ PEIVQLLMENEQTDITSQDSRGNNILHALVTVAEDFKTQNDFVKRMYDMILLRSGNWELETMRNNDG LTPLQLAAKMGKAEILKYILSREIKEKPLRSLSRKFTDWAYGPVSSSLYDLTNVDTTTDNSVLEIIVYNT NIDNRHEMLTLEPLHTLLHMKWKKFAKYMFFLSFCFYFFYNITLTLVSYYRPREDEALPHPLALTHKM SWLQLLGRMFVLIWATCISVKEGIAIFLLRPSDLQSILSDAWFHFVFFVQAVLVILSVFLYLFAYKEYLAC LVLAMALGWANMLYYTRGFQSMGMYSVMIQKVILHDVLKFLFVYILFLLGFGVALASLIEKCSKDKK DCSSYGSFSDAVLELFKLTIGLGDLNIQQNSTYPILFLFLLITYVILTFVLLLNMLIALMGETVENVSKES ERIWRLQRARTILEFEKMLPEWLRSRFRMGELCKVADEDFRLCLRINEVKWTEWKTHVSFLNEDPGPI RRTADLNKIQDSSRSNSKTTLYAFDELDEFPETSV
>Lesser Egyptian Jerboa	XP_004672442.1	MNAHPKEMVPLMGRRTTAPSGNSVVLTEKRPAELTPTKKSAHFFLEIEGFEPNPTVTKTSPPIFSKPMD SNIRQCISGNCDDMDSPQSPQDDVTETPSNPNSPSANLAKEEQRQKKKHLKKYIFMAVSEGCVEELME LLLELQELCSRRRGLDVPDFLMHKLTASDTGKTCLMKALLNINPSTKEIVRILLAFAEENGILDRFINAE YTEEAYEGQTALNIAIERRQGDITALLIAAGADVNAHAKGVFFNPKYQHEGFYFGETPLALAACTNQP EIVQLLMENDQTDITSQDSRGNNILHALVTVAEDFRTQNDFVKHMYDMILLRSGNWELETMRNNDGL TPLQLAAKMGKAEILKYILSREIKEKPLRSLSRKFTDWAYGPVSSSLYDLTNVDTMTDNSVLEIIVYNT NIDNRHEMLTLEPLHTLLHMKWKKFAKYMFFLSFCFYFFYNITLTLVSYYRPREEEALPHPLALTHKM GWLQLLGRMFVLIWATCISVKEGIAIFLLRPSDLQSILSDAWFHFVFFVQAVLVILSVFLYLFAYKEYLA

		CLVLAMALGWGNMLYYTRGFQSMGMYSVMIQKVILHDVLKFLFVYILFLLGFGVALASLIEKCSKDK KDCSSYGSFSDAVLELFKLTIGLGDLNIQQNSTYPILFLFLLITYVILTFVLLLNMLIALMGETVENVSKE SERIWRLQRARTILEFEKMLPEWLRSRFRMGELCKVAEGDFRLCLRINEVKWTEWKTHVSFLNEDPGP IRRTADFNKIQDSSRSNSKTTLNAFDEIDEFPETSV
>Degu	XP_004638337.1	MNAHPREMVPLMGRKANISSGNPAVLTEKRPAEVTPTKKSAHFFLEIEGFEPNPTVAKTSPPVFSKPMD SNIRQCISGNCDDMDSPQSPQDDVTETPSNPNSPSANQAKEEQRRKKKRLKKRIFTAVSEGFVEELVEL LVELQELCKRRRGLDVSDFLMHKLTASDTGKTCLMKALLNINPNTKEIVHILLTFADENDILDQFVNAE YTEEAYEGQTALNIAIERRQGDIAAVLIAAGADVNAHAKGVFFNPKYQHEGFYFGETPLALAACTNQP EIVQLLMENEQTDITSQDSRGNNILHALVTVAEDFRTQNDFVKHMYDMILLRSGNWELETMRNNDGL TPLQLAAKMGKAEILKYILSREIKEKPLRSLSRKFTDWAYGPVSSSLYDLTNVDTTTDNSVLEIIVYNTN IDNRHEMLTLEPLHTLLHMKWKKFAKYMFYLSFCFYFFYNITLTLVSYYRPREPEDLPHPLALSHNMG WLQLLGRMFVLIWATCISVKEGIAIFLLRPSDLQSILSDAWFHFVFFIQAVLVILSVFLYLFAYKEYLAFL VLAMALGWANMLYYTRGFQSMGMYSVMIQKVILHDVLKFLFVYIVFLLGFGVALASLIEKCSDDNK DCSSYGSFSDAVLELFKLTIGLGDLKIQQNSTYPILFLFLLITYVILTFVLLLNMLIALMGETVENVSKES ERIWRLQRARTILEFEKMLPEWLRSRFRMGELCKVAEDDFRLCLRINEVKWTEWKTHVSFLNEDPGPI RRTVDFNKIQDSSRSNSKTTLNAFEEIDEFPETSV
>Naked Mole-Rat	XP_004857266.1	MNAHPKEMVPLMGRKVNVASGNPAVLTEKRPAEVTPTKKSAHFFLEIEGFEPNPTITKTSPPIFSKPMD SNIRQCLSGNCEDMDSPQSPQDDVTETPSNPNSPSANQAKEEQRRKKKRLKKCIFTAVSEGCVEELVEL LVELQELCKRRCGLDVSDFLMHKLTASDTGKTCLMKALLNINPNTKEIVRILLTFADENDILDQFINAE YTEEAYEGQTALNIAIERRQGDIAAVLIAAGADVNAHAKGVFFNPKSQHEGFYFGETPLALAACTNQP EIVQLLMENEQTDITSQDSRGNNILHALVTVAEDFKTQNDFVKRMYDMILLRSGNWELETMRNNDGL TPLQLAAKMGKAEILKYILSREIKEKPLRSLSRKFTDWAYGPVSSSLYDLTNVDTTTDNSVLEIIVYNTN IDNRHEMLTLEPLHTLLHMKWKKFAKYMFFLSFCFYFFYNITLTLVSYYRPREKEDLPHPLALSHKMG WLQLLGRMFVLIWATCISVKEGIAIFLLRPSDLQSILSDAWFHFVFFIQAVLVILSVFLYLFAYKEYLACL VLAMALGWANMLYYTRGFQSMGMYSVMIQKVILHDVLKFLFVYIVFLLGFGVALASLIEKCSDDSED CSSYGSFSDAVLELFKLTIGLGDLKIQQNSTYPILFLFLLITYVILTFVLLLNMLIALMGETVENVSKESE RIWRLQRARTILEFEKMLPECLRSRFRMGELCKVAEDDFRLCLRINEVKWTEWKTHVSFLNEDPGPIR RTVDFNKIQDSSRSNSKTTLNAFEEIDEFPETSV
>Aardvark	XP_007935665.1	MNTHPKEMVPLMGRRVTAPSGNPAVLQEKRPTELTPTKKSAHFFLEIEGFEPNPTVAKTSPPIFSKPMDS NIRQCISGNCDDMDSPQSGQDDVTETPSNPNSPSANLAKEEHRRNKKRLKKRIFTAVSEGCVEELVELL VELQELCRRRRGLDVPDFLMHKLTASDTGKTCLMKALLNINPNTKEIVRILLTFAEENDILDRFINAEY TEEAYEGQTALNIAIERRQGDITAALIAAGADVNAHAKGVFFNPKYQHEGFYFGETPLALAACTNQPE IVQLLMENEQTDITSQDSRGNNILHALVTVAEDFKTQNDFVKHMYDMILLRSRNWELETMCNNDGLN PLQLAAKMGKAEILKYILSREIKEKPLRSLSRKFTDWAYGPVSSSLYDLTDVDTMTDNSVLEIIVYNTNI DNRHEMLTLEPLHTLLHMKWKKFAKYMFFLSFCFYFFYNITLTLVSYYRPREEEALPHPLALTHKMG WLQLLGRMFVLIWAMCISVKEGIAIFLLRPSDLQSILSDAWFHFVFFIQAVLVILSVFLYLFAYKEYLAC LVLAMALGWANMLYYTRGFQSMGMYSVMIQKVILHDVLKFLFVYIVFLLGFGVALASLIEKCAPDSS NCSSYGSFGDAVLELFKLTIGLGDLNIQQNSKYPVLFLFLLITYVILTFVLLLNMLIALMGETVENISKES ERIWRLQRARTILEFEKMLPEWLRSRFRMGELCKVAEEDFRLCLRINEVKWTEWKTHVSFLNEDPGP VRRTADFNKIQNSSRSNSKTTLNAFDEIDEFPETSV
>Cape Golden Mole	XP_006863324.1	MNAHPKEMVPLMGRRAVAPSGNPAILQEKRPTELTPTKKSAHFFLEIEGFEPNPTVNKTSPPVFSKPMD SNIRQCISGNCDDMDSPQSPQDDVTETPSNPNSPSANLAKEEQRRNKKRLKKRIFAAVSEGCVEELVEL LMELQELSRRRRRGLDGPDFLMHKLTASDTGKTCLMKALLNINSNTKEIVRILLTFAEENGILTRFINAE YTEEAYEGQTALNIAIERRQGDITAALIAAGADVNAHAKGVFFNPKYQHEGFYFGETPLALAACTNQP EIVQLLMENEQTDITSQDSRGNNILHALVTVAEDFKTQNDFVKRMYDMILLRSRNWDLETMCNNEGL NPLQLAAKMGKAEVLKYILSREIKEKPLRSLSRKFTDWAYGPVSSSLYDLTDVDTTTDNSVLEIIVYNT NIDNRHEMLTLEPLHTLLRMKWKKFAKYMFFLSFCFYFFYNITLTLVSYYRPREEEALPHPLALTHKM GWLQLLGRMFVLIWAMCISVKEGIAIFLLRPSDLQSILSDAWFHFVFFIQAVLVILSVFLYLFAYKEYLA CLVLAMALGWANMLYYTRGFQSMGMYSVMIQKVILHDVLKFLFVYIVFLLGFGVALASLIEKCSKEN NDCSSYGSFSDAVLELFKLTIGLGDLNIQQNSKYPILFLFLLITYVILTFVLLLNMLIALMGETVENISKE SERIWRLQRARTILEFEKMLPEWLRSRFRMGELCKVAEDDFRLCLRINEVKWTEWKTHVSFLTEDPGP VKRTADLNKIQNVSRSNSKTTLNAFDEIDEFPETSV
>Cape Elephant Shrew	XP_006899806.1	MNTQSKETVPLMGRRAAAPSGNPAIMQEKRPTELTPTKKSAHFFLEIEGFEPNPIVAKTSPPIFSKPMDS NIRQCISGNCDDMDSPQSPQDDVTETPSNPNSPSANLAKEEQRRNKKRLKKRIFAAVSEGCVEELVELL LELQELCRRRRGLDVPDFLMHKLTASDTGKTCLMKALLNINPNTKEIVRILLAFAEENDILDRFINAEY TEEAYEGQTALNIAIERRQGDITAALIAAGADVNAHAKGVFFNPKYQHEGFYFGETPLALAACTNQPE IVQLLMENEQTDIMSQDSRGNNILHALVTVAEDFKTQNDFVKRMYDMILLRSRNWELETMCNNDGL NPLQLAAKMGKAEILKYILSREIKEKPLRSLSRKFTDWAYGPVSSSLYDLTNVDTVTDNSVLEIIVYNT NIDNRHEMLTLEPLHTLLRMKWKKFAKYMFFLSFCFYFFYNITLTLVSYYRPREEEALPHPLALTHNLA WLQLLGRMFVLIWATCISVKEGIAIFLLRPSDLQSILSDAWFHFVFFIQAVLVILSVFLYLFAYKEYLACL VLAMALGWANMLYYTRGFQSMGMYSVMIQKVILHDVLKFLFVYIVFLLGFGVALASLIEKCPKDSNE CSSYGSFGDAVLELFKLTIGLGDLNIQQNSKYPILFLFLLITYVILTFVLLLNMLIALMGETVENISKESE RIWRLQRARTILEFEKMLPEWLRSRFRMGELCKVAEEDFRLCLRINEVKWTEWKTHVSFLTEDPGPVR RTADISKIQNSSRSNSKTTLNAFDEIDDFPETSV
>Platypus	XP_001508712.2	MNKTQKELIPLMGKKTNPPSSASAGLLEKKPSEVTPTKKSSHFFLEIEGFEPNPAVSKPSPPIFSKPMDS NIRQCISGNCEDMDSPQSPQDDITETPSNPNSPCVNLAREQNRNKKKLKKCIFAAVSEGNVEELNSLLV ELKELSKRRRNMDIQDYLMHKFTASDTGKTCLMKALLNINPNTKEIVRHLLSFAEENGILERFINAEYT EEAYKGQTALNIAIERRQCEITETLIEKGADVNVQAKGLFFNPKYKHEGFYFGETPLALAACTNQPEIV QMLMDNNKTDIASQDSRGNTILHALVTVAEDFKTQNDFVKQMYDRILLRSKNMALETMQNNDGLTP LQLAAKMGKSEILKYILSREIKEKPKRSLSRKFTDWAYGPVSSSLYDLTKVDTTTDNSVLEIIVYNTNID NRHEMLTLEPLHTLLRMKWKKFAKYMFFMSFCLYFFYNITLTLVSYYRPREEEALPHPLALTHKMGW LQLLGRMFVMIWATCITVKEGIAIFLLRPSDLQSILSDAWFHFAFFIQAVLVILSVFLYLFAYKEYLACLV LAMALGWANMLYYTRGFQSMGMYSVMIQKVILHDVLKFLFVYIVFLLGFGVALASLIEKCPQNDSEC SSYGSFSDAVLELFKLTIGLGDLDIQQNSKYPILFLFLLITYVILTFVLLLNMLIALMGETVENISKESERI

		WRLQRARTILEFEKLLPEWLRSKFRLGELCKVADNDFRLCLRINEVKWTEWKTHVSFISEDPGPGRHS GTFGFNKIQDVSRSNSKTTLNAFDEIEDFPETSV
>Northern Fulmar	XP_009577964.1	MIKDNNEIIPLMGKKTNPSGIPPSNQQEKKPTESTPTKKSSHFFLEIDGFESNATPNNTSPPVFSKPMDSN IRPCASGNGEDMDSPQSLQDDATEYSPNVDSCCANISQGPEQTSARKKLKRYIFRAVSEGNIEELQCLL AELKERSNACTNMTVPDYLMKKFTASDTGKTCLMKALLNINQNTNEIVNTLLSFAEENGIMERLINA AYTEEAYKGQTALNIAIERRQYEITQSLIEKGADVNAYAQGIFFNPKHKHEGFYFGETALALAACTNQP DIIQLLMDNTRTNITSQDSRGNNILHALVTVAEDFKTQNDFVIRMYDMILLKSKDRNLEKTKNKEGLTP LQLAAKTGKLEILKYILSREIRDKPNRSLSRKFTDWAYGPVQSSLYDLTELDTTTDNSVLEIIVYNTNIG NRHEMLTLEPLNSLLRMKWKKFARHMFFMSCCFYFLYNVTLTLVSYHRPNENEAPPYPLALTRGVGW LQLSGQVMVMLGAIFLAIKESVAIFLLRPSDLQSILSDAWFHFAFFIQALLVIFSVFLYLFSYKEHLVCLV LAMALGWANMLYFTRGFQSMGIYSVMIQKVILQDVIKFLVVYIVFLLGFGVALAALIETCQDGSECHS NSSLGPVLMDLFKLTLGLGDLEIQQNSKYPVLFLLLLITYVVLTFVLLLNMLIALMGETVEDISKESEHI WKLQRARTILEFEKFLPKCLRKKFQLGERCKVAENDTRVCLRINEVKWTEWKTHVSFINEDPGPTDPS KVQDNSRTNSKNTLNTFEEMDDLPETSV
>Adelie Penguin	XP_009326905.1	MIKDNNEIIPLMGKKTNPSGIPPSNQQEKKPTESTPTKKSSHFFLEIDGFESNATPNNTSPPVFSKPMDSN IRPCASGNGEDMDSPQSLQDDATEYSPNVDSCCANLSQGPEQTSARKKLKRYIFRAVSEGNVEELQCL LAELKERSNACTNMTVPDYLMKKFTASDTGKTCLMKALLNINQNTNEIVNMLLSFAEENGILERFINA AYTEEAYKGQTALNIAIERRQYEVTQSLIEKGADVNAHAQGIFFNPKHKHEGFYFGETALALAACTNQ PDIIQLLMDNTRTNITSQDSRGNNILHALVTVAEDFKTQNDFVIRMYDMILLKSKDRNLETTKNKEGLT PLQLAAKTGKLEILKYILSREIRDKPNRSLSRKFTDWAYGPVQSSLYDLTELDTTADNSVLEIIVYNTNI GNRHEMLTLEPLNSLLRMKWKKFARHMFFMSCCFYFIYNVTLTLVSYHRPNENEAPPYPLALTHGVG WLQLSGQVMVMLGAIFLAIKESVAIFLLRPSDLQSILSDAWFHFAFFIQALLVIFSVILYLFSYKEHLVCL VLAMALGWANMLYFTRGFQSMGIYSVMIQKVILQDVIKFLVVYIVFLLGFGVALAALIETCQDGGECH SNSSLGPVLMDLFKLTLGLGDLEIQQNSKYPVLFLLLLITYVVLTFVLLLNMLIALMGETVEDISKESEH IWKLQRARTILEFEKFLPKCLRKKFQLGERCKVAENDTRVCLRINEVKWTEWKTHVSFINEDPGPTDP SKVQDNSRTNSKNTLNTFEEMDDLPETSV
>Emperor Penguin	XP_009276461.1	MIKDNNEIIPLMGKKTNPSGIPPSNQQEKKPTESTPTKKSSHFFLEIDGFESNATPNNTSPPVFSKPMDSN IRPCASGNGEDMDSPQSLQDDATEYSPNVDSCCANLSQGPEQTSARKKLKRYIFRAVSEGNVEELQCL LAELKERSNACTNMTVPDYLMKKFTASDTGKTCLMKALLNINQNTNEIVNMLLSFAEENGILERFINA AYTEEAYKGQTALNIAIERRQYEVTQSLIEKGADVNAHAQGIFFNPKHKHEGFYFGETALALAACTNQ PDIIQLLMDNTRTNITFQDSRGNNILHALVTVAEDFKTQNDFVIRMYDMILLKSKDRNLETTKNKEGLT PLQLAAKTGKLEILKYILSREIRDKPNRSLSRKFTDWAYGPVQSSLYDLTELDTTADNSVLEIIVYNTNI GNRHEMLTLEPLNSLLRMKWKKFARHMFFMSCCFYFVYNVTLTLVSYHRPNENEAPPYPLALTHGVG WLQLSGQVMVMLGAIFLAIKESVAIFLLRPSDLQSILSDAWFHFAFFIQALLVIFSVFLYLFSYKEHLVCL VLAMALGWANMLYFTRGFQSMGIYSVMIQKVILQDVIKFLVVYIVFLLGFGVALAALIETCQDGGECH SNSSLGPVLMDLFKLTLGLGDLEIQQNSKYPVLFLLLLITYVVLTFVLLLNMLIALMGETVEDISKESEH IWKLQRARTILEFEKFLPKCLRKKFQLGERCKVAENDTRVCLRINEVKWTEWKTHVSFINEDPGPTDP SKVQDNSRTNSKNTLNTFEEMDDLPETSV
>Great Cormorant	XP_009501827.1	MIKDNNEIIPLMGKKTNPSGIPPSNQQEKKPTESTPTKKSSHFFLEIDGFESNATPNNTSPPVFSKPMDSN IRPCASGNGEDMDSPQSLQDDATEYSPNVDSCCANISQGPEQTSARKKLKKYIFWAVSEGNIEELQCLL AELKERSNACTNMTVPDYLMKKFTAVDTGKTCLMKALLNINENTKEIVNALLSFAEENGILERFINAA YTEEAYKGQTALNIAIERRQYEITQSLIEKGADVNAHAQGIFFNPKHKHEGFYFGETALALAACTNQP DIIQLLMDNTRTNITSQDSRGNNILHALVTVAEDFKTQNDFVIRMYDMILLKSKDRNLEKTKNKEGLTP LQLAAKTGKLEILKYILSREIRDKPNRSLSRKFTDWAYGPVQSSLYDLTELDTTADNSVLEIIVYNTNIG VRSDMKCLEPLNSLLRMKWKKFARHMFFMSCCFYFLYNITLTLVSYHRPNEKEAPPYPLALTRGVGW LQLLGQVMVMLGAIFLAIKESVAIFLLRPSDLQSILSDAWFHFAFFIQALLVIFSVFLYLFSYKEHLVCLV LAMALGWANMLYFTRGFQSMGIYSVMIQKVILQDVIKFLVVYIVFLLGFGVALAALIETCQDGSECHS NSSLGPVLMDLFKLTLGLGDLEIQQNSKYPVLFLLLLITYVVLTFVLLLNMLIALMGETVEDISKESEHI WKLQRARTILEFEKFLPKCLRKKFQLGERCKVAENDTRVCLRINEVKWTEWKTHVSFINEDPGPTDPS KVQDNSRTNSKITLNTFEEMDDLPETSV
>Little Egret	XP_009632246.1	MIKDNNEIIPLMGKKSNPSGIPPSNQQEKKTTEGTPTKKSSHFFLEIDGFESNTTSNNTSPPVFSKPMDS NIRPCASGNGEDMDSPQSLQDDATEYSPNVDSCCANISQGPEQTSGRKKLKRYIFRAVSEGNIEELQCL LAELKERSNACTNMTVPDYLMKKFTASDTGKTCLMKALLNISQNTNEIVNTLLSFAEENGILERFINA AYTEEAYKGQTALNIAIERRQYEITQSLIEKGADVNAHAQGIFFNPKHKHEGFYFGETALALAACTNQP DIIQLLMDNTRTNISSQDSRGNNILHALVTVAEDLKTQNDFVIRMYDMILLKSKDRYLETTRNKEGLTP LQLAAKTGKLEILKYILSREIRDKPNRSLSRKFTDWAYGPVQSSLYDLTELDTTADNSVLEIIVYNTNIG NRHEMLTLEPLNSLLRMKWKKFARHMFFMSCCFYFLYNITLTLVSYHRPNENEAPPYPLALTRGVGW LQLSGQVMVMLGAIFLAIKESVAIFLLRPSDLQSILSDAWFHFAFFIQALLVIFSVFLYLFSYKEHLVCLV LAMALGWANMLYFTRGFQSMGIYSVMIQKVILQDVIKFLVVYIVFLLGFGVALAALTETCPGGSECHS NSRLGPVLMDLFKLTLGLGDLEIQQNSKYPVLFLLLLITYVVLTFVLLLNMLIALMGETVEDISKESEHI WKLQRARTILEFEKFLPKRLRKKFQLGERCKVAENDTRVCLRINEVKWTEWKTHVSFINEDPGPTDPS KVQDNSRTNSKNTLNTFEETDDLPETSV
>Dalmatian Pelican	XP_009477903.1	MIKDNNEIIPLMGKKTNPSGIPPSNQQEKKPTESTPTKKSSHFFLEIDGFESNVTPNNTSPPVFSKPMDS NIRPCASGNGEDMDSPQSLQDDATEYSPNVDSCCANISQGPEQTSARKKLKRYIFRAVSEGNIEELQCL LAELKERSNACTNMTVPDYLMKKFTASDTGKTCLMKALLNINQNTNEIVNTLLSFAEENGILERFINA AYTEEAYKGQTALNIAIERRQYEITQSLIEKGADVNAHAQGIFFNPKHKHEGFYFGETALALAACTNQP DIIQLLMDNTRTNITSQDSRGNNILHALVTVAEDFKTQNDFVIRMYDMILLKSKDRNLETTKNKEGLTP LQLAAKTGKLEILKYILSREIRDKPNRSLSRKFTDWAYGPVQSSLYDLTELDTTADNSVLEIIVYNTNIG NRHEMLTLEPLNSLLRMKWKKFARHMFFMSCCFYFLYNITLTLVSYHRPNENEAPPYPLALTRGVGW LQLLGQVMVMLGAIFLAIKESVAIFLLRPSDLQSILSDAWFHFAFFIQALLVIFSVFLYLFSYKEHLVCLV LAMALGWANMLYFTRGFQSMGIYSVMIQKVILQDVIKFLVVYIVFLLGFGVALAALIETCQGGSECHS NSSLGPVLMDLFKLTLGLGDLEIQQNSKYPVLFLLLLITFVVLTFVLLLNMLIALMGETVEDISKESEHI WKLQRARTILEFEKFLPKCLRKKFQLGERCKVAENDTRVCLRINEVKWTEWKTHVSFINEDPGPTDPS KVQDNSRTNSKNTLNMFEETDDLPETSV

>Crested Ibis	XP_009462803.1	MIKDSNEIIPLMGKKTNPSGIPPSNQQEKKPTESTPTKKSSHFFLEIDGFESNTTPNNTSPPVFSKPMDSNIRPCASGNGEDMDSPQSLQDDATEYSPNIDSCCANISQGPEQTSARKKLKRYIFRAVSEGNIEELQCLLAELKERSNACTNMTVPDYLMKKFTASDTGKTCLMKALLNINQNTNEIVNTLLSFAEENGILERFINAAYTEEAYKGQTALNIAIERRQYEITENLIEKGADVNAQAKGIFFNPKHKHEGFYFGETALALAACTNQPDIIQLLMDNTRTNITSQDSRGNNILHALVTVAEDFKTQNDFVIRMYDMILLKSKDRNLETTKNKEGLTPLQLAAKTGKLEILKYILSREIRDKPNRSLSRKFTDWAYGPVQSSLYDLTELDTTADNSVLEIIVYNTNIGNRHEMLTLEPLNSLLRMKWKKFARHMFFMSCCFYFLYNITLTLVSYHRPNENEAPPYPLALTRQVGWLQLSGQVMVMLGAIFLAIKESVAIFLLRPSDLQSILSDAWFHFAFFIQALLVIFSVFLYLFSYKEHLVCLVLAMALGWANMLYFTRGFQSMGIYSVMIQKVILQDVIKFLVVYIVFLLGFGVALAALIETCQDGSECHSNSSLGPVLMDLFKLTLGLGDLEIQQNSKYPVLFLLLLITFVVLTFVLLLNMLIALMGETVEDISKESEHIWKLQRARTILEFEKFLPKCLRKKFQLGERCKVAENDTRVCLRINEVKWTEWKTHVSFINEDPGPTDPSKVQDNSRTNSKTTLNTFEEMDDLPETSV
>Golden-Collared Manakin	XP_008928724.1	MIKDNNEVVPLMGKKTNPSGIPPSNQQEKKVTESTPTKKSSHFFLEIDGFESNATPNNTSPPVFSKPMDSNIRPCASGNGEDMDSPQSLQDDATEYSPNVDSCCANISQGPEQTSARKKLKRFLFRAVSEGNVEELQCLLGELKERSRACTNMTVPDYLMKKFTASDTGKTCLMKALLNINENTNEIVNMLLSFAEENGILERFINAAYTEEAYKGQTALNIAIERRQYEITQSLIEKGADVNAHAQGIFFNPKHKHEGFYFGETALALAACTNQPDIIQLLMDNARTNISSQDSRGNNILHALVTVAEDSKTQNDFVIRMYDMILLKSKDKNLETTKNKEGLTPLQLAAKTGKLEILKYILSREIREKPNRSLSRKFTDWAYGPVQSSLYDLTELDTTADNSVLEIIVYNTNIGNRHEMLTLEPLNSLLRMKWKKFARHMFFMSCCFYFLYNVTLTLVSYHRPNENEAPPYPLALTRGVGGLQLSGQVMVMLGAIFLAIKESVAIFLLRPSDLQSILSDAWFHFAFFIQALLVIFSVFLYLFSYKEHLVCLVLAMALGWANMLYFTRGFQSMGIYSVMIQKVILQDVIKFLVVYIVFLLGFGVALAALIETCHEGGECHSNSSLGPVLMDLFKLTLGLGDLEIQQNSKYPVLFLLLLITFVVLTFVLLLNMLIALMGETVEDISKESEHIWKLQRARTILEFEKFLPKCLRKKFQLGERCKVAENDTRVCLRINEVKWTEWKTHVSFINEDPGPTDPSKIQDNSRTNSKNTLNTFEEMDDLPETAV
>Downy Woodpecker	XP_009901562.1	MIKDNNEIIPLMGKKTNPSGIPPSNQPEKKSTESTPTKKSSHFFLEIEGFESNATPNNTSPPVFSKPMDSNIRPCASGNGEDMDSPQSLQDDATEYSPNADTCGANISQGPEQTRARKKLKRDLFRAVSEGNPEELQRLLGELRERSSACTSATVPDYLMKKFTASDTGKTCLMKALLNINQNTHEIVNMLLSFAEENGILERFINAAYTEEAYKGQTALNIAIERRQYEITQSLIEKGADVNAYAQGVFFNPKHKHEGFYFGETALALAACTNQPDILQLLMDNTRTNITSQDSRGNNILHALVTVAEDFKTQNDFVIRMYDMILLKSKDRNLETTKNKAGLTPLQLAAKTGKLEILKYILSREIRDKANRSLSRKFTDWAYGPVQSSLYDLTDLDTTSDNSVLEIIVYNTNIGNRHEMLTLEPLNSLLRMKWKKFARHMFFISCCFYFLYNVTLTLVSYHRPNENEAPPYPLALTRGVGWLQLCGQVMVMLGAIFLAIKESVAIFLLRPSDLQSILSDAWFHFAFFIQAMLVIFSVFLYLFSYKEHLVCLVLAMALGWANMLYFTRGFQSMGIYSVMIQKVILQDVIKFLVVYIVFLLGFGVALAALIDTCQDGSDCHSNSSLGPVLMDLFKLTLGLGDLEIQQNSKYPVLFLLLLITYVVLTFVLLLNMLIALMGETVEDISKESEHIWKLQRARTILEFEKFLPKCLRKKFQLGERCKVAENDTRVCLRINEVKWTEWKTHVSFINEDPGPTDPSKVQDNSRTNSKNTLNTFEEMDDLPETSV
>Common Cuckoo	XP_009556781.1	MIKDNNDIIPLMGKKTNPSGTPPSNQQEKKPTESTPTKKSSHFFLEIDGFESNASPNNTSPPVFSKPMDSNIRPCASGNGEDMDSPQSLQDDATEYSPNVDSCCANISQGAEQTSARKKLKKYIFRAVSEGNIEELQCLLAELKERSNACRNMTVPDYLMKKFTAVDTGKTCLMKALLNINENTNEIVNTLLSFAEENGILERFINAAYTEEAYKGQTALNIAIERRQYEITQSLIEKGADVNAHAQGVFFNPKHKHEGFYFGETALALAACTNQPDIIQLLMDNARTNISSQDSRGNNILHALVTVAENLKTQNDFVIRMYDMILLKSKDRNLETTRNKEGLTPLQLAAKTGKLEILKYILSREIRDKPNRSLSRKFTDWAYGPVQSSLYDLTELDTTTDNSVLEIIVYNTNIGNRHEMLTLEPLNSLLRMKWKKFARHMFFMSCCFYFLYNITLTLVSYHRPNENEAPPYPLALMHGVGWLQLSGQVMVMLGAIFLAIKESVAIFLLRPSDLHSILSDAWFHFAFFIQALLVIFSVFLYLFSYKEHLVCLVLAMALGWANMLYFTRGFQSMGIYSVMIQKVILQDVIKFLVVYIVFLLGFGVALAALIETCQDGSECHSHSSLGPVLMDLFKLTLGLGDLEIQQNSKYPVLFLLLLITFVVLTFVLLLNMLIALMGETVEDISKESEHIWKLQRARTILEFEKFLPKCLRKKFQLGERCKVAENDTRVCLRINEVKWTEWKTHVSFINEDPGPTDPSKVQDNSRTNSKTTLNTFEETDDLPETSV
>Anna's Hummingbird	XP_008493324.1	MIKDNNEIVPLMGKKTNPSGIPPSNQQEKKPTESTPTKKSSHFFLEIDGFESNATPNNTSPPVFSKPMDSNIRPCASGNGEDMDSPQSLQDDATEYSPNVDSCCANMSQGPEQRSARKKLKRYIFRAVSEGNIEELQELLTELKERSNACTNMTVPDYLMKKFTASDTGKTCLMKALLNINENTNEIVNTLLAFAEENGILERFINAAYTEEAYKGQTALNIAIERRQYEITQSLIEKGADVNAHAQGIFFNPKHKHEGFYFGETALALAACTNQPDIIQLLMDNARTNITSQDSRGNNILHALVTVAEDFKTQNDFVIRMYDMILLRSKDRNLETTKNKEGLTPLQLAAKTGKLEILKYILSREIRDKPNRSLSRKFTDWAYGPVQSSLYDLTELDTTADNSVLEIIVYNTNIGNRHEMLTLEPLNSLLRMKWKKFARHMFFMSCWFYFLYNVTLTLVSYHRPNENEAPPYPLALTRGVGWLQLLGQVMVMLGAIFLAIKESVAIFLLRPSDLQSILSDAWFHFAFFIQALLVIFSVFLYLFSYKEHLVCLVLAMALGWANMLYFTRGFQSMGIYSVMIQKVILQDVIKFLVVYIVFLLGFGVALAALIETCQEGSECRHYNSSLGPVLMDLFKLTLGLGDLEIQQNSKYPVLFLLLLITFVVLTFVLLLNMLIALMGETVEDISKESEHIWKLQRARTILEFEKFLPKCLRKKFQLGERCKVAENDTRVCLRINEVRWTEWKTHVSFINEDPGPTDPSKVQDNSRTNSKNTLNTFEEMDDLPETSV
>Red-Legged Seriema	XP_009699809.1	MIKDNNEIIPLMDKKINPSGIPPPNQQEKKLTESTPTKKSSHFFLEIDGFESNATPNNTSPPVFSKPMDSNIRPCASGNGEDMDSPQSLQDDATEYSPNVDSCCANISQGPEQTSARKKLKRYIFRAVSEGNIEELQCLLTELKERSNACTNMTVQDYLMKKFTALDTGKTCLMKALLNINQNTNEIVNTLLSFAEENGILERFINAAYTEEAYKGQTALNIAIERRQYEITQSLIEKGADVNAHAQGIFFNPKHKHEGFYFGETALALAACTNQPDIIQLLMDNARTNITSQDSRGNNILHALVTVAEDFKTQNDFVIRMYDTILLKSKDRNLETTKNKEGLTPLQLAAKTGKLEILKYILSREIRDKPNRSLSRKFTDWAYGPVQSSLYDLTELDTTADNSVLEIIVYNTNIGNRHEMLTLEPLNSLLRMKWKKFAQQMFFMSCCFYFLYNVTLTLVSYHRPNENEAPPYPLALTRGVGWLQLSGQVMVMLGAIFLAIKESVAIFLLRPSDLQSILSDAWFHFAFFIQALLVIFSVFLYLFSYKEHLVCLVLAMALGWANMLYFTRGFQSMGIYSVMIQKVILQDVIKFLVVYIVFLLGFGVALAALIETCQDGSECHSNSSLGPVLMDLFKLTLGLGDLEIQQNSKYPVLFLLLLITYVVLTFVLLLNMLIALMGETVEDISKESEHIWKLQRARTILEFEKFLPKCLRKKFQLGERCKVAENDTRVCLRINEVKWTEWKTHVSFINEDPGPTDPSKVQDNSRTNSKTTLNTFEEMDDLPETSV
>Sunbittern	XP_010153216.1	MIKDNSEIIPLMGKKNPSGIPPSNQQEKKPTESTPTKKSSHFFLEIDGFESNATPHNTSPPVFSKPMDSNIRPCASGNGEDMDSPQSLQDDATEYSPNVESCCANISQGPEQTRARKKLKRYIFRAVSEGNIEELQCLLAELKERSNACTSMTVPDYLMKKFTDVDTGKTCLMKALLNINQNTKEIVNMLLSFAEENGILERFINAAY

		TEEVYKGQTALNIAIERRQYEITQSLIEKGADVNAHAQGIFFNPKHKHEGFYFGETALALAACTNQPDI IQLLMDNARTNITSQDSRGNNILHALVTVAEDLKTQNDFVIRMYDMILLKSKDRNLETTKNKEGLTPL QLAAKTGKLEILKYILSREIRDKPNRSLSRKFTDWAYGPVQSSLYDLTELDTTADNSVLEIIVYNTNIGN RHEMLTLEPLNSLLRMKWKKFARHMFFMSCCFYFLYNVTLTLVSYHRPNQNEAPPYPLALTRGVGWL QLSGQVMVMLGAIFLAIKESVAIFLLRPSDLQSILSDAWFHFAFFIQALLVIFSVFLYLFSYKEHLVCLVL AMALGWANMLYFTRGFQSMGIYSVMIQKVILQDVIKFLVVYIVFLLGFGVALAALIETCRDGTGCHSN SSLGPVLMDLFKLTLGLGDLEIQQNSKYPVLFLLLLITYVVLTFVLLLNMLIALMGETVEDISKESEHIW KLQRARTILEFEKFLPKCLRKKFQLGEQCRVAENESRVCLRINEVKWTEWKTHVSFINEDPGPTDPNK VQDNSRTSSKNTLNTFEETDDLPETSV
>Barn Owl	XP_009970996.1	MIKDNNEIIPLMGKKTNPSGIPPSNQQEKKPTEGTPTKKSSHFFLEIDGFESNATPNNTSPPVFSKPMDS NIRPCASGNGEDMDSPQSLQDDATEYSPNVDSCCANISQGPEQTSARKKLKRYIFRAVSEGNIEELQCL LAELKERSNACTNMTVPDYLMKKFTASDTGKTCLMKALLNINQNTNEIVNTLLSFAEENGILERFINA AYTEEAYKGQTALNIAIERRQYEITQSLIEKGADVNAHAQGIFFNPKHKHEGFYFGETALALAACTNQP DIIQLLMDNTRTNITSQDSRGNNILHALVTVAEDSKTQNDFVIRMYDMILLRSKDRNLETTRNKEGLTP LQLAAKTGKLEILKYILSREIRDKPNRSLSRKFTDWAYGPVQSSLYDLTELDTTADNSVLEIIVYNTNIG NRHEMLTLEPLNSLLRMKWKKFARHMFFMSCWFYFLYNVTLTLVSYHRPNENEAPPYPLALTRGVG WLQLSGQVMVMLGAIFLAIKESVAIFLLRPSDLQSILSDAWFHFAFFIQALLVIFSVFLYLFSYKEHLVCL VLAMALGWANMLYFTRGFQSMGIYSVMIQKVILQDVIKFLVVYIVFLLGFGVALAALIETCQDGSECH SNSSLGPVLMDLFKLTLGLGDLEIQQNSKYPVLFLLLLITYVVLTFVLLLNMLIALMGETVEDISKESEH IWKLQRARTILEFEKFLPKCLRKKFQLGERCKVAENDTRVCLRINEVKWTEWKTHVSFINEDPGPTDP SKVQDNSRTNSKNTLNTFEEMDDLPETSV
> Stinkbird	XP_009944089.1	MIKDNNEIIPLMGKKTNPSGIPPSNQQEKKPTESTPTKKSSHFFLEIDGFESNATPNNVSPPVFSKPMDS NIRPCVSRNGEDMDSPQSLQDDATEYSPNVDSCCANRSQGPEQTSARKKLKRYIFRAVSEGNLEDLQC LLAELKERSNVCTNMTVPDYLMKRFTASDTGKTCLMKALLNINQNTNEIVKTLLSFAEENGILERFIN AAYTEEAYKGQTALNIAIERRQYEITQSLIEKGADVNAHAQGIFFNPKHKYEGFYFGETALALAACTN QPDIVQLLMDNTRTNITSQDSRGNNILHALVTVAEDFKTQNDFVIRMYDMILLKSKDRNLETTKNKEG LTPLQLAAKTGKLEILKYILSREIRDKPNRSLSRKFTDWAYGPVQSSLYDLTELDTTANNSVLEIIVYNT NIGNRHEMLTLEPLNSLLRMKWKKFARHMFFMSCWFYFLYNITLTLVSYHRPSENEAPPYPLALTRGM GWMQLSGQVMVMLGAIFLAIKESVAIFLLRPSDLQSILSDAWFHFAFFIQASLVIFSVFLYLFSYKEHLV CLVLAMALGWANMLYFTRGFQSMGIYSVMIQKVILQDVIKFLVVYIVFLLGFGVALAALIETCQDGSE CHSNNSLGPVVMDLFKLTLGLGDLEIQQNSKYPVLFILLLITFVVLTFVLLLNMLIALMGETVEDISKES EHIWKLQRARTILEFEKFLPKRLRKKFQLGERCKVAENDTRVCLRINEVKWTEWKTHVSFINEDPGPT DPSKIQDNSRTNSKNTLNTFEEMDDLPETSV
>Red-Throated Loon	XP_009816957.1	MIKDNNEIIPLMGKKTNPSGIPPSNQQEKKPTESTPTKKSSHFFLEIDGFESNATPNNTSPPVFSKPMDSN IRPCASGNGEDMDSPQSLQDDATEYSPNVDSCCANISQGPEQTSARKKLKRYIFRAVSEGNIEELQCLL AELKERSNACTNMTAPDYLMKKFTASDTGKTCLMKALLNINQNTNEIVNTLLSFAEENGILERFINAA YTEEAYKGQTALNIAIERRQYEITQSLIEKGADVNARAQGIFFNPKHKHEGFYFGETALALAACTNQPD IIQLLMDNTRTNITSQDSRGNNILHALVTVAEDFKTQNDFVIRMYDMILLKSKDRHLETTKNKEGLTPL QLAAKTGKLEILKYILSREIRDKPNRSLSRKFTDWAYGPVQSSLYDLTELDTTTDNSVLEIIVYNTNIGN RHEMLTLEPLNSLLRMKWKKFARHMFFMSCWFYFLYNVTLTLVSYHRPNENEAPPYPLALTRGVGW LQLSGQVMVMLGAIFLAIKESVAIFLLRPSDLQSILSDAWFHFAFFIQALLVIFSVFLYLFSYKEHLVCLV LAMALGWANMLYFTRGFQSMGIYSVMIQKVILQDVIKFLVVYIVFLLGFGVALAALIETCQDGSECHS NSSLGPVLMDLFKLTLGLGDLEIQQNSKYPVLFLLLLITYVVLTFVLLLNMLIALMGETVEDISKESEHI WKLQRARTILEFEKFLPKCLRKKFQLGERCKVAENDTRVCLRINEVKWTEWKTHVSFINEDPGPTDPS KVQDNSRTNSKNTLNTFEEMDDLPETSV
>Dog	XP_005625015.1	MNAHPKEMVPLMGRRAAVPSGNPAILQEKRPAEITPTKKSAHFFLEIEGFDPNPTVSKTSPPIFSKPMDS NIRQCLSGNCDDMDSPQSPQDDVTETPSNPNSPSANVAKEEQRRKKKRLKKRIFAAVSEGCVGELLEL LVELQELCKRRRGLDVADFLMHKLTASDTGKTCLMKALLNINTKTKEIVRILLAFAEENDILDRFVNA AYTEEAYEGQTALNIAIERRQGDLTALLIAAGADVNAHARGVFFNPKYQHEGFYFGETPLALAACTNQ PEIVQLLMENEQTDITSQDSRGNNILHALVTVAEDFKTQNDFVKRMYDMILLRSGTWELETMHNNDG LTPLQLAAKMGKAEILKYILSREIKEKPLRSLSRKFTDWAYGPVSSSLYDLTNVDTTTDNSVLEIIVYNT NIDNRHEMLTLEPLHTLLHMKWKKFAKYMFFLSFCLYFFYNITLTLVSYYRPREEEALPHPLALTHKM GWLQLLGRMFVLIWAMCISVKEGIAIFLLRPSDLQSILSDAWFHFVFFVQAVLVVLSVFLYLFAYKEYL ACLVLAMALGWANMLYYTRGFQSMGMYSVMIQKVILHDVLKFLFVYIVFLLGFGVALASLIEKCPSD NKDCSSYGSFSDAVLELFKLTIGLGDLNIQQNSKYPILFLFLLITYVILTFVLLLNMLIALMGETVENVSK ESERIWRLQRARTILEFEKMLPEWLRSRFRMGELCKVAEEDFRLCLRINEVKWTEWKTHVSFLNEDPG PGRRTADFNKIQDSSRSNSKTTLNAFDEIDEFPETSV
>Domestic Cat	XP_006940018.1	MNVHTKEMVPLMGRRAAVPSGNPAILQEKRSAEITPTKKSAHFFLEIEGFDPNPTVSKTSPPVFSKPMD SNIRQCLSGNCDDMDSPQSPQDDVTETPSNPNSPSANLAKEEQRRKKRRLKKRIFAAVSEGSVEELLEL LVELQELCKRRRGLEVADFLMHKLTASDTGKTCLMKALLNINPNTKEIVRILLAFAEENNILDRFINAA YTEEAYEGQTALNIAIERRQGDVTALLIAAGADVNAHASGVFFNPKYQHEGFYFGETPLALAACTNQP EIVQLLMENEQTDITSQDSRGNNILHALVTVAEDFKTQNDFVKRMYDMILLRSGTWELETMCNNDGL TPLQLAAKMGKAEILKYILSREIKEKPLRSLSRKFTDWAYGPVSSSLYDLTNVDTTTDNSVLEIIVYNTN IDNRHEMLTLEPLHTLLHMKWKKFAKYMFFLSFCFYFFYNITLTLVSYYRPREEEALPHPLALTHKMG WLQLLGRMFVLIWATCISVKEGMAIFLLRPSDLQSILSDAWFHFVFFVQAVLVILSVFLYLFAYKEYLAC LVLAMALGWANMLYYTRGFQSMGMYSVMIQKVILHDVLKFLFVYIVFLLGFGVALASLIEKCSSDNK DCSSYGSFSDSVLELFKLTIGLGDLNIQQNSKYPILFLFLLITYVILTFVLLLNMLIALMGETVENVSKES ERIWRLQRARTILEFEKMLPEWLRSRFRMGELCKVAEEDFRLCLRINEVKWTEWKTHVSFLNEDPGP VRRTADFNKIQDSSRSNSKTTLNAFDEIDEFPETSV
>Water Buffalo	XP_006079771.1	MSICRTAMKAHPKEMVPLTGRRATIPFVNPAIMQEKRPSEITPTKKSAHFFLEIEGFEPNPTVAKTSPPIFS KPMDSNIRQCVSGNCDDMDSPQSPQDDVTETPSNPNSPSANLAKEEQRRKKKRLKKRIFMAVSEGCV EELLELLGELQELCKRRHSLDVPDFLMHKLTALDTGKTCLMKALLNINPNTKEIVRTLLAFAEENDILD RFINAEYTEEAYEGQTALNIAIERRQGDITAALIAAGADVNAHAKGVFFNPKYQHEGFYFGETPLALA ACTNQPEIVQMLMENEQTDITSQDSRGNNILHALVTVAEDFKTQNDFVKRMYDMILLRSRTWELETT RNNDGLTPLQLAAKMGKAEILKYILSREIKDKRLRSLSRKFTDWAYGPVSSSLYDLTNVDTTTDNSVL

		EIIVYNTNIDNRHEMLTLEPLHTLLHMKWKKFAKYMFFLSFCFYFFYNITLTLVSYYRPREEEALPHPL ALTHKMGWLQLLGRMFVLIWAMFISVKEGIAIFLLRPSDLQSILSDAWFHFVFFAQAVLVILSVFLYLFA YKEYLACLVLAMALGWANMLYYTRGFQSMGMYSVMIQKVILHDVLKFLFVYIVFLLGFGVALASLIE KCPKSHENCSSYGSFSDAVLELFKLTIGLGDLNIQQNSKYPILFLFLLITYVILTFVLLLNMLIALMGETV ENISKESECIWRLQRARTILEFEKILPEWLRSRFRMGELCKVAEDDFRLCLRINEVKWTEWKTHVSFLN EDPGPGRRTADSDKIQDSSRSNSKTTLNAFEEIDEFPETSV
>Wild Yak	XP_005906744.1	MKAHPKEMVPLTGRRATIPFVNPAIMQEKRPSEITPTKKSAHFFLEIEGFEPNPTVAKTSPPIFSKPMDSN IRQCVSGNCDDMDSPQSPQDDVTETPSNPNSPSANLAKEEQRRKKKRLKKRIFTAVSEGCVEELLELL GELQELCKRRHSLDVPDFLMHKLTALDTGKTCLMKALLNINPNTKEIVRILLAFAEENDILDRFINAEY TEEAYEGQTALNIAIERRQGDITAALIAAGADVNAHAKGVFFNPKYQHEGFYFGETPLALAACTNQPE IVQMLMENEQTDITSQDSRGNNILHALVTVAEDFKTQNDFVKRMYDMILLRSRTWELETTRNNDGLT PLQLAAKMGKAEILKYILSREIKDKRLRSLSRKFTDWAYGPVSSSLYDLTNVDTTTDNSVLEIIVYNTNI DNRHEMLTLEPLHTLLHMKWKKFAKYMFFLSFCFYFFYNITLTLVSYYRPREEEALPHPLALTHKMG WLQLLGRMFVLIWAMFISVKEGIAIFLLRPSDLQSILSDAWFHFVFFAQAVLVILSVFLYLFAYKEYLAC LVLAMALGWANMLYYTRGFQSMGMYSVMIQKVILHDVLKFLFVYIVFLLGFGVALASLIEKCPKSHE NCSSYGSFSDAVLELFKLTIGLGDLNIQQNSKYPILFLFLLITYVILTFVLLLNMLIALMGETVENVSKES ERIWRLQRARTILEFEKILPEWLRSRFRMGELCKVAEDDFRLCLRINEVKWTEWKTHVSFLNEDPGPG RRTADSNKIQDSSRSNSKTTLNAFEEIDEFPETSV
> American Buffalo	XP_010845784.1	MKAHPKEMVPLTGRRATIPFVNPAIMQEKRPSEITPTKKSAHFFLEIEGFEPNPTVAKTSPPIFSKPMDSN IRQCVSGNCDDMDSPQSPQDDVTETPSNPNSPSANLAKEEQRRKKKRLKKRIFTAVSEGCVEELLELL GELQELCKRRHSLDVPDFLMHKLTALDTGKTCLMKALLNINPNTKEIVRILLAFAEENDILDRFINAEY TEEAYEGQTALNIAIERRQGDITAALIAAGADVNAHAKGVFFNPKYQHEGFYFGETPLALAACTNQPE IVQMLMENEQTDITSQDSRGNNILHALVTVAEDFKTQNDFVKRMYDMILLRSRTWELETTRNNDGLT PLQLAAKMGKAEILKYILSREIKDKRLRSLSRKFTDWAYGPVSSSLYDLTNVDTTTDNSVLEIIVYNTNI DNRHEMLTLEPLHTLLHMKWKKFAKYMFFLSFCFYFFYNITLTLVSYYRPREEEALPHPLALTHKMG WLQLLGRMFVLIWAMFISVKEGIAIFLLRPSDLQSILSDAWFHFVFFAQAVLVILSVFLYLFAYKEYLAC LVLAMALGWANMLYYTRGFQSMGMYSVMIQKVILHDVLKFLFVYIVFLLGFGVALASLIEKCPKSHE NCSSYGSFSDAVLELFKLTIGLGDLNIQQNSKYPILFLFLLITYVILTFVLLLNMLIALMGETVENVSKES ERIWRLQRARTILEFEKILPEWLRSRFRMGELCKVAEDDFRLCLRINEVKWTEWKTHVSFLNEDPGPG RRTADSNKIQDSSRSNSKTTLNAFEEIDEFPETSV
>Sheep	XP_004012614.1	MNAHPKEMVPLTGRRATIPFVNPAILQEKRPSEVTPTKKSAHFFLEIEGFEPNPTVAKTSPPIFSKPMDSN IRQCVSGNCDDMDSPQSPQDDVTETPSNPNSPSANLAKEEQRRKKKRLKKRIFTAVSEGCVEELLELL GELQELCKRRHSLDVPDFLMHKLTALDTGKTCLMKALLNINPSTKEIVRILLAFAEENDILDRFINAEY TEEAYEGQTALNIAIERRQGDIPAVLIAAGADVNAHAKGVFFNPKYQHEGFYFGETPLALAACTNQPEI VQMLMENEQTDITSQDSRGNNILHALVTVAEDFKTQNDFVKRMYDMILLRSGTWELETTRNNDGLTP LQLAAKMGKAEILKYILSREIKDKRLRSLSRKFTDWAYGPVSSSLYDLTNVDTTTDNSVLEIIVYNTNID NRHEMLTLEPLHTLLHMKWKKFAKYMFFLSFCFYFFYNVTLTLVSYYRPREEEALPHPLALTHKMGW LQLLGRMFVLIWAMFISVKEGIAIFLLRPSDLQSILSDAWFHFVFFAQAVLVILSVFLYLFAYKEYLACLV LAMALGWANMLYYTRGFQSMGMYSVMIQKVILHDVLKFLFVYIVFLLGFGVALASLIEKCPQNHENC SSYGSFSDAVLELFKLTIGLGDLNIQQNSKYPILFLFLLITYVILTFVLLLNMLIALMGETVENVSKESERI WRLQRARTILEFEKILPEWLRSRFRMGELCKVAEDDFRLCLRINEVKWTEWKTHVSFLNEDPGPGRRT DFNKIQDTSRSNSKTTLNAFEEIDEFPETSV
>Sperm Whale	XP_007125526.1	MDAHPREMVPLVGRIATLPSGNTAILQEKRPAEITPTKKSAHFFLDIEGFEPNPTVTNNSPLIFSKPMDS NIRQCLLDSCDDMDSPQSPQDDGRETPFNPNCPSANLAKQEQRHKKKWLKKHIFVAVSEGCVEKLLE LLMELQELCEQCRSLDVPDFLMHKLTASDTGKTCLMKALLNINPSTKETVRILLAFAKENNILDRFINA KYTEEAYEGQTALNIAIERRQGDITAVLIEAGADVNAHAKGVFFNPKYQHEGFYFGETPLALAACTNQ PEIVQLLMDNKQTDITSQDSRGNNILHALVTVAEDFKTQNDFVNHMYDMILLRSGNWELETMRNND GLTPLQLAAKMGKAEILKYILSREIKEKRLRSLSRKFTDWAYGPVSSSLYDLTNVDTMTDNSVLKIIVY NTNIDNRHDMLTLEPLHTLLHMKWKKFARYMFFLSFCSYFFYNITLTFISYYLPREEEALPRPLALTYK MGCLQLLGSMFVLIWATCISVKEGIAIFLLRPSDLQSILSDAWFHFVFFVQAVLVVLSVFLYLFGYKEYL ACFVLAMALGWANMLYYTRGFQSMGMYSVMIQKVILHDVLKFLFVYIVFLLGFGVALASLIEKRSKV NEDYSSYGSFNDTVLELFKLTIGLGDLKIQQNSKYPILFLFLLITYVTLTFVLLLNMLIALMGETVENISK ESERIWRLQRARTILEFEKMLPAWLRSRFQMGELCKVAEQDFRLCLRINEVKWTEWKTHVSFLNEDP GPGRRTADFNKIQDSSRSNSKTTLNASDEIDEFPETSV
>Pig	XP_005669174.1	MNAHPKEMVPLVGKRAVIPSGNPAILQEKRPAEITPTKKSAHFFLEIEGFEPNPTVAKTSPPIFSKPMDSN IRQCISGNCDDMDSPQSPQDDVTETPSNPNSPSAHLAKEEQRRKKKRLKKRIFAAVSEGCVEELVELL MELQELGKRRRGLDVSDFLMHKLTASDTGKTCLMKALLNINPNTKEVVRILLAFAEENDILDRFINAE YTEEAYRGQTALNIAIERRQGDITALLIHAGADVNAHAKGVFFNPKYQHEGFYFGETPLALAACTNQP EIVQLLMEHEQTDITSQDSRGNNILHALVTVAEDFKTQNDFVKRMYDMILLRSGTWGLETTRNKDGL TPLQLAAKMGKAEILKYILSREIKDKRLRSLSRKFTDWAYGPVSSSLYDLTNVDTTTENSVLEIIVYNTN IDNRHEMLTLEPLHTLLHMKWKKFAKYMFFLSFCFYFFYNITLTLVSYYRPREVEALPHPLALTHKMG WLQLLGRMFVLIWAMCISVKEGIAIFLLRPSDLQSILSDAWFHFVFFVQAVLVILSVFLYLFAYKEYLAC LVLAMALGWANMLYYTRGFQSMGMYSVMIQKVILHDVLKFLFVYIVFLLGFGVALASLIEKCSKDNK DCTSYGSFSDAVLELFKLTIGLGDLNIQQNSKYPILFLFLLITYVILTFVLLLNMLIALMGETVEDVSKES ERIWRLQRARTILEFEKMLPEWLRSRFRMGELCKVAEEDFRLCLRINEVKWTEWKTHVSFLNEDPGP GRRTADFNKIQDSSRSNSKTTLNAFDEMEEFPETSV
>European Shrew	XP_004605021.1	MNTIPKEMVPLMGRRGAVPNVNPGVLQEKRPAELTPTKKSAYFFLEIEGFEPNPAVAKNSPPVFSKPMD SNIRQCISGNCEDMDSPQSPQDDVTETPSNPNSPCANLAKEEQRRKKKRLKKRIFAAVSEGCVEELLEL LVELQELCKRRRGLDVPDFLMHKLTASDTGKTCLMKALLNINPNTKEIVRILLAFAEENHILARFINAE YTEEAYEGQTALNIAIERRQGDITAVLIAAGADVNAHAKGVFFNPKYLHEGFYFGETPLALAACTNQP EIVQLLMENEQTDITSQDSRGNNILHALVTVAEDFKTQNDFVKRMYDMILLKSGNWELETMRNNDGL TPLQLAAKMGKAEILKYILSREIKEKPLRSLSRKFTDWAYGPVSSSLYDLTNVDTTTDNSVLEIIVYNTN IDNRHEMLTLEPLHTLLHMKWKKFAKYMFFLSFCFYFFYNITLTLVSYYRPREEEAFPHPLALTHKMG WLQLLGRMFVLIWAMCITVKEGIAIFLLRPSDLQSILSDAWFHFVFFVQAVLVILSVFLYLFAYKEYLAC LVLAMALGWANMLYYTRGFQSMGMYSVMIQKVILHDVLKFLFVYIVFLLGFGVALASLIEKCSEDNK

		DCSSYGSFSDAVLELFKLTIGLGDLNIQQNSKYPILFLFLLITYVILTFVLLLNMLIALMGETVENVSKES ERIWRLQRARTILEFEKMLPEWLRSRFRMGELCKVAEEDFRLCLRINEVKWTEWKTHVSFLNEDPGP GRRTADFNKIQDSSRSNSKTTLNAFDEIEEFPETSV
>Bat	XP_006761558.1	MNAHPKEMVPLMGRKATVTSGNQVVLQEKRPAEITPTKKSAHFFLEIEGFEPNPTVAKTSPPIFSKPMD SNIRQCLSGNCDDMDSPQSPQDDATETPSNPNSPSANLAKEEQRRKKKRLKKCLFAAVSEGCVEELVQ LLVELQELCKRRRNLDVPDFLMHKLTASDTGKTCLMKALLNINPNTKEIVRILLAFADENDILDRFINA EYTEEAYEGQTALNIAIERRQRDITALLIAAGADVNAHAKGVFFNPKYQHEGFYFGETPLALAACTNQ PEIVQLLMENEQTDITSQDSRGNNILHALVTVAEDFKTQNDFVKRMYDMILLRSGNWELETMRNNDG LTPLQLAAKMGKAEILKYILSREIKEKRLRSLSRKFTDWAYGPVSSSLYDLTNVDTTTDNSVLEIIVYNT NIDNRHEMLTLEPLHTLLRIKWKKFAKYMFFLSFFFYFFYNITLTLISYYRPREEEALPHPLALTHKMG WLQLLGRMFVLIWAMCISVKEVIVLFELTPSDLQSILSDAWFHFVFFVQAVLVILSVFLYLFAYKEYLAC LVLAMALGWANMLYYTRGFQSMGMYSVMIQKVILHDVLKFLFVYIVFLLGFGVALASLIEKCPKDHK DCSSYGSFSDAVLELFKLTIGLGDLNIQQNSKYPILFLFLLITYVILTFVLLLNMLIALMGETVENVSKES ERIWRLQRARTILEFEKMLPEWLRSRFRTGELCKVAEEDFRLCLRINEVKWTEWKTHVSFLNEDPGSV RRTADFNKIQDSSRSNSKTTLNAFEEIDEFPETSV
>Black Flying Fox	XP_006922255.1	MNAHPKEMMPLMGRKATIPSGNPAILQEKRPAEITPTKKSAHFFLEIEGFEPNPTVAKTSPPVFSKPMDS NIRQCVSGNCDDMDSPQSPQDDMTETPSNPNSPSANLAKEEQRRKKKRLKKCIFVAVSEGCVEELLEL LVDLQELCKRRRGLDVPDFLMHKLTSSDTGKTCLMKALLNINPNTKEIVRILLTFAEENDILDRFINAE YTEEAYEGQTALNIAIERRQGDITALLIAAGADVNAHAKGVFFNPKYQHEGFYFGETPLALAACTNQP EIVQLLMENEQTDITSQDSRGNNILHALVTVAEDFKTQNDFVKRMYDMILLRSGNWELETMRNNDGL TPLQLAAKMGKAEILKYILSREIKEKPLRRLSRKFTDWAYGPVSSSLYDLTNVDTTTDNSVLEIIVYNTN IDNRHEMLTLEPLHTLLHMKWKKFAKYMFFLSFCFYFFYNITLTLVSYYRPREKEAFPHPLALTHKMG WLQLLGRMFVLIWATCISVKEGIAIFLLRPSDLQSILSDAWFHFVFFVQAVLVILSVFLYLFAYKEYLAC LVLAMALGWANMLYYTRGFQSMGMYSVMIQKVILHDVLKFLFVYIVFLLGFGVALASLIEKCPDDKK DCSSYGSFSDAVLELFKLTIGLGDLNIQQNSKYPILFLFLLITYVILTFVLLLNMLIALMGETVENISKESE RIWRLQRARTILEFEKMLPEWLRSRFRMGELCKVAEEDFRLCLRINEVKWTEWKTHVSFLNEDPGPV RRTADFNKIQDSSRSNSKITLNAFEELDEFPETSV
>Golden Snub-Nosed Monkey	XP_010380522.1	MNAHPKETVPLMGKRVAAPSGNPAILPEKRAAEITPTKKSAHFFLEIEGFDPNPTVAKTSPPVFSKPMD SNIRQCISGNCDDMDSPQSPQDDATETPSNPNSPGAHLAKEEQRRKKRRLKKRIFAAVSEGCVEELVEL LVELQELCRRRRDEDVPDFLMHKLTASDTGKTCLMKALLNINPNTKEIVRVLLAFAEENDILGRFINAE YTEEAYEGQTALNIAIERRQGDIAAVLIAAGADVNAHAKGAFFNPKYQHEGFYFGETPLALAACTNQP EIVQLLMDHEQMDITSQDSQGNNILHALVTVAEDFKTQNDFVKRMYDMILLRSGNWELETTRNNDGL TPLQLAAKLGKAEILKYILSREIKEKRLRSLSRKFTDWAYGPVSSSLYDLTNVDTTTDNSVLEITVYNTN IDNRHEMLTLEPLHTLLRMKWKKFAKYMFFLSFCFYFFYNITLTLVSYYRPREEETFPHPLALTHKMG WLQLLGRMFVLIWATCISVKEGIAIFLLRPSDLQSILSDAWFHFVFFIQAVLVILSVFLYLFAYKEYLACL VLAMALGWANMLYYTRGFQSMGMYSVMIQKVILHDVLKFLFVYIVFLLGFGVALASLIEKCPKDNK DCSSYGSFSDAVLELFKLTIGLGDLNIQQNSKYPILFLFLLITYVILTFVLLLNMLIALMGETVENVSKES ERIWRLQRARTILEFEKMLPEWLRSRFRMGELCRVAEEDFRLCLRINEVKWTEWKTHVSFLNEDPGPV RRTADFNKIQDSSRNNSKTTLNAFEEIEDFPETSV
>Small Madagascar Hedgehog	XP_004716220.1	MNTNPKEMVPLLGRRTVVPSGNPAVLQEKRATELTPTKKSAHFFLEIEGFEPNPIVSKTSPPIFSKPMDS NIRQCISGNCDDMDSPQSPQDDVTETPSNPNSPSAHLAKEEQRRNKKRLKKRLFAAVSEGCAEEVVEL LMELQERCRRRRGLDVPDFLMHKLTASDTGKTCLMKALLNINPNTKEIVRILLTFAEENDILDWLINAE YTEEAYEGQTALNIAIERRQGDITAELIAAGADVNAHAKGFFFNPKSQHEGFYFGETPLALAACTNQPE IVQLLMENEQTDITSQDSRGNNILHALVTVSEDFKTQNDFVKRMYDMILLRSGNWELETTCNNDGLN PLQLAAKMGKAEILKYILSREIKEKPLRSLSRKFTDWAYGPVSSSLYDLTNVDTTTDNSVLEIIVYNTNI DNRHEMLTLEPLHTLLRMKWKKFAKYMFFLSFCFYFFYNITLTLVSYYRPREDEALPHPLALTHKMG WLQLLGRMFVLIWAMCISVKEGIAIFLLRPSDLQSILSDAWFHFVFFVQAVLVILSVFLYLFAYKEYLAC LVLAMALGWANMLYYTRGFQSMGMYSVMIQKVILHDVLKFLFVYIVFLLGFGVALASLIEKCPEDSG DCSSYGSFSDAVLELFKLTIGLGDLNIQQNSKYPILFLILLITYVILTFVLLLNMLIALMGETVEKISQESE RIWRLQRARTILEFEKMLPEWLRSRFRMGELCKVAEEDFRLCLRINEVKWTEWKTHVSFLNEDPGPG RRTADLNKVQNSSRSNSKTTLYAFDEIDDFPETSV
>Yellow-Throated Sandgrouse	XP_010081996.1	MIKDNNEIIPLMGKKTNPSGIPPSNQQEKKLTESTPTKKSSHFFLEIDGFESNATPNNTSPPVFSKPMDSN IRPCASGNGEDMDSPQSLQDDATEYSPNVDSCCANISQGPEQTSARKKLKRYIFRAVSEGNIEELQCLL AELKERSNACRNMTVPDYLMKKFTAADTGKTCLMKALLNINQNTNEIVNTLLSFAEENGILERFINAA YTEEAYKGQTALNIAIERRQYEITRSLIEKGADVNAHAQGIFFNPKHKHEGFYFGETALALAACTNQPD IIQLLMDNTRTNITSQDSRGNNILHALVTVAEDSKTQNDFVIRMYDMILLKSKDRNLETMKNKEGLTPL QLAAKTGKLEILKYILSREIRDKPNRSLSRKFTDWAYGPVQSSLYDLTELDTTADNSVLEIIVYNTNIGN RHEMLTLEPLNSLLRMKWKKFARHMFFMSCCFYFLYNITLTLVSYHRPNENEAPPYPLALTRGVGWL QLSGQVMVMLGAIYLAIKESVAIFLLRPSDLQSILSDAWFHFAFFIQALLVIFSVFLYLFSYKEHLVCLVL AMALGWANMLYFTRGLQSMGIYSVMIQKVILHDVIKFLVVYIVFLLGFGVALAALIETCQDGSECNSN SSLGPVLMDLFKLTLGLGDLEIQQNSKYPVLFLLLLITFVVLTFVLLLNMLIALMGETVEDISKESEHIW KLQRARTILEFEKFLPKRLRKKFQLGERCKVAENDTRVCLRINEVKWTEWKTHVSFINEDPGPTDPSK VQDNSRTNSKNTLNTFEETFEEMDDLPETSV
>Killer Whale	XP_004267084.1	MDAHLKEMVPLTGRIATMPSGNAAILQEKRLAEITPTKSAHFFLEIEGFEPSPTVTKTSPLIFSKPMDSNI RQCLPGSCDDMDSPHSPQDDVTETPFNPNSPSANLAKQEQRHKQKRLKKHIFAAVSEGCVQQLLELL MELQELCEQRHSLEVPDFLMRNLTALDTGKTCLMKALLNVNPSTKEIVRILLAFAEENDILDRFINAKY TEEAFEGQTALNIAIERRQGDIAAVLIEAGADVNAHAKGVFFNPKYQHEGFYFGETPLALAACTNQPEI VELLMGNEQTDITSQDSRGNNILHALVTVAEDFKTQNDFVKHMYDMILLRSGNWELETMRNNNGLT PLQLAAKMGKAEILKYILSREIKEKRLRSLSRKFTDWAYGPVSSSLYDLTNVDTMTDNSVLKIIVYNTTI DNRHEMLTLEPLHTLLHMKWKKFAKYMFFLSFCSYFFYNITLTIISYYHTRGEEALKHPLANKMGWL QLLGRMFVLIWAMCISVKEGIAIFLLRPSDMQSILSDAWFHFVFFVQALLVILSVLLYLFACKEYLACLV LAMALGWANMLYYTRGFQSMGMYSVMIQKVILHDVLKFLFVYIVFLFGFGVALASLIEKCSKDNEDC TSYGSFSDTVLELFKLTIGLGDLKIQQNSKYPILSLILLITYVTLTFVLLLNMLIALMGETVENISKESERI WRLQRARTILEFEKMLPEWLKSRFQMGELCKVAEQDFRLCLRINEVKWTEWKTHVSFLNEDPGPGRR SDFNKIQDSSRNNSKTTLNAFDDIDEVPETSV

>Horse	XP_005597720.1	MNAHPKEMMPLMGRRATIPGAHPAILQEKRPAELTPTKKSAHFFLEIEGFEPNPTVTKTSPPVFSKPMD SNIRQCVSGNCDDMDSPQSPQDDVTETPSNPNSPSANLAKEERRRKKRRLKKRIFGAVSEGCVEELLE LLAELLEICKRRRSVDVPDFLMHKLTASDTGKTCLMKALLNINPNTKEIVRILLAFAEENDILDRFINAA YTEEAYEGQTALNIAIERRQGDITAALIAAGADVNAHAKGVFFNPKYQHEGFYFGETPLALAACTNQP EIVQLLMENEQTDITSQDSQGNNILHALVTVAEDFKTQNDFVKRMYDMILLRSGNWELETTRNKDGL TPPQLAAKLGKAEILKYILSREIREKPLRSLSRKFTDWAYGPVSSSLYDLTNVDTTTDNSVLEIIVYNTTI DNRHEMLTLEPLHTLLHMKWKKFAKYMFFLSFCFYFFYNITLTLVSYYRPREEEALPHPLALTHKMG WLQLLGRMFVLIWAMCISVKEGIAIFLLRPSDLQSILSDAWFHFVFFVQAVLVILSVFLYLFAYKEYLAC LVLAMALGWANMLYYTRGFQSMGMYSVMIQKVILHDVLKFLFVYIVFLLGFGVALASLIEKCSKDNK NCSSYGSFSDAVLELFKLTIGLGDLNIQQNSKYPILFLFLLITYVILTFVLLLNMLIALMGETVENISKESE RIWRLQRARTILEFEKMLPEWLRSRFQMGELCKVAEEDFRLCLRINEVKWTEWKTHVSFLNEDPGPG RRTDDFNKIQDSSRSNSKTTLNAFDEIEEFPETSV
>Green Sea Turtle	XP_007057812.1	MKLNNYESIYYRNMIKDNKENIPLMAKRTNTSGPPTTNHQEKKPTENTPTKKSSQFFFEIEGFESNSSP RQTSPPVFSKPMDSNIRPCASVNGEDMDSPQSLQDDITEYATNIDSYCTNMLQGGHWNNARKKLKKY MFRAVSEGNIEELQCLLMQVKERSNACRNMTVQDYLMKKLTDSDTGKTCLMKALLNINQNTNEIVK MLLSFGEENSFLERLINAEYTEEAYKGQTALNIAIERRQYDIAQTLIEKGADVNAHSQGVFFNPKHKHE GFYFGETPLALAACTNQPDIVQLLMDNRRTDITSQDSRGNNILHALVTVAEDFKTQNDFVIRMYDMIL LKSKSRTLETMKNKDGLTPLQLAAKSGKLEILKYILSREIKDKPKRSLSRKFTDWAYGPVQSSLYDLTE LDTTADNSLLEIIVYNTNIGNRHEMLTLEPLHSLLRMKWKKFARHMFFMSCCFYFIYNIMLTLVSYYRP RRDEAPPYPLDLTGNLGWLQLLAQVLIMIAAIFLAIKESVAIFLLRPSDLQSILSDAWFHFAFFIQAVLVIF SVFLYLFSYKEHLVCLVLAMALGWANMLYFTRGFQSMGIYSVMIQKVILQDVLKFLVVYIVFLLGFGV ALAALIDTCPNDSKCYTHSSLGAVLMELFKLTIGLGDLEIQQNSKYPVLFLLLLITYVLLTFVLLLNMLI ALMGETVENISKESEHIWRLQRARTILEFEKMLPKYLKKRFQLGELCKVAENDTRVCLRINEVKWTE WKTHVSFINEDPGPTGYNRIQDTSRSNSKNTLNTFDEMDYLLETTV
>American Alligator	XP_006275259.1	MGKKPNPPGTPPTHHQDKKATESTLPKKSSHFFLELDGFDSNSTPSHASPPVFSKPMDSNIRPCASGNG EDIDSPQSLQDDITNTDSCCNYFTAQPSQQNNVRKKLKKYLFRAVSEGNIEELCHLLIEIKERSNACRN MTVPEYLMKKLTASDTGKTCLMKALLNINRNTNEIVNILLSFAEENSILEIFINAAYTDEAYKGQAALNI AIERRQYDIAKTLIEKGADVNAHAEGVFFNPKYKHEGFYFGETPLALAACTNQPDIVQLLMANSRTDI TSQDSRGNNILHALVTVAEDFKTQNDFVIKMYDMILLKSKARMLETMKNKDGLTPLQLAAKTGKVEI LKYILSREIKDKPNRSLSRKFTDWAYGPVQSSLYDLTELDTTVDNSLLEIIVYNTNIGNRHDMLTLEPLN SLLRMKWKKFARHMFFISCCFYFIYNVTLTLVSYHKPHGEEDPPYPLILTRNMGWLHLMGQLFVMLG ALGLAVRESVAIFLLRPSDLQSILSDAWFHFAFFIQAVLVIFSVFLYYFSYKEHLVCLVLAMALGWANML YFTRGLQSMGIYSVMIQKVILHDVIKFLVAYIIFLLGFGVALAALVDPCPKNTECHSYSSLGKVLMELFK LTIGLGDLEIQQNSKYPLLFLLILITYVILTFILLLNMLIALMGETVENISKESEHIWKLQRARTILEFEKIL PKYLRKKFKLGELCKVAENDTRLCLRINEVKWTEWKTHVSFINEDPGATDYNRIQDNSRSNSKNTLN TFDEMDDLRETTV
>Chinese Alligator	XP_006033191.1	MIKDNKETIPLMGKKPNPPGTPPTNHQDKKATESTLPKKSSSHFFLELDGFDSNSSPSHASPPVFSKPM DSNIRPCASGNGEDIDSPQSLQDDITNTDSCCTNLPHGAQQNNVRKKLKKYLFRAVSEGNIEELCHLLI EIKERSNACRNMTVPEYLMKKLTASDTGKTCLMKALLNINRNTNEIVNILLCFAEENSILEIFINAAYTD EAYKGQAALNIAIERRQYDIAKTLIEKGADVNAHAEGVFFNPKYKHEGFYFGETPLALAACTNQPDIV QLLMANSRTDITSQDSRGNNILHALVTVAEDFKTQNDFVIRMYDMILLKSKARMLETMKNKDGLTPL QLAAKTGKVEILKYILSREIKDKPNRSLSRKFTDWAYGPVQSSLYDLTELDTTVNNSLLEIIVYNTNIGN RHDMLTLEPLNSLLRMKWKKFARHMFFISCCFYFIYNVTLTLVSYHKPHGEEDPPYPLILTGNMGWLH LMGQLFVMLGALGLTVRESVAIFLLRPSDLQSILSDAWFHFAFFIQAVLVIFSVFLYYFSYKEYLVCLVL AMALGWANMLYFTRGLQSMGIYSVMIQKVILHDVIKFLVAYIIFLLGFGVALAALIDPCPNNTECHSYS SLGKVLMELFKLTIGLGDLEIQQNSKYPLLFLLILITYVILTFILLLNMLIALMGETVENISKESEHIWKL QRARTILEFEKILPKYLRKKFELGELCKVAENDTRLCLRINEVKWTEWKTHVSFINEDPGATDYNRIQD NSRSNSKNTLNTFDEMDDLRETTV
>Western Clawed Frog	NP_001243218.1	MINKHPGEMSPLISRERLAPGTPPRSPRHTENGLKRNDTTDFSRSNPLWLSTQMDTNNYSNEKKNEDT DTPQTTQTAFSPCYGWQGRKPALTRNTRKPTKKLLFKAVSEGDTEMLTDLLSEAKSSSRVYSVTQAKE FFMHKLTSKDTGKTCLMKALLNINEKTPEVVRSLLTFAEENDILETFINAEYTEENYKGQTALNIAIERR QVELVKYLIEKGAKIDVRAQGRFFNPKNKYEGFYFGETPLALAACTNQPEIVQLIMDKSPTIGTIQDSL GNTVLHALVNVADNSEAQNDFIIGMYDTILRNCKNKSLEQIPNNEGLTSMQLAAKLGKTEILHYILSRE IKEKENMVLSRKFTDWAYGPVSSSLYDLTSIDTCWPNSVLEIVVYNTDIDNRHELLTLEPLHTLLQMK WKKFARYMFFLSFLLSFTYNIALTLVSYYRPRGEQDVYPLNLSYENGWLQLVGQMFIIVCATYLMVKE AVVMFLVKQSDLKSVLSDAWFHILFFIQAVLVIVSVFCYLFGVDFYLVFLVLAMALGWMNLLYYTRGF QSLGIYSVMIQKVILNDVLKFLFVYILFLLGFGVALASLLENCEDGEECQSLSTAILELFELTIGLRGLEM DKDPKYPVLFLFLLITFVILTFVLLLNMLIALMGETVEKISQESEHIWRLQRARTILEFEKSLPAWLQAR FQLGESCTVSKGDNNRICLRINEVKWTEWNNHVTCIKEEPGLTFFPDTKDTNTASEDELDSFEKFAGISI SVGDLEDQAMETTV
>Elephant Shark	XP_007894728.1	MIKFRARRELRMMDKNLRVLLATEVDSCTPDPCNEMKIKQRKLQNRVWVDFYRSIAEGDLGEFDKFL QLFQESKTKLTAEWLRDPRTGKTCLMKALLNLNDNTQEMVEKLISFAEASDSLEQLINAEYTDREYK GQTALHIAIERRCKTIVQLLVEKGADINAKAQGRFFKPKKLKHGFYFGELPLSLAACTNQPDIVTLLMA SGRTDVRAQDAWGNCILHALVTVADDSEDNTTFVTEMYDMILMSSQDHNLEGICNLRGLNPLQLAA KLGKFKIFSHILCREFKDKKHLNLSRKITDWAYGPVSSSLYDITEVDTNHQNSVLEIVVHNTKIQNRHE LLSVEPLNTLLEEKWLTFGAHMFTITCIVYVLYIIGFTTVYYNQAERYQSLISENLTSTTSLQLFGEISSFT AAWVVIIKEGLVLVRLRPSDLRSIVTDAWFHILFFLQALMTASSAVLCWARVEAHLLLLVPALALGWIN ILYFTRGFKSMGIYSVILQKVLLTDVLLFLFVYLLFLIGFSVALASLIDSCPNSLECSPYLTFNTVILELFK LTLGLGDLQIQQHAKYPQLFLLLLGVYVVLTFVLLLNMLIALMSETVEDTAKESKNIWKLQRARMILN LERSLPKCLRRRFQLGTILKNSQGHSRRYIRINEVNWTKWKTSVARIHEDPGNEEEEQEDKSSDEVEH KICPGTTLQSVQTTSGPSDSEKEEPRCKRIGKLRIKAKNMNTLHSEAVLEQETYPLQEPSNTTQ
>Western Painted Turtle	XP_008167187.1	MLHVVMTIIHVLQGHNFSSSSSLCPSFMGVAPELRSPWKSRNMIKDNKENIPLMGKRTNTSGPIANHQ EKKPSENTPTRKSSQFFFEIEGFESNSSPRQTSPPVFSKPMDSNIRPCASGNGEDMDSPQSLQDDITEYAT NVDSYCTNMLQGDHQNNARKKLKKYMFRAVSEGNIEELQCLLMEVKERSNACRNMTVQDYLMKK LTDSDTGKTCLMKALLNINQNTNEIVKILLSFGEENNFLERLINAKYTEEAYKGQTALNIAIERRQYDIA

		QTLIQKGADVNAHSQGVFFNPKHKHEGFYFGETPLALAACTNQPEIVQLLMDNRRTDITSQDARGNNI LHALVTVAEDFKTQNDFVIRMYDMILLKSKSRTLETMKNKDGLTPLQLAAKSGKLEILKYILSREIKDK PNRSLSRKFTDWAYGPVQSSLYDLTELDTTADNSLLEIIVYNTNIGNRHEMLTLEPLHSLLRMKWKKFA RHMFFMSCCFYFIYNIILTLVSYYRPRRDEAPPYPLALTRNMGWLQLLVQVLIMIAAIFLAIKESVAIFLL RPSDLQSILSDAWFHFAFFIQAVLVIFSVFLYLFSYKEHLVCLVLAMALGWANMLYFTRGFQSMGIYSV MIQKVILQDVIKFLVVYIVFLLGFGVALAALIETCPNDSKCHSHSSLGAVLMELFKLTIGLGDLEIQQNS KYPVLFLLLLITYVLLTFVLLLNMLIALMGETVENISKESEHIWRLQRARTILEFEKMLPKYLKKKFQL GELCKVAENDTRVCLRINEVKWTEWKTHVSFINEDPGPTGYNRIQDTSRSNSKNTLDTFDEMDYLLET TV
>Burmese Python	XP_007438955.1	MIKDIKEMVPLMGNKKPGPRETPPAADQDKRAAEGAPAKKRLNPASLLFPSTLSWRVQHRQIPNVTPH LGSSHFFLEIEAFESNVSPSRTSPPIFSKPMDSNIRPCASANCEDMDSPQSIQDDMTEYTPNAESSCTNST HNAQQNNYRKKLKKYLFRAVSEGNLEDLQRLLVEMKDRSQRCQNLTVQEYLMNKMTSSDTGKTCL MKALLNINQHTKEIVNMLLSFAEENQILEKLINASYTEEAYRGQTALNIAIERRQYDITQTLIEKGADV NARAQGVFFNPKRKHEGFYFGETPLALAACTNQPDIVQLLMENSKTDIMSQDARGNNILHALVTVAE DFKTQNDFVRRMYDTILLKSRSRDLETMKNKAGLTPLQLAAKTGKLEILKYILSREIKEKPIRSLSRKF TDWAYGPVQSSLYDLTELDTTSENSLLDIIVYNTNIGNRHEMLALEPLHSLLRMKWKRFARHVFFLSC CLYFFYNLILTLISYYRPHTTQPPPYPLALIGDLNWLQLAGQAAVILGAVFIAIKESVALFLLRPSDLQTIL SDAWFHFAFFIQAVLVIFSVFLYLFSYKGHLPCLVLAMSLGWANMLYFTRGLQSMGIYSVMIQQVILHD VIKFIVVYLVFLFGFGVALAALVDSCPEDSKCNEYSVLGSIEIDLFMLTLGLGELDVPKNAKYPILFLLL LISFVILTFVLLLNMLIALMGETVEDISKESEHIWRLQRARTIVEIEKLLPQFLRRRFQLGEWCKVADSD SRLCLRINEVKWTEWKTHVAFINEDPGSTDCSRMQDTSRSNSKTTLNAFEEIYDLPETTV
>Nanorana parkeri	XP_018413135	MSKNDGVALLAKDRIPPGTPPRTHKPLDNGLKKSDTTDFPVAPSKSSFPVFSKPMDSNIKHCDIRKSEDI DSPQTSPEVSEYLLKKYNNGVDSISPKKTPKRPPKNLLFKAVSEGDIESLNRLLQEAKESAATYTQKEA QDFFVYKLTSKDTGKTCLMKALLNINDNTPEIVCILMSFAEENGFLERLINAAYTEENYKGQTALNIAI ERRQSDLAKCLIRKGANINVRAQGRFFNPKHKHEGFYFGETPLALAACTNQPDVVQLLMENSQTNVT IQDSLGNTVLHALVTVAENSEAQNVFIIRMYDTILRTCKNKSLESIENNEGLTPMQLAAKTGKTEILHYI LSREIKEKENRVLTRKFTDWAYGPVSSCLYDLKDVDTCSRNSLLEIVVYNTNTNNRHELLALEPLHTLL QLKWKKFARYMFLLSFLLSLTYNVALTLISYYRPRGEQALYPLSLTYDRGWLQLVGQMFIIVCATYLMI KEGVVIFLVKPSDLRYVLSDAWFHVLFFIQAVLVILSVFCYLFGVKEYLAFLVLAMALGWANMLYYTR GFQSLGIYSVMIQKVILNDVLKFLFVYILFLFGFGVALASLIENCTDGDECSAYKSFSTAIVELFKLTIGL GDLEIQHDSKYPVLFLLLLIAYVILTFVLLLNMLIALMGETVEKVSKESEHIWRLQRARTILEFEKNLPM WLKGKFQLGESCTVSKNDNRTCLRINEVKWTEWHNHVTCINEEPGFAMCSGTSYANFNAEDEPDSFE NDQPVTIEFKDVVEPCIETTV
>Xenopus laevis	XP_018101159	MKRQKMINKHPGEMSPLISRMPPGTPPPRSPRHTENGLKRNDTTDFSRSQPLLLSTQMDTKNFSDDRK PEDIDTPQTTQTVFPCSWQARKLALASNTRKPIKKLLFKAVSEGDTEMVTELLAEAKSYSMVFAKTQA KDFLIHKLTSKDTGKTCLMKALLNINEMTPEIVRILLTFAEENDILQPLVNAEYTEENYRGQTALNIAIE RRQLELVKYLIEKGAGIDVRAQGRFFNPKNKYEGFYFGETPLALAACTNQPDIVQLIMDKCPTIGTMQ DSLGNTVLHALVIVADNSEAQNDFIIRMYDTILRNCKNKSLEQIPNNEGLTSMQLAAKLGKTEILHSILS REIKEKENMVLSRKFTDWAYGPVSSSLYDLTGIDTCWPNSVLEIAVYNTKINNRQELLTLEPLHTLLQM KWKKFARYMFFMSFLLSFTYNIVLTLVSYYRPREEQDRYPLNLSYENGWIQLIGQMFIIVCATYMMVK EAVVIFLVKQSDLKSVLSDAWFHILFFIQAVLVIVSVFCYLFGVTIYLVFLVLAMALGWLNLLYYTRGF QSLGIYSVMIQKVILNDVLKFLFVYILFLLGFGVALASLLEDCKDGEQCQSLSTTIMELFELTIGLRGLE MDNEPKYPALFLLLLITFVILTFVLLLNMLIALMGETVEKISQESEHIWRLQRARTILEFEKNLPTWLQS RFQLGESCTVSKGDNNRICLRINEVKWTEWNNHVTCINEEPGLMFVADTKETNTASEDELDSFEKFPG ISISIGDLEDQVMETAV
>V3-like isoform X2 [Latimeria chalumnae]	XP_006010861.1	MEDSAAEGILLMERAGSNISIDNETIVPLQDHSEEMDSEDDKCPDHMDIPYFVVPIETVLECSNPKETRI GELSEAICDGSLEKVKAILNELPSKTFEEFKVSANGQTYLMKALLNFNEKTKETVELLLTFAEDNGFLK VLINAEYENGDYKGQTALHIAIERRCKDIVKLLLNKGADVDAKACGDFFNPKMNMDGFYFGETPLAL AACTNQLEIVQMLLEKGSDTGFQDSRGNTVLHALVEVADDSENYINSIKQIYEEILTKHEGENLEAVTN NKNLTPVHLAAQRGKRWILKYILERELKDKKTRNLSRKHTTWAYGPVSSSVYDLTGLDADQDISVLK LIVYNSEIPERHEMLALEPLNTVLCMKWEKFASKMFSISFLFYFTYNVILTLISYYRPNRDKFPVPLDLS RHSGRLHFSGQVFVFICAIYLMIKESIELILLRPSDLKIVLSDAWFHITFFLQAALIIVSSIMCWSSLKECV IVLVLGLSLGWINMLYYTRGFETLGIYSVMVQKVILNDVLKFLLVYALFLLGFGVALASLVNTCPDNN DCSPYSSYHTTVLELFKLTLGLGDLELQKHSLYPELFLALLVLYVLLTFVLLLNMLIALMGETVEELSK KSKNIWKLQRARTILDLERRLPPYFRKKFRIGQFYHFNDNHRWCIRINELNWTEFNTSVACTEEDPAKK EHNGSTRRMSPLLPEESS